

The potential application of rapeseed pomace extracts in the prevention and treatment of neurodegenerative diseases.

POHL, F.

2019

The author of this thesis retains the right to be identified as such on any occasion in which content from this thesis is referenced or re-used. The licence under which this thesis is distributed applies to the text and any original images only – re-use of any third-party content must still be cleared with the original copyright holder.

*THE POTENTIAL APPLICATION OF
RAPESEED POMACE EXTRACTS IN
THE PREVENTION AND TREATMENT
OF NEURODEGENERATIVE DISEASES*

FRANZISKA POHL

A thesis submitted in partial fulfilment of the
requirement of the
Robert Gordon University (Aberdeen)
for the degree of Doctor of Philosophy

This research programme was carried out
in collaboration with the
Life and Health Sciences Research Institute (ICVS),
Universidade do Minho and the
Rowett Institute of Nutrition and Health,
Aberdeen University

January 2019

Dedication

"This thesis is dedicated to all those suffering from neurodegenerative disease and those caring for them."

"Unless someone like you cares a whole awful lot, nothing is going to get better. It's not."

~Dr. Seuss~

ABSTRACT

Rapeseed pomace (RSP) is the waste/by-product obtained after edible oil production from *Brassica napus* and is currently used as animal feed. In an attempt to revalorize this by-product as a potential nutraceutical for the treatment or prevention of neurodegenerative disease, this project aimed to determine (i) a suitable extraction technique, (ii) the phytochemical composition and *in vitro* activity of the extract, in relation to neuroprotective properties, (iii) the neuroprotective potential of the extract in a cellular model (SH-SY5Y neuroblastoma cells) and (iv) the extracts potential to prevent/treat neurodegenerative disease in one Machado-Joseph disease (MJD) and three Parkinson's disease (PD) *C. elegans* (nematode) models.

To achieve this aim at the start of the project, three extraction techniques i.e. Soxhlet, ultrasonic assisted and accelerated solvent extraction were employed using a solvent mixture of ethanol and water (95:5) on the RSP samples obtained from the north east of Scotland. Based on the chemical composition of the extracts and their antioxidant properties, Soxhlet extraction was revealed as the most promising and practical extraction technique. Bulk extraction was carried out, to obtain enough RSP extract that would last for the duration of the project. Thereafter, the composition of the extract was further investigated, to show sinapine to be the most abundant secondary metabolite, together with other phenolic acids, such as sinapic, ferulic, caffeic and syringic acid. The final extract showed *in vitro* antioxidant and acetylcholinesterase inhibition activity, the potential to protect plasmid DNA from oxidative damage, copper ion chelating potential and the inhibition of self-mediated β -amyloid (1–42) aggregation. The latter *in vitro* characteristics and properties could be beneficial for the protection of neurons from oxidative stress induced degeneration.

In the SH-SY5Y neuroblastoma cell line, the RSP extract was found to be non-toxic up to a concentration of 1.5 mg/mL. Subsequent cellular studies using 1 mg/mL or less of the RSP extract, showed its ability to protect the cells from reactive oxygen species (ROS) and oxidative DNA strand breakage induced by hydrogen peroxide. In addition, using protein array technology, the RSP extract was able to down regulate cell stress associated proteins SIRT2 and SOD2.

In the *C. elegans* nematode model, the RSP extract showed no toxicity up to 5 mg/mL. The RSP extract was able to improve the disease phenotype in the MJD model (motility deficiency) as well as in all three PD models (dopaminergic neuronal loss). This improvement was at least partially dependent on the activation of the antioxidant gene glutathione-s-transferase (*gst-4*) in *C. elegans*. Overall, the RSP extract showed very positive *in vitro* characteristics and valuable *in vivo* effects in 4 disease *C. elegans* models, thus warranting further detailed studies on the use of RSP extract to help prevent and/or treat neurodegenerative diseases.

Keywords: rapeseed pomace/cake/meal, canola, antioxidants, phenolics, neurodegeneration, *C. elegans*, SH-SY5Y, oxidative stress, acetylcholinesterase, β -amyloid, antioxidant pathways, Machado-Joseph disease, Parkinson's disease, Alzheimer's disease

ACKNOWLEDGEMENTS

Most of all I would like to thank my main supervisor Prof Kong Thoo Lin. He has been a great support throughout the last 4 years and especially his encouragement right from the beginning on writing papers made it possible for me to get the most out of my research project (hopefully at least 3 papers and one review). He encouraged me to continue even when things were not going well on more than one occasion. Only his contact to Portugal made it possible for me to work in Braga at the ICVS, which is where I found my passion for *C. elegans*. Thank you very much for all the support, I hope there is room for further collaboration in the future.

I would also like to thank Dr Marie Goua for her help with the flowcytometry work as well as for her support during the protein array experiment and her feedback on my thesis draft. Furthermore, I would like to thank Dr Giovanna Bermano for her help in ordering *C. elegans* strains for RGU and letting me use some of her equipment for the nematode related work. Both of them also deserve thanks for their support through supervisory meetings.

In addition, I would also like to thank Prof Susan Duthie, who although not part of my supervisory team was of great support regarding the comet assay. Her and Dr Elena Lendoiro were very kind in teaching me the comet assay and both were open for all kinds of questions regarding the experiment. Dr Susan Duthie also assisted with advice on the creation on the comet assay graphs and was available for meetings regarding all kinds of issues project or university related.

There are a number of other people I would like to thank at RGU, including Iain Tough and Emily Hunter, for their help with all microscopy related questions, Julia Kennedy for her support with all ERASMUS related issues, Gemma Barron for her support with the SH-SY5Y cell line and general molecular biology related questions and Fiona Aitcheson for her help with booking my flight to a conference in Philadelphia, when I thought I would not be able to go after the initial booking was cancelled. In addition, there is Andrea MacMillan from the graduate school to thank for her administration and mental support, especially in the first three years of the PhD, Noelle O'Driscoll, who let me help her teach the third year pharmacy students which provided me with valuable teaching experience and Kyari Yates, who helped

supervising one of the exchange students on my project, which led to the production of a further paper and the proof of the presence of sinapine within the extract.

There are also numerous project students to thank for who were either directly or indirectly involved in my project and which presented me with the possibility to get great supervisory experience. These students include Sarah Wynants, who helped with the initial set up of all the antioxidant assays as well as the Ellman assay, Lisa Leyser, who tested the antioxidant activity of a number of compounds individually and in synergy, Annika Mozer and Maike Busch for their further determination of phenolic acids in the extract at RGU and initial studies of the Fenton reaction in the DNA plasmid protection assay, Annette Lenaerts and her unfortunately unsuccessful attempts to produce beta amyloid peptide for us as well as her experiments on the acetylcholinesterase inhibition potential of some of the found compounds in the extract, Louis Watters, who helped us to determine the sinapine in the extract, he set up the metal chelating assays and determined the acetylcholinesterase inhibition potential and antioxidant activity of phenolic acids and sinapine, which were essential for the production of the second paper. Last but not least also thanks to Victoria Lindsay, who took the opportunity to follow in my footsteps and did her masters project in Portugal in collaboration with Patricia Maciel and Andreia Teixeira-Castro. This made it possible for us to get a closer look into the importance of *gst-4* when treating *C. elegans* with RSP extract. Having her as a student also helped to teach me to support students before and while they are on an exchange program. She took the time before her exchange to learn the basics of *C. elegans* from me which saved a huge amount of time during her stay in Portugal. Her work will add to the third paper, which we hope to publish after the preparation of this thesis, which will include all the *C. elegans* results.

This brings me to another very important group of people I would like to thank, which is Patricia Maciel and her MJD group at the ICVS in Braga. Patricia has been a great support throughout the entire project, with advice and comments on abstracts and presentations, especially in relation to the *C. elegans* work. She introduced me to the ataxia community by suggesting submitting an abstract to the national ataxia investigators meeting 2018 and was always welcoming me in her lab, where I now spend more than one year

in total over the last 5 years. Working in a different lab and lab environment was the best part of my PhD time and I wouldn't want to miss it. Patricia's research group is amazing, and I need to express a special thanks to Andreia, who helped with the experimental set up of the work in Portugal especially at my last stay and is responsible for all the counted neurons and confocal imaging presented in this thesis. Special thanks also to Marta who was of great help to me and Victoria during our project and Ana, who was not in the lab at my last visit in 2017 but was of great supported for the previous two visits. There are also Carlos, Sarah, Andreia, Joana, Juliana and Daniela, all of which helped me out in Braga as well as so many other people from the ICVS which have made my stay so much more enjoyable. I hope that there will be further collaborations in the future. You are a great research team. Obrigada!

I would also like to thank Prof Wendy Russell for her help and support, especially in the beginning of the project by initiating the initial LC-MS/MS studies at the Rowett Institute. Wendy and her research team including Lorraine Scobbie, Lesley Milne and Madalina Neacsu provided the necessary support for the secondary metabolite composition analysis of the rapeseed pomace and the RSP extracts, including the glucosinolates analysis. I also need to thank her for her feedback on the draft of my thesis.

Also, friends in the office and in the labs need to be thanked, including Cameron, Benedicta, PJ, Maria, Steve, Josh, Calum, Matteo, Serena, Mhairi, Hazel, Prisila, Katia, Quirin, Tesnime, Elena who made the last four years more enjoyable Danke, Grazie, Ευχαριστώ, Obrigada, Gracias, شكر. In this category also fall my two German friends Johana and Julia, who where a big part of the last four years. Especially Julia, who had started the "Aberdeen adventure" with me in 2011 and has been a great friend ever since, Danke. Also, a great thanks to all my other friends at home and aboard which I was able to visit during the last 4 years, which gave me a break from all the lab work and research.

I am also deeply grateful to TENOVUS Scotland (Grampian) who funded this project for 4 years and let me have an inside into the workings of a charity. Without their support this project would not have been possible. For my periods abroad, I have to thank the ERASMUS program for funding, they

supported me for all my trips to Portugal. Without this funding the research exchange might not have been possible. I would also like to acknowledge Gregor Mackintosh, who provided the RSP for the project and allowed me to view his farm and the production process of the rapeseed oil.

My last thanks go out to my family, who supported my decisions on going to Aberdeen in 2011 and ever since have been supportive of all my decisions, including doing this PhD. Finally, thanks to my fiancé Jeremy, who was always there for me, had to hear all the complains up until the very end and still wants to marry me and supported my choice to go to Portugal; and thanks, also to the newest member of the family Jango, who made the last weeks of writing a bit more enjoyable and challenging at the same time. I love you all.

RESEARCH OUTPUT

Oral conference presentations:

- Natural Product Biotechnology 2014, 18th-20th November Inverness, Scotland "The potential use of Rapeseed Pomace extracts against neurodegenerative disease in a *C. elegans* model"
- ICMAN IUPHAR From Nutraceuticals to Pharmaceuticals-Common Challenges and Approaches 2017, 26th-29th September Aberdeen, Scotland "A study into antioxidant and DNA protective properties (in vitro) of a RSP extract and its effects on neurodegenerative disease *C. elegans* models", published abstract:
 - Pohl, F. et al. O18 Revalorisation of rapeseed pomace (RSP): A study into antioxidant and DNA protective properties (in vitro) of a RSP extract and its effects on neurodegenerative disease *C. elegans* models. *Biochemical Pharmacology*. **139**, 115 (2017)
- 12th World Congress on Polyphenols Applications 2018, 25th-28th September Bonn, Germany "Utilization of rapeseed pomace (RSP) extract: A study into its phenolic contents, *in vitro* anti-oxidant properties and *in vivo* activation of oxidative stress response enzymes"

Poster conference presentations:

- Phytochemicals and health: new perspectives on plant based nutrition 2016, 21st-22nd March Edinburgh Scotland "Study into the polyphenol content and antioxidant activity of rapeseed pomace extracts", published abstract:
 - Pohl, F. et al. Study into the polyphenol content and antioxidant activity of rapeseed pomace extracts. *Proceedings of the Nutrition Society*. **75**, E59 (2016)
- 7th Ataxia Investigators Meeting (AIM) 2018, 2nd-5th April Philadelphia, USA "Utilization of Rapeseed Pomace (RSP) Extracts in the Prevention of Neurological Impairment in a *C. elegans* Model of Machado-Joseph Disease (MJD)"

Published Paper (page xv/xvi):

Pohl F, Goua M, Bermano G, Russell W, Scobbie L, Maciel P. et al. Revalorisation of rapeseed pomace extracts: An in vitro study into its anti-oxidant and DNA protective properties. Food Chemistry. 239, 323–332 (2018).

Yates K, Pohl F, Busch M, Mozer A, Watters L, Shiryaev A et al. Determination of Sinapine in Rapeseed Pomace Extract: its antioxidant and acetylcholinesterase inhibition properties. Food Chemistry. 276, 768-775 (2019).

Pohl F, Kong Thoo Lin, P. The Potential Use of Plant Natural Products and Plant Extracts with Antioxidant Properties for the Prevention/Treatment of Neurodegenerative Diseases: In Vitro, In Vivo and Clinical Trials. Molecules. 23, 3283 (2018).

Paper in preparation:

*Pohl F et al. Activation of *gst-4* in *C. elegans* by rapeseed pomace extract prevents neurodegeneration in models of Parkinson's and Machado-Joseph disease (working title)*



Contents lists available at ScienceDirect

Food Chemistry

journal homepage: www.elsevier.com/locate/foodchem

Revalorisation of rapeseed pomace extracts: An *in vitro* study into its anti-oxidant and DNA protective properties



Franziska Pohl^a, Marie Goua^a, Giovanna Bermano^b, Wendy R. Russell^c, Lorraine Scobbie^c, Patrícia Maciel^{d,e}, Paul Kong Thoo Lin^{a,*}

^a School of Pharmacy and Life Science, Robert Gordon University, Aberdeen AB10 1GJ, Scotland, United Kingdom

^b Centre for Obesity Research and Education (CORE), Robert Gordon University, Aberdeen AB10 1GJ, Scotland, United Kingdom

^c Rowett Institute of Nutrition and Health, University of Aberdeen, AB25 2ZD, Scotland, United Kingdom

^d Life and Health Sciences Research Institute (ICVS), School of Medicine, University of Minho, Braga, Portugal

^e ICVS/3B's – PT Government Associate Laboratory, Braga/Guimarães, Portugal

ARTICLE INFO

Article history:

Received 16 March 2017

Received in revised form 12 May 2017

Accepted 21 June 2017

Available online 23 June 2017

Keywords:

Rapeseed pomace

Soxhlet extraction

Reducing capacity (FC)

Phenolics

Radical scavenging activity (DPPH)

Ferric iron reducing antioxidant power

(FRAP)

Oxygen-radical absorbance capacity assay

(ORAC)

pBR322 plasmid DNA

ABSTRACT

Rapeseed pomace (RSP) is a waste product obtained after edible oil production from *Brassica napus*. Analysis of ubiquitous secondary metabolites in RSP samples (two breeds, harvested in 2012/2014 respectively from North East of Scotland) and their ethanol/water (95:5) Soxhlet extracts were carried out. Soxhlet extraction of the RSP (petroleum ether followed by 95% ethanol) gave a solid extract. LC-MS/MS data of the extracts revealed several secondary metabolites, with Sinapic acid being the most abundant. Strong antioxidant activities of the Soxhlet extracts were confirmed from the results obtained in the FRAP, DPPH and ORAC assays. Furthermore, for the very first time, RSP extracts (13.9 µg/ml) provided complete DNA protection, from oxidative stress induced by AAPH (3.5 mM). Therefore the strong antioxidant and DNA protecting properties demonstrated by the RSP extracts in this study warrants further investigation for their revalorisation and potential use as reliable source of antioxidants in different food applications.

© 2017 Elsevier Ltd. All rights reserved.



Contents lists available at ScienceDirect

Food Chemistry

journal homepage: www.elsevier.com/locate/foodchem

Determination of sinapine in rapeseed pomace extract: Its antioxidant and acetylcholinesterase inhibition properties



Kyari Yates^a, Franziska Pohl^a, Maik Busch^{a,b}, Annika Mozer^{a,b}, Louis Watters^{a,c}, Andrey Shiryaev^d, Paul Kong Thoo Lin^{a,*}

^a School of Pharmacy and Life Sciences, Robert Gordon University, Aberdeen AB10 7GJ, United Kingdom

^b Department of Natural Science, Hochschule Bonn-Rhein-Sieg, Rheinbach, Germany

^c Artesis Plantijn University College Antwerp, Belgium

^d Chemistry Department, Samara State Technical University, Russia

ARTICLE INFO

Keywords:

Rapeseed pomace

Canola

Sinapine

Phenolic acids

Antioxidant assays

Plasmid DNA (pBR322)

LC-MS/MS

Acetylcholinesterase (AChE)

ABSTRACT

Sinapine is the main secondary metabolite present in rapeseed pomace (RSP) with its concentration being dependent on rapeseed processing, growing conditions, extraction parameters and the country of origin. Here we report, the concentration of sinapine from an extract of defatted RSP harvested in the North East of Scotland. Using liquid chromatography tandem mass spectrometry, the most abundant phenolic compound in the RSP extract was, as expected, sinapine (109.1 mg/g RSP extract). Additionally, sinapic, caffeic, ferulic and syringic acids were identified (0.159–3.91 mg/g RSP extract). Sinapine together with the phenolics at the concentration present in the RSP extract, exhibited ≥ 50% activity relative to the extract in antioxidant assays. Furthermore, sinapine provided plasmid DNA (pBR322) protection, from 2,2'-azobis(2-amidinopropane) dihydrochloride and inhibited acetylcholinesterase activity by 85%. Molecular docking was utilised to explain the inhibitory activity. RSP can be an excellent source of bioactive compounds for pharmaceuticals, food additive and nutraceutical applications.

Review

The Potential Use of Plant Natural Products and Plant Extracts with Antioxidant Properties for the Prevention/Treatment of Neurodegenerative Diseases: In Vitro, In Vivo and Clinical Trials

Franziska Pohl and Paul Kong Thoo Lin *

School of Pharmacy and Life Sciences, Robert Gordon University, Aberdeen AB10 7GJ, UK; f.pohl@rgu.ac.uk

* Correspondence: p.v.s.kong-thoo-lin@rgu.ac.uk; Tel.: +44-122-426-2818

Academic Editor: Isabel C.F.R. Ferreira

Received: 8 November 2018; Accepted: 30 November 2018; Published: 11 December 2018



Abstract: Neurodegenerative disorders, including Alzheimer’s disease, Parkinson’s disease and Huntington’s disease, present a major health issue and financial burden for health care systems around the world. The impact of these diseases will further increase over the next decades due to increasing life expectancies. No cure is currently available for the treatment of these conditions; only drugs, which merely alleviate the symptoms. Oxidative stress has long been associated with neurodegeneration, whether as a cause or as part of the downstream results caused by other factors. Thus, the use of antioxidants to counter cellular oxidative stress within the nervous system has been suggested as a potential treatment option for neurological disorders. Over the last decade, significant research has focused on the potential use of natural antioxidants to target oxidative stress. However, clinical trial results have lacked success for the treatment of patients with neurological disorders. The knowledge that natural extracts show other positive molecular activities in addition to antioxidant activity, however, has led to further research of natural extracts for their potential use as prevention or treatment/management of neurodegenerative diseases. This review will cover several in vitro and in vivo research studies, as well as clinical trials, and highlight the potential of natural antioxidants.

Keywords: antioxidants; natural products; in vitro; in vivo; clinical trials; plant extracts; phytochemicals; phenolics; Ginkgo biloba; secondary metabolites

CONTENTS

1 INTRODUCTION	1
1.1 NATURAL PRODUCTS FOR MEDICINAL USE	2
1.1.1 <i>Natural waste/by-products from food production</i>	<i>3</i>
1.1.2 <i>Secondary metabolites</i>	<i>5</i>
1.1.3 <i>Phenolic secondary metabolites</i>	<i>9</i>
1.2 RAPESEED AND RAPESEED POMACE	13
1.2.1 <i>Phytochemicals in rapeseed/RSP</i>	<i>18</i>
1.3 NEURODEGENERATION	23
1.3.1 <i>Alzheimer’s Disease (AD).....</i>	<i>27</i>
1.3.2 <i>Machado-Joseph Disease (MJD).....</i>	<i>37</i>
1.3.3 <i>Parkinson’s disease (PD)</i>	<i>47</i>
1.4 OXIDATIVE STRESS IN NEURODEGENERATION AND THE POTENTIAL USE OF ANTIOXIDANTS TO PREVENT NEUROLOGICAL DISORDERS	51
1.4.1 <i>Oxidative stress</i>	<i>53</i>
1.4.2 <i>Antioxidants to counteract oxidative stress</i>	<i>56</i>
1.4.3 <i>Exogenous antioxidants - natural products: direct and indirect antioxidant activity</i>	<i>58</i>
1.5 OVERALL AIM AND THESIS STRUCTURE.....	64
2 SECONDARY METABOLITE COMPOSITION AND ANTIOXIDANT ACTIVITY OF RAPESEED POMACE EXTRACTS – COMPARISON BETWEEN 2 HARVEST YEARS AND 3 EXTRACTION TECHNIQUES	65
2.1 INTRODUCTION	66
2.1.1 <i>Extraction.....</i>	<i>66</i>
2.1.2 <i>Determination of secondary metabolites in extracts</i>	<i>77</i>

2.1.3	<i>Antioxidant/Reducing Capacity Assays</i>	80
2.1.4	<i>Objectives</i>	87
2.2	MATERIALS AND METHODS	88
2.2.1	<i>Chemicals and Equipment</i>	88
2.2.2	<i>Methods</i>	90
2.3	RESULTS AND DISCUSSION.....	98
2.3.1	<i>Secondary metabolite composition of RSP from free, alkali-labile and acid-labile fractions</i>	98
2.3.2	<i>Comparison of SOX, UAE and ASE extraction techniques</i>	103
2.3.3	<i>Folin-Ciocalteu (FC) Assay</i>	105
2.3.4	<i>HPLC-MS/MS</i>	107
2.3.5	<i>FRAP assay</i>	111
2.3.6	<i>DPPH assay</i>	114
2.3.7	<i>Correlation of the data from FC, FRAP and DPPH assay</i>	118
2.3.8	<i>Partial least squares analysis of data from the DPPH, FC and FRAP assay</i>	120
2.3.9	<i>ORAC assay</i>	122
2.3.10	<i>Partial least squares analysis (ORAC)</i>	125
2.3.11	<i>Determination of Antioxidant activity of single compounds within the extract as well as their mixtures</i>	127
2.4	CONCLUSION/FUTURE WORK	131
3	PHYTOCHEMICAL CHARACTERISATION AND NEUROPROTECTIVE PROPERTIES OF RSP EXTRACT <i>IN VITRO</i>	133
3.1	INTRODUCTION	134
3.1.1	<i>Determination of additional secondary metabolites in the RSP extract</i>	134

3.1.2 Metal chelating properties.....	142
3.1.3 Acetylcholinesterase (AChE)/Acetylcholinesterase inhibitors....	146
3.1.4 Inhibition of self-mediated β -amyloid (1–42) aggregation.....	150
3.1.5 DNA protection.....	152
3.1.6 Objectives	154
3.2 MATERIALS AND METHODS.....	155
3.2.1 Chemicals and Equipment.....	155
3.2.2 Methods	157
3.3 RESULTS AND DISCUSSION	167
3.3.1 Extraction replicates differences in FC, FRAP and DPPH	167
3.3.2 Antioxidant activity of final RSP extract	168
3.3.3 LC-MS/MS analysis of final RSP extract	170
3.3.4 Additional secondary metabolite analysis.....	175
3.3.5 Metal chelating potential.....	191
3.3.6 AChE inhibition potential	194
3.3.7 Inhibition of self-mediated β -amyloid (1–42) aggregation.....	199
3.3.8 Inhibition of Supercoiled Plasmid DNA Strand Breakage.....	201
3.4 CONCLUSION/FUTURE WORK.....	205
4 CELL PROTECTIVE PROPERTIES OF RSP EXTRACT IN SH-SY5Y NEUROBLASTOMA CELL LINE	209
4.1 INTRODUCTION	210
4.1.1 Neuronal cell culture	210
4.1.2 Cell toxicity/viability assays	213
4.1.3 ROS in the cell system	217

4.1.4 Cellular DNA damage/ Comet assay.....	220
4.1.5 Cell stress related proteins	224
4.1.6 Objectives.....	226
4.2 MATERIALS AND METHODS	227
4.2.1 Chemicals and Equipment	227
4.2.2 Methods.....	229
4.3 RESULTS AND DISCUSSION.....	237
4.3.1 Cellular toxicity of RSP extract.....	237
4.3.2 Protection of SH-SY5Y cells by RSP extract from ROS induced by H ₂ O ₂	241
4.3.3 Protection of SH-SY5Y cells by RSP extract from H ₂ O ₂ -induced DNA strand breakage-Comet assay.....	244
4.3.1 Study into the cell stress related protein expression induced by RSP extract using micro array technology	250
4.3.2 AChE inhibition study by RSP extract in SH-SY5Y cells	256
4.4 CONCLUSION/FUTURE WORK	258
5 AN <i>IN VIVO</i> STUDY OF THE ANTIOXIDANT AND NEUROPROTECTIVE PROPERTIES OF RSP EXTRACT IN <i>C. ELEGANS</i> NEMATODE MODELS	261
5.1 INTRODUCTION	262
5.1.1 <i>C. elegans</i>	262
5.1.2 <i>C. elegans</i> disease models and their application in neurodegeneration studies.....	269
5.1.3 Determination of potential pathways of action using <i>C. elegans</i> as model organism	280
5.1.4 Objectives.....	287
5.2 MATERIALS AND METHODS	288

5.2.1 Chemicals and Equipment.....	288
5.2.2 Methods.....	290
5.3 RESULTS AND DISCUSSION	312
5.3.1 Toxicity/Food Clearance assay.....	312
5.3.2 Machado-Joseph disease <i>C. elegans</i> model	317
5.3.3 AChE inhibition hypothesis.....	323
5.3.4 Parkinson's Disease <i>C. elegans</i> model	329
5.3.5 <i>In vivo</i> study of antioxidant activity: the indirect antioxidant activity pathway theory	338
5.4 CONCLUSION/FUTURE WORK.....	347
6 OVERALL CONCLUSION ON THE POTENTIAL OF THE RSP EXTRACT	
351	
7 REFERENCES	355
APPENDICES	423

LIST OF TABLES

TABLE 1.1 ESTIMATED FOOD LOSS AND WASTAGE IN THE U.S. SUPPLY CHAIN	4
TABLE 1.2 TOTAL AMOUNT OF PHENOLICS IN OILSEED FLOURS	18
TABLE 1.3 NEURODEGENERATIVE DISEASE WITH THEIR RESPECTIVE MICROSCOPIC LESIONS, LOCATION AND AGGREGATED PROTEINS.....	25
TABLE 1.4 COLLECTION OF THE 9 POLYGLUTAMINE EXPANSION DISEASE AND SOME OF THEIR CHARACTERISTICS ^{79,157,169}	40
TABLE 1.5 CYTOPROTECTIVE ENZYMES AND THEIR ANTIOXIDANT FUNCTION ⁵⁴	57
TABLE 1.6 PLANT, PLANT PRODUCTS AND BY-PRODUCTS AND THEIR PREVENTATIVE/MEDICINAL PROPERTIES IN NEURODEGENERATION.....	62
TABLE 2.1 SOLVENTS USED FOR EXTRACTION OF SPECIFIC PLANT SECONDARY METABOLITE GROUPS (ADAPTED FROM ²⁵⁶⁻²⁵⁸).....	69
TABLE 2.2 UV-VIS METHODS FOR THE DETECTION OF SECONDARY METABOLITES IN PLANT EXTRACTS.....	78
TABLE 2.3 CHEMICALS, REAGENTS AND KITS.....	88
TABLE 2.4 EQUIPMENT	89
TABLE 2.5 PETROLEUM ETHER AND ETHANOL/WATER (95:5) SOXHLET EXTRACTION PARAMETERS	93
TABLE 2.6 CONCENTRATIONS (MG/KG POMACE) OF THE MOST ABUNDANT SECONDARY METABOLITES FOUND IN BOTH RSP SAMPLES AFTER FREE, ALKALI-LABILE AND ACID-LABILE EXTRACTIONS	98
TABLE 2.7 COMPARISON OF FREE PHENOLIC ACIDS DETECTED FROM RAPESEED FLOUR IN KRYGIER <i>ET AL.</i> ³⁵⁴ TO THE TWO HARVESTS IN THIS STUDY (2012, 2014)	100
TABLE 2.8 IMPACT OF SOLID TO SOLVENT RATIO ON ANTIOXIDANT ACTIVITY OF EXTRACTS	103
TABLE 2.9 EXTRACTION YIELDS IN MG PER G POMACE AND IN PERCENT, SUBDIVIDED BY EXTRACTION TECHNIQUE AND HARVEST YEAR	104

TABLE 2.10 PHENOLICS, AMINES AND FLAVANOIDS/COUMARINS FOUND IN RSP EXTRACTS	108
TABLE 2.11 CORRELATION BETWEEN FC, FRAP AND DPPH ASSAY.....	118
TABLE 2.12 SEVEN SINGLE COMPOUNDS AND THEIR FRAP AND DPPH ACTIVITY ³⁸³	127
TABLE 2.13 COMPARISON OF FRAP ACTIVITY OF SINGLE PHENOLICS FOUND IN THIS STUDY AND MUDNIC <i>ET AL.</i> ³⁸⁴	129
TABLE 2.14 MIXTURES OF SECONDARY METABOLITES CREATED FOR ANALYSIS OF THEIR ANTIOXIDANT AND RADICAL SCAVENGING ACTIVITY AND THE DETERMINATION OF POTENTIAL SYNERGISTIC EFFECTS ³⁸³	130
TABLE 3.1 CHEMICALS, REAGENTS AND KITS	155
TABLE 3.2 EQUIPMENT	156
TABLE 3.3 EXTERNAL GLUCOSINOLATE STANDARDS FOR HPLC	160
TABLE 3.4 MOBILE PHASE HPLC GRADIENT FOR THE DETECTION OF GLUCOSINOLATES	160
TABLE 3.5 CONCENTRATION OF SECONDARY METABOLITES IN FIRST AND FINAL RSP EXTRACT AND PUBLISHED BIOLOGICAL ACTIVITIES	171
TABLE 3.6 MS/MS FRAGMENTATIONS OF UNKNOWN PEAKS WITHIN THE CHROMATOGRAM	182
TABLE 3.7 GLS FOUND IN RS EXTRACT (BLUE ARROWS IN FIGURE 3.24).....	186
TABLE 3.8 SECONDARY METABOLITES PREVENTING OR MODULATING B-AMYLOID AGGREGATION	200
TABLE 4.1 TETRAZOLIUM BASED CELL VIABILITY ASSAYS (ADAPTED FROM ^{525,527,528})	214
TABLE 4.2 COMET ASSAY TYPES AND SOME EXAMPLES OF THEIR USAGE ^{541,545,546} ...	221
TABLE 4.3 CHEMICALS, REAGENTS AND KITS	227
TABLE 4.4 EQUIPMENT	228
TABLE 4.5 COMET SCORING CRITERIA	234
TABLE 4.6 HUMAN CELL STRESS PROTEINS INCLUDED IN THE PROTEIN ARRAY ⁵⁵⁶	250

TABLE 5.1 SCIENTIFIC CLASSIFICATION OF <i>C. ELEGANS</i>	263
TABLE 5.2 POTENTIAL KNOCK OUT STRAINS FOR SOD-3, GST-4 AND GCS-1.....	286
TABLE 5.3 CHEMICALS, REAGENTS AND KITS.....	288
TABLE 5.4 EQUIPMENT	289
TABLE 5.5 LIST OF STRAINS.....	291
TABLE 5.6 LIST OF STRAINS CREATED	291
TABLE 5.7 PRIMERS FOR CROSSES AND BACK-CROSSES	293
TABLE 5.8 PCR MASTER MIXES	294
TABLE 5.9 EXPECTED DNA FRAGMENTS FOR GENOTYPED ACE-1, ACE-2 AND GST-4 (KO) WORMS.....	295
TABLE 5.10 GENETIC CROSS OF HERMAPHRODITE SELF-FERTILIZATION	296
TABLE 5.11 GENETIC CROSS FOR PROGENY OF THE 24 ISOLATED ANIMALS*	298
TABLE 0.1 EXPECTED DNA LENGTH* FOR THE THREE DIFFERENT GENOTYPES	459
TABLE 0.2 GENOTYPICAL OUTCOME OF CROSSING MALE OBTAINED FROM FIRST CROSS (WT/WT; AT3Q130/WT) WITH ACE-1 HERMAPHRODITE (ACE-1/ACE-1; WT/WT)	461

LIST OF FIGURES

FIGURE 1.1 WORLD POPULATION ESTIMATES FROM 1950-2015	3
FIGURE 1.2 COMMON ALKALOIDS.....	7
FIGURE 1.3 SUBDIVISIONS OF TERPENES	8
FIGURE 1.4 COMMON TERPENES.....	8
FIGURE 1.5 NUMBER OF PUBLICATIONS ON SCIENCEDIRECT.COM WITH THE SEARCH WORD "PHENOLIC" FROM 2000-2018	9
FIGURE 1.6 POLYPHENOLS SUB-DIVISIONS AND THEIR BASIC CHEMICAL STRUCTURE, ADAPTED FROM SHAHIDI <i>ET AL.</i> ⁴¹ AND FIRUZI ⁴²	10
FIGURE 1.7 RAPESEED FIELD NEAR ST. CYRUS IN KINCARDINESHIRE, SCOTLAND (F. POHL, MAY 2018).....	13
FIGURE 1.8 A: WORLD VEGETABLE OIL PRODUCTION IN 2012/2013 (ADAPTED FROM USDA ⁷⁸) B: RAPESEED PLANT (F. POHL, MAY 2018)	14
FIGURE 1.9 UNITED KINGDOM/WORLD PRODUCTION OF RAPESEED, INDICATING HARVEST AREA AND THE AMOUNT OF PRODUCED RAPESEED AND RAPESEED OIL, ADAPTED FROM FAOSTAT ^{85,86}	16
FIGURE 1.10 CHEMICAL STRUCTURE OF SINAPIC ACID (SA) AND SA DERIVATIVES COMMON IN RAPESEED.....	19
FIGURE 1.11 DIFFERENT TOCOLS	20
FIGURE 1.12 PHYTOSTEROLS IN RAPESEED, ADAPTED FROM ^{75,106,107}	21
FIGURE 1.13 LOCATION OF RAPESEED HARVEST/OIL PRODUCTION BY MACKINTOSH OF GLENDAVENY	22
FIGURE 1.14 NEUROPATHOLOGY OF ALZHEIMER'S DISEASE.....	29
FIGURE 1.15 FRAGMENTATION OF AMYLOID PRECURSOR PROTEIN (APP) INTO TOXIC AND NON-TOXIC FRAGMENTS	32
FIGURE 1.16 CHEMICAL STRUCTURE OF DONEPEZIL, GALANTAMINE AND RIVASTIGMINE, CURRENT TREATMENTS FOR SYMPTOMS OF ALZHEIMER'S DISEASE	35

FIGURE 1.17 NMDA RECEPTOR ANTAGONIST MEMANTINE, ADAPTED FROM ^{153,154}	36
FIGURE 1.18 CORRELATION BETWEEN THE NUMBER OF CAG REPEATS AND THE AGE OF ONSET OF 8 POLYGLUTAMINE DISORDERS	38
FIGURE 1.19 MUTANT ATAXIN-3, CAUSED BY INCREASED CAG REPEATS, LEADING TO POLYQ AMINO ACID SEQUENCE AND ELONGATED AND MISFOLDED PROTEINS	39
FIGURE 1.20 GENERAL STRUCTURE ASSOCIATED WITH ATAXIN-3	41
FIGURE 1.21 SIMPLE SKETCH OF THE UBIQUITIN-PROTEASOME PATHWAY	42
FIGURE 1.22 PROBLEMS ASSOCIATED WITH MUTATED ATAXIN-3	45
FIGURE 1.23 POSSIBLE THERAPEUTIC DRUG TARGETS ASSOCIATED WITH MJD	46
FIGURE 1.24 MECHANISM OF LEVODOPA	50
FIGURE 1.25 EXAMPLES OF DRUG TARGETS FOR NEURODEGENERATION	51
FIGURE 1.26 DIFFERENCE BETWEEN THE NORMAL AND THE DISEASE STATE OF OXIDATIVE STRESS BALANCE	54
FIGURE 1.27 CAUSES OF OXIDATIVE STRESS IN NEURODEGENERATION.....	54
FIGURE 1.28 NATURAL ANTIOXIDANTS CATEGORISED WITH EXAMPLES	56
FIGURE 1.29 ACTIVATION OF NRF2-KEAP1 PATHWAY	60
FIGURE 2.1 EXTRACTION OF PHYTOCHEMICALS FROM RSP.....	71
FIGURE 2.2 AUTOMATED SOXHLET EXTRACTION APPARATUS.....	72
FIGURE 2.3 SCHEMATIC OF UAE USING A ULTRASOUND WATER BATH	74
FIGURE 2.4 SCHEMATIC OF ASE EQUIPMENT.....	75
FIGURE 2.5 FC REAGENT REACTION WITH PHENOLIC COMPOUND	82
FIGURE 2.6 FRAP REACTION MECHANISM	83
FIGURE 2.7 DPPH REACTION WITH RADICAL SCAVENGER (H-AO)	84
FIGURE 2.8 REACTION MECHANISM OF REACTION BETWEEN FLUORESCHEIN AND AAPH85	
FIGURE 2.9 GRAPHICAL REPRESENTATION OF THE ORAC ASSAY.....	86

FIGURE 2.10 OVERVIEW OF <i>IN VITRO</i> METHODS USED IN THE ASSESSMENT OF RSP AND RSP EXTRACTS.....	90
FIGURE 2.11 FC ASSAY RESULTS, COMPARING THE THREE EXTRACTION TECHNIQUES TOGETHER WITH THE TWO HARVEST YEARS/BREEDS	105
FIGURE 2.12 CALIBRATION GRAPH EXAMPLE FOR FRAP ASSAY USING 1.56-15.6 $\mu\text{G}/\text{ML}$ TROLOX	111
FIGURE 2.13 FRAP RESULTS IN TROLOX EQUIVALENCE PER G RSP EXTRACT	112
FIGURE 2.14 DPPH ASSAY IC_{50} DETERMINATION.....	114
FIGURE 2.15 DPPH RESULTS AS IC_{50} ($\mu\text{G}/\text{ML}$)	115
FIGURE 2.16 HYPOTHETICAL REACTION KINETIC COMPARISON	117
FIGURE 2.17 CORRELATION BETWEEN FRAP AND DPPH ASSAYS	119
FIGURE 2.18 PLS PLOT INCLUDING THE SIX EXTRACTS AND THEIR SECONDARY METABOLITE COMPOSITION, IN RELATION TO THEIR	121
FIGURE 2.19 ORAC RESULTS IN μMOL TROLOX EQUIVALENCE PER G RSP EXTRACT	122
FIGURE 2.20 EXAMPLE OF ORAC ABSORBANCE MEASUREMENT FOR SOX2012	123
FIGURE 2.21 PLS PLOT INCLUDING THE SOX AND UAE EXTRACTS AND THEIR SECONDARY METABOLITE COMPOSITION, IN RELATION	126
FIGURE 2.22 HBA AND HCA ANALYSED IN MUDNIC <i>ET AL.</i> ³⁸⁴ FOR THEIR FRAP ACTIVITY	128
FIGURE 3.1 CHEMICAL STRUCTURE OF SINAPINE IN COMPARISON TO ACETYLCHOLINE	135
FIGURE 3.2 GLUCOSINOLATES BASIC STRUCTURE	137
FIGURE 3.3 11 GLUCOSINOLATES COMMONLY PRESENT IN <i>BRASSICA</i> PLANTS ANALYSED IN THIS STUDY	139
FIGURE 3.4 GENERAL STRUCTURE OF ANTHOCYANINS (FLAVYLIUM CATION).....	140
FIGURE 3.5 CHEMICAL REACTION OF THE COLOUR CHANGE EXPECTED FOR THE ANTHOCYANIN PELARGONIDIN (ADAPTED FROM ²⁹⁵)	141
FIGURE 3.6 REACTION MECHNISM FOR THE <i>IN VITRO</i> IRON CHELATING ASSAY	143

FIGURE 3.7 REACTION COLOUR SCHEME FOR THE IRON(II) CHELATING ACTIVITY ASSAY	143
FIGURE 3.8 REACTION MECHANISM FOR THE <i>IN VITRO</i> COPPER CHELATING ASSAY ..	144
FIGURE 3.9 REACTION COLOUR SCHEME FOR THE COPPER (II) ION CHELATING ACTIVITY ASSAY	144
FIGURE 3.10 ACETYLCHOLINE LEVELS AND NEUROTRANSMISSION IN AD PATIENTS WITH AND WITHOUT ACETYLCHOLINESTERASE INHIBITORS	147
FIGURE 3.11 REACTION MECHANISM OF THE ELLMAN METHOD FOR THE DETECTION OF ACHE INHIBITION, ADAPTED FROM BADAWY AND EL-ASWAD ⁴⁴²	148
FIGURE 3.12 AMPLEX® RED ACETYLCHOLINE/ACETYLCHOLINESTERASE ASSAY REACTION SCHEME	149
FIGURE 3.13 THT ASSAY	151
FIGURE 3.14 REACTION OF pBR322 PLASMID DNA WITH AAPH.....	152
FIGURE 3.15 OVERVIEW OF METHODS USED IN THE ASSESSMENT OF THE RSP EXTRACT FOR ITS CHEMICAL COMPOSITION AND <i>IN VITRO</i> NEUROPROTECTIVE PROPERTIES	157
FIGURE 3.16 DPPH, FC AND FRAP RESULTS OBTAINED FROM 3 EXTRACTION REPLICATES	167
FIGURE 3.17 DPPH, FC AND FRAP AND ORAC RESULTS OBTAINED FROM THREE EXTRACTION REPLICATES	169
FIGURE 3.18 RSP EXTRACT (AT 1 MG/ML) CHROMATOGRAM IN BOTH/POSITIVE/NEGATIVE ION MODE AFTER LC-MS ANALYSIS	176
FIGURE 3.19 MS/MS DATA OBTAINED FOR THE BREAKDOWN OF THE M/Z 310.1 PEAK	177
FIGURE 3.20 CHROMATOGRAM OF SINAPINE	178
FIGURE 3.21 ANTIOXIDANT ACTIVITY OF SINAPINE AND PHENOLIC ACIDS AND THEIR MIXTURE COMPARED TO THE RSP EXTRACT ACTIVITY, DETERMINING UNKNOWN ACTIVITY IN THE EXTRACT, ADAPTED FROM YATES <i>ET AL.</i> ⁴⁵⁶	180
FIGURE 3.22 +/- ESI TOTAL ION CHROMATOGRAM OF A 1 MG/ML RSP EXTRACT ..	181

FIGURE 3.23 GLUCOSINOLATE STANDARD MIXTURE HPLC CHROMATOGRAM	183
FIGURE 3.24 HPLC GLUCOSINOLATES CHROMATORGRAM FOR STANDARD MIXTURE AND RSP EXTRACT (OVERLAY)	184
FIGURE 3.25 ABSORBANCE SPECTRA FOR PROGOITRIN STANDARD AND RSP EXTRACT (190-360 NM)	185
FIGURE 3.26 CALIBRATION CURVE OBTAINED FOR PROGOITRIN (0.005-0.5 MG/ML)	185
FIGURE 3.27 PH DIFFERENTIAL METHOD	189
FIGURE 3.28 ABSORBANCE SPECTRA FOR RSP AND GP EXTRACTS AT PH 4.5 AND PH 1.0 FOR THE DETERMINATION OF TOTAL ANTHOCYANINS	189
FIGURE 3.29 COPPER CHELATING PROPERTIES OF THE RSP EXTRACT	192
FIGURE 3.30 ABSORBANCE SPECTRA AND REACTION OF DTNB TO 5-THIO-2-NITROBENZOATE (ADAPTED FROM ^{442,492})	194
FIGURE 3.31 ABSORBANCE SPECTRA OVERLAY OF 5-THIO-2-NITROBENZOATE AND THE RSP EXTRACT	194
FIGURE 3.32 TIME DEPENDENT ACHE ACTIVITY.....	195
FIGURE 3.33 ACHE ACTIVITY INHIBITION BY RSP EXTRACT (0.001-1.00 MG/ML) AND NEOSTIGMINE (5 µG/ML).....	196
FIGURE 3.34 TIME DEPENDENT ACHE INHIBITION STUDY OF RSP EXTRACT SECONDARY METABOLITES	198
FIGURE 3.35 B- AMYLOID SELF-MEDIATED AGGREGATION INHIBITION STUDY	199
FIGURE 3.36 PROTECTION OF PBR322 PLASMID DNA	201
FIGURE 3.37 QUANTIFICATION OF THE PLASMID DNA PROTECTION EFFECT	202
FIGURE 3.38 DNA PROTECTIVE PROPERTIES OF THE RSP EXTRACT SECONDARY METABOLITES	203
FIGURE 4.1 UNDIFFERENTIATED SH-SY5Y CELLS IN DMEM MEDIA (40X MAGNIFICATION)	212
FIGURE 4.2 MTT REACTION IN METABOLIC ACTIVE CELLS	215

FIGURE 4.3 REDUCTION OF RESAZURIN TO RESORUFIN WITHIN CELLS	216
FIGURE 4.4 H ₂ DCFDA <i>IN VITRO</i> REACTION IN THE PRESENCE OF ROS/RNS.....	217
FIGURE 4.5 SCHEMATIC OF FLOW CYTOMETRY IN THE PRESENCE OF FLUORESCENT AND NON-FLUORESCENT CELLS.....	218
FIGURE 4.6 COMET ASSAY OVERVIEW	223
FIGURE 4.7 PRINCIPLE OF PROTEIN MICRO ARRAYS	224
FIGURE 4.8 OVERVIEW OF METHODS USED TO DETERMINE THE EXTRACTS ACTIVITY IN SH- SY5Y NEUROBLASTOMA CELLS	229
FIGURE 4.9 MTT-ASSAY RESULTS FROM SH-SY5Y CELLS INCUBATED WITH RSP EXTRACT (24 H TREATMENT).....	237
FIGURE 4.10 MTT REDUCTION BY SINAPIC ACID IN A CELL FREE SYSTEM (24 H) ...	238
FIGURE 4.11 RESAZURIN CELL VIABILITY ASSAY USING RSP EXTRACT (0.1-5.0 MG/ML, 24 H TREATMENT).....	239
FIGURE 4.12 ROS PRODUCTION IN SH-SY5Y CELLS CAUSED BY H ₂ O ₂ CONTROL (1 MM, 30 MIN) AND DIFFERENT CONCENTRATIONS OF RSP EXTRACT (0.25-1.0 MG/ML)241	
FIGURE 4.13 ROS PRODUCTION AFTER PRE-TREATMENT WITH RSP EXTRACT (24 H) FOLLOWED BY TREATMENT WITH H ₂ O ₂ (1 MM, 30 MINUTES)	242
FIGURE 4.14 IMAGES OF COMET CLASSES OBTAINED FOR SH-SY5Y CELLS.....	245
FIGURE 4.15 CONCENTRATION DEPENDENT DNA STRAND BREAKS INDUCED BY H ₂ O ₂ (30 MINUTES).....	246
FIGURE 4.16 CELLULAR DNA PROTECTION FROM H ₂ O ₂ INDUCED DNA STRAND BREAKS BY THE RSP EXTRACT (1MG/ML, 24 H PREINCUBATION)	247
FIGURE 4.17 DEVELOPED FILMS OF HUMAN CELL STRESS PROTEIN ARRAYS	251
FIGURE 4.18 EXPRESSION OF HUMAN CELL STRESS PROTEINS IN SH-SY5Y CELLS EXPOSED TO RSP EXTRACT (1 MG/ML, 24 H) IN COMPARISON TO MEDIA CONTROL.....	252
FIGURE 4.19 REACTION OF SUPEROXIDE TO H ₂ O ₂ CATALYSED BY MNSOD (SOD2)254	
FIGURE 4.20 AChE ACTIVITY IN SH-SY5Y CELLS	256

FIGURE 5.1 ADVANTAGES OF <i>C. ELEGANS</i> AS RESEARCH MODEL ORGANISM	262
FIGURE 5.2 MICROSCOPY IMAGES (BRIGHT-FIELD ILLUMINATION) AND SCHEMATICS OF HERMAPHRODITE AND MALE <i>C. ELEGANS</i>	264
FIGURE 5.3 COMPLETE LIFE CYCLE OF <i>C. ELEGANS</i>	265
FIGURE 5.4 FOOD CLEARANCE ASSAY EXAMPLE READOUT FOR DMSO TOXICITY TEST	268
FIGURE 5.5 COMPARISON OF AT3Q14, AT3Q75 AND ATQ130 <i>C. ELEGANS</i> STRAIN	270
FIGURE 5.6 LOCOMOTION DEFECT OF AT3Q130 IN THE CLASSICAL MOTILITY ASSAY	271
FIGURE 5.7 <i>C. ELEGANS</i> CEP NEURONS	273
FIGURE 5.8 <i>C. ELEGANS</i> ADE NEURONS.....	274
FIGURE 5.9 <i>C. ELEGANS</i> PDE NEURONS.....	274
FIGURE 5.10 DA BIOSYNTHESIS.....	275
FIGURE 5.11 DAERGIC NEURONAL DAMAGE OBSERVED IN GENETIC (UA44 AND UA57) AND CHEMICAL INDUCED (6-OHDA) <i>C. ELEGANS</i> MODELS OF PD.....	276
FIGURE 5.12 CHEMICAL STRUCTURE FOR 6-HYDROXYDOPAMINE (6-OHDA) COMPARED TO DOPAMINE (DA)	277
FIGURE 5.13 GENES FOR ACHE (ACE1-4) IN THE <i>C. ELEGANS</i> GENOME.....	281
FIGURE 5.14 GSH SYNTHESIS FROM GLU, CYS AND GLY CATALYSED THROUGH γ -GCS AND GS	285
FIGURE 5.15 HYPOTHETICAL RESULTS FOR THE RSP EXTRACTS' DEPENDENCE ON EXPRESSION OF SOD-3 USING DOUBLE MUTANTS (SOD-3(KO);AT3Q130).....	286
FIGURE 5.16 OVERVIEW OF METHODS USED TO DETERMINE THE EXTRACTS ACTIVITY IN DIFFERENT <i>C. ELEGANS</i> MODELS	290
FIGURE 5.17 BACKCROSSING SCHEMATIC FOR ACE-1 WORMS, DELETION OF ACE-1 ON THE X CHROMOSOME	297
FIGURE 5.18 SCHEMATIC DEPICTING THE CROSSING FOR ACE-1 (ON CHROMOSOME X) X AT3Q130 (ON CHROMOSOME II) WORMS FOR THE CREATION OF DOUBLE MUTANTS	300

FIGURE 5.19 FOOD CLEARANCE ASSAY/TOXICITY ASSAY FOR EVALUATING THE TOXICITY OF THE RSP EXTRACT IN <i>C. ELEGANS</i>	302
FIGURE 5.20 SCHEMATIC OF THE MOTILITY ASSAY OF N2 AND AT3Q130 WORMS..	307
FIGURE 5.21 6-OHDA INDUCED PD MODEL EXPERIMENTAL SETUP USING BZ555 ANIMALS	309
FIGURE 5.22 TOXICITY ASSESSMENT OF RSP EXTRACT (0.01-5.0 MG/ML) USING THE FOOD CLEARANCE ASSAY, DMSO AS NEGATIVE (1%) AND POSITIVE (5%) CONTROL	312
FIGURE 5.23 TOXICITY ASSESSMENT OF SINAPINE (0.001-1.0 MG/ML) USING THE FOOD CLEARANCE ASSAY, DMSO AS NEGATIVE (1%) AND POSITIVE (5%) CONTROL	314
FIGURE 5.24 TOXICITY ASSESSMENT OF NEOSTIGMINE (0.01-10 MM) USING THE FOOD CLEARANCE ASSAY, DMSO AS NEGATIVE (1%) AND POSITIVE (5%) CONTROL	316
FIGURE 5.25 RSP EXTRACT IMPROVES LOCOMOTION DEFECTIVE BEHAVIOUR OF MJD (AT3Q130) ANIMALS.....	317
FIGURE 5.26 SINAPINE SHOWS LIMITED POSITIVE EFFECT IN MJD STRAIN (AT3Q130)	318
FIGURE 5.27 RSP EXTRACTS EFFECT ON MJD STRAIN IS DISEASE SPECIFIC.....	320
FIGURE 5.28 NO CHANGES IN THE ATAXIN-3 AGGREGATION LOAD INDUCE BY RSP EXTRACT IN THE MJD MODEL	321
FIGURE 5.29 LOCOMOTION DEFECTIVE BEHAVIOUR OF AT3Q130 ANIMALS AFTER NEOSTIGMINE TREATMENT.....	323
FIGURE 5.30 LOCOMOTION DEFECTIVE BEHAVIOUR OF AT3Q130 ANIMALS AFTER LOWER CONCENTRATIONS OFNEOSTIGMINE TREATMENT	324
FIGURE 5.31 LOCOMOTION DEFECTIVE BEHAVIOUR OF AT3Q130 ANIMALS COMPARED TO DOUBLE MUTANT	326
FIGURE 5.32 PROTECTIVE EFFECTS OF RSP EXTRACT ON THE DAERGIC NEURODEGENERATION IN <i>C. ELEGANS</i>	331
FIGURE 5.33 DAERGIC NEURON LOSS IS DEPENDENT ON 6-OHDA CONCENTRATION AS WELL AS CLASS OF DAERGIC NEURONS	332

FIGURE 5.34| EFFECT OF RSP EXTRACT TREATMENT IN GENETIC *C. ELEGANS* PD STRAINS335

FIGURE 5.35|RSP EXTRACT TREATMENT ACTIVATES ANTIOXIDANT PATHWAYS GST-4 AND SOD-3 IN *C. ELEGANS*339

FIGURE 5.36| CONDITIONS AND STRAINS USED TO DETERMINE THE RSP EXTRACTS DEPENDENCE ON GST-4 IN THE UA44 STRAIN342

FIGURE 5.37| PROTECTION OF DAERGIC NEURONS IN UA44 STRAIN DEPENDENT ON GST-4 ACTIVATION.....343

FIGURE 5.38|ACTIVATION PATHWAY OF GST-4 THROUGH EPIDERMAL GROWTH FACTOR (EGF) SIGNALLING BY ROYALACTIN345

FIGURE 5.39| OXIDATIVE STRESS AND METAL HOMEOSTASIS IMPLICATIONS IN PD..346

LIST OF ABBREVIATIONS AND ACRONYMS

6-OHDA	6-hydroxydopamine
A	Absorbance
AA	Ascorbic acid
AAPH	2,2'-Azobis(2-amidinopropane) dihydrochloride
ACD	Acid labile
Ach	Acetylcholine
AChE	Acetylcholinesterase
AChEI	Acetylcholinesterase inhibitor
AD	Alzheimer's disease
ADE	Anterior deirid neuron
ALK	Alkali labile
ALS	Amyotrophic lateral sclerosis
ANOVA	Analysis of variance
APP	Amyloid precursor protein
ARE	Antioxidant response element
ASE	Accelerated solvent extraction
ATP	Adenosine triphosphate
ATXN3	Ataxin-3
AU	Arbitrary unit
Aβ	Amyloid-beta (β -amyloid)
BC	Back crossed
<i>C. elegans</i>	<i>Caenorhabditis elegans</i>
CA	Caffeic acid
CAT	Catalase
CAT-2	Tyrosine hydroxylase
CE	Capillary electrophoresis
CEP	Cephalic sensilla neuron
CGC	Caenorhabditis Genetics Center
ChAT	Choline acetyltransferase
CNS	Central nervous system
Cul3	Cullin-3
cyn-3-glu	Cyanidin-3-glucoside
DA	Dopamine
DAD	Diode array detector
DAPI	4',6-diamidino-2-phenylindole
DCF	2', 7' -dichlorofluorescein
DF	Dilution factor
DMEM	Dulbecco's Modified Eagle Medium
DMSO	Dimethylsulfoxide
DNA	Deoxyribonucleic Acid
DNC	Dorsal nerve cord
DPPH	2,2-diphenyl-1-picrylhydrazyl
DRPLA	Dentatorubral-pallidoluysian atrophy
DTNB	5,5'-dithiobis-(2-nitrobenzoic acid)
dw	Dry weight
<i>E. coli</i>	<i>Escherichia coli</i>
EDTA	Ethylenediaminetetraacetic acid
EGCG	(-)epigallocatechin-3-gallate

EGF	Epidermal growth factor
EMA	European Medicines Agency
ERK1/2	Extracellular signal-regulated kinase 1/2
ESI	Electro-spray ionization
ET	Electron transfer
EtOAc	Ethyl acetate
FA	Ferulic acid
FBS	Foetal bovine serum
FC	Folin-Ciocalteu
FDA	Food and Drug Administration (U.S.)
ff.	Following
FOXO	Forkhead box O
FRAP	Ferric ion reducing antioxidant power
FSC	Forward scattered
GAE	Gallic acid equivalence
GC	Gas chromatography
GCL, GCS	γ -glutamylcysteine ligase, γ -glutamylcysteine synthetase
GFP	Green fluorescence protein
GLS	Glucosinolate
GP	Grape pomace
GSH	Glutathione
GST	Glutathione s transferase
h	Hour
H₂DCFDA	2',7' -dichlorofluorescein diacetate
H₂O₂	Hydrogen peroxide
HAT	Hydrogen atom transfer
HBA	Hydroxybenzoic acids
HCA	Hydroxycinnamic acids
HD	Huntington's disease
HET/het	Heterozygous
HO-1	Heme oxygenase-1
HPLC	High performance liquid chromatography
IAA	Indole-3-acetic acid
IC50	Inhibitory Concentration
IPA	Indole-3-pyruvic acid
IR	Infrared
Keap1	Kelch-like ECH-associated protein 1
ko	Knock out
l	Length
L1-L4	Larva stages of <i>C. elegans</i>
LAFA	Loss Adjusted Food Availability
LB	Luria broth
LC	Liquid chromatography
LDH	Lactate dehydrogenase
L-DOPA	Levodopa
LMP	Low melting point
LOD	Limit of detection
LOQ	Limit of quantification

m/z	Mass/charge ratio
M9	<i>C. elegans</i> buffer solution
MDA	Malonaldehyde
min(s)	Minute(s)
MJD	Machado-Joseph disease
MPTP	1-methyl-4-phenyl-1,2,3,6-tetrahydropyridine
mRNA	Messenger RNA
MS	Mass spectrometry
MTT	3-(4,5-dimethylthiazol-2-yl)-2,5-diphenyltetrazolium bromide
MUT/mut	Mutant
MW	Molecular Weight
NEAA	Non-essential amino acids
NFT	Neurofibrillary tangles
NFκB	Nuclear factor kappa-light-chain-enhancer of activated B cells
NGM	Nematode growth media
NII	Neuronal intranuclear inclusion
NMDA	N-methyl-D-aspartic acid
NMR	Nuclear magnetic resonance
NP	Natural product
NQO1	NAD(P)H dehydrogenase (quinone 1)
Nrf2	Nuclear factor erythroid 2 [NF-E2]-related factor 2
OD	Optical density
OP50	Strain of <i>Escherichia coli</i> used for maintenance of <i>Caenorhabditis elegans</i> cultures
ORAC	Oxygen radical absorbance capacity
p.	Page
PBS	Phosphate Buffered Saline
PCR	Polymerase chain reaction
PD	Parkinson's disease
PDE	Posterior deirid neuron
Pen/Strep	Penicillin/Streptomycin
PLS	Partial least analysis
polyQ	Poly glutamine
PUFA	Polyunsaturated fatty acids
q14, q75, q130	number of CAG repeats in the <i>C. elegans</i> model
RNA	Ribonucleic acid
ROS	Reactive oxygen species
rpm	Round per minute
RSP	Rapeseed pomace
RT	Retention time
rt	Room temperature
rt-PCR	Reverse transcription polymerase chain reaction
SA	Sinapic acid
SBMA	Kennedy's disease
SCA	Spinocerebella ataxia
SCGE (comet)	Single cell gel electrophoresis
SERT	Serotonin transporter
SH-SY5Y	Human neuroblastoma cel line

SIRT2	Sirtuin2
sMaf	Small musculoaponeurotic fibrosarcoma protein
SMP	Standard melting point
SNpc	Substantia nigra pars compacta
SOD	Superoxide dismutase
SOX	Soxhlet extraction
SSC	Side scattered
SyA	Syringic acid
TAE buffer	Tris base, acetic acid and EDTA buffer
TE	Trolox equivalents
TEAC	Trolox equivalent antioxidant capacity
TFC	Total flavanoid content
ThT	Thioflavin T
TIC	Total ion chromatogram
TLC/HPTLC	Thin layer chromatography/high performance thin layer chromatography
TPTZ	2,4,6-Tris(2-pyridyl)-s-triazine
TRAP	Total peroxy radical trapping antioxidant parameter
UAE	Ultra sonic assisted extraction
UIM	Ubiquitin-Interacting Motif
UK	United kingdom
USDA	United States Department of Agriculture
UV	Ultraviolet
v/v	Volume per volume
VIS	Visible
VNC	Ventral nerve cord
w/v	Weight/volume
WT/wt	Wild type
YFP	Yellow fluorescence protein
ε	Molar extinction coefficient

LIST OF COLLABORATORS/SUPERVISORS AND THEIR CONTRIBUTIONS TO THIS WORK

Supervisors:

Prof Kong Thoo Lin (Robert Gordon University, Aberdeen, Scotland)

- primary supervisor of the project

Prof Patricia Maciel (ICVS, Universidade do Minho, Braga, Portugal)

- main supervisor on all *C. elegans* related work in Braga, Portugal

Prof Wendy Russell (The Rowett Institute, Aberdeen University, Aberdeen, Scotland)

- supervisor of the work conducted at the Rowett Institute, including preliminary secondary metabolite, glucosinolate and PLS analysis

Dr Marie Goua (Robert Gordon University, Aberdeen, Scotland)

-project supervisor at RGU

Dr Giovanna Bermano (Robert Gordon University, Aberdeen, Scotland)

-project supervisor at RGU

Collaborators:

Dr Andreia Teixeira-Castro (ICVS, Universidade do Minho, Braga, Portugal)

- supervisory role at ICVS, help with all *C. elegans* related issues and confocal imaging for disease strains

Dr Marta Costa (ICVS, Universidade do Minho, Braga, Portugal)

- supervisory role at ICVS, help with all *C. elegans* related issues

Dr Kyari Yates (Robert Gordon University, Aberdeen, Scotland)

- supervisory role at RGU on work related to the secondary HPLC analysis (e.g. sinapine) including supervision of project students and their projects (L. Watters, M. Busch and A. Mozer)

Dr Madalina Neacsu (The Rowett Institute, Aberdeen University, Aberdeen, Scotland)

- supervisory role at Rowett Institute with glucosinolate analysis related issues

Lorraine Scobbie (The Rowett Institute, Aberdeen University, Aberdeen, Scotland)

- help with RSP extract three-way extraction and extracts preparation for Rowett based secondary metabolite analysis

Lesley Milne (The Rowett Institute, Aberdeen University, Aberdeen, Scotland)

- help with sample preparation and HPLC for glucosinolate analysis at Rowett Institute

Garry Duncan (The Rowett Institute, Aberdeen University, Aberdeen, Scotland)

- Rowett based HPLC analysis of secondary metabolites

Prof Andrey Shiryaev (Samara State Technical University, Samara, Russia)

- conducting of AChE binding study (modelling) included in sinapine paper

Victoria Lindsay (Robert Gordon University, Aberdeen, Scotland)

- RGU project student working at the ICVS, conducting of the AT3q130;ace-2 motility assay, involved in the back crossing of *gst-4(ko)* worms and crossing of *gst-4(ko)* with AT3q130 worms, conducted experiment of AT3q130;*gst-4(ko)* worms with RSP extract

Louis Watters (Artesis Plantijn Hogeschool, Antwerp, Belgium)

- RGU project student, involved in the secondary HPLC-MS/MS analysis of e.g. sinapine under supervision of F. Pohl, K. Yates and P. Kong Thoo Lin, collaboration with F. Pohl on metal chelating assays and AChE inhibition activity of sinapine, conducted experiments comparing RSP extracts antioxidant activity to phenolic acid mixture and sinapine

Sarah Wynants (Artesis Plantijn Hogeschool, Antwerp, Belgium)

- RGU project student, set-up of 96-well plate antioxidant assays from cuvette assays using single compounds (DPPH, FC, FRAP, ORAC and AChE inhibition Ellman) under supervision and in collaboration with F. Pohl and P. Kong Thoo Lin

Lisa Leyser (Robert Gordon University, Aberdeen, Scotland & Hochschule Bonn Rhein Sieg, Rheinbach, Germany)

- RGU project student, antioxidant analysis of single secondary metabolites from RSP extract and their potential synergistic effect under supervision and in collaboration with F. Pohl and P. Kong Thoo Lin

Maïke Busch and Annika Mozer (Robert Gordon University, Aberdeen, Scotland & Hochschule Bonn Rhein Sieg, Rheinbach, Germany)

- RGU project student, help with HPLC-MS/MS analysis set up at RGU used for following sinapine analysis, contribution to sinapine based paper under supervision and in collaboration with F. Pohl, K. Yates and P. Kong Thoo Lin

Contributions from all collaborations are further highlighted in the result/discussion section of each chapter in the Figure/Table details.

1 INTRODUCTION

Contents

1.1 Natural products for medicinal use	2
1.1.1 Natural waste/by-products from food production	
1.1.2 Secondary metabolites	
1.1.3 Phenolic secondary metabolites	
1.2 Rapeseed and Rapeseed pomace	13
1.2.1 Phytochemicals in rapeseed/RSP	
1.3 Neurodegeneration	23
1.3.1 Alzheimer's Disease	
1.3.2 Machado-Joseph Disease	
1.3.3 Parkinson's Disease	
1.4 Oxidative stress in neurodegeneration and the potential use of antioxidants to prevent neurological disorders	51
1.4.1 Oxidative stress	
1.4.2 Antioxidants to counteract oxidative stress	
1.4.3 Exogenous antioxidants - natural products: direct and indirect antioxidant activity	
1.5 Overall Aim	64

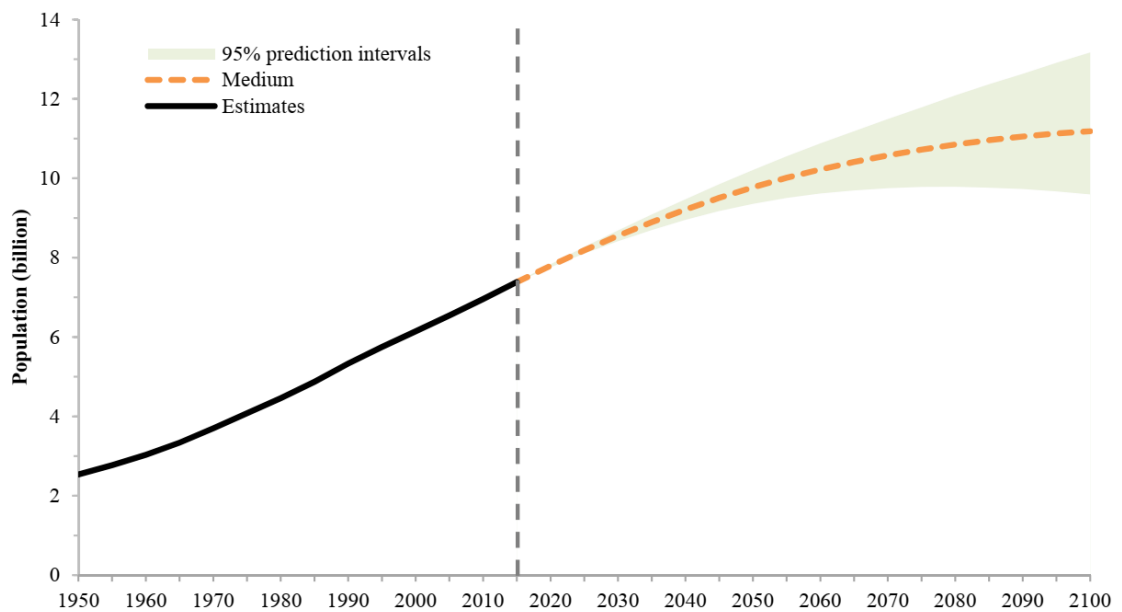
This chapter will give a brief introduction to the general topics associated with this thesis, including waste products and their current use, rapeseed and rapeseed pomace production and research. Furthermore, the chapter will introduce topics on oxidative stress, direct/indirect antioxidants as well as neurodegenerative disease in general. Focus will be drawn to Alzheimer's-, Parkinson's- and Machado-Joseph disease, as these are of interest in subsequent chapters of this thesis. At the end, this chapter provides a summary of the overall aims of the project.

1.1 Natural products for medicinal use

The plant kingdom has always offered a great variety of remedies¹. The oldest so far found written evidence of plant exploitation for medical use was found in a Sumerian chunk of clay, dating back 5000 years². Natural products (NPs) can be defined as substances produced and/or found in nature, more often referring to compounds with pharmacological effects³. These compounds have always played a significant role in the development of new drugs. This is still the case as shown in a recently published paper by Newman *et al.*⁴, covering "Natural products as Sources of New Drugs over the 30 Years from 1981 to 2010". Although synthetic drugs are still the main contributors for drug development, natural, biological or natural derived products are significantly contributing in numbers. Natural compounds can be obtained from plants, microbes, minerals as well as animals and are very often secondary metabolites (1.1.2 Secondary metabolites, p.5)⁵⁻⁷. Recent papers have reported on berry extracts⁸, nut extracts⁹ and extracts obtained from grape by-products in the wine making process^{10,11} indicating the great potential of NPs in drug development and research. The active ingredients in these plant and plant by-products are phytochemicals (secondary metabolites) produced by the plants, non-essential for plant growth and developments but with important defensive activity. Plants and especially secondary metabolites have long served as an important resource for the development of small-molecule therapeutics, due to their mostly unique chemical characteristics and bioactivity. Historically a few of the best known natural products are aspirin (acetylsalicylic acid), from the parental compound salicin, which was first isolated from the bark of the willow tree (*Salix alba*), as well as morphine isolated from opium poppy (*Papaver somniferum*) and quinine isolated the bark of *Cinchona spp.*¹². Interest has also increased in the extraction of biological active secondary metabolites from food sources, such as berries or fruits. However, this has certain disadvantages, as those foods are lost as food source for the ever growing world population. Also, the extraction from other plants is not ideal as they fulfil other ecological purposes in nature. However, food waste/by-products are ideal for the extraction of valuable phytochemicals.

1.1.1 Natural waste/by-products from food production

The food processing industry is fast growing in most countries, due to the ever-increasing world population. Understanding population growth is very important when trying to achieve sustainable food production for the next generations. In 2017, the world reached a population of 7.6 billion. This number is expected to increase further to over 8 billion in 2030, and almost 10 billion in 2050 (Figure 1.1), with Africa being expected to be the fastest-growing continent in population numbers¹³.



Source: United Nations, Department of Economic and Social Affairs, Population Division (2017). *World Population Prospects: The 2017 Revision*. New York: United Nations.

Figure 1.1 | World population estimates from 1950-2015

including medium-variant projection with 95 % confidence interval from 2015-2100, reproduced with copy right agreement from *World Population Prospects: The 2017 Revision*¹³

This means that within the next 82 years almost 1.5 times as many people will have to be sustained. Already in 2050 a 50% production increase will be necessary to feed the growing population¹⁴. The demand on producers as well as on food waste management will increase with this demand. The use of food waste and/or by-products for the extraction of phytochemicals could help to cope with the increased need for food while decreasing the amount of waste. Currently food waste and by-products are created but their potential is not exploited at all or not efficiently enough. Common by-products from the agricultural food industry are hulls, shells, husks, pods, stems, stalks, bran, seeds, washings, pulp refuse, stones, press cake/pomace¹⁵. All these are obtained after the production of nutritional valuable products, from

vegetables, oilseeds or fruit, and often considered to be waste products. Food waste is accumulated in all stages, in the food production industry, retail and on the side of the consumers. The extent and magnitude of the accumulated waste of some food products in the US is presented in Table 1.1.

Table 1.1| Estimated food loss and wastage in the U.S. supply chain

Food Group	Industry ^a	Retail ^b	Consumer ^b
	Million metric tonnes		
Vegetables	17.4 (31%) ^c	3.2 (8%)	8.3 (22%)
Fruit	6.4 (19%)	2.7 (9%)	5.7 (19%)
Dairy	– ^d	4.2 (11%)	7.3 (20%)
Meat poultry fish	12.0 (32%)	1.2 (5%)	5.8 (22%)
Grain products	–	3.3 (12%)	5.1 (19%)
Eggs	0.07 (2%)	0.3 (7%)	1.0 (21%)
Fats and oils	–	2.4 (21%)	2.0 (17%)
Sugar and sweeteners	–	2.0 (11%)	5.6 (30%)
Tree nuts and peanuts	0.01 (1%)	0.1 (6%)	0.1 (9%)
SUM	35.9 (15%)	19.5 (10%)	40.8 (21%)

Note(s): Reprinted under the terms of the Creative Commons Attribution-NonCommercial-No Derivatives License (CC BY NC ND) from Dou et al.¹⁶. ^acalculations from Dou et al.¹⁶ based on USDA ERS Loss Adjusted Food Availability (LAFA) databases;2012 data. ^bBuzby et al.¹⁷ based on USDA ERS LAFA databases;2010 data. ^c values in () represent percent of food entering each of the supply chain sectors that is lost and wasted in this sector. ^dfor some food groups, processing losses were 0 in the LAFA tables, see Food Availability tables for details (USDA-ERS, 2015a)

The disposal of these waste products is presenting a continuously growing problem. Plant material for example is prone to microbial spoilage, which might limit further exploitation. Also, legal restrictions on disposing of by-products present an issue. Hence, the interest in efficient, inexpensive and environmentally responsible utilization of these materials is raising in importance^{18,19}. Some of the produced by-products such as brewers grains²⁰, soybean meal and soy husks, wheat by-products such as middlings and bran, cotton seed meal and rapeseed pomace/meal are used as live stock or fish feed and so have some value²¹. One issue for the farmers producing the feed from those by-products is the constantly fluctuating sales value. A paper by Carré and Pouzet²², for example summarizes the meal prices for rapeseed meal from 1998 to 2013, showing prices below 100 €/t in 1998 up to over 300 €/t in June 2013 with significant fluctuations in between. Similar changes in value were also seen for sunflower and soybean meals. This is due to the

fact that demand for feed varies and depends on agricultural yields². To increase the commercial and ecological value of by-products, research has started to investigate the exploitation/utilization of these by-products for use apart from animal feed and to prevent them from going to waste treatment plants. This would add value to the by product, reducing strain on farmers selling the product and would give the product extra value.

One potential option is the use of by-products for the extraction of fibres. The isolation of dietary fibre has risen in interest, due to its common availability in a significant number of food by-products, and because its use has shown success in the prevention and cure of a diverse range of common diseases, especially related to gut health²³. Fibres have been extracted from a wide variety of food production left overs such as fruit pomace (e.g. apple); peel and pulp refuse (citrus fruits, potatoes and bananas); oil cakes (e.g. olive, rapeseed and cotton seed); as well as bran and other plant components^{15,23}. A report by Sharma *et al.*¹⁵ provides an overview of the studies on fibres obtained from by-products. In addition, plant by-products have also been suggested as new sources of protein, e.g. cauliflower leaves and stems²⁴, tomato seed meal²⁵, flaxseed meal²⁶, rapeseed stems²⁷ and Kiwi fruit seeds²⁸.

One of the most researched areas in revalorisation of plant by-products however is the extraction of phytochemicals. Phytochemicals (from Greek phuton, "plant") are biologically active compound found in different plant species. Most phytochemicals are secondary metabolites, which are not directly involved in plant growth, development, or reproduction. However, they are important for their defence against herbivores, pests and pathogens²⁹. These secondary metabolites, including alkaloids, terpenes and phenolics, can be extracted from plant products but also from food production by-products.

1.1.2 Secondary metabolites

Plants produce a significant number of metabolites, which can be separated into two main groups, primary and secondary metabolites. Primary metabolites are the ones necessary for plant growth and development, without them the plant would not survive. In contrast, secondary metabolites are not involved in growth and development and their absence will not lead to instant plant death³⁰. Initially secondary metabolites were considered plant

waste products, but in recent years they have been found to play a significant role in the plant's survivability. A lack of secondary metabolites can for example cause a deficiency in the plants defence system (against herbivorous animals, viruses, microbes or competing plants). Whilst other organisms can flight or fight for defence, plants developed a different system i.e. the production of secondary metabolites²⁹⁻³¹. They can fulfil a variety of different ecological roles apart from defence they also help them compete for water, light and nutrients. In addition, they can also act as signalling compounds to attract pollinating and seed-dispersing animals, help to protect from external stress, such as UV light or physical harm or have selected physiological functions and hence provide advantage for survival³².

Plants usually produce complex mixtures of secondary metabolites, often representing different classes. Because the structures of secondary metabolites have been shaped and optimized during more than 500 million years of evolution, many of them exert interesting biological and pharmacological properties which make them useful for medicine or as bio-rational pesticides³⁰. There are a number of factors that contribute to the secondary metabolite composition (qualitative and quantitative) of different plants, e.g. agronomic conditions (plant species, cultivar, developmental stage, plant part, plant competition, fertilization, pH), season, climatic factors, water availability, light (intensity, quality, duration) and carbon dioxide³³.

Plant secondary metabolites are a diverse group of compounds, which can be divided into three main groups, (i) terpenes, (ii) phenolics and (iii) alkaloids/nitrogen containing compounds. Different classes within these groups are often separated according to their biosynthetic pathways and certain classes are associated with certain set of species within a phylogenetic group and so can be used as taxonomic markers. In general plants will produce a mixture of different secondary metabolites from different classes, which can act additively or synergistically on different molecular targets^{29,30}. The structure and shape of these compounds have been optimized throughout evolution and many of them show interesting biological and pharmacological characteristics, which can and have been employed in the pharmaceutical industries³¹.

The alkaloids represent a structurally diverse group of secondary metabolites containing nitrogen. They are one of the larger groups of secondary metabolites³⁴. Most of these alkaloids are derivatives of amino acid precursors, such as ornithine, arginine, lysine, leucine, tyrosine, tryptophan or nicotinic or anthranilic acid. Depending on the precursor, these classes can be further separated into minor divisions³⁵. The biosynthetic pathways of many alkaloids have already been elucidated on the enzyme and even at the gene level³⁶. Well known alkaloids include morphine, nicotine and caffeine (Figure 1.2).

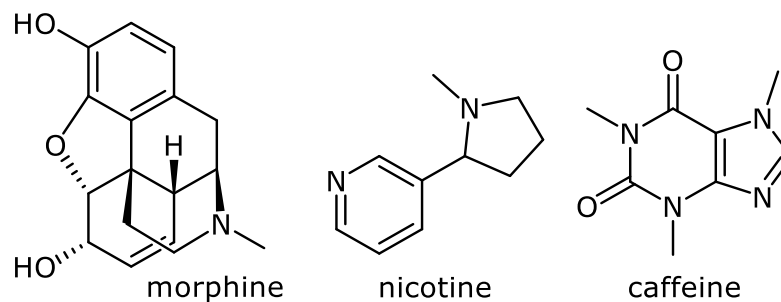


Figure 1.2| Common alkaloids

More than 20,000 different alkaloids have been discovered, with certain plant families being particularly rich in alkaloids, e.g. nightshades and amaryllis. Alkaloids represent an immense number of phytochemicals, with toxicological, pharmacological, nutritional and cosmetic interests. The alkaloids belong to a general group of nitrogen containing secondary metabolites, also non-protein amino acids, amines, cyanogenic glycosides, alkamides, lectins, peptides, polypeptides and glucosinolates all belong to this group. However, apart from the latter (3.1.1.2 Glucosinolates (GLSs) p. 136) no other nitrogen containing compounds were closely investigated in this project, hence they only get a brief mention here. Similar is true for the terpenes. The latter are hydrocarbons with a basic C₅-unit (isopentenyl pyrophosphate or dimethylallyl pyrophosphate) as a building block and can be subdivided into hemiterpenes (C₅H₈), monoterpenes (C₁₀H₁₆), sesquiterpenes (C₁₅H₂₄), diterpenes (C₂₀H₃₂), triterpenes (C₃₀H₄₈), tetraterpenes (C₄₀H₆₄), and polyterpenes ((C₅H₈)_n) such as rubber (Figure 1.3, p. 8)³⁷.

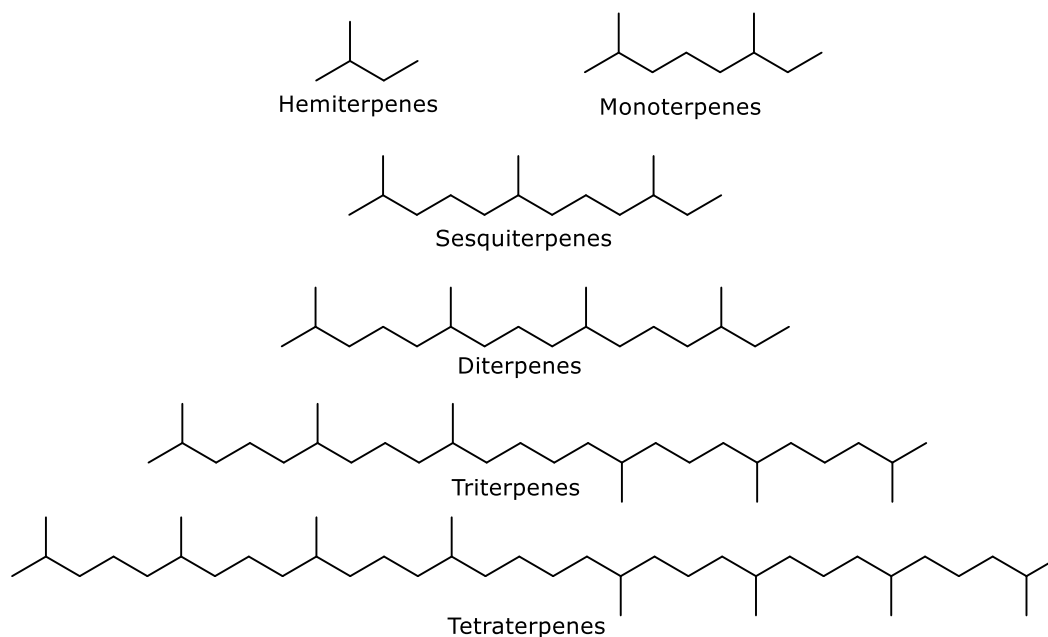


Figure 1.3| Subdivisions of terpenes

Terpenoids are usually terpenes with additional functional groups. The latter are the largest group of secondary metabolites³⁸. Most of the terpenes readily interact with cell components, such as biological membranes and proteins within them, changing their normal function, which can lead to cell death. This activity is mostly non-specific; which makes terpenes cytotoxic to a wide range of organisms. Due to structural similarity, some terpenes can also act as analogues to natural substrates such as hormones or neurotransmitters. Some of the most commonly known terpenes are eucalyptol, limonene and myrcene (Figure 1.4).

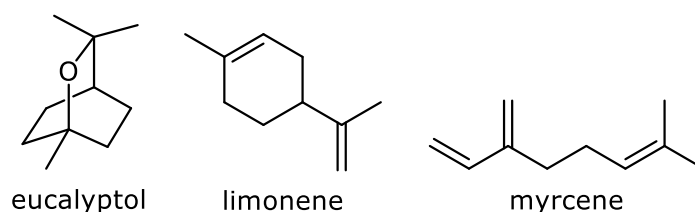


Figure 1.4|Common terpenes

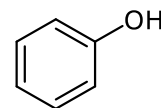
All the above characteristics make them and the alkaloids/nitrogen containing compounds very interesting research material. However, these have not been widely reported in rapeseed by-products and were not part of this project. The third main group of secondary metabolites are the phenolics and in

contrast to terpenes and alkaloids, they are widely researched in rapeseed by-products and so are the focus of this work.

1.1.3 Phenolic secondary metabolites

Phenolics are secondary metabolites with at least one hydroxyl group attached to one or more aromatic rings.

Currently, there are more than 8,000 known phenolic structures ranging from simple molecules to highly polymerized complex



phenolics basic structure

substances^{39,40}. These phenolic compounds can again be further classified according to their chemical structure (Figure 1.6 p.10).

The interest in phenolics has been increasing linearly over the last 20 years, as presented in Figure 1.5. This is mainly due to their interesting biological activities.

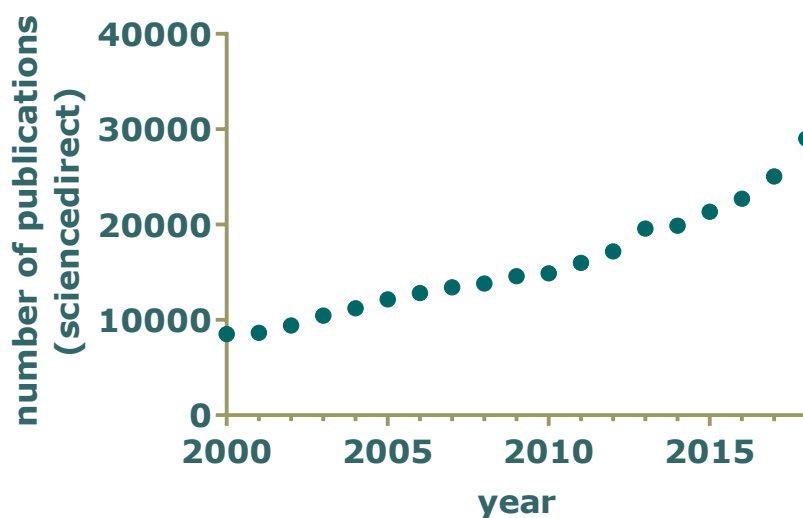


Figure 1.5| Number of publications on sciencedirect.com with the search word "phenolic" from 2000-2018

The data for the year 2018 so far shows that the number of publications (29023) on phenolics has exceeded the number of publications in 2017 (25047) by over 4000 papers. A total number of 5139 publications are already published for 2019 (as of December 2018).

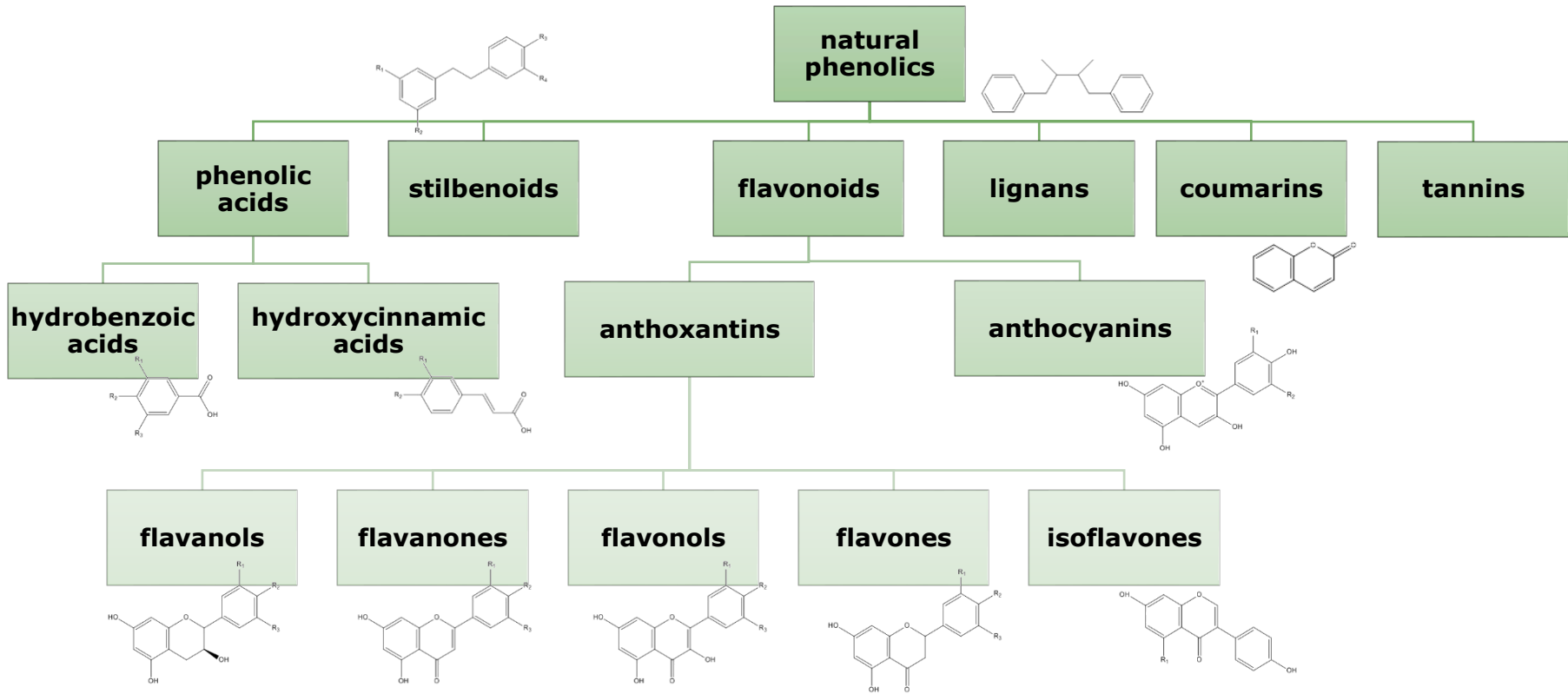


Figure 1.6| Polyphenols sub-divisions and their basic chemical structure, adapted from Shahidi *et al.*⁴¹ and Firuzi⁴²

Amongst all the phenolics, flavonoids are the largest family with more than 2000 individual natural compounds. Phenolics are produced in plants as secondary metabolites *via* the shikimic acid pathway⁴⁰, an overview of which can be found in Maeda *et al.*⁴³. In general, plant genetics/cultivar, soil composition, growing conditions, maturity state, season of harvest and post-harvest processes can effect quantity and quality of the phenolics present in plant foods and by-products^{44,45}. Just like the phytochemicals in general, phenolics are particularly known for their biological activity and beneficial effects for human health and wellbeing. They have for example been associated with a number of valuable physiological properties, including anti-inflammatory⁴⁶, antimicrobial^{47,48}, cardioprotective^{49,50} and anti-atherogenic⁵¹ effects.

In addition, the antioxidant properties of phenolics have been widely studied, in both, *in vitro* and *in vivo* systems producing very interesting data and making them potential candidates for the pharma-, food- and cosmetic-industry⁵²⁻⁵⁴. Various studies have also shown that a diet rich in fruits and vegetables can contribute to the delay of aging and in particular reduce the risk of oxidative stress, associated with a number of chronic disorders (e.g., cardiovascular diseases, arteriosclerosis, cancer, diabetes and neurological diseases)⁵⁵. On a molecular level, different mechanisms have been observed, for the action of secondary metabolites, which are responsible for their biological activity especially related to neuroprotection. For example green tea polyphenols such as (-)-epigallocatechin-3-gallate (EGCG) have been found to exhibit antioxidant activity by chelating metal ions⁵⁶. Tea extracts (green and black) have been shown to suppress lipid peroxidation and protected neuroblastoma cells (SH-SY5Y) from 6-hydroxydopamine induced neuronal death⁵⁷ while EGCG also inhibits β -amyloid-induced cognitive function⁵⁸. Lin *et al.*⁵⁹ suggested that polyphenolic compounds from magnolia extracts (honokiol and magnolol) protect neurons (rat cerebellar granule cells) from hydrogen peroxide, glutamate and N-methyl-D-aspartic acid (NMDA) induced toxicity, suspecting neuroprotection to be related to their antioxidant properties. Similar results were also found for blueberry^{8,60-62}, ginkgo bilboa⁶³⁻⁶⁵ and grape pomace^{10,66,67} extracts. These and other biological activities relevant for neuronal protection, have made phenolics very interesting compounds in the research for drugs to prevent or treat neurodegeneration associated diseases.

This project also connects food waste and the biological activity of phenolic compounds (both topics briefly discussed above) in a neurodegeneration associated study. To decrease the amount of food waste, or at least to improve the value of food waste, attention was focused on the rapeseed pomace (RSP). The latter is the leftover product after the production of rapeseed oil, with the aim of determining its chemical secondary metabolite composition as well as studying its biological activity related to neurodegenerative diseases. Food process by-and/or waste-products such as pomace are ideal for the search of new and interesting compounds. Pomace in general, is the waste product obtained after for example fruit juice, wine or oil production. It can comprise of only one or all of the following plant components: fruit skins, pulp or seeds, plant stems and leaves or any other solid or soft plant parts ^{1,11}. A variety of different plant pomace such as grape ^{10,11,68}, apple ^{1,69}, berry ^{70,71} and olive ^{72,73} had already been analysed and were found to contain significant amounts of phytochemicals. This project is based on determining the potential use of rapeseed pomace extracts and its functional ingredients in the treatment and/or prevention of neurodegenerative diseases. A brief introduction to both rapeseed/RSP and neurodegenerative disease will be provided following, to provide a background for the project (1.2 Rapeseed and Rapeseed pomace and 1.3 Neurodegeneration). The section on rapeseed will give an overview of the plant as well as a literature review on the current knowledge of rapeseed pomace research, including its secondary metabolite composition. The section on neurodegenerative disease will entail a general introduction on the three neurodegenerative diseases investigated in this project i.e. Alzheimer's disease, Parkinson's disease and Machado-Joseph disease (Spinocerebellar Ataxia 3).

1.2 Rapeseed and Rapeseed pomace

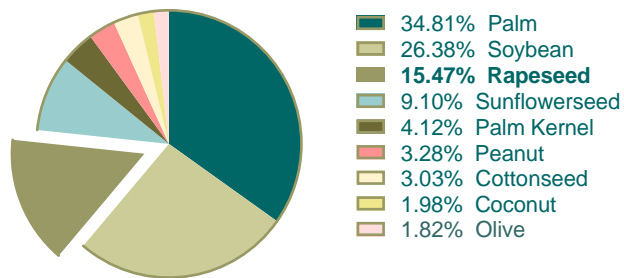
Rapeseed (*Brassica napus*) also known as oil rape, oilseed rape, swede rape, Argentine rape or colza belongs into the *Brassicaceae* family (formerly *Cruciferae*). Plants belonging to the *Brassicaceae* family are widely distributed in nature, with approximately 350 genera and 3500 species⁷⁴, including amongst others a number of well known vegetables such as broccoli, cabbage, kale, turnip and horseradish. The bright-yellow flowering rapeseed cultivar (Figure 1.7 and Figure 1.8B) is believed to have originated through spontaneous hybridization between turnip rape (*B. rapa* L.) and cabbage (*B. oleracea* L.) genotypes⁷⁵. The plant can grow between 50-200 cm in height⁷⁶.



Figure 1.7 | Rapeseed field near St. Cyrus in Kincardineshire, Scotland (F. Pohl, May 2018)

A species previously used as industrial lubricant is now one of the top three oilseeds worldwide, after palm and soybean oil production (Figure 1.8A)^{77,78}.

World vegetable oil supply and distribution 2013/2014



A

Total=170.57 million metric tons



B

Figure 1.8| A: World Vegetable Oil Production in 2012/2013 (adapted from USDA⁷⁸) B: Rapeseed plant (F. Pohl, May 2018)

Canola, a registered trade mark in Canada, is a different name for rapeseed mainly used in the USA and Canada. It describes the same plant, with some genetic modifications, obtained through traditional breeding in Canada starting in the 1970's⁷⁷. This species was created to decrease anti-nutritional components of rapeseed, namely glucosinolates and erucic acid. Both provide an unfavourable bitter taste. In Europe rapeseed oil in this form was introduced in 1977 as low-erucic acid rapeseed (LEAR) oil containing <5% erucic acid and low amounts of glucosinolates⁷⁷. Today, the same breed used in the European Union, is still referred to as rapeseed. In general, the oil which can be obtained from rapeseed seeds, contains little (<10%) saturated fatty acid and high concentrations of monounsaturated fatty acids (45-75%)⁷⁹. Furthermore it is high in α -linolenic acid (C18:3), giving it a low ratio (1.7-2.4⁸⁰) of omega – 6/omega – 3 fatty acids (essential fatty acids) making it better for human consumption than many other plant oils in this respective⁸⁰⁻⁸³. Increased intake of omega-6 polyunsaturated fatty acids (PUFA) and hence an increase in omega-6/omega-3 ratio, are associated with the increased risk of many disease including cardiovascular disease, cancer, inflammatory- and autoimmune diseases⁸⁴. In contrast, increased levels of omega-3 PUFA (a low omega-6/omega-3 ratio) has shown to suppress these effects⁸⁴.

Rapeseed can be cultivated as winter (Europe), semi-winter (Asia) and spring-sown (Canada, China, Australia and northern European countries) crop⁷⁵. The production of rapeseed crop and oil has seen a huge increase over the last 50 years across the world (bottom, Figure 1.9 p.16). But not only the

overall world production has increased, also the UK's rapeseed crop production has increased almost 180 times in over 30 years, from nearly nothing in 1972 (14000 t) to 2.46 million tonnes in 2014 (top, Figure 1.9 p.16). With these values, the UK was 8th top producer in 2014 after Canada, China (mainland), India, Germany, France, Australia and Poland. The harvest of these almost 2.5 million tonnes of rapeseed crop lead to a production of about 831200 tonnes of rapeseed oil, giving a yield of about 34%. The total oil content of rapeseed is most times given as being around 40% which can also be seen in Figure 1.9 from the world production^{80,83,85,86}. Differences between the general oil content and the percentage of oil produced in a single country (e.g. United Kingdom) can be explained by the potential processing of grown crops in other countries or the processing process itself (i.e. cold pressing and/or solvent extraction).

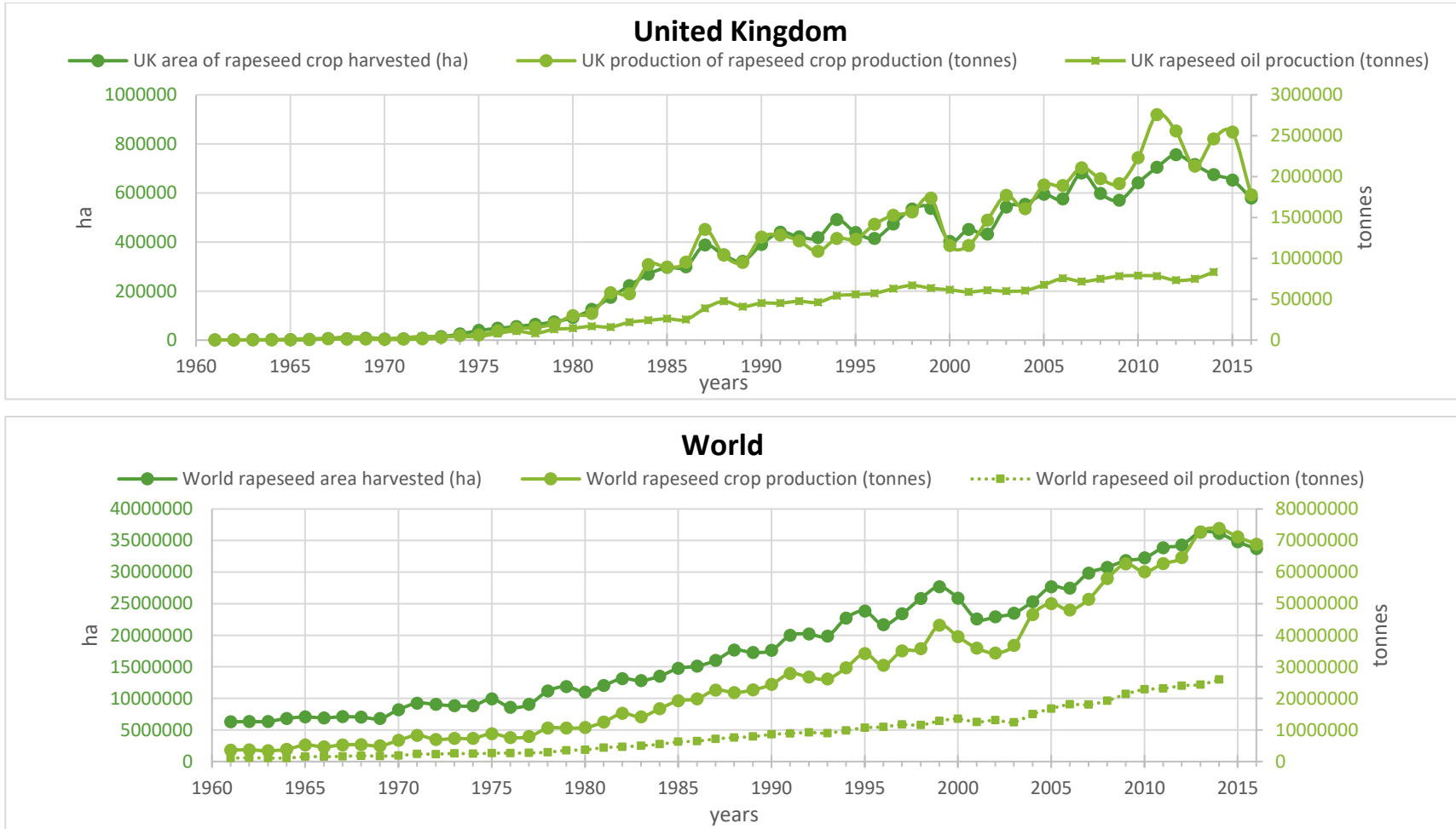


Figure 1.9| United Kingdom/World production of Rapeseed, indicating harvest area and the amount of produced rapeseed and rapeseed oil, adapted from FAOstat^{85,86}

However, increasing production of rapeseed oil also accumulates a higher amount of solid rapeseed waste/by-product called rapeseed pomace (RSP) or rapeseed cake/meal. Depending on the process of oil production, cold pressed or heat/solvent aided, the RSP can still contain more or less amounts of oil respectively.

Currently this by-product is used as an addition to livestock feed due to its high protein content⁸³ and is sold for a considerable but fluctuating price²². However, there might be potential to improve the value of this material. As previously described, plants contain different phytochemicals, some of which have been found beneficial for human health. However, only small amounts of these are found in the rapeseed oil itself, most of them are left in the by-products, after oil production. Options to improve the oils properties have been suggested: (i) developing rapeseed varieties, that apart from the low erucic acid and glucosinolates, have higher amounts of bioactive components, (ii) modification of rapeseed pre-treatment before the oil production process, (iii) the use of enzymes in the production process, and (iv) the potential supplementation of the rapeseed oil with phytochemical rich extracts^{80,87-90}. The latter was taken into consideration by Thiyam *et al.*⁹¹, which in 2004 reported the potential use of RSP extracts in preventing lipid oxidation in rapeseed oil, due to significant amount of phenolic compounds present in the extracts. Suggestions were not only made to use RSP extracts to stabilize oils, but also other food products. This utilization of rapeseed oil by-product would have a large contribution to the plant meal industry⁹¹. A review by Szydłowska-Czerniak⁷⁵ on bioactive compounds from rapeseed and its products described the presence of many biologically active compounds such as tocopherols, phytosterols, phospholipids and phenolic compounds and their distribution in rapeseed, rapeseed oil or the pomace. Some of the compounds present have antioxidant properties, suggesting their potential use in the food, pharmaceutical or cosmetic industry⁷⁵.

1.2.1 Phytochemicals in rapeseed/RSP

The number of papers covering the composition of rapeseed oil and its importance for the food industry are significant. However, research related to the rapeseed oil production by-product rapeseed pomace/meal/cake, and its potential application in the food and pharma industry is less attainable. The total phenolic content of rapeseed is known to be higher than in any other oilseed flours/cakes as shown in Table 1.2.

Table 1.2| Total amount of phenolics in oilseed flours

MEAL	Total Phenolics (mg/100g, dry weight)
SOYBEAN FLOUR^A	23.4
COTTON FLOUR^A	56.7
PEANUT FLOUR^A	63.6
RAPESEED/CANOLA FLOUR^A	639.9
CANOLA MEAL^B	1540-1840
SOYBEAN MEAL^B	460
CANOLA SEED CAKE (DEFATTED)^C	~2200
HEMP SEED CAKE (DEFATTED)^C	~900
FLAX SEED CAKE (DEFATTED)^C	~800

Note(s): data adapted from A⁹², B⁹³ and C⁹⁴ (in mg gallic acid equivalence/100 g, extraction techniques: ^Anot provided, ^Btwo phase solvent extraction (10% ammonia/methanol and methanol/5% water), ^Cultra sound assisted extraction

Extracts of rapeseed mainly contain phenolic acid, flavonoid and condensed tannins derivatives⁹⁵. Rapeseed and RSP have been found to contain high amounts of sinapic acid (SA) and SA derivatives (Figure 1.10) together between 6390 and 18370 µg/g RSP cake, depending on variety, growing conditions and pressing method. SA belongs to the group of naturally occurring hydroxycinnamic acids and makes up over 73% of the free phenolic acids in rapeseed cakes⁹⁶.

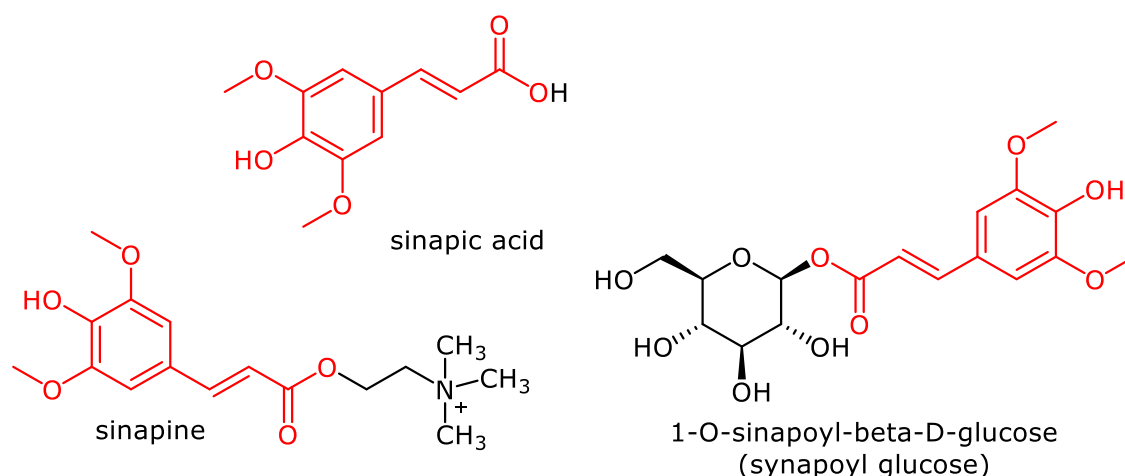


Figure 1.10| Chemical structure of sinapic acid (SA) and SA derivatives common in rapeseed

Sinapine (Figure 1.10), a choline ester of sinapic acid, is the most abundant phenolic ester in rapeseed extracts⁹². According to Thiyam *et al.*⁹⁷ sinapine constitutes between 55-70% of rapeseed extract while sinapic acid constitutes between 6-14%. They also found significant amounts of sinapoyl glucose (14–27%, Figure 1.10) in the rapeseed extracts. All three of which showed antioxidant activity in the following order sinapic acid > sinapoyl glucose > sinapine⁹⁷. A detailed overview of sinapic acid, its derivatives (including sinapine) their natural sources and biological activity is available from Nićiforović and Abramovič⁹⁶.

Furthermore, other phenolics such as caffeic, chlorogenic, ferulic, gallic, cinnamic, p-coumaric, p-hydroxybenzoic, protocatechuic and syringic acids have been found in some rapeseed varieties^{80,93}. These together with other phenolics, such as benzoic and cinnamic acid derivatives are present as free, insoluble bound form and as soluble esters (glycosides)⁹⁵. Phenolics such as those named above are known for their radical scavenging activity, quenching of ROS, chelation of transition metals and their inhibition of oxidative enzymes⁹⁸. Phenolics in rapeseed are thought to protect from ultraviolet-B (UV-B) stress⁹⁹.

Another group of compounds often found in rapeseed and RSP, are the glucosinolates, one of the nitrogen containing secondary metabolites. Identified glucosinolates in rapeseed include progoitrin, epiprogoitrin, glucoraphanin, gluconapin and others⁹⁹⁻¹⁰¹. Further details about glucosinolates can be found under 3.1.1.2 Glucosinolates (GLSs) (p. 136).

In addition, tocopherols have been identified in rapeseed. They can be classified into two groups, the tocopherols and tocotrienols, with four isomers (α , β , γ , δ) in each group (Figure 1.11)⁷⁵. The principal tocopherols in rapeseed are α and γ tocopherol but also plastochromanol-8 and tocotrienols can be found¹⁰²⁻¹⁰⁴. The latter are among some of the major antioxidants in food¹⁰⁵. However, as they are lipid soluble compounds, most of the time either rapeseed seeds or rapeseed oil is analysed for their presence, not rapeseed pomace. An extensive list of references regarding the tocopherol content of rapeseed and rapeseed oil can be found in Szydłowska-Czerniak⁷⁵.

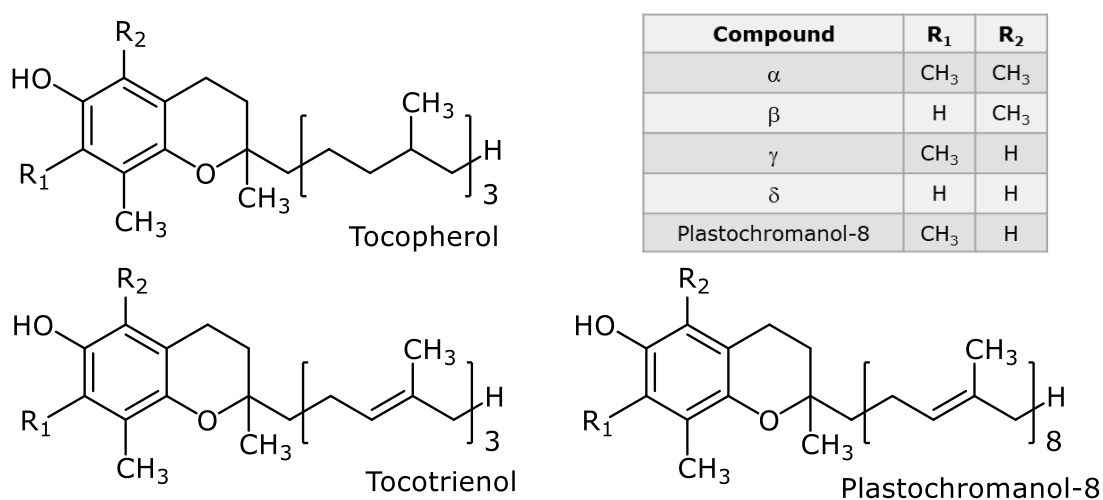


Figure 1.11 | Different Tocopherols

Also phytosterols (steroid alcohols), including plant sterols and stanols have been reported in rapeseed. Stanols are saturated (no double bond in the sterol ring structure) sterols. Just like many other secondary metabolites, phytosterols can be free or bound to other compounds such as esters and glucosides. Phytosterols found in rapeseed include sitosterol, campesterol, brassicasterol, Δ^5 -avenasterol, stigmasterol and cholesterol (Figure 1.12)^{75,106}.

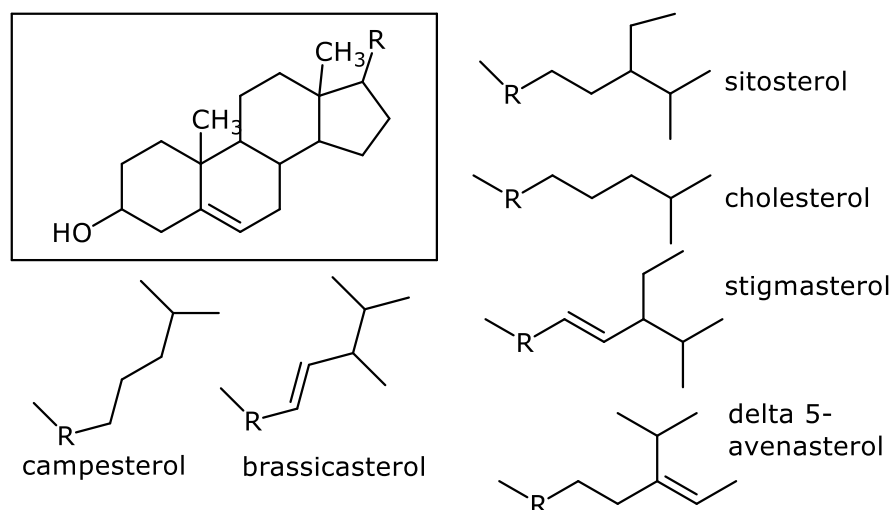


Figure 1.12|Phytosterols in rapeseed, adapted from^{75,106,107}

In contrast to phytosterols and tocopherols, which are mostly found in the oil, phenolics are often retained in the meal after pressing of the rapeseed seeds¹⁰⁸. This had prompted researchers to investigate the leftover product rapeseed pomace/meal for the presence of phenolics. Research has shown that the previously mentioned phenolic compounds e.g. sinapic acid, sinapine, and ferulic acid are retained in the pomace/meal after oil extraction (cold press or solvent extraction). Hence, these can be extracted from the de-oiled pomace using different solvent systems, e.g. alcoholic solvents such as ethanol or methanol or water (2.1.1.2 Extraction solvents, p.69) in conjunction with different extraction methods (2.1.1.3 Extraction technique, p.70), e.g. Soxhlet, microwave, or ultrasonic assisted extraction^{91,109,110}. *In vitro* studies of a number of different RSP extracts by e.g. Hassas-Roudsari *et al.*¹¹¹, Wanasundara and Shahini⁸⁷ and Szydłowska-Czerniak *et al.*⁹⁰, have previously reported their antioxidant activity. An overview of the rapeseed metabolome was recently also provided by Misra¹¹², which included a table that summarized all the so far detected secondary metabolites and their corresponding references, including compound class, their MS m/z ratio as well as MS/MS breakdown products.

Although a lot of work has been done on the chemical composition of rapeseed and RSP, most of the work was done on seed/plants grown in Canada¹¹³, Korea¹¹⁰, Poland^{80,109}, China¹¹⁴ Germany^{80,91,113} or France⁸⁰, little literature is however available on rapeseed grown in Scotland/UK¹¹⁵. The rapeseed pomace obtained for this project was kindly provided by Gregor

Mackintosh, the owner of Mackintosh of Glendaveny. This family owned farm is located in Glendaveny, in Aberdeenshire, near the town of Peterhead (Figure 1.13). Mackintosh of Glendaveny was established in 2009 and since then produces cold pressed rapeseed oil. The rapeseed pomace is currently sold to surrounding farmers as animal feed.



Figure 1.13| Location of rapeseed harvest/oil production by Mackintosh of Glendaveny

1.3 Neurodegeneration

With the continual growth and improvement of medical services as well as the constant access to food and cleaner water, especially in the developed countries of the world, the average human longevity has been increasing continuously over the last decades¹¹⁶. In the United States for example, the average human life span has seen a rise of around 6 years over the last century, increasing the average expected age for men to 74 and for women to almost 80 years¹¹⁷. This increase in life expectancy is a consequence of the positive impact of medical research and development as well as easier access to basic human needs i.e. clean water, food and shelter. Although the increase in life expectancy is a great achievement for mankind, it presents itself as double-edged sword, because it also leads to an increase of age related diseases.^{79,117,118}

Age related diseases refer to those ailments that are closely associated with ageing and are known to increase in prevalence with rising age. In addition, factors such as advanced medical diagnostic tools and enhanced awareness of neurodegenerative disease markers have added to the raising numbers¹¹⁹. The problem is further exacerbated by the lack of treatment options for some of these medical conditions. Treatment is either unavailable, only partially effective or only treats the symptoms of the disease but does not impact on the actual origin of the diseases. Conspicuous is the fact, that there are a lot of neurodegenerative disease in that list of age related conditions, such as Alzheimer's disease (AD), Huntington's disease (HD) and Parkinson's disease (PD).

Neurodegenerative diseases are the consequence of the gradual and progressive degradation and loss of neurons, which inevitably leads to nervous system dysfunction¹²⁰. The increasing rise in such debilitating chronic neurodegenerative disease is closely associated with the ageing population. This inevitably also intensifies the obligations of scientists and medical researchers to (i) acquire sophisticated knowledge of these neurodegenerative diseases and (ii) implement the necessary research to develop and find new therapeutics¹²¹. Increased research in this area and possible treatment will improve the elderly's quality of life, by preventing, curing or at least delaying the onset of such disease. On the other hand, costs

related to the health system and the burden on carers will also be reduced, proving a great benefit to mankind. The treatment of neurodegenerative diseases is thought to cost the United States billions of dollars every year, the frontrunner being AD, with estimated costs of \$100 billion alone¹²⁰.

Many neurodegenerative diseases share a common pathogenic mechanistic element, the aggregation and deposition of misfolded proteins in the central nervous system, although these proteins are expressed systemically in most cells¹²². AD, HD, PD, Creutzfeldt-Jakob disease, multiple system atrophy as well as many of the spinocerebellar ataxias (SCAs) are only some of the common and well known neurodegenerative diseases showing such protein misfolding. Although the type of protein aggregation, their location and the temporal and regional pattern of deposition pattern varies in all these diseases (Table 1.3), they are however thought to be linked by comparable protein aggregation pathways¹²². Furthermore, the patients' innate response together with environmental factors can influence the aggregations¹²³.

Table 1.3| Neurodegenerative disease with their respective microscopic lesions, location and aggregated proteins

Disease	Onset	Microscopic lesion	Location	Aggregated Protein
Alzheimer's Disease (AD)	Usually 6 th decade or older	Amyloid plaque	Extracellular/ Intracellular	Amyloid- β (A β)
		Neurofibrillary tangle	Intracytoplasmic (neurons)	Tau
		Lewy bodies	Intracytoplasmic (neurons)	α -synuclein
Amyotrophic lateral sclerosis (ALS)	About 60 years of age	Hyaline inclusions	Intracytoplasmic (neurons)	Superoxide dismutase-1 (SOD1)
Huntington disease (HD)	Dependent on poly-Q repeats, usually 30-50	Neuronal inclusions	Intranuclear (neurons)	Huntingtin (containing polyglutamine repeats)
Multiple system atrophy	6 th decade of life	Glial cytoplasmic inclusions	Intracytoplasmic (oligodendroglia)	α -synuclein
Parkinson's disease (PD)	Over the age of 50	Lewy bodies	Intracytoplasmic (neurons)	α -synuclein
Pick's disease	Typically, before the age of 60	Prion plaques	Extracellular	Protease-resistant prion protein
Spinocerebellar ataxia (SCA)	Dependent on poly-Q repeats, usually 30-50	Neuronal inclusions	Intranuclear (neurons, plasma)	Ataxin (containing polyQ repeat expansion)

Note(s): adapted from^{116,122,124-128}, as previously published in⁷⁹

Not only the type of aggregates and their position of occurrence, but also the disease symptoms can differ significantly amongst these diseases. Possible symptoms are dementia (AD), movement deficits (SCA's and HD) and personality changes (HD, AD)^{120,129}. Despite all their differences, all the aforementioned neuronal conditions can nevertheless be associated with the aggregation of proteins and a mostly adult onset of the disease. This has led to the idea that it might be possible to treat all these diseases by the same therapeutic approach/target¹³⁰. Research, however, is still in its early stages and the reason behind the neurotoxicity in these diseases has not been fully elucidated. Much more effort and work are necessary to evaluate their mechanisms and the possibilities of treatment. On that account, in this

project RSP extract was employed to study its neuroprotective properties *in vitro* and *in vivo*.

The work undertaken here was based on neurodegeneration and oxidative stress and in particular on three neurodegenerative diseases, Alzheimer's-, Machado-Joseph- and Parkinson's disease. For this reason, the following three neurodegenerative diseases will be introduced in more detail, followed by a section on the significance of oxidative stress in neurodegeneration (1.4 Oxidative stress in neurodegeneration and the potential use of antioxidants to prevent neurological disorders p.51 ff.).

1.3.1 Alzheimer's Disease (AD)

Alzheimer's disease (AD) is, a progressive neurodegenerative disease with a late onset in life. With 60-80% of cases, it is the most common form of dementia in the elderly¹³¹. Furthermore, statistics from 2016 show that it is the 5th leading cause of death, whilst in 2000 it was only the 14th ¹³². These numbers indicate the major increase of prevalence of AD, which is related to the general increase in life expectancy and better diagnosis. The risk of developing AD is increasing by a factor of two per 5 years, starting from the age of 65¹²⁰. Alone the number of people with dementia in the UK, is over 900,000. This is set to rise to just over 2 million by 2051. Of these approximately 62% are AD related¹³³. The costs associated with the care of AD patients are tremendous, in 2014 the costs in the UK alone were estimated to about £26.3 billion, with an average yearly cost of £32,250 per patient¹³³. This figure will have increased over the last 4 years and will probably double till 2051 with the doubling of patient numbers. Just like for most neurodegenerative disease, the main risk factor for AD is age¹³⁴.

1.3.1.1 Symptoms

There are major problems giving a clinical definition for AD and it is hard to implement a uniform diagnosis, because of the many different symptoms and their severities. Usually AD can be diagnosed in patients with some or all the following symptoms at the beginning of onset: (i) slight memory loss, (ii) disorientation, (iii) restlessness, (iv) incoherent conversations and (v) occasional confusion. This is soon followed by severe mental impairment, which can even lead to personality changes of the patient^{120,128}. Also the decrease in cognitive function and an impairment of daily living activities are common¹³⁵. For example, even simple tasks can become confusing and more of a challenge with ongoing disease progression. In the later stages of the disease this might even become impossible. In the last years of the disease, symptoms will worsen and might even be followed with the patient being incontinent, bedridden and often mute and unresponsive¹³⁶. In addition, AD patients have language difficulties that show early in the disease, usually with reduced verbal fluency and naming abilities¹³⁷.

Pathologically, AD is associated with a progressive degeneration of nerve cells (mainly cholinergic neurons) in the brain regions (especially hippocampus),

which are critically for memory, cognitive performance and personality, leading to the above mentioned recognizable symptoms in the patient^{119,136}. All these symptoms are a reduction of life quality, for the patients as well as all the surrounding people associated with the patients. This in addition to the associated costs for the health care system, highlight the importance of a cure for AD.

1.3.1.2 Mechanisms/pathophysiology associated with AD

AD was first described by Alois Alzheimer in 1907, who identified salient clinical and pathological aspects of the disease. It was not till later however, that AD was discovered as being the most common cause for dementia in elderly people *by Blessed et al.*^{135,138}.

In general, Alzheimer's disease can be characterized by the hallmark of abnormal aggregations of harmful proteins. The most common aggregated proteins include β -amyloid ($A\beta$) peptide and tau, leading to plaques and neurofibrillary tangles (NFTs) respectively, visualized in Figure 1.14¹³⁹.

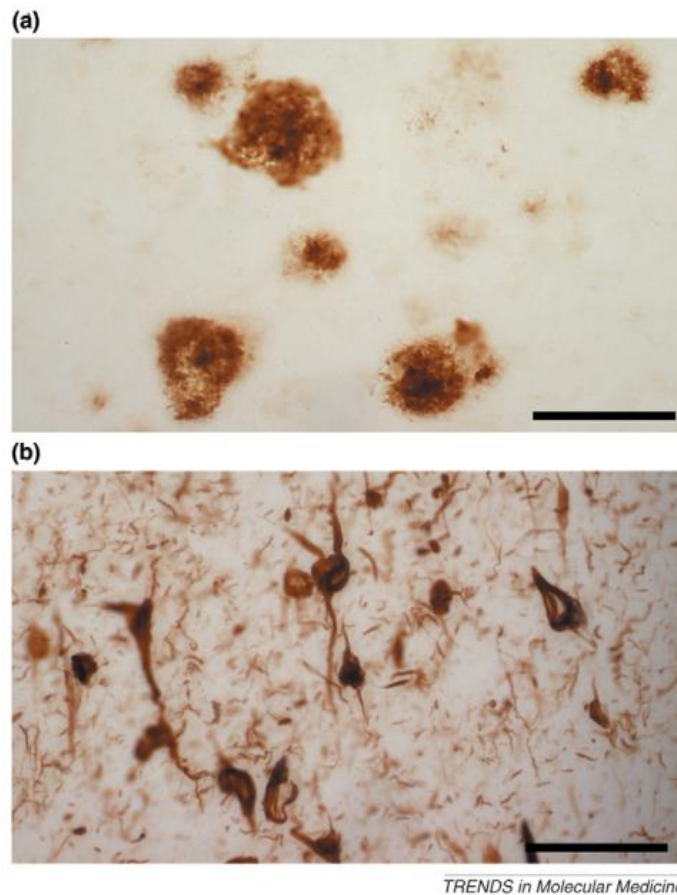


Figure 1.14| Neuropathology of Alzheimer's disease

(a) Microphotograph of amyloid plaques in the AD brain, visualized by immunostaining with anti- $A\beta_{42}$ specific antibody; scale bar: 125 μ m. (b) Microphotograph of neurofibrillary tangles, visualized by immunostaining with an anti-PHF1 specific antibody; scale bar: 62.5 μ m. Reprinted with copyright permission from LaFerla and Oddo¹³⁹

The affected proteins have unrelated functions, but their aggregation is further downstream associated with oxidative stress and inflammatory damage that lead to energy failure and synaptic dysfunction and neuronal loss¹³⁴. Both proteins will be further discussed following.

A Tau

AD belongs into a group of tauopathies, with other disease such as Pick's disease, frontotemporal dementia with parkinsonism and progressive supra nuclear palsy, due to the presence of aggregates formed by tau in patients' brains. In AD patients, tau levels (total and phosphorylated tau) are increased in the brain as well as the cerebrospinal fluid (CSF). The mechanisms behind the increase in aggregated tau are still under investigation¹⁴⁰. The tau protein normally binds to microtubules and is responsible for their stabilization and assembly as well as for vesicle transport. Tau is controlled by the level of phosphorylation^{122,134}. When this stabilization process is no longer given, for example due to hyperphosphorylation of the protein (insoluble and lacks affinity for microtubules), the formation of NFTs is possible, after its self-association into paired helical filament structures¹³⁴. Hyperphosphorylation is not the only explanation for the accumulation of NFTs and there are other factors that also modify the interaction of tau with microtubules or even with the cytoskeleton, leading to toxicity¹²⁰. A paper published by Arriagada *et al.*¹⁴¹, suggests that the formation of NFTs by hyperphosphorylated forms of tau has a higher correlation with the progression and severity of AD, than the amyloid plaques (described below) and are also thought to be the main mechanism of neuronal death¹³⁵. However, opinions on that are still divided. Tangles are preferentially situated in specific brain regions, for example areas of the hippocampus (correlating with some clinical features, such as memory loss) as well as nerve cells of the basal forebrain, leading to cholinergic neurotransmitter deficits¹³⁵. The exact mechanisms of why these aggregates or previous intermediate stages lead to the outbreak of the disease are still under investigation.

B β -amyloid

In addition to the tau tangles β -amyloid plaques can also be found in the brains of AD patients. Amyloid plaques are compact and spherical extracellular deposits mainly consisting of the amyloid β -peptide ($A\beta$)¹³⁹. These usually start to assemble in the 5th decade of life and at the 8th decade about 75% of the population is thought to be affected. In general, the density of senile plaques is not assumed to increase slowly with age but thought to go from a plaque free status to a plaque-bearing status in a very short time. The mechanism and the reason for this behavior however, are not established so far¹³⁵. They start developing as diffuse plaques first (mostly non-toxic β -amyloid), in some individuals thus they undergo changes and soon form senile neuritic plaques. The main constituent of these plaques is β -amyloid ($A\beta$) but they can also contain other proteins, metal ions and cholinesterase's (Figure 1.15 p.32)¹⁴². $A\beta$ is a heterogeneous group of small peptides containing between 38 or 43 amino acids (AAs) and is cleaved from the amyloid precursor protein (APP, Figure 1.15)¹⁴⁰. This protein can be fragmented by different secretases, during proteolytic processing¹³⁶, which will cleave at different locations of the protein (Figure 1.15). The left hand side of Figure 1.15 presents the "normal", non-neurotoxic cleavage of the protein via α - and γ - secretase. β -amyloid ($A\beta_{40}$ or $A\beta_{42}$) thus is produced by cutting with γ - and β -secretase. In non-AD patients, the shorter, less aggregatory $A\beta_{40}$ peptide is most prevalent. However, in sporadic and most cases of familial AD either the ratio of $A\beta_{42}$ to $A\beta_{40}$ is raised or the total concentration of $A\beta_{42}$ is increased.

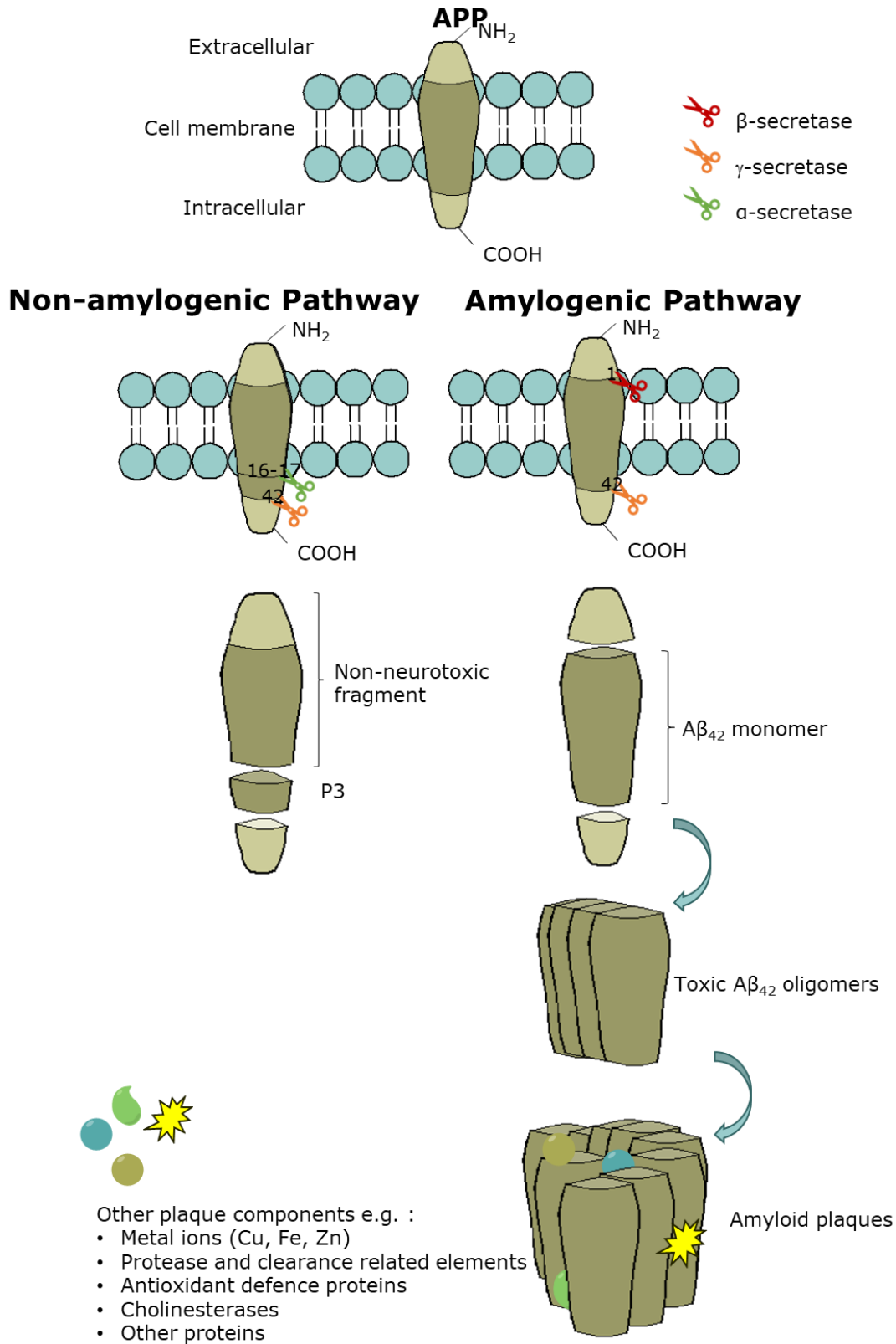


Figure 1.15| Fragmentation of amyloid precursor protein (APP) into toxic and non-toxic fragments

Non-neurotoxic fragmentation on the left (a), neurotoxic cleavage on the right (b), schematic altered from^{135,142,143}

Plaques form by aggregation of a number of A β monomers. Although plaques are closely associated with AD, more recent research has focused on the oligomers, as they seem more likely to be causing the neurotoxicity instead of the plaques. This was indicated by a few patients with visible plaques in the brain which failed to present symptoms of dementia. Also, other studies showed that learning defects do not require the presence of large visible plaques, suggesting that already small intracellular accumulations of A β are enough to lead to deficits in the learning process¹⁴⁴.

However, the aggregation of A β amyloid just like tau tangles are not the origin of AD, but a downstream effect. Research had shown, that there are usually at least a number of possible discrete genetic mutations or polymorphisms preceding and causing the aggregation and hence the accumulation of A β ¹⁴⁵. Although it was shown that the aggregation levels of A β have an effect on phenotypes, the aggregation rate and level alone does not determine the pathogenicity¹²⁰. It is also known that some genetic mutations in the coding gene for β -APP on chromosome 21 might even lead to an early onset (autosomal dominated inherited) familial AD¹³⁵ (see C Genetic implications p.34).

Nevertheless, how exactly these A β plaques and Tau NFTs in AD lead to the progression and pathology of the disease is still unclear and controversial. Some people with AD brain pathology showing tau and β -amyloid aggregates e.g. sometimes stay dementia free¹⁴⁶. It was also established, that environmental factors and the comorbid (co-occurring medical condition) brain pathology can have an important impact on the outbreak of the disease¹³⁵. The relevance of environmental factors has been suggested by studies of monozygotic twins, which showed that not always both developed the disease¹⁴⁷.

C Genetic implications

AD can be classified into two types, early-onset, which typically develops before the age of 65 years, and late-onset which usually starts in those older than 65. Early-onset AD (familial AD) is caused by rare and dominantly inherited mutations in APP, or the proteins cleaving APP, PSEN1 (component of the γ -secretase complex), and PSEN2 (component of the γ -secretase complex along with PSEN1) all of which are involved in β -amyloid₄₂ production^{139,148,149}. But also late-onset AD (sporadic AD) can have genetic components, with high heritability, but genetic as well as environmental factors play a role in onset, progression, and severity of these cases^{148,150}. One of the genes known to be involved in sporadic AD is *APOE* ($\epsilon 4$ allele). The *APOE* protein is responsible for cholesterol carriage in the brain and is also involved in control of inflammation, cholesterol metabolism, lipid transport, neurogenesis, or the generation and trafficking of APP and $A\beta$ ¹⁴⁸. Due to the genome-wide association study researchers were able to identify a great number of other genes, which when mutated can increase the chance of AD later in life. A comprehensive summary of these was provided by Giri *et al.* in 2016¹⁴⁸.

Although both proteins (tau and $A\beta_{42}$) have been positively associated with AD as well as some genetic mutations, AD is a multifactorial and complex disease, which is still not well understood. And researchers are still in the dark on the actual cause. Other factors might play a significant role in the disease origin or development, e.g. oxidative stress (1.4 Oxidative stress in neurodegeneration and the potential use of antioxidants to prevent neurological disorders), which is one of the main points of interests in this project.

1.3.1.3 Treatment (current and future)

Although there are some drugs currently available for the treatment of AD, which slowdown the progression of the disease, no treatment has been found to cure this neurodegenerative disease¹²⁰. There are 2 classes of FDA (Food and Drug Administration) approved drugs which can be prescribed to AD patients, acetylcholinesterase inhibitors (AChEIs) and N-methyl-D-aspartate (NMDA) receptor antagonist¹⁵¹ or a combination of both¹⁵².

A Acetylcholinesterase inhibitors

As previously described, AD is caused by the death of neurons, in particular cholinergic neurons, which leads to a decrease in acetylcholine neuronal signaling. To alleviate this decrease, acetylcholinesterase (AChE) inhibitors are used, which as their name states, inhibit acetylcholinesterase, the enzyme responsible for the breakdown of acetylcholine in the synaptic cleft (Figure 3.10 p.147). By using AChE inhibitors, acetylcholine is retained in the synaptic cleft for neurotransmission. The three currently used AChE inhibitors are galantamine, rivastigmine and donepezil (Figure 1.16).

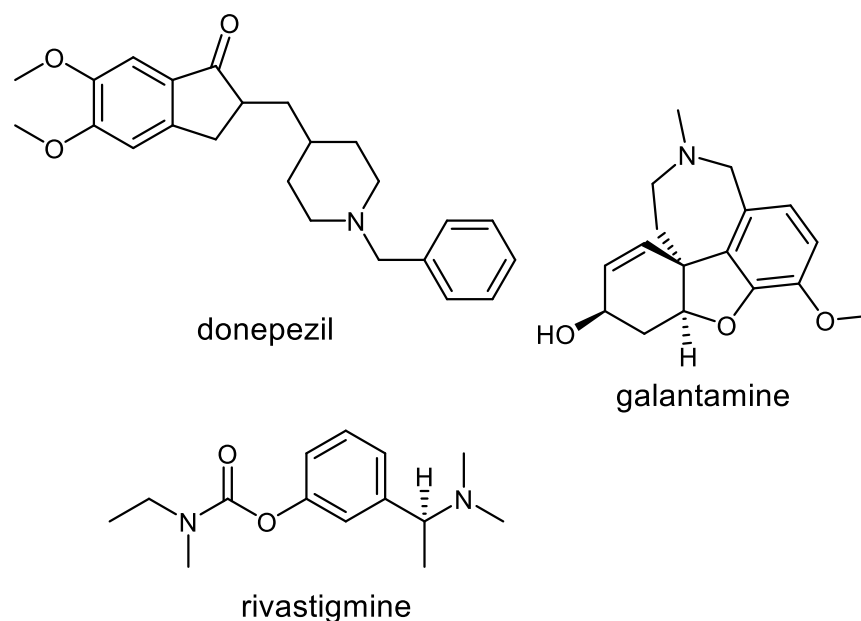


Figure 1.16 | Chemical structure of donepezil, galantamine and rivastigmine, current treatments for symptoms of Alzheimer's disease

B N-methyl-D-aspartate receptor antagonists

N-methyl-D-aspartate (NMDA) receptor antagonists inhibit NMDA receptors and fall into four categories, those that bind to and block the binding sites for either (i) glutamate or (ii) glycine or noncompetitive antagonists, which inhibit NMDA receptors by binding to (iii) the allosteric sites, (iv) those that block the ion channel by binding to a site within the channel (Figure 1.17 left). Memantine, the currently approved NMDA receptor antagonist is a non-competitive blocker of the NMDAR channel and prevents entry of excess calcium¹⁵³ (lower level of noise Figure 1.17 p.36).

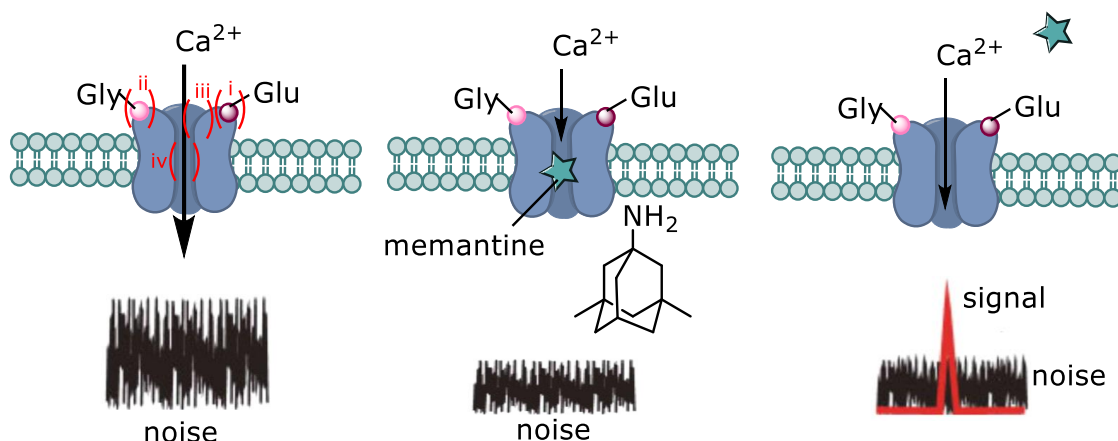


Figure 1.17| NMDA receptor antagonist memantine, adapted from^{153,154}

Nevertheless, there is currently no drug available that can cure the disease itself. All the introduced drugs only ease the symptoms and might delay further progression. However, research is in progress, as reported by Cummings *et al.*¹⁵⁵, currently (stand May 2017) a total of 25 agents are in 29 phase I trials, 52 agents are in 68 phase II trials and a total of 28 agents are in 42 phase III trials. The mechanism of action of all these agents are covering a wide area, including drugs which are (i) neurotransmitter based, (ii) anti-tau, (iii) anti-amyloid, (iv) neuroprotective, (v) anti-inflammatory as well as (vi) antiviral and (vi) metabolic based. All the agents currently in trials are summarized and discussed by Cummings *et al.*¹⁵⁵. The number of agents in clinical trials has increased over the last years. A similar review written by Cummings *et al.*¹⁵⁶ in 2014 presented data on agents and their registration years, whilst there was only a total of 5 agents that were registered for clinical trials in 2002, this number increased to 12 in 2003, 14 in 2004, 32 in 2005 till a maximum of 72 registrations in 2009. From then on (2010-2012) the number of registered agents was constantly around 50.

1.3.2 Machado-Joseph Disease (MJD)

Machado-Joseph disease (MJD), also named spinocerebellar ataxia 3 (SCA3) is one of the types of spinocerebellar ataxias. There is a wide range of SCAs, such as SCA1, SCA2, SCA6 and SCA17, but SCA3 is by far the most prevalent worldwide^{157,158}. In Portugal, for example, MJD covers 58% of all known dominant ataxias¹⁵⁹. The prevalence however is strongly dependent on geographic places. The Flores Island, in the North Atlantic Ocean (one of the Azores Islands) is associated with the highest prevalence of MJD worldwide (1/239)^{79,160}.

This adult-onset neurodegenerative disease obtained its name from the affected families of Antone Joseph and William Machado, both originating from the Portuguese Azores Islands¹⁴⁴. Due to the first mentioning of MJD symptoms in this family it was first named "Azorean disease of the nervous system"¹⁵⁹. Initially, MJD was described as three independent clinical entities found in two other families (Thomas and Joseph), described between 1972 and 1976. This indicates the immense differences in phenotypical symptoms, which can be observed in SCA3 patients. Only a paper published a couple years later proposes the presence of a single disease¹⁶¹. Although the condition was first reported in the mentioned families, it has since been found in families with different ethnical background and geographical origin^{79,162}.

1.3.2.1 Symptoms and Onset of MJD

In general, the symptoms of MJD show a gradual progression, which subsequently leads to the death of the patient. Most obvious is the progressive neuron loss, which can be associated with a decline in motor and cognitive function. The usual onset of symptoms is relatively late in life (midlife, 3rd or 4th decade), with death occurring 10 to 30 years (with an average of 21 years¹⁵⁹) after the first symptoms have been noticed. The age of onset and severity is also dependent on the number of CAG-repeats (Figure 1.18)^{158,163}. The green line in this graph (highlighted with arrow) shows the decreased age for onset of SCA3 with increased number of CAG repeats¹⁶⁴. In comparison to some of the other polyQ disease (e.g. SCA7 and HD) the slope for MJD is particularly steep, i.e. only slight changes in the number of repeats have a significant impact on the age of onset⁷⁹.

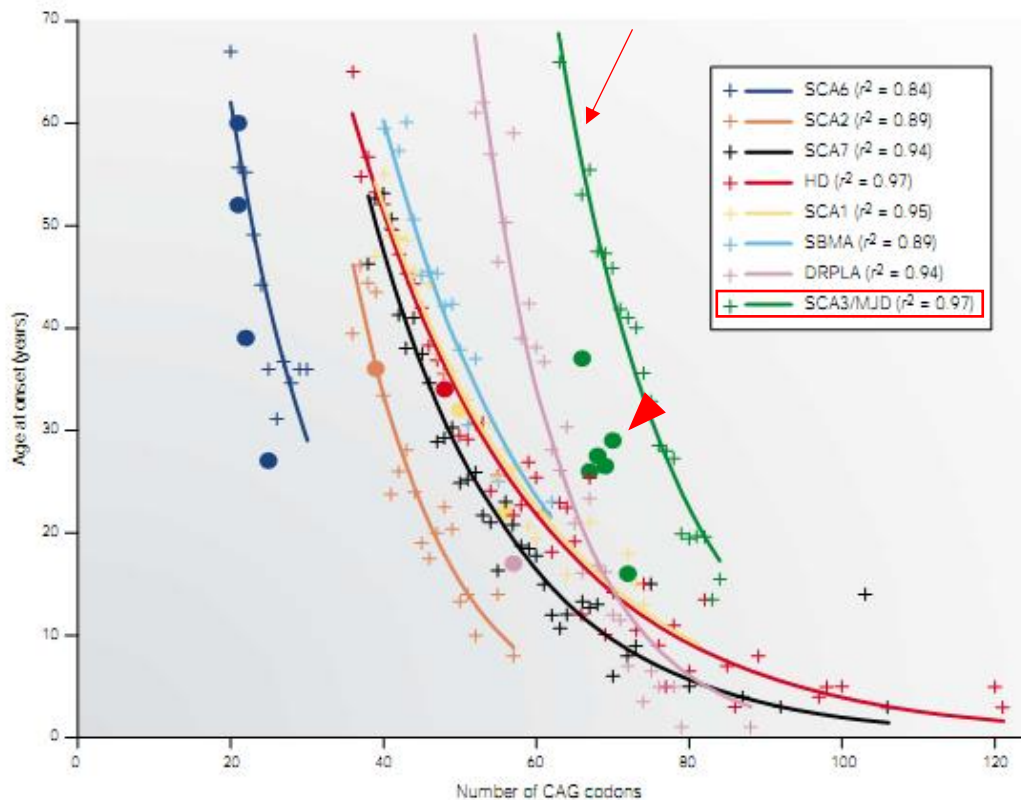


Figure 1.18| Correlation between the number of CAG repeats and the age of onset of 8 polyglutamine disorders

crosses heterozygous (indicated by arrow) and circles homozygous (indicated by arrow head) patients, reprinted with copyright permission from Gusella et al.¹⁶⁴

Even people with the same number of repeats, do not necessarily start showing symptoms at the same age. This demonstrates that there are also other factors that have an influence on the outbreak of the disease¹⁶⁵. Although MJD has an average onset age of 40 years, extremes of 4 and 70 years have been reported¹⁵⁹.

Since MJD is a dominantly inherited disorder, the onset, clinical features and progression should be similar in homozygote and heterozygote patients. Nevertheless, few homozygous affected patients were reported to present more severe phenotypes than what is observed in heterozygote individuals¹⁶⁶. Also, from Figure 1.18 this conclusion can be drawn, where homozygote patients are depicted with green circles (highlighted with arrow head), showing an earlier onset for all MJD cases¹⁶⁴. Very common for polyQ disease is also a decreasing age of onset in successive generations, also called anticipation, which results from paternal transmission^{79,167}.

In general, ataxia is associated with problems to coordinate voluntary muscle movements, which usually can be seen in unsteady movement and staggering gait. Progressive ataxia also shows the following symptoms: cerebellar syndrome (uncoordinated gait), dysarthria (speech disorder), spasticity, nystagmus (involuntary eye movement), and oropharyngeal dysphagia (swallowing disorder)^{158,167}. This however, is not a comprehensive catalogue of symptoms of MJD. These symptoms severely decrease life quality for patients and a cure is urgently needed, even though the number of affected patients in comparison to AD is low.

1.3.2.2 Mechanisms/pathophysiology associated with MJD

MJD is caused by an increased expansion of unstable CAG-repeats in the coding region of the gene encoding the protein ataxin-3 (Figure 1.19), a protein with ubiquitous expression in the body^{157,163}.

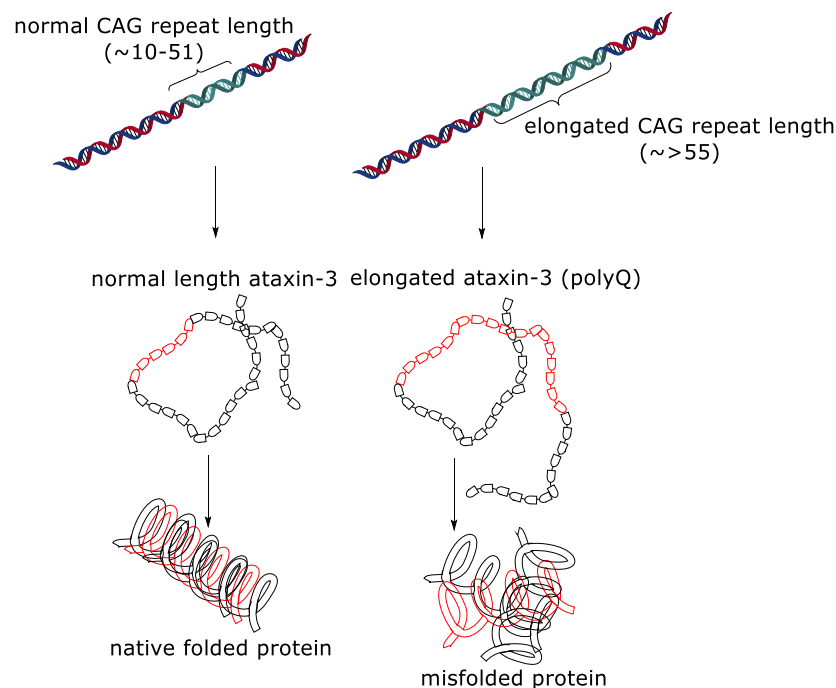


Figure 1.19|Mutant ataxin-3, caused by increased CAG repeats, leading to polyQ amino acid sequence and elongated and misfolded proteins

The disease thus only occurs when a certain threshold of repeats is exceeded¹⁶⁸ (Table 1.4, p.40). The three letter code CAG encodes the amino acid glutamine (Gln), which has the one letter code Q. Hence, SCA3 is also known to be one of at least 9 so far recognised polyglutamine diseases (polyQ disease, Table 1.4, p.40)^{79,168}.

Table 1.4|Collection of the 9 polyglutamine expansion disease and some of their characteristics^{79,157,169}

Disease	Affected protein	Gene location	Regular CAG repeat	Pathogenic CAG repeat	Intracellular protein localization	Intracellular localization of aggregates
SBMA (Kennedy's disease)	Androgen receptor	Xq11-12	9-36	38-65	Cytoplasm/ nucleus	Nuclear
HD	Huntingtin	4p16.3	6-35	36-121	Cytoplasm/ nucleus	Nuclear/ cytoplasmic
DRPLA	Atrophin-1	12p13	3-35	49-88	Cytoplasm/ nucleus	Nuclear
SCA1	Ataxin-1	6p23	6-38	39-83	Cytoplasm/ nucleus	Nuclear
SCA2	Ataxin-2	12q24.1	14-31	32-77	Cytoplasm	Nuclear/cytoplasmic
SCA3	Ataxin-3	14q32.1	10-51	55-87	Cytoplasm/ nucleus	Nuclear/cytoplasmic
SCA6	CACNA1A	19p13.1	4-19	20-33	Cytoplasm	Nuclear/cytoplasmic
SCA7	Ataxin-7	3p12-13.5	4-35	37-306	Cytoplasm/ nucleus	Nuclear
SCA17	TBP	6q27	47-55	47-55	Nucleus	Nuclear

Note(s): SBMA- Spinal and bulbar muscular atrophy, HD-Huntington's disease, DRPLA- Dentatorubral-pallidoluysian atrophy, SCA-Spinocerebellar ataxia, TBP- gene, encoding the TATA-box-binding protein

MJD, like most other polyQ diseases, is an autosomal dominant inherited disorder. The precise numbers of repeats that cause MJD symptoms are open to interpretation. Although Table 1.4 provides the range of 55-87 repeats to show the abnormal phenotype¹⁵⁷, other sources suggest, that only repeats above a number of 61 are associated with the condition^{159,160}. This can be explained by the relative rarity of the occurrence of intermediate alleles. In addition, some people with an intermediate number of repeats show an abnormal phenotype, whilst others do not^{170,171}. This again indicates that other, possible environmental, factors might have an influence on the disease's outbreak and appearance.

The increased number of CAG repeats is assumed to originate from a DNA strand slippage during the process of DNA replication or DNA repair, leading to a looping out of one or more repeats in the newly formed DNA strand. After a further replication these loops can be converted to expansions. These expandable repeats were shown to form unusual hair-pin-like structures, predisposing them to instability^{79,172}.

A MJD Associated Protein Ataxin-3

The MJD associated gene encodes ataxin-3, a protein with a molecular weight of approximately 42kD, in its original form, it is the smallest of the known polyglutamine-containing proteins¹⁷³. It belongs to a family of cysteine-proteases, composed of 339 amino acids plus the variable polyQ part. An overview of the general protein structure is given in Figure 1.20.



Figure 1.20| General structure associated with ataxin-3

not showing possible isoforms, adapted from Costa et al.¹⁷⁴ as presented in⁷⁹

The figure above shows the overall organisation of ataxin-3, containing a conserved N-terminal Josephin domain, which is followed by two Ubiquitin-Interacting Motif (UIM) domains, the polyQ region and sometimes by another UIM domain. The existence of this protein in the nucleus and cytoplasm in

various kinds of tissues, suggests its importance in eukaryotic cells. This is reinforced by findings of highly homologous sequences in other organism's genes (mouse, chicken, *C. elegans*)^{79,174}.

Due to the UIM regions (short, conserved and 11 amino acids long) in ataxin-3 (Figure 1.20, p.41), this protein is thought to bind polyubiquitin chains and play a role as deubiquinating enzyme in the ubiquitin-proteasome pathway (Figure 1.21), as shown *in vitro*^{159,168}. In general these UIM regions are found in proteins taking part in ubiquitination and ubiquitin recognition¹⁵⁷.

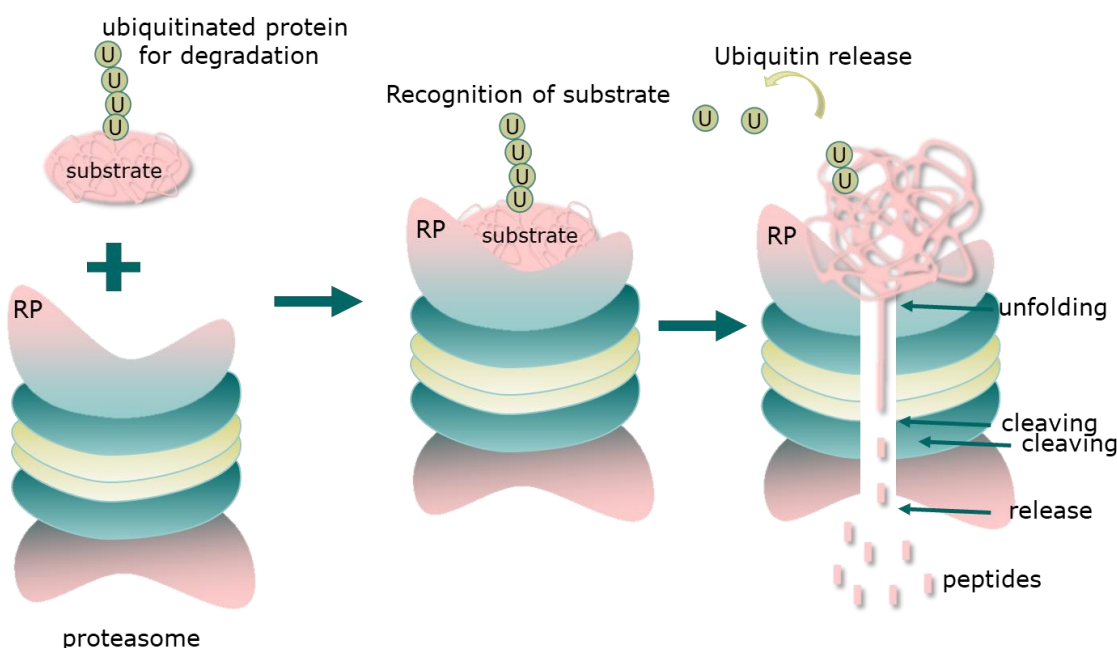


Figure 1.21 | Simple sketch of the ubiquitin-proteasome pathway
adapted from Hochstrasser et al.¹⁷⁵

This pathway is responsible for the degradation of proteins, which are either regulatory (and not needed anymore), misfolded or otherwise abnormal proteins, which might lead to aggregation or toxicity, when not degraded¹⁶⁸. Due to ubiquitin receptors associated with the proteasome (regulatory particle-RP in Figure 1.21), ubiquitinated substrates are recognised and will be degraded.

On the other hand, ataxin-3 has also been linked to protein homeostasis maintenance¹⁷⁶, cytoskeleton organisation¹⁷⁷, transcription regulation¹⁷⁸ as well as myogenesis¹⁷⁴, thus its specific biological function is still not completely elucidated. This also limits the understanding, of why a mutation

in this protein leads selectively to the death of neurons in patients with MJD^{79,168}.

B Protein Aggregations and Inclusions found in neurons

The CAG expansions cause glutamine repeats in the affected proteins, which then can lead to irregular protein conformations and polyglutamine aggregates or neuronal intranuclear inclusions (NIIs) in the brain¹⁵⁷. If these aggregates cannot be degraded, they tend to build up into neuronal inclusion. Both the full-length ataxin-3 proteins and their polyQ fragments can act as an origin for aggregations. Misfolded proteins can undergo different mechanisms of degradation, including autophagy and degradation *via* proteasomes. If degradation does not occur, they can form oligomers that can lead to the formation of insoluble aggregates (Figure 1.22, p.45), which are observable in certain neurons in MJD patients.

Conspicuous however is the fact that, although the proteins are expressed ubiquitously, it only leads to aggregations in neurons at certain regions of the brain (central nervous system, CNS), such as the deep cerebellar nuclei, *substantia nigra*, cranial nerve motor-, vestibular- and pontine nuclei and Clarkes's columns. Hence, it is thought that there are specific cellular conditions only present in some neurons, which cause the discriminating cytotoxicity only in these cells. However, the presence of these aggregations is still an issue and widely controversial¹⁷⁹. For example it is not clear whether the toxicity of polyQ disease is related to the presence of these inclusions or due to the intermediate species (oligomeric species such as protofibrils and microaggregates¹⁷⁹), produced during the process of aggregation¹⁷³. Hence, it could be that the inclusions are only a cellular strategy to trap pathogenic proteins, to prevent their toxic effect and thus might only be the end product of an upstream toxic event¹⁷⁹. However, inclusions are usually found in the patients and progression of the disease can so far only be associated with the increasing amount of inclusions. This clearly shows that inclusions are still a good indicator for the presence and progression of the disease.

C Pathogenic Mechanism of MJD

Although the genetic background is identified as discussed above, the molecular mechanism is still unclear and the question “How does the mutated protein trigger the pathogenic process?” still needs to be answered. Many different proposals about the mechanism of pathogenesis and the progressing neuronal death have been introduced, including a) alterations induced by the polyQ sequence, leading to functional changes and/or the generation of protein aggregations and the formation of toxic oligomers, b) transcription dysregulation, c) decreased axonal transport, d) inhibition of ubiquitin-proteasome system, e) synaptic and mitochondrial dysfunction and f) apoptotic cell death¹⁵⁷ as well as others (Figure 1.22). However, due to the close relationship found between age of onset and the number of CAG-repeats a connection between the expanded polyQ sequence and the mechanism (leading to the disease) can be suspected^{79,168}.

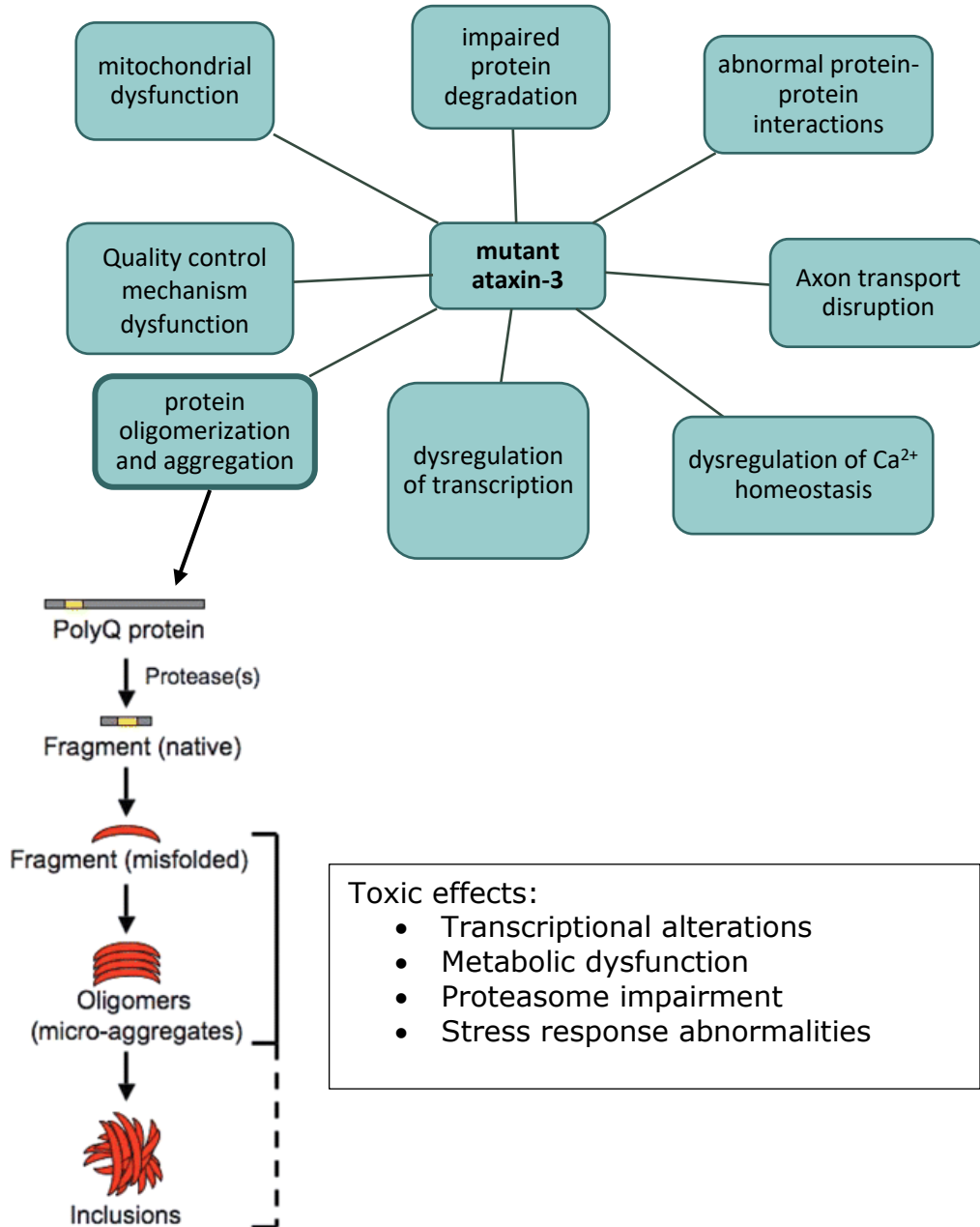


Figure 1.22| Problems associated with mutated ataxin-3

top: pathogenic mechanism of mutant ataxin-3 , altered from¹⁸⁰; bottom formation of oligomers and inclusions and their toxic effects, reprinted with copyright permission from Shao et al.¹⁸¹, adapted from Pohl⁷⁹

1.3.2.3 Therapeutic Strategies for MJD

There are two main categories in which the therapeutic strategies for MJD can be divided into: A) those having an impact on the downstream effect of the expanded polyQ protein and B) treatments targeting the mutant protein itself¹⁷³. Possible pathways of treating MJD are shown in Figure 1.23. However, to date no cure or effective treatment has been found for MJD.

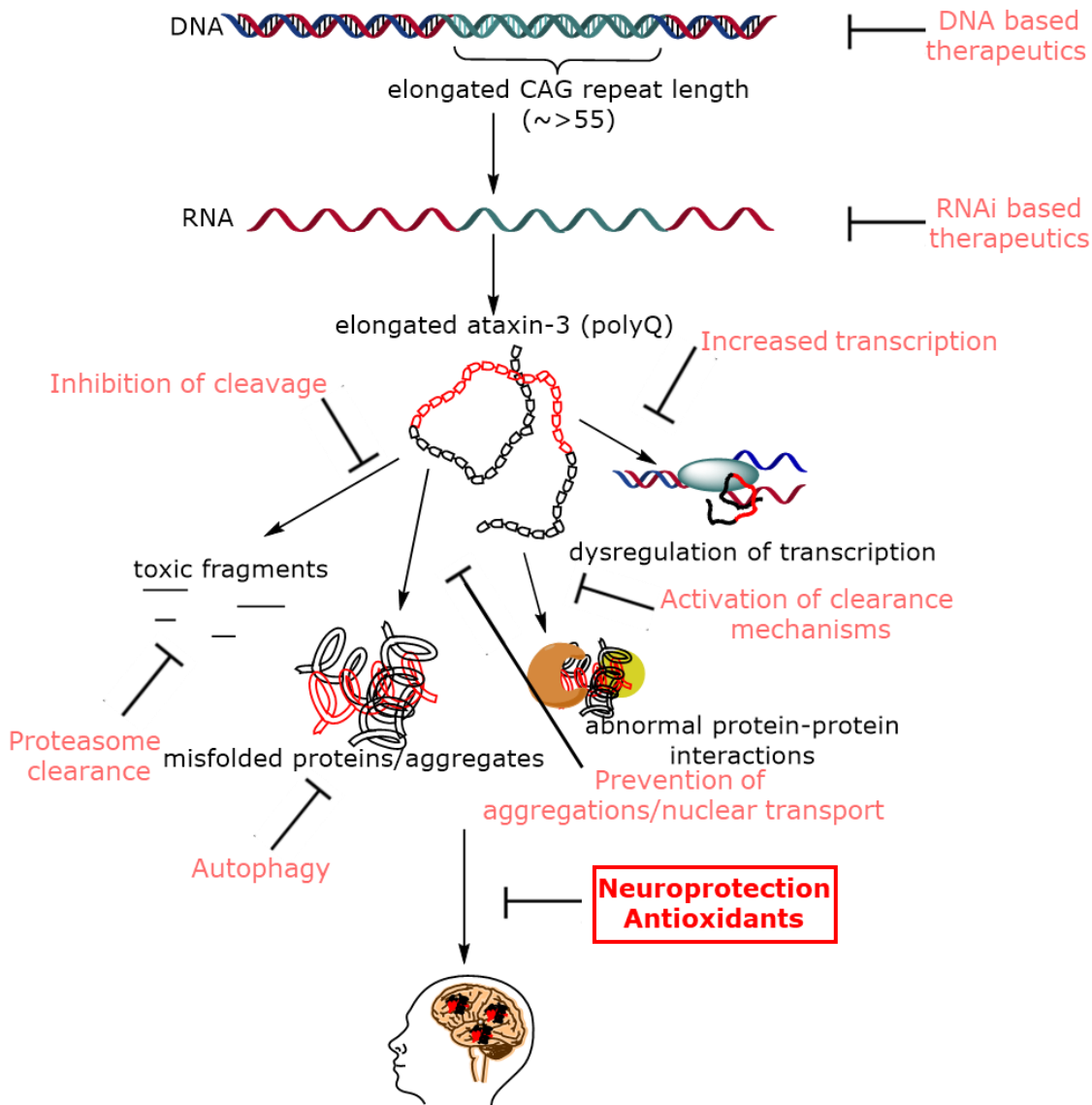


Figure 1.23| Possible therapeutic drug targets associated with MJD highlighting the therapeutic target associated with this project (red box); adapted from^{79,180,181}

The importance of oxidative stress and the potential treatment with antioxidants in MJD or neurodegeneration in general is further highlighted in section “1.4 Oxidative stress in neurodegeneration and the potential use of antioxidants to prevent neurological disorders” p.51 ff.

1.3.3 Parkinson's Disease (PD)

PD is a progressive neurodegenerative disease with a combination of motor and non-motor symptoms. After AD (in conjunction with other dementias), PD is the second highest cause of death for neurological disorders and the numbers are still increasing significantly. Whilst in the year 2000 the crude rate of death was 1.7 per 100,000 people globally, this number has almost doubled till 2016 to 2.9¹³². PD is slightly more prevalent in males and numbers significantly increase with rising age. The first descriptions of PD were made two centuries ago by James Parkinson in 1817. These findings were further refined and expanded by Jean-Martin Charcot in the mid 1800's, including the separation from other disorders such as multiple sclerosis, although showing similar symptoms. Since then PD has become one of many complex neurological disorders under constant investigation¹⁸². Up until today the exact cause and path of the disease is still not fully understood. Both environmental and genetic causes have been investigated and associated with the disease. A complex interplay of both seem to cause complex cellular dysfunction in the brain. The most common feature is the loss of dopaminergic (DAergic) neurons.

1.3.3.1 Symptoms/clinical features

The key symptoms of PD are rest tremor, rigid and stiff muscles, postural and gait impairment as well as bradykinesia (slowness of movement). However, these symptoms strongly differ from patient to patient (heterogeneous). Also, non-motor function related symptoms have been described, such as cognitive impairment, sleep disorders, pain, constipation, fatigue and olfactory dysfunction. Some of these non-motor symptoms can start before the onset of the PD classical motor symptoms^{182,183}.

The progression of the disease can be seen through the worsening of the bodily motor functions, which still can be managed with treatment (1.3.3.3 Treatment, p.49). However, the long-time treatment of PD can lead to complications, which create challenges for the management of later stages of the disease. Treatment-resistant symptoms such as postural instability, freezing of gait, falls, dysphagia, and speech dysfunction become more pronounced about 17 years after disease onset. Common non-motor features at this age are urinary incontinence, constipation, and symptomatic postural

hypotension. Also dementia is a common clinical feature in the later stages of the disease^{182,183}. PD symptoms, especially in the later stages significantly impair the patients' normal living and most often need considerable care once treatment residence sets in.

1.3.3.2 Mechanisms/pathophysiology associated with PD

The most prevalent brain pathological feature in PD is the loss of DAergic neurons, especially in the substantia nigra pars compacta (SNpc). Loss of these DAergic neurons within this area leads to the previously introduced symptoms. Normally functioning dopamine (neurotransmitter) is responsible for excitatory and inhibitory synaptic transmission ensuring smooth directed movements¹⁸⁴.

Also, the presence of eosinophilic protein deposits (Lewy bodies) is a common hallmark of PD. As previously described in AD, many neurodegenerative diseases are associated with the abnormal formation of proteins, and PD is one of them. The aggregated protein in PD patients is α -synuclein, which in the misfolded state becomes insoluble and forms intracellular inclusions called Lewy bodies within the cells. These inclusions can also occur in neuronal processes and are then called Lewy neurites. α -synuclein is a 14-kDa protein found in neuronal cells, belonging to a family of structural related proteins. Under non-disease physiological conditions, α -synuclein promotes the association of the SNARE machinery, a large protein complex responsible for vesicle fusion, in the presynaptic terminal. It has also been suggested to play a role in neurotransmitter release and protection of nerve terminals against injury¹⁸⁵. However, under disease physiological conditions, inclusions are formed containing mainly misfolded α -synuclein. These inclusions were first described by F.J.H. Lewy in 1912 and were named after him by K.N. Tretiakoff in 1919¹⁸⁶. Lewy body formation is hypothesised to be a biological marker for PD and some even give them a causal role in the disease development. However, PD is more complex, and neurodegeneration is most likely not only caused by Lewy bodies. Just like for AD and β -amyloid, other aggregation types have been revealed (e.g. oligomers), which might play an important role in the degeneration process¹⁸⁵. Also, other misfolded proteins (e.g. tau and β -amyloid) have been found in PD patients brains¹⁸². Furthermore, also neuroinflammation and oxidative stress (1.4 Oxidative

stress in neurodegeneration and the potential use of antioxidants to prevent neurological disorders p.51 ff.) are common features in PD^{187,188}.

1.3.3.3 Treatment

Initial treatment for PD has included venesection and other methods to divert blood and inflammatory pressure away from the brain and spinal cord (beginning of the 19th century). Later, anticholinergic drugs (e.g. belladonna alkaloids or hyoscyamine, a tropane alkaloid) were used as well as other compounds and apparatus, which are summarised by Goetz¹⁸⁹. It was not until the finding of the synthetic pathway of dopamine in 1910 and later the discovery of dopaminergic deficits in Parkinson's disease patients' brains in the mid 1900's that levodopa was introduced as treatment for PD. Levodopa was first administered to patients in 1961 with exceptionally good results¹⁹⁰ and remains the most used drug for the treatment of PD motor symptoms up until today. In the clinic, it slows the progression of motor disabilities (assessed by the Hoehn and Yahr staging system) and furthermore it reduces mortality. In addition, it is one of the better tolerated drugs for PD treatment particularly in the elderly population¹⁹¹.

Levodopa is a prodrug which metabolizes after administration into the pharmacologically active compound, in this case to dopamine *via* L-aromatic amino acid decarboxylase (Figure 5.10, p.275). Levodopa can cross the blood brain barrier in contrast to dopamine and so can restore synaptic DA concentrations (Figure 1.24, p.50).

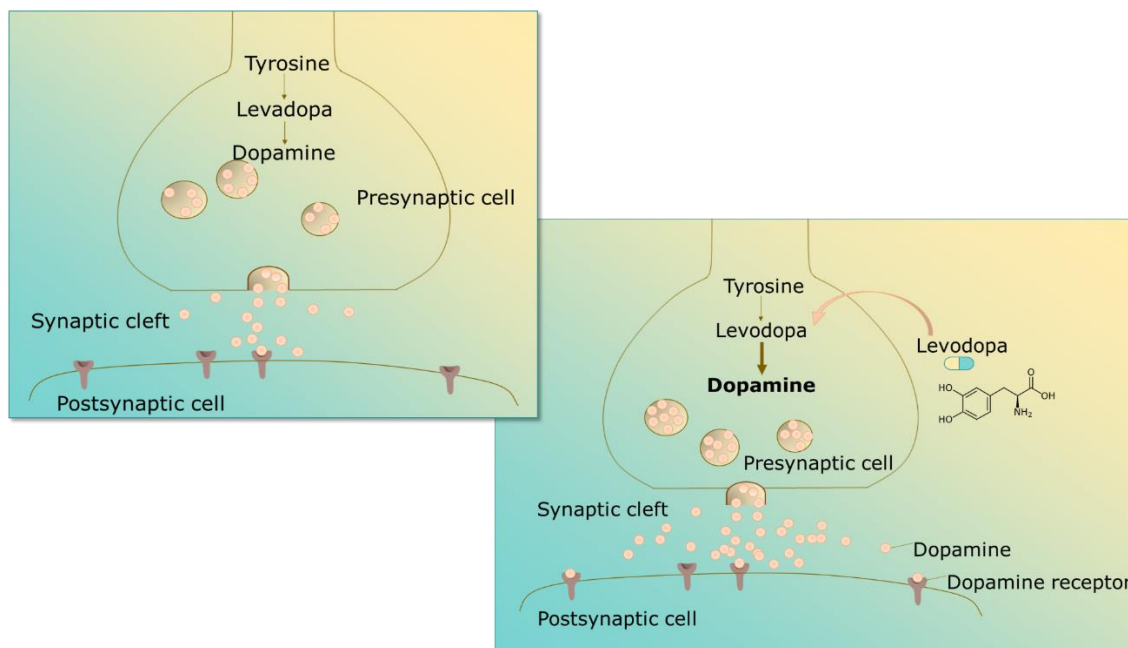


Figure 1.24| Mechanism of Levodopa

Apart from levodopa there are other treatments (for motor-symptoms) available that effect the DA concentrations or excite the dopamine receptors and these include (i) dopamine agonists (Piribedil, Rotigotine and Bromocriptine), (ii) monoamine oxidase type B inhibitors (Rasagiline and Selegiline) (iii) catechol-O-methyltransferase inhibitors (Entacapone, Tolcapone) and others (Amantadine, Anticholinergics, clozapine)¹⁸². However, current treatment options still only treat the symptoms of the disease, not the origins of the disease. Current research is actively seeking to find drugs that stop or at least slow the neurodegenerative process associated with PD¹⁸².

The three introduced neurodegenerative disease (AD, PD and MJD) covered here, have varying symptoms and backgrounds. However, they also have common features, such as the aggregation of proteins in neuronal cells. For all of them the exact pathology leading to the neuronal death has not been completely elucidated. They also share the notion that oxidative stress could be involved in the disease pathology. The medication with exogenous antioxidants could be a potential treatment or prevention not just for a certain neurodegenerative disease, but for all of them in general^{192,193}. Thus, the following section will introduce oxidative stress and the potential of natural antioxidants in the fight against these conditions.

1.4 Oxidative stress in neurodegeneration and the potential use of antioxidants to prevent neurological disorders

Current research has been focusing on a wide variety of different potential drug targets. In AD these have included for example N-Methyl-D-aspartate (NMDA) receptor antagonists ^{194,195}, acetylcholinesterase inhibitors ^{195,196}, radical scavengers ¹⁹⁷, monoamine oxidase inhibitors ¹⁹⁶ and A β and tau aggregation inhibitors/dissolver¹⁹⁸. In PD, treatment is mainly based on levodopa. Currently there is no treatment specifically for MJD. Drugs employed for the treatment of neurodegenerative diseases have helped to alleviate some of the symptoms associated with the diseases, but they are currently neither a cure nor do they halt the progression of the disease in any way. The number of current and future drug targets under investigation, might potentially lead to a cure for many neurodegenerative diseases. Some of those targets are summarized in Figure 1.25, highlighting targets of interest in this study in red.

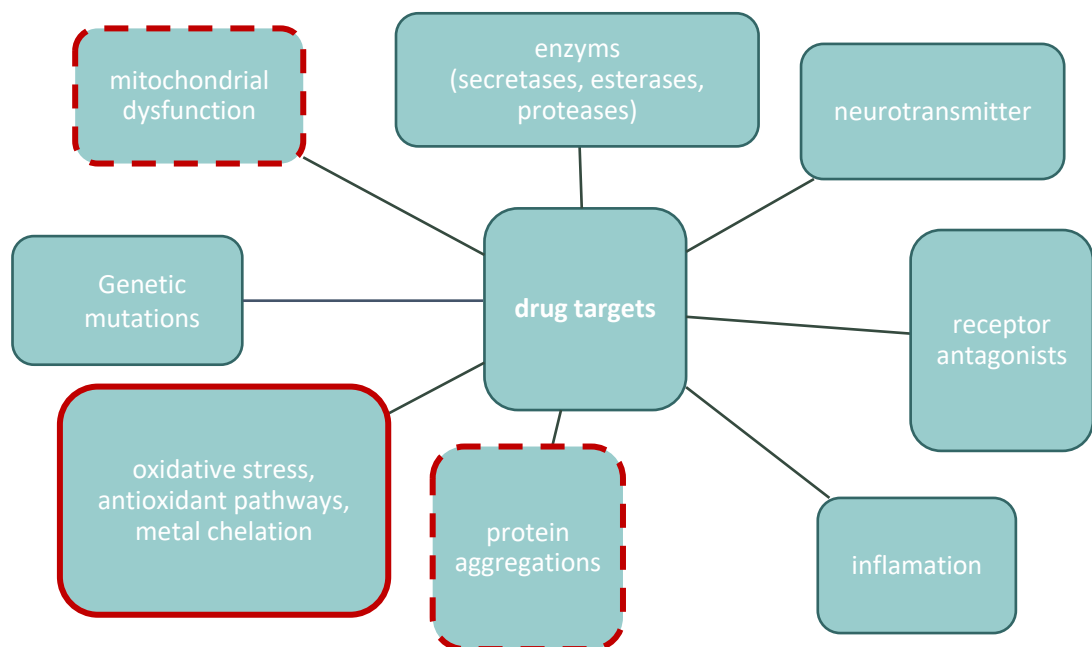


Figure 1.25| Examples of drug targets for neurodegeneration
highlighting the targets under investigation in this project (red outline)

In this project, the focus is the prevention of oxidative stress, using phenolic antioxidants, and to determine their potential to decrease the neurodegenerative pathology. Furthermore, mitochondrial dysfunction is

often associated with oxidative stress, hence this is partially highlighted in Figure 1.25 (p.52) together with protein aggregations, which are also part of this investigation.

Aging, one of the main risk factors of many neurodegenerative disease has first been associated with free radicals (oxidative stress) by Harman "Aging: A theory based on free radical and radiation chemistry" in 1956¹⁹⁹. Since then, reactive oxygen species (ROS) have shown to be the cause of oxidative stress, the latter has been linked to a range of neurological disorders such as AD, PD, ALS and MJD^{157,193}. It is assumed, that reducing oxidative stress within the human body could at least be part of future treatment options; maybe in conjunction with other drugs, pursuing multiple drug targets simultaneously. This could be of advantage, as most neurodegenerative disease have been associated with a number of different pathways involved in the disease development^{200,201}.

1.4.1 Oxidative stress

Oxidative stress, a condition where the balance of reactive oxygen (ROS) and reactive nitrogen species (RNS) to antioxidants is in favour of ROS/RNS, is one of the causes associated with many neurodegenerative diseases. ROS, such as superoxide ($O_2^{\bullet-}$), hydrogen peroxide (H_2O_2) and hydroxyl radical (OH^{\bullet}) are generated during normal aerobic respiration of the cells. Other sources of oxidants are bacteria or virus infected cells, which are destroyed by phagocytosis, generation of by-products in peroxisomes (lipid and fatty acid degradation) as well as by-products generated by cytochrome P450 (enzyme responsible for metabolism of many medications (phase1))¹⁹³.

It is well known, that the production of ROS increases with age, whilst some of the endogenous defence mechanisms can decrease. If the balance between ROS and antioxidants is disturbed, the excessive amounts of ROS will damage the cells, by protein oxidation, DNA/RNA strand breakage, lipid peroxidation or the formation of advanced glycosylation end-products. These changes in the body with increased age lead to the aging phenotype that relates to the neurodegenerative disease. However, it is important to remember, that under normal conditions, a balance slightly on the pro-oxidant side (Figure 1.26) is optimal for essential cellular processes, because ROS fulfil an important regulatory role, affecting a variety of cellular processes e.g. proliferation, metabolism, differentiation, apoptosis, antioxidant and anti-inflammatory responses, iron homeostasis as well as the adaptive stress response of cells⁵⁴. Therefore, the antioxidant defence system should minimize the levels of harmful ROS, while enabling enough ROS to remain in the cell²⁰².

The Potential Application of Rapeseed Pomace Extracts in the Prevention and Treatment of Neurodegenerative Diseases

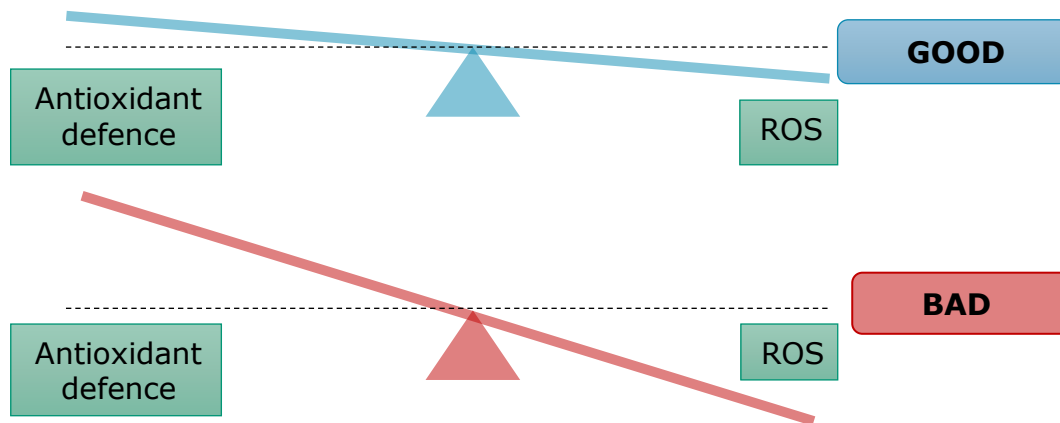


Figure 1.26| Difference between the normal and the disease state of oxidative stress balance

adapted from Poljsak et al.²⁰² as presented in Pohl and Kong Thoo Lin²⁰³

Redox dysregulation can be caused by the ineffectiveness of the endogenous antioxidant system to handle an increase in the production of free radicals (e.g. disease, mitochondrial dysfunction, exposure to environmental factors) or because of a decreased effectivity of the endogenous antioxidant system itself. The additional stress that relates damage to biological molecules can lead to a rapid cell death, which if occurring in the brain, this will result in neurodegeneration^{192,204}.

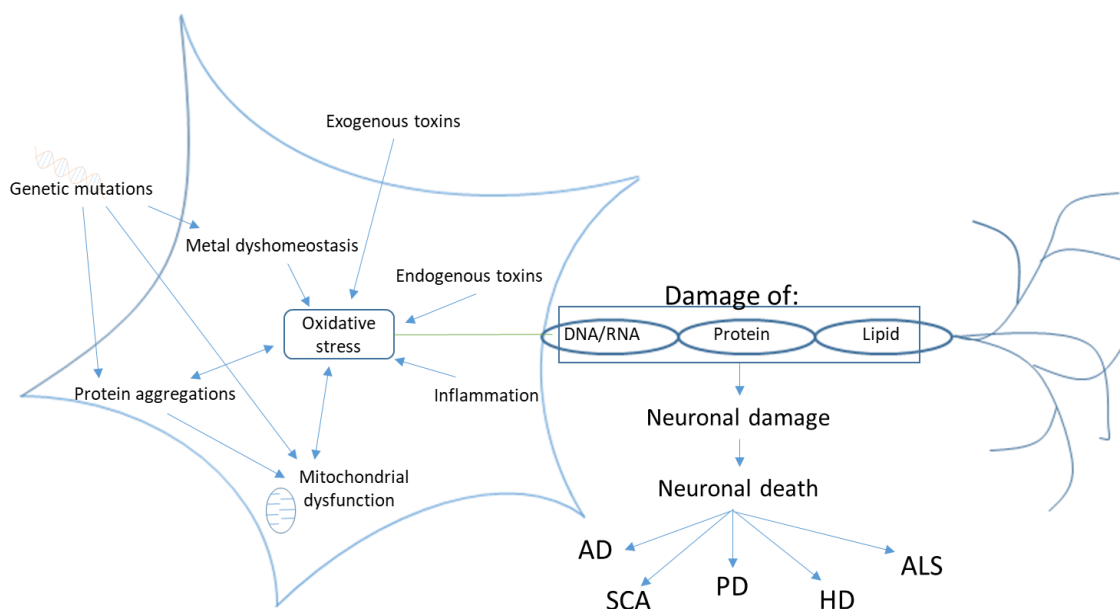


Figure 1.27| Causes of oxidative stress in neurodegeneration

adapted from^{205,206} as presented in Pohl and Kong Thoo Lin²⁰³

In addition, inflammation, protein aggregations (e.g. amyloid in AD) as well as excessive presence of metal ions such as iron (Fe^{2+}) and copper (Cu^{2+}) can lead to oxidative stress (Figure 1.27)^{205,206}. ROS can damage cell components

like DNA/RNA, proteins and lipids. DNA damage can lead to mutations and possibly cancer, if the damage cannot be reversed by DNA repair mechanisms in time. Damage to the lipids in the cell can result in decline in physiological function and cell death, whereas protein damage can e.g. cause enzyme inhibition, denaturation or protein degradation, all of which cause a disruption of regular cellular mechanisms which can lead to cell death/neurodegeneration⁵⁴. In general, eukaryotic cells control reactive compounds through an elaborate detoxification system in which lipophilic molecules are solubilized (cytochrome P450; phase 1), thereafter, reactive species, including ROS, and products of the phase 1 system are inactivated (phase 2) and can then be transported out of the cell (phase 3)²⁰⁷.

1.4.2 Antioxidants to counteract oxidative stress

Antioxidant molecules are those that can prevent the oxidation of other molecules i.e. biomolecules (DNA/RNA, proteins or lipids) in the human body. Generally, the human body has its own in-built antioxidant system (Figure 1.28), which ought to keep a balance between the production of ROS and the antioxidants defence system. Keeping this biological equilibrium is especially important for neurons. Due to their very high oxygen consumption, long life time and the additional formation of reactive nitrogen species and the prominent role of nitric oxide in the signalling processes, neuronal cells are even more susceptible to oxidative stress^{192,193,208}. The natural human antioxidant system can be divided in two groups, enzymatic and non-enzymatic¹⁹³ (Figure 1.28).

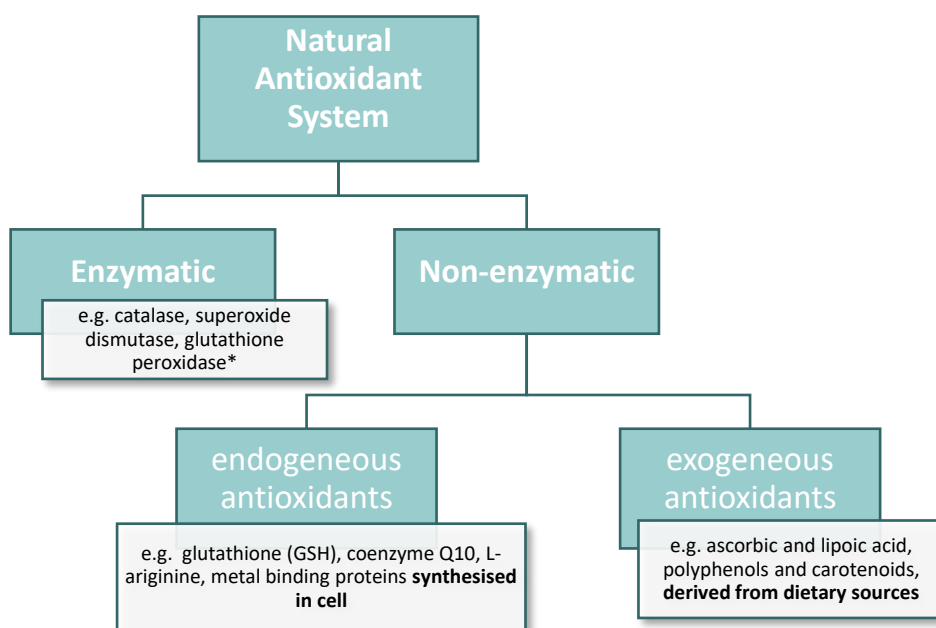


Figure 1.28| Natural antioxidants categorised with examples

*adapted from^{54,193,209,210}; * further detailed in Table 1.5*

A number of the important enzymatic antioxidants and their functions are presented in Table 1.5. In addition to the enzymatic anti-oxidants, the body also produces non-enzymatic antioxidants. These can also be called metabolic antioxidants (endogenous), that are produced by metabolism in the body, such as α -lipoic acid, metal binding proteins (e.g. ferritin), glutathione (GSH), L-arginine, coenzyme Q10, melatonin and uric acid all of which are summarized by Mirończuk-Chodakowska *et al.*²¹¹.

Table 1.5|Cytoprotective enzymes and their antioxidant function⁵⁴

Enzyme/ Protein	Function
<i>Catalase (CAT)</i>	Elimination of H ₂ O ₂
<i>Glutathione peroxidase (GPx)</i>	Elimination of H ₂ O ₂
<i>Glutathione reductase (GR)</i>	Reduces glutathione disulfide to the sulfhydryl form glutathione, which is an important cellular antioxidant
<i>Glutathione S-transferase (GST)</i>	Phase 2 enzyme (glutathionylation)
<i>Heme oxygenase-1 (HO-1)</i>	Heme catabolism, stress response
<i>Superoxide dismutase (SOD)</i>	Elimination of superoxide radical
<i>Thioredoxin (TXN)</i>	Cysteine thiol-disulfide exchange
<i>Thioredoxin reductase (TrxRs)</i>	Reduction of oxidants and oxidized thiols

In addition to endogenous antioxidants the body also receives exogenous antioxidants e.g. ascorbic acid (vitamin C), tocopherols (vitamin E) and phenolics through dietary sources. The latter are the focus of this project (Figure 1.28, p.56). When the endogenous antioxidant system is not functioning well enough, an increased amount of exogenous antioxidants could reduce the cumulative effect of oxidative stress²⁰⁹, and hence prevent oxidative cell damage and neuron loss. Sources of exogenous antioxidants can either be synthetic or natural. There are a large variety of synthetic antioxidant compounds previously discussed by Augustyniak *et al.*²¹⁰ and Carocho and Ferreira²¹². However, these synthetic antioxidants are sometimes associated with a negative reputation e.g. toxicity²¹². For that reason, in most antioxidants studies nowadays, compounds from natural sources are employed. One source of natural antioxidants is in the human diet; especially plant products provide a good source of plant secondary metabolites of which many have previously demonstrated positive antioxidant activities *in vitro*²¹³.

1.4.3 Exogenous antioxidants - natural products: direct and indirect antioxidant activity

In drug discovery pipelines, natural products (mostly plant sources) have always been a rich source of antioxidant compounds (1.1 Natural products for medicinal use p.2 ff.) Even in the case of synthetic derivatives plant metabolites can be an inspiration for the drug development process²¹⁴. Extracts from plants, animals, microbes and minerals were the only medication in hand before the 20th century and are still widely used in Asia⁶. In the last two decades however their use had decreased, due to technical barriers for screening natural products in high-throughput assays for specific molecular targets and with issues associated with the synthesis of natural compounds for the pharmaceutical industry²¹⁵ as well as advances in metagenomics and combinatorial chemistry²¹⁶. However, their importance has risen again in recent years. This is due to improved fractionation techniques and advanced NMR techniques for structural elucidation as well as profiling and isolation techniques such as HPLC-MS/MS, high-resolution Fourier-transform mass spectrometry and photo-diode arrays for metabolomics; the use of natural extracts has become more attractive again^{203,215}.

Antioxidant activity detected in plant extracts or isolated compounds are mostly due to secondary metabolites, which occur in plants in high levels of structural diversity and number (1.1.2 Secondary metabolites, p.5 ff.). Although some secondary plant metabolites are thought to have disease-protecting properties *in vivo*, they are non-essential nutrients for humans. Phytochemicals from plants were shown to exhibit different biological activities, such as anti-inflammatory^{9,76,217,218}, anti-microbial^{83,219}, anti-carcinogenic^{219,220} and anti-diabetic properties^{10,221}. Some of which, are due to the regulation of several cellular molecular pathways²²². Hence, the *in vitro* and *in vivo* effects of phytochemicals have been shown intense interest as testified in the literature, including their ability to treat and prevent neurodegeneration^{6,10,83,203,223}.

Exogenous antioxidants can be further separated into direct and indirect antioxidants, based on their mode of action. Direct antioxidants on the one hand are compounds that are redox active and can directly scavenge ROS²²⁴.

Some well-known exogenous antioxidants are e.g. ascorbate (mineral salts of ascorbic acid), tocopherols as well as phenolics⁵⁴. These direct antioxidants are short-lived because they are either consumed or chemically modified during the process of their redox action. To keep the system in balance, these direct antioxidants need to be replenished or regenerated²²⁴. The number of secondary metabolites in plants with direct antioxidant activity is huge, including phenolics (phenolic acids, flavonoids, anthocyanins, coumarins lignans and stilbenes (Figure 1.6, p.10), carotenoids (xanthophylls and carotenes) and vitamins (vitamin E and C)^{225,226}.

Indirect antioxidants on the other hand are not always redox active. Their mode of action is the activation of antioxidant regulatory pathways (e.g. Kelch-like ECH-associated protein 1- nuclear factor erythroid 2-related factor 2- antioxidant response element (Keap1-Nrf2-ARE))^{54,227}. Under normal circumstances Nrf2 is bound to Keap1 for maintaining normal (inactive) levels of Nrf2 and degraded *via* proteasome if not needed. However, compounds with e.g. an α,β -unsaturated carbonyl group (quercetin)⁵⁴ or an isocyanate group (sulforaphane)²²⁸, which are highly reactive towards nucleophiles (electron donator), can be inducers of cytoprotective proteins (Figure 1.29). The reactive protein (e.g. Keap1 with cysteine thiols) within the cell act as nucleophile in the addition reaction. Through a nucleophilic attack of the thiol group by e.g. sulforaphane, a covalent bond can be formed and so activate the Keap1-Nrf2-ARE regulatory pathway (Figure 1.29)⁵⁴. This activation also occurs on the impact of oxidative or electrophilic stress (ROS)²²⁹. Once released Nrf2 moves into the nucleus to bind the ARE in the DNA, which upregulates the transcription of ARE-responsive genes i.e. a number of antioxidant and phase 2 detoxification enzymes, e.g. NAD(P)H:quinone acceptor oxidoreductases 1 (NQO1), heme oxygenase 1 (HO-1), catalase (CAT), glutathione peroxidase (GPx) and glutathione S-transferases (GSTs)²³⁰.

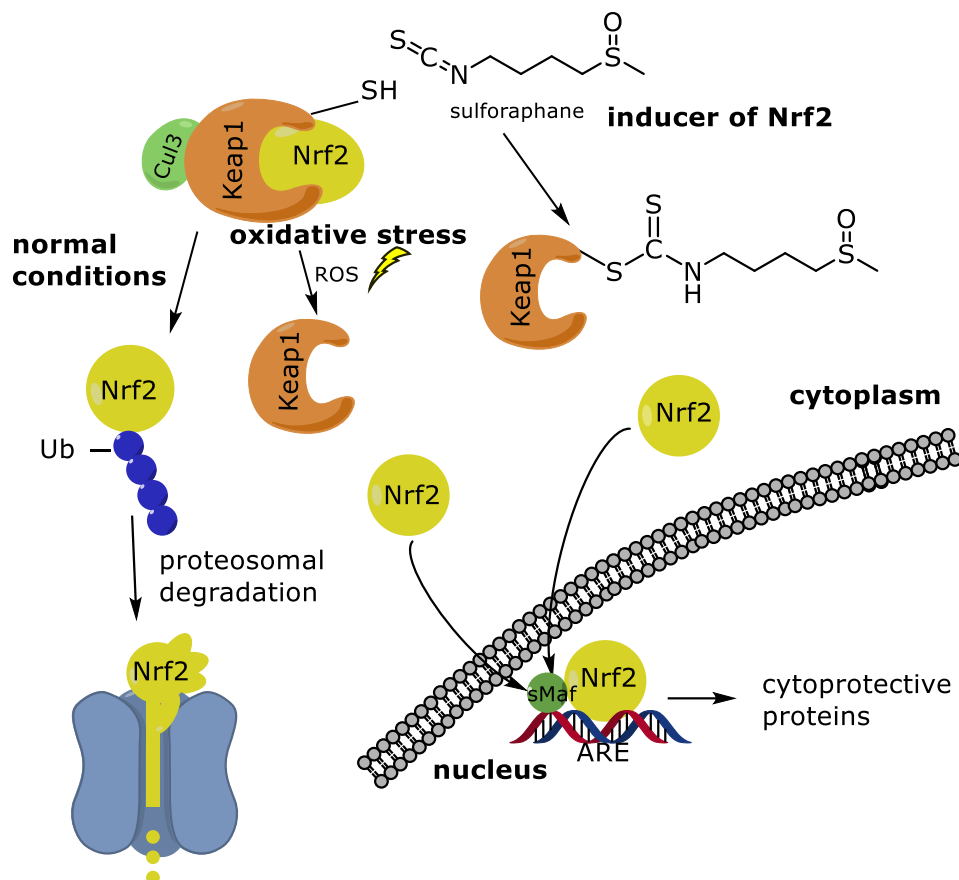


Figure 1.29| Activation of Nrf2-Keap1 pathway
via oxidative stress and indirect antioxidant sulforaphane, adapted from^{54,228}

Sulforaphane and quercetin are not the only natural Nrf2-Keap1 pathway activator, also other compounds such as resveratrol (grape), curcumin (turmeric), naringenin, ferulic acid (cabbage) and diallyl sulphide (garlic) can induce the pathway (concentration dependent)²³¹. The cytoprotective proteins (catalysts) induced during this process are not consumed during their reactions with ROS and have a longer half-life than direct antioxidants. This means they do not need to be replenished as quickly as direct antioxidants²²⁷. That is why inducers for these pathways, which leads to the upregulation of genes for the production of these cytoprotective/detoxification proteins play an important role in the bodies protection from ROS⁵⁴.

In addition, there are a few other antioxidants, that are neither direct nor indirect antioxidants in the way described above e.g. metal chelators. Through their action the production of radicals can be inhibited due to a

decreased availability of redox active metals²³². Antioxidant-based therapies or MJD/SCA3 have been scarcely researched, however the use of natural antioxidants has been shown more interest in AD and PD. Table 1.6 (p.62), highlights just a few of natural antioxidant extracts/compounds, which have shown neuroprotective properties in *in vitro* and *in vivo* models for those three diseases. Additional natural products with promising effects in neurodegeneration studies will be presented throughout the following chapters.

This chapter gave an introduction on the main topics covered during this research, followed by the overall aim of the project. In the end of the introductions, provided for each of the following four experimental chapters, the objectives to achieve this aim will be further discussed.

Table 1.6| Plant, plant products and by-products and their preventative/medicinal properties in neurodegeneration

		Disease/ condition	Substance/plant	Outcome	Ref.
Cell culture	SH-SY5Y	Oxidative stress	Scutellaria baicalensis extracts	- radical scavenging and antioxidative activity - nitric oxide and lipid peroxidation inhibition - protection against H ₂ O ₂ -induced cell injury	233,234
		Neurodegeneration in general	Vanillin	- attenuated rotenone induced mitochondrial dysfunction, ROS generation, oxidative stress, and apoptosis	235
	Primary human neurons	PD	Pomegranate Juice Extracts	- ameliorate MPTP-induced neurotoxicity	236
	SK-N-SH-MJD78	MJD/SCA3	Caffeic Acid and Resveratrol	- decreased reactive oxygen species (ROS), mutant ataxin-3 and apoptosis and increased autophagy in pro-oxidant tert-butyl hydroperoxide (tBH)-treated cells	237
Model Organism	<i>C. elegans</i>	AD	Ginkgo biloba Extract EGb 761	- alleviates A β -induced pathological behaviors - inhibits A β oligomerization and A deposits (not by reducing oxidative stress) - attenuated the basal as well as the induced levels of H ₂ O ₂ -related reactive oxygen species	64,65
		AD, aging	Tea Seed Pomace (<i>Camellia tenuifolia</i>)	- decreased intracellular reactive oxygen species - prolonged lifespan - reduced amyloid- β (A β) toxicity in transgenic <i>C. elegans</i> expressing human A β	238
		Aging, oxidative stress	Green Tea (epigallocatechin gallate)	- EGCG decreased the formation of lipofuscin, an aging related pigment - EGCG reduced beta amyloid (A?) deposits and inhibited A β oligomerization	239
	<i>Drosophila</i>	MJD/SCA3	Caffeic Acid and Resveratrol	- improved survival and locomotor activity and decreased mutant ataxin-3 and ROS levels in tBH-treated SCA3 <i>Drosophila</i>	237

		PD	Natural antioxidants of <i>Decalepis Hamiltonii</i>	<ul style="list-style-type: none"> - significantly improved climbing ability and circadian rhythm of locomotor activity - reduced levels of ROS and LPO and enhanced catalase (CAT) and superoxide dismutase (SOD) activity 	240
	mice	AD, dementia	Sinapic acid, Sodium sinapate	<ul style="list-style-type: none"> - rescued neuronal cell death and attenuated the increase of iNOS expression, glial cell activations and nitrotyrosine expressions induced by Aβ1-42 protein - attenuated memory impairment - cerebral protective and cognition-improving effects 	241,242
		AD	Grape seed polyphenol extract	<ul style="list-style-type: none"> - attenuated the development of tau neuropathology in a TMHT mouse model of AD through mechanisms associated with attenuation of extracellular signal-receptor kinase 1/2 signaling in the brain - interference with the assembly of tau peptides into neurotoxic aggregates 	67
	rats	PD	Ferulic acid	<ul style="list-style-type: none"> - rescued dopamine neurons in substantia nigra pars compacta area and nerve terminals in the striatum from the rotenone insult - restored antioxidant enzymes, prevented depletion of glutathione, and inhibited lipid peroxidation - attenuation of microglial and astrocytic activation 	243

1.5 Overall Aim and thesis structure

The overall aim of this study was to determine the potential use of the by-product RSP, obtained after edible rapeseed oil production in Scotland, for the treatment or prevention of neurodegenerative disease *in vitro* and *in vivo* models.

To achieve the aim several objectives were set out, leading to the following four chapters of this thesis:

Chapter	Title
2	Secondary Metabolite Composition and Antioxidant Activity of Rapeseed Pomace Extracts – comparison between 2 harvest years and 3 extraction techniques
3	Phytochemical Characterisation and Neuroprotective Properties of RSP Extract <i>in vitro</i> Phytochemical Characterisation and Neuroprotective Properties of RSP Extract
4	Cell Protective Properties of RSP Extract in SH-SY5Y Neuroblastoma Cell Line
5	An <i>in vivo</i> Study of the Antioxidant and Neuroprotective Properties of RSP Extract in <i>C. elegans</i> Nematode Models

Each chapter will have its own introduction, including the objectives and general information covering techniques as well as background information necessary for the chapter. Materials and methods, results and discussion as well as a conclusion, summarizing the found results in context and leading to the following chapter, will follow the introduction. All the results obtained will be drawn together in an overall conclusion at the end of the thesis (Chapter 6). References (Chapter 7) and supplementary data (Appendices) follow there after.

2 SECONDARY METABOLITE COMPOSITION AND ANTIOXIDANT ACTIVITY OF RAPESEED POMACE EXTRACTS – COMPARISON BETWEEN 2 HARVEST YEARS AND 3 EXTRACTION TECHNIQUES

Contents

2.1 Introduction	66
2.1.1 Extraction	
2.1.2 Determination of secondary metabolites in extracts	
2.1.3 Antioxidant/Reducing capacity assays	
2.1.4 Objectives	
2.2 Materials and Methods	88
2.2.1 Chemicals and Equipment	
2.2.2 Methods	
2.3 Results and Discussion	98
2.3.1 Secondary metabolite composition of RSP from free, alkali-labile and acid-labile fractions	
2.3.2 Comparison of SOX, UAE and ASE extraction techniques	
2.3.3 Folin-Ciocalteu (FC) assay	
2.3.4 HPLC-MS/MS	
2.3.5 FRAP assay	
2.3.6 DPPH assay	
2.3.7 Correlation of the data from FC, FRAP and DPPH	
2.3.8 Partial least squares analysis of data from the DPPH, FC and FRAP	
2.3.9 ORAC assay	
2.3.10 Partial least squares analysis (ORAC)	
2.3.11 Determination of antioxidant activity of single compounds within the extract as well as their mixtures	
2.4 Conclusion/Future work	131

This chapter will cover the analysis of free and bound secondary metabolites of the RSP as well as RSP extracts obtained via three different extraction techniques. All three extractions were done using two harvest years of rapeseed (2012 and 2014). These extracts were compared regarding their secondary metabolite composition, antioxidant and radical scavenging activity as well as their ease of handling, to select a viable extraction technique for further in vitro and in vivo experiments.

2.1 Introduction

2.1.1 Extraction

The use of plants and their secondary metabolites has gained much interest over the last few years (as described in chapter 1 Introduction"). However, to determine their potential activity, their active ingredients are required to be extracted from the starting material. This can then be followed by their chemical characterisation and assessment of their *in vitro* and *in vivo* biological activities. Extraction is necessary as most activity experiments are undertaken in solution and applied to multi well formats; whole plant leaves, stems, seeds or by-products are difficult to assess. The use of organic solvents is the most popular process of extraction from solid matter. Extraction also leads to the concentration of the compounds in question, opening the possibilities to test the extract from high to very low concentrations in all assays. To extract the secondary metabolites of interest it is important to pick the right extraction technique and conditions, as well as extraction solvent/solvents (2.1.1.2 Extraction solvents, p.69/2.1.1.3 Extraction technique, p.70) for the sample matrix²⁴⁴. Parameters such as solvent polarity, temperature and pressure of the solvent can influence the extracts composition. There is not one general extraction technique for all plant material; hence, the experimental set up is unique for each project.

2.1.1.1 Pre- extraction preparations

Before the start of extraction, the pre-extraction preparations of samples need to be considered. Pre-extraction preparations are important, to preserve the molecules of interest within the plant sample²⁴⁵.

A. Dry or fresh samples

Plant material can be utilized either fresh or dried, both having certain advantages and disadvantages. Analysing fresh samples gives the advantage of being representative for what is in the plant when consumed immediately as fresh product. However, being of organic content, plant material will not stay fresh for long and would need to be analysed within a few hours of harvesting²⁴⁶. In comparison, when drying or freezing samples, they can be preserved for much longer without affecting the contents of the sample.

Dry materials allow the expression of components from the sample on a dry mass basis and thus remove the problems associated with water content in crude samples²⁴⁷. There are a number of drying processes available and these include air-, microwave-, oven- and freeze-drying (lyophilisation) all of which are described in more detail in a review by Azwanida²⁴⁵. Using different drying techniques and temperatures can lead to materials with different characteristics, which might affect the subsequent extraction process²⁴⁸. In general, the drying process can change the plant composition, and consequently does not present a reliable comparison of the plants initial composition. However, since dried samples can nowadays be effectively stored, they are used more regularly than fresh ones. Vongsak *et al.*²⁴⁹ studied different extraction techniques such as decoction and maceration on fresh and dry samples of drumstick tree (*Moringa oleifera*) leaves. Their findings showed no significant differences in phenolic contents, between the fresh and dried samples when extracting using decoction. In general, their results show that the extraction technique and solvent composition are more important than the decision on whether to use fresh or dry samples. In contrast, a study by Vaidya *et al.*²⁵⁰, on the "Antioxidant Capacity of Fresh and Dry Leaf Extracts of Sixteen Scutellaria Species" demonstrated significant differences of total polyphenol content, Trolox equivalent antioxidant capacity (TEAC) as well as total flavonoid content. The found differences are not consistently better for one or the other, the outcome was dependent on the species as well as the analysis method.

Mulinacci *et al.*²⁵¹ published a paper on the effects of pre-extraction preparations, comparing fresh rosemary sample to frozen, freeze-dried and room temperature dried samples. Freezing of the fresh material was not appropriate for rosemary, due to a loss of rosmarinic acid. Freeze-drying gave better results than drying at room temperature, for total flavonoids, terpenoids and phenols content. Overall, fresh samples still showed the highest results for all the analysed characteristics.

The deciding factor on whether to use dried, frozen or fresh samples depends on the experimental procedure as well as the project length, the questions of interest as well as the source material available for analysis.

B. Whole plant versus ground samples


As part of the extraction process one has to decide whether to use whole plant parts or ground/powdered samples. Grinding can be accomplished with a conventional pestle and mortar or electric grinders and mills. By grinding the sample, the particle size is lowered, resulting in an increased surface area between sample and extraction solvent. Theoretically, the smaller the particle size, the bigger the surface contact area, the better the extraction efficiency due to a better mass transfer of active particles from plant material to solvent²⁵². However, in practice this does not always seem to be the case. In a study by Mankanjuola²⁵³ for example it was shown, that for the aqueous extracts the smallest particle size always showed the highest antioxidant properties. However, for both ethanoic and aqueous ethanoic extracts no single particle size (0.425, 0.710 and 1.180 mm) was able to show significant different results in any of the antioxidant assays²⁵³. This led to the conclusion, that (i) the optimal particle size depends on the solvent; (ii) the optimal particle size depends on the antioxidant properties measured (assay type) and (iii) not always the smallest particle size yields the best antioxidant properties. In a different study, by Kossah *et al.*²⁵⁴, it was shown, that with decreasing particle size, the extracted phenolic content increased. However, no significant difference was observed between the smallest particle sizes 0.5 and 1 mm. This leads to the conclusion that the difference between particle size, below a certain size (such as 1 mm), potentially has a smaller or no impact on the extraction efficiency. Although grinding seems to positively affect the extraction efficiency in most cases, it also adds an additional step to the process, costing time and money. Khan *et al.*²⁵⁵ provide one example, where a decreased particle size reduced the extraction efficacy of polyphenols from orange peel. A range of five particle sizes (0.5, 1.0, 1.5, 2.0 and 2.5 cm²) was tested and polyphenol yields of 3.44%, 3.65%, 4.32%, 4.41% and 4.38% were found respectively. In this case, the highest concentration of polyphenols was reached with particles of 2.0 cm². One suggested explanation for this observation was that smaller particle sizes of orange peel float at the top of the extraction solvent, leading to less efficient extraction. Considering the examples provided here, the decision on whether to grind

samples and if so to which size must be made with economic reasoning and considering the sample characteristics and the extraction technique.

2.1.1.2 Extraction solvents

A very important factor to consider for the extraction of phytochemicals apart from the extraction technique (2.1.1.3 Extraction technique p.70) is the solvent. There is a large number of solvents available for the different extraction techniques. The choice on what solvent to use depends on the following factors: (i) used extraction technique, (ii) compounds of interest, (iii) environmental impact, (iv) costs, (v) safety and (vi) ease of use, e.g. low boiling point for solvent removal. The table below provides an overview of which liquid solvents to use, when interested in a particular group of secondary metabolites.

Table 2.1| Solvents used for extraction of specific plant secondary metabolite groups (adapted from²⁵⁶⁻²⁵⁸)

solvent	Water	Methanol	Ethanol	Acetone	Chloroform	Ether
Extraction of:	Tannins Saponins Terpenoids Lectins Poly-peptides Antho-cyanins	Anthocyanin Terpenoids Saponins Tannins Flavones Polyphenols Quassinoids	Tannins Polyphenols Flavonol Terpenoids Alkaloids Poly-acetylenes Sterols Ethanol	Flavonoids	Terpenoids Flavonoids	Alkaloids Terpenoids coumarins Fatty acids
polarity	polar  non-polar					

By mixing two or more of the solvents, presented above, for extraction, different compounds can be extracted. In a recent study by Ngo²⁵⁹, four different pure solvents (acetone, methanol, ethanol and water) together with water mixtures (50% v/v) were used for extraction. Mixtures of the solvents showed higher results for most of the measured parameters e.g. total phenolics and flavonoids, radical scavenging activity, ferric ion reducing capacity and cupric reducing antioxidant capacity.

Apart from the solvent or mixture of solvent of choice, also the solid to solvent ratio plays a role in the extraction efficiency. In a study by Wong *et al.*²⁶¹ it was shown, that a 1:5 solid to liquid ratio showed lower results in the activity assays (Folin-Ciocalteu(FC), total flavonoid content (TFC), ABTS and DPPH)

than for example a 1:15 or 1:20 ratio. The difference between the 1:15 and the 1:20 ratio only showed significant differences for one of the assays (FC). It can be assumed that a further increase of the ratio would show less of an effect in extraction efficiency. Also in Radojković *et al.*²⁴⁴, a higher solvent to sample mixture showed better results, which is consistent with the mass transfer principle. The transfer of compounds into the solvent is dependent on a concentration gradient between solid and solvent, meaning higher solvent to solid ratio shows better extraction.

2.1.1.3 Extraction technique

Extraction is the process of separating compounds of interest from a solid or liquid starting material using selected individual or a mixture of solvents. The extraction of phytochemicals from plant and plant by-products has always been of interest, especially in Asia, where herbal remedies have commonly been used throughout the centuries. Also, in the western world, the interest in extracting active compounds from plants and plant by-products has seen a significant increase over the last few years. Extraction is the process used to separate the soluble metabolites from the plants. The procedure leaves behind the insoluble residue (cellular marc)^{245,252}. The plant extracts can contain various secondary plant metabolites such as phenolics, flavonoids, alkaloids, glycosides and terpenes. Products obtained through extraction of for example medicinal plants are usually impure liquids, semisolids or powders (depending on post-extraction procedures). They can be used for oral administration or external application. Some of the common extraction techniques are explained briefly in Table A1 (appendix, p.424 ff.), including some advantages and disadvantages as well as examples of papers where they were used for the extraction of plant metabolites.

For the extraction of RSP in this project, three different extraction techniques, Soxhlet (SOX)-, ultrasonic assisted (UAE)- and accelerated solvent (ASE) extraction were initially evaluated and the extracts compared *in vitro*. These three extraction techniques are described in more detail below.

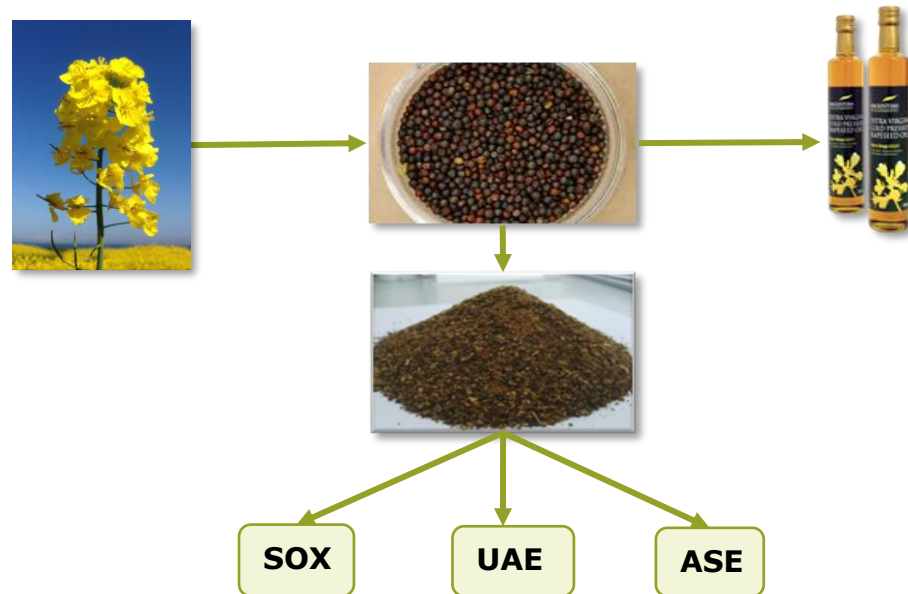


Figure 2.1 | Extraction of phytochemicals from RSP

A. Soxhlet Extraction (SOX)

One of the working extracts was obtained *via* automated Soxhlet extraction, a technique often used for lipid extractions^{262,263}. However, this user friendly method of extraction has previously also been used for the extraction of phytochemicals^{264,265}. For automated Soxhlet extraction, the sample is weighed into a cellulose thimble, which is inserted into a metal wire holder and then introduced to the solvent in the extraction beaker. In most automated systems a number of these beakers (2-6) can be run in the same machine and sometimes a number of machines can be run at the same time all managed by one controller (multistat)²⁶⁶. The extraction starts with the heating of the solvent to a set temperature (hot extraction, see Figure 2.2 A, p.72).

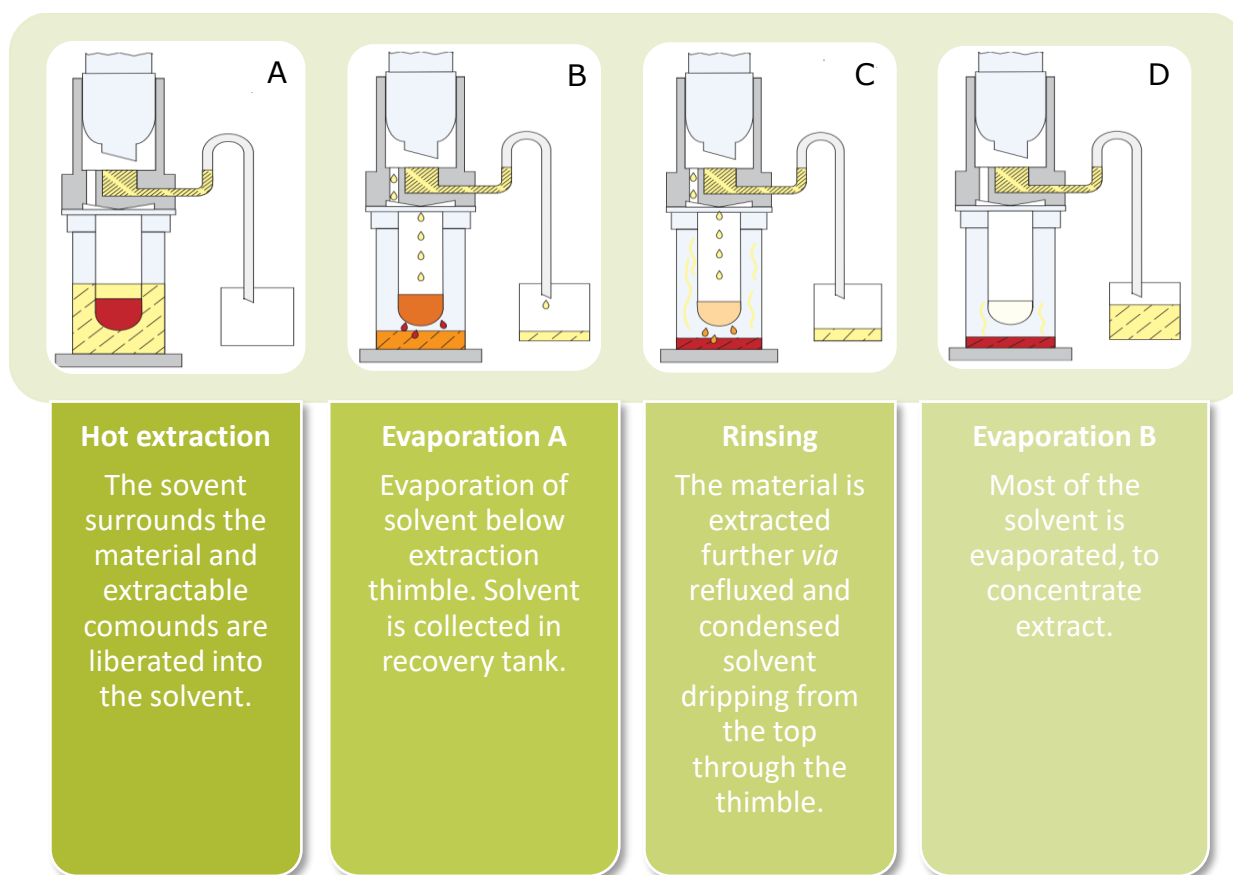


Figure 2.2| Automated Soxhlet extraction apparatus

*adapted from Gerhardt instruction manual*²⁶⁶

The cellulose thimble lets the solvent pass through, and the sample is in direct contact with the solvent throughout the whole extraction time (Figure 2.2 A). The extraction can be set to any desired time between 0 and 99 minutes²⁶⁶. Leakage of the sample into the beaker is prevented by using glass wool in the top of the thimble. After a period of extraction, the first evaporation process starts, to allow the solvent, to reach levels below the cellulose thimble. For this, the outlet at the top of the beaker is opened, to let the solvent evaporate. The evaporated solvent is cooled down and then collected in a recovery tank in the back (Figure 2.2 B). This makes it possible to recycle the solvent for a considerably lower environmental impact. After the solvent has evaporated below the level of the thimble/sample, the rinsing process starts, by closing the outlet at the top. This way the evaporating solvent condenses just above the beaker and can drop back down through the sample and rinse out further compounds of interest with the condensed solvent (Figure 2.2 C). The rinsing time can also be set to any desired time between 0-99 minutes²⁶⁶. There after the final evaporation takes place to lower the

amount of solvent in the extract, to shorten the post-extraction preparations needed (Figure 2.2 D). After the extraction finished, necessary modifications can be applied during post –extraction processing (2.1.1.4).

Previously extractions of the rapeseed pomace involving two step extractions with petroleum ether (40-60°C) and an ethanol/water (95/5%, v/v) mixture showed high levels of phenolic compounds. In addition those extracts exhibited radical scavenging activity, ferric ion reducing antioxidant power and partial rescue of a MJD *C. elegans* disease strain^{79,267}. Due to these positive results, the same extraction method will be undertaken, and the extracts tested to confirm the previously observed results.

B. Ultrasound Assisted Extraction (UAE)

An additional extraction method used is conventional solvent liquid extraction, assisted by ultra sound (UAE) as previously undertaken by for example Londoño-Londoño *et al.* and Khan *et al.*^{255,268}. When using UAE, two different ultrasound options can be used, either ultrasonic baths (indirect sonication) or ultrasound probes. Ultrasonic baths are common laboratory equipment and were used for this project. For the extraction process, the sample and solvent are mixed in glass jars and immersed in the ultrasound bath for the desired time. The solvent is in constant contact with the sample. When the ultrasound passes through the solvent, small vacuum filled bubbles, also called cavitations are created. These can implode with further rarefaction and compression cycles (Figure 2.3, p.74). When they burst an area of increased temperature and pressure is created, which improves the extraction because of the higher mass transfer^{269,270}. A review recently published in Ultrasonics Sonochemistry by Chemat *et al.*²⁷¹ provides details on recent advances on the use of UAE for food and natural products and references other papers for more detailed background literature.

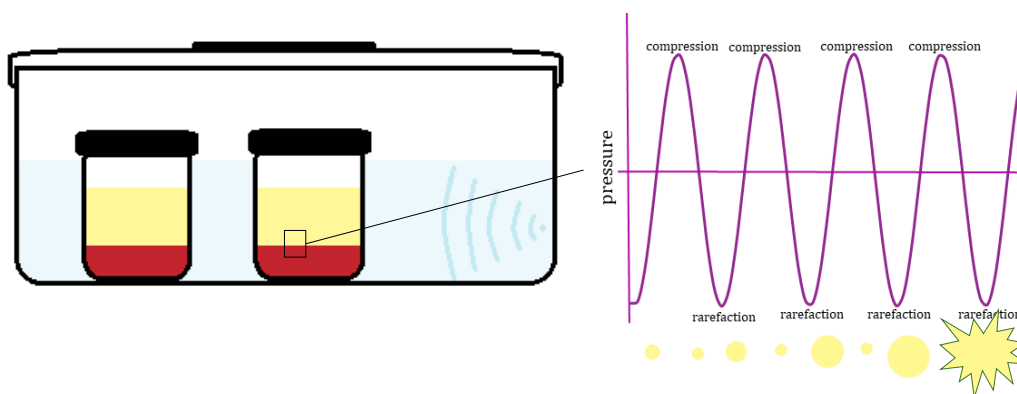


Figure 2.3| Schematic of UAE using a ultrasound water bath
description on cavitation adapted from^{272,273}

Extractions from RSP had been undertaken using UAE before with promising results. The obtained extraction product showed phenolic content, radical scavenging activity, ferric ion reducing antioxidant power as well as the partial rescue of a *C. elegans* model of MJD^{79,267}. Research published by Yu *et al.*²⁷ demonstrated the positive effect of UAE (ultrasonic probe) in the extraction of protein and polyphenols from rapeseed green biomass. Also other publications have shown successful use of UAE for plants and plant by-products^{255,274}, including rapeseed⁵².

C. Accelerated Solvent Extraction (ASE)

Both above methods use a large amount of solvent. In case of the Soxhlet extraction the sample is also heated up to the boiling point of the solvent (140°C-260°C) which might decompose some of the phytochemicals²⁷⁵. For those reasons, a third extraction method is employed for comparison purposes. Accelerated solvent extraction (ASE), also known as pressurized fluid/liquid extraction¹⁰, is an extraction technique working with smaller volumes of solvents. To avoid the use of very high temperatures, which might decompose the secondary metabolites of interest in the sample, high pressure is applied, enhancing the extraction kinetics at lower temperatures and shortening the extraction time. The equipment available allows the user to run multiple sample cells at the same time without human intervention. The solvent is pumped into the extraction cell, which is located in an oven and the extract solution collected in a separate vessel (Figure 2.4).

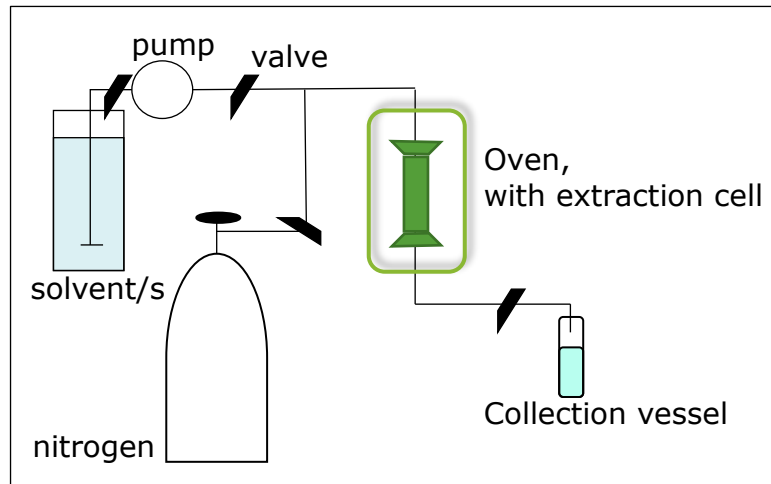


Figure 2.4| Schematic of ASE equipment

(adapted from Shahid *et al.*³⁹)

Parameter such as extraction time and cycle number, solvent mixture and temperature can be adapted. Vergara-Salinas *et al.*¹¹ successfully used ASE for the extraction of phenolics from deodorized thyme (*Thymus vulgaris*). Their results showed the best phenolics extraction was with a 5-minute extraction at 100°C, using water. However, the highest antioxidant activity was obtained with extracts from a higher temperature (200°C) and longer extraction time (30 minutes)¹¹. Similarly, Hossain *et al.*²⁷⁶ found that extracts obtained with higher extraction temperatures (129°C) exhibited better antioxidant activity than extracts from lower extraction temperatures (66°C). They also compared different mixtures of methanol (32-88%) and water as extraction solvent on three plants of the *Lamiaceae* family. Their findings showed, that for different plant species different methanol/water mixtures were optimal²⁷⁶.

2.1.1.4 Post-extraction preparations

In post extraction methodology most extracts are liquid, consisting of the extracted compounds dissolved in the utilized solvent/s. The extract solution can be analysed as it comes, as long as the solvent does not interfere with the subsequent experiments. Long-time storage of extracts in this condition however, can have a strong impact on their activity *in vitro* as well as their phenolic and anthocyanins contents as reported by Srivastava *et al.*²⁷⁷. When storing blueberry extracts in their liquid form in glass bottles, a significant decrease in phenolic and anthocyanin content and antioxidant activity trolox equivalent antioxidant capacity (TEAC) assay was found within the first

month of storage at $23\pm 1^{\circ}\text{C}$ and $35\pm 1^{\circ}\text{C}$. Even storage at temperatures of $6\pm 1^{\circ}\text{C}$ and $-20\pm 1^{\circ}\text{C}$ showed a significant decrease in phenolic and anthocyanin content after 60 days. The antioxidant activity (TEAC) was not significantly changed at -20°C ²⁷⁷. These significant changes for phenolic and anthocyanin content even at -20°C (60 days) when stored as liquid extracts must be borne in mind when planning long-term projects. Therefore, the solvent is usually evaporated using rotary evaporation and/or a vacuum drying oven. Leftover water/moisture can be evaporated by freeze-drying (lyophilisation).

Thus, a solid final product provides a material, that is easy to handle (homogeneous sample taking), more stable for storage and less prone to degradation. In a study by Maisuthisakul *et al.*²⁷⁸ the antioxidant activity of freeze dried Thai mango seed kernels was tested over a period of 0-182 days under different storage temperatures. DPPH radical scavenging as well as antioxidant efficiency decreased significantly at room ($28-32^{\circ}\text{C}$) and fridge (7°C) temperatures. The appropriate storage temperature was found to be -20°C , as the extracts activity did not change (aluminium foil packaging)²⁷⁸.

2.1.2 Determination of secondary metabolites in extracts

To determine the chemical composition of extracts several methods are available. Simple chemical reactions can be used for qualitative analysis, e.g. Mayer's and Wagner's test for the determination of alkaloid²⁷⁹, froth test for saponins²⁸⁰, Salkowski's and Libermann Buchard's test for steroids/triterpenoids²⁸¹ and the gelatine test for the presence of tannins²⁸².

For a general overview of total amounts of certain groups of secondary metabolites, UV-VIS spectrophotometric methods have successfully been used for qualitative and quantitative analysis. A few examples are detailed in Table 2.2 (p.78).

Table 2.2| UV-VIS methods for the detection of secondary metabolites in plant extracts

Secondary metabolite	UV-VIS detection			chromatography	
	specific	Chemical test/reaction chemicals used	Example, with reference	method	Example, with reference
Alkaloids	Total alkaloids	reaction between alkaloid and bromocresol green (BCG)	Chitrakadivati ²⁸³ , Sankezhen (roots of Berberis plant) ²⁸⁴	HPLC	Sankezhen (roots of Berberis plant) ²⁸⁴
Glucosinolates	Total glucosinolates	sodium tetrachloropalladate	Mustard cake (de-oiled) ²⁸⁵ , cruciferous seeds ²⁸⁶	HPLC-DAD	Rapeseed meal ¹¹⁵
Terpenoids	Total triterpenoids	vanillin-acetic solution, sulfuric acid/perchloric acid and acetic acid	<i>Jatropha curcas</i> leaves ²⁸⁷ , medicinal plants ²⁸⁸	GC-MS Fast-GC LC-MS/MS	Plant leaves (<i>Ocimum basilicum</i> and <i>Nicotiana langsdorffii</i>) ²⁸⁹ Pine ²⁹⁰ Ginko ²⁹¹
Phenolics	Total phenolics	Folin-Ciocalteu reagent (2.1.3.1 Folin-Ciocalteu- (FC) Assay)	medicinal plants ²⁸⁸ , oil cake extracts ²⁹² , Root of <i>Salacia chinensis</i> L. ²⁵⁹	HPLC/LC-MS HPLC-DAD	fruits ²⁹³ Trochuda cabbage ²⁹⁴
	Total flavonoids	NaNO ₂ , AlCl ₃ *6H ₂ O solution and NaOH	medicinal plants ²⁸⁸	LC-MS/MS	Ginko ²⁹¹
	Total anthocyanins	pH differential method (0 Total Monomeric Anthocyanin Pigment Content)	Juices, wine, food colorants ²⁹⁵ , Chilean berry extracts ²⁹⁶	HPLC-ESI-MS	Acai species ²⁷⁵

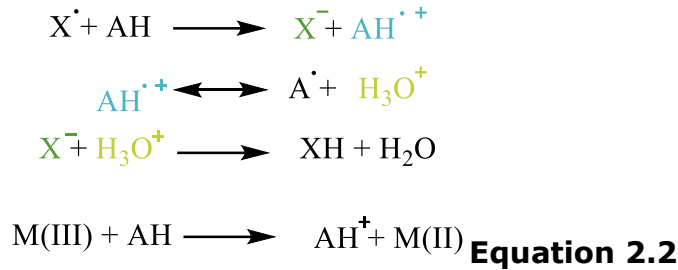
Apart from spectroscopy other methods such as indirect desorption electrospray ionization imaging mass spectrometry²⁹⁷, GC-MS²⁹⁸, thin layer chromatography (TLC) and high performance thin layer chromatography (HPTLC)²⁹⁹, infrared spectroscopy (IR)³⁰⁰, NMR²⁴⁶, capillary electrophoresis (CE)²⁸⁰ and others can be used for the isolation and determination of secondary metabolites. However, the most common method for the qualitative/quantitative determination of single secondary metabolites in plant, plant components or plant extracts are high performance liquid chromatograph (HPLC), liquid chromatography coupled to mass spectrometry (LC-MS or LC-MS/MS), gas chromatograph (GC) or gas chromatography mass spectrometry (GC-MS). Secondary profiling of different groups of secondary metabolites can be undertaken and the present metabolites can be qualified and quantified (Table 2.2).

2.1.3 Antioxidant/Reducing capacity assays

There are a number of assays available to analyse *in vitro* antioxidant/reducing capacity. These chemical assays are based on different mechanisms and hence provide distinct information on the interactions of the antioxidant and the respective ROS/RNS species created/used³⁰¹. Depending on the reaction involved, these can be broadly divided into hydrogen atom- (HAT) and electron transfer (ET) reactions as described by Huang *et al.*³⁰². As previously reported by Apak *et al.*³⁰³, HAT-based assays measure the capability of substances to quench free radicals by donation of hydrogen atoms, like demonstrated in the following reaction (Equation 2.1), where the H-atom of e.g. the phenol (Ar-OH) is transferred to a peroxy radical (ROO•).



The aryloxy radical (ArO•) formed in the reaction is stabilized and non-reactive, due to resonance, hydrogen bonds and conjugation³⁰³⁻³⁰⁵. To protect biomolecules (BioH) effectively, the antioxidants need to react faster with the free radicals than the biomolecules themselves. This mechanism of competitive reaction is reflected in HAT-based assays such as the total peroxy radical-trapping antioxidant parameter (TRAP)³⁰⁶ and the crocin bleaching³⁰⁷ assay both of which use the peroxy radical generator 2,2'-Azobis(2-amidinopropane) dihydrochloride (AAPH) as radical source. The latter measures the inhibition capacity of compounds to prevent the bleaching of crocin (natural carotenoid) by AAPH³⁰², whereas the TRAP assay employs R-phycoerythrin as fluorescence probe and analyses the lag time of fluorescence decay induced by antioxidants³⁰⁸. The oxygen radical absorbance capacity (ORAC, 2.1.3.4) assay is another example for a HAT based reaction, whereas the Folin-Ciocalteu (FC, 2.1.3.1) assay and the ferric ion reducing antioxidant power (FRAP, 2.1.3.2) assay are ET based³⁰². The latter reactions are based on the ability of antioxidants to transfer one of their electrons (e⁻) to either free radicals, carbonyls or for example metals^{232,309} (Equation 2.2)



The 2,2-diphenyl-1-picrylhydrazyl (DPPH) assay in contrast has been found to be based on both, electron and hydrogen atom transfer³¹⁰. Depending on the solvent of choice and the pH, one or the other can be favoured. Although most often it is referred to as an ET reaction³⁰². A summary of a number of common assays to determine antioxidants from natural sources is provided in Ndhlala *et al.*³¹¹, where the mechanism, advantages and disadvantages are described. None of the above *in vitro* assays can accurately reflect all the radical sources and reaction characteristics/mechanisms involved, within living organisms, alone. That is why for most studies two to four different assays are often undertaken^{90,312,313}.

Following, a brief summary and the reaction mechanism behind all four assays, used in this study, together with their advantages are explained in detail. Limitations of each technique will follow in results and discussion (2.3 Results and Discussion, p.98).

2.1.3.1 Folin-Ciocalteu- (FC) Assay

This assay, often referred to as “total phenolic assay” or “Gallic acid equivalence method”, measures the samples reducing capacity and not total phenolic content of samples. A variation of this assay was described as early as 1912 in a paper published by Folin and Denis³¹⁴. Later in 1927 Folin and Ciocalteu then described the reagent for the detection of tyrosine (containing phenol group) and tryptophan^{302,315}. As early as 1965 Singleton and Rossi described the use of Folin-Ciocalteu reagent, in favour over the original Folin-Denis reagent, for the determination of phenolics in wine samples using gallic acid as standard³¹⁶. The method was even adopted by the European Communities for the analysis of wine in 1990³¹⁷ but is also described in more recent publications³¹⁸. Although the reagent can be prepared, as described by Huang *et al.*³⁰² and the European commission^{317,318}, most often is just bought as ready to use reagent from chemical suppliers. The reagent is a mixture of

tungstate (W^{6+}) and molybdate (Mo^{6+})³¹⁹, when in contact with phenolics changes its colour from yellow to blue in an alkaline environment (sodium carbonate). It is assumed, that the molybdenum in the complex is easier to reduce and electron transfer occurs between reductants and Mo^{6+} (Figure 2.5).

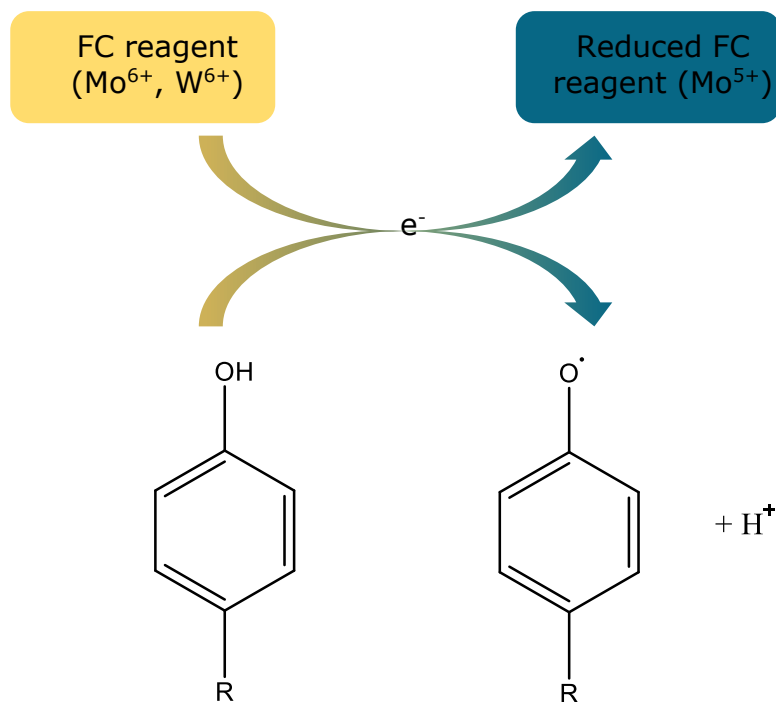


Figure 2.5| FC reagent reaction with phenolic compound

The intensity of the blue colour relates to the concentration of phenolics as described by Singleton and Rossi³¹⁶. Gallic acid is used as phenolic standard and the final results are given as mg gallic acid equivalence (GAE)/g sample or per mL of a solution/extract. The analysis is quick and does not require excessive amounts of preparations, when using prepared FC reagent directly. It is usually one of the first experiments undertaken when analysing samples of unknown phenolic composition such as plant extracts^{244,276}, fruit juice/beverages^{236,320} or extracts from plant waste/by-products^{68,113,292}.

2.1.3.2 Ferric Reducing Antioxidant Power (FRAP) assay

As with the FC assay, the FRAP assay is based on an ET reaction. The ferric salt, $Fe(III)(TPTZ)_2Cl_3$ (Figure 2.6) is the oxidant; the antioxidant provides

an electron, which leads to the reduction of Fe (III) to Fe (II), yielding an intense blue colour, which can be measured at 593 nm.

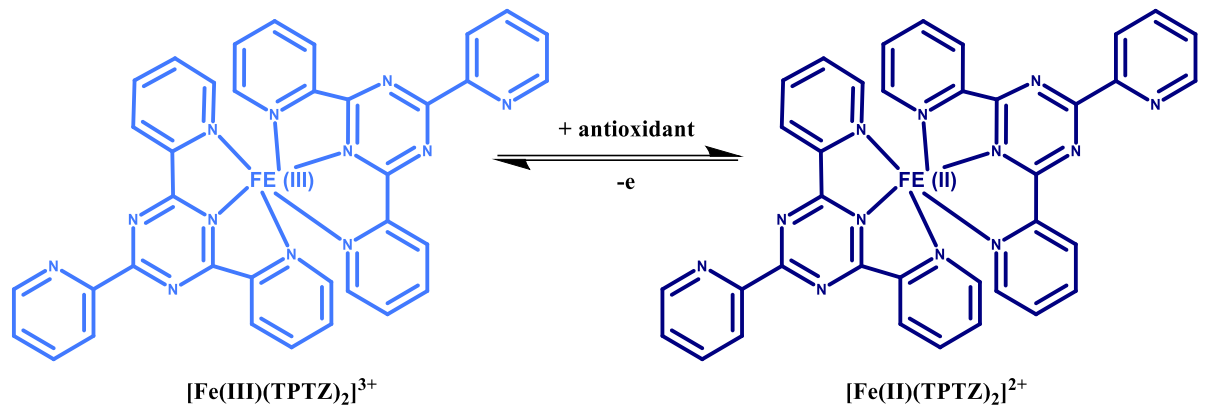


Figure 2.6 | FRAP reaction mechanism

This assay was first described by Benzie and Strain^{321,322} for the measurement of reducing power in plasma but it was quickly adapted for the determination of antioxidants in botanicals^{323,324}. The redox potential of Fe (III) salt (~ 0.7 V) is close to the one of ABTS^{•-} (~ 0.68 V) the oxidant used in an additional antioxidant assay called Trolox Equivalent Antioxidant Capacity Assay (TEAC), the only difference being the pH which they are run at. The FRAP is conducted under acidic aqueous conditions (pH 3.6), whereas the TEAC is carried out at a neutral pH. These two assays usually show good positive linear correlation^{325,326}, warranting the use of only the FRAP assay in this project. The FRAP is a rapid method for the determination of reducing power of unknown samples. Although the preparation of the FRAP reagent is slightly more time consuming than the ready to use solution in the FC assay, the assay is still quick and easily conductible with common laboratory equipment.

2.1.3.3 2,2-diphenyl-1-picrylhydrazyl (DPPH) assay

DPPH, a stable radical was first suggested for the determination of antioxidant content by Blois in 1958³²⁷, since then it has been adapted and is mostly used to determine radical scavenging activity of samples with antioxidant property. The experiment is simple and can be undertaken even in laboratories equipped with little instrumentation. As previously mentioned, the reaction (Figure 2.7, p.84) can be based on electron or hydrogen atom transfer depending on the chemical environment of the experiment, making the DPPH assay a bit more complex in determining reaction mechanisms^{310,328}.

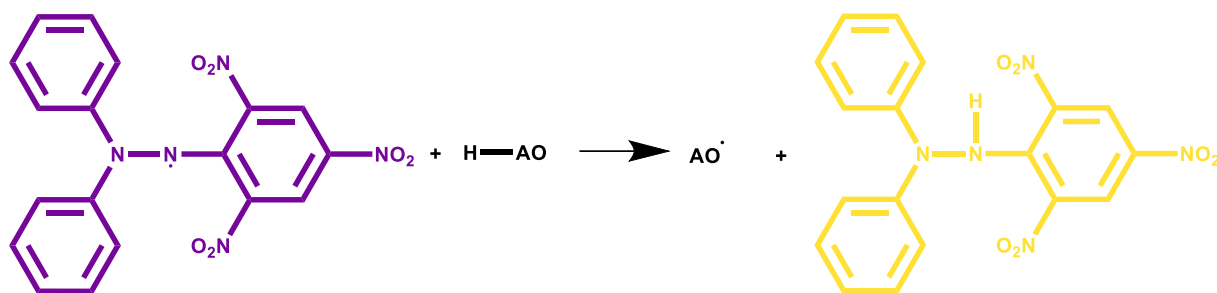


Figure 2.7| DPPH reaction with radical scavenger (H-AO)

example of HAT based reaction

Once the DPPH radical, with an unpaired valence electron at the atom of the nitrogen bridge (dissolved in methanol purple), reacts with a radical scavenging compound, it is converted into the reduced DPPH₂, resulting in a colour change from purple to yellow, as indicated in Figure 2.7. In this reaction DPPH acts as both, the radical and the probe³²⁹.

This assay has been used for a wide variety of antioxidants, such as the radical scavenging of different plant extracts^{249,330-332}, food by-products^{292,333}, beverages^{320,329} as well as single compounds^{310,328}.

2.1.3.4 ORAC

The ORAC assay is based on early work by Glazer³³⁴ and was further developed by Cao et al.³³⁵. In this assay AAPH is used to create peroxy radicals, which react with the fluorescent probe, causing oxidation of the latter, to produce a non-fluorescent product. The initial fluorescence probe introduced by Cao *et al.*³³⁵ was B-phycoerythrin (B-PE), an isolated protein from red alga (*Porphyridium cruentum*). This probe was replaced in 2001 with fluorescein, due to its advantages over B-PE, such as decreased experimental costs, less interaction with other compounds and higher stability in the absence of AAPH³⁰⁵. The kinetics of the reaction between fluorescein and AAPH (Figure 2.8) can be monitored using fluorescence spectroscopy, over a set period of time³²³.

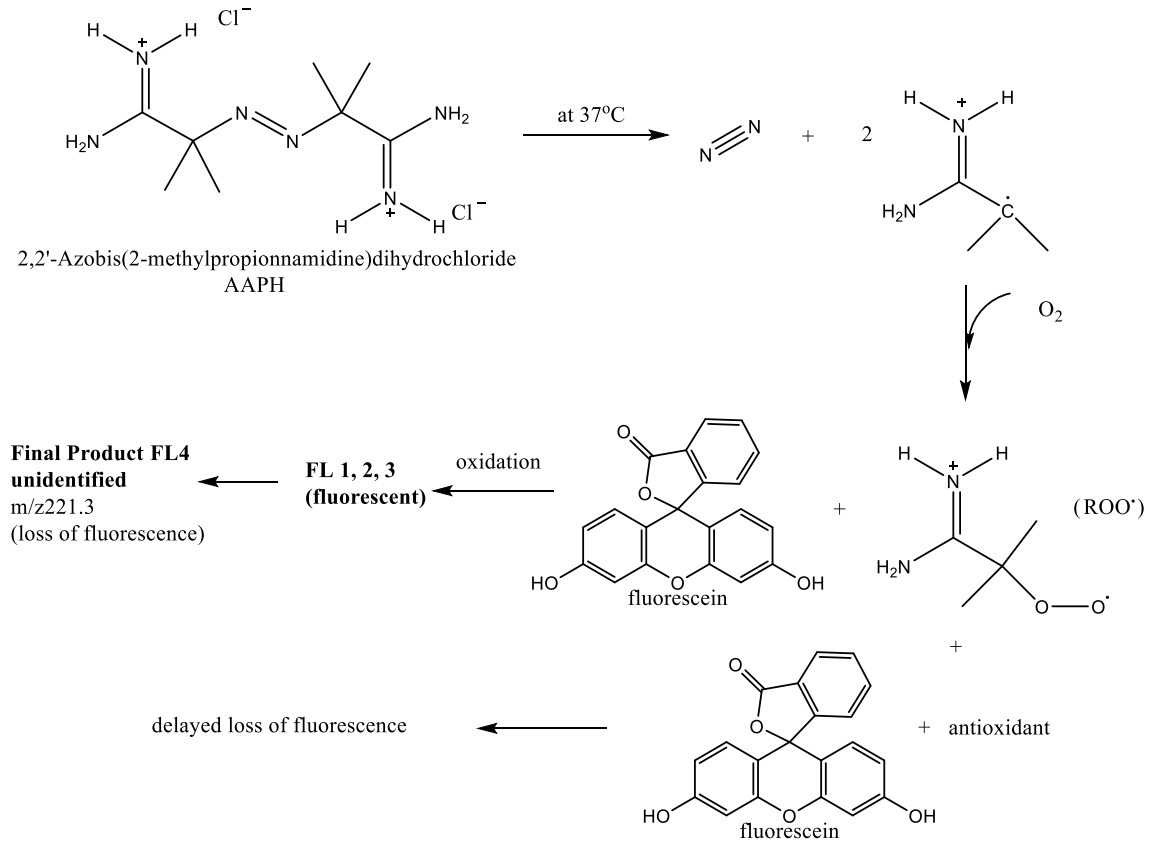


Figure 2.8| Reaction mechanism of reaction between fluorescein and AAPH
(adapted from^{305,336})

This HAT-based reaction uses a competitive reaction scheme between the antioxidant and the fluorescein probe for the constantly generated peroxy radical (hydrophilic). These are created by AAPH, *via* spontaneous thermal decomposition³³⁷. The stronger the antioxidant activity of the compound in question the better the elimination of the created radical and hence the better protection of the fluorescence probe (Figure 2.9, p.86).

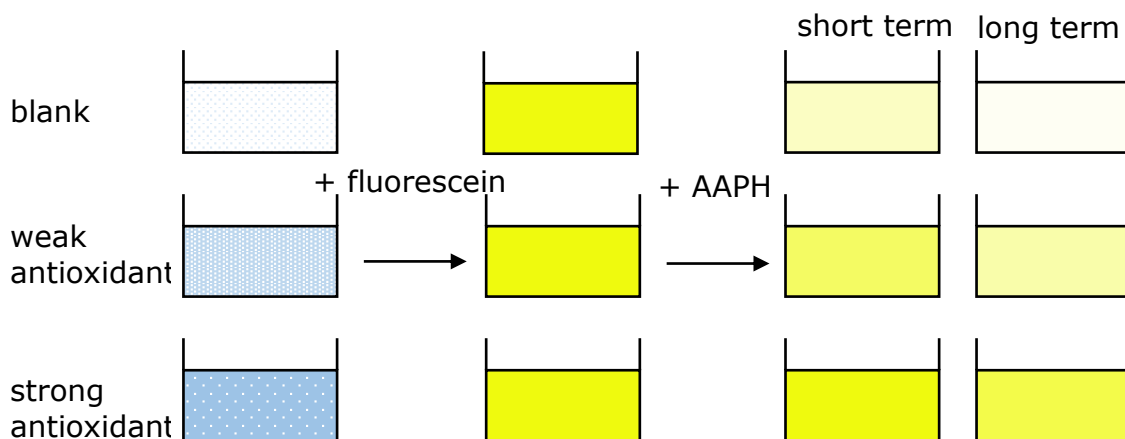


Figure 2.9| Graphical representation of the ORAC assay

comparing a blank to a weak and strong antioxidant in the reaction mix

The results are presented using fluorescence decay curves, determining inhibition time and degree³⁰⁵. Since its introduction this assay has widely been used for the determination of antioxidant capacity of beverages³²⁹, plants/plant extracts³³⁸⁻³⁴⁰ as well as biological samples e.g. urine or serum³⁰⁵.

Compared to the FRAP assay that follows a single electron transfer mechanism and measures the specific oxidant -reducing power, ORAC measures chain-breaking antioxidants that interrupt the radical chain reaction. More specifically, the ORAC assay determines the hydrophilic (aqueous condition) antioxidant activity for the AAPH created peroxy radicals^{305,319}. Use of the peroxy radical offers advantages over some of the other assays, providing a better model for ROS in food and *in vivo* than for example DPPH radicals. Also, the continuous production of radicals, caused by the temperature of the assay (37°C), in a timely manner are closely associated with *in situ* reactions³⁴¹.

Determination of antioxidant activity of the different RSP extracts together with their secondary metabolite composition, will aid to determine a favourable extraction technique for further investigations. This and the other objectives set out for this part of the project are highlighted next.

2.1.4 Objectives

The list below describes the objectives set out for this chapter:

- Determine the secondary metabolite composition of the RSP (free and bound fraction)
- Compare three different extraction techniques and determine the most suitable using antioxidant activity assays as well as LC-MS/MS analysis of secondary metabolites
- Compare pomace samples from two harvest years and decide on most appropriate using antioxidant activity assays as well as LC-MS/MS analysis of secondary metabolites
- Determine secondary metabolites responsible for the shown activity via partial least squares analysis (PLS) analysis

2.2 Materials and Methods

2.2.1 Chemicals and Equipment

For the experiments discussed in this chapter, the following chemicals (Table 2.3) and equipment (Table 2.4) were used.

Table 2.3| Chemicals, reagents and kits

Chemicals	Provider
1,1-Diphenyl-2-picryl-hydrazyl (DPPH)	Sigma-Aldrich
Methanol (HPLC grade)	Sigma-Aldrich
Gallic acid	Sigma-Aldrich
Trolox	Sigma-Aldrich
Folin & Ciocalteu's phenol reagent	Sigma-Aldrich
Sodium acetate trihydrate	Sigma-Aldrich
2,4,6-Tris(2-pyridyl)-s-triazine (TPTZ)	Sigma-Aldrich
Hydrochloric acid (HCl)	Sigma-Aldrich
Ferric chloride	Sigma-Aldrich
Sodium carbonate (Na ₂ CO ₃)	Sigma-Aldrich
Sodium hydroxide (NaOH)	Sigma-Aldrich
2,2'-Azobis(2-amidinopropane) dihydrochloride (AAPH)	Sigma-Aldrich
Monopotassium phosphate (KH ₂ PO ₄)	Sigma-Aldrich
Ethylenediaminetetraacetic acid (EDTA)	Sigma-Aldrich
Sodium fluorescein	Sigma-Aldrich
Sinapic acid (SA)	Sigma-Aldrich
Glacial acetic acid (CH ₃ CO ₂ H)	Fisher Scientific
Ethanol	Fisher Scientific
Tris-base	Fisher Scientific
Petroleum ether, extra pure (C ₆ H ₁₄ ; boiling point 40-60°C)	Fisher Scientific
Naringenin	Sigma-Aldrich
Syringic acid (SyA)	Sigma-Aldrich
Ferulic acid (FA)	Sigma-Aldrich
Caffeic acid (CA)	Sigma-Aldrich
Vanillic acid (VA)	Sigma-Aldrich
Vanillin (V)	Sigma-Aldrich

Table 2.4| Equipment

Equipment	Manufacturer/Details
Freeze Dryer	Modulyo Edwards
Coffee grinder	De Longhi KG39
Freeze-mill	Spex 6700, Edison
LC MS/MS (Rowett)	Agilent 1100
Automatic Soxhlet	Gerhardt; Soxtherm SE 416
Plate reader	BioTek μ Quant
Ultrasonic bath (extraction)	Fisher Scientific FB15060
Evaporator	gene vac (EZ-2)
Accelerated solvent extractor	Dionex ASE 350
Rotary evaporator	Büchi Rotavapor R-114
Oven	Techne Hybridiser HB-10
Fridge	DEAWOO
Freezer -20°C	Blomberg
Freezer -80°C	New Brunswick Scientific U725
pH meter	Denver Instruments Basic
Balance	OHAUS Pioneer™PA114
Ultrasonic bath	Ultrawave SFE5901
Balance	Mettler BB1200
Centrifuge (molecular)	Heraeus Multifuge 1 L-R

2.2.2 Methods

The methods described in this chapter were employed to determine the best possible extraction technique for further investigations. The chapter aims to determine a quick and reliable extraction method for the RSP and to determine any significant differences between the two harvest years/breeds. Figure 2.10 gives a general overview of the methods used.

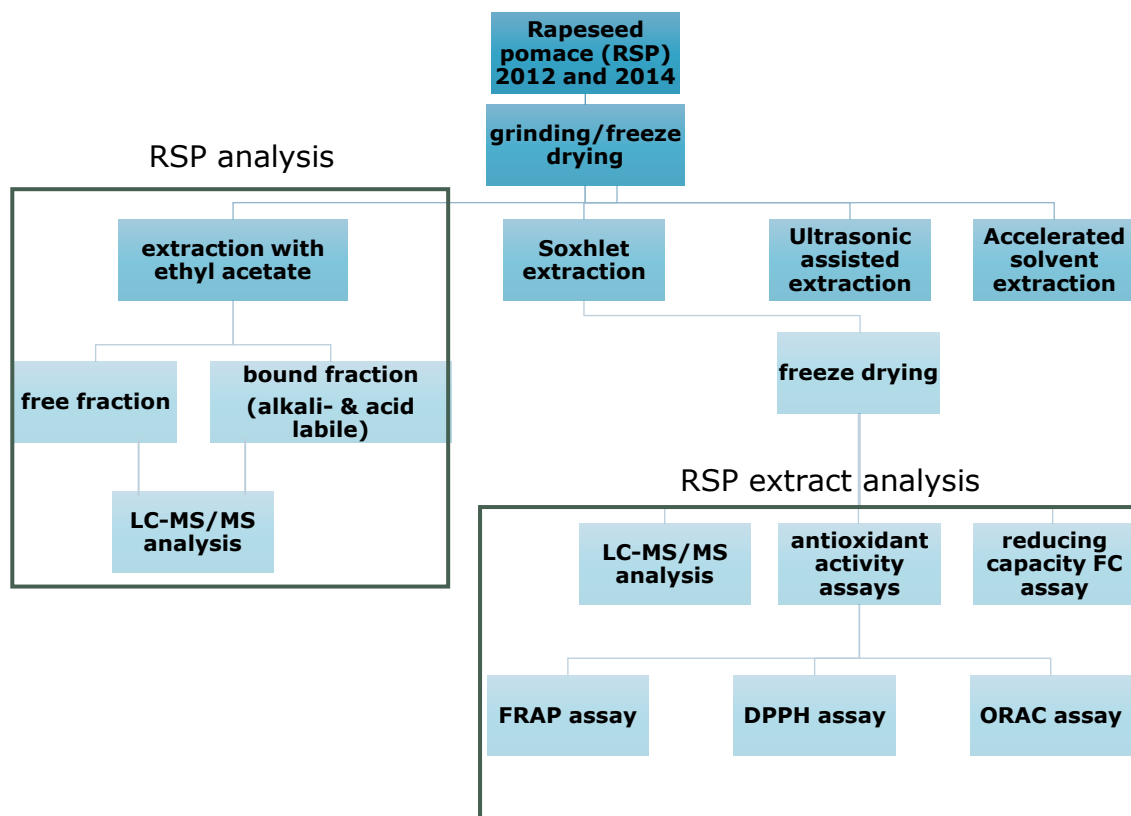


Figure 2.10| Overview of *in vitro* methods used in the assessment of RSP and RSP extracts

2.2.2.1 Plant Material

The RSP utilized throughout this project was provided by Gregor Mackintosh of Glendaveny (Mains of Buthlaw, Glendaveny, Peterhead), Scotland. Two RSP samples were obtained, one breed harvested in 2012 and a second breed harvested in 2014 and stored in plastic bags at -80°C upon arrival. The pomace from the 2014 harvest was freeze dried (Edwards, Freeze Dryer Modulyo) prior storage at -80°C .

Before extraction the pomace samples were individually ground in a coffee grinder (De Longhi KG39) to a particle size between 710 and 125 μm and then freeze dried (Edwards, Freeze Dryer Modulyo). Ground dried samples

were kept at -20°C until extraction (short time storage). For long-term storage, the pomace was kept at -80°C.

2.2.2.2 Secondary Metabolite Analysis of Rapeseed Pomace

To characterise the major secondary metabolites (free and bound fractions) in the RSP three extractions on freeze-milled (Spex 6700, Edison) pomace samples were performed, to determine free (FA) and bound (alkali (ALK)- and acid labile (ACD)) secondary metabolites, using extraction processes previously described by Russell *et al.*²⁹³.

Free Acids

In brief, RSP sample (0.1 g dry weight) was suspended in HCl (0.2 M; 3 mL) followed by the addition of ethyl acetate (EtOAc; 5 mL). The mixture was shaken, vortexed and sonicated for 5 mins, followed by centrifugation (1800 x g; 5 mins; 18°C). The EtOAc layer was collected and filtered into a round bottom flask (50 mL), by passing through Whatman No 1 filter paper containing a small amount of sodium sulphate (anhydrous). This process was repeated two more times, with a final centrifugation (3200 x g; 10 mins; 18°C). The solvent in the round bottom flask was removed *via* a rotary evaporator at temperatures not exceeding 40°C. Samples were stored in a desiccator until preparation for analysis. The remaining aqueous fraction (obtained after the EtOAc extraction) was neutralised (pH 6.5-7.0) using NaOH (4 M), frozen and then freeze dried.

Alkali-labile Phenolic Acids

To the freeze dried aqueous fractions, NaOH (1 M; 3 mL) was added and stirred at room temperature for 4 hours under nitrogen, then the pH was reduced to pH 2 with HCl (10 M). The fraction was then extracted with EtOAc (5 mL), shaken, vortexed and sonicated (5 mins). The solvent (EtOAc) layers were separated by centrifugation (1800 x g; 5 mins; 18°C), and then processed as above.

Acid-labile Phenolic Acids

To the freeze dried aqueous fractions, HCl (2 M; 3 mL) was added and the sample incubated at 95°C for 30 mins with intermittent mixing, then cooled

to room temperature and extracted with EtOAc (5 mL), shaken, vortexed and sonicated (5 mins). The solvent (EtOAc) layers was separated by centrifugation (1800 x g; 5 mins; 18°C), and then processed as above.

Chemical Analysis of the free and bound phenolic Extracts (HPLC-MS/MS)

The three RSP extract fractions (free, alkali- and acid- labile) were subject to LC-MS/MS analysis, to determine their phytochemical profile. The freeze-dried extracts were dissolved in 0.5 mL methanol. For analysis, each sample (100 µL) was mixed with an internal standard (400 µL) and then analysed as previously described by Russell and Neacsu *et al.*^{342,343} on an Agilent 1100 HPLC system, fitted with a Zorbax Eclipse 5 µm, 150 mm x 4 mm column (both Agilent Technologies, Wokingham, UK). This analysis was kindly undertaken by Garry Duncan as a service of the Rowett Institute of Nutrition and Health, Aberdeen University.

2.2.2.3 Rapeseed Pomace Extraction techniques

Soxhlet Extraction (SOX)

For the Soxhlet (Gerhardt; Soxtherm SE 416) extraction both RSP samples from 2012 and 2014 (dissimilar breeds) were used; these will be referred to as SOX2012 and SOX2014 respectively. First, both pomace samples were defatted according to Wanasundara *et al.*³⁴⁴ and Sagdic *et al.*³⁴⁵ with some modifications. Ground pomace (6.0 g) was transferred into cellulose thimbles (Fioroni S.A X25 Extraction thimble 33x80mm) for the Soxhlet extraction. The lipids were extracted with petroleum ether (140 mL) as previously described by Qin Liu *et al.*³⁴⁶, in a shorter procedure with the settings shown in Table 2.5. The de-fatted pomace filled thimbles were left to dry overnight in a fume hood, to remove any traces of solvent.

After 16 hours, a second extraction with an ethanol/water mixture (95:5, 140 mL, pH 7.9) according to Sagdic *et al.*³⁴⁵ was undertaken, with minor modifications (Table 2.5). The total ethanol/water extraction lasted three hours. The final evaporation (B) was aborted before complete dryness, to avoid charring of the extracts. Extracts from the 6 extraction beakers were

pool into one pre-weight round bottom flasks (150 mL), evaporated on a rotary evaporator (Büchi Rotavapor R-114), frozen and freeze dried (Edwards, Freeze Dryer Modulyo) to yield a powdered dry product. The extraction yield was determined by weight.

Table 2.5|Petroleum ether and ethanol/water (95:5) Soxhlet extraction parameters

step	petroleum ether	ethanol/water
Extraction	45 mins, 150°C	45 mins, 240°C
Evaporation A	4 x interval	4 x interval
Rinsing	45 mins	45 mins
Evaporation B	1 x interval	1 x interval

Ultrasound Assisted Extraction (UAE)

Rapeseed pomace, from both harvest years (3 g), and extraction solvent (95:5(v/v) ethanol/water, 70 mL, pH 7.9) were transferred into brown glass jars and then placed in an ultrasonic bath (Fisher Scientific FB15060) for 45 min. Following extraction, the extracts were transferred in falcon tubes (50 mL) and centrifuged at 2600 x g for 15 minutes. The supernatant was then transferred into a pre-weight round bottom flasks, evaporated on the rotary evaporator (Büchi Rotavapor R-114), frozen (-20°C), freeze dried (Edwards, Freeze Dryer Modulyo) and the extraction yield determined. Following, these two extracts will be referred to as UAE2012 and UAE2014 respectively.

Accelerated Solvent Extraction (ASE)

For the accelerated solvent extraction, the sample cells were prepared, by weighing 6 g Ottawa sand and 0.5 g sample (2012 and 2014 pomace) into an extraction cell. The latter was then packed with Ottawa sand. Cellulose filter (27 mm) were fitted at the bottom and top of the extraction cell. The extraction method was set up, to run 4 extraction cycles, using the same ethanol/water mixture as previously described for SOX and UAE (5 mL), at 80°C with a static time of 5 min and a purge time of 300 s. The extract was collected in pre-weight brown glass vials and evaporated in the Genevac (EZ-2), frozen (-20°C), freeze died (Edwards, Freeze Dryer Modulyo) and the extraction yield determined. Following these two extracts are referred to as ASE2012 and ASE2014 respectively.

2.2.2.4 Folin-Ciocalteu-(FC) Assay

The FC assay was conducted according to Waterhouse *et al.*³⁴⁷ with minor modifications. Gallic acid was prepared to give final concentrations from 0.01 to 0.20 mg/mL. The extracts were dissolved (ethanol:water, 4:10) and further diluted with deionised water. For the reaction to occur, test solutions (25 µL) were mixed with distilled water (200 µL) and FC reagent (20 µL) (n = 3, technical replicates in plate). After a short incubation time (3 mins at room temperature), 20% Na₂CO₃ solution (25 µL) was added. After a second incubation (37°C; 30 mins), the absorbance was read at 750 nm (BioTek µQuant). Sinapic acid (SA), as most abundant phenolic acid, was analysed for comparison in the FC assay. The results are expressed as mg GAE/ g dry RSP extract (C) by using the following formula, where *c* equals the found concentration from the gallic acid calibration graph (mg/mL), *V* is the used volume (mL) of the extract and *M* is the total mass (g) of extract used in one well (Equation 2.3).

$$C(\text{mgGAE}/1\text{g}) = c(\text{mg}/\text{mL}) * \left(\frac{V(\text{mL})}{M(\text{g})} \right) \text{ Equation 2.3}$$

2.2.2.5 Chemical Analysis of the RSP Extracts (HPLC-MS/MS)

The extracts obtained from the three extraction techniques (SOX, UAE, ASE) were subject to LC-MS/MS analysis, to determine their phytochemical profile. Solutions of the freeze-dried extracts with a concentration of 1 mg/mL were prepared (methanol/deionized water, 95/5 (v/v)). For analysis, each sample (100 µL) was mixed with a standard (400 µL) and then analysed as previously described by Russell *et al.*^{342,343} on an Agilent 1100 HPLC system using a Zorbax Eclipse 5 µm, 150 mm x 4 mm column (both Agilent Technologies, Wokingham, UK). Garry Duncan kindly undertook this analysis, as a service of the Rowett Institute of Nutrition and Health, Aberdeen University.

2.2.2.6 In vitro antioxidant activity

Ferric Reducing/Antioxidant Power (Plasma)- (FRAP) Assay

The FRAP assay was performed according to Arya *et al.*³⁴⁸. To freshly prepare FRAP reagent, acetate buffer (25 mL; 300 mM; pH 3.6), TPTZ (2.5 mL; 10

mM in 40 mM HCL) and $\text{FeCl}_3 \cdot 6\text{H}_2\text{O}$ (2.5 mL; 20 mM in dH_2O) were mixed and incubated (37°C) until use. Trolox was prepared with concentrations ranging from 31.20 to 312.5 $\mu\text{g}/\text{mL}$. The samples were prepared in ethanol:water (4:10) and diluted further with water to obtain absorbance values in the range of the calibration curve. Sample/blank/standard (10 μL) were mixed with the FRAP reagent (190 μL) and the absorbance at 593 nm (BioTek μQuant) was read after incubation (30 mins, at room temperature, in the dark). The results are given as mg TE/g dry extract (C) by using the following formula (Equation 2.4), where c is the concentration obtained from the Trolox calibration graph (mg/mL), V is the volume (mL) of extract and M is the total mass (g) of extract used in each well (Equation 2.4).

$$C(\text{mgTE}/1\text{g}) = c(\text{mg}/\text{mL}) * \left(\frac{V(\text{mL})}{M(\text{g})}\right) \quad \text{Equation 2.4}$$

2,2-Diphenyl-1-picrylhydrazyl- (DPPH) Assay

The radical scavenging activity of the samples was measured using the method by Sagdic *et al.*³⁴⁵ with minor modifications. Serial dilutions of all the extracts (3.9-1000 $\mu\text{g}/\text{mL}$) were prepared in methanol and 50 μL mixed with freshly prepared DPPH solution (100 μL ; 0.1 mM in methanol) for final extract concentrations between 1.3 and 333.3 $\mu\text{g}/\text{mL}$. The 96-well plates were incubated in the dark (30 mins; at room temperature) and the absorbance was read at 517 nm (BioTek μQuant). The percentage of present radicals was calculated as below (Equation 2.5), where A is the absorbance. The linear part (including the 50% mark) of the obtained curve was used to determine the IC_{50} value, by plotting a linear graph and using the trend line for IC_{50} calculations.

$$\% \text{ of present radicals} = \frac{(100 * A_{\text{sample}})}{A_{\text{blank}}} \quad \text{Equation 2.5}$$

Oxygen Radical Absorbance Capacity (ORAC) Assay

Samples were analysed according to Roy *et al.*³²⁹ and Huang *et al.*³⁴⁹ with minor modifications. From a Trolox stock solution, a series of dilutions (10 to 125 μM) was made in PBS (75 mM; pH 7.4). To start the ORAC reaction, Trolox (25 μL) and sodium fluorescein (150 μL ; 25 nM) were incubated (30 mins, 37°C). After the incubation, 2,2'-Azobis (2-amidnopropane)

dihydrochloride (AAPH, 25 μ L, 150 mM) was added and the reaction was monitored (over 2 hours at 2 mins intervals) at an excitation and emission wavelengths of 485/20 and 525/20 nm respectively (BioTek Synergy HT). RSP extract solutions were prepared (1 to 50 μ g/mL) in PBS, giving final well concentrations of 0.125 to 6.25 μ g/mL. RSP extract samples were treated in the same way as the Trolox standard solutions described above. The Trolox standard series was run with all samples to determine μ mol Trolox equivalents (TE)/g of dry extract (C) from the net AUC calibration curve (see calculations below Equation 2.6-2.8). *AUC* is the area under the curve, $f_{x\text{min}}$ the fluorescence measurement at the respective minute, c is the concentration obtained from the Trolox calibration graph (μ mol/L), V is the volume (L) of extract and M is the total mass (g) of extract used in one well.

$$AUC = 0.5 + \frac{f_{2\text{min}}}{f_{0\text{min}}} + \frac{f_{4\text{min}}}{f_{0\text{min}}} + \frac{f_{6\text{min}}}{f_{0\text{min}}} + \dots + \frac{f_{118\text{min}}}{f_{0\text{min}}} + 0.5 \left(\frac{f_{120\text{min}}}{f_{0\text{min}}} \right)$$

$$\text{net } AUC = AUC_{\text{sample}} - AUC_{\text{neg control}}$$

$$C(\mu\text{molTE}/1\text{g}) = c(\mu\text{mol}/L) * \left(\frac{V(L)}{M(g)} \right)$$

Equation 2.6-2.7-2.8

2.2.2.7 In vitro antioxidant activity of single compounds in RSP extract/PLS

To see if it is possible to determine the compounds responsible for the antioxidant activity in the RSP extract, seven different compounds were selected, using the following criteria:

- i. Highest concentration in extract
- ii. Most likely responsible for DPPH, FC, FRAP activity
- iii. Most likely responsible for ORAC activity

The first criteria (i) was determined using the results obtained from HPLC-MS/MS analysis, (ii) and (iii) were determined after PLS analysis of the data obtained above, using the 6 extracts, their secondary metabolite profile as

well as their *in vitro* activity from results obtained in the DPPH, FC, FRAP and ORAC assay.

The overall activity of these seven compounds was tested as well as their activity at the extract specific (SOX2014) concentration at 1 mg/mL using the same methods as described in 2.2.2.4 Folin-Ciocalteu-(FC) Assay (p.94) and 2.2.2.6 *In vitro* antioxidant activity (p.94 ff.)

2.2.2.8 Statistical analysis

Statistical analysis was carried out using GraphPad Prism 7 and Umetrics software. Specific methods used for statistical comparison and correlation analysis for each experiment are detailed in the results section. P-values below 0.05 were considered to be significant. All experiments were repeated at least three times unless otherwise stated and results shown as mean±standard deviation.

2.3 Results and Discussion

2.3.1 Secondary metabolite composition of RSP from free, alkali-labile and acid-labile fractions

To determine the secondary metabolite composition of the starting RSP material, a number of extractions were undertaken. The reasoning of applying three different ethyl acetate extractions was to analyse which secondary metabolites would be available should RSP be used directly for human consumption. Since free phenolic acids are easily absorbed in the small intestine³⁵⁰, these compounds can be measured by simple solvent extraction into ethyl acetate (free) (Table 2.6, Table A2 p.429 ff.).

Table 2.6| Concentrations (mg/kg pomace) of the most abundant secondary metabolites found in both RSP samples after free, alkali-labile and acid-labile extractions

Secondary metabolite	extraction	RSP 2012 (mg/kg pomace)	RSP 2014 (mg/kg pomace)	Significant difference
<i>sinapic acid</i>	free	224.24 ± 3.58	161.40 ± 25.55	*
	alkali-labile	917.650 ± 43.78	1072.14 ± 32.38	**
	acid-labile	11.31 ± 1.38	10.54 ± 1.25	
<i>indol-3-pyruvic acid</i>	free	3.04 ± 0.39	53.54 ± 87.11	
	alkali-labile	76.17 ± 131.93	197.68 ± 37.96	
	acid-labile	381.40 ± 71.97	223.58 ± 123.48	
<i>kaempferol</i>	free	0.19 ± 0.01	0.75 ± 0.53	
	alkali-labile	0.11 ± 0.01	0.20 ± 0.01	***
	acid-labile	141.30 ± 6.77	152.62 ± 5.54	
<i>ferulic acid</i>	free	12.25 ± 0.30	9.570 ± 1.63	*
	alkali-labile	64.55 ± 39.37	38.65 ± 2.07	
	acid-labile	1.53 ± 0.17	1.23 ± 0.06	*
<i>protocatechuic acid</i>	free	2.52 ± 0.04	5.40 ± 0.81	**
	alkali-labile	16.54 ± 3.76	24.12 ± 1.20	*
	acid-labile	17.14 ± 0.53	17.42 ± 0.94	

Note(s): Further metabolites can be found in Table A2 (p.429 ff.), statistical analysis was performed using multiple *t*-tests without correction for multiple comparison in Graph Pad Prism6 (statistical significance with alpha=5.000%, $p < 0.05^*$, $p < 0.01^{**}$, $p < 0.001^{***}$), HPLC-MS/MS analysis conducted by Garry Duncan (Rowett)

However, most of the secondary metabolites were found to be esterified to other plant components, like sugars and complex carbohydrates. When bound to cell wall components, such as polysaccharides and lignin, they are unlikely to be absorbed in the small intestine and will only be available after microbial

release and metabolism in the colon^{351,352}. Bound metabolites were measured after alkali (ALK) and acid (ACD) extraction. Although this does not allow the determination of the conjugate, it allows for a more accurate phenolics quantification³⁵³.

Table 2.6 shows the five most abundant secondary metabolites found. The table distinguishes among the three extraction techniques (free, ALK, ACD) used for total metabolite analysis. A part of the results presented here have previously been published in F. Pohl *et al.*³⁵³ in 2018. A more detailed list of all the analysed metabolites is presented in Table A2 in the appendix (p.429 ff.), including compounds analysed for, but not present in the extracts.

There are significant differences between the two harvest years, when comparing the results found for the metabolites from the different extractions. Sinapic acid shows significantly higher ($p < 0.5$) results in the free metabolite fraction for 2012, but for the alkali labile fraction concentrations were found to be significantly higher in the 2014 pomace. Whereas there is no significant difference for the acid-labile fraction. In general, there is no trend visible for both samples/years and the extraction techniques studied.

As expected, most metabolites were found following alkali and/or acid extractions e.g. approximately 80% of sinapic acid was extracted after alkali treatment, while most of the kaempferol (more than 99%) was obtained after acid treatment. Only for a small number of compounds such as *m*-hydroxybenzoic acid and chlorogenic acid as well as cinnamic acid and phenyllactic acid no/or smaller concentrations were extracted during alkali/acid-labile extraction respectively (Table A2, p.429 ff.). In general, only few studies have been carried out on the accessible secondary metabolites after ethyl acetate extraction of rapeseed pomace/meal. Most times the solvents of choice are methanol, ethanol, water or mixtures of these^{91,338}.

Similar free phenolic acids were found previously by Krygier *et al.*³⁵⁴, in 3 different defatted rapeseed cultivars (flour), showing the presence of *p*-hydroxybenzoic, vanillic, gentisic, protocatechuic, syringic, *p*-coumaric, ferulic, sinapic, and chlorogenic acid at different concentrations depending on the cultivar. Sinapic acid was found to be the most abundant in all 3 samples (Table 2.7, p.100). The analysis of RSP itself gives a very good idea on what

can be extracted when using different extraction methods such as SOX, UAE and ASE.

A series of papers by Krygier *et al.* and Sosulski *et al.*³⁵⁴⁻³⁵⁶ looked into free and bound fractions of phenolic acids in defatted rapeseed and other vegetable flours. Their method of extraction was slightly different to the one used here, e.g. no acid labile extraction was undertaken. However, it gives a good indication about free and bound fractions in the three varieties of rapeseed (Yellow Sarson, Indian; Candle and Tower, Canadian) studied. They found trans-sinapic acid to be the most abundant phenolic acid in both, the free (37 mg/kg-801 mg/kg, Table 2.7) and from esters liberated fraction 7123-11162 mg/kg.

Table 2.7| Comparison of free phenolic acids detected from rapeseed flour in Krygier *et al.*³⁵⁴ to the two harvests in this study (2012, 2014)

<i>Phenolic acid</i>	Yellow Sarson^a	Candle^a	Tower^a	Scottish Rapeseed pomace	
				2012	2014
<i>p</i> -hydroxybenzoic	1	5	trace	3.8	5.2
<i>Vanillic</i>	trace	3	8	1.8	2.6
<i>Gentisic</i>		4	trace	Not analysed	
<i>Protocatechuic</i>	3	6		2.5	5.4
<i>Syringic</i>	11	6	15	2.4	5.7
<i>p</i> -coumaric		11	31	2.2	1.9
<i>cis</i> -ferulic		trace	0.6	12.3 ^b	9.6 ^b
<i>trans</i> -ferulic	8	68	27		
<i>Caffeic</i>	1	3	4	5.5	7.5
<i>cis</i> -sinapic	trace	7	90	224.2 ^b	161.4 ^b
<i>trans</i> -sinapic	37	732	801		
<i>Chlorogenic</i>		trace	trace	1.0	1.0
Total	61	845	982	254.7	200.3

Notes(s): All concentrations given as mg/kg dry pomace/flour

^a values adapted from publication³⁵⁴ transferred from mg/100g to mg/kg

^b not distinguished between *cis*- and *trans*-forms

HPLC-MS/MS analysis of Scottish Rapeseed pomace conducted by Garry Duncan (Rowett)

When comparing the concentrations of free phenolic acids measured by Krygier *et al.*³⁵⁴ with ours (Table 2.7), similar results were obtained for most phenolics. Surprisingly, the amount of total sinapic acid was very low for their Yellow Sarson variety (37 mg/kg) compared with Candle (739 mg/kg) and Tower (891 mg/kg) cultivar. However, our Scottish RSP gave concentrations within the minimum and maximum values obtained.

Some differences can be explained by the pre-extraction preparations. In our study, the pomace was obtained from a family farm that obtains oil purely by cold pressing³⁵⁷. In contrast, the samples used in Krygier's study were first defatted using hexane as solvent. The defatting process makes the starting material lighter implying that more flour/pomace was initially weighed in for further extraction when compared to this project. Furthermore, the difference in extraction solvent and the different growing conditions can have an impact on the results. Unfortunately, the alkali/acid-labile extraction in our work cannot be compared with Krygier's paper, due to differences between the methods.

Other publications also suggest the usage of acid and alkali extractions to find the bound fractions of secondary metabolites^{358,359}. The same alkali/acid-labile extraction undertaken in this project, have previously been undertaken to determine bound secondary metabolites in different fruits in Russell *et al.*²⁹³ and cereals in Neacsu *et al.*³⁴³. For better comparison in the same plant family (*Brassica*), selected secondary metabolite compositions of e.g. cabbage, kale, broccoli and cauliflower are provided in Table A3 (p. 440, unpublished data³⁶⁰). This set of data was provided by Wendy Russell from the Rowett Institute, where they form part of a study on secondary metabolite composition of different plants. The table shows, that the RSP shows a similar secondary metabolite composition to the other *Brassica* plants. The sinapic acid concentration of the RSP for example is less than in red cabbage and kale, but more than in white cabbage, broccoli and cauliflower. A similar distribution is true for other metabolites such as coumaric acid, ferulic acid and p-hydroxybenzoic acid. For some of the metabolites the RSP has the highest content e.g. indole-3-pyruvic acid (IPA), kaempferol and benzoic acid. For both kaempferol and IPA the higher concentrations were obtained from the acid-labile fraction³⁵³, meaning these might have been bound to other plant components. Different kaempferol derivatives have previously been identified in rapeseed, e.g. kaempferol-3-O- β -D-glucopyranosyl-(1 \rightarrow 2)- β -D-glucopyranoside-7-O- β -D-glucopyranoside and kaempferol-3-O-(2-O-sinapoyl)- β -D-glucopyranosyl-(1 \rightarrow 2)- β -D-glucopyranoside-7-O- β -D-glucopyranoside⁹⁹, from which kaempferol could have been liberated during the acid labile extraction. IPA is part of the IPA pathway for the production of

indole-3-acetic acid (IAA) from tryptophan in plants, where it acts as regulator of growth and development³⁶¹.

The analysis of free and bound secondary metabolites in the RSP was undertaken to analyse the starting material to get a general overview in metabolite distribution. The extraction technique used to obtain the three fractions are not amenable for commercial application due to the time consuming extraction. For this reason, here three extraction different techniques were chosen for the secondary metabolite extraction of RSP. The final chosen technique should provide an extract with easy handling for further experiments.

2.3.2 Comparison of SOX, UAE and ASE extraction techniques

For the SOX and UAE extraction techniques a solid to solvent ratio of 1:18.8 (g/g) or 1:23.3 (g/mL) was used. The ratio for ASE was 1:10 for 4 extractions in sequence (total of 1:40). Kankara *et al.*³⁶², Wong *et al.*²⁶¹ and Muñiz-Márquez *et al.*²⁷⁴ had previously demonstrated, that the solid to solvent ratio can have an impact on the extraction efficiency (Table 2.8, p.103).

Table 2.8|Impact of solid to solvent ratio on antioxidant activity of extracts

reference	Ratios tested	Antioxidant assays	outcome
<i>Kankara et al.</i> ³⁶²	1:10, 1:15 or 1:20	FC, DPPH or FRAP	No sig. difference
	1:30	FC, DPPH	Slightly less active than the above
<i>Wong et al.</i> ²⁶¹	1:5	FC, ABTS, DPPH, total flavonoids	Significant less active than 1:10, 1:15 and 1:20
	1:10	FC, ABTS, DPPH, total flavonoids	Better than 1:5 in FC, ABTS and DPPH
	1:15 and 1:20	FC, ABTS, DPPH, total flavonoids	Both significantly better than 1:10 in FC, total flavonoid and DPPH 1:20 only sig. better activity in FC assay
<i>Muñiz-Márquez et al.</i> ²⁷⁴	1:12, 1:8 and 1:4	FC	1:12 sig. better than 1:4 and 1:8

The solvent of choice for the secondary metabolite extraction in this project was an ethanol water mixture (95:5, v/v) for all three extraction techniques. Considering Table 2.1 (p.69), this should provide a wide variety of secondary metabolites. This solvent mixture was also chosen due to positive preliminary results²⁶⁷ and the smaller environmental impact of ethanol compared to other organic solvents³⁶³.

2.3.2.1 Yield of extraction

The amount of extract obtained after the extraction is very important, especially if the product is made commercially viable, then the higher the yield the higher the earnings on the product. Furthermore, the physical characteristics of the extracts are important for ease of handling.

The most efficient extraction technique during this project was found to be accelerated solvent extraction (ASE), followed by ultrasonic assisted extraction (UAE) and Soxhlet (SOX) respectively (Table 2.9).

Table 2.9| Extraction yields in mg per g pomace and in percent, subdivided by extraction technique and harvest year

<i>extraction</i>	<i>year</i>	<i>yield [mg/g pomace]</i>	<i>yield [%]</i>
SOX	2012	79.55	7.96
	2014	75.59	7.56
UAE	2012	158.59	15.86
	2014	175.46	17.55
ASE	2012	362.31	36.23
	2014	344.67	34.47

However, due to the nature of the techniques higher yields in overall mass were obtained for SOX and UAE, because higher amounts of pomace can be used as starting material. In comparison, for the ASE only 0.5 g were employed per extraction cell, while 6 or 12 times more starting material was used for UAE and SOX respectively. An advantage of SOX, over the other two extraction techniques, was that a dry extract was obtained after extraction followed by freeze drying. Extracts from both UAE and ASE yielded oilier extracts in nature, which were difficult to handle. Homogeneous sample taking was challenging for the latter ones. The difference in the physical state of the extract is most likely due to the additional defatting step undertaken during the SOX extraction, which is a common step with Soxhlet extraction. However, previous results presented by Wagener²⁶⁷ had shown positive antioxidant activity for both the SOX and the UAE, which is why the extraction parameters were kept very similar. ASE was added as an additional extraction technique for comparison and due to its ease of use and lower solvent consumption.

2.3.3 Folin-Ciocalteu (FC) assay

The first step in determining whether there is a difference in phenolic content in the 6 different extracts (three extraction methods of two harvest years (2012/2014) each), the Folin-Ciocalteu (FC) method was chosen. As previously mentioned, this method is often referred to as analysing the phenolic content but is actually measuring the samples reducing capacity (2.1.3.1 Folin-Ciocalteu- (FC) Assay, p.81). The results obtained for the FC assay performed on the six RSP extracts are presented in Figure 2.11.

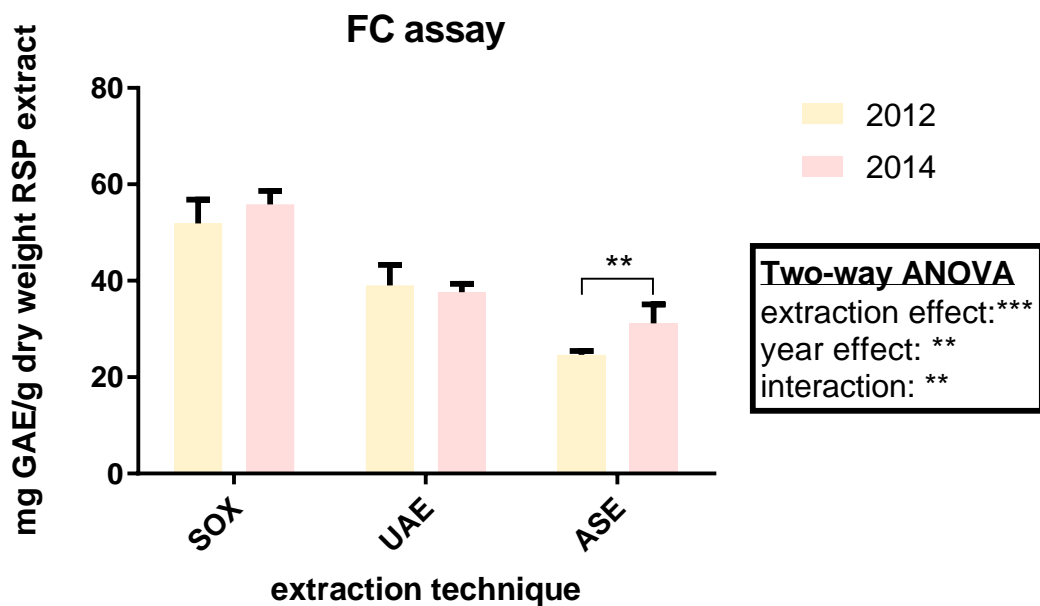


Figure 2.11| FC assay results, comparing the three extraction techniques together with the two harvest years/breeds

Results are given as mg gallic acid equivalence (GAE) per g dry weight of RSP extract. Significant difference via Two-way ANOVA (box) and Bonferroni's multiple comparisons test between years for each extraction technique; $p \leq 0.01$ **, $p \leq 0.001$ ***

The highest reducing capacity was found for the SOX extract (51.92 ± 4.91 (2012) and 55.84 ± 2.83 (2014) mg GAE per g dry weight of RSP extract), followed by UAE (39.03 ± 4.28 and 37.61 ± 1.79 mg GAE per g dry weight of RSP extract for 2012 and 2014 respectively) and ASE (24.63 ± 0.83 and 31.17 ± 3.91 mg GAE per g dry weight of RSP extract for 2012 and 2014 respectively). Two-way ANOVA showed that the extraction technique ($p < 0.001$) had a higher significant difference than the harvest years ($p < 0.01$) on the reducing capacity. However, an interaction was found which makes the interpretation of the results more complex. For example, the extract obtained from the 2014 harvest did not show better results in the FC assay

for all three extraction techniques. Whereas, better results were exhibited after SOX and ASE extraction, the 2012 extract was found to show slightly better results after UAE. Additional multiple comparison analysis (Bonferroni's) revealed, that only ASE extraction showed significant differences between the two harvest years.

The FC results especially for the SOX extracts are in close agreement with previous reports. Cvjetko *et al*³⁶⁴. reported: 51.7 (80% ethanol), 54.0 (60% ethanol) and 55.7 (70% methanol) mg GAE/g using defatted rapeseed pomace/meal and ultrasonic assisted extraction at 45°C for 40 minutes. Data on the reducing capacity of rapeseed oil itself is not readily available, except in one publication it was shown that cold pressed rapeseed oil had polyphenol equivalents to 1.56 mg GAE/g³⁶⁵. This implies that the extract from our RSP has about 35 times (SOX) more reducing capacity than the oil itself.

Although the FC method has widely been used^{68,113,244}, due to its fast and easy procedure, it has its limitations. The resulting colour change is due to the oxidation of the phenolics and the reduction of molybdenum, which leads to the blue colour. However, this oxidation can also be found for non-phenolics, such as aromatic amines, sugars and ascorbic acid³¹¹, which is why the assay should be referred to as measuring the samples reducing capacity. An issue one encounters when analysing samples with this technique, is the lack of a standard method for solid samples. Although the European commissions have a method for the analysis of wine a standard method for solid samples is not available. This has led to a vast amount of results that are not comparable with other laboratories unless the same operating procedure is used. A further problem is the use of different phenolics as standard, whereas most papers show their results as GAE, such as Cvjetko *et al*.³⁶⁴ others choose to give results as sinapic acid equivalence, as in the case of Szydłowska-Czerniak and Tułodziecka⁵². In their study sinapic acid was chosen, because it is known to be one of the most common phenolic acids in rapeseed. Testing strongly coloured substances in this assay can lead to interferences, if they absorb at the FC specific wavelength (750 nm). Although the extract is yellow, once dissolved, the tested concentrations are faint enough not to interfere with the 750 nm wavelengths. However, for a better qualitative and quantitative overview of present secondary

metabolites, HPLC-MS/MS analysis was applied to analyse for the presence of e.g. phenolics, indoles, amines, flavonoids and coumarins.

2.3.4 HPLC-MS/MS

The most abundant phenolic found during HPLC-MS/MS analysis of all the extracts (SOX, UAE, ASE) is sinapic acid (Table 2.10, p.108). This confirms previously found results in the literature^{80,366} as well as results obtained during the analysis of the pomace starting material using the same HPLC-MS/MS method (2.3.1 Secondary metabolite composition of RSP from free, alkali-labile and acid-labile fractions, p.98 ff.).

Other phenolics with high concentrations are ferulic acid, caffeic acid, syringic acid and 4-hydroxyphenylpyruvic acid (Table 2.10, p.108). Surprising were the high amounts of spermidine (amine) and indole-3-pyruvic acid (indole) found in the extracts. These could be present due to the degradation of protein, particularly through fermentation or storage³⁶⁰. The most abundant flavonoids/coumarins are kaempferol (SOX14; UAE12) and luteolin (SOX12; UAE14; ASE12,14). Additional found phenolics, indoles, amines, flavonoids and coumarins are presented in Table 2.10, excluding the metabolites not found in either of the six extracts.

In general, the total amount of phenolic compounds found, appears to mirror the results obtained by the FC assay, showing the following general order SOX>UAE>ASE. However, when comparing the total concentrations, the order considering the extraction technique and year (*SOX12>SOX14>UAE12> UAE14>ASE12>ASE14*, Table 2.10) slightly deviates from the results found in the FC assay (*SOX14>SOX12>UAE12>UAE14>ASE14>ASE12*, Figure 2.11, p.105) as for the ASE and SOX the years are switched. This shows that simple chemical reaction assays with spectroscopically measurement, such as the FC assay, can give a general overview of the phenolic content; however, they are not as accurate as separation techniques, such as HPLC analysis.

The phenolics, sinapic and ferulic acid found in the RSP extracts are well known antioxidants and they have shown interesting chemical and biological activity in previous research. Sinapic acid (SA) for example has shown DPPH

radical scavenging⁹⁷, superoxide $O_2^{\bullet-}$, hydroxyl ($\bullet OH$), nitric oxide ($\bullet NO$), and peroxy nitrite ($ONOO^-$) scavenging as well as the suppression of lipid peroxidation³⁶⁷. In further studies using rodent models, SA was found to protect rats from arsenic induced toxicity³⁶⁸, exhibited neuroprotective effects in a amyloid $\beta(1-42)$ protein-induced Alzheimer's disease mouse model²⁴¹ and attenuated kainic acid-induced hippocampal neuronal damage in mice³⁶⁹. Other phenolics such as ferulic acid have also been found to show neuroprotective potential in e.g. a rotenone model of Parkinson's disease²⁴³. In a oxidative stress induced ($A\beta_{42}$) sea urchin (*Paracentrotus lividus*) embryo model, ferulic acid neutralized ROS, blocked apoptotic pathways and recovered mitochondrial membrane potential³⁷⁰. For others phenolics such as syringic acid and 4-hydroxyphenylpyruvic acid not much research on their biological availability and potential activity are available.

Also the flavonoids luteolin, kaempferol and naringenin, previously found in the pollen of *Brassica napus*³⁷¹, exhibit interesting biological activity. For example luteolin has shown to have cancer chemopreventive and chemotherapeutic potential as well as antioxidant, anti-inflammatory and antimicrobial activity³⁷². Kaempferol was shown to exhibit similar activity (anti-inflammatory, cardio-protective, antitumor and antioxidant)^{373,374}.

Table 2.10| Phenolics, Amines and Flavanoids/Coumarins found in RSP extracts

Extraction technique	SOX		UAE		ASE	
	2012	2014	2012	2014	2012	2014
<i>Harvest year</i>	2012	2014	2012	2014	2012	2014
Benzoic Acids						
<i>p-hydroxybenzoic acid</i>	48.90 ± 1.82	74.89 ± 9.51	27.23 ± 1.56	36.37 ± 1.90	12.08 ± 1.65	17.46 ± 0.64
<i>syringic acid</i>	44.82 ± 2.45	224.2 ± 16.54	20.35 ± 0.71	113.3 ± 8.78	7.52 ± 6.52	73.59 ± 4.22
<i>vanillic acid</i>	41.85 ± 0.79	44.72 ± 2.61	18.29 ± 1.08	16.39 ± 14.21	3.63 ± 6.29	-
<i>protocatechuic acid</i>	32.27 ± 1.51	72.59 ± 1.14	14.66 ± 1.02	35.75 ± 2.15	9.17 ± 1.26	24.20 ± 2.04
<i>salicylic acid</i>	11.47 ± 1.82	14.99 ± 1.72	10.81 ± 0.66	8.24 ± 1.27	7.01 ± 2.58	13.99 ± 1.58

<i>p-anisic acid</i>	-	28.11 ± 3.94	-	-	-	-
Benzaldehydes						
<i>syringin</i>	64.30 ± 4.19	33.58 ± 3.15	10.20 ± 0.87	8.16 ± 0.61	8.23 ± 1.72	8.04 ± 0.60
<i>protocatachaldehyde</i>	54.46 ± 3.56	48.83 ± 1.38	-	-	6.52 ± 0.85	9.65 ± 0.82
<i>vanillin</i>	17.26 ± 1.60	15.08 ± 1.34	-	-	-	-
Cinnamic Acids						
<i>sinapic acid</i>	7496.7 ± 198.89	4896.9 ± 281.68	4610.2 ± 61.59	2769.3 ± 79.64	2682.1 ± 58.02	1923.3 ± 18.45
<i>ferulic acid</i>	226.54 ± 8.37	182.70 ± 9.82	126.48 ± 7.13	91.28 ± 3.85	70.97 ± 2.40	60.92 ± 1.76
<i>cinnamic acid</i>	107.94 ± 11.67	69.59 ± 3.35	68.41 ± 11.10	56.05 ± 2.25	55.41 ± 3.81	84.96 ± 3.24
<i>caffeic acid</i>	97.28 ± 7.26	110.82 ± 9.57	50.00 ± 2.13	61.12 ± 2.61	30.08 ± 0.91	41.24 ± 1.65
<i>p-coumaric acid</i>	46.97 ± 0.89	32.10 ± 2.94	15.69 ± 1.18	15.87 ± 0.45	8.97 ± 0.84	-
Phenylpyruvic Acids						
<i>4-hydroxyphenylpyruvic acid</i>	172.74 ± 43.61	149.77 ± 39.56	160.35 ± 14.50	128.57 ± 5.23	117.88 ± 8.36	161.31 ± 13.54
Other Phenolics						
<i>4-hydroxy 3-methoxy benzyl alcohol</i>	-	0.76 ± 1.32	-	-	-	-
Indoles						
<i>indole-3-pyruvic acid</i>	480.81 ± 80.64	336.05 ± 89.09	630.38 ± 46.73	351.63 ± 33.77	270.97 ± 31.69	311.73 ± 17.77
<i>indole-3-carboxylic acid</i>	17.36 ± 0.23	11.78 ± 0.59	6.01 ± 0.91	4.81 ± 0.20	4.96 ± 0.24	4.42 ± 0.90
Amines						
<i>spermidine</i>	524.93 ± 12.38	433.56 ± 41.44	389.52 ± 22.87	345.30 ± 20.72	408.39 ± 55.54	456.14 ± 82.34

The Potential Application of Rapeseed Pomace Extracts in the Prevention and Treatment of Neurodegenerative Diseases

<i>spermine</i>	2.68 ± 0.57	1.82 ± 0.05	1.97 ± 0.18	1.50 ± 0.21	1.80 ± 0.42	2.21 ± 0.20
Flavanoids/Coumarins						
<i>Kaempferol</i>	123.6 9 ± 100.8 8	22.32 ± 6.92	12.26 ± 3.32	-	-	-
<i>Isorhamnetin</i>	27.89 ± 12.97	7.85 ± 1.30	6.41 ± 0.67	1.26 ± 1.13	4.46 ± 0.19	-
<i>Luteolin</i>	18.75 ± 1.49	44.66 ± 3.43	7.07 ± 0.55	3.16 ± 0.17	4.68 ± 0.45	4.35 ± 0.03
<i>Apigenin</i>	4.78 ± 0.30	2.31 ± 0.42	2.78 ± 0.29	0.19 ± 0.33	0.89 ± 0.09	0.95 ± 0.15
<i>Naringenin</i>	3.53 ± 0.24	2.58 ± 0.25	-	-	0.85 ± 0.13	-
<i>Tangeretin</i>	1.09 ± 0.04	0.93 ± 0.10	0.75 ± 0.19	0.75 ± 0.05	0.61 ± 0.16	0.85 ± 0.12
<i>Quercetin-3-Glucoside</i>	-	6.72 ± 0.81	-	2.44 ± 0.34	2.62 ± 4.53	-
<i>Phloridzin</i>	-	2.09 ± 0.29	-	-	-	-
<i>e-lac</i>	-	-	-	0.51 ± 0.05	0.51 ± 0.05	1.12 ± 0.23
total	9669	6872	6190	4052	3720	3200

Note(s): determined using HPLC-MS/MS analysis, in mg/kg extract (mean) ± standard deviation, excluding compounds found in neither of the samples, HPLC-MS/MS analysis conducted by Garry Duncan (Rowett)

2.3.5 FRAP assay

This assay determines the antioxidant power by the extracts potential of reducing the ferric-tripyridyl triazine complex to the ferrous-tripyridyl triazine complex by electron transfer reaction (Figure 2.6, p.83). This reduction leads to a colour change of the solution, measured at 593 nm³⁰². To verify this absorbance maximum suggested by other papers the absorbance spectrum of different concentration of Trolox, a common reducing agent, as well as a negative control (no reducing agent) were recorded. The results of this study are presented in Figure A1 (p.440); verifying that the absorption maximum is at 593 nm.

Figure 2.12 shows an example of one of the calibration curves obtained for the FRAP assay, using Trolox as standard, because following results of the extracts will be expressed as Trolox equivalents (TE). For all the experiments similar curves were obtained, with R² values above 0.999 for all experiments.

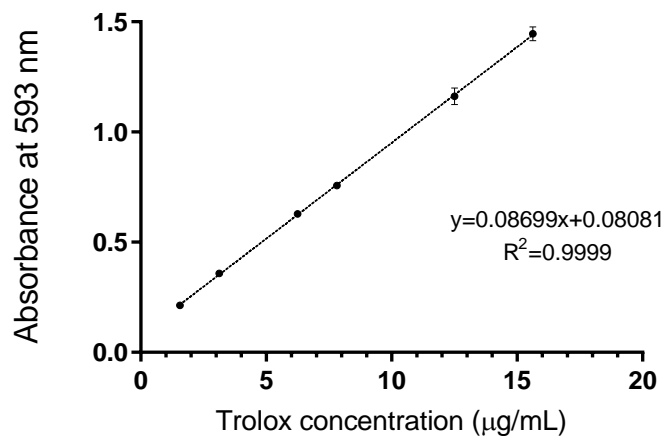


Figure 2.12| Calibration graph example for FRAP assay using 1.56-15.6 µg/mL Trolox

Using the Trolox calibration curves, the FRAP activity in mg TE/g dw RSP extract can be calculated for each of the six extracts. The order of reducing activity in the FRAP assay for all the extracts is similar to the FC assay results obtained previously. SOX gave the best ferric reducing antioxidant power along all the extracts with values of 163.4 ± 3.8 and 172.4 ± 3.8 mg TE/g per dry weight for the 2012 and 2014 sample respectively (Figure 2.13, p. 112).

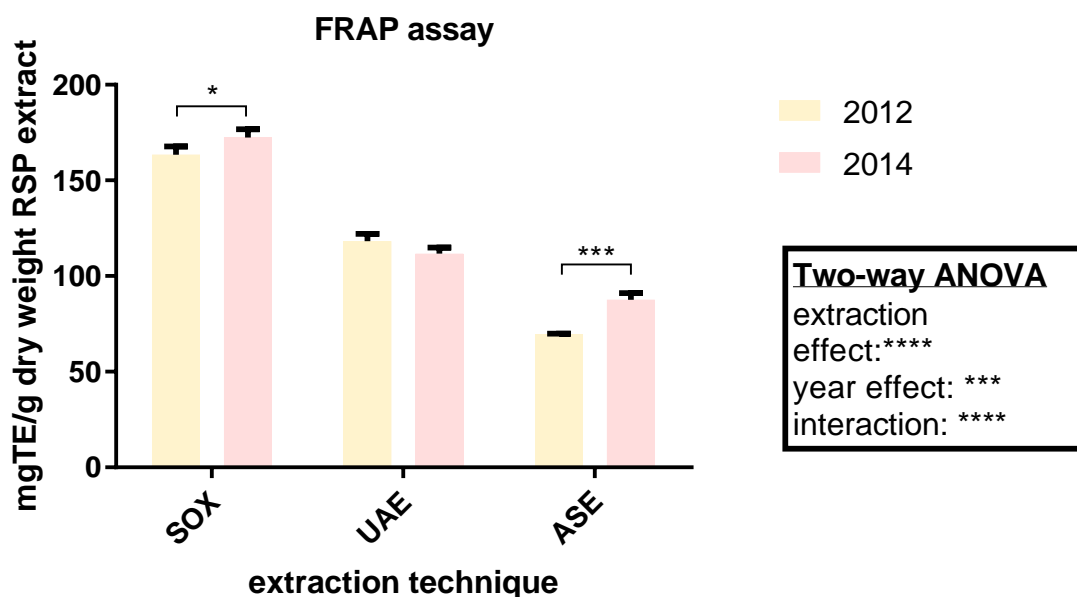


Figure 2.13 | FRAP results in Trolox equivalence per g RSP extract
 Dry weight, significant difference via Two-way ANOVA (box), Bonferroni's multiple comparisons test between years for each extraction technique; $p \leq 0.05^*$, $p \leq 0.001^{***}$

The extraction technique applied showed higher significant differences ($p < 0.0001$) than the harvest year ($p = 0.0002$). However, a significant interaction ($p < 0.001$) is present too as previously seen in the FC assay. The *post hoc* Bonferroni's multiple comparison test showed that the differences between the years are highly significant ($p < 0.0001$) for the ASE. A smaller significant difference ($p = 0.0314$) between the two years is present for SOX, whereas UAE does not show any significant difference between the years. In general, the outcomes from the FRAP assay are similar to the FC assay giving the following order of ferric ion reducing antioxidant power potential: *SOX 14* > *SOX 12* > *UAE 12* > *UAE 14* > *ASE 14* > *ASE 12* (Figure 2.13).

In the FRAP assay (as in the FC assay) not the SOX 2012 extract, with the highest total amount of phenolics (Table 2.10, p.108), but SOX 2014 showed the best reducing capacity. This has led to the assumption that maybe not sinapic acid, the main secondary metabolite, but one of the compounds with higher concentration in SOX 2014 is contributing more to the FRAP and FC activity. Potentially compounds such as p-hydroxybenzoic acid, syringic acid, protocatechuic acid, caffeic acid or luteolin (higher in SOX14) have a more significant impact on the *in vitro* antioxidant activity assays.

When comparing results from the FRAP assay with the methanol extracts of waste and by-products of other plants reported by Wijngaard *et al.*³⁷⁵, the RSP extracts showed very promising results. For example, the SOX extracts showed antioxidant activity 10 times higher than for example kiwifruit, pink grapefruit and apple pomace extracts. Furthermore up to 20 times higher results were obtained when compared to vegetable by-products such as white cabbage cut-offs, cauliflower cut-offs and broccoli stems (methanol extracts)³⁷⁵. In a paper by Szydłowska-Czerniak *et al.*⁹⁰ it was shown that the FRAP and DPPH activity as well as the concentrations of erucic acid and total glucosinolates were dependent on the breed/variety and their origin. Here in our study, the origin for both samples (2012 and 2014) was the same. The rapeseed used in the production of the Mackintosh of Glendaveny rapeseed oil is harvested in the north east of Scotland. However, the breed and the year of harvest were different for both samples and either could have contributed the difference in the FRAP activity.

One disadvantage about using the FRAP assay is the requirement of an acidic pH (3.6) environment; this is far from physiological conditions. A similar assay to the FRAP assay is the CUPRAC, this is done at pH 7.0 and emulates normal physiological conditions better³⁰¹. Just like for the FC assay the FRAP reaction is nonspecific, any compound will cause the reduction of the Fe(III)-TPTZ, if they have a suitable redox potential³¹⁹.

2.3.6 DPPH assay

For the DPPH assay, the IC_{50} values were determined for each sample. The latter is the concentration of the sample required to scavenge half of the number of initial radicals. The lower the concentration needed to scavenge these, the better the scavenging activity of the sample. To verify the absorbance maximum for DPPH at 517 nm³²⁷, absorbance spectra were recorded for the DPPH solution and DPPH reacted with sinapic acid, a well-known antioxidant found in the RSP extracts. The results are presented in Figure A2 (p.440), verifying the absorption maximum at 517 nm.

This wavelength was then used to determine the radical scavenging activity of different concentrations of RSP extract, when in contact with the free radicals of the DPPH solution. Concentrations between 1.3 and 333.33 $\mu\text{g/mL}$ of the extract (e.g. SOX14) showed the decay course of absorbance presented in Figure 2.14 (A). The straight part of this curve, including the 50% mark, was used to determine the IC_{50} via linear regression (B).

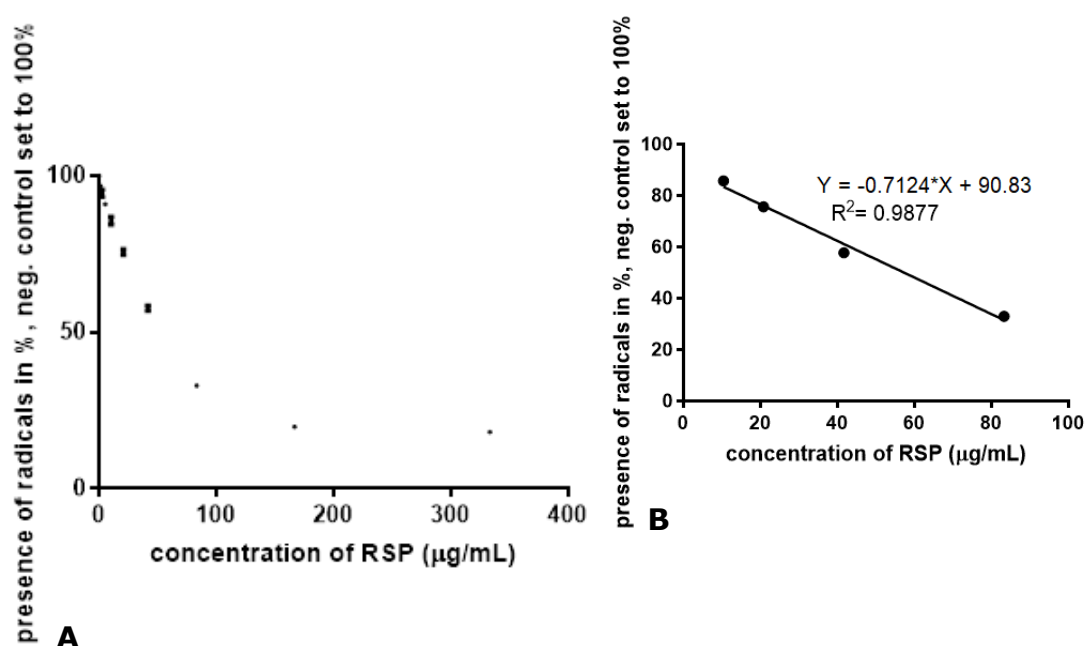


Figure 2.14 | DPPH assay IC_{50} determination

A) representative example of the course of the curve for the scavenging potential of one of the RSP extracts (SOX14) from 333.3 $\mu\text{g/mL}$ down till 1.3 $\mu\text{g/mL}$ B) linear regressing of A) including 50% mark for determination of IC_{50} , Graph Pad Prism

When considering all three extraction techniques, the order of activity determined from the previous antioxidant assays (FC, FRAP) is maintained.

SOX is the extraction technique that gave the extract with the best radical scavenging activity, followed by UAE and ASE (Figure 2.15). The trend related to the harvest year for each extraction technique is also the same as previously identified *via* FC and FRAP assay, given the following order of activity: SOX14 (49.23 ±14.01 µg/mL) > SOX12 (60.09±1.343 µg/mL) > UAE12 (100.9±0.8049 µg/mL) > UAE14 (109.1±2.601) > ASE14 (131.4±4.659 µg/mL) > ASE12 (180.3±16.16 µg/mL).

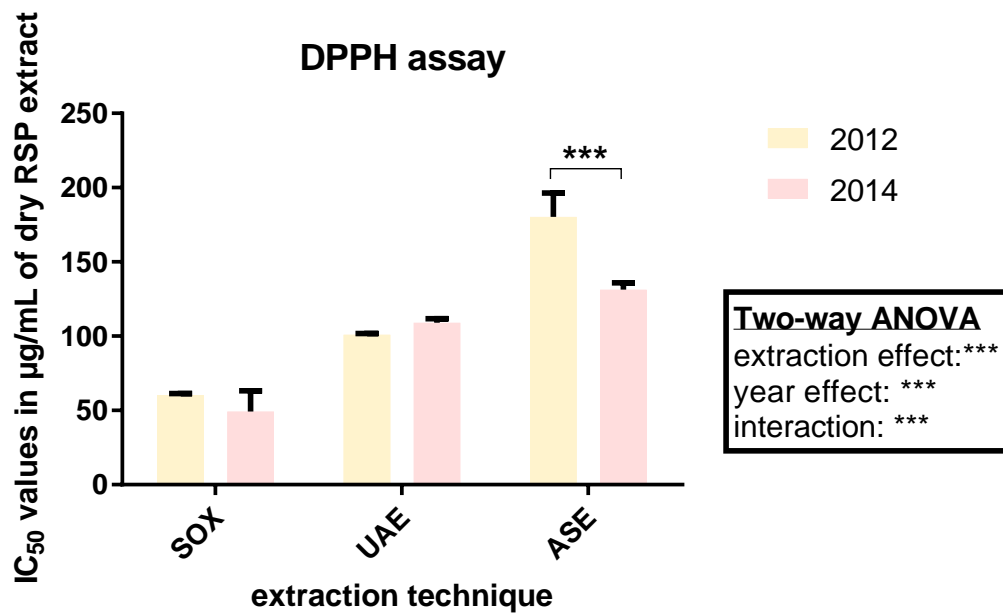


Figure 2.15| DPPH results as IC₅₀ (µg/mL)

Significant difference via Two-way ANOVA (box), Bonferroni's multiple comparisons test between years for each extraction technique; $p \leq 0.001$ ***

Although this assay is commonly used in many laboratories interested in radical scavenging activity, a lack of (i) standardization of the experimental procedures, (ii) sample and DPPH solutions preparation, (iii) reaction conditions and (iv) the expression of the results in different ways makes it difficult to compare results obtained from different laboratories and different plant materials^{310,376}. Szydłowska-Czerniak and Tułodziecka⁵² for example test RS extracts (UAE) in the DPPH assay, but decided to show their results as mmol TE/100g. Radojković *et al.*²⁴⁴ determined IC₅₀ values for the radical scavenging activity of black mulberry leaf extracts showing a range between 10 and 60 µg/mL²⁴⁴. When comparing rapeseed pomace extracts to mulberry leaf extracts, the latter showed better radical scavenging activity than the

RSP extracts. However, the slight differences in experimental set up need to be taken into consideration when comparing results with other research papers. For example in their method description an incubation time of 60 minutes was used, compared to 30 minutes in this project. Although a steady state is expected to be reached after 30 minutes, slight changes could significantly influence the IC₅₀ value determination. Furthermore the authors fail to mention the concentration of DPPH used and also, how the IC₅₀ value was obtained. Another DPPH method, described in more detail by Phani Kumar *et al.*³⁷⁷, uses a similar experimental setup as in this project (30 minutes incubation, 0.1 mM DPPH in methanol). For extracts from *Terminalia arjuna* bark (Indian traditional medicine) they found higher IC₅₀ values ranging between 270±12 µg/mL and more than 500 µg/mL for different extraction solvents. The initial alcoholic extract (ethanol) was carried out using Soxhlet extraction (72h), thereafter the extract was further partitioned using additional solvents³⁷⁷. Having a mixture of solvents might have increased the chances of extracting other groups of secondary metabolites (Table 2.1, p.69), which decreased the concentration necessary to scavenge DPPH radicals.

Another draw back of this assay is that although determination of the IC₅₀ provides valuable input on the stoichiometry of the reaction, it does not provide any information on the kinetics of the reaction, as measurements are undertaken after the steady state is reached (measurement after 30 minutes). Compared to the DPPH radicals that are stable in solution for hours, most physiologically relevant radicals have lifetimes of milliseconds or seconds, only some ROS/RNS e.g. non radicals such as organic peroxides (ROOH), hypochlorous acid (HOCl) or peroxyntrous acid (ONOOH) are slightly more stable^{310,378}. So for the positive activity of radical scavengers within the living system, the number of reactive groups is not as important as the velocity of the reaction. To better understand the reaction kinetics, measurements should be taken continuously starting right after the addition of DPPH to the compound/s of interest. However, not many papers show kinetic analysis and so comparison between different compounds/lab/research projects is not possible. Interestingly, Sharma and Bhat³⁷⁶ reported a kinetic comparison between common antioxidants,

demonstrating an instantant reaction of ascorbic acid. BHT however, reacted relatively slowly. Although they might show a similar absorbance after 30 minutes, their reaction kinetics for the first 30 minutes can be very different (e.g. Figure 2.16)³⁷⁶.

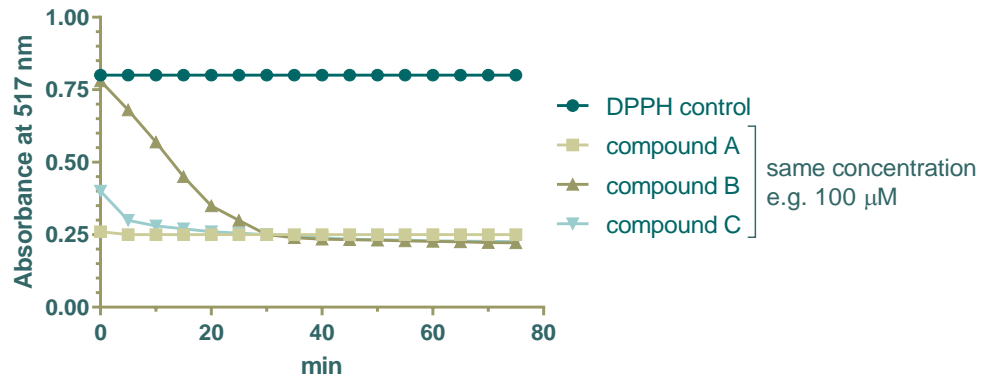


Figure 2.16| Hypothetical reaction kinetic comparison

Compounds A, B and C, with same absorbance at 30 minutes but different reaction times (adapted from Sharma et al.³⁷⁶)

For better explanation a graph is presented in Figure 2.16 above, comparing the reaction kinetics for three hypothetical compounds A, B and C. Although these compounds show the same absorbance at 30 minutes their initial reaction kinetics are very different. Whilst compound A reacts immediately after reaction initiation with DPPH radicals. Compound C in comparison has a slightly delayed reaction but reaches the same absorbance as compound A after about 20 minutes. In contrast, compound B reacts even slower within the first 30 minutes, before reaching the same absorbance as compound A and C. As described before, the reaction velocity however is important, considering the very short lifetime of some radicals. For better comparison of compounds, both reaction kinetics as well as concentration dependent reaction curves should be obtained. In addition, Sharma and Bhat³⁷⁶ also highlighted the lack of standard operation procedures. Unequal DPPH concentration, reaction media and incubation times are used within laboratories, leading to different IC₅₀ values for the same compounds. For better intra and inter laboratory comparison of results, standard operating procedures are necessary, not just for DPPH but also for the FC and FRAP assay.

2.3.7 Correlation of the data from FC, FRAP and DPPH assay

To determine whether there is a relationship between two variables (numerical, continuous) correlation analysis is used. Having a positive value close to 1.0, demonstrates a positive relationship between these two variables. The fact, that the data from the three antioxidant experiments show the same trend in activity of all the samples, would suggest a strong correlation among the three assays used. This was confirmed using correlation analysis as shown in Table 2.11.

Table 2.11 | Correlation between FC, FRAP and DPPH assay

	FC	FRAP	DPPH#
FC	-	0.9987	0.9798
FRAP	0.9987	-	0.9756
DPPH#	0.9798	0.9756	-

Note(s): using the mean activity values for all six extracts via Pearson correlation in GraphPad Prism; #to address the inverted values of the DPPH assay, 1/IC₅₀ values were used for correlation

Obtaining a very high correlation for all the six extracts would suggest that in our case, not all three experiments were necessary to determine the extracts order of antioxidant activity. Similar high correlations were reported by Dudonné *et al.*³³⁰, DPPH and FRAP (R=0.822) followed by FRAP and FC (R=0.906) and DPPH to FC (R=0.939). Here in our case, the correlation between DPPH and FRAP is the smallest with R=0.9756, followed by R=0.9798 (DPPH/FC) and highest for FRAP and FC with R=0.9987. Similar to Dudonné *et al.*³³⁰, also Vergara-Sallinas *et al.*³³⁹ found high correlation among DPPH, ORAC and FRAP, when analysing effect of different temperatures and times of the extraction towards the antioxidant activity of thyme. The high correlation obtained in this project is probably due to the fact that our results are from (i) the same plant species, (ii) are grown in the same region and (iii) involved only a small sample number (n=6). Figure 2.17 shows an example graph for the correlation of FRAP and DPPH, including the equation and the R²-value obtained from the linear regression analysis.

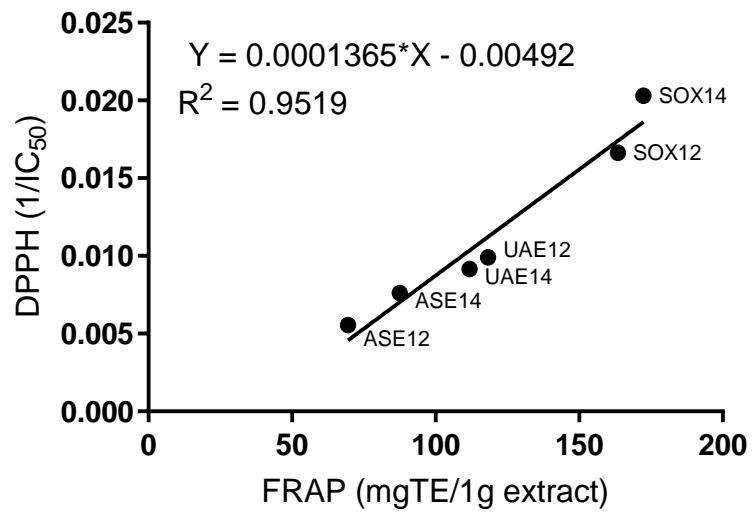


Figure 2.17 | Correlation between FRAP and DPPH assays

Correlation coefficient $R = 0.9756$ (Pearson) and linear regression analysis using GraphPad Prism

2.3.8 Partial least squares analysis of data from the DPPH, FC and FRAP assay

Data review using partial least squares (PLS) analysis was undertaken including secondary metabolite composition and antioxidant activity results (FC, FRAP, DPPH) for both harvest years (2012 and 2014) and the three extraction techniques (SOX, UAE and ASE). A Loadings Bi-plot was created with umetrics software (Figure 2.18). The plot displays similarity and dissimilarity among observations by creating a model of the data (extraction technique (observation), phenolic analysis (variable x) and *in vitro* antioxidant tests (variable y)). The closer the data points, the more likely these variables are affecting each other.

All the results from the three assays (FC, FRAP, DPPH) are in close proximity to SOX2014, showing similarity, with better activity. SOX2014 is closely followed by SOX2012 in proximity to the activity assays. When measuring the distances the following order concerning activity can be classified: *SOX14>SOX12>UAE12>UAE14>ASE14>ASE12*, thus confirming the order previously determined (2.3.3 Folin-Ciocalteu (FC) assay p.105 ff., 2.3.5 FRAP assay p.111 ff. and 2.3.6 DPPH assay p.114 ff.).

In addition, the secondary metabolites found in the extracts were included in the created model. As a result, it is possible to determine metabolites that might be responsible for the activity found for the extracts. Both, vanillic acid and caffeic acid are in close proximity to FC, FRAP and DPPH assay, suggesting their importance for activities found in the extract.

Furthermore, the proximity of metabolites to extracts shows which compounds are found in higher concentrations in certain extracts, e.g. protocatechuic acid is most prevalent in SOX14, whereas the flavonoids apigenin and kaempferol are at the highest concentration in SOX12 (Table 2.10, p.90). In brief the PLS plot creates an overview of the data obtained so far and displays them in connectivity manner. However, it is noteworthy to mention that this is only a statistical theoretical model and the information provided must be used with caution. Just because caffeic acid is found the closest to the antioxidant activity, does not mean that caffeic acid is causing the most activity in practice. An additional drawback is that this model only considers parameters entered into the software, unknown secondary metabolites are not included.

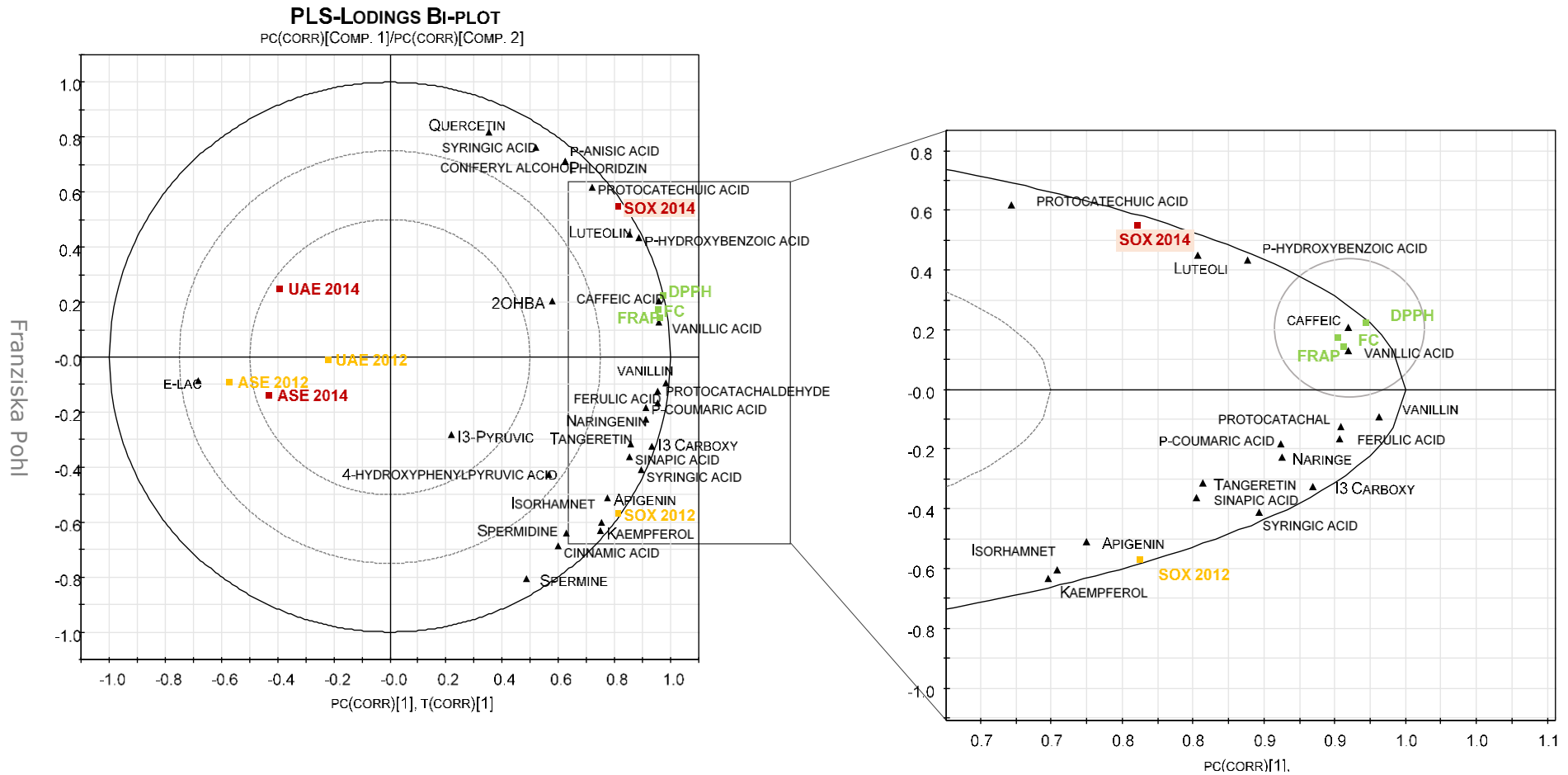


Figure 2.18| PLS plot including the six extracts and their secondary metabolite composition, in relation to their found FC, FRAP and DPPH activity

2.3.9 ORAC assay

After concluding that ASE showed the lowest activity in all antioxidant assays carried out, experiments using these extracts were discontinued and only SOX and UAE extracts were taken further for ORAC analysis.

The ORAC analysis gave mean values of 2825 ± 87 and 2607 ± 212 $\mu\text{mol TE/g dry weight}$ for SOX12 and SOX14 respectively. Lower values of 1729 ± 91 (2012) and 1618 ± 327 (2014) $\mu\text{mol TE/g dry weight}$ were found for both UAEs (Figure 2.19).

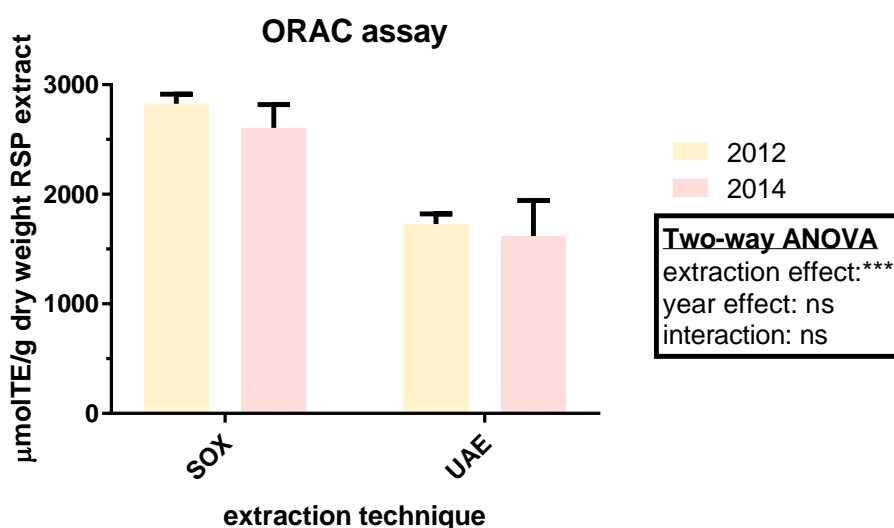


Figure 2.19| ORAC results in $\mu\text{mol Trolox equivalence per g RSP extract}$

*Dry weight, significant difference via Two-way ANOVA (box), Bonferroni's multiple comparisons test between years for each extraction technique; $p \leq 0.001^{***}$*

Two-way ANOVA analysis showed a significant difference between the extraction techniques. However, the harvest year had no effect on the activity. Multiple comparison analysis also showed insignificant differences between the breeds/harvest years (Figure 2.19). All four extracts inhibit and/or delay the probes (fluorescein) oxidation caused by the free radical-generating azo compound AAPH. The latter produces a peroxy free radical upon thermal decomposition (Figure 2.8, p.85) which is commonly found in the body, making this reaction more relevant to biological systems than for example the FRAP or DPPH assay³⁷⁹.

Figure 2.20 shows the kinetic curves obtained for the SOX 2012 extract at different concentrations (0.25-6.25 $\mu\text{g/mL}$), showing clear protection

properties over time, when compared to control (--- 0 µg/mL). Even at low concentration (— 0.25 µg/mL) of the extract partial protection of the fluorescence probe, fluorescein, from the damaged caused by AAPH, is observed (Figure 2.20 --- vs. — curve).

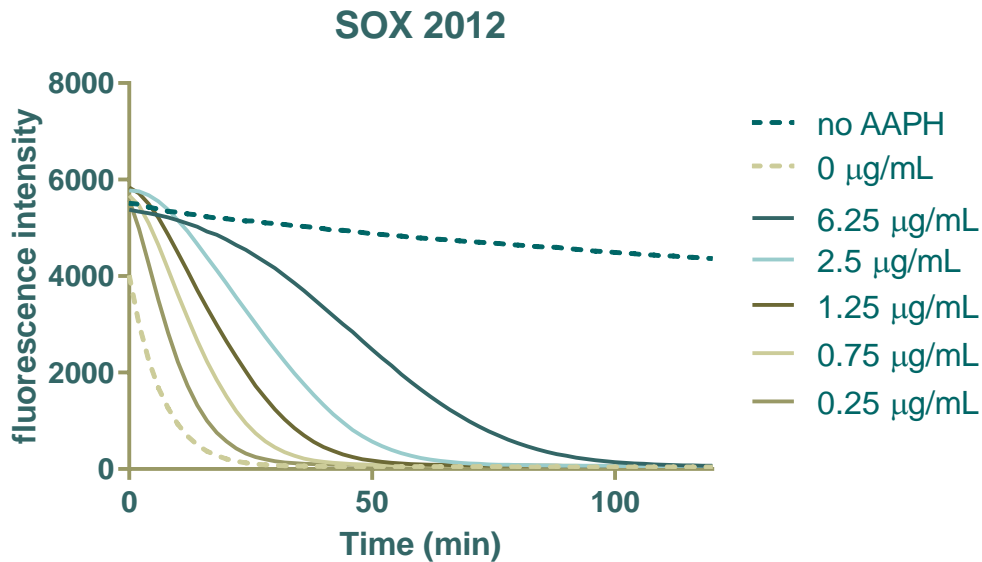


Figure 2.20| Example of ORAC absorbance measurement for SOX2012

Concentrations between 0 and 6.25 µg/mL (final concentration) compared to the fluorescein control (120 min)

The ORAC results obtained for the SOX extraction (>2500 µmol TE/g RSP extract) are about eight times higher than those obtained by Chandrasekara *et al.*³³⁸. The latter reported values between 0.24 ± 0.02 mmol TE/g dw and 0.37 ± 0.06 mmol TE/g dw for canola extracts, extracted using an ethanol/water mix (80:20) and 4 different extraction techniques at temperatures of 60°C or less. The conditions together with the origin of the rapeseed, could have contributed to their lower ORAC activity values.

Although the ORAC assay employs a biological relevant radical source (peroxyl radical, ROO•)¹⁰, it cannot be considered a total antioxidant activity assay. It measures the hydrophilic antioxidant activity of the extracts specifically against peroxyl radicals. To determine the overall antioxidant activity of a sample they would need to be tested against various ROS/RNS in different environments³⁰⁵. A limitation of this experiment is also the need of a more sophisticated plate reader, which can undertake thermostated

fluorescence measurement, compared to the previously described antioxidant assays. Although this assay is mostly seen as more biological relevant due to the radical source created by AAPH, its nutritional relevance has recently been questioned³¹⁹. Seeing the kinetics of the measurement however is very useful to understand the reaction, as shown in Figure 2.20. Amarati and Valgimigli³¹⁹ suggest that determining the AUC mixes both the duration and the efficacy of protection, giving more weight to the former, which might lead to misleading interpretations of the AUC results³¹⁹.

ORAC data collected on food, mostly provided by Wu *et al.*^{380,381} were provided in a data base by the United States Department of Agriculture (USDA) in 2007. However, after the release of a second version, the database was deleted by the USDA due to a couple of reasons described on the USDA web page (<http://www.ars.usda.gov/Services/docs.htm?docid=15866>)³⁰⁹:

- i) evidence indicates that the antioxidant capacity values have no relevance to the effects of the tested compounds, including polyphenols on human health
- ii) the metabolic pathways associated with antioxidants are not completely understood and potential non-antioxidant mechanisms (undefined) might be responsible for the activity
- iii) misused of ORAC values by the food and dietary supplement industry to promote products
- iv) lack of evidence that the positive effects of polyphenol-rich foods are caused by the antioxidant properties

Never the less, new ways of potentially using a number of different reactive oxygen species (ORAC using multiple radical, ORAC_{MR}) are suggested by Prior and Prior *et al.*^{309,382}. These might increase the knowledge obtained from this *in vitro* assay. The potential use of more relevant probes might influence the current opinion on antioxidant assays. Schaich *et al.*³⁴¹ also suggested the replacement of fluorescein with a probe, which does not interact with itself or phenols by non-radical mechanisms. Unfortunately, they fail to provide potential options.

2.3.10 Partial least squares analysis (ORAC)

From the ORAC results of all four extracts (SOX2012/2014 and UAE2012/2014), an additional PLS plot was created, including the secondary metabolites and the ORAC activity (Figure 2.21). In this plot, as well as the last one (Figure 2.18, p.121), SOX extracts are closer to the ORAC activity, suggesting better activity. However, the order of the harvest years is different to the previous three assays (FC, FRAP and DPPH). SOX12 is closer to ORAC than SOX14, followed by UAE12 and then UAE14. This order of activity was also shown in the ORAC results (Figure 2.19, p.122). In contrast to the previous PLS plot (Figure 2.18, p.121) the secondary metabolites closest associated with the ORAC activity are naringenin, vanillin and protocatechaldehyde, followed by vanillic acid and p-coumaric acid. As previously highlighted, this theoretical model only shows indications of potential relation of secondary metabolites to activity in the respective assays. However, it is only a model and any assumptions taken need to be experimentally proven.

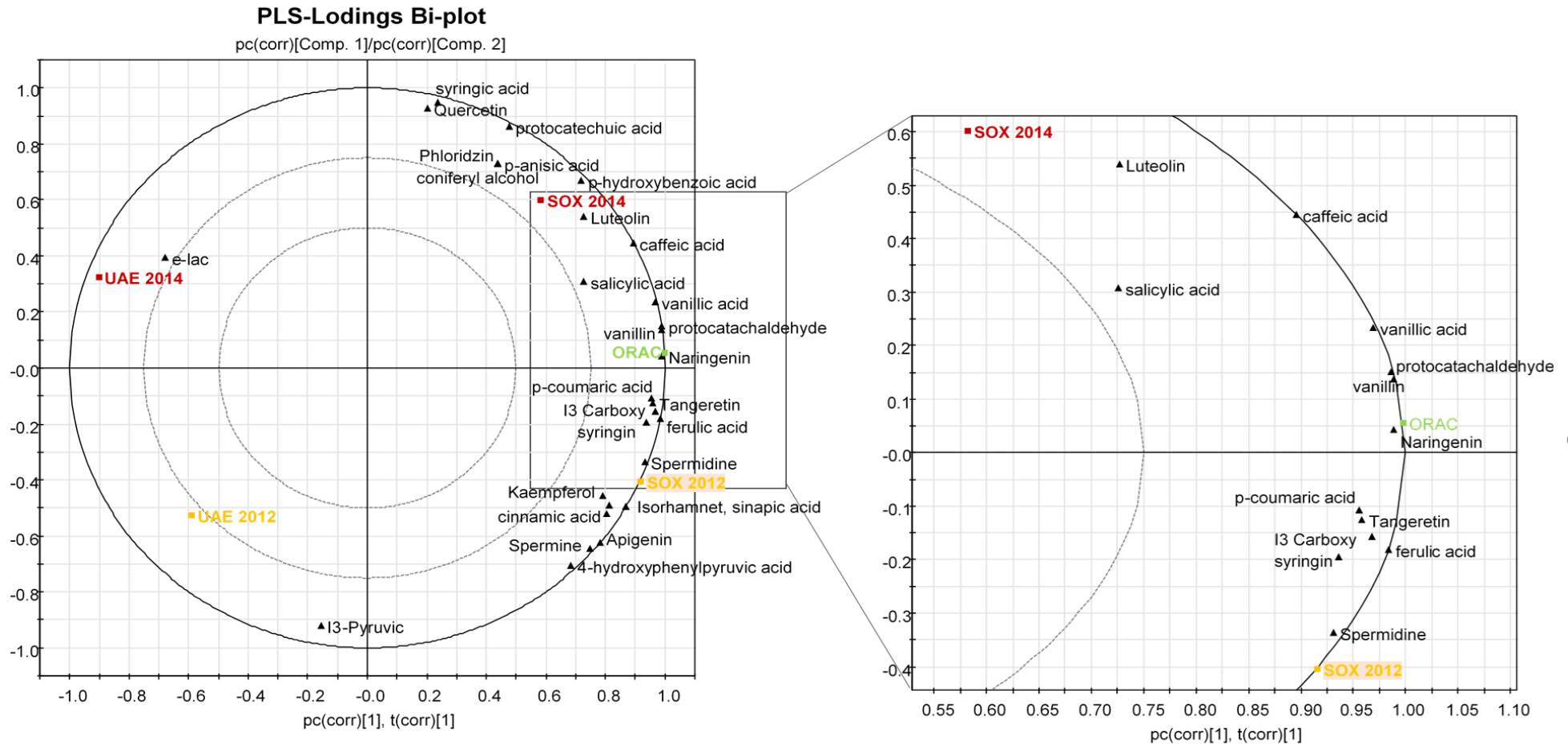


Figure 2.21| PLS plot including the SOX and UAE extracts and their secondary metabolite composition, in relation to their found ORAC activity

2.3.11 Determination of antioxidant activity of single compounds within the extract as well as their mixtures

To determine whether the theoretical models created during PLS analysis are representative for the activity caused by the individual compounds in the *in vitro* assays, seven compounds were chosen and analysed using ORAC, FRAP and DPPH assay, to determine their activity as single compound and to determine whether a synergistic effect contributes to the activity among those chosen compounds.

Two compounds, caffeic acid (CA) and vanillic acid (VA), were selected because they showed close proximity to the FC, FRAP and DPPH activity in the PLS plot (Figure 2.18 p.121). The phenolic aldehyde vanillin (V) and the flavanone naringenin (N) were chosen since they showed more relevance to the ORAC activity in the second PLS graph (Figure 2.21, p.126). Three further metabolites (sinapic-(SA), syringic- (SyA) and ferulic acid (FA)) were also analysed due to their high concentration in the RSP extracts. The RSP extract was analysed in parallel as control. For comparison purposes, initially the single compounds activity, in the FRAP and DPPH assay, was analysed and compared to the RSP extract (Table 2.12)³⁸³.

Table 2.12| Seven single compounds and their FRAP and DPPH activity³⁸³

compound	FRAP (mgTE/g DW)	DPPH IC ₅₀ (µg/mL)	
sinapic acid	1336.95 ± 260.51	4.76 ± 0.84	High abundance in RSP extract (Table 2.10)
syringic acid	2171.47 ± 263.18	2.76 ± 0.51	
ferulic acid	1332.60 ± 7.96	5.11 ± 0.22	
caffeic acid	1908.34 ± 162	2.51 ± 0.52	FC, FRAP, DPPH PLS plot (Figure 2.18)
vanillic acid	344.86 ± 21.3	682.09 ± 180.38	
vanillin	99.69 ± 7.49	1036.58 ± 522.79	ORAC PLS plot (Figure 2.21)
naringenin	0	>3000	
RSP extract	147.54 ± 3.01	61.52 ± 3.10	

Note(s): results obtained in collaboration with Lisa Leyer

The DPPH and FRAP results for the different secondary metabolites showed to be diverse. The three compounds selected due to their high abundance in

the extract (SA, SyA, FA) showed high activity in both FRAP and DPPH assay. Although they are situated further away from the activity assays in the PLS plot than CA and VA. CA, which showed the second best activity of the tested compounds in the FRAP and the best results in the DPPH, was suggested to be an active compound by its close proximity to the assays (Figure 2.18, p.121). However, VA, also suggested to have the potential for high activity in the PCA plot, showed to be less active than SA, SyA and FA in both assays. In a similar study, Mudnic *et al.*³⁸⁴ looked at FRAP activity of hydroxybenzoic acids (HBA); p-hydroxybenzoic-, protocatechuic-, vanillic-, gallic- and syringic acid as well as hydroxycinnamic acids (HCA); p-coumaric- caffeic-, ferulic- and sinapic acid (Figure 2.22).

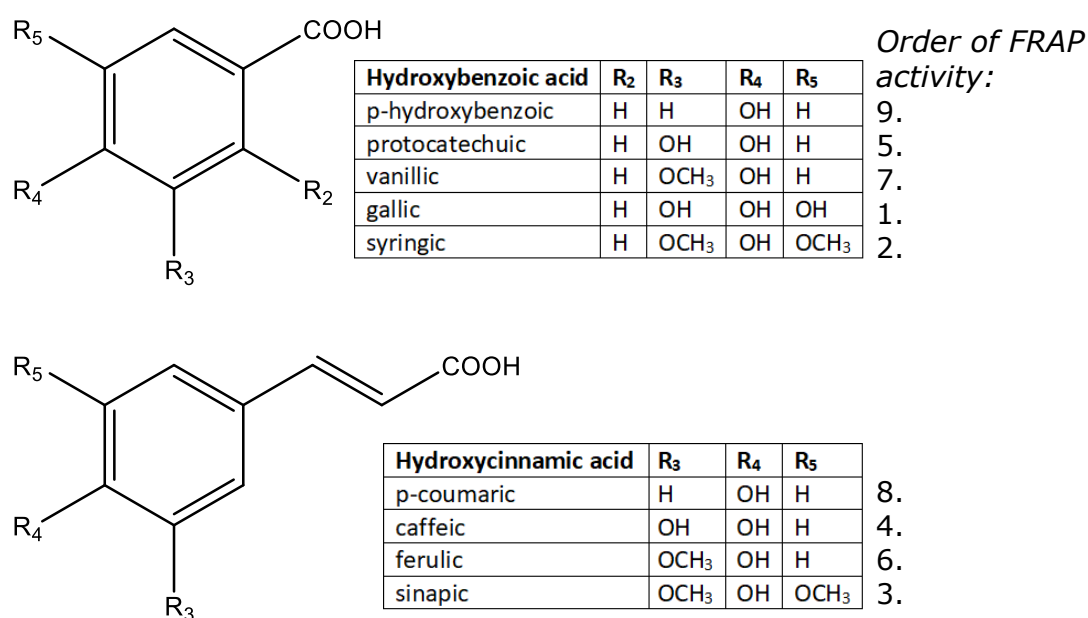


Figure 2.22| HBA and HCA analysed in Mudnic *et al.*³⁸⁴ for their FRAP activity

For comparison of results, compounds analysed in both studies are shown in Table 2.13 with their respective order determined in both studies. Included in this table are the allocations of the compounds to their respective HCA/HBA group. Comparing both, no general conclusion can be drawn on whether HBA or HCA perform better in this assay. More important seems to be the number of -OH or -OCH₃ groups present in HBA and HCA. Gallic-, syringic- and sinapic acid which all have three -OH or OCH₃ groups show the best activity. This is followed by caffeic-, protocatechuic-, ferulic- and vanillic acid which have two of these sidechains, whereas both p-coumaric- and p-hydroxybenzoic acid

each only have one. Although both groups impact the activity, when comparing compounds with the same number of R's, the ones with a higher number of –OH groups are better than the ones with more –OCH₃ e.g. gallic acid compared to syringic acid. Already in 1996 Rice-Evans *et al.*³⁸⁵ suggested the importance of hydroxyl groups in phenolics and flavonoids antioxidant activity. However, Mudnic *et al.*³⁸⁴ as well as this study shows that the number of hydroxyl as well as the number of methoxy groups are important, e.g. syringic vs. protocatechuic acid.

Table 2.13| Comparison of FRAP activity of single phenolics found in this study and Mudnic *et al.*³⁸⁴

compound	HBA/HCA	Mudnic <i>et al.</i> [mmol/L TE]	Order in Mudnic <i>et al.</i>	Leyer and Pohl (Table 2.12)
Syringic acid	HBA	1.47	1.	1. =
Sinapic acid	HCA	1.26	2.	3. ↓
Caffeic acid	HCA	1.11	3.	2. ↑
Ferulic acid	HCA	0.99	4.	4. =
Vanillic acid	HBA	0.37	5.	5. =

Sevgi *et al.*³⁸⁶ also analyses a number of selected phenolic acids, including caffeic-, ferulic-, syringic- and vanillic acid. Their order of activity for both DPPH radical scavenging and reducing power deviate from this study and Mudnic *et al.*'s³⁸⁴ results. In their study caffeic acid shows the best activity in both assays. Variations found between their activities are very minor in Sevgi *et al.*³⁸⁶ Differences between their and this study could be due to the different ways of calculating results and experimental set up.

During our study we also analysed V and N due to their proximity to the ORAC assay in the PLS plot (Figure 2.21, p.126). V, thus much closer situated to the activity in the plots than e.g. SyA, showed lower activity. Also, N showed very little or no activity in either assay, although close in proximity to e.g. FA in the PLS plot (Figure 2.18, p.121). Out of the seven individual compounds tested, only naringenin did not exhibit any activity in the FRAP assay. This was also observed by Csepregi *et al.*³²⁸ who reported a value of 0 myricetin-3-Oglucoside equivalents. Those results show that the PLS analysis can give an initial indication of potentially active compounds, as found with caffeic acid however it is advised to verify theoretical models like the PLS analysis using the same *in vitro* experiment.

To assess the contribution of these compound to the extracts activity the concentrations present in the extract were measured in FRAP, DPPH and ORAC. At the test concentrations, none of the compounds showed any significant activity. To investigate a potential synergistic effect, mixtures were prepared (Table 2.14), containing the same concentrations of metabolites found in the extract.

Table 2.14| Mixtures of secondary metabolites created for analysis of their antioxidant and radical scavenging activity and the determination of potential synergistic effects³⁸³

MIXTURE	COMPOSITION
A	SA, SyA, FA, CA, VA, V, N
B	SA, SyA, FA, CA, VA, V
C	SA, SyA, FA, CA, VA
D	SA, SyA, FA, CA
E	SA, SyA, FA
F	SA, SyA
G	SA

Note(s): results obtained in collaboration with Lisa Leyer

The six mixtures and SA were then analysed using FC, FRAP and DPPH assay to determine their activity and potential synergistic effects. The results obtained for the absorbance/fluorescence were very close the negative control. No significant contribution of these mixtures of compounds at the extract specific concentration was observable³⁸³.

These results suggested, that the secondary metabolites tested here are not responsible for the *in vitro* antioxidant activity observed in the RSP extract. There are a few potential reasons for this outcome:

- (i) One of the other known compounds of lesser concentration (Table 2.10, p.108) is responsible
- (ii) A number of other known compounds (Table 2.10, p.108) work in synergy with either the tested compounds (Table 2.14, p.130) or other unknown compounds to cause the activity
- (iii) There are other secondary metabolites in the extract, which have not yet been identified responsible for the activity, either by themselves or in synergy with known/unknown compounds

2.4 Conclusion/Future work

All six RSP extracts obtained throughout this initial study of extraction techniques and antioxidant activity, have shown to be active in the FC, FRAP and the DPPH assay. However, taking all six extracts further in this study was not possible. Thus, the results obtained in this chapter, allowed the selection of SOX extraction as the method of choice for subsequent experiments discussed in later chapters of this thesis. All the *in vitro* assays show that the SOX extraction method demonstrated the best antioxidant activity that was substantiated in both PLS plots. In addition, the SOX extracts also demonstrated better activity in the ORAC antioxidant assay. Using a preliminary defatting step during this extraction method created an easily workable starting material for further investigation. The results obtained for the Soxhlet extraction for both years (2012 and 2014) were published in Pohl *et al.* 2018³⁵³.

The decision of the harvest year was reached after detailed observations of the results obtained as well as considering handling and storage circumstances. SOX2014 showed significantly higher results for the FRAP assay as well as slightly better results for the FC and DPPH assay. The lower activity of the SOX2014 extract for the ORAC assay was found to be non-significant. In addition, the HPLC-MS/MS analysis demonstrated a similar general secondary metabolite composition for both harvest years. Furthermore, the 2014 pomace was obtained within the first couple of months of this project. On arrival, the pomace was freeze dried and stored at -80°C (long term storage). The process after the arrival of the 2012 harvest was not clear. The impact of the longer storage time of the 2012 harvest was also considered. All these factors led to the decision to continue research with the RSP from 2014.

Besides, the study showed, that the compounds suggested to be responsible for the extract's *in vitro* activity by the PLS plots were not responsible for the found activity of the RSP extract. Further research into the extract's composition could lead to the identification of the responsible compounds. Literature research suggests the presence of e.g. sinapine and other phenolic compounds^{88,110}, canolol¹⁰⁸, glucosinolates⁹⁹, tocopherols¹⁰², phytosterols¹⁰⁶ and phospholipids³⁸⁷. That is why the following chapter will focus on determining

the reproducibility of the SOX extraction technique and the further characterisation of the final extract, including glucosinolate, anthocyanin and sinapine analysis. In addition, further *in vitro* studies looking into the extract's potential in the prevention or treatment of neurodegenerative disease will be shown.

To optimise the extraction of phytochemicals on the one hand other extraction techniques could be tested such as described in Table A1 (p.424). On the other hand different solvent combinations and ratios³³⁸, extraction temperature and time³⁸⁸ and the solid to solvent ratio²⁶¹ will have an effect on the extraction efficiency as well as the composition of the extract and should be optimised for the RSP. Further research into the Soxhlet extraction technique should consider eliminating the petroleum ether extraction, as the latter solvent is not environmentally friendly. However, this might lead to a less dry end product, such as seen for the UAE and the ASE extraction, where no de-oiling was undertaken. Hence, if the elimination of this de-oiling is not possible, the Soxhlet equipment should be used to its capacity and the solvent collected at the end of the run reused, after verifying that this has no impact on the de-oiling procedure. By re-using the solvent, the environmental impact of the Soxhlet extraction could be decreased. When changing the extraction technique or the solvent composition, a parameter for optimization of extraction needs to be chosen. Here we used the *in vitro* antioxidant activity as a read out, however this might not be the optimal read out, other parameters, such as *in vivo* activity or the concentration of a certain secondary metabolite might be more appropriate depending on the further use of the extract. In addition, further research should also consider the analysis of the leftover product after the initial Soxhlet extraction. This powdery material might still contain valuable components e.g. proteins which can add additional value to the product.

3

PHYTOCHEMICAL CHARACTERISATION AND NEUROPROTECTIVE PROPERTIES OF RSP EXTRACT *IN VITRO*

Contents

3.1 Introduction	134
3.1.1 Determination of additional secondary metabolites in the RSP extract	
3.1.2 Metal chelating properties	
3.1.3 Acetylcholinesterase (AChE)/Acetylcholinesterase inhibitors	
3.1.4 Inhibition of self-mediated β -amyloid (1–42) aggregation	
3.1.5 DNA protection	
3.1.6 Objectives	
3.2 Materials and Methods	155
3.2.1 Chemicals and Equipment	
3.2.2 Methods	
3.3 Results and Discussion	167
3.3.1 Extraction replicates differences in FC, FRAP and DPPH	
3.3.2 Antioxidant activity of final RSP extract	
3.3.4 Additional secondary metabolite analysis	
3.3.5 Metal chelating potential	
3.3.6 AChE inhibition potential	
3.3.7 Inhibition of self-mediated β -amyloid (1–42) aggregation	
3.3.8 Inhibition of supercoiled plasmid DNA strand breakage	
3.4 Conclusion/Future Work	205

This chapter will cover the characterisation of the final extract (SOX2014), determining a number of different secondary metabolite groups, including phenolics, glucosinolates and anthocyanins. In addition, results for in vitro chemical activities, such as antioxidant-, metal chelating-, acetylcholinesterase inhibition-, self-mediated β -amyloid (1–42) aggregation inhibition and plasmid DNA protective activities will be presented.

3.1 Introduction

The following chapter is focused on the chemical characterisation of the final chosen RSP pomace extract. As determined in the previous chapter, SOX extraction was the chosen extraction technique and the RSP from 2014 was used for the extraction. Initially the repeatability of the extraction technique was assessed on three independent extracts based on their *in vitro* activity (FC, FRAP and DPPH). This helped to determine whether a bulk extraction of the RSP would be necessary for a more homogeneous extract. A final characterisation using DPPH, FC, FRAP, ORAC and LC-MS/MS (chapter 2) analysis, for the previously analysed secondary metabolites, was undertaken, to characterise the final extract.

3.1.1 Determination of additional secondary metabolites in the RSP extract

For the last decade, interest in rapeseed secondary metabolites has increased. A large number of papers recently reported the analysis of secondary metabolites^{81,112,353} and biological/chemical activity of rapeseed, RSP, RSP extracts or respective single metabolites found in rapeseed^{76,111,353,366,389}. Those reports suggested the presence of phenolics, such as sinapic acid, caffeic acid, ferulic acid and others which agree with our data described in chapter 2. Furthermore, other secondary metabolites have been reported in the *Brassica* plant, these include sinapine (a choline ester of sinapic acid), sinapic acid derivatives, other phenolics^{99,110,113,390} and glucosinolates^{99,391}. The characterisation of these metabolites from the RSP extract formed the basis of this chapter (3.1.1.1 Sinapine and additional phenolic derivatives, p.135 and 3.1.1.2 Glucosinolates (GLSs), p.136). A further group of secondary metabolites often cited for their positive antioxidant activity is the anthocyanins. The latter are flavonoids, mostly associated with causing red/blue colours in fruits, vegetables and other plants/plant parts. As RSP does not show the indicative colour, the anthocyanin content has not been of great interest so far but will however be part of this investigation (3.1.1.3 Anthocyanins, p.140).

3.1.1.1 Sinapine and additional phenolic derivatives

In the last few years, sinapic acid and its derivatives such as syringaldehyde, sinapoyl ester, 4-vinylsyringol and sinapine have received increase attention due to their various biological activities⁹⁶. Sinapine (sinapoyl choline) for example is known to be present in the *Brassicaceas/Cruciferae* plant family, to which rapeseed/canola belongs to. It was first isolated by Henry, Fils and Garot in 1825³⁹² from black mustard seeds and named sinapine, but its chemical structure was not proposed till 1897³⁹³. Sinapine has been reported to be the most abundant phenolic ester in rapeseed^{92,110}. It is produced in the plants through the shikimate/phenylpropanoid pathway and accumulates in brassicaceous plants together with a number of sinapate esters of flavonol glycosides, glucose and gentiobios^{40,110,394,395}. In the past, breeding programs had aimed to decrease the content of these metabolites in *Brassica napus*, due to their associated anti-nutritive properties³⁹⁵.

In many Asian countries research on sinapine has received much attention due to its significant biological activity. Brassica plants such as turnip (*Brassica rapa var. rapa L.*) and mustard (*Brassica juncea*), or parts of these, contain significant amounts of sinapine^{396,397} and are known to be used in Tibetan or Traditional Chinese Medicine³⁹⁶. Sinapine is also considered an acetylcholinesterase inhibitor due to structural similarity to acetylcholine (Figure 3.1)³⁹⁸.

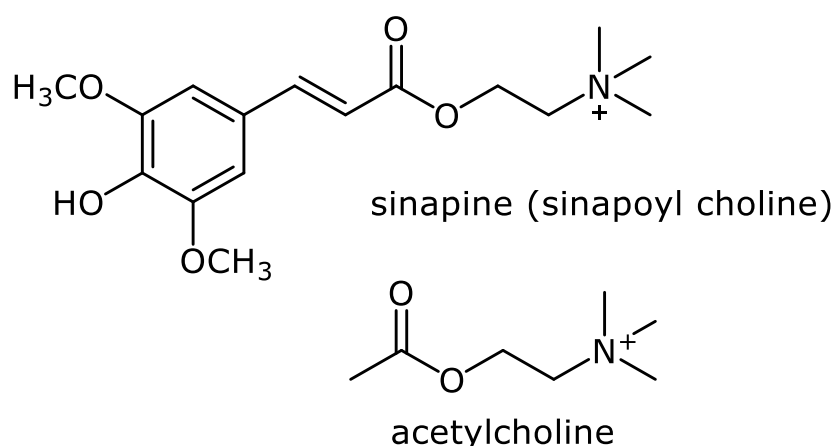


Figure 3.1| Chemical structure of sinapine in comparison to acetylcholine

The patent "Use of sinapine in preparing medicine for preventing and curing senile dementia" (CN1259045C, language Chinese), granted in June 2006,

demonstrated the AChE inhibiting potential of sinapine³⁹⁹. Another Chinese patent application (CN105732402A) described the preparation of sinapine thiocyanate from rapeseed cakes and suggested its application in AD, due to its AChE inhibition activity⁴⁰⁰. He *et al.*⁴⁰¹ (only abstract available in English) reports the compounds activity in cerebral homogenate and blood serum of rats with IC₅₀ values of 3.66 and 22.1 µmol/L respectively and suggests sinapine's potential for the prevention and cure of Alzheimer's disease⁴⁰¹. Apart from AChE inhibition activity, sinapine present in *Brassica rapa var. rapa* L., had shown hepatoprotection in CCl₄-induced hepatotoxicity mice models³⁹⁶. In a PC12 (rat pheochromocytoma) hypoxia damage model, sinapine showed protection from Na₂S₂O₄-induced apoptosis and mitochondrial transmembrane potential disruption. Furthermore, it decreased malonaldehyde (MDA) production and lactate dehydrogenase (LDH) leakage⁴⁰². Sinapine was also able to increase maximum, average and median life spans of *Drosophila melanogaster* at 10 and 50 mg/L concentrations⁴⁰³. The immense research undertaken in the Asian countries shows the potential importance of sinapine to human health.

Other secondary metabolites of interest are for example 1-O-β-D-glucopyranosyl sinapate as this was found to be the most active antioxidant metabolite in canola meal³⁴⁴. A vast number of other phytochemicals have also been identified in rapeseed; including derivatives of some of the secondary metabolites determined in the rapeseed as described in Chapter 2 e.g. kaempferol, quercetin and ferulic acid^{101,110,404-406}. To analyse the additional secondary metabolites in the RSP extract, LC-MS/MS analysis will be employed.

3.1.1.2 Glucosinolates (GLSs)

Glucosinolates (GLSs), sulphur-containing secondary-metabolites are characteristic for *Brassica* plants such as rapeseed/canola. They all share a β-thioglucoside N-hydroxysulfate configuration with a variable side-chain derived from amino acids¹⁰¹. Glucosinolates are known to be present in at least 15 botanical families of the order Capparales including Brassicaceae⁴⁰⁷. When GLSs are exposed to hydrolytic enzymes such as myrosinase (β-thioglucosidase) after tissue disruption, such as cutting, processing (pressing) or chewing, their breakdown leads to products such as

isothiocyanates, thiocyanates or nitriles that act as repellents towards generalist herbivores (Figure 3.2)⁴⁰⁷⁻⁴⁰⁹.

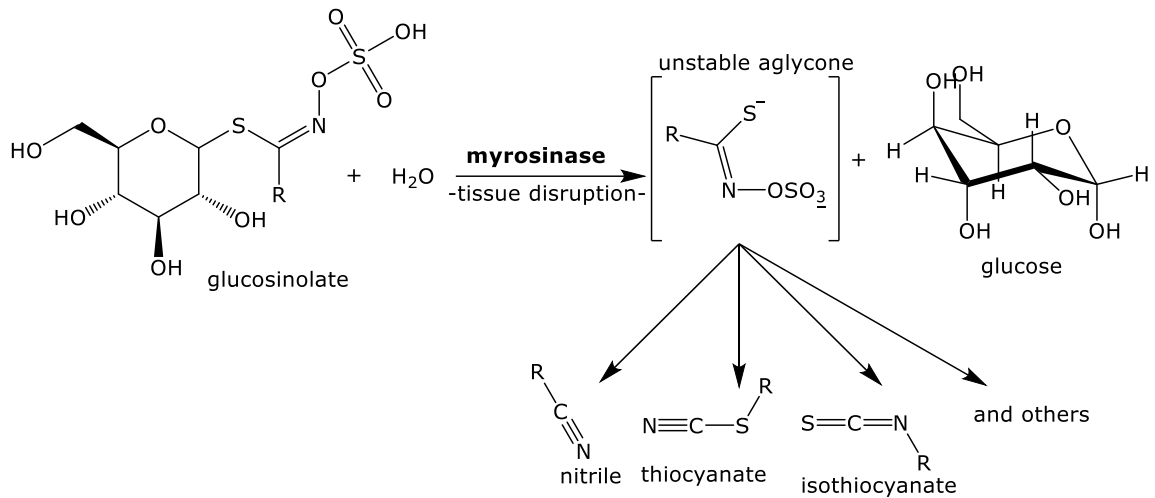


Figure 3.2| Glucosinolates basic structure

Side chain -R depending on specific glucosinolate and their products after myrosinase hydrolysis (adapted from^{409,410})

The content of GLSs in rapeseed depends on the presence of certain nutrients (nitrogen and sulphur) in the growing environment⁴¹¹. In general, they account for between 3-8% of rapeseed meal in conventional cultivars, or 0.5-1.0%, in low-GLS cultivars⁹⁹. Just like sinapine, GLSs were undesirable due to their anti-nutritional properties, which prompted the creation of low-GLS cultivars⁹⁰. However, positive biological activities have been identified for some isothiocyanates. Sulforaphane for example, which is produced in *Brassica* plants by the enzymatic reaction between glucoraphanin (GRa, Figure 3.3, p.139) and myrosinase, was shown to activate Nrf2 (redox sensitive transcription factor) that once activated, induces a number of phase II drug metabolising enzymes (Figure 1.29 p.60)⁴¹². A review by Giacoppo *et al.*⁴¹³ presents further data on the neuroprotective effects of isothiocyanates for the treatment of neurodegenerative disease. Hence, in recent years, researchers have attempted to selectively increase certain GLSs in rapeseed such as glucoraphanin, the precursor for the isothiocyanate sulforaphane⁴⁰⁷. Although myrosinase is a plant specific enzyme, GLSs can be hydrolysed at a much lower rate by thioglucosidase enzymes⁴¹⁴ or bacteria found in the gut flora^{415,416}, which can lead to the presence of isothiocyanates in the gut, even in the absence of myrosinase.

The glucosinolate-myrosinase system, in conjunction with the break down products, found in rape and other Brassica species is a well-studied chemical defence systems against herbivores and fungi⁹⁹. However, very little has been reported about the biological activities and advantages of GLSs themselves. A review by Vig *et al.*⁴¹⁷ summarised their biocidal, bioherbicidal, antimutagenic, antiproliferative and indirect antioxidant activity caused by their hydrolysis products. A number of different glucosinolates have previously been identified in the seeds of the rapeseed plant, and these include (i) progoitrin; (ii) epiprogoitrin; (iii) glucoraphanin; (iv) gluconapoleiferin; (v) glucoalyssin; (iv) gluconapin; (vii) 4-hydroxyglucobrassicin; (viii) glucobrassicinapin; (ix) glucoerucin; (x) glucoberteroin; (xi) gluconasturtiin and (xii) neoglucobrassicin⁹⁹⁻¹⁰¹. Figure 3.3 shows structures of the 11 GLSs analysed in this study. HPLC analysis with external GLS standards will be used to detect and quantify GLSs present in the RSP extract.

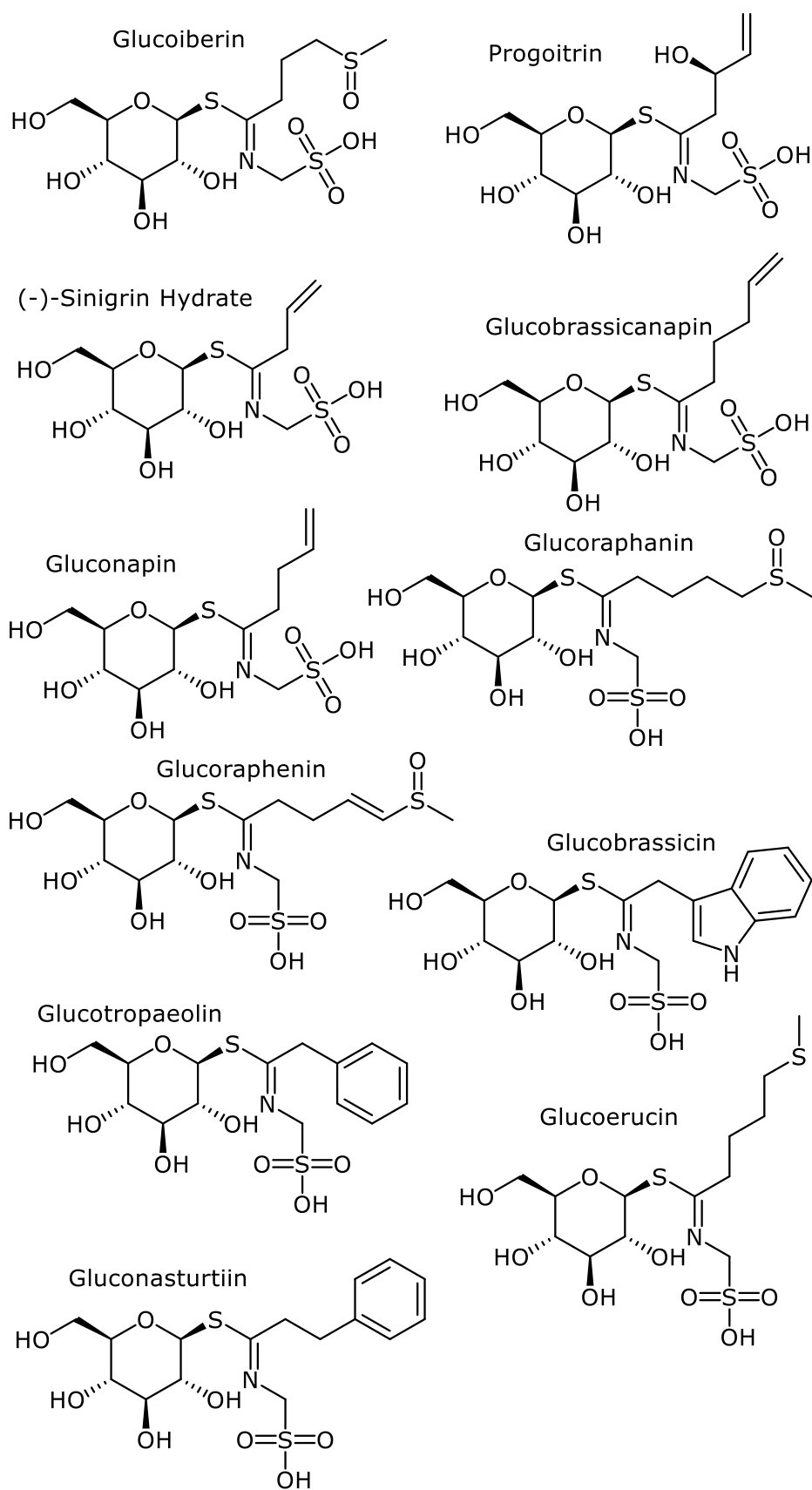


Figure 3.3| 11 glucosinolates commonly present in *Brassica* plants analysed in this study

3.1.1.3 Anthocyanins

Anthocyanins (Figure 3.4), a subclass of flavonoids, can be found in 27 plant families, including the Brassicaceae family and the Brassica genera. They are most abundant in red/purple/blue coloured flowering plants as well as coloured vegetables and fruit, such as berries, black grapes and red cabbage⁴¹⁸. The disease preventing properties of anthocyanin-rich extracts have been well documented for both *in vitro* and *in vivo* models and they are as follows: (i) antioxidant; (ii) anti-mutagenic; (iii) anti-inflammatory; (iv) anti-neurodegenerative and (v) anti-aging^{419,420}. The most common anthocyanins in plants are pelargonidin, peonidin, cyanidin, malvidin, petunidin and delphinidin⁴¹⁸.

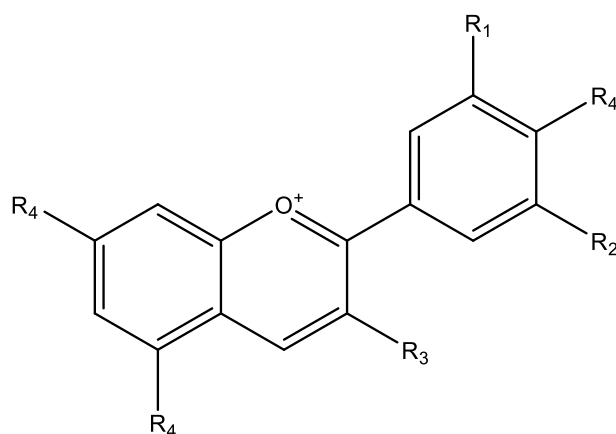


Figure 3.4| General structure of anthocyanins (flavylium cation)

*R*₁ and *R*₂ can be H, OH or OCH₃; *R*₃ a glycosyl or H and *R*₄ a glycosyl or OH, adapted from Kong et al.⁴¹⁸

Anthocyanins have been reported in many different Brassica plants such as *Brassica oleracea var capitata* (red cabbage)⁴²⁰, *Brassica campestris var. chinensis* (Beninabana)⁴²¹, *B. oleracea L. var. botrytis* (violet cauliflower)⁴²² and *Brassica juncea* Coss variety (red mustard greens)⁴²³. However, anthocyanin content in *Brassica napus* has not been widely published. The only papers available were those investigating the potential increase of anthocyanin content in genetically modified rapeseed. Those papers showed an insignificant amount of anthocyanin in the unmodified plants. However, those analysis were done on the leaves rather than the seeds^{424,425}. Limited data on the anthocyanin content of RSP extracts had therefore prompted us to analyse the anthocyanin content of RSP extract in this project. The analysis

of the presence of anthocyanin can initially be undertaken spectroscopically using the pH differential method. The latter method was first proposed by Fuleki and Francis in 1968⁴²⁶. It is based on a pH dependent colour change of anthocyanins (Figure 3.5). At a low pH of 1.0, anthocyanin pigments are brightly coloured (oxonium form, pink). In contrast, at pH 4.5 these pigments turn colourless (hemiketal form). In the presence of any anthocyanins in the extract, a colour change from colourless to pink is anticipated at pH 1.0, with a maximum absorbance at a wavelength of 520 nm²⁹⁵.

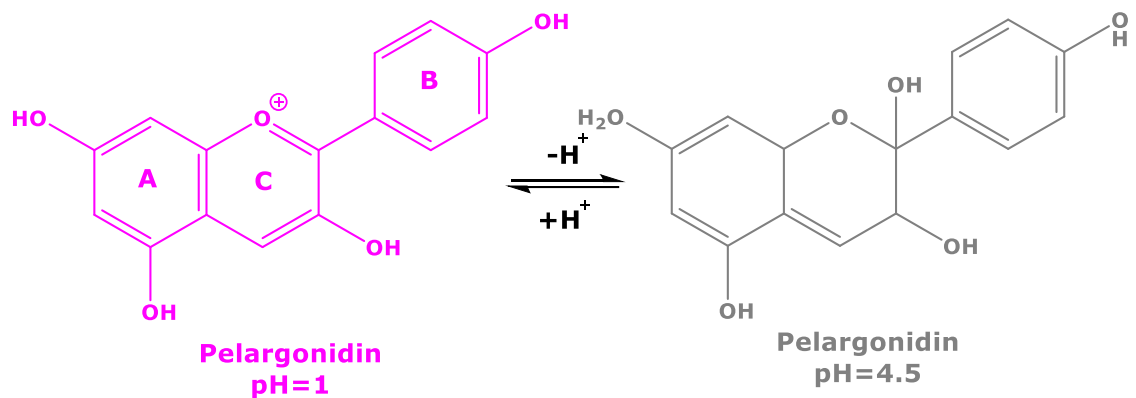
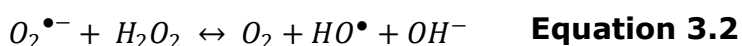
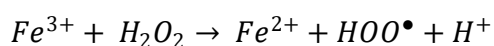
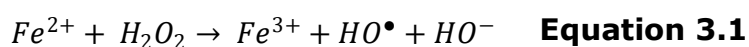


Figure 3.5| Chemical reaction of the colour change expected for the anthocyanin Pelargonidin (adapted from²⁹⁵)

3.1.2 Metal chelating properties

Redox-active metals, such as Iron (Fe^{2+}) and Copper (Cu^{2+}) have important functions within the human body. Iron for example participates in several biochemical reactions, such as DNA, RNA and protein synthesis. It is also a co-factor for certain enzyme reactions (e.g. heme synthesis) and contributes to the synthesis of myelin which is necessary for normal brain function⁴²⁷. Copper on the other hand is just as important; it is a co-factor and structural component of numerous enzymes involved in essential cellular processes including energy metabolism, antioxidative defence, iron metabolism, neuropeptide and neurotransmitter synthesis^{428,429}. Dis-homeostasis of iron and copper can lead to severe disorders e.g. Copper: Menkes disease, Wilson's disease⁴²⁸; Iron: Iron deficiency⁴³⁰. Impaired metal homeostasis has also been associated with a number of neurodegenerative diseases, such as PD, AD and ALS⁴³¹. An increase in either Fe^{2+} or Cu^{2+} can lead to higher oxidative stress caused by the generation of free radicals *in vivo* via the Fenton (Equation 3.1) and Haber-Weiss reactions (Equation 3.2)



Metal chelators have shown improvements in *in vitro* and *in vivo* models of neurodegenerative disease. In an AD mouse model for example the metal chelators clioquinol reduced the amount of amyloid deposits in the brain⁴³². Desferrioxamine, one of the earliest iron chelators has shown promising results in PD animal model studies, using MPTP (1-methyl-4-phenyl-1,2,3,6-tetrahydropyridine) as inducer of neurodegeneration, by inhibiting iron accumulation while elevating dopamine to normal levels⁴³³. Metal chelating activity together with the known antioxidant activity of the extract could add to the extract's potential to prevent neurodegeneration.

In a paper by Santos *et al.*²³² high-throughput assays for the determination of iron and copper chelating properties were proposed. The iron chelating activity assay employs ferrozine (3-(2-pyridyl)-5,6-diphenyl-1,2,4-triazine-*p,p'*-disulfonic acid monosodium salt hydrate) for the detection of chelating properties, which was first introduced by Carter⁴³⁴. In this assay, the

compounds/extracts in question are in competition with ferrozine, to bind Fe^{2+} ions provided by iron(II)sulfate (Figure 3.6; e.g. caffeic acid). The stronger the binding of the tested compound, the smaller the amount of Fe^{2+} that can bind to ferrozine. When ferrozine binds to iron ions, a colour change from clear to blue is observed²³².

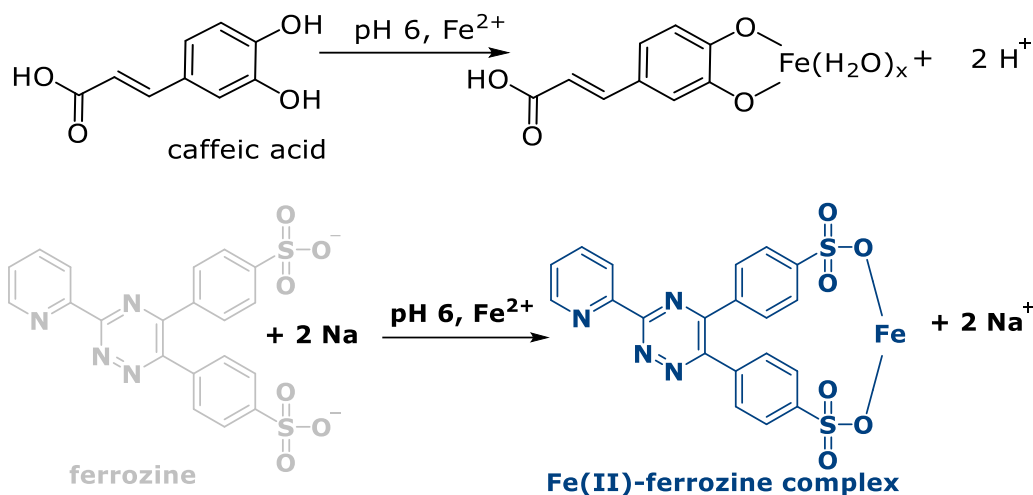


Figure 3.6| Reaction mechanism for the *in vitro* iron chelating assay

The intensity of the observed blue colour depends on this chelating ability of the tested compounds, i.e. the better the binding, the less intense the blue colour (Figure 3.7). This change in absorbance is measured at a wavelength of 562 nm. No change in the absorbance compared to the control (solvent instead of tested compounds) suggests no chelating activity.

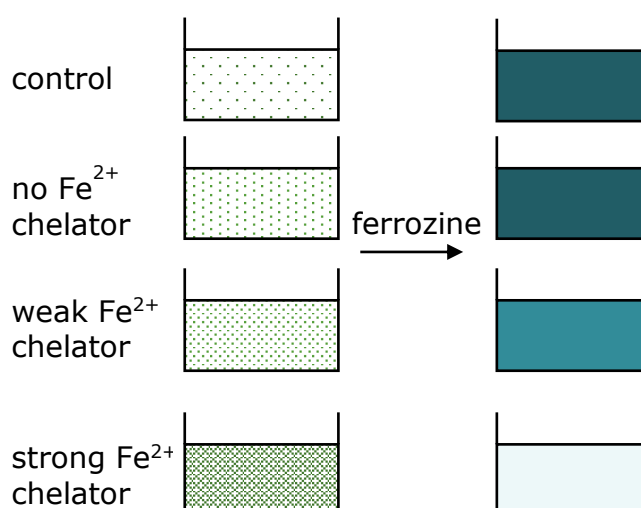


Figure 3.7| Reaction colour scheme for the iron(II) chelating activity assay

The copper (II) chelating assay employs pyrocatechol violet (3,3',4-trihydroxyfuchson-2''-sulfonic acid) for the determination of Cu^{2+} chelating potential. Similar to the iron chelating assay, the compounds/extracts of interest are in a competitive relationship with pyrocatechol violet for the binding of copper(II) ions. An example for the reaction mechanism is depicted below using quercetin as example phenolic (Figure 3.8).

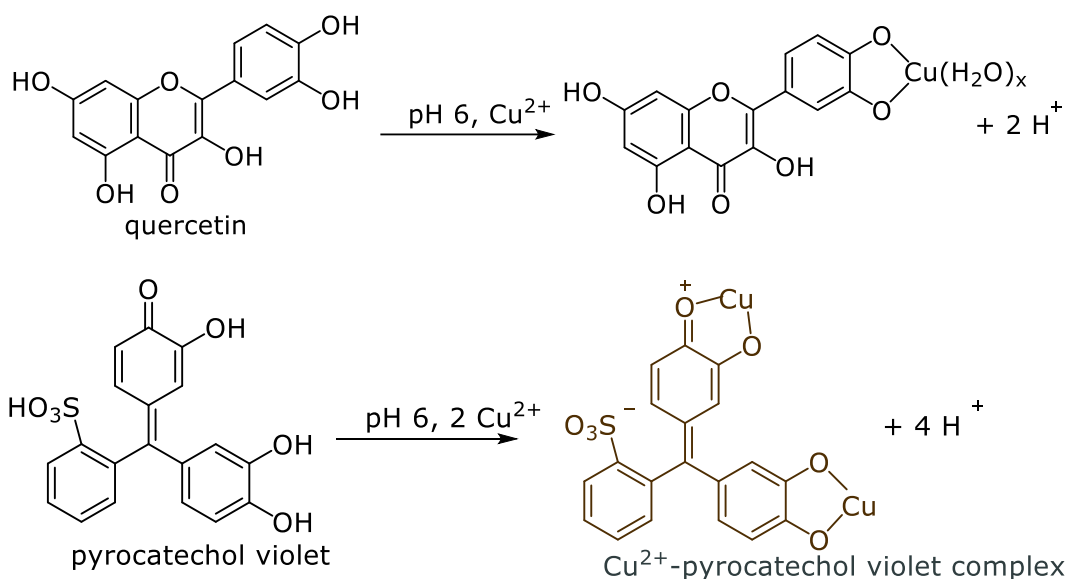


Figure 3.8| Reaction mechanism for the *in vitro* copper chelating assay

When pyrocatechol violet binds Cu^{2+} the absorbance increases at a wavelength of 632 nm due to the brown/blue coloured complex formation. In contrast, if this complex formation is inhibited by copper chelating agents, the reaction mix is yellow.

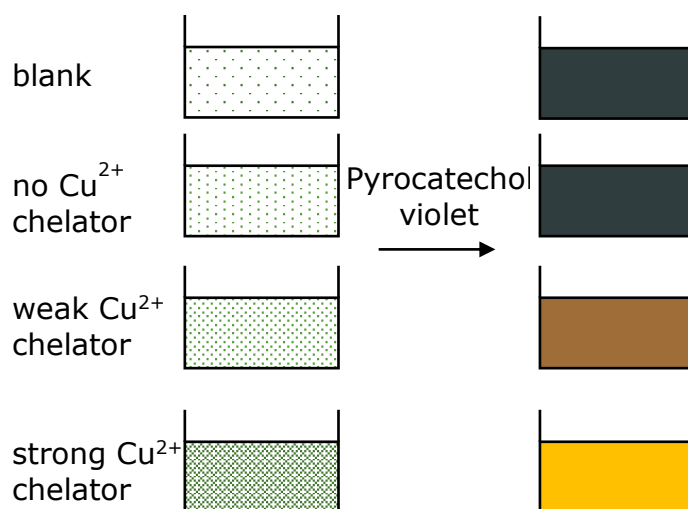


Figure 3.9| Reaction colour scheme for the copper (II) ion chelating activity assay

Both assays are easy to perform and can be applied in any laboratory. As described previously for the ORAC, FC and FRAP assay, these experiments use EDTA as standard and the extracts' activity are given as EDTA equivalence. In Santos *et al.*²³² the technique was tested on coffee extracts found to have good reproducibility and repeatability and a mean recoveries of over 96%.

3.1.3 Acetylcholinesterase (AChE)/Acetylcholinesterase inhibitors

Current treatments for AD are mostly acetylcholinesterase inhibitors (AChE) such as Donepezil (synthetic), Rivastigmine (semi-synthetic derivative of physostigmine) and Galantamine (alkaloid present in plants e.g. members of the family *Amaryllidaceae* or synthetic production). All of which are reversible AChE inhibitors⁴³⁵. AChE is an enzyme (serine-protease), responsible for the breakdown of the neurotransmitter acetylcholine (ACh), *via* the hydrolysis of carboxylic ester of ACh in the synaptic cleft⁴³⁶ (Figure 3.10). The endogenous neurotransmitter ACh was first discovered by Otto Loewi (German-born pharmacologist), who received the Nobel Prize in Physiology or Medicine in 1936 for his discovery of the first known neurotransmitter. Systematic biochemical investigations of AD patients, to elucidate the cause for AD and to find potential drug targets started in the 1960s and early 1970s. In the mid-1970s, low levels of choline acetyltransferase (ChAT), the enzyme responsible for the production of ACh were found^{437,438}. Later studies confirmed the deficiency in presynaptic ACh. This together with the known importance of ACh in learning and memory led to the cholinergic hypothesis of Alzheimer's disease^{437,439}, which initiated the use of AChE inhibitors for the treatment of AD. Figure 3.10, shows a schematic of ACh transmission in untreated AD patients and those treated with AChE inhibitors. AChE inhibitors, apart from the ones currently used in clinic, are continuously being discovered, especially in plant extracts such as from *Globularia alypum*²¹⁸, *Solanum leucocarpum* Dunal and *Witheringia coccoloboides* (Damm) (*Solanaceae* family)⁴⁴⁰ as well as *Hypericum undulatum* and *Sanguisorba minor*³³².

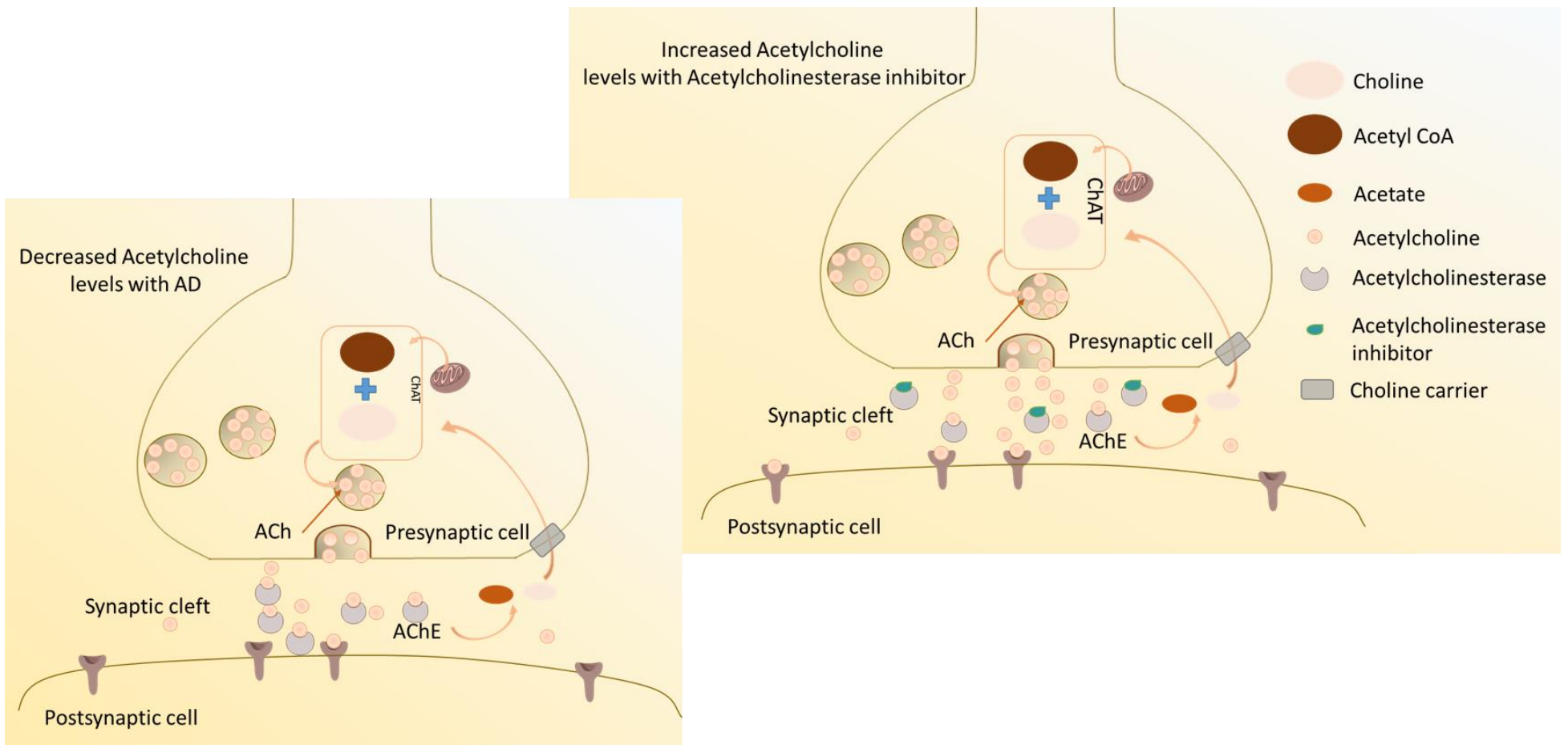


Figure 3.10| Acetylcholine levels and neurotransmission in AD patients with and without acetylcholinesterase inhibitors

Franziska Pohl

3.1.3.1 Ellman method for AChE inhibition studies

To determine the acetylcholinesterase inhibition activity of the RSP extract initially the Ellman method⁴⁴¹ was applied. In this assay acetylthiocholine iodide is used as substrate which is hydrolysed by acetylcholinesterase to thiocholine and acetic acid, thereafter thiocholine reacts with the oxidizing agent 5,5'-dithiobis-(2-nitrobenzoic acid) (DTNB) to form 5-thio-2-nitrobenzoate as a yellow coloured product with an absorption maximum at 412 nm (Figure 3.11).

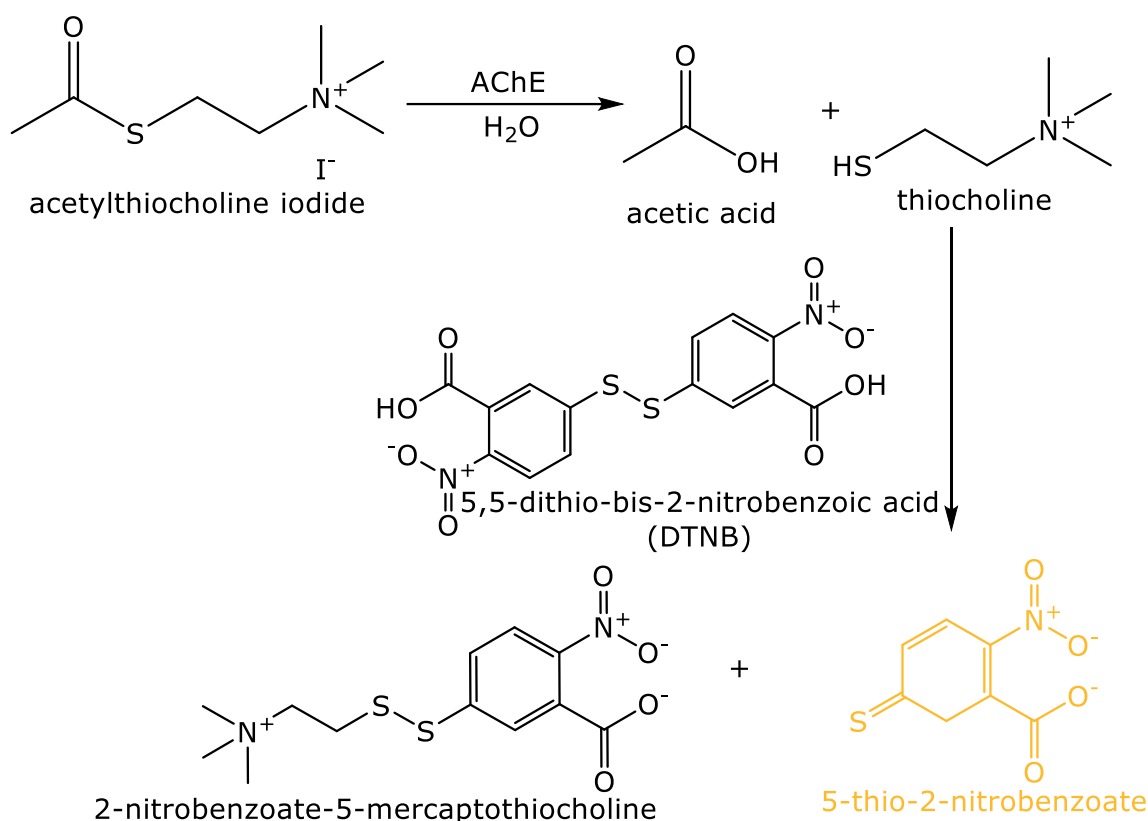


Figure 3.11| Reaction mechanism of the Ellman method for the detection of AChE inhibition, adapted from Badawy and El-Aswad⁴⁴²

In the presence of AChE inhibitors, 5-thio-2-nitrobenzoate will not be formed, showing no increase in absorbance, thus differentiating between inhibitors and non-inhibitors.

3.1.3.2 Amplex Red Assay kit for AChE inhibition studies

A second method for the determination of AChE inhibition activity is a fluorescent based assay known as the Amplex Red AChE kit. It is more sensitive and less prone to interference than the Ellman assay (UV/VIS-absorbance based). In this assay the AChE activity is measured indirectly

through 10-acetyl-3,7-dihydroxyphenoxazine (Amplex Red reagent), which reacts with H_2O_2 and acts as fluorogenic probe. Acetylcholine chloride, used as acetylcholine substrate, is converted to choline by AChE (Figure 3.12). Thereafter, choline is oxidized by choline oxidase, which leads to the formation of betaine and H_2O_2 . The fluorogenic probe Amplex red reacts with the formed H_2O_2 (in the presence of horseradish peroxidase) in a 1:1 stoichiometric ratio to form the fluorescent end-product resorufin, with an excitation and emission wavelength of 530-560 nm and ~ 590 nm respectively⁴⁴³.

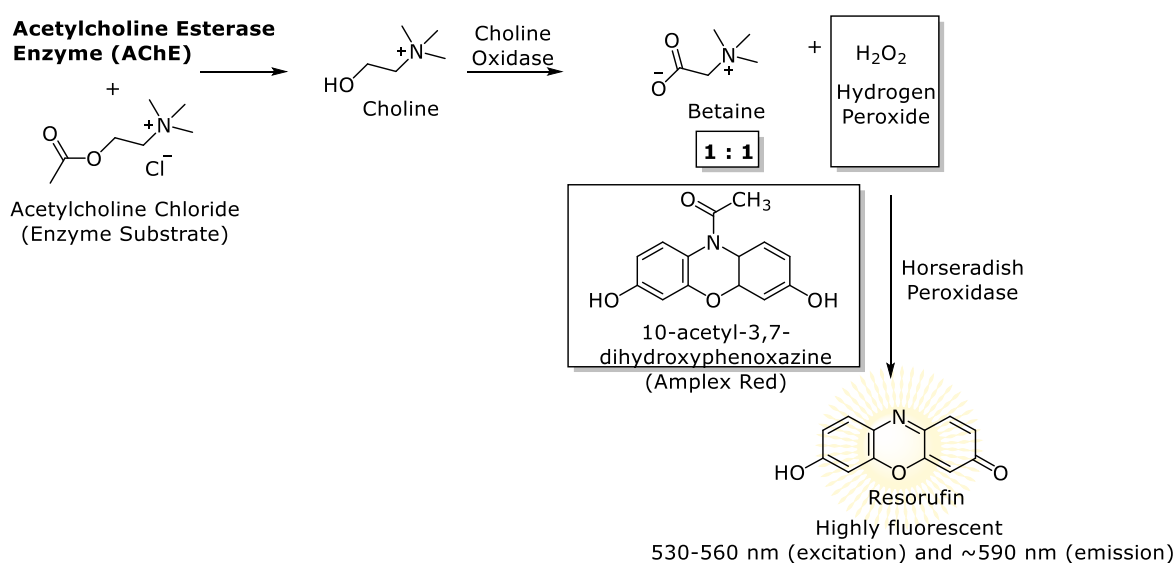


Figure 3.12| Amplex® Red Acetylcholine/Acetylcholinesterase Assay reaction scheme

By using a fluorescence-based assay, potential absorbance interferences can be avoided. The increased sensitivity is also of significant advantage, especially for compounds showing little AChE inhibition activity.

3.1.4 Inhibition of self-mediated β -amyloid (1–42) aggregation

The progressive deposition of misfolded and aggregated proteins is a hallmark of a number of different neurodegenerative disease e.g. AD (β -amyloid peptide, tau), PD (α -synuclein), HD (Huntingtin), SCA3 (ataxin-3) and ALS (superoxide dismutase) (1.3 Neurodegeneration, p.23 ff.). These misfolded proteins are fundamental for the progressive development of neurodegenerative disease. The question on which form of mutated protein (monomers, oligomers or insoluble aggregates) is causing the disease is still unknown. Also, the fact on whether the aggregations are causing the disease or are a downstream effect of it is still unclear. Although protein aggregates are a common target for drug treatments, the issue of missing knowledge about protein aggregations is generating a unique challenge for the drug development process⁴⁴⁴.

In AD for example, the prevention of self-mediated β -amyloid aggregation is a well-studied potential mechanism of disease prevention. A number of natural compounds such as curcumin, caffeic acid, ferulic acid, β -carotene and sulforaphane have been identified as peptide aggregation inhibitors⁴⁴⁵. However, although these compounds have been found to inhibit the aggregation formation, their specific target and chemical mechanisms underlying this prevention is still unclear. Research has shown different covalent and non-covalent inhibition mechanisms⁴⁴⁵.

Some of the above stated compounds, i.e. caffeic acid and ferulic acid have been positively identified in the RSP extract (Table A2, p.429). To assess the extracts ability to inhibit self-mediated β -amyloid aggregation, the thioflavin T (ThT) fluorescence method was used (Figure 3.13). The use of ThT for the detection of β -amyloid aggregations was first described by Vassar and Cullin in 1959⁴⁴⁶.

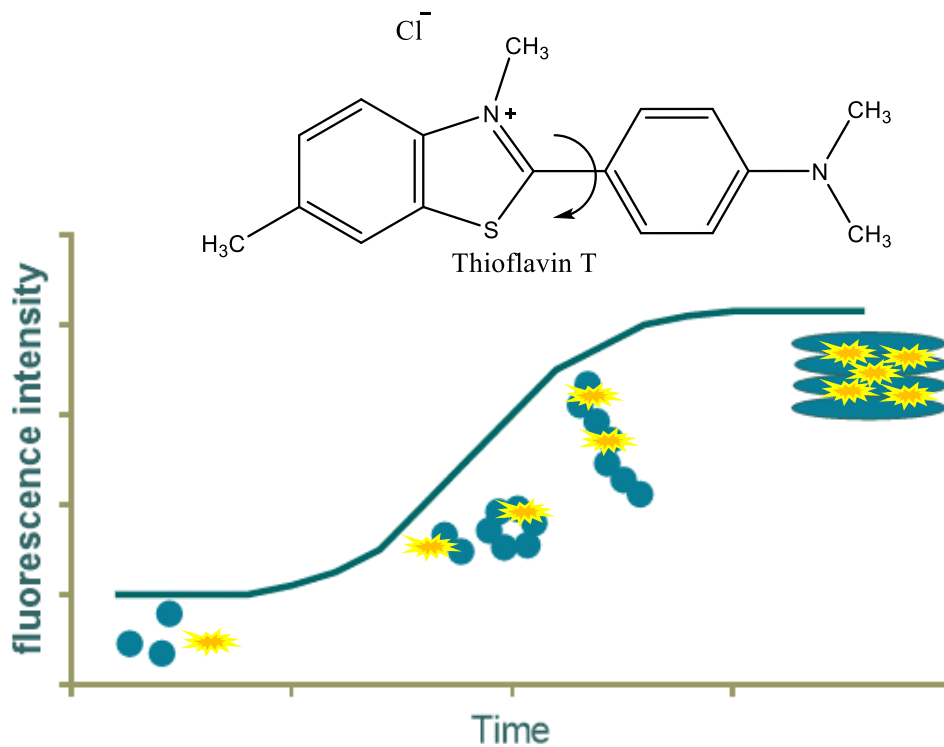


Figure 3.13| ThT assay

Increase of fluorescence reading during the formation of β -amyloid fibril formation adapted from Wallin et al.⁴⁴⁷

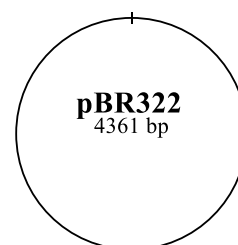
The fluorescence intensity of ThT increases when bound to protein fibrils. A smaller increase of fluorescence intensity suggests the inhibition of aggregation.

A positive outcome of this study would supplement the extracts known antioxidant activity and support further investigation into the extracts potential to prevent or treat neurodegenerative disease. Extracts from plant material such as Mulberry leaves⁴⁴⁸, grape seeds⁴⁴⁹ and maple syrup⁴⁵⁰ have previously shown prevention of β -amyloid aggregation.

3.1.5 DNA protection

Cells in the human body are under constant stress from chemicals produced *in vivo* during normal cellular metabolism or from external factors, such as environmental chemicals or radiation. This stress, mostly oxidative, can cause DNA damage (Figure 1.27, p. 54). Damage to DNA is exceptionally harmful, as DNA builds the basis for the formation of proteins necessary for cellular function. This is especially worrying for neurons, as these are not like for example epithelial cells, lining the intestine, replaced every five days, but are retained for life. This increases the importance of protecting neurons from DNA damage⁴⁵¹.

To determine the DNA protection potential of the RSP extract a simple *in vitro* assay using plasmid DNA will be employed. Plasmid DNA such as pBR322, created in 1977 by postdoctoral researchers (Bolivar and Rodriguez) in Herbert Boyers lab at the University of California, San Francisco is used as DNA source. The pBR322 plasmid is circular DNA



consisting of 4361 base pairs. In its native state pBR322 plasmid DNA is mostly super coiled (over- and under- wind). However, once it is exposed to ROS (e.g. peroxy- or hydroxyl radicals) the supercoiled form is broken into an open circular or even linear formation (Figure 3.14). ROS can be introduced *in vitro* via e.g. AAPH, a peroxy radical producer (2.1.3.4 ORAC, p.84 ff.), or the Fenton reaction, leading to the formation of hydroxyl radicals.

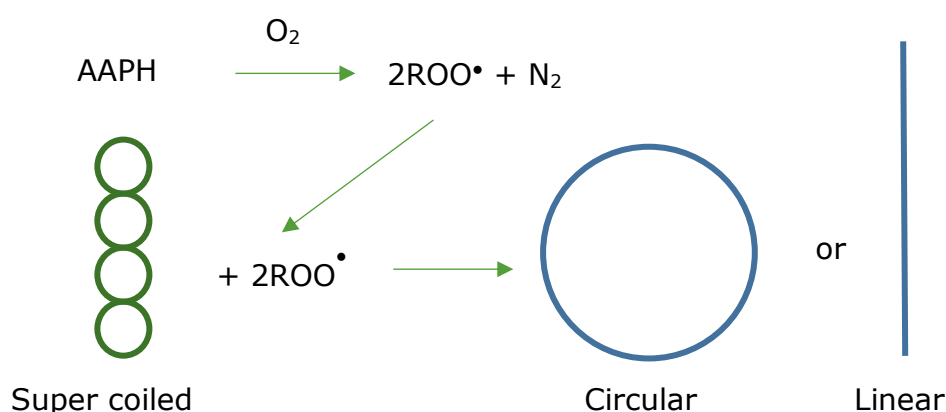


Figure 3.14| Reaction of pBR322 plasmid DNA with AAPH

This change is associated with a conformational change of the plasmid DNA, which leads to a delay of movement; in e.g. agarose gels, compared to the supercoiled form. This assay has previously been used to determine DNA protective properties for various extracts and single compounds, e.g. polyphenols extracted from green tea⁴⁵² and *Terminalia arjuna* bark extracts³⁷⁷, with promising results. The same experiment using pUC19 plasmid DNA showed protecting properties for onion extracts (*allium cepa* L.)⁴⁵³. These and other plasmids (pMK 3⁴⁵⁴, pUC18⁴⁵⁵) have previously been used to determine the protection of DNA from oxidative stress *in vitro*.

The plasmid DNA protection assay together with the other anticipated experiments described in this introduction will enhance our knowledge of the composition and *in vitro* activity of the RSP extract regarding neuroprotective potential. All the set out objectives for this chapter are briefly summarised following.

3.1.6 Objectives

The list below describes the objectives set out for this chapter:

- Determine repeatability of Soxhlet extraction technique, to assess whether bulk extraction is necessary
- Analyse antioxidant activity of the final extract
- Determine secondary metabolite composition of final extract, including previously shown method as well as additional LC-MS/MS, HPLC and spectroscopic methods
- Establish the extracts metal chelating (Fe(II) and Cu(II))- , DNA protecting-, β -amyloid (1-42) self-mediated aggregation inhibiting- and AChE inhibiting properties

3.2 Materials and Methods

3.2.1 Chemicals and Equipment

For the experiments discussed in this chapter, the following chemicals/kits (Table 3.1) and equipment (Table 3.2) were used.

Table 3.1| Chemicals, reagents and kits

Chemicals	Provider
1,1-diphenyl-2-picryl-hydrazyl (DPPH)	Sigma-Aldrich
Methanol (HPLC grade)	Fisher Scientific/Sigma-Aldrich
Gallic acid	Sigma-Aldrich
Trolox	Sigma-Aldrich
Folin & Ciocalteu's phenol reagent	Sigma-Aldrich
Sodium acetate trihydrate	Sigma-Aldrich
2,4,6-tris(2-pyridyl)-s-triazine (TPTZ)	Sigma-Aldrich
Hydrochloric acid (HCl)	Sigma-Aldrich
Ferric chloride (FeCl ₃ *6H ₂ O)	Sigma-Aldrich
Sodium carbonate (Na ₂ CO ₃)	Sigma-Aldrich
Sodium hydroxide (NaOH)	Sigma-Aldrich
2,2'-azobis(2-amidinopropane) dihydrochloride (AAPH)	Sigma-Aldrich
Monopotassium phosphate (KH ₂ PO ₄)	Sigma-Aldrich
Ethylenediaminetetraacetic acid (EDTA)	Sigma-Aldrich/Alfa Aesar
Sodium fluorescein	Sigma-Aldrich
Sinapic acid	Sigma-Aldrich
Glacial acetic acid (CH ₃ CO ₂ H)	Fisher Scientific
Ethanol	Fisher Scientific
Tris-base	Fisher Scientific
Petroleum ether (C ₆ H ₁₄ ; boiling point 40-60°C)	Fisher Scientific
Syringic acid	Sigma-Aldrich
Ferulic acid	Sigma-Aldrich
Caffeic acid	Sigma-Aldrich
Acetonitrile	Fisher Scientific
Glacial acetic acid	Fisher Scientific
Trifluoroacetic acid (TFA)	Fisher Scientific
FeSO ₄ *5H ₂ O	Sigma-Aldrich
Ferrozin	Sigma-Aldrich
CuSO ₄ *5H ₂ O	Sigma-Aldrich
Penicillamine	Sigma-Aldrich
Pyrocatechol	Sigma-Aldrich
Green tea	Meßmer, Kaufland, Germany

Grapeseed pomace	Portugal, Brancellao red grapes
Plasmid DNA pBR322	Fisher Scientific
GelRed dye	Fisher Scientific
Agarose	Fisher Scientific
β -amyloid peptide (1-42)	calbiochem
Na_2HPO_4	Fisher Scientific
NaH_2PO_4	BDH (The British Drug Houses)
Sodium chloride (NaCl)	Fisher Scientific
Glycine	Fisher Scientific
Thioflavin T	Acros Organic
DMSO	Fisher Scientific
Curcumin	Sigma-Aldrich
PBS	OXOID
Amplex® Acetylcholine / Acetylcholinesterase Assay Kit	Fisher Scientific
Sinapine thiocyanate	ChemFaces
pBR322 plasmid DNA	Fisher Scientific
Choline chloride	Sigma-Aldrich
DTNB	Sigma-Aldrich
Gel Red™ (10000x in water)	VWR
AChE (electric eel)	Sigma-Aldrich
Hepes	Sigma-Aldrich
Acetylthiocholine iodide	Sigma-Aldrich

Table 3.2| Equipment

Equipment	Manufacturer/Details
Freeze Dryer	Modulyo Edwards
Coffee grinder	De Longhi KG39
LC-MS/MS	Agilent MassHunter 6420 Triple Quad
LC MS/MS (Rowett)	Agilent 1100
Gel tank	Life Technologies Horizon®58
Automatic Soxhlet	Gerhardt; Soxtherm SE 416
Plate reader	BioTek μ Quant
Fluorescence spectrophotometer	Perkin Elmer LS55
Rotary evaporator	Büchi Rotavapor R-114
Oven	Techne Hybridiser HB-10
Fridge	DEAWOO
Freezer -20°C	Blomberg
Freezer -80°C	New Brunswick Scientific U725
pH-meter	Denver Instruments Basic
Balance	OHAUS Pioneer™PA114
Balance	Mettler BB1200
Ultrasonic bath	Ultrawave SFE5901
Power pack	E-C Apparatus Corporation EC 105
Plate shaker (molecular)	Heidolph Polymax 1040
Microwave	Panasonic NN-E255W

3.2.2 Methods

The methods in this chapter (Figure 3.15) were applied to further elucidate the chemical composition of the RSP extracts and to determine which compounds within the extract were responsible for antioxidant activity. Furthermore, the RSP extracts neuronal protection potential, was evaluated *in vitro*, in order to evaluate the extracts' potential in preventing or treating neurodegenerative disease.

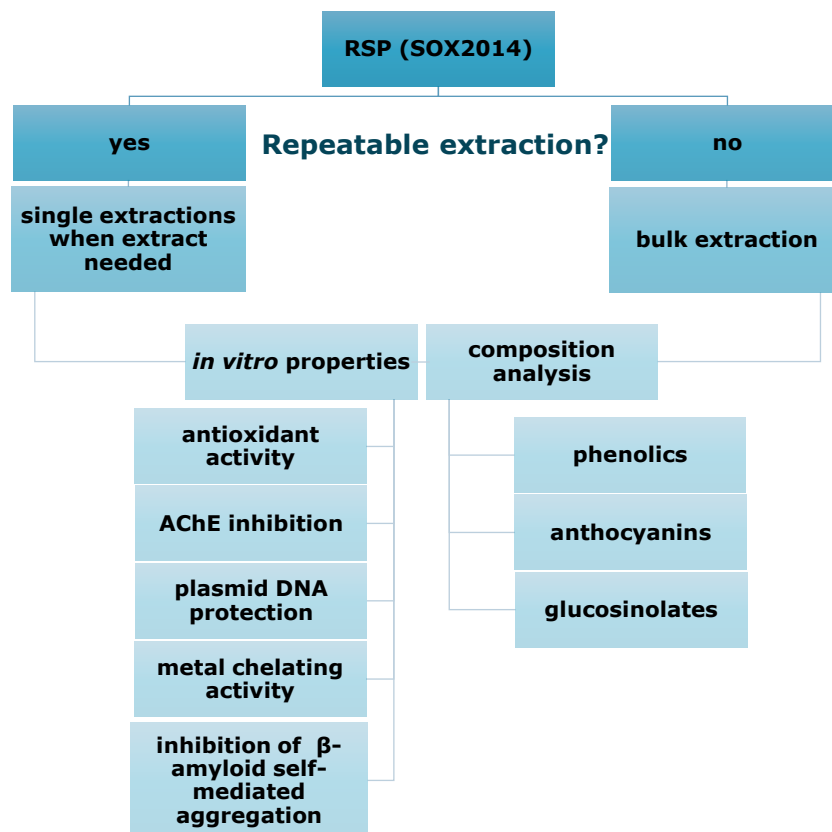


Figure 3.15| Overview of methods used in the assessment of the RSP extract for its chemical composition and *in vitro* neuroprotective properties

3.2.2.1 Determination of repeatability of Soxhlet extraction

In this chapter repeatability of the extraction technique was determined for three independent extracts (2.2.2.3 Rapeseed Pomace Extraction techniques, Soxhlet, p.92 ff.), by determining their antioxidant activity using the DPPH, FC, FRAP assays (2.2.2.4 Folin-Ciocalteu-(FC) Assay, p.94/2.2.2.6 *In vitro* antioxidant activity, p.94 f.).

3.2.2.2 Production of final RSP extract and antioxidant activity and secondary metabolite analysis

A final RSP extract was obtained by carefully mixing the extracts from nine separate extractions together to obtain one homogeneous mixture. In the following chapters this will be called RSP extract. Dried RSP extract aliquots (1-3 g) were sealed into plastic packages using a vacuum sealer and stored at -80°C until further use. The extract package in use at the time of experiments was stored at -20°C in 25 mL tubes in the presence silica gel as desiccant, to avoid moisture. That final extract was further characterised using the previously described antioxidant assays ((2.2.2.4 Folin-Ciocalteu- (FC) Assay, p.94/2.2.2.6 *In vitro* antioxidant activity, p.94)). In addition, the final extract was submitted to LC-MS/MS analysis at the Rowett Institute, as previously described (2.2.2.5 Chemical Analysis of the RSP Extracts (HPLC-MS/MS), p.94).

3.2.2.3 Determination of additional secondary metabolites in the extract

Additional secondary metabolites in the RSP extract were determine using different analytical techniques. Sinapine and other phenolic derivatives were determined using LC-MS/MS, glucosinolates using HPLC and total monomeric anthocyanin content was determined in a simple colorimetric reaction (UV-VIS spectroscopy).

Sinapine and similar

Chromatographic separation was performed as previously described by Yates *et al.*⁴⁵⁶, according to Neacsu *et al.*³⁴³ with minor modifications, on an Agilent 1200 Infinity Series HPLC (Cheshire, UK) using a Zorbax Eclipse Plus C18 Rapid Resolution column (100 x 4.6 mm; 3.5 µm) maintained at 25°C. The mobile phase consisted of 0.1% acetic acid in water (A) and 0.1% acetic acid in acetonitrile (B) operated under gradient conditions at a flow rate of 0.4 mL/min over 69 min with an injection volume of 10 µL. The gradient programme was: 90% A – 10% B initially, changed to 45% A – 55% B over 45 min, then to 20% A – 80% B over 15 min and held for 3 min. Thereafter, conditions were changed back to the starting conditions of 90% A – 10% B in 1 min and kept for a final 5 min. The HPLC system was allowed to equilibrate after each run. The HPLC was coupled to an Agilent 6420 MS/MS

triple quadrupole. Electro-spray ionization (ESI) was utilised in both negative and positive ionisation modes. The capillary voltage for both negative and positive ionisation modes was set to 4 kV. The desolvation temperature was kept at 350°C with a gas flow rate of 12 L/min and nebulising pressure of 50 psi. Nitrogen gas was used as the nebulising, desolvation and collision gas. Full-scan MS spectra were obtained by scanning from 40 – 1000 m/z. Retention times and two multiple reaction monitoring (MRM) transitions were monitored for each analyte for quantification and confirmation purposes⁴⁵⁷.

Linearity was established *via* a six point calibration curve ranging in concentration from 0.05 to 1 µg/mL sinapine in mobile phase (90:10% acetonitrile:water). Intra-day and inter-day precision and accuracy was determined by triplicate injection of 0.1 and 1 µg/mL (0.8 µg/mL for sinapine) standards over two different days, respectively⁴⁵⁶.

Antioxidant activity of sinapine in comparison to a mixture of phenolic acids (sinapic acid, caffeic acid, ferulic acid and syringic acid) and the RSP extract was tested as previously described (2.2.2.4 Folin-Ciocalteu-(FC) Assay, p.94, 2.2.2.6 *In vitro* antioxidant activity, p.94 ff.).

Glucosinolates (GLSs) analysis

For the determination of GLSs in the rapeseed pomace as well as in the final RSP extract the procedure by Raikos *et al.*¹¹⁵ was followed with minor modifications. In brief, 50 mg of sample (RSP and RSP extract) were weighed in triplicate into 15 mL falcon tubes. A water bath was set to 100°C and a bottle containing milliQ water heated to the same temperature. Once the water reached the required temperature, all samples were made up to 25 mg/mL, with hot water, vortexed, and placed into the water bath for extraction. The samples were vortexed regularly every 5 minutes. After 15 minutes, the tubes were left to cool to room temperature and centrifuged (4000 rpm, 10 min, rt). The supernatant was collected into 5 mL Eppendorf tubes. Then filtered into two separate Eppendorf tubes (1.5 mL), collecting the initial and the final filtrate in one and the middle filtrate in the other one. The latter one was used for HPLC analysis. Samples were stored at -70°C until analysis. A serial dilution of all tested standards (external) was prepared

for external calibration and the limit of detection and quantification calculated.

Table 3.3| External Glucosinolate Standards for HPLC

- (-)-Sinigrin Hydrate •Gluconapin •Progoitrin •Glucobrassicin
- Glucobrassicinapin •Glucoraphanin •Glucoiberin •Glucoerucin
- Glucotropaeolin •Gluconasturtiin •Glucoraphenin

Note(s): for chemical structure of GLSs see Figure 3.3 p.139

The analysis was undertaken on an Agilent 1260 Infinity HPLC with a diode array detector (DAD), using a Phenomenex Synergi 4 µm Hydro-RP 80A HPLC column (250 x 4.6 mm) with Phenomenex Synergi Polar-RP pre-column. DAD spectra were recorded between 190-700 nm and chromatograms monitored at 229 nm wavelength due to high absorption of glucosinolates at this wavelength. A gradient programme was used with mobile phase A, 0.05 M KH₂PO₄ buffer (pH 2.3), filtered (0.2 µm) and purged with nitrogen for 36 hours protected from light and mobile phase B was HPLC grade acetonitrile.

The column temperature was set to 25°C and the auto sampler thermostat to 4°C. Samples (20 µL) were injected and a flowrate of 1 mL/min was applied. The injection needle was washed with 100% acetonitrile between injections.

Table 3.4| Mobile phase HPLC gradient for the detection of glucosinolates

<i>Time (min)</i>	<i>%A</i>	<i>%B</i>
0-6	100	0
6-35	67	33
35-36	67-30	33-70
36-42	30	70
42-43	30-100	70-0
43-55	100	0

Limit of detection (LOD) and quantification (LOQ) were calculated based on the standard deviation of the response (S_y) and the slope of the calibration curve (S) (Equation 3.3):

$$LOD = 3.3 * \frac{S_y}{S} \quad LOQ = 10 * \frac{S_y}{S} \quad \text{Equation 3.3}$$

Total Monomeric Anthocyanin Pigment Content

The pH differential method was applied according to Lee *et al.*²⁹⁵ with minor modifications. Briefly, RSP extract (final extract) was made up in methanol to a final concentration of 1 mg/mL. This solution was diluted with two buffers (i) potassium chloride (0.025 M) buffer, pH 1.0 (ii) sodium acetate (0.4 M) buffer, pH 4.5, to give final concentrations of 200 µg/mL.

The absorbance was measured at 520 nm. To correct for the presence of turbidity a measurement is also taken at 700 nm and subtracted from the 520 nm reading. The measurements were taken 30 min after the preparation of solutions and the results are given as anthocyanin pigment cyanidin-3-glucoside (cyn-3-glu) equivalents in mg/L (Equation 3.4)

$$\text{anthocyanin pigment cyn - 3 - glu equivalents in mg/L} = \frac{A * MW * DF * 10^3}{\epsilon * l}$$

Equation 3.4

Where A = (A_{520 nm} - A_{700 nm}) pH 1.0 - (A_{520 nm} - A_{700 nm}) pH 4.5; MW (molecular weight) = 449.2 g/mol for cyanidin-3-glucoside (cyd-3-glu); DF = dilution factor; l = pathlength in cm; ε = 26900 molar extinction coefficient, in (L/(mol*cm), for cyd-3-glu; and 10³ = factor for conversion from g to mg.

As this method is measuring mg of anthocyanin pigment cyanidin-3-glucoside equivalents in liquids, the obtained results are for the starting solution of 1 mg/mL. To obtain more useful results, this was transferred to mg of anthocyanin pigment cyanidin-3-glucoside equivalents per g extract. As positive control, grape pomace (GP) extract was prepared as described previously for the RSP (2.2.2.3 Rapeseed Pomace Extraction techniques, p.92) and analysed simultaneously. Wine production by-products have previously shown to contain anthocyanins³⁴⁰.

3.2.2.4 Metal chelating properties (Iron and copper)

Iron (Fe²⁺) chelating

The iron chelating activity of the extracts was assessed according to Santos *et al.*²³². EDTA was used as a standard and concentration between 5-50 µg/mL prepared in deionized water. Both, the extract and sinapine were

similarly prepared in deionized water (1 mg/mL and 120 µg/mL respectively). Green tea was used as positive control⁴⁵⁸. A 96-well plate set-up was used, and wells filled with 50 µL sample/EDTA/negative control and 160 µL deionized water followed by 20 µL of Fe₂SO₄ (0.3 mM in deionized water). After a 5-minute reaction time, 30 µL ferrozine (0.8 mM in deionized water) were added and plates incubated for 15 minutes (rt). Thereafter, the absorbance was recorded at 562 nm. EDTA calibration curves were created and mg EDTA equivalence (equ.)/g RSP extract calculated (Equation 3.5).

$$C(\text{mg EDTA equivalence/1g RSP}) = c(\text{mg/mL}) * \left(\frac{V(\text{mL})}{M(\text{g})}\right) \quad \text{Equation 3.5}$$

Limit of detection (LOD) and quantification (LOQ) were calculated as previously described based on the standard deviation of the response (Sy) and the slope of the calibration curve (S) (Equation 3.3, p. 160).

Copper (Cu²⁺) chelating

The extracts ability to chelate copper ions was assessed following the method by Santos *et al.*²³² using pyrocatechol violet as indicator. EDTA was used as a standard and concentration between 5-75 µg/mL were prepared in deionized water. Both, the extract and sinapine were similarly prepared in deionized water (1 mg/mL and 120 µg/mL respectively). As positive control Penicillamine was employed⁴²⁹. Briefly, 30 µL of sample/EDTA/negative and positive control were mixed with 200 µL sodium acetate buffer (50 mM, pH 6.0) and 30 µL CuSO₄* 5H₂O (0.4 M) and were left to react for 2 min. To initiate the reaction, 8.5 µL pyrocatechol violet (2 mM) were added and the 96-well plate shaken for 10 minutes followed by an additional 10 minutes reaction (25°C) thereafter, the absorbance was recorded at 632 nm. EDTA calibration curves were made and mg EDTA equivalence/g RSP extract calculated using the same formula (Equation 3.5) as for the iron chelating properties. Limit of detection (LOD) and quantification (LOQ) were calculated based on the standard deviation of the response (Sy) and the slope of the calibration curve (S) (Equation 3.3).

3.2.2.5 Acetylcholinesterase inhibition potential

Ellman acetylcholinesterase (AChE) inhibition assay

To determine AChE inhibition activity, the procedure detailed by Khelifi *et al.*²¹⁸ based on the Ellman method⁴⁴¹ was used with slight modifications. For this, a 22 U/mL stock solution of acetylcholinesterase was prepared in Tris-HCl buffer (20 mM, pH 7.5). Prior to starting the experiment this solution was again diluted 1/100. The extract as well as the positive control neostigmine were dissolved in methanol, to obtain stock solutions of 1 mg/mL, which were further diluted in methanol to receive a serial dilution, to determine the IC₅₀ value. In a 96-well plate 125 µL DTNB (3 mM) are mixed with 25 µL sample or positive/negative control and 25 µL of the diluted AChE and the plate incubated for 10 minutes at room temperature. Thereafter 25 µL Acetylthiocholine iodide (15 mM) were added and the plate incubated for 10 minutes at 37°C. Absorbance readings were recorded at 412 nm. IC₅₀ values were calculated, using the linear part of the curve created after determining % of AChE inhibition (Equation 3.6).

$$\% \text{ of AChE inhibition} = \frac{(100 * A_{\text{sample}})}{A_{\text{blank}}} \quad \text{Equation 3.6}$$

Amplex® Red Acetylcholine/Acetylcholinesterase Assay Kit (A12217)

For this assay, the instructions given by Molecular Probes⁴⁴³ were followed. All stock solutions were prepared as per instructions. Briefly, a ~20 mM stock solution of Amplex red reagent was prepared by dissolving one vial of the Amplex Red reagent (1 mg) in 200 µL DMSO. A 1X working solution of the reaction buffer was prepared by diluting the provided 5X stock solution 1:5 in deionized water. The 200 U/mL stock solution of horse radish peroxidase (HRP) was prepared by adding 1 mL 1X reaction buffer to the vial of HRP. A 20 mM H₂O₂ working solution was prepared daily by diluting the 3.6% stock solution with 1X buffer. The choline oxidase stock solution (20 U/mL) was prepared by dissolving the content of the provided vial (12 U) in 600 µL 1X buffer, which was aliquoted for the following experiments. To prepare 100 mM acetylcholine, 5 mg of acetylcholine chloride was dissolved in 275 µL deionized water. This solution was made daily before each new set of

experiments. By dissolving the provided 60 U acetylcholinesterase (from electric eel) in 600 μ L 1X reaction buffer a 100 U/mL stock solution was prepared. All prepared stock solutions, 5X buffer, H₂O₂ as well acetylcholinchloride were contained in the freezer (-20°C) until needed for the experiment.

There after the instructions for the Acetylcholinesterase Assay⁴⁴³ were follow with minor modifications, to allow for the determination of acetylcholinesterase inhibition. The extract was dissolved in 1X reaction buffer and diluted to give a concentration gradient from 4 to 0.04 mg/mL with final well concentrations ranging from 1-0.001 mg/mL. As positive control, neostigmine was dissolved and diluted in 1X reaction buffer to 0.02 mg/mL giving a final well concentration of 0.005 mg/mL (22.39 μ M). The 100 U/mL acetylcholinesterase stock solution was diluted to 0.2 U/mL (in 1X reaction buffer), of which 50 μ L were used in each well, together with 50 μ L RSP extract/neostigmine/1Xreaction (neg. control) buffer to determine the inhibition activity of the samples. A second positive control was prepared by diluting the 20 mM H₂O₂ working solution to 10 μ M in 1X reaction buffer. For this reaction control instead of 50 μ L AChE and 50 μ L sample 100 μ L H₂O₂ were pipetted into the well. To all the wells, 100 μ L of Amplex Red reagent (400 μ M Amplex Red, containing 2 U/mL HRP, 0.2 U/mL choline oxidise and 100 μ M acetylcholine), were added to start the reaction. After addition of the Amplex Red reagent, the plate was immediately transferred into a preheated (37°C) fluorescence plate reader, running a program with the following settings, excitation wave length 530/25 nm and emission wave length 590/35 nm and a gain of 35 for 150 minutes.

In addition, after determination of the sinapine concentration in the extract, the extract (0.25 mg/mL) in comparison with the respective sinapine concentration as well as mixture of four phenolic acids (SA, SyrA, FA, CA) were analysed for AChE inhibition activity.

3.2.2.6 Inhibition of self-mediated β -amyloid (1–42) aggregation

The assessment of the extracts ability to inhibit self-mediated β -amyloid (1-42) aggregation was done according to Bolognesi *et al.*⁴⁵⁹, with minor modifications. The amyloid peptide (0.25 mg) was dissolved in DMSO (110

µL) to prepare a 500 µM (2.27 mg/mL) stock solution. Curcumin (2.27 mg/mL) and the extract (2.27 and 22.7 mg/mL) were similarly prepared in DMSO. For the reaction mix, 2 µL of peptide and 2 µL of the compounds were added to 96 µL of Phosphate/NaCl buffer (10 mM, pH 8.0). For the negative control, the extract was exchanged for 2 µL of DMSO. After 24 hours incubation, 300 µL of glycine/NaOH buffer (50 mM, pH 8.5) containing 5 µM ThT were added to each reaction mix. The resulting solutions were analysed using fluorescence spectroscopy (Perkin Elmer LS55) with an excitation wavelength of 446 nm and an emission of 490 nm, the values were averaged after subtracting the fluorescence background reading of the blank ThT solution. In addition, also extract controls were analysed, where the 2 µL peptide in the reaction mix were exchanged for DMSO.

3.2.2.7 Inhibition of Supercoiled Plasmid DNA Strand Breakage

The inhibition of supercoiled plasmid DNA strand breakage was performed according to Camargo *et al.*⁴⁶⁰ and Shahidi *et al.*³¹², 1 µL pBR322 plasmid DNA (0.5 µg/µL) was incubated with 6 µL PBS, 8 µL AAPH (10 mM, final concentration 3.48 mM) and 8 µL RSP extract (60-10 µg/mL, final concentration 20.9-3.5 µg/mL) or 8 µL sinapic acid (60-0.29 µg/mL, final concentration 20.9-0.102 µg/mL) for comparison. AAPH and/or extracts/sinapic acid were substituted with PBS for controls. The mixture was vortexed, centrifuged briefly (10000rcf, Eppendorf centrifuge 5415D) and incubated in the dark (37°C, 60 mins). Thereafter, 2 µL loading dye (500 µL glycerol; 500 µL dH₂O; 5 mg bromophenol blue) were added, the sample vortexed and loaded (10 µL) onto a 0.7% agarose gel, prepared with TAE buffer (40 mM Tris acetate, 1mM EDTA), stained with gel red dye (0.01%) and electrophoresed (70 mins; 80 V (Life Technologies Horizon 58 gel tank and Thermo EC 105 power pack) in TAE buffer. The gels were visualized and photographed using Peqlab Fusion FX7 (Fusion 15.11 software) under UV-light. ImageJ software (v1.51) was used to analyse the band intensity. Inhibition of DNA strand breakage (%) was calculated (Equation 3.7).

$$\text{Inhibition of DNA strand breakage (\%)} = \frac{\text{DNA content with the oxidative radical and extract (band intensity)}}{\text{DNA content without the oxidative radical (band intensity)}} * 100\% \quad \text{Equation 3.7}$$

After the sinapine concentration in the extract was determined (3.1.1.1 Sinapine and additional phenolic derivatives), the extract (20 µg/mL) in

comparison with the respective sinapine concentration as well as mixture of four phenolic acids (SA, SyrA, FA, CA) were analysed for DNA protective properties, along with two additional sinapine concentrations (20 and 0.2 µg/mL).

3.2.2.8 Statistical analysis

Statistical analysis was performed using GraphPad Prism 7. Specific methods used for statistical comparison of each experiment are detailed in the results section. P-values below 0.05 were considered significant and results shown as mean ± standard deviation.

3.3 Results and Discussion

3.3.1 Extraction replicates differences in FC, FRAP and DPPH

To determine the reliability of the 95% ethanoic extraction technique (SOX), three independent extractions were undertaken, and their antioxidant activities were determined *via* the DPPH, FC and FRAP assays. Among the three extracts significant differences were found only in the DPPH assay. In contrast, the FC and FRAP assays showed no significant differences among the samples studied (Figure 3.16).

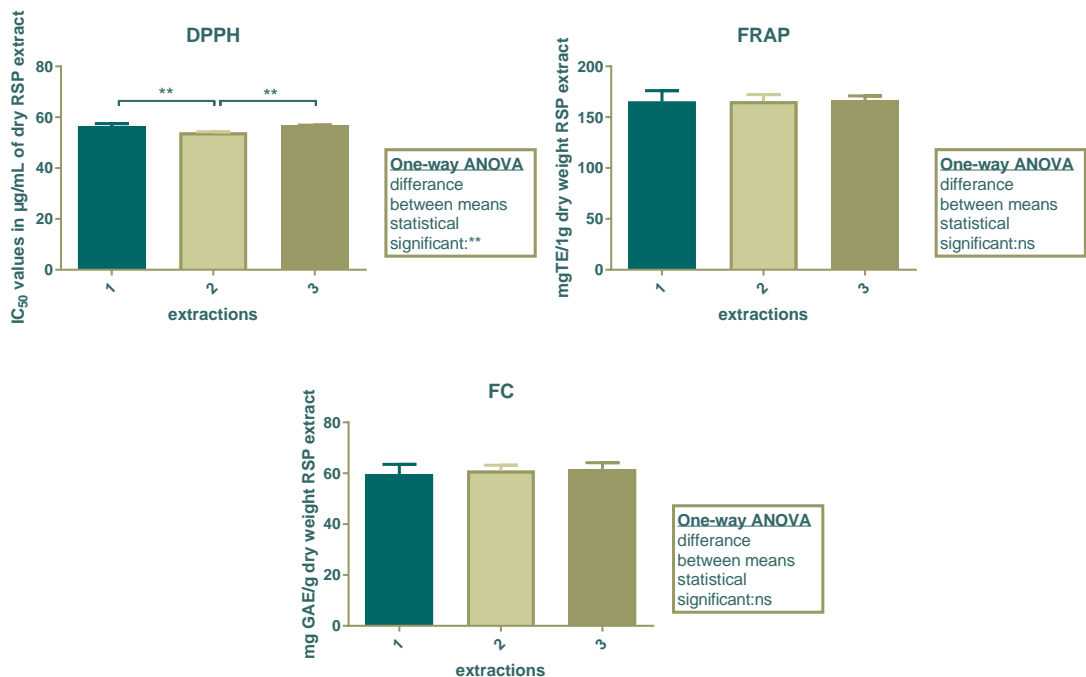


Figure 3.16| DPPH, FC and FRAP results obtained from 3 extraction replicates

*Significant difference via One-way ANOVA (box), Bonferroni's multiple comparisons test between extractions; $p \leq 0.01$ (**)*

Apart from the very small differences for the DPPH assay (only extract number 2), the results suggest that the extraction technique is reproducible, when using the same RSP harvest/breed (2014). However, to reduce the differences among the extractions, several extractions were undertaken in succession. Then, after freeze drying the extracts from all these extractions,

they were pooled together and mixed, to yield a homogeneous RSP extract. Subsequently, the extract was proportioned into smaller samples (1-3 g), which were vacuum packed and stored at -80°C . This procedure provided a homogeneous RSP extract that was used in all the experiments for the rest of the project. Of note, working RSP extract samples were stored at -20°C . All subsequent experiments were based on this extract, which will be referred to as RSP extract from now on.

3.3.2 Antioxidant activity of final RSP extract

To verify the homogeneity of the final extract in terms of its antioxidant properties, DPPH, FC, FRAP and ORAC assays were applied. Three independent samples from the mixture of the different extractions were taken and analysed. The results obtained clearly showed that the three independent samples taken from the final extract show no significant difference in all the assays (Figure 3.17). Therefore, samples used for further analysis should exhibit the same activity throughout the project.

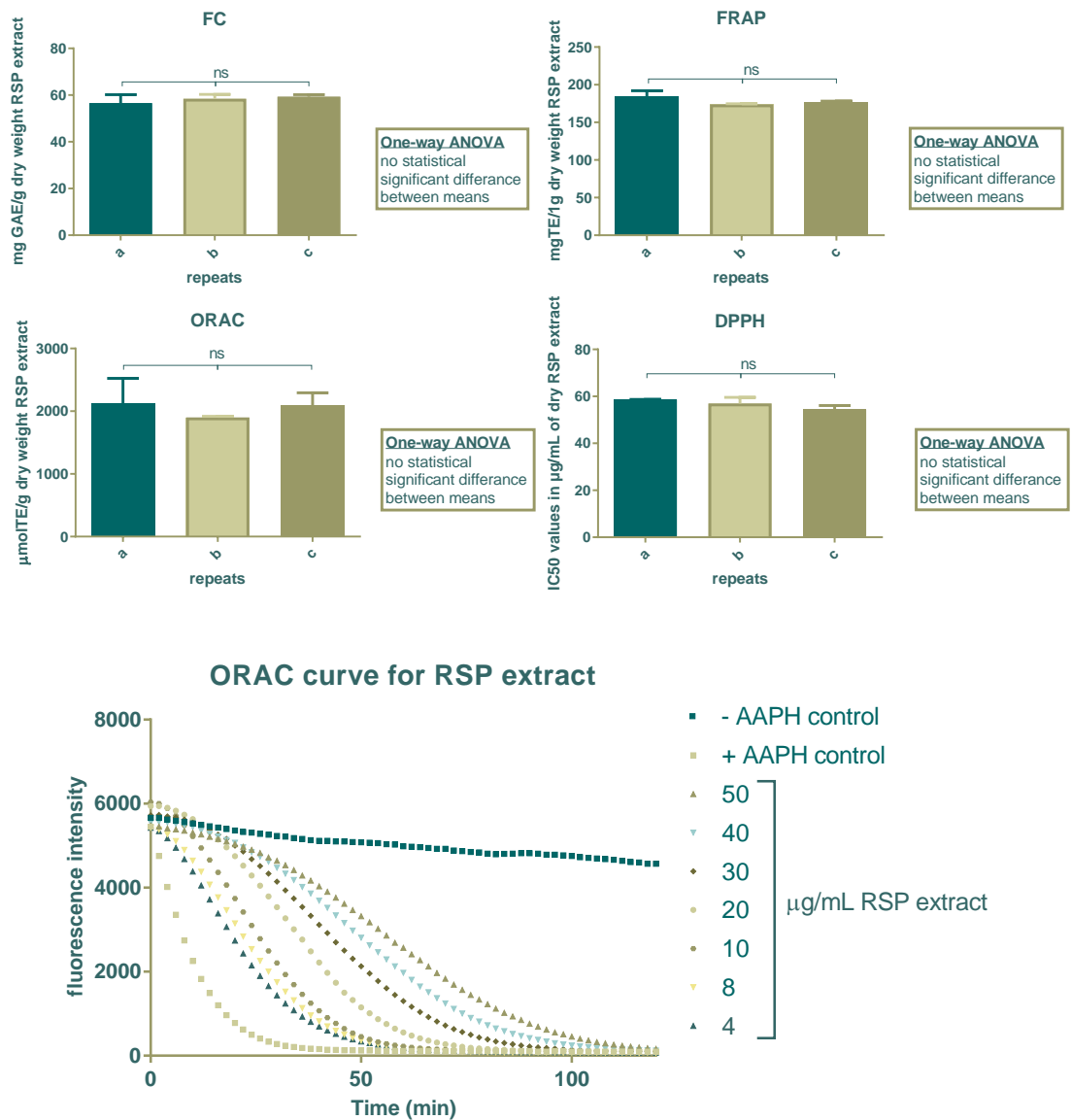


Figure 3.17| DPPH, FC and FRAP and ORAC results obtained from three extraction replicates
 Indicating mean and standard deviation (technical replicates), significant difference via One-way ANOVA (box), Bonferroni's multiple comparisons test between samples, ns-not significant

3.3.3 LC-MS/MS analysis of final RSP extract

In addition to the antioxidant assays, the secondary metabolite analysis was repeated, to determine the final extracts composition and to compare it to the previous SOX 2014 extract (Table A2, p.429 ff.). Most of the secondary metabolites initially found in the SOX extract from the 2014 harvest were also present in the final RSP extract (Table 3.5). The most abundant compounds in the final extract are sinapic acid, indole-3-pyruvic acid, syringic acid, 4-hydroxyphenylpyruvic acid and ferulic acid. Multiple t-test was carried out between the two extracts (SOX2014 from Chapter 2 and the new SOX2014 extract from chapter 3) and they showed significant differences for some of the compounds present. These differences might occur due to the way the original sample is processed and stored. The pomace itself is a biological sample and not completely homogeneous and can contain left over plant particles from leaves and stems as well as the seed pomace. Samples taken for the extraction are not necessarily completely homogeneous. Hence, when comparing the initial extract SOX2014 from chapter 2 (2.3.4 HPLC-MS/MS p.107 ff., first extract Table 3.5) to the final extract here in chapter 3 (final extract; Table 3.5), differences between the composition were expected.

Sinapic acid, the most abundant compound with 3993 ± 49.89 mg/kg only represents about 0.4% of the extract. As described in chapter 2 (2.3.11 Determination of antioxidant activity of single compounds within the extract as well as their mixtures, p.127 ff.) these low concentrations of phenolics do not contribute a great deal towards the antioxidant activity of the extract. Therefore, these results have led to further investigations in finding other abundant secondary metabolites in the extract which might be responsible for the observed antioxidant activity (3.3.4 Additional secondary metabolite analysis, p.175 ff.). Although most of the secondary metabolites found so far are present in small concentrations and do not contribute significantly to the antioxidant activity of the extract; they might have different activity *in vitro* or *in vivo* for which smaller concentrations are sufficient. Table 3.5 below, lists some of these additional activities for the secondary metabolites found in the RSP extract. Some of these activities have been closely associated with the potential treatment of neurodegenerative diseases.

Table 3.5| Concentration of secondary metabolites in First and Final RSP extract and published biological activities

Extraction technique	SOX [mg/kg RSP extract]			
<i>Harvest year</i>	2014 (first extract)	2014 (final extract)	t-test	activity
Benzoic Acids (in mg/kg extract)				
<i>benzoic acid</i>	-	21.59 ± 7.21	ns	
<i>p-hydroxybenzoic acid</i>	74.89 ± 9.51	71.20 ± 9.07	ns	-AChE/BChE inhibition ⁴⁶¹ -metal chelating and DNA protection <i>in vitro</i> ³⁸⁶
<i>syringic acid</i>	224.23 ± 16.54	317.77 ± 16.15	*	-metal chelating and DNA protection <i>in vitro</i> ³⁸⁶ - neuro protection, elevation of SOD activity reduction of oxidative stress ⁴⁶²
<i>vanillic acid</i>	44.72 ± 2.61	12.83 ± 6.94	*	-metal chelating and DNA protection <i>in vitro</i> ³⁸⁶
<i>protocatechuic acid</i>	72.59 ± 1.14	98.78 ± 4.70	*	-metal chelating and DNA protection <i>in vitro</i> ³⁸⁶ -nerve regeneration potential ⁴⁶³ - inhibition of Aβ ₄₂ ⁴⁴⁵
<i>salicylic acid</i>	14.99 ± 1.72	5.59 ± 0.30	*	-antioxidant activity ⁴⁶²
<i>p-anisic acid</i>	28.11 ± 3.94	-	**	
<i>gallic acid</i>	-	48.67 ± 2.34	***	-metal chelating and DNA protection <i>in vitro</i> ³⁸⁶ -inhibition of Aβ ₄₂ ⁴⁴⁵
Benzaldehydes				
<i>syringin</i>	33.58 ± 3.15	14.19 ± 8.53	ns	-protects Aβ (25-35)-induced toxicity in neuronal cells ⁴⁶⁴
<i>protocatechualdehyde</i>	48.83 ± 1.38	21.87 ± 2.49	**	- decreased reactive oxygen species (ROS) production and increased Nrf2/HO-1 expression ⁴⁶⁵

The Potential Application of Rapeseed Pomace Extracts in the Prevention and Treatment of Neurodegenerative Diseases

<i>vanillin</i>	15.08 ± 1.34	-	**	-neurosupportive role on rotenone induced neurotoxicity (SH-SY5Y) ²³⁵
Cinnamic Acids				
<i>sinapic acid</i>	4896.91 ± 281.68	3993.67 ± 49.89	ns	-AChE/BChE inhibition ⁴⁶¹ -neuroprotection AD model (<i>in vivo</i>) ²⁴¹
<i>ferulic acid</i>	182.70 ± 9.82	199.84 ± 1.62	ns	-AChE/BChE inhibition ⁴⁶¹ -neuroprotection ²⁴³ -metal chelating and DNA protection <i>in vitro</i> ³⁸⁶ -inhibition of Aβ ₄₂ ⁴⁴⁵
<i>cinnamic acid</i>	69.59 ± 3.35	19.35 ± 0.23	***	-metal chelating and DNA protection <i>in vitro</i> ³⁸⁶
<i>caffeic acid</i>	110.82 ± 9.57	94.48 ± 8.00	ns	-anti dementia activity ⁴⁶⁶ -metal chelating and DNA protection <i>in vitro</i> ³⁸⁶ -inhibition of Aβ ₄₂ ⁴⁴⁵
<i>p-coumaric acid</i>	32.10 ± 2.94	26.87 ± 0.48	ns	-AChE/BChE inhibition ⁴⁶¹
Phenylpyruvic Acids				
<i>4-hydroxyphenylpyruvic acid</i>	149.77 ± 39.56	249.62 ± 20.34	ns	-AChE inhibition ⁴⁶⁷
<i>phenylpyruvic acid</i>	-	15.39 ± 0.42	***	
Acetophenes				
<i>3,4,5-trimethoxyacetophenone</i>	-	2.23 ± 0.52	*	
Phenylactic Acids				
<i>phenylactic acid</i>	-	5.82 ± 0.31	***	
Other Phenolics				
<i>4-hydroxy 3-methoxybenzyl alcohol</i>	0.76 ± 1.32	6.49 ± 0.40	*	-antioxidant activity ⁴⁶⁸
<i>anthranilic acid</i>	-	3.09 ± 0.06	***	
<i>chlorogenic acid</i>	-	19.46 ± 2.90	**	-metal chelating and DNA protection <i>in vitro</i> ³⁸⁶ -antioxidant activity ⁴⁶²

<i>hydroxytyrosol</i>	-	10.12 ± 0.13	***	-neuroprotective effect in rat brain slices ⁴⁶⁹
-----------------------	---	--------------	-----	--

Indoles

<i>Indole</i>	-	13.34 ± 1.10	**	
<i>indole-3-pyruvic acid</i>	336.05 ± 89.09	412.36 ± 72.43	ns	
<i>indole-3-carboxylic acid</i>	11.78 ± 0.59	9.57 ± 2.01	ns	

Amines

<i>Spermidine</i>	433.56 ± 41.44	-	**	-protects against a-synuclein neurotoxicity ⁴⁷⁰
<i>Spermine</i>	1.82 ± 0.05	13.61 ± 0.74	***	-neuroprotective by induction of autophagy ⁴⁷¹

Flavanoids/Coumarins

<i>8-methylpsoralen</i>	-	2.06 ± 0.25	**	
<i>Bergapten</i>	-	1.86 ± 0.55	ns	
<i>Kaempferol</i>	22.32 ± 6.92	3.09 ± 0.50	ns	-inhibition of Aβ ₄₂ ⁴⁴⁵
<i>Isorhamnetin</i>	7.85 ± 1.30	-	*	-protective effects against amyloid β-induced cytotoxicity and amyloid β aggregation ⁴⁷²
<i>Luteolin</i>	44.66 ± 3.43	67.59 ± 1.34	*	-inhibition of Aβ ₄₂ ⁴⁷³
<i>Apigenin</i>	2.31 ± 0.42	11.31 ± 0.21	***	-inhibition of Aβ ₄₂ ⁴⁴⁵
<i>Glycitein</i>	-	1.26 ± 0.18	**	-suppress Aβ toxicity through combined antioxidative activity and inhibition of Aβ deposition (<i>in vivo C. elegans</i>)
<i>Epicatechin</i>	-	22.50 ± 0.32	***	-inhibition of Aβ ₄₂ ⁴⁴⁵
<i>Phloretin</i>	-	0.50 ± 0.03	***	-neuroprotective <i>via</i> ROS scavenging, normalizing mitochondrial transmembrane

The Potential Application of Rapeseed Pomace Extracts in the Prevention and Treatment of Neurodegenerative Diseases

				potential and consequently avoiding energy depletion ⁴⁷⁴
<i>Imperatorin</i>	-	3.63 ± 0.29	***	-anti-inflammatory and antioxidant activities ⁴⁷⁵
<i>Naringenin</i>	2.58 ± 0.25	2.00 ± 0.18	ns	-neuroprotective effect through suppression of NF-κB signalling pathway and upregulates the antioxidant status ⁴⁷⁶
<i>Tangeretin</i>	0.93 ± 0.10	4.82 ± 0.53	**	-antioxidant and anti-inflammatory effects, attenuate cholinergic deficits and reduction of abnormal accumulation of neurotoxic amyloid-beta peptides ⁴⁷⁷
<i>Quercetin</i>	-	30.61 ± 0.54	***	-inhibition of Aβ ₄₂ ⁴⁴⁵
<i>Quercetin-3-Glucoside</i>	6.72 ± 0.81	3.24 ± 0.28	*	
<i>Quercitrin</i>	-	0.61 ± 0.03	***	-attenuated Aβ (25-35)-induced neurotoxicity ⁴⁷⁸
<i>Hesperidin</i>	-	1.24 ± 0.21	*	-antioxidant, inhibiting lipid peroxidation ⁴⁷⁹
<i>Taxifolin</i>	-	1.17 ± 0.06	***	-inhibition of Aβ ₄₂ ⁴⁴⁵
<i>Phloridzin</i>	2.09 ± 0.29	2.92 ± 0.30	Ns	-neuroprotective effect through activation of Nrf2 defence pathway (<i>in vivo</i> , rats) ⁴⁸⁰
<i>I3-carboxaldehyde</i>	Not analysed	19.38 ± 1.80	-	
<i>total</i>	6902.27	5887.60		

Note(s): Statistical significance determined using the Holm-Sidak method, with alpha = 0.05. Each row was analysed individually, without assuming a consistent SD. ns-not significant, *p≤0.05, ** p≤0.01, *** p≤0.001, given from adjusted p-values; HPLC-MS/MS analysis conducted by Garry Duncan (Rowett)

3.3.4 Additional secondary metabolite analysis

3.3.4.1 Sinapine

The secondary metabolite composition of the extract described in Table 3.5, (p.171 ff.) was provided by the Rowett Institute. This service only determines concentrations of secondary metabolites that already exist in their reference library. Therefore, this prompted further HPLC analyses of the RSP extract, using similar parameters as described in the methods by Russell and Neacsu *et al.*^{342,343}. This extended analysis was carried at RGU using LC-MS/MS methodology and was published in Yates *et al.*⁴⁵⁶.

Initially the extract was analysed to obtain a chromatogram in the positive as well as negative ion mode (Figure 3.18). The chromatogram shows several, differently sized peaks. As published in Yates *et al.*⁴⁵⁶, standards of previously found secondary metabolites (sinapic acid RT=17.3 min, caffeic acid RT=12.0 min, ferulic acid RT=17.5 min and syringic acid RT=12.1 min, highlighted with arrows in Figure 3.18, p.176) were analysed separately and their concentration determined in 5 mg/mL RSP extract samples. Their retention times are highlighted in the negative ion mode chromatogram (Figure 3.18, p.176). The peak sizes for caffeic, ferulic and syringic acid are relatively small compared to some of the other peaks observed for example at a RT of 2.5, 3 and 8.8 mins. This initiated further analysis of those and a number of other peaks (Figure 3.22, p.181).

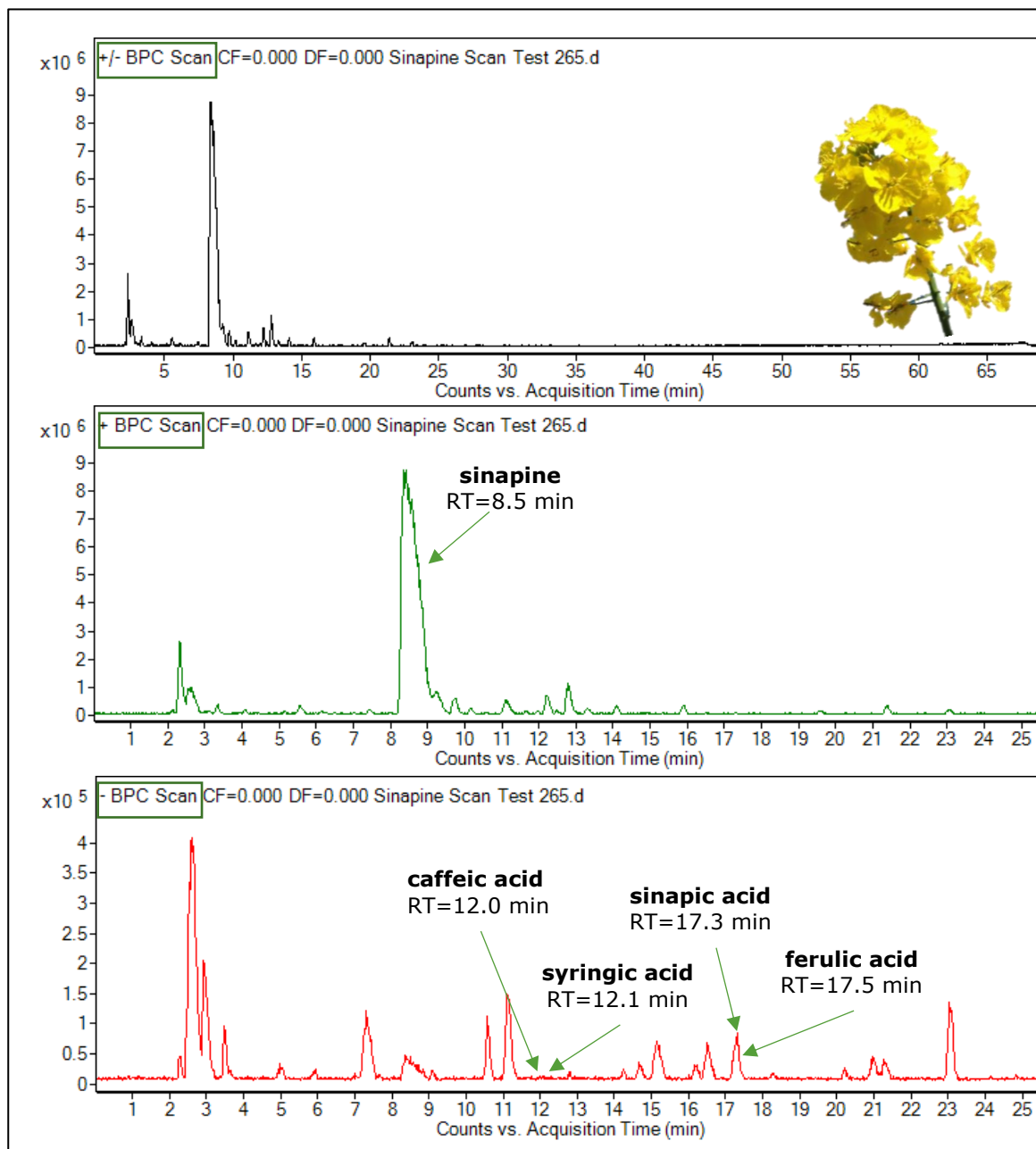


Figure 3.18| RSP extract (at 1 mg/mL) chromatogram in both/positive/negative ion mode after LC-MS analysis

Results obtained in collaboration with Louis Watter and Kyari Yates

The most significant peak found in the extract is eluting between 8.1 – 9.0 minute retention time. This peak was most prominent in the positive ion mode (Figure 3.18). When conducting MS/MS analysis of this peak with a m/z ratio of 310.1 the following fragmentation peaks (m/z ratio) were found: 251.0, 206.8 and 174.9 (Figure 3.19). These are the same MS/MS break down products suggested by Yang *et al.* as being sinapine, a secondary metabolite very common in rapeseed¹¹⁰.

Chapter 3: Phytochemical Characterisation and Neuroprotective Properties of RSP
Extract *in vitro*

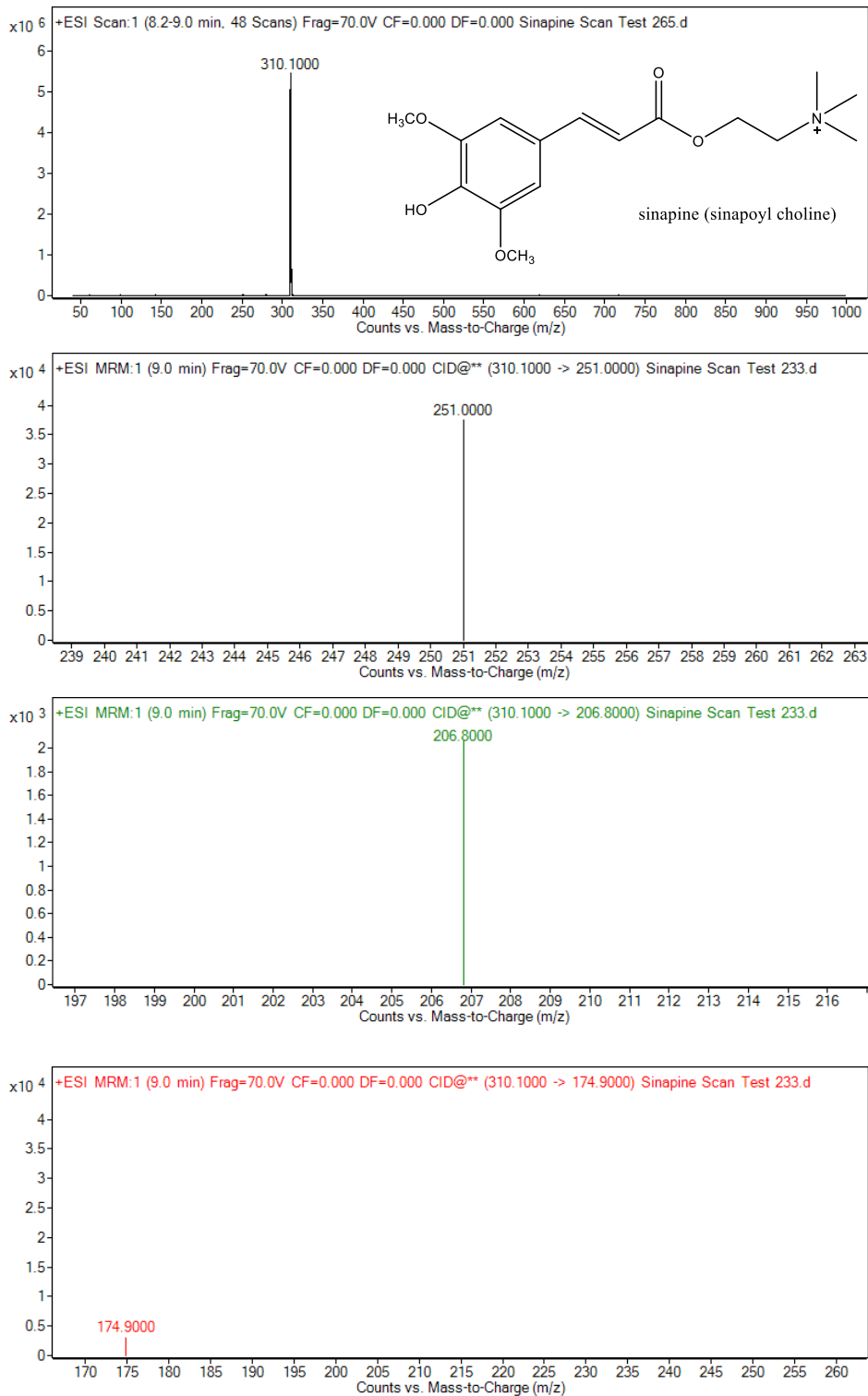


Figure 3.19| MS/MS data obtained for the breakdown of the m/z 310.1 peak

Results obtained in collaboration with Louis Watter and Kyari Yates

This result was compared with a commercially available sinapine thiocyanate standard (chemface). Equal break down products and a similar retention time were found, corresponding to those found for the extract (comparison of Figure 3.18, p.176 with Figure 3.20). By creating a sinapine calibration curve, using the sinapine thiocyanate standard, the concentration of sinapine in the RSP extract was determined to be 109.1 mg/g RSP extract (10.9 %). Further details on the analysis of sinapine and the four phenolic acids (sinapic-, ferulic-, syringic- and caffeic acid) can be found in Yates *et al.*⁴⁵⁶.

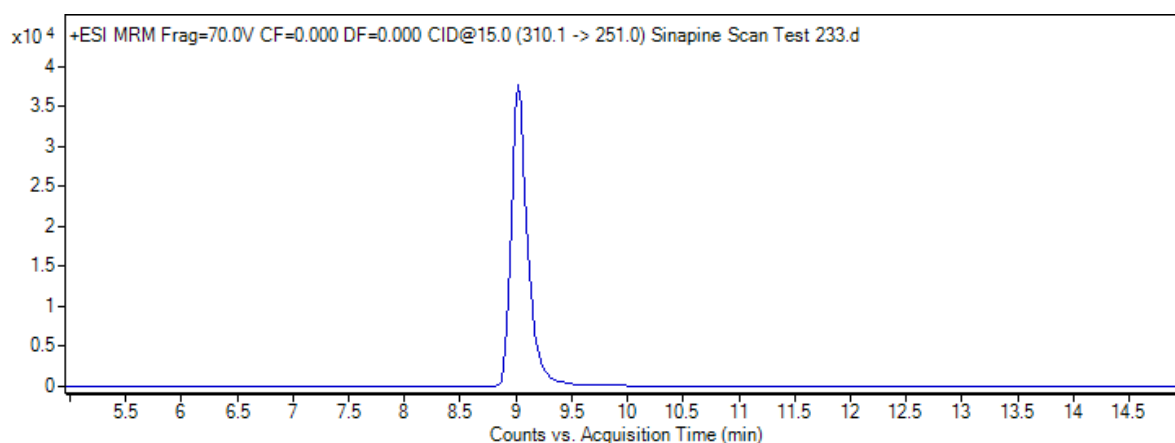


Figure 3.20| Chromatogram of sinapine






Results obtained in collaboration with Louis Watter and Kyari Yates

It is noteworthy to mention that direct comparison with other published data can be difficult. This is due to the fact that most papers express sinapine content in mg/g dry weight meal/cake. Here the concentration of sinapine is given per g RSP extract. The calculation of sinapine per g meal/pomace can be made by using the previously obtained extraction yields (Table 2.9, p.104) of about 76 mg extract/g RSP. A concentration of 109.1 μg sinapine per 1 mg of extract would mean a concentration of 8291.6 $\mu\text{g/g}$ of pomace or 8.3 mg/g RSP. Zago *et al.*¹⁰⁸ found a concentration of 9.80 ± 1.27 mg/g in their (un-oiled) methanol extracted rapeseed cake. This is comparable to results found here, although our results are presented for the cold pressed RSP, still containing certain amounts of oil. Much higher values of sinapine were shown by Yang *et al.*¹¹⁰, ranging from 29.74 ± 4.81 to 52.24 ± 3.64 mg/g RSP meal. The extraction in the latter was carried out on de-oiled rapeseed meal, using 10% methanol and 0.1% phosphoric acid. The extraction technique along with the different crop growing conditions and potentially different processing for the de-oiling steps (no details given in Yang *et al.*¹¹⁰) could have led to

these high values. Another explanation is the potential of additional sinapine in the leftover product after the first aqueous ethanol extraction, because the determination of extraction efficiency was not part of this project.

In that case, the current value of 8.3 mg/g dry RSP (cold pressed) would not be the maximum concentration of sinapine in the RSP used in this study.

Antioxidant activity of Sinapine

To determine whether sinapine is responsible for the antioxidant activity of the RSP extract, the following samples at the extract concentration were put through a few antioxidant assays: (i) sinapine, (ii) a mixture of phenolic acids (sinapic acid, caffeic acid, ferulic acid and syringic acid) (iii) a mixture of sinapine and the phenolic acids. The results obtained for the FC, FRAP, DPPH and ORAC assay are presented in Figure 3.21 (p.180). The results show that sinapine is the main contributor to the antioxidant activity observed in the extract. Together with the phenolic acid mixture, less than 50% of the activity for the extract is unexplained (Figure 3.21 ). Furthermore, the mixing of sinapine with the phenolic acids leads to an addition effect in all four experiments (Figure 3.21 ). No synergistic or antagonistic effect was observed. This can be seen when comparing the height of the bars for the phenolic acid and sinapine mixture () to sinapine () and the phenolic acid mix (.

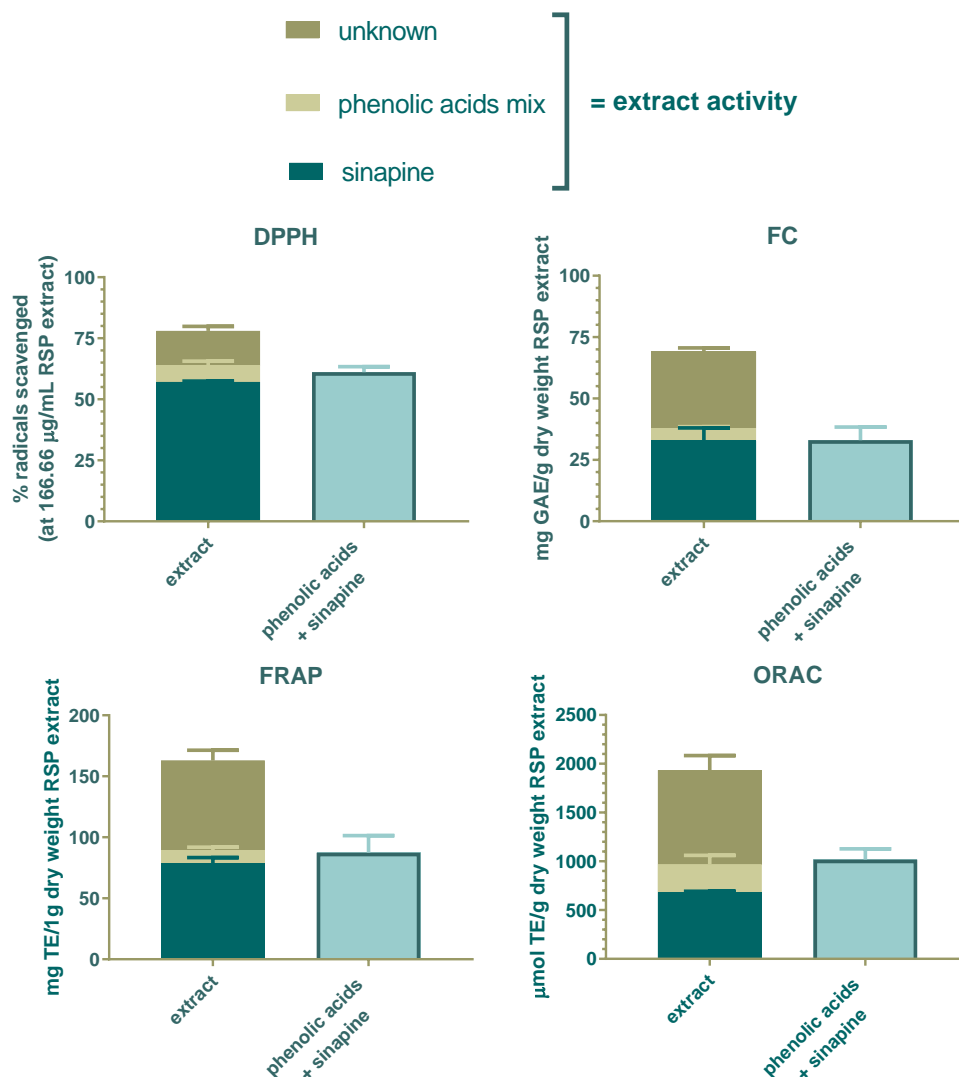


Figure 3.21 | Antioxidant activity of sinapine and phenolic acids and their mixture compared to the RSP extract activity, determining unknown activity in the extract, adapted from Yates *et al.*⁴⁵⁶

Results obtained in collaboration with Louis Watter

The FC assay shows that sinapine is responsible for about 47% of the phenolic content (Figure A3, p.442). Slightly higher results were obtained by Thiyam *et al.*⁹⁷, where sinapine alone, was found to be responsible for between 55-70% of the phenolic content. In contrast, for the DPPH assay, they found sinapine to be responsible for only between 25-50% of the radical scavenging activity. Whereas in our study sinapine is responsible for more than 70% at the tested extract concentration (Figure A3, p.442). A comparison of sinapic acid (SA), sinapine (Sin) and sinapoyl glucose (SG) in the DPPH assay showed the following order of scavenging activity in their study SA>SG>Sin⁹⁷.

However, they did not investigate the activity of sinapine in the FRAP or ORAC assay.

The results in Figure 3.21 show that sinapine appears to exhibit a better radical scavenging activity (DPPH) than reducing capacity (FRAP/FC). The ORAC activity was found to be even lower and demonstrated that not all of the extract's activity can be explained using sinapine and some of the phenolic acids found within the extract. Figure 3.18 (p.176) however indicated the presence of other compounds within the extract, which have not been identified yet. Some of the peaks have a larger peak area compared to the phenolic acids, these were investigated using MS/MS analysis following.

3.3.4.2 Additional phenolic derivatives and other secondary metabolites identified via LC-MS/MS

To determine some of the unknown peaks (1-7) within the chromatogram (Figure 3.22), MS/MS analysis was employed. The found m/z ratios for the molecular ion and the fragmentations are shown in Table 3.6 (p.182).

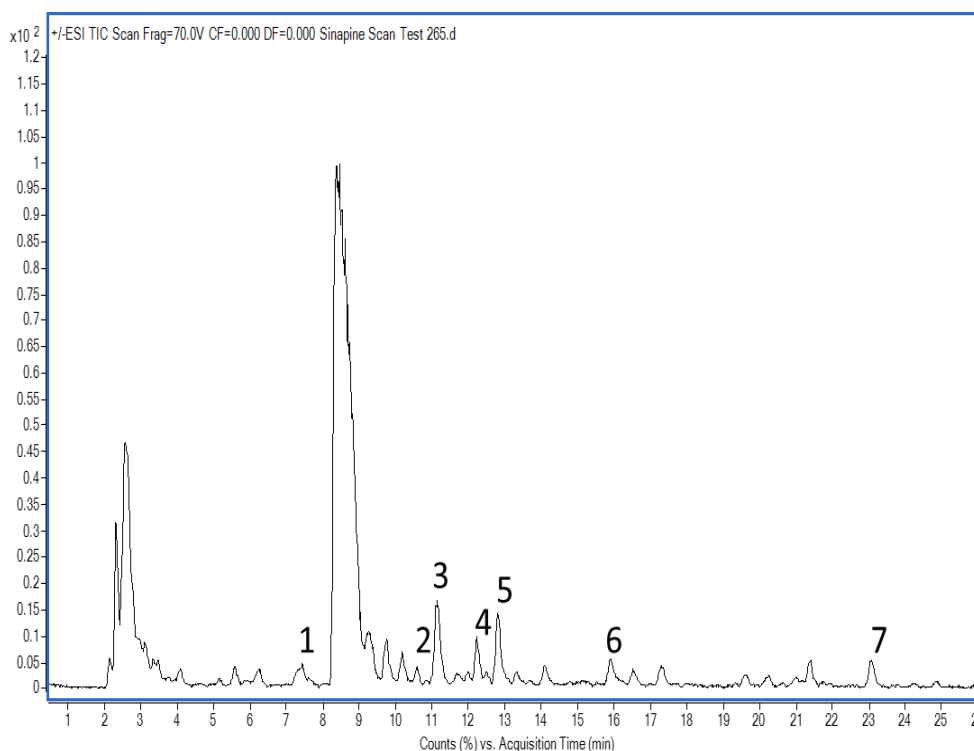


Figure 3.22| +/- ESI total ion chromatogram of a 1 mg/mL RSP extract

Showing additional peaks, some of which have been identified from existing literature (Table 3.6), adapted from Yates et al.⁴⁵⁶; results obtained in collaboration with Louis Watter and Kyari Yates

Table 3.6| MS/MS fragmentations of unknown peaks within the chromatogram

Peak #	Compound name	Rt (min)	quasi-molecular ion type	MS-MS fragments following CID m/z	References used in identification
1	Benzoylcholine	7.5	[M+H] ⁺	208	149.1, 105.1 Clauß <i>et al.</i> (2011) ⁴⁰⁴
2	Kaempferol-3-O-(sinapoyl)-diglucoside-7-O-glucoside	10.7	[M-H] ⁻	977	815.2 Ferrerres <i>et al.</i> (2009) ³⁹⁸
3	Sinapoyl glucoside	11.2	[M-H] ⁻	385	325.1, 265.2, 247, 223, 205 Ferrerres <i>et al.</i> (2009) ³⁹⁸ , Thiyam <i>et al.</i> (2009) ⁴⁰⁵ , Oszmianski <i>et al.</i> (2013) ⁴⁰⁶
4	Sinapine (4-O-8') guaiacyl	12.3	[M+H] ⁺	506	446.9, 251, 207, 175, 147 Clauß <i>et al.</i> (2011) ⁴⁰⁴
5	Cyclic spermidine conjugate (alkaloid)	12.9	[M+H] ⁺	496	478, 425, 408.2, 381.9, 351, 324.9, 280.8, 231.9, 198, 191, 175 Clauß <i>et al.</i> (2011) ⁴⁰⁴ , Yang <i>et al.</i> (2015) ¹¹⁰
6	Feruloyl choline (5-8') guaiacyl	16.0	[M+H] ⁺	458	399, 381, 369.1 Clauß <i>et al.</i> (2011) ⁴⁰⁴ , Yang <i>et al.</i> (2015) ¹¹⁰
7	1,2-disinapoyl glucoside	23.1	[M-H] ⁻	591	367, 223, 205 Ferrerres <i>et al.</i> (2009) ³⁹⁸ , Yang <i>et al.</i> (2015) ¹¹⁰

Note(s): Including suspected names after literature comparison, adapted from Yates *et al.*⁴⁵⁶; results obtained in collaboration with Louis Watter and Kyari Yates

The identification of these metabolites was based on their mass spectra results and hence the proposed identity of each peak is not absolute. To verify their identity and determine concentrations found within the extract, standards are required. To date, these metabolites are not commercially available. However, these secondary metabolites have previously been identified in *Brassica* species^{110,398,404–406}, which made identification using MS/MS spectra analysis possible. There are no reports on the antioxidant activity of these secondary metabolites, but they could contribute to the unknown antioxidant activity of the RSP extract (Figure 3.21 ■, p.180). Due to the lack of standards, one other way to positively identify these compounds and determine their activity would be the use of preparative/semi-preparative HPLC, to isolate and collect each individual peak followed by their subsequent NMR and antioxidant analysis.

3.3.4.3 Glucosinolate (GLS) analysis

To determine the presence of GLSs in the RSP extract HPLC methodology was utilized. Eleven GLSs were used as external standards (Figure 3.3, p.139). A chromatogram of this mixture is presented in Figure 3.23.

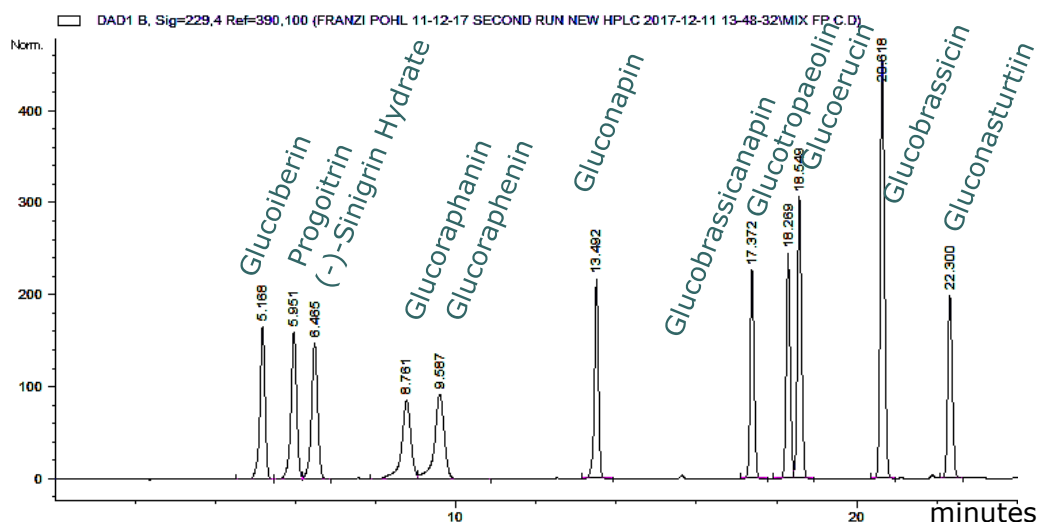


Figure 3.23| Glucosinolate standard mixture HPLC chromatogram

When overlaying the chromatogram obtained from the standard mix with the chromatogram from the extract (Figure 3.24, p.184), a number of peak retention times, match those from the standards, implying that the extract could contain these GLSs (Figure 3.24, indicated by blue and red arrows, p.184).

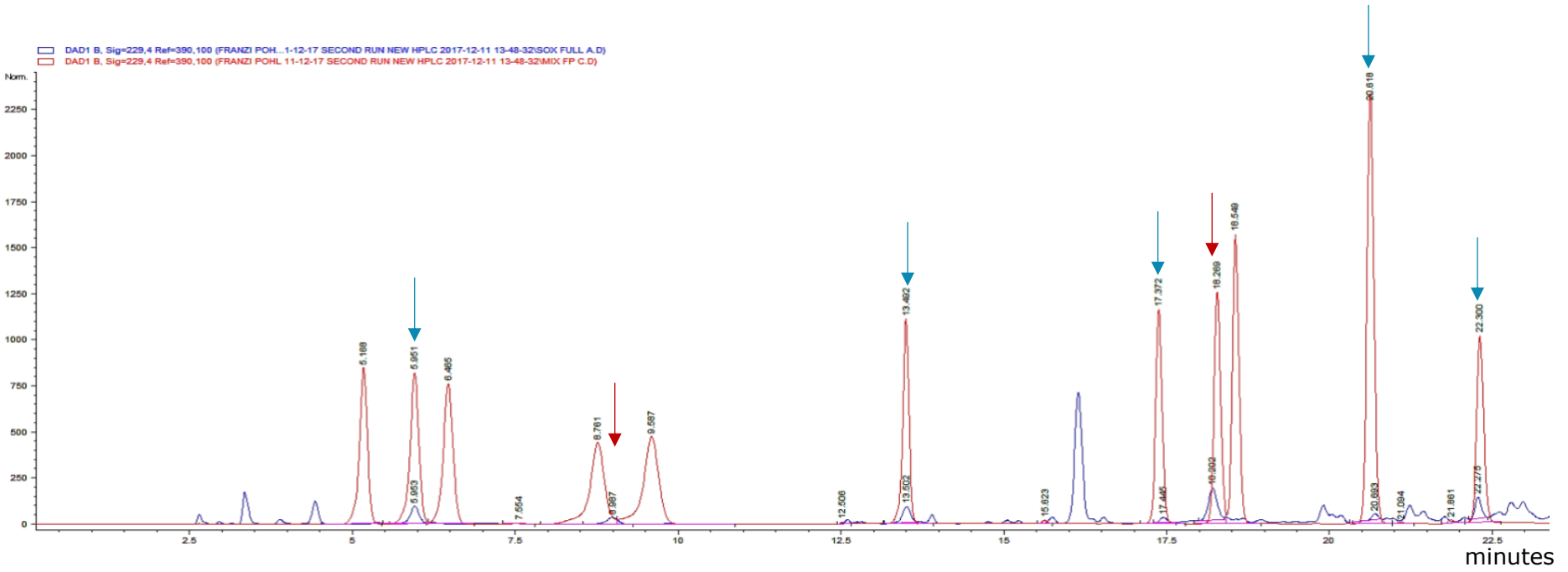


Figure 3.24| HPLC glucosinolates chromatogram for standard mixture and RSP extract (overlay)

Standard mixture of glucosinolates (0.091 mg/mL) and their retention times (red) overlaid with the chromatogram obtained for the RSP extract (blue, 25 mg/mL), highlighting potential glucosinolate peaks (red and blue arrows)

To confirm the presence of the GLS at these specific retention times, absorbance spectra of each standard was compared to the extract at the specific retention time (e.g. GLS progoitrin Figure 3.25). If it was possible to overlay the extract absorbance spectra with the spectra obtained from the respective standard, as seen with progoitrin (Figure 3.25), the GLS was considered for concentration calculations in the extract. A small difference in the DAD spectra (GLS standard vs. RSP extract) can be explained by a potential co-elution of the GLS with other compounds (Figure A4, p. 442 ff.). Thus, their determination in the RSP extract is not conclusive.

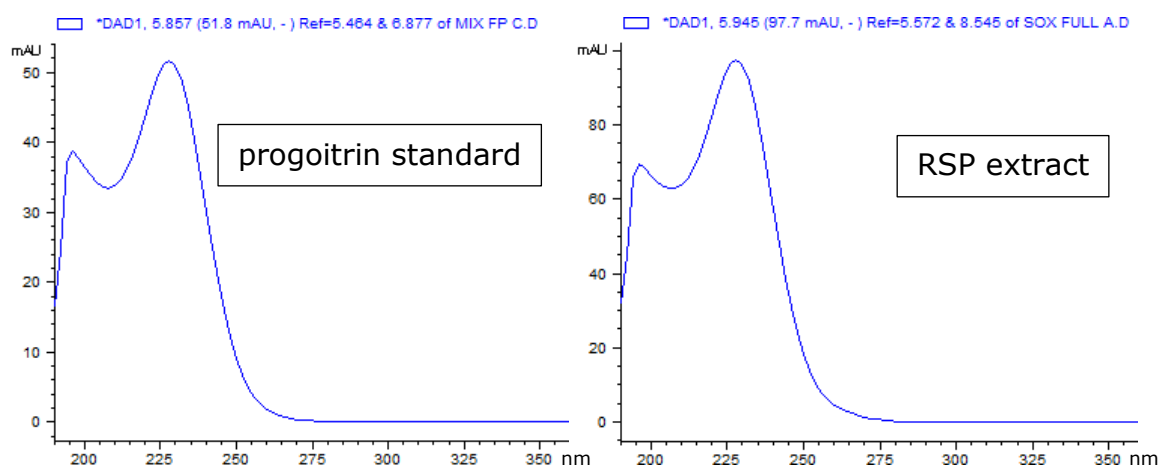


Figure 3.25| Absorbance spectra for progoitrin Standard and RSP extract (190-360 nm)

Calibration curves were obtained for each GLS and concentrations in the extract calculated if the obtained peak area was above the limit of quantification, as demonstrated in Figure 3.26 on the example of progoitrin.

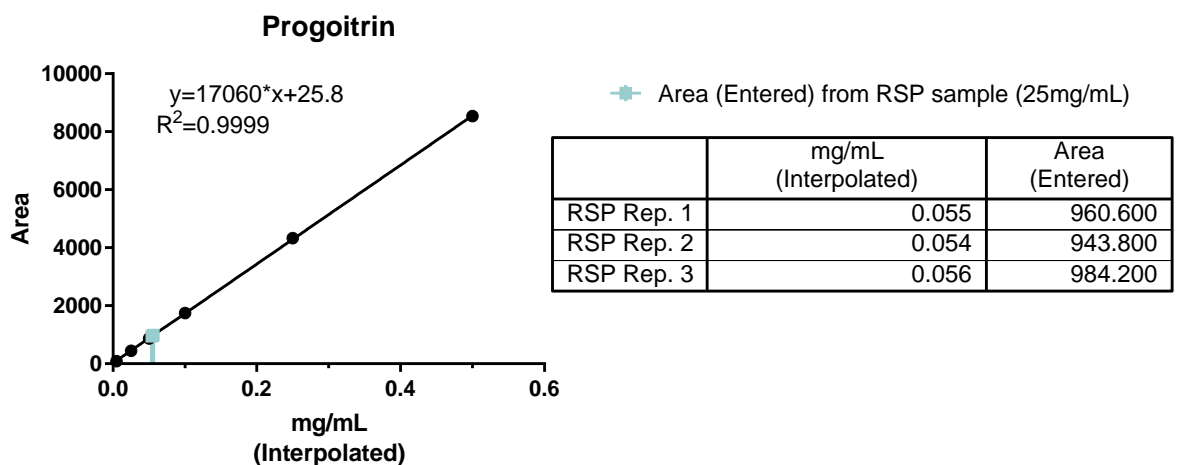


Figure 3.26| Calibration curve obtained for progoitrin (0.005-0.5 mg/mL)

The concentrations obtained in mg/mL were then transformed into mg GLS/g extract, giving progoitrin concentrations of 2.20 ± 0.05 mg/g RSP extract, making it the most abundant GLS in the extract. Other GLSs found above the LOD and LOQ were gluconapin and gluconasturtin (Table 3.7). Glucobrassicinapin was detected but the peak area was below the LOQ, so no concentration was calculated. Similarly, the spectra at 20.6 minutes retention time can be matched with the spectra of glucobrassicin (Figure A4, p.442 ff.) however, the detected peak area is below the LOD.

Table 3.7| GLS found in RS extract (blue arrows in Figure 3.24)

GLS	concentration [mg/mL]		RSP [mg/g extract]	
	LOD	LOQ	mean	std
PROGOITRIN	0.005148	0.01560	2.197	0.04759
GLUCONAPIN #	0.005781	0.01752	1.959	0.04021
GLUCOBRASSICANAPIN #	0.009727	0.02948	below LOQ	
GLUCOBRASSICIN #	0.02899	0.08784	below LOD	
GLUCONASTURTIIN #	0.01546	0.04685	1.899	0.03623

Note(s): #compounds potentially co-eluting with other compounds, absorption spectra inconclusive (Figure A4, p.442 ff.)

Progoitrin has previously been shown to be the main GLS in RSP from Scotland, followed by gluconapin and glucobrassicinapin¹¹⁵. These three GLSs were also detected in our RSP extract. In a different study by Millán *et al.*⁴⁸¹ a wider variety of GLS was found. Samples for their study were obtained from a field experiment studying the effect of different nitrogen and sulphur fertilizer on the level of GLS; the most abundant GLSs were also progoitrin, gluconapin and glucobrassicinapin. In addition, they also found high amounts of 4-hydroxyglucobrassicin as well as epiprogoitrin and gluconapoleiferin which were not analysed in this study; and glucobrassicin, gluconasturtiin. The total amount of GLSs present in rapeseed are known to be dependent on the nitrogen and sulphur content⁴¹¹. Other factors affecting the GLS concentrations in rapeseed are the cultivar, physiological age, health, and environmental factors (e.g. climate condition). The production process of the rapeseed also has a big impact on the GLS content of RSP sample, due to the activity of the enzyme myrosinase. The latter can act upon GLSs once the plant tissue is harmed (e.g. cutting, milling, chewing). In the study by Millán *et al.*⁴⁸¹ harvested seeds were dried, then crushed and immediately extracted, giving the myrosinase little time to hydrolyse the GLSs. This could be the

reason for the additionally found GLSs. For this research project however, RSP was obtained, which was cold pressed and transported later to RGUs research facility. The exact storage condition at the farm as well as the time the RSP was store, before it was brought to RGU are unclear. The concentration of GLSs however is strongly dependent on storage time^{410,482}. This uncertainty in storage time and environment suggests, that myrosinase might have had much longer time to act upon the glucosinolates in our samples. The action of myrosinase, at least partially, could have transformed the GLSs into GLS hydrolysis products (3.1.1.2 Glucosinolates (GLSs), p.136). An overview, summarizing parameters influencing the formation of different hydrolysis products are discussed in Holst *et al.*⁴⁰⁷.

It is difficult to compare the quantitative results obtained in this study to other studies, because in most research papers concentrations are given in mg or μmol per gram or kg dry seed or de-oiled pomace. In contrast, the concentrations in this study are given per gram of extract, since the latter is the end-product of interest here.

For better comparison with the literature, also the RSP itself was extracted with boiling water and analysed according the same method (3.2.2.3 Determination of additional secondary metabolites in the extract, p.158 ff.). However, the peak areas obtained through HPLC analysis were much smaller or not visible for the GLSs studied (Figure A5, p. 445). No concentrations could be determined for any of the positively identified compounds *via* spectra comparison. However, GLS concentrations can be back calculated (Figure A6, p.445) to the cold pressed RSP by using the extraction yield of 76 mg RSP extract/g RSP (Table 2.9, p.104), leading to values of: progoitrin:0.167 g/kg RSP, gluconapin:0.149 g/kg RSP and gluconasturtiin:0.144 g/kg RSP which are much lower than the results found by for example Raikos *et al.*¹¹⁵ for cold-pressed rapeseed pomace (progoitrin: 2.52 ± 0.16 g/kg; gluconapin: 0.68 ± 0.12 g/kg; glucobrassicinapin 0.45 ± 0.02 g/kg).

Since GLSs have not been reported to have significant direct antioxidant activity⁴⁸³, their presence most probably does not contribute to the unknown antioxidant activity found for the extract (Figure 3.21, p.180). However, GLS hydrolysis products (Figure 3.2, p.137) can be indirect antioxidants, by

inducing phase II enzymes, responsible for the antioxidant and xenobiotic metabolizing response pathway involving e.g. heme oxygenase 1 (HO-1) or glutathione S transferases (GSTs) through Keap1-Nrf-2-ARE signalling (1.4.3 Exogenous antioxidants - natural products: direct and indirect antioxidant activity, p.58 ff.)^{409,484}. Their presence *in vivo* or in a cell system could induce an oxidative stress response pathway and aid in metabolising endogenous compounds and xenobiotics. A variety of isothiocyanines have previously been identified in rapeseed and rapeseed pomace, e.g. butenyl-, butenyl- and pentenyl- isothiocyanates^{485,486}. Their analysis was unfortunately not part of this project due to time restrictions.

3.3.4.4 Determination of total monomeric anthocyanin pigment content

A further group of secondary metabolites often associated with positive biological activity are the anthocyanins, which belong to the flavonoid group of secondary metabolites (Figure 1.6, p.10). Anthocyanins are well known antioxidants and if present in the RSP extract, might play a role in the extracts antioxidant activity⁴⁸⁷. Here, the pH differential method was employed to confirm or preclude the presence of any anthocyanin.

No colour change was visible, when mixing a stock solution of the RSP extract (1 mg/mL) with the highly acidic buffer (pH 1.0) 1:5. A slight turbidity occurred once the extract was introduced to the pH 1.0 buffer. In contrast, the grape pomace (GP) extract at the same concentration, showed a significant colour change, suggesting the presence of anthocyanins (Figure 3.27).



Figure 3.27| pH differential method

Visual observation of colour change, comparing RSP (left) with GP (right)

When measuring the absorbance for the solution, a clear difference between peak intensity (520 nm) can be seen between the pH 4.5 and pH 1.0 solution for the GP extract (Figure 3.28, ■ and ■ line respectively). For the RSP extract however, no peak is visible. The slight overall increase of the curve (Figure 3.28, ■ compared to ■) between 390 and 800 nm is most likely caused by the increased turbidity of the sample (Figure 3.27).

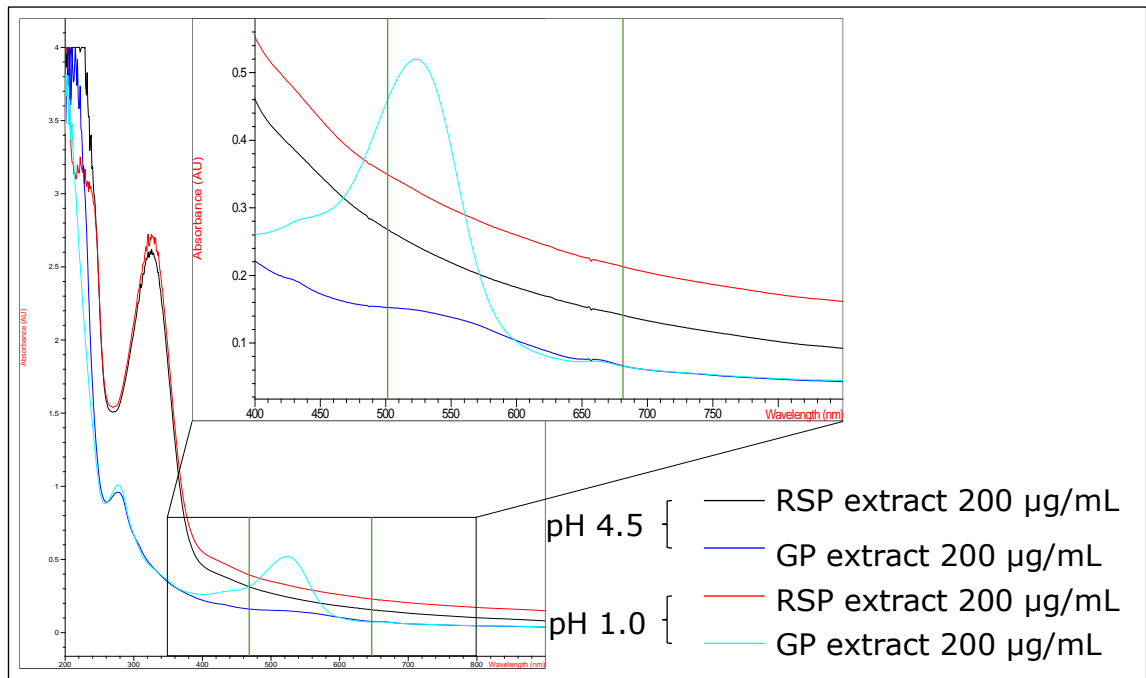


Figure 3.28| Absorbance spectra for RSP and GP extracts at pH 4.5 and pH 1.0 for the determination of total anthocyanins

The calculation of the anthocyanin content showed the presence of 31.4 ± 1.1 mg total monomeric anthocyanin pigment content per g GP extract. The value

obtained for the RSP extract was much lower with 1.28 ± 0.35 mg/g. However, this value is not arising from an actual peak but from the general absorbance increase (turbidity of sample at pH 1.0) over the 390-800 nm range. Hence, the obtained anthocyanin concentration is most likely not the actual value for the anthocyanin content. Even the correction using a reading at 700 nm was not able to correct for the turbidity caused increase of absorbance. However, the fact that there is no peak visible at 520 nm suggests the lack of anthocyanins in the RSP extract.

Searching the literature for the presence of anthocyanins in rapeseed seeds or pomace, was unsuccessful. No papers were found showing anthocyanin content in RSP but neither did papers show the negative outcome of anthocyanin analysis. Anthocyanins most often cause a plant to be strongly coloured (red, blue or purple; e.g. red grapes). As rapeseed does not show any sign of this colouration, the assumption might have formed, that no anthocyanins are present in rapeseed seeds, which was confirmed, after determination using the pH differential method. Interestingly, a paper published by Li *et al.*⁴²⁵ used genetic manipulation to significantly increase the amount of anthocyanins in the leaves of *Brassica napus* with the aims to (i) improve the plants potential to produce pharmaceutical antioxidants and (ii) provide protection against potential disease⁴²⁵. A paper by Dai *et al.*⁴⁸⁸ also suggests the potential for (iii) increased resistance to droughts and cold stress. However, neither failed to show data for anthocyanin content in the seeds.

This pH differential method gives an indication of total anthocyanin content but is not very sensitive to low amounts of anthocyanins. For a 100% exclusion of their presence, techniques that are more sophisticated should be used, such as HPLC-MS/MS methods. In a paper by Lee *et al.*⁴⁸⁹ for example, both methods showed good correlation. However, the HPLC results gave higher values than the pH differential values, in most of their samples. Because the pH differential method showed no indication for the presence of anthocyanins, it was decided to not look further into the HPLC analysis of anthocyanins within the RSP extract, due to time limitations.

3.3.5 Metal chelating potential

The *in vitro* analysis of the metal (iron and copper) chelating activity of the extract, showed no significant iron chelating properties. The absorbance showed no significant differences to the negative control and values were outside the LOD and LOQ (Figure A8, p. 447). There is currently no research into the iron chelating properties of RSP extracts. However, the results are in contradiction to findings by Andjelković *et al.*⁴⁹⁰ who found iron chelating ability for both benzoic (weaker) and cinnamic acids (stronger) such as protocatechuic acid, gallic acid and caffeic acid, which are present in the RSP extract (Table 3.5, p.171). Sevgi *et al.*³⁸⁶ also found ferrous iron chelating properties for caffeic-, chlorogenic-, cinnamic-, ferulic-, gallic-, p-hydroxybenzoic-, protocatechuic-, syringic- and vanillic acid, all of which are present in the RSP extract (Table 3.5, p.171). An explanation for the negative results in the iron chelating assay in this study could be the low concentrations of those single phenolic acids within the extract. An extract concentration of 1 mg/mL was prepared, however within the assay final extract concentrations only reach 0.19 mg/mL (3.2.2.4 Metal chelating properties (Iron and copper), p.161). In comparison, Sevgi *et al.*³⁸⁶ run final concentrations of 0.89 mg/mL of the phenolic acids. The highest concentration of the phenolic acids tested by Sevgi *et al.* in the RSP extract is syringic acid with 318 mg/kg (Table 3.5, p.171). In 0.19 mg of extract there are only about 0.06 µg of syringic acid, which is much lower than the tested concentrations in Sevgi *et al.*³⁸⁶.

In contrast, the copper chelating activity assay showed the extracts potential to chelate Cu²⁺ ions, absorbance values measured were within the LOD and LOQ. The copper chelating activity was calculated and expressed as 29.23 mg EDTA equivalents/1 g RSP extract (Figure 3.29, p.192). This shows that only very high concentrations of the extract can chelate copper, meaning the extract is not as efficient as EDTA.

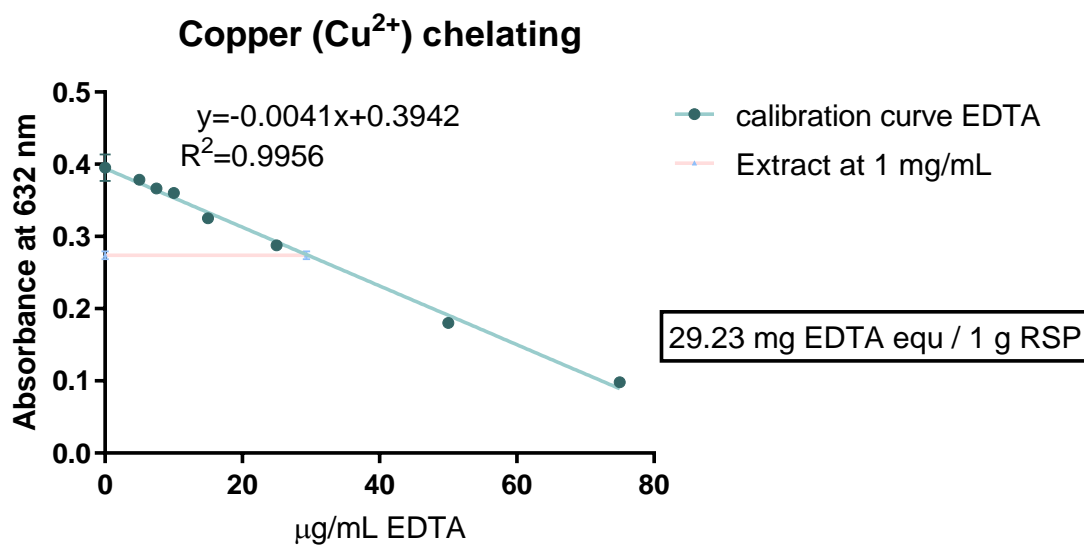


Figure 3.29| Copper chelating properties of the RSP extract

Results obtained in collaboration with Louis Watters

To determine whether sinapine is responsible for the copper chelating activity, the extract specific concentration of sinapine* was analysed in the same experiment, no change in absorbance compared to the negative control was observed. This leads to the conclusion, that sinapine is not acting as copper chelating agent in the RSP extract. The observed activity for the extract must therefore, be from other compounds within the extract. For example, Řiha *et al.*⁴⁹¹ found copper chelating properties for a number of flavonoids, using two different methods, the hematoxylin assay (for less competitive compounds) and the bathocuproinedisulfonic acid disodium salt (BCS) assay (for more competitive compounds). In the hematoxylin assay 24 out of a tested 26 compounds, including kaempferol, luteolin, apigenin, epicatechin and quercetin, all of which were found in the extract (Table 3.5, p.171 ff.). In the more competitive BCS assay, all the previous except epicatechin showed copper ion chelating properties⁴⁹¹.

Although the copper chelating properties are weak, they can add a positive attribute to the extract. In addition to the antioxidant properties found, the copper chelating activity, might further contribute to its potential activity *in vitro* and *in vivo*, as copper dis-homeostasis has been associated with a number of neurodegenerative diseases⁴³¹. The outcome from this experiment also suggests that sinapine, although responsible for a significant amount of

* 120 µg/mg RSP extract, exact concentration (109.1 µg/mg RSP extract) was still unknown at time of experiment

the antioxidant activity, is not accountable for all the different activities found for the RSP extract. Outcomes like this imply that the use of extracts might be preferable over the use of a single secondary metabolite, such as sinapine, from the plant extracts for further *in vitro* and *in vivo* studies.

3.3.6 AChE inhibition potential

Initially AChE inhibition activity was analysed using the Ellman method, for which the absorption of 5-thio-2-nitrobenzoate (yellow solution) with an absorption maximum at 412 nm is measured (Figure 3.30).

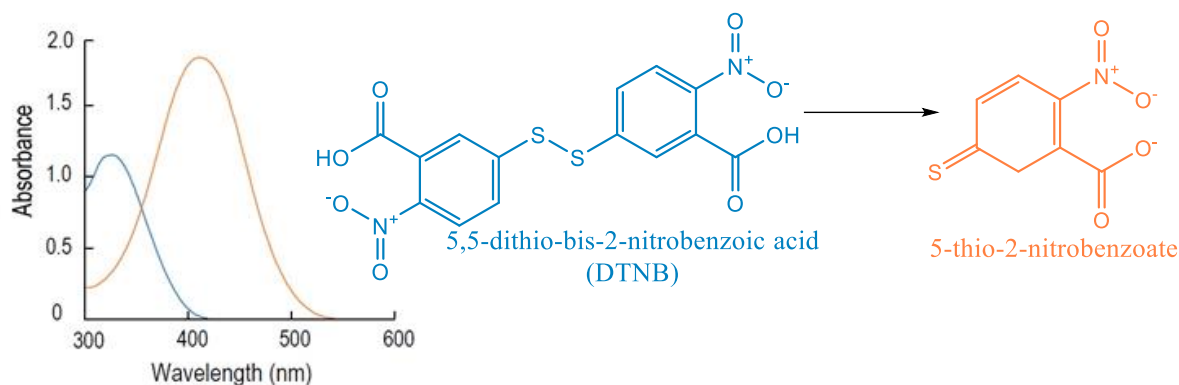


Figure 3.30| Absorbance spectra and reaction of DTNB to 5-thio-2-nitrobenzoate (adapted from^{442,492})

However, when dissolving the extract, a similar colour (yellow) to the reaction product 5-thio-2-nitrobenzoate can be observed. To reveal potential interference of the extracts colour, when using the Ellman method for the determination of AChE inhibition activity, a complete spectrum (400-900 nm) for the extract was obtained (0.156-2.5 mg/mL) and compared to the absorbance spectra of 5-thio-2-nitrobenzoate (Figure 3.31).

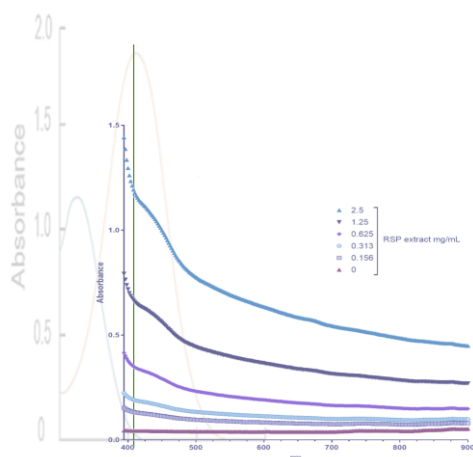


Figure 3.31| Absorbance spectra overlay of 5-thio-2-nitrobenzoate and the RSP extract

Demonstrating the interference with the Ellman assay

The results obtained therefore confirm issues with interference, since the extract absorbs at 412 nm. Furthermore, the formation of turbidity at high

extract concentrations showed absorbance at higher wavelengths (500-900 nm). However, turbidity interference can be corrected by subtracting the absorbance obtained at 700 nm from the wavelength of interest (412 nm) as done in the anthocyanin assay. Despite this, the presence of much higher absorbance readings at 412 nm (Figure 3.31), makes this method unreliable to use for the determination of the extracts AChE inhibition potential.

Instead, the fluorescent Amplex Red assay kit was used. The results obtained from this *in vitro* assay showed the extracts potential to inhibit AChE in a concentration and time dependent manner. As a positive control for the assay neostigmine (5 µg/mL ◆) showed significant inhibition throughout the full 150 minutes the assay was conducted. Very similar inhibition results were found for 1.00 (▼) and 0.75 (▲) mg/mL RSP extract. With decreasing concentrations of the extract and increasing time however, the inhibition of AChE activity of was reduced (Figure 3.32).

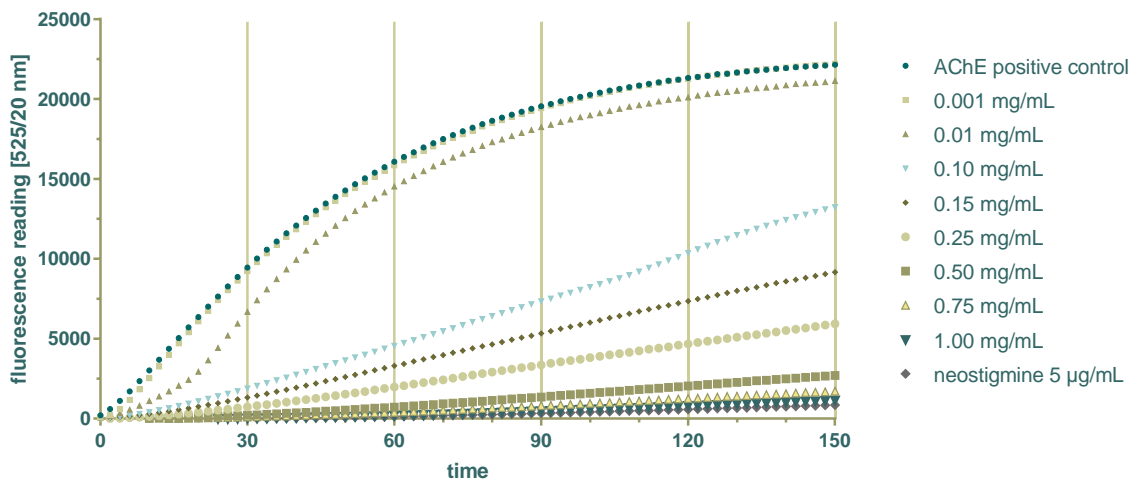


Figure 3.32| Time dependent AChE activity

Showing one of the three replicates, including the AChE positive control, co-incubation with the RSP extract (0.001-1.00 mg/mL) and neostigmine (0.005 mg/mL) as positive control for AChE inhibition

At 0.001 mg/mL (■) no significant inhibition activity was detected. Whereas at 0.1 mg/mL (▲) of RSP extract significant AChE inhibition activity was observed at 30 minutes ($p < 0.0001$, Figure 3.33, p.196). This inhibition decreased after 60 minutes ($p = 0.0214$) and after 90 minutes, the significance had disappeared

completely (Figure 3.33). Extract concentrations over 0.1 mg/mL of RSP extract, show a significantly decreased AChE activity at all time points.

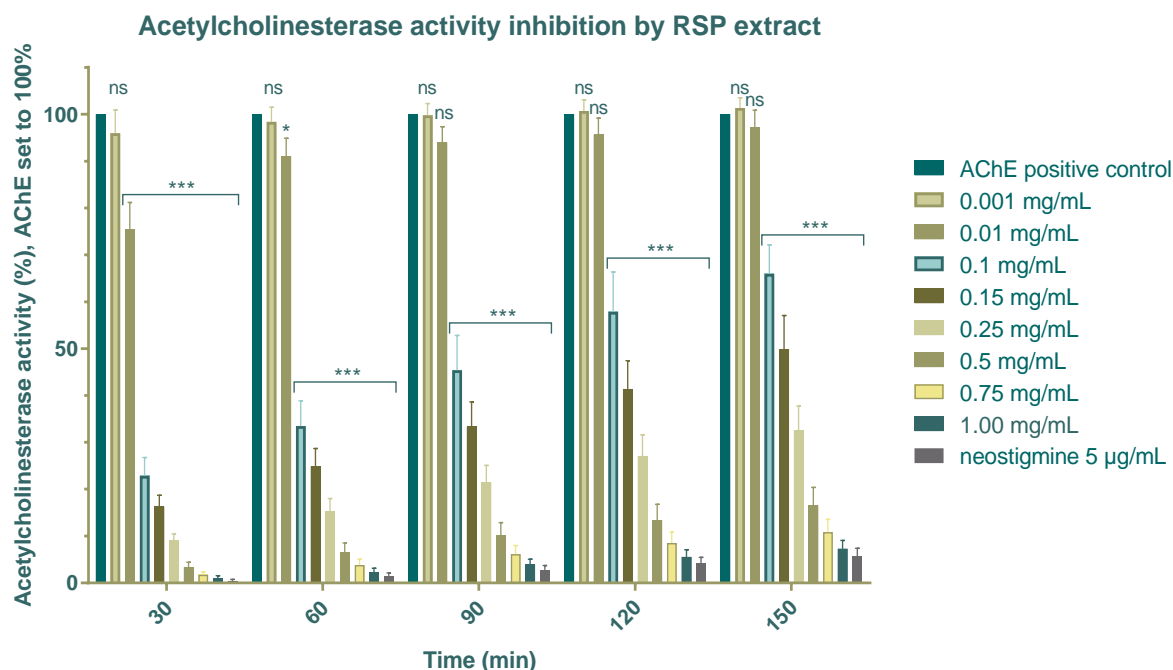


Figure 3.33| AChE activity inhibition by RSP extract (0.001-1.00 mg/mL) and neostigmine (5 µg/mL)

Significant difference via One-way ANOVA and Bonferroni's multiple comparisons test with AChE control (ns-not significant, $p \leq 0.05^*$, $p \leq 0.001^{***}$)

Calculating the IC_{50} (50% inhibition of AChE activity) gave results ranging from 0.055 mg/mL at 30 minutes to 0.13 mg/mL at 150 minutes. IC_{50} values were calculated as previously demonstrated for the DPPH assay (Figure 2.14, p.114) for individual time points of the assay. The concentration needed to show significant AChE inhibition throughout the whole experiment (0.1 mg/mL and higher) are much higher than for neostigmine, which shows significant inhibition at 0.005 mg/mL throughout the whole assay. This was to be expected due to the nature of the extract. The extract contains a number of components, only some of which might be AChE inhibitors, in contrast, neostigmine is a pure compound known to inhibit AChE. However, the fact that most often higher concentrations of plant extracts are tolerated in cell systems or *in vivo* compared to single compounds, the higher concentration of extract necessary to inhibit AChE are not concerning. Other plant extracts have previously shown AChE inhibition activity *in vitro* and *in vivo*, such as black chokeberry and lemon juice⁴⁹³, mulberry flavonols⁴⁹⁴ and

poly-phenol rich blueberry extracts⁴⁹⁵. Comparisons are difficult to make, as they all use the Ellman method for AChE inhibition potential.

A review published by Chen³⁸⁹ in 2015 suggested the AChE inhibition potential of sinapine, by referring to two other papers published by He *et al.*⁴⁰¹ and Ferreres *et al.*³⁹⁸. These indications had led us to analyse the AChE inhibition properties of sinapine alone together with the extract, the phenolic acid mixture (sinapic-, ferulic, caffeic and syringic acid) and the phenolic acids and sinapine in one mixture. Results obtained from this analysis, showed strong AChE inhibition activity for sinapine (▼ Figure 3.34, p.198). Interestingly the phenolic acids mixture also exhibits weak AChE inhibition activity. The activity of both sinapine and the phenolic acids mixture together (◆) showed a stronger AChE inhibition activity than sinapine on its own. However, the extract still shows better activity than the mixture of sinapine and the phenolic acids which is only observable after 90 minutes (■ Figure 3.34). The result obtained for the extract here (Figure 3.34, p.198), gave similar curve as the previous results for the extract at 0.25 mg/mL (Figure 3.32 p.195), suggesting the experiments repeatability. The same analysis was undertaken using 1 mg/mL of the extract and the respective concentrations for sinapine and the phenolic acids. Increasing the sinapine concentration 4 times, to 109.1 µg/mL (present in 1 mg/mL of the RSP extract) led to complete inhibition of AChE for 150 minutes (Figure A7, p.446).

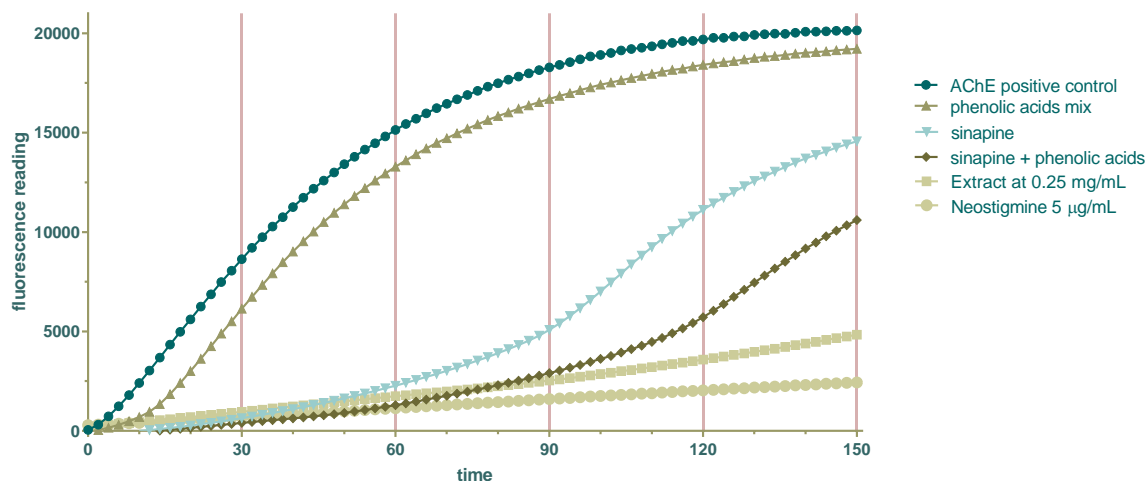





Figure 3.34 | Time dependent AChE inhibition study of RSP extract secondary metabolites

Including the AChE positive control, co-incubation with the RSP extract (0.25 mg/mL), phenolic acid, sinapine and a mixture of sinapine and phenolic acids at the extract specific concentration and neostigmine (5 µg/mL) as positive control for AChE inhibition, showing one of the three replicates. Results obtained in collaboration with Louis Watters.

A Chinese patent, suggests the use of sinapine in the treatment of AD (CN1259045C³⁹⁹). A further Chinese patent application “Method for preparing sinapine thiocyanate from rapeseed cakes and application” (CN105732402A) even describes the isolation of sinapine thiocyanate from rapeseed⁴⁰⁰. In comparison, no such patents were found in the American or European patent offices. The results obtained for the AChE inhibition activity for the extract as well as for sinapine in this study are promising indicators in addition to the patents for sinapine’s potential as AChE inhibitors in the clinic.

In addition to the *in vitro* AChE inhibition activity, molecular docking studies on sinapine were performed by Andrej Shiryaev, from the chemistry department at Samara State Technical University, Russia. The *in silico* results are presented in Yates *et al.*⁴⁵⁶.

3.3.7 Inhibition of self-mediated β -amyloid (1–42) aggregation

To test for the inhibition of self-mediated β -amyloid aggregation the ThT assay was used. Curcumin, a natural phenolic found in e.g. turmeric, had previously showed aggregation inhibition⁴⁹⁶ and was used as positive control in our study. Statistical analysis of the obtained data shows a significantly ($p \leq 0.001$) reduced formation of β -amyloid aggregations while co-incubated with curcumin (Figure 3.35 , 0.0455 mg/mL). At the same concentration as the peptide (0.0455 mg/mL) the extract also shows a significant ($p \leq 0.05$) inhibition of peptide aggregation. However, the ability of the RSP extract to inhibit the self-mediated β -amyloid aggregation, is lower than curcumins (Figure 3.35  vs. ).

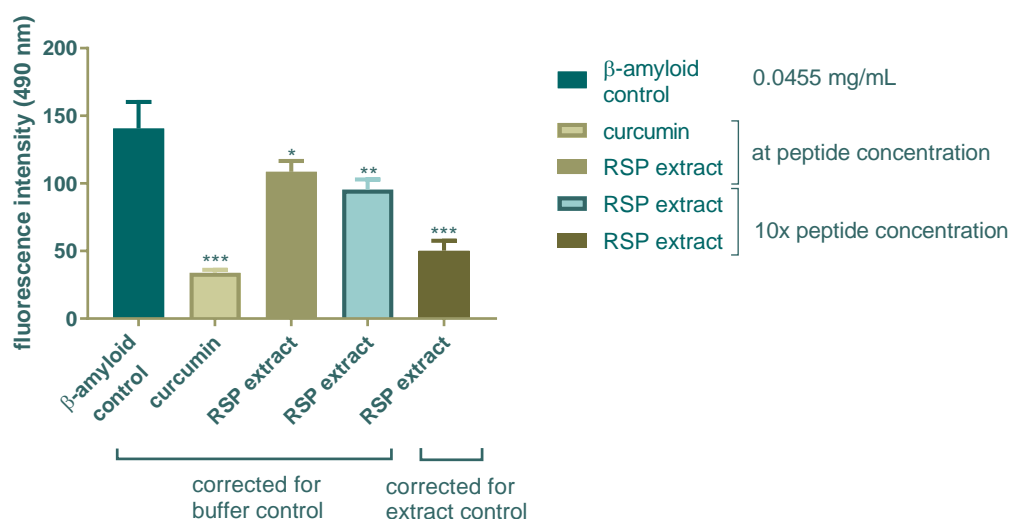




Figure 3.35| β - amyloid self-mediated aggregation inhibition study
Comparing co-incubation with curcumin (peptide concentration) and the RSP extract (peptide and 10x peptide concentration). Statistical significant difference analysis via One-way ANOVA and Bonferroni's multiple comparisons analysis between the β -amyloid control and treatments, $p \leq 0.05$ *, $P \leq 0.01$ **, $p \leq 0.001$ ***

When increasing the concentration of the extract 10-fold (0.455 mg/mL), the RSP extract control (no β -amyloid peptide) showed a significant increase in fluorescence at the emission wavelength (490 nm). This could be due to the wide variety of compounds present in the RSP extract one or a few of which might show fluorescence at the specific excitation (446 nm) and emission wavelength. That is why Figure 3.35 above shows the results for both, the ThT buffer control () as well as the RSP extract control () corrected emission (see determined emission values in Table A4, p.445). Both show a

significant decrease in aggregation formation i.e. lower emission readings. When correcting for the RSP extract control, the significance ($p \leq 0.001$) is bigger than that for the buffer (ThT) control corrected sample. A similar but much stronger interference was observed by Weinberg *et al.*⁴⁹⁷, when trying to determine the aggregation inhibition of β -amyloid by oil palm phenolics. To overcome this issue, they used the Congo Red dye binding assay.

In general, the results showed that the extract can inhibit the self-mediated aggregation of β -amyloid, but to a lesser extent than curcumin. This result is not surprising, as curcumin was tested at a much higher concentration than any single compound in the extract (3.3.4 Additional secondary metabolite analysis, p.175 ff.). When testing the extract at the peptide specific concentration, the most abundant known metabolite is sinapine, with only about 0.005 mg/mL. For the other determined compounds within the extract, their respective concentration is even less. At the higher concentration of the extract (0.455 mg/mL), a better inhibition was observed. At this concentration, the amount of sinapine (0.0496 mg/mL) is similar to the concentration of the peptide (0.0455 mg/mL). Literature research into the inhibition of amyloid aggregation by sinapine did not show any previous research in this direction. However, other compounds found in the extract (Table 3.8) have previously been identified to prevent or modulate amyloid aggregations^{445,473}. These components could be responsible for the extract's A β peptide aggregation preventative properties. Further in depth analysis of these compounds at the extract specific concentrations either by themselves or in a mixture could shed light on this subject.

Table 3.8| Secondary metabolites preventing or modulating β -amyloid aggregation

Flavonoids	Other phenolics
Apigenin	Caffeic acid
Epicatechin	Ferulic acid
Kaempferol	Gallic acid
Quercetin	
Taxifolin	
Luteolin	

Note(s): adapted from^{445,473}

3.3.8 Inhibition of supercoiled plasmid DNA strand breakage

As previously demonstrated in the ORAC assay (2.3.9 ORAC assay p.122 ff.), AAPH is able to decrease the fluorescence intensity of the fluorescence probe, by radical generation. AAPH is also able to cause oxidative DNA strand breakage in pBR322 plasmids⁴⁵², from the supercoiled to both an opened circular and linear form of the plasmid DNA (lane 2 Figure 3.36 A+B)³⁵³. Previous research had shown that certain natural compounds, such as green tea polyphenols⁴⁵², *Terminalia arjuna* bark extracts³⁷⁷ and phenolic extracts from *Sphallerocarpus gracilis* seeds⁴⁹⁸ are able to prevent this AAPH induced plasmid DNA strand breakage.

Similar observations were made, for the RSP extract in the present study³⁵³. Concentrations of the RSP extract between 13.9 and 20.9 µg/mL showed almost complete protection from the AAPH induced oxidative damage (Figure 3.36/ Figure 3.37, p.202). Lower RSP extract concentrations, e.g. 7.0 and 10.4 µg/mL, still showed partial DNA protection. However, no visible DNA protection was observed at a RSP extract concentration 3.5 µg/mL³⁵³.

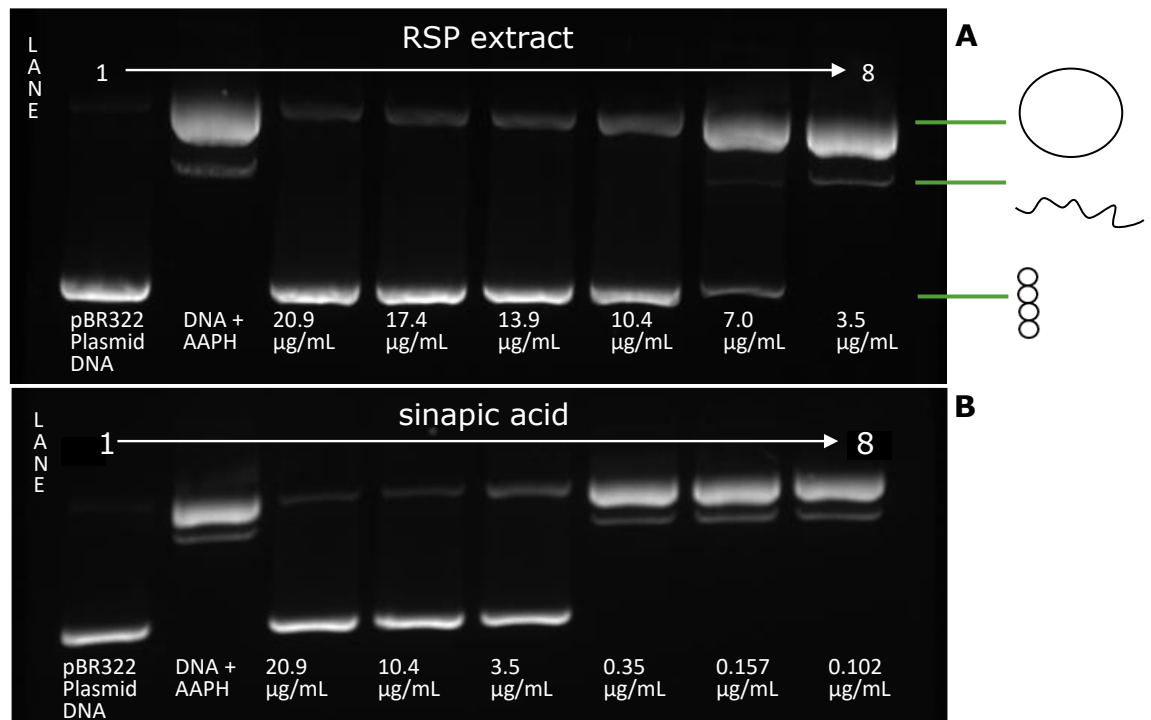


Figure 3.36| Protection of pBR322 plasmid DNA

Plasmid DNA control (lane 1), AAPH (3.48 mM) induced damage (lane 2) protection by A: RSP extract (3.5-20.9 µg/mL, lane 3-8) and B: sinapic acid (0.102-20.9 µg/mL, lane 3-8)³⁵³

To investigate whether the presence of the most abundant phenolic acid, sinapic acid, in the RSP extract, is contributing to the DNA protection, the respective concentrations found in 20.9 µg/mL of the two RSP extracts obtained in chapter 2* (Ext. SOX 2012: 0.157 and SOX 2014: 0.102 µg/mL, Table 2.10, p.108) were tested. In addition, concentrations of SA between 0.35 and 20.9 µg/mL were assessed. While the three highest tested concentrations (20.9, 10.4 and 3.5 µg/mL) of sinapic acid show very good protective properties, lower sinapic acid concentrations i.e. 0.35 µg/mL and the relevant extract concentrations (SOX 2012: 0.157 and SOX 2014: 0.102 µg/mL in 20.9 µg/mL extract*) showed little or no visible protection respectively (Figure 3.37).

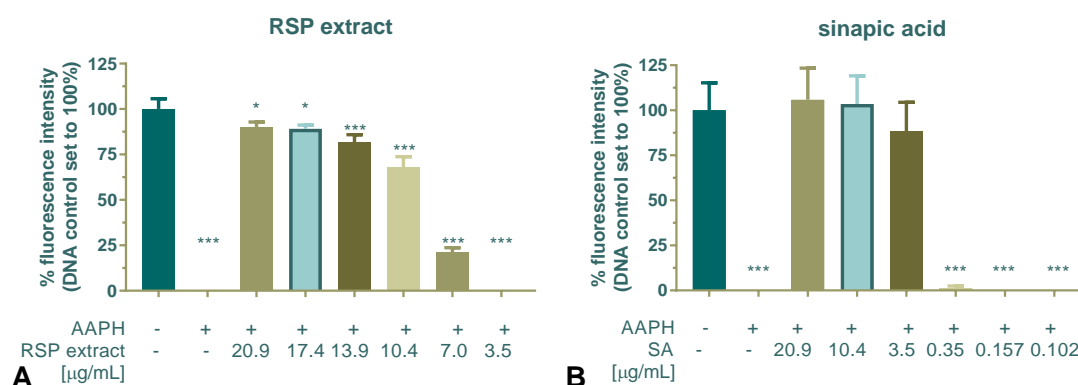


Figure 3.37 | Quantification of the plasmid DNA protection effect
 Protection of pBR322 plasmid DNA from AAPH (3.48 mM) induced damage by (A) RSP extract and (B) sinapic acid. Statistical significant difference analysis via One-way ANOVA and Bonferroni's multiple comparisons analysis in comparison to DNA control column, $p \leq 0.05$ *, $p \leq 0.001$ ***, $n=3^{353}$

The above results confirm that although SA is the most abundant phenolic acid present in the extracts, it is not the main contributor to the DNA protective activity of the RSP extract.

To determine whether sinapine and/or the mixture of phenolic acid (3.1.1.1 Sinapine and additional phenolic derivatives p.135 ff.) could be responsible for the found DNA protective properties of the RSP extract, they were also tested in this assay. For this experiment RSP extract was analysed at 20 µg/mL along with the respective concentrations of the 4 phenolic acids (PA) mixed, sinapine (Sin) and a mixture of the phenolic acids and sinapine. The AAPH converts supercoiled plasmid DNA into open circular DNA, as previously

* experiment was undertaken before the production of final extract (sinapic acid conc. = 0.083µg/mL)

seen (Figure 3.36, p.201). Co-incubation of the extract (20 µg/mL) with AAPH can prevent this DNA damage (Figure 3.38). When testing the phenolic acid mixture, no DNA protection was observed. Similar to SA (Figure 3.37 B) the concentration of phenolic acids present in the extract are not high enough to demonstrate DNA protective properties (Figure 3.38).

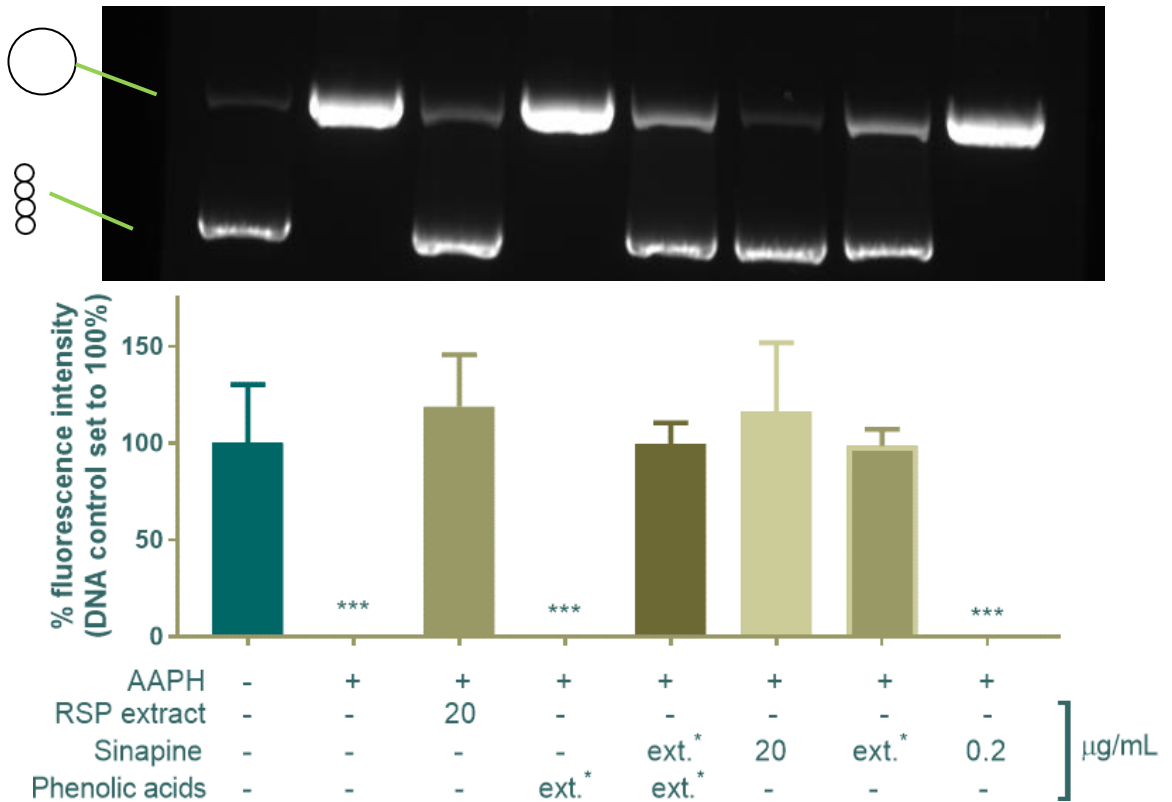


Figure 3.38| DNA protective properties of the RSP extract secondary metabolites

Including phenolic acid mixture, sinapine (0.2-20 µg/mL) and a mixture containing sinapine and phenolic acids (*concentration present in 20 µg/mL extract). Statistical analysis via One-way ANOVA and Bonferroni's multiple comparisons analysis between DNA control and AAPH treated samples, *** $p \leq 0.05$, $n=3$); results obtained in collaboration with Louis Watters.

In comparison, sinapine, at the extract specific concentration (2.18 µg/mL), is showing protective properties. Statistical analysis showed no significant differences between the DNA control and samples incubated with AAPH and the extract (■), sinapine (■, at extract concentration) and the sinapine/phenolic acids mixture (■ extract concentration). Also, 20 µg/mL sinapine (■) shows DNA protective properties, with no significant difference

to the DNA control. However, when diluting sinapine to 0.2 µg/mL no protective properties were observed (Figure 3.38, p.203).

This is the only known study so far looking into the protection of plasmid DNA from AAPH induced oxidative damage by RSP extract and sinapine. No papers showing similar rapeseed related research were found in the literature. Compared to the copper chelating properties (3.3.5 Copper (Cu²⁺) chelating, p.191 f.), where sinapine was not responsible for the activity; or the antioxidant activity, where it was causing between 35-73% of the activity (3.3.4.1 Antioxidant activity of Sinapine, p.175 ff.); in the plasmid DNA protection assay it seems to be responsible for most if not all of the DNA protection.

3.4 Conclusion/Future Work

The final extract obtained through bulk extraction (Soxhlet) from RSP showed a similar antioxidant activity and LC-MS/MS secondary metabolite profile to the preliminary extract (SOX 2014) characterised in chapter 2. For further phytochemical characterisation of the extract, additional LC-MS/MS analysis was undertaken to determine additional secondary metabolites. This investigation demonstrated a significant presence of sinapine, as well as additional phenolic derivatives in the RSP extract. Sinapine contributed mostly to the antioxidant activity (35-73%, depending on assay) of the RSP extract. These results were published in Yates *et al.* 2019⁴⁹⁹. In addition, the presence of three glucosinolates (progoitrin, gluconapin* and gluconasturtiin*) was confirmed, while no indication for the presence of anthocyanins was observed. Although some peaks found during the additional LC-MS/MS analysis (Figure 3.22 p.181) are still unknown, less than 50% of the extracts antioxidant activity is of unknown origin (Figure A3, p. 442), because the phenolic acids and sinapine explain the majority of the activity. The further identified compounds, e.g. sinapoyl glucoside or feruloyl choline (5-8') guaiacyl (Table 3.6 p.182), but not with standards verified metabolites, could explain some of the additional activity. Potentially in conjunction with some of the undetermined peaks.

Metal chelating properties of the extract were studied for copper(II) and iron(II) ions. The extract only demonstrated positive chelating ability for copper and this was not associated with the sinapine present in the extract. Additional investigations are needed to determine whether the other present secondary metabolites or unknown compounds in the RSP extract are responsible for the copper chelating activity. Furthermore, it was found that a major part of the AChE inhibition activity of the extract, is due to the presence of sinapine and some of the phenolic acids present in the extract. However, a small fraction of the AChE inhibition activity is still unexplained and requires further investigation. The RSP extract also inhibited self-mediated β -amyloid (1-42) aggregation although inhibition observed was less than that with positive control curcumin but significant when compared with the untreated β -amyloid control. The RSP extract also demonstrates *in vitro*

plasmid DNA protective properties in the presence of radical initiator AAPH. In this case the activity was mainly attributed to the concentration of sinapine within the extract. The DNA protective properties of the RSP extract in comparison to sinapine and the mixture of phenolic acids formed part of the publication Yates *et al.*⁴⁹⁹. Metal chelating properties, inhibition of AChE as well as the inhibition of protein aggregations are all positive characteristics important for the potential treatment of neurodegenerative disease, because metal dis-homeostasis^{206,431,500}, Ach levels⁵⁰¹ as well as protein aggregations^{122,157,444,502} have all been associated with neurodegeneration.

Overall, the extract demonstrates several positive *in vitro* activities, some of which can be explained by the presence of sinapine in the RSP extract. Extracts with similar activities have previously gone on to show very good results in different cellular or *in vivo* models of neurodegenerative disease. The AChE inhibition activity of the extract for example although much lower than for example neostigmine is promising, since it would provide a natural alternative to the commonly used AD drugs. Especially with the additional antioxidant and copper chelating properties, it could be advantageous (multi-target) over compounds purely inhibiting AChE. More and more researchers explore the use of a mixture of drugs or extracts for the treatment of neurodegenerative disease, due to their complex and multifactorial nature (1.3 Neurodegeneration, p.23 ff.). The one drug one disease theory might not be applicable for this type of disease. Extracts showing multiple positive characteristics might show the long sought effects for the treatment or prevention of neurodegenerative disease.

However, as raised by López-Alarcón and Denicola³⁰¹ *in vitro* methods are not sufficient to assess compounds activity *in vivo*, due to the complexity involved in their mechanism of action. Most of these simple *in vitro* assays also ignore important parameters in biological environments, such as pH, bioavailability and the blood-brain barrier. Particularly the induction of antioxidant pathways within model systems is ignored using these *in vitro* methods. In conclusion, the *in vitro* assays presented in this chapter, only verify chemical activity. For the extract to be of biological relevance, similar activity in cell systems and/or *in vivo* is crucial for the potential use of the extract in health and wellbeing. Thus, the next two chapters will focus on exploring the biological activity of

the extracts *in vitro* (SH-SY5Y cells, Chapter 4) and *in vivo* (*C. elegans*, chapter 5).

The Potential Application of Rapeseed Pomace Extracts in the Prevention and Treatment of Neurodegenerative Diseases

4 CELL PROTECTIVE PROPERTIES OF RSP EXTRACT IN SH-SY5Y NEUROBLASTOMA CELL LINE

Contents

4.1 Introduction	210
4.1.1 Neuronal cell culture	
4.1.2 Cell toxicity/viability assays	
4.1.3 ROS in the cell system	
4.1.4 Cellular DNA damage/ Comet assay	
4.1.5 Cell stress related proteins	
4.1.6 Objectives	
4.2 Materials and Methods	227
4.2.1 Chemicals and Equipment	
4.2.2 Methods	
4.3 Results and Discussion	237
4.3.1 Cellular toxicity of RSP extract	
4.3.2 Protection of SH-SY5Y cells by RSP extract from ROS induced by H ₂ O ₂	
4.3.3 Protection of SH-SY5Y cells by RSP extract from H ₂ O ₂ -induced DNA strand breakage-Comet assay	
4.3.1 Study into the cell stress related protein expression induced by RSP extract	
4.3.2 AChE inhibition study by RSP extract in SH-SY5Y cells	
4.4 Conclusion/Future Work	258

This chapter will cover experiments designed to study the antioxidant properties of RSP extract activity in a cell-based system. The SH SY-5Y neuroblastoma cell line was employed to determine the extracts toxicity and its potential to (i) reduce the production of reactive oxygen species and (ii) to prevent DNA damage induced by hydrogen peroxide. Furthermore, the effect of the RSP extracts on oxidative stress related protein makers and the enzyme acetylcholinesterase at cellular level were explored.

4.1 Introduction

4.1.1 Neuronal cell culture

When undertaking research to study the effect of plant extracts in the field of neurodegeneration the best option for cell-based research is the use of primary neurons. Primary mammalian neurons can be derived from embryonic central nervous system tissue. However, they do come with certain limitations. Once terminally differentiated into neurons, these cells will no longer propagate and so the number of cells available for experiments is limited^{503,504}. In addition, recent developments in stem cell research have made it possible to generate induced pluripotent stem cells, from differentiated patient-derived cells, which have the capacity to self-renew by dividing and to develop into all cells of the adult body e.g. neurons, in the laboratory⁵⁰⁵. Advancing this research even further has led to the creation of 3D cell models using human stem cells⁵⁰⁶⁻⁵⁰⁸. These and further advances in cell based research, could lead to new experiments and future discoveries in neuroscience.

To overcome the issue of non-propagating neuronal cells, very often secondary cell lines, derived from neuronal tumours, which have become immortalized, are used. Advantages of these include (i) unlimited number of cells which, grow easily under cell culture conditions (ii) less variability (iii) less challenging preparation (iv) approval from ethics committees is easier and (v) facile transfection. There are several cell lines currently being used for the search of potential neurodegenerative treatment from natural antioxidants. These include the neuroblastoma cell line SH-SY5Y, the human neuronally committed teratocarcinoma cell line NT2 or NTera as well as the PC12 cell line derived from rat pheochromocytoma of the adrenal medulla^{503,504}. However, there are disadvantages in using these neuron like cell lines, for example they bear more physiological differences to mature neurons, thus making them less likely to exhibit similar properties as neurons *in vivo*⁵⁰⁴. Depending on the field of interest, the right cell line/type needs to be chosen carefully. To study the effect of RSP extracts in neuronal like cells, the SH-SY5Y neuroblastoma is the cell line of choice in this study,

since this cell line is commonly used, as testified by their presence in the literature. Thus, this also will facilitate comparison of results.

4.1.1.1 Background on SH-SY5Y cells

The neuroblastoma cell line SH-SY5Y was created by subcloning the original cell line SK-N-SH three times. The SK-N-SH cell line (first reported in 1973⁵⁰⁹) was isolated from a bone marrow biopsy from a four-year old female patient with neuroblastoma, a cancer that is formed in immature nerve tissue mostly in children. The initial cell line SK-N-SH, first cultured in 1970, was subcloned to SH-SY, followed by SH-SY5, to the final cell line SH-SY5Y^{504,510}.

Since SH-SY5Y cells were derived from human, they express a number of human-specific proteins, which would not be present in rodent culture, giving them an advantage over for example the PC12 cell line mentioned before. SH-SY5Y cells are commonly used *in vitro*, for experiments requiring neuron-like cells such as for research in PD, AD and ALS⁵¹¹⁻⁵¹⁴. Advantages for the use of this cell line include its human origin, catecholaminergic neuronal properties and easy maintainance⁵¹². In the nervous system catecholaminergic neurons synthesise and release neurotransmitters dopamine and noradrenaline. In addition SH-SY5Y cells express tyrosine hydroxylase (rate-limiting enzyme for the production of dopamine) and exhibit, noradrenaline specific, moderate levels of dopamine- β -hydroxylase activity, which is part of the synthetic pathway of noradrenaline in neurons⁵¹⁵.

Both the use of differentiated and undifferentiated SH-SY5Y cells has been reported in the search for treatment of neurodegenerative disease. Similar to working with primary neurons, differentiated cells (e.g. with retinoic acid) cannot further propagate, due to cell population growth inhibition⁵¹⁶. Differentiation of the cells in every experiment is time and work intensive and thus it was decided against in this project. Also the higher number of papers using undifferentiated SH-SY5Y (Figure 4.1, p.212) cells in for example PD research (81.5%)⁵¹², aided the decision to use undifferentiated cell for better comparison with previous research. Also Cheung *et al.*⁵¹⁷ suggests the use of undifferentiated SH-SY5Y cells in research related to neurotoxicity or neuroprotection, due to the changes, e.g. reduced susceptibility to 6-hydroxydopamine or MPP⁺(inducer of PD), induced by for example retinoic

acid as differentiating agent. In general undifferentiated SH-SY5Y cells lack long neurite outgrowth and tend to grow in clusters as demonstrated in Figure 4.1⁵¹⁶.

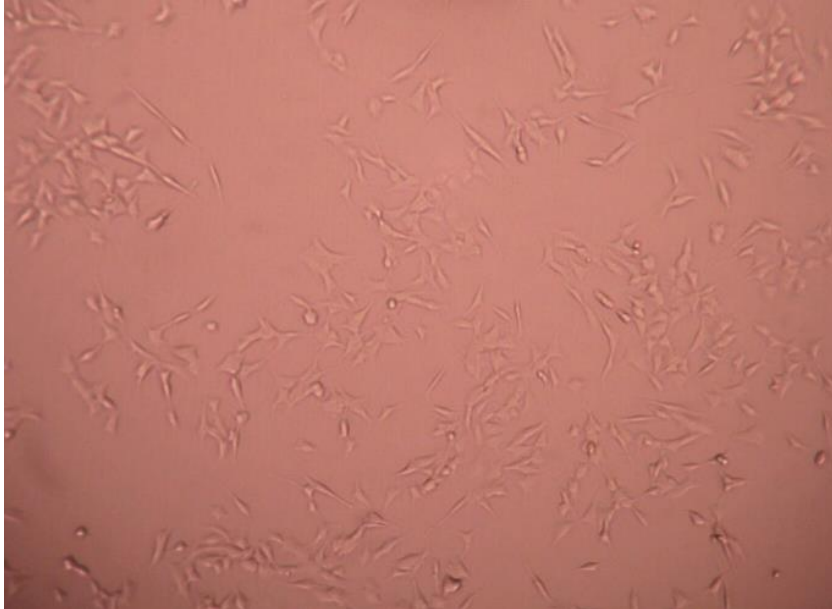


Figure 4.1| Undifferentiated SH-SY5Y cells in DMEM media (40x magnification)

SH-SY5Y cell lines have been maintained in several different basal media with various types of serum and other cell culture supplements. In a systematic review by Xicoy *et al.*⁵¹² on the use of this cell line in PD research the most common culture media in articles was Dulbecco's Modified Eagle Medium (DMEM, 434 articles) with 10% foetal bovine serum (FBS, 770 articles). In addition, several articles also showed the supplementation of the culture media with antibiotics (631), glutamine (230), non-essential amino acids (94) and sodium pyruvate (61).

In the field of natural products and neurodegeneration this cell line was used extensively. Hu *et al.*⁵¹⁸ for example, tested 3,6'-disinapoyl sucrose (DISS) from Radix Polygala (root of *Polygala tenuifolia*) in association with the cell line, Seoposengwe *et al.*⁵¹⁹ demonstrated the potential of four medical plants from Africa (*Lannea schweinfurthii*, *Zanthoxylum capense*, *Scadoxus puniceus* and *Crinum bulbispermum*) against rotenone-induced toxicity and many others⁵²⁰⁻⁵²³.

4.1.2 Cell toxicity/viability assays

Cell viability assays are fundamental in the field of cell biology and drug discovery⁵²⁴. To work with compounds/natural extracts within a cell system, their initial toxicity needs to be determined. This information provides knowledge on safe working concentrations for further investigation. These working concentrations strongly depend on the aim of the research, for cancer research for example a certain amount of cell death is desirable. In contrast, when studying neuroprotection, concentrations must be chosen that are not harmful to the cells. The toxicity of compounds towards cell lines can be determined using a number of different assays, with each one of them having their own advantages and disadvantages. In general these assays either look into the viability of cell populations or individual cells⁵²⁵. One of the earliest methods to determine cell viability was trypan blue, the latter cannot cross intact cell membranes, so only dead cells will take up the dye. Viable versus non-viable cells can be counted manually (e.g. using a haemocytometer) or using automated systems, such as automated cell counters or flow cytometry. However, manual counting is labour intensive while sophisticated equipment in the case of automation is associated with high costs. Alternatives are the use of radiolabelled nucleotides (e.g. ³H-thymidine) and monitoring the rate of their incorporation into the DNA, which can be correlated to the rate of proliferation. This approach is sensitive but requires operation and safe handling of radio isotopic waste^{525,526}.

Nowadays the use of dyes in toxicity assays is more common. The dyes are transformed in the presence of metabolically active cells. Most of these assays can be performed on adherent cells in multi-well format and are evaluated using plate readers. The use of plate readers increases the number of samples and replicates that can be analysed at the same time. Tetrazolium salts are the most common dyes, the latter form colourless or weakly coloured aqueous solutions. They are converted to brightly coloured formazan compound by the reduction of the tetrazole ring in the presence of metabolically active cells⁵²⁷ (4.1.2.1 MTT assay, p.215). Both water soluble (sulfonated) and water insoluble formazans can be formed, depending on the starting compound (Table 4.1, p.214). The formation of aqueous insoluble formazans is used in endpoint assays, whereas soluble formazans, can be

used for continuous real time assays⁵²⁷. An overview of some commonly used dyes is given in Table 4.1. More specific details on these can be found in reviews by Berridge *et al.*⁵²⁷ and Stockert *et al.*⁵²⁸.

Table 4.1| Tetrazolium based cell viability assays (adapted from^{525,527,528})

Compound	Full name	Tetrazolium salt	Formazan-water
MTT*	3-(4,5-dimethylthiazol-2-yl)-2,5-diphenyltetrazolium bromide	mono	insoluble
MTS	5-[3-(carboxymethoxy)phenyl]-3-(4,5-dimethyl-2-thiazolyl)-2-(4-sulfophenyl)-2H-tetrazolium inner salt	mono	soluble
CTC	5-cyano-2,3-di-(p-tolyl) tetrazolium chloride	mono	insoluble
NBT	nitroblue tetrazolium chloride	di	insoluble
XTT	sodium 2,3-bis(2-methoxy-4-nitro-5-sulfophenyl)-5-[(phenylamino)-carbonyl]-2H-tetrazolium inner salt	mono	soluble
WST	sodium 5-(2,4-disulfophenyl)-2-(4-iodophenyl)-3-(4-nitrophenyl)-2Htetrazolium inner salt	mono	soluble

Note(s): * used in this project

These methods are cost effective and easy to undertake. However, they do lack high sensitivity and potential interactions with reducing groups from drugs are possible, limiting their use for certain experiments⁵²⁴.

Fluorescence based assays such as Alamar Blue (resazurin, see 4.1.2.2 Resazurin assay, p.215) can overcome the issue of low sensitivity and interference. These are increasingly being used for the determination of cell viability. Other methods such as using cellular ATP production or real-time methods, such as engineered luciferase and a small molecule pro-substrate are used. In the case of the luciferase assay, the pro-substrate is reduced by the cells with active metabolism and diffuses into the culture media to react with the luciferase yielding a luminescent signal. Even multiplex assays using the continuous viability data in conjunction with other cell based downstream effects can be undertaken, as long as reagents used for either do not interfere with each other^{525,529}. These and other possibilities for viability measurements are reviewed in the book "Mammalian Cell Viability" by Stoddart⁵²⁵. Both, the MTT and the resazurin, assays used in this project are further discussed following.

4.1.2.1 MTT assay

The MTT (3-(4,5-dimethylthiazol-2-yl)-2,5-diphenyltetrazolium bromide) assay is a colorimetric assay that assesses cell viability *via* their metabolic activity. It was first introduced in 1957 by Pearse for the detection of dehydrogenase activity⁵³⁰. For this assay the MTT solution is added to the adherent cells in a well plate format and incubated for a set amount of time (between 2-4 hours). If the cells are metabolic active, the MTT will be reduced to the purple formazan forming water insoluble crystals (Figure 4.2). These can be dissolved by the addition of e.g. dimethyl sulfoxide (DMSO) after removal of the culture media. The reduction takes place due to the presence of the coenzyme NAD(P)H and glycolytic enzymes within the cell.

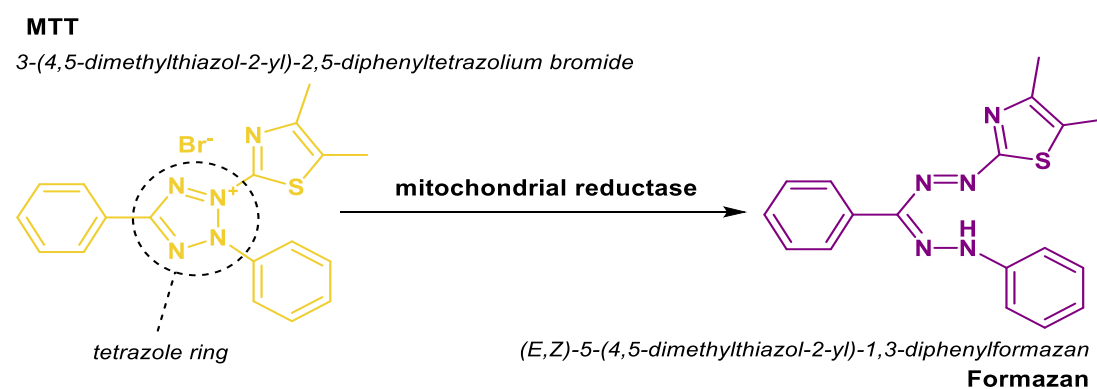


Figure 4.2| MTT reaction in metabolic active cells

The higher number of the metabolically active cells present, the more formazan crystals will be formed giving higher absorbance at 560 nm after dissolving the formazan crystals. The MTT assay is one of the most widely used assays for cell viability, cytotoxicity, proliferation and chemo- and radio sensitivity analysis *in vitro*⁵²⁸. It is simple and less time consuming compared to for example trypan blue cell counting methods, since it can be undertaken in a multi-well plate format, testing several drugs or drug concentrations at the same time by using plate readers for detection.

4.1.2.2 Resazurin assay

Resazurin (7-Hydroxy-3H-phenoxazin-3-one 10-oxide), first introduced as alamarBlue®, is a blue dye with weak fluorescence. In viable cells resazurin (an oxazone chromophore) is irreversibly reduced to the pink coloured resorufin due to the electron transfer from NADH/H⁺ to resazurin (Figure 4.3, p.216)⁵²⁸. Resorufin can be detected either using colourimetry or fluorimetry.

The fluorescence measurement shows better sensitivity, as little as 80 cells can give reproducible signals^{531,532}.

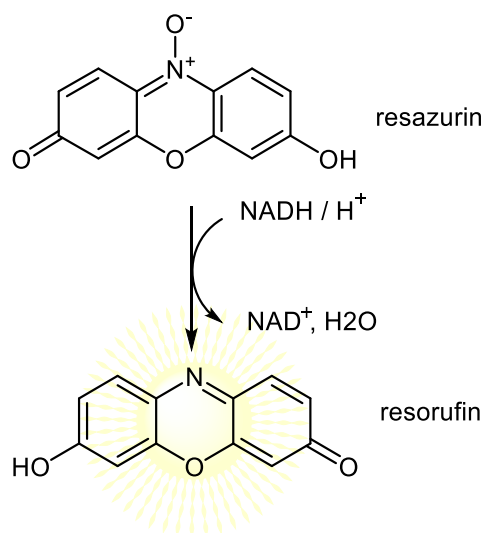


Figure 4.3| Reduction of resazurin to resorufin within cells

Being able to add resazurin straight to the culture media and the formation of the aqueous soluble resorufin eliminates certain steps necessary for e.g. the MTT assay. Resazurin has also been found to be less toxic than the former. As cells are not killed in the process of toxicity assessment, further analysis can be undertaken with the same set of cells⁵³². However, incubation times suggested by the manufacturer need to be adhered to otherwise cell toxicity might be observed⁵³³. A disadvantage is also that further reduction of resorufin can give a final colourless/non-fluorescent product called hydroresorufin^{528,532}, again suggesting to adhere to manufacturers incubation times. Furthermore, to determine potential interference issues, wells without cells with the compound in question should be analysed simultaneously. Interference in this assay can occur if the compound/extract in question shows similar absorbance/fluorescent signalling.

4.1.3 ROS in the cell system

Indications on the importance of ROS production in the neurodegenerative disease development has been described in "1.4 Oxidative stress in neurodegeneration and the potential use of antioxidants to prevent neurological disorders" (p. 51 ff.). This makes the detection of ROS within cell systems and the potential prevention of ROS production very important. The dye H₂DCFDA (2',7'-dichlorofluorescein diacetate, (Figure 4.4, top) is widely used to measure the production of hydroxyl-, peroxy- and other ROS activity in cells. In general, H₂DCFDA is resistant to oxidation, but once taken up by cells, it is deacetylated by intracellular esterases to form the more hydrophilic non-fluorescent dye 2',7'-dichlorohydrofluorescein DCFH, which is retained in the cells⁵³⁴. In the presence of oxidizing species, it is rapidly oxidized to form the highly fluorescent DCF (2', 7' -dichlorofluorescein)⁵³⁵.

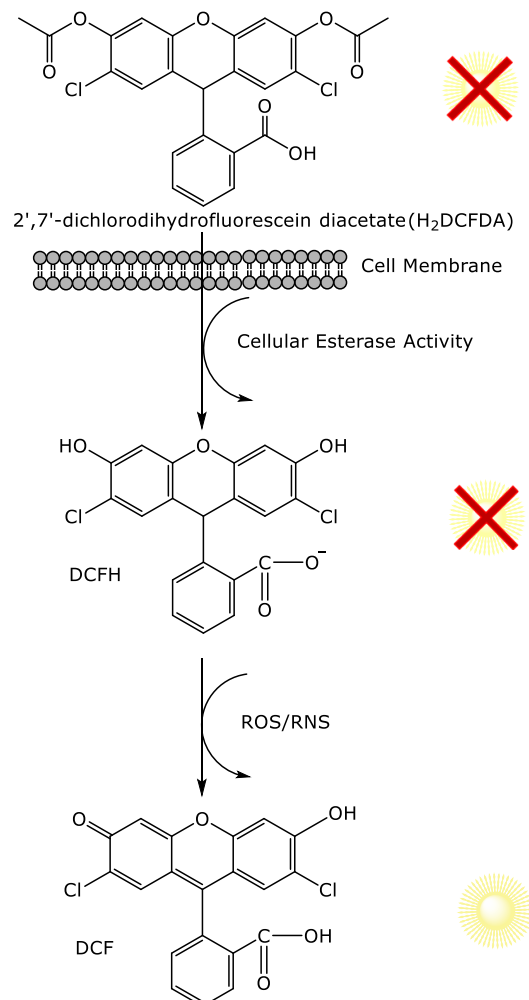


Figure 4.4| H₂DCFDA *in vitro* reaction in the presence of ROS/RNS
(adapted from Eruslanov and Kusmartsev⁵³⁵)

The occurring fluorescent signal can be detected by using (i) a multi-well plate system and a fluorescence plate readers, (ii) fluorescence microscopy, (iii) fluorimeter or (iv) flow cytometry with excitation sources and emission filters appropriate for fluorescein (Ex: ~492–495 nm; Em: ~517–527 nm).

Although plate readers bring the advantage of being quick and easy, they are only able to measure total fluorescence, since intra- and extracellular fluorescence cannot be distinguished from each other. In contrast, flow cytometry provides the possibility to measure the intracellular fluorescence of cells as well as optical cell characteristics. Total number of cells emitting fluorescence can be determined, compared to relative fluorescence units in the plate reader^{535,536}. During flow cytometry analysis (Figure 4.5), cells are transported from the sampling tube into the flow cell system and cells are surrounded by sheath fluid (physiological buffer).

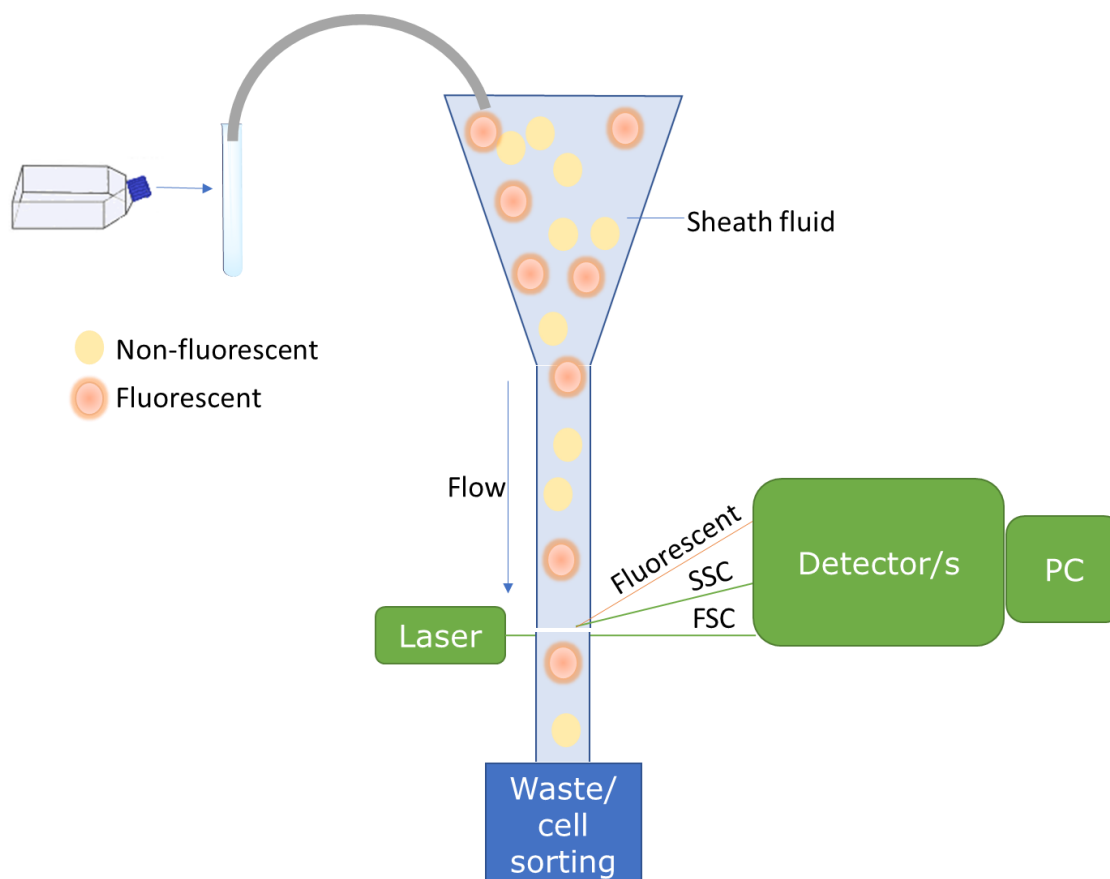


Figure 4.5] Schematic of flow cytometry in the presence of fluorescent and non-fluorescent cells

The fluidic system, consisting of the sheath fluid and pressurized lines, funnels the cells into single file, where they will eventually pass through the

excitation laser (interrogation point). Detectors can collect data on forward scattered (FSC), side scattered (SSC) and fluorescent emissions. The scattered light is related to structural and morphological properties (FSC: size and SSC: internal complexity) of the cells under investigation. The fluorescence emission is directly proportional to the quantity of fluorescent probe (e.g. DCF) within a cell. For further information on the principles and applications of flow cytometry can be found in a review published by Adan *et al.*⁵³⁶ gives a detailed overview. By using the number of detected events (cells) and their respective fluorescence, the level of ROS within a cell sample can be measured and compared with different samples, e.g. H₂O₂ stressed cells or cells treated with other compounds of interest.

4.1.4 Cellular DNA damage/ Comet assay

Oxidative stress (1.4 Oxidative stress in neurodegeneration and the potential use of antioxidants to prevent neurological disorders p. 51 ff.), amongst others factors can lead to DNA damage, which together with protein and lipid damage is associated with neurodegeneration. The question of whether DNA damage is a cause or a consequence (or both) of the neurodegenerative process is still unclear⁵³⁷. Already in 1994 Mecocci *et al.*⁵³⁸ observed a significant increase in oxidative DNA damage marker, 8-hydroxy-2'-deoxyguanosine (using HPLC), in the mitochondrial and nuclear DNA, of post-mortem brain tissue from AD patients. Furthermore DNA strand breaks have previously been detected in samples from e.g. AD⁵³⁹ and PD⁵⁴⁰ patients.

Here, to determine the potential of the extract to protect nuclear DNA from H₂O₂ induced strand breakage in SH-SY5Y cells, the comet assay was employed. The comet assay, also known as single cell gel electrophoresis (SCGE), is one common technique available to measure nuclear DNA breakage and repair in individual eukaryotic cells⁵⁴¹. Ostling and Johanson⁵⁴² first introduced the use of microgel electrophoresis in 1984 for the detection of radiation-induced DNA damage in mammalian cells. This method was modified by Singh *et al.*⁵⁴³ in 1988 using alkaline conditions⁵⁴⁴. The comet assay has successfully been employed in genotoxicity testing, ecologic monitoring and human studies⁵⁴¹. The modified alkaline version of the assay was used in this project, to detect single and double strand breakage as well as alkali-labile sites. There are a few variants of the assay which are briefly described in Table 4.2.

Table 4.2| Comet assay types and some examples of their usage^{541,545,546}

Un-/common	Type	Short description	Examples of application
Common	Alkaline[#]	Detection of double and single DNA strand breaks, including alkali-labile sites such as base or phosphate alkylations and intermediates in base excision repair, the base-less sugars left by glycosylase action, which are transformed into strand breaks by high pH	<ul style="list-style-type: none"> - Potential mutagenic/carcinogenic action of inhalation anaesthetics⁵⁴⁷ - Evaluation of sperm DNA quality⁵⁴⁸ - Oxidative DNA damage protection and repair by polyphenolic compounds in PC12 cells⁵⁴⁹
	Neutral	Detection of double and single strand breaks predominantly facilitates the detection of double strand breaks	<ul style="list-style-type: none"> - Environmental exposures to phthalates (industrial chemicals) and DNA damage in human sperm⁵⁵⁰
	Lesion-specific enzymes	Convert altered bases to strand breaks e.g. <ul style="list-style-type: none"> - Endonuclease III converts oxidised pyrimidines - Formamidopyrimidine DNA glycosylase (FPG) converts 8-oxoguanine and some other oxidised purines - 3-methyladenine DNA glycosylase II (AlkA) converts alkylated bases to AP (apurinic/apyrimidinic) sites - T4 endonuclease V converts cyclobutane pyrimidine dimers - UDG detects uracil misincorporated in DNA 	<ul style="list-style-type: none"> - Evaluate the genotoxicity of oregano essential oil in rats - Genotoxicity of the herbicide⁵⁵¹
	DNA repair	a) Cells are given time, after removal of stressor, for DNA repair, thereafter one of the above techniques is used to determine the DNA repair efficiency of the cells or b) Comet-based <i>in vitro</i> assay: DNA nucleoids containing a specific lesion are incubated with a cell extract containing a certain amount of repair enzymes; enzymes, as a part of the repair process, produce breaks at the sites of the lesions in the DNA that are measured using the alkaline comet assay protocol; the capacity of the cell extract to carry out the incisions, is considered to be the rate-limiting step of the repair process and is taken as an indicator of the DNA repair activity of those cells	a) Assessment of DNA repair efficiency in drug naïve schizophrenia patients ⁵⁵² b) Oxidative DNA damage protection and repair by polyphenolic compounds in PC12 cells ⁵⁴⁹
Un-common	Bromodeoxy-uridine labelling	Identification of replicating DNA	<ul style="list-style-type: none"> - Cancer research, Detection of Maturation of Recently Replicated DNA⁵⁵³
	Fluorescence in situ hybridization (FISH) comets	Detection of damage on specific chromosomes	<ul style="list-style-type: none"> - Test for radio sensitivity of specific genes: compare DNA damage and repair in p53 and hTERT genes⁵⁵⁴

Note(s): [#] version of comet assay used in this project

Cultured cells, primary cells or tissue samples can be employed for the comet assay⁵⁴⁶. When studying the protection of DNA by compounds/extracts from oxidative stress induced DNA strand breakage, cells can be exposed to e.g. H₂O₂. This exposure can take place before cell collection, in the culture flasks or after cell collection in Eppendorf tubes. To determine whether certain compounds can prevent DNA damage, pre-treatment for a chosen time occurs just before the introduction of the stressor. Once cells are harvested, cell pellets are obtained *via* centrifugation and cells are resuspended in low-melting point agarose gel (1% in PBS (#2 Figure 4.6). The cells in the agarose suspension are then evenly distributed (#3 Figure 4.6) onto squares of thin agarose layers (1% standard melting point agarose in PBS), prepared on top of microscopy slides (frosted or agarose coated, #1 Figure 4.6), and covered with cover slides for an even dispersal of cells in the gel layer. The cells on the slides are then lysed, using detergent and a high salt solution to remove membranes, cytoplasm and nucleoplasm and to dissolve the nucleosome, leaving only the DNA (supercoiled in a negative sense) in the nucleoids (#4 Figure 4.6). Subsequent alkali treatment leads to supercoil unwinding and unzipping of the double DNA strands (#5 Figure 4.6). During the process of electrophoresis, DNA with strand breakages, is more likely traveling towards the positive electrode of the electrophoresis tank (comet tail). DNA without strand breakage, lacks free ends and so the large size prevents the migration, and the DNA stays in place, forming the comet head (#6 Figure 4.6). The difference in number of DNA strand breakages leads to different shapes of the comets. After electrophoresis, the slides are immersed into neutralisation buffer, which leads to the joining of the unzipped DNA strands (#7 Figure 4.6). This prepares the DNA for DAPI staining. DAPI is a DNA intercalating dye which binds to adenine–thymine rich regions of double stranded DNA. This staining makes the observation of the comets possible, using fluorescence microscopy (#8 Figure 4.6). The comets are then scored (#9 Figure 4.6) according their head/tail size and intensity, given an arbitrary number between 0 (no DNA strand breaks, circular comets) and 4 (high number of DNA strand breaks, comets with a small head and big tail, Table 4.5, p.234).

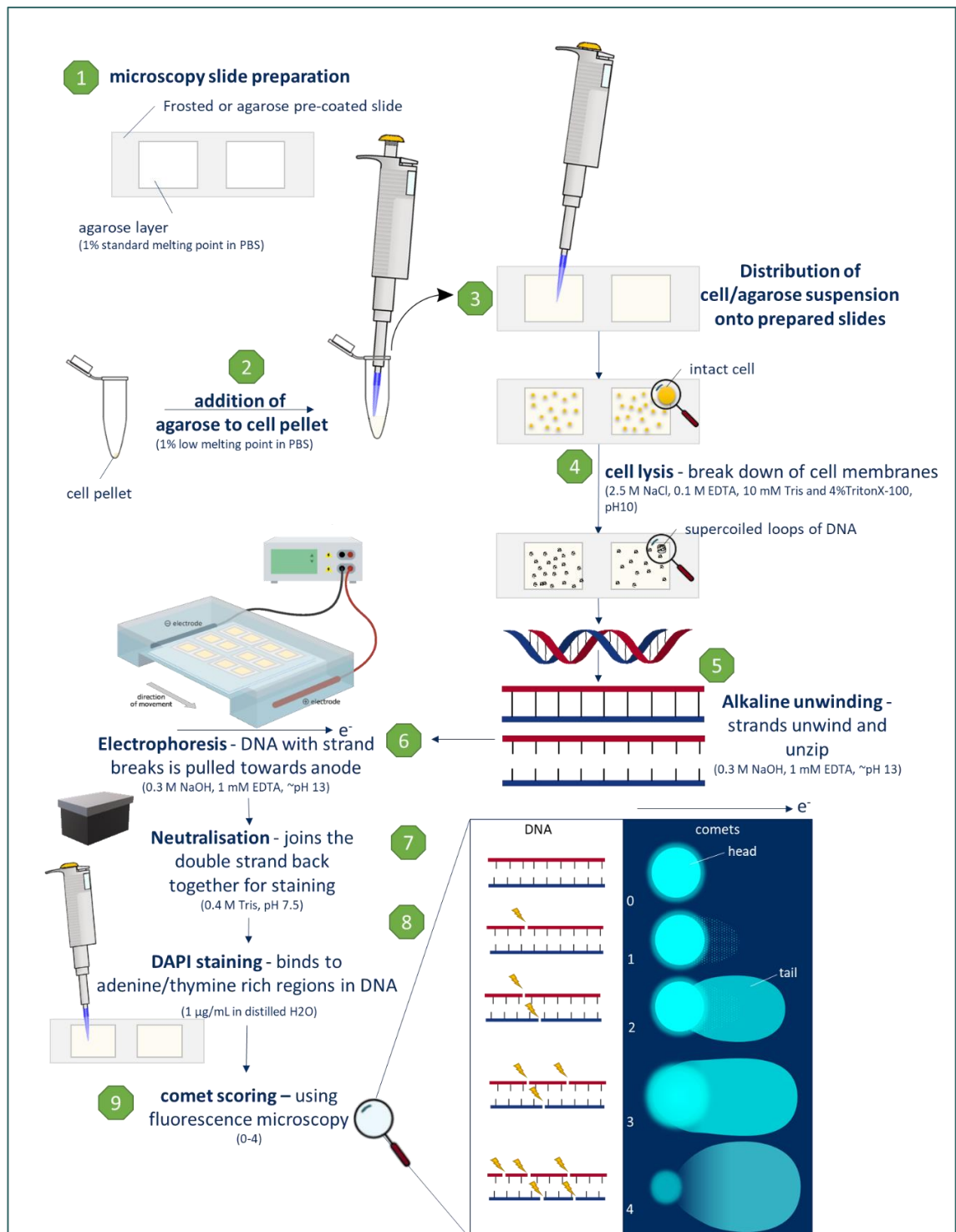


Figure 4.6| Comet assay overview

4.1.5 Cell stress related proteins

Oxidative stress can have an impact on many cellular components such as DNA (see chapter 4.1.4), lipids and protein. Cellular stress can activate a number of cell stress related proteins within the cell system (e.g. Nrf2 pathway, Figure 1.29, p.60). The most common technique to study the expression levels of certain proteins is western blotting. With these, expression levels of proteins can be detected. When investigating several different proteins, this technique becomes laborious and very time consuming. To address this, protein micro array technology has been developed and is now commonly used in many laboratories. With this system, the expression levels of several different proteins can be determined at the same time, thus making this method extremely time efficient⁵⁵⁵.

These protein arrays are membrane-based antibody arrays for the detection of selected human proteins. Cell as well as tissue lysates have been validated for detection in these assays. Initially cell/tissue lysates are usually incubated with the biotinylated detection antibodies (#1 Figure 4.7), in the presence of the protein in question, the latter will bind to the antibodies. The mixture of the cell lysate and the antibodies is thereafter added to the array membrane (#2 Figure 4.7)⁵⁵⁶.

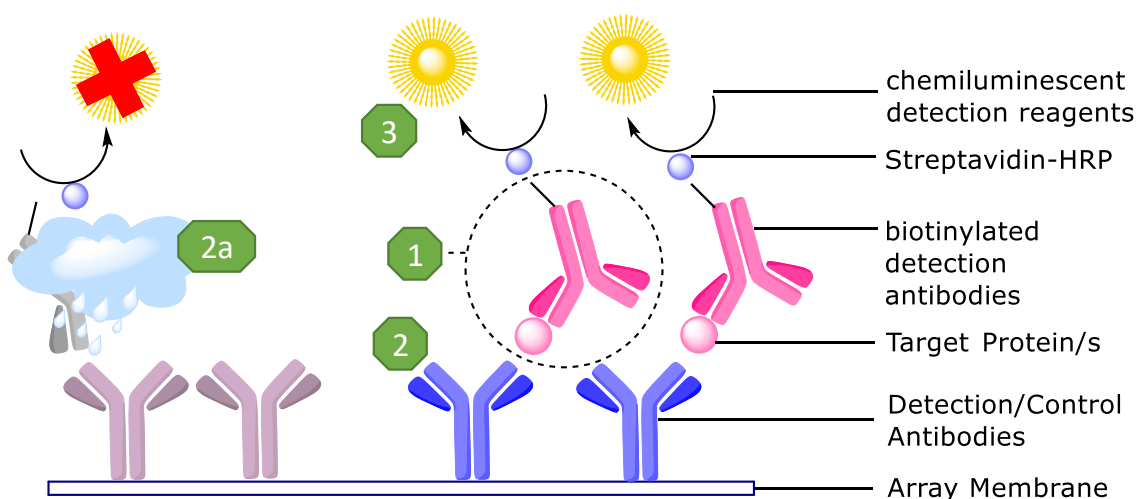


Figure 4.7| Principle of protein micro arrays
(HRP-horse radish peroxidase)

After overnight incubation, the membranes are washed. If the protein/s in question are not present in the cell lysate, the biotinylated detection antibodies are washed off (#2a Figure 4.7). Thereafter, streptavidin-HRP and

chemiluminescent detection reagents are added to make the detection possible (#3 Figure 4.7). In the case of absent proteins in the cell lysate, no signal is produced.

To determine whether the RSP extract induces cell stress, the Proteome Profiler Human Cell Stress Array Kit (R&D systems) was employed. This kit contains 4 membranes, which are spotted in duplicate with 26 cell stress related capture antibodies and allows the detection of relative levels of these proteins. Amongst other the kit determines protein levels for (i) heat shock proteins (HSPs), induced in response to environmental, physical and chemical stresses⁵⁵⁷, (ii) superoxide dismutase (SOD), an enzyme responsible for the catalysis of the superoxide (O_2^-) anion to molecular oxygen (O_2) or hydrogen peroxide (H_2O_2) (4.3.1 Study into the cell stress related protein expression induced by RSP extract using micro array technology p.250), (iii) Serum paraoxonase/arylesterases (PONs), which are enzymes responsible for hydrolysing exogenous toxic organophosphate compounds⁵⁵⁸, (iv) hypoxia-inducible factors (HIFs), induced under a lack of oxygen (hypoxia)⁵⁵⁹ as well as (v) transcription factor NF κ B1, which can activate a vast number of genes related to cell survival and death, inflammation and immunological responses⁵⁶⁰.

A similar human cell stress array kit had previously been used to determine the effect of marine oils, digested with human fluids, on human intestinal Caco-2 cells, which showed down regulation of certain cell stress proteins (e.g. HSP-70 and SOD2)⁵⁶¹.

The determination of stress related protein levels in the SH-SY5Y cells, after RSP extract treatment, together with the other experiments set out for this part of the project will aid to elucidate the RSP extract's potential to prevent or treat neurodegeneration associated with oxidative stress. Following the objectives for this chapter, used to assess the overall aim of the project (1.5 Overall Aim and thesis structure, p.64), are introduced.

4.1.6 Objectives

The list below describes the objectives set out for this chapter:

- Examine the RSP extracts cytotoxic effects in SH-SY5Y neuroblastoma cells
- Assess the extracts potential to prevent ROS production within the cell system
- Analyse the extracts DNA damaging and protective properties in the cellular model
- Inspect the extracts activity on cell stress specific proteins
- Determine the extracts AChE inhibition activity in SH-SY5Y cells

4.2 Materials and Methods

4.2.1 Chemicals and Equipment

The following chemicals/kits (Table 4.3) and equipment (Table 4.4) was used in the aid of the experiments in this chapter.

Table 4.3| Chemicals, reagents and kits

Chemicals	Provider
MTT	Sigma-Aldrich
Resazurin	R&D systems
DMEM, high glucose, pyruvate	Fisher Scientific
FBS	Fisher Scientific
Pen/Strep	Sigma-Aldrich
NEAA	Sigma-Aldrich
Trypsin-EDTA solution	Sigma-Aldrich
H ₂ DCFDA	Invitogen, Life Technologies by Fisher Scientific
Sheath buffer	Beckman Coulter Inc.
DMSO	Fisher Scientific
PBS	OXOID, Fisher Scientific
Amplex® Acetylcholine/ Assay Kit	Fisher Scientific
Proteome Profiler Human Cell Stress Array Kit	R&D systems
H ₂ O ₂	Sigma-Aldrich
AAPH	Sigma-Aldrich
agarose gel (high melting point)	Fisher Scientific
agarose gel (low melting point)	Sigma-Aldrich
EDTA	Alfa Aesar
Triton-X100	Acros Organics
NaOH	Fisher Scientific
Tris base	Fisher Scientific
Developer and Fixer (RP X-OMAT LO)	KODAK, Carestream
DCTM Protein Assay Kit	Bio-Rad

Table 4.4| Equipment

Equipment	Manufacturer/Details
Plate reader	BioTek μ Quant
Oven	Techne Hybridiser HB-10
Fridge	DEAWOO
Freezer -20°C	Blomberg
Freezer -80°C	New Brunswick Scientific U725
pH-meter	Denver Instruments Basic
Balance	OHAUS Pioneer™PA114
Balance	Mettler BB1200
Ultrasonic bath	Ultrawave SFE5901
Incubator (cells)	Nuaire™ DH Autoflow
Incubator (media)	Stuart Scientific co.LTD SI50
Fridge (cell culture)	Zanussi
Flow chamber	Thermo Electron Corporation Hera safe
Freezer (cell culture)	AEG Öko_ARCTIS
Flow cytometer	Coulter Epics XL-MCL
Scanner	Canon 4225i
Centrifuge (cell culture)	MSE centaur 2
Centrifuge (molecular)	Heraeus Multifuge 1 L-R
Microscope (cell culture)	Leica DMIL
Microscope (comet assay)	Leica DMRB
microwave	Panasonic NN-E255W
Comet electrophoresis tank	Anachem 3003
Power source	Consort E831
Plate shaker (molecular)	Heidolph Polymax 1040
CL-XPosure X-ray film	Thermoscientific

4.2.2 Methods

The methods employed in this chapter (Figure 4.8) were used to study the effect of RSP extract on neuronal like cells. The results from these methods also aid the evaluation of the potential application of RSP extract as treatment or prevention of neurodegenerative diseases.

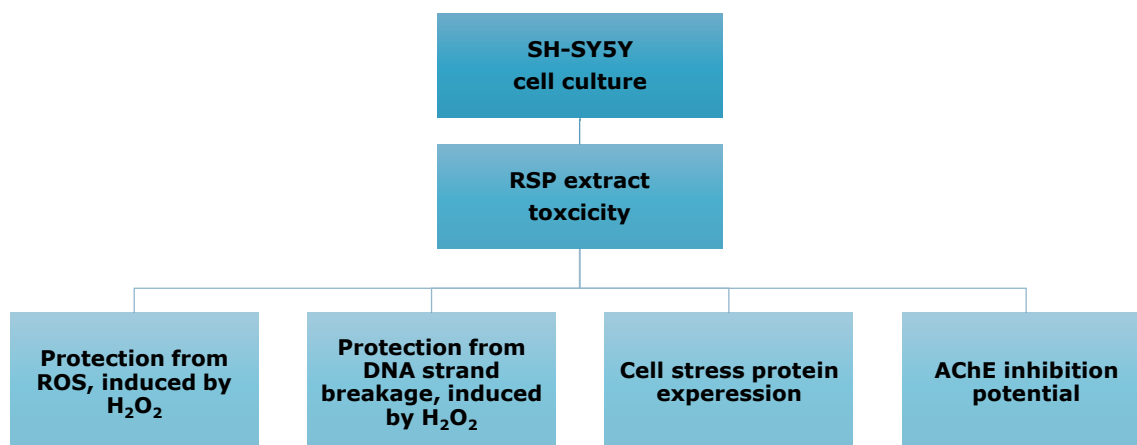


Figure 4.8| Overview of methods used to determine the extracts activity in SH-SY5Y neuroblastoma cells

4.2.2.1 General cell culture techniques

Maintenance

SH-SY5Y cells were cultured as previously described⁵⁶² with minor modifications, using DMEM media (Gibco™ DMEM, high glucose, pyruvate) supplemented with 10% FBS, 1% non-essential amino acids (NEAA) and 1% Penicillin/Streptomycin (Pen/Strep). Maintenance cell culture flasks and experimental plates/flasks were maintained in a 5 % CO₂ humidified incubator at 37°C. Cells were passaged once 80% to 90% confluence levels were reached. For passage or cells collection, old media was discarded, cells were washed with PBS and then trypsinized for 2-5 minutes (37°C). Trypsin activity was stopped by addition of fresh supplemented media and cells centrifuged (1500 rpm, 5 minutes). Then the media/trypsin supernatant was discarded, and cells suspended in fresh media for passage or in experimental buffer for further analysis. When necessary, cells were counted using a haemocytometer and cell numbers adjusted with media/ experimental buffer depending on cell density needed for experiment and/or stock of cells.

Cell lysis

Cell pellets were collected by centrifuging of the cell suspensions for 5 minutes at 2000 rpm (4°C) and the supernatant discarded. Collected cell pellets were suspended in lysis buffer (~200 µL, 150 mM NaCl, 50 mM Tris pH 8.0, 1.0% Triton-X100) for 30 minutes on ice and then sonicated for an additional 15 minutes (4°C). Thereafter cell lysates were centrifuged for 10 minutes at 14,000 g and the supernatant transferred into new Eppendorf tubes for protein analysis.

Protein determination

Both, the Bradford and the DC protein assays were applied, to determine the appropriate assay compatible with the lysis buffer. Since the Bradford assay showed strong interferences with the used lysis buffer (1% Triton-X100), it was not use for protein determination. However, the DC protein assay (BIO-RAD) showed no interferences and was used for protein determinations, using the protocol provided by the "DC Protein Assay Instruction Manual"⁵⁶³. Briefly, a working reagent A' was prepared fresh daily by adding 20 µL reagent S per 1 mL reagent A. A bovine serum albumin (BSA) standard was prepared (25 mg/mL) and further diluted (2.5 mg/mL) with cold deionized water. Standard solutions of this BSA stock were prepared ranging from 0.125-1.5 mg/mL. Cell lysate samples were diluted 1:10 in deionized water. The BSA standard solutions as well as the diluted samples (5 µL) were pipetted into a clear flat bottom 96-well plate in triplicates. Thereafter 25 µL of reagent A' followed by 200 µL reagent B were added to each well. The plate was incubated on a shaking platform for 15 minutes and then analysed at 750 nm in a plate reader. The BSA standards were employed to create a standard curve, which was used to calculate the protein amount in the 10-fold diluted sample, which was converted into the concentration of the actual sample. Protein concentrations for each sample were adjusted with deionized water or experimental buffer to required concentration in each of the experiments.

4.2.2.2 Cell viability

MTT assay

The MTT assay was carried out according to Barron *et al.* ⁵⁶⁴. Briefly, 10⁴ cells (100 µL) were seeded in 96-well plates and left to attach for 24 hours. Thereafter, 100 µL of the RSP extracts (concentrations as specified in 4.3.1, p.250) or other compounds under investigation (diluted with media) were added and cells incubated for an additional 24 hours. On the following day cells were observed under the microscope (DMIL Leica) before the cell culture medium was removed and 100 µL of freshly made and sterile-filtered (0.22 µm) MTT solution (1 mg/mL, in serum free media) were added. After 4 hours incubation (37°C), the MTT solution was carefully removed and 200 µL DMSO were added to each well and the plate shaken to dissolve the metabolised MTT product. After 20 minutes, the absorbance was measured at 560 nm. IC₅₀ concentrations were determined, normalising to the media control mean (Equation 4.1).

$$\% \text{ of viable cells} = \frac{(100 * A_{\text{treatment}})}{A_{\text{control}}} \quad \text{Equation 4.1}$$

All experiments contained at least three technical replicates per plate and statistical analysis was done on at least 3 independent experiments.

Resazurin assay

For the resazurin assay, 10⁴ cells, in 100 µL media were seeded in 96-well plates (white, clear bottom) and left to attach for 24 hours. Thereafter the RSP extract was added at final concentrations between 0.1-5 mg/mL (in 100 µL media) and cells incubated for an additional 24 hours. The next day cells were observed under the microscope (DMIL Leica) before the addition of 20 µL of resazurin (ready to use buffered solution, 0.2 µm filtered; R&D systems) to each well and incubation for 4 hours. The fluorescence intensity was read at wavelengths of 530/25 nm and 590/35 nm for excitation and emission respectively. IC₅₀ concentrations were determined, as described for the DPPH assay before (Figure 2.14, p.114). All experiments had three technical

replicates per plate, statistical analysis was done on at least 3 independent experiments.

4.2.2.3 Measurement of intracellular ROS accumulation

To determine the ROS production in SH SY-5Y cells, 2,7'-dichlorofluorescein diacetate (H₂DCFDA) was used. Cells (7×10^5) were cultured in T25 culture flasks (in duplicate), 24 hours later cells were treated with RSP extract/media (control cells) and cells incubated for an additional 24 hours. The next day, H₂O₂ (1mM) was added in 5 mL fresh media, to avoiding co-incubation of H₂O₂ with the RSP extract, removed after 30 minutes and H₂DCFDA dye (5 μ L, 0.58 μ g/ μ L) added (in 5 mL fresh media). After 4 hours incubation, the cells were washed twice with PBS, trypsinized and collected using PBS. The supernatant was removed after centrifugation (1500 rpm, 5 min) and cells re-suspended in fresh PBS for flow cytometer analysis. Duplicates of every condition were run in each independent experiment. A total number of 4 independent experiments were carried out.

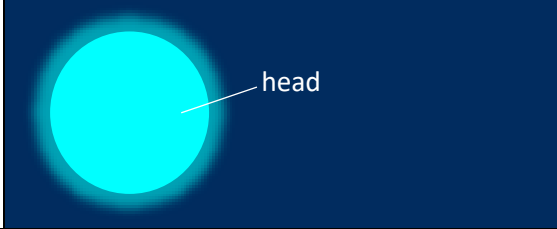
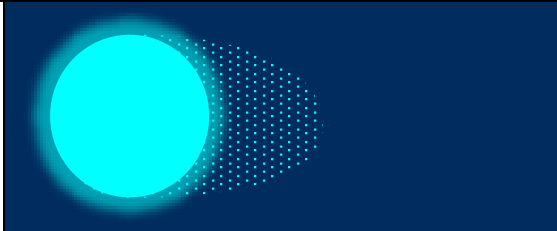
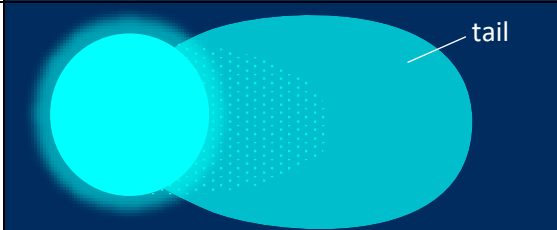
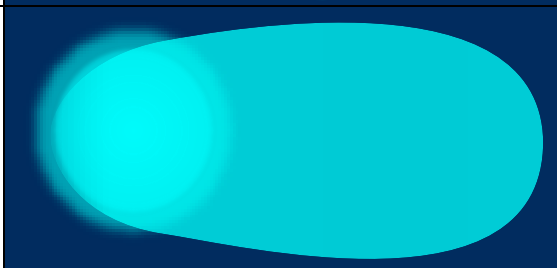
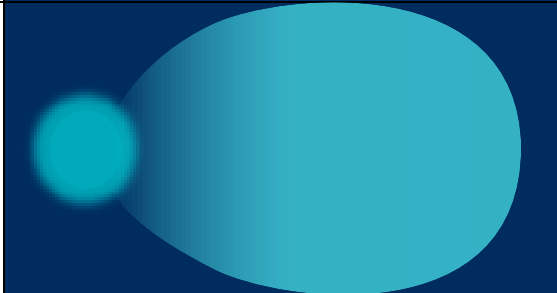
4.2.2.4 Comet assay (alkaline)

For the comet assay, cells were seeded (10^5 in 800 μ L media) in 12 well plates. After 24 h, the RSP extract (5 mg/mL in 200 μ L) or media (control cells) was added and left for an additional 24 h. All conditions were run in duplicate wells. The next day, the culture media was replaced with 1 mL fresh media (control) or media containing H₂O₂ (concentration depending on experiment, 4.3.3 Protection of SH-SY5Y cells by RSP extract from H₂O₂-induced DNA strand breakage-Comet assay, p.244) and left to incubate for 30 minutes respectively. Thereafter cells were washed with PBS and detached using 100 μ L trypsin per well. To inactivate the trypsin 900 μ L supplemented media were added after detachment and cells were collected in Eppendorf tubes and counted using a haemocytometer (cell numbers usually between 2×10^5 and 2.7×10^5). Cells were centrifuged for 5 minutes (4°C, 2000 rpm), and the supernatant carefully removed, without disturbing the pellet. The pellets were kept on ice until further use.

The comet assay was run according to Duthie *et al.*⁵⁶⁵ with minor modifications (Figure 4.6, p.223). First the bottom 1% (w/v) agarose gels (standard melting point, SMP) was prepared on frosted microscopy slides (Richardson Supply Ltd). For this, a 1% (w/v) standard melting point SMP

agarose was prepared and kept in a 40°C water bath, to avoid solidification. The SMP agarose (85 µL) was pipetted onto frosted microscopy slides and covered carefully with 18x18 mm microscope coverslips (#1 0.13-0.16 mm; Fisher Scientific) to form an even square agarose layer. Two slides were prepared per experimental condition, with two gels on each slide. After preparation of the gel layer, the slides were left to solidify (4°C for 5-10 minutes). A 1% (w/v) low melting point (LMP) agarose was prepared, and the cell pellet carefully suspended in an appropriate amount of LMP agarose to achieve about $2-5 \times 10^4$ cells in 85 µL agarose. The latter were then added on top of the SMP agarose layer, after removing the coverslip. This second layer of agarose containing the cells was also covered with 18x18 mm cover slips and left to solidify as before. Then the coverslips were removed, and the slides suspended in lysis buffer (2.5 M NaCl, 0.1 M EDTA, 10 mM Tris and 4% TritonX-100, pH 10) for one hour (4°C protected from light). Thereafter slides were placed into the electrophoresis buffer (0.3 M NaOH, 1 mM EDTA, ~pH 13) in the electrophoresis tank. After 40 minutes incubation, the electrophoresis was started using 25V. For both the alkaline treatment and the electrophoresis, the tank was kept protected from light (4°C). After 40 minutes of electrophoresis, slides were washed for 5 minutes using neutralisation buffer (0.4 M Tris, pH 7.5) in microscopy slide boxes. This was repeated 2 more times (fresh buffer (4°C)). Thereafter gels were covered using 22x22 mm microscope coverslips (#1.5 0.16-0.19 mm; Fisher Scientific) and stored protected from light (4°C, up to 3 days) until comet scoring. For the comet scoring, coverslips were removed, 20 µL DAPI staining solution (1 µg/mL in distilled H₂O) added and slides covered again with 22x22 mm coverslips. Comets were scored manually according to Heuser *et al.*⁵⁶⁶ using a fluorescence microscope with an excitation wavelength from 340-380 nm and an emission wavelength of 425 nm (Leica DMRB 200x magnification). Comet scores and criteria for moving to the next level of comet are detailed in Table 4.5, p.234. In case not all the criteria for the next level were present, comets were scored into the lower number category. A total number of 100 comets were scored leading to arbitrary numbers between 0-400 for each scored gel. For each condition three gels were scored, and their mean value determined. Statistical analysis was done on at least three independent experiments.

Table 4.5| Comet scoring criteria

Comet score	Schematic	Criteria
0		<ul style="list-style-type: none"> • Bright big circular comet head • No indication of tail
1		<ul style="list-style-type: none"> • Big and bright circular comet head (same as 0) • Sparkle like tail visible; at least the length of the head
2		<ul style="list-style-type: none"> • Bright circular comet head, same size as 0 and 1 • Comets show significant tail • Tail is less bright than head • Head still has a sharp outer contour
3		<ul style="list-style-type: none"> • Big head, but fainter in brightness, similar to tail brightness • Tail and head begin to merge in shape • Head loses sharp circular contour
4		<ul style="list-style-type: none"> • Small head with decreased brightness • Head is smaller in diameter than tail and looks separated from tail

4.2.2.5 Proteome Profiler (Human Cell Stress Array Kit)

To determine the relative levels of selected human cell stress related proteins the proteome profiler was used according the manufacturer's instructions⁵⁵⁶ with minor modifications. Cells were grown and treated (1 mg/mL RSP extract) in T25 culture flasks in duplicates (as described in 4.2.2.3, p.232). After 48 hours, the cells were harvested as previously described and treated with Lysis Buffer 6 (1×10^7 cells/mL) for 30 minutes, after which the

suspension was centrifuged at 14000 x g for 5 minutes and the supernatant transferred into a clean Eppendorf tube. The protein content was determined as described before (4.2.2.1 General cell culture techniques, p.229). To prepare the membranes, 2 mL of Array Buffer 6 were dispensed into each well of the 4-well multi-dish provided with the kit and membranes were immersed into the solution (one well each, 2 for each condition) for 1 hour on a rocking platform (rt). The samples were prepared in Array Buffer 6 to a total of 1 mL (300 µg protein each) and 0.5 mL of Array Buffer 4 were added. To each sample in addition 20 µL detection antibody cocktail (reconstituted in 100 µL deionized water) were added and samples mixed and incubated for one hour (rt).

After blocking of the membranes with Array Buffer 6, the buffer was removed from the 4-well plate and prepared samples with antibody mixture added to each membrane. The samples were incubated with the membranes overnight on a rocking platform shaker (rt).

The next day membranes were carefully removed and placed into individual plastic containers containing 20 mL of 1x washing buffer, prepared from the 25x washing buffer provided. Membranes were washed individually for 10 minutes three times. Streptavidin-HRP was diluted in Array Buffer 6 (1:1000) and 2 mL pipetted into each well of the 4-well plate. Membranes were added to the Streptavidin-HRP solution after draining the wash buffer and incubated on a rocking platform shaker for 30 minutes (rt). After incubation each membrane was washed individually in wash buffer 3 times as previously described. Before placing the membranes on foil (saran film), each membrane was drained by blotting the lower edge onto paper towel. Once membranes were placed on the foil 1 mL of Chemi Reagent Mix (1:1 mixture of chemi reagents 1 and 2) was pipetted onto each membrane and covered with more foil and incubated for 1 minute. The membranes were placed into an autoradiography film cassette and exposed to X-ray film (CL-Xposure, Thermoscientific) for 15 minutes. Thereafter, the film was developed, washed, fixed (Kodak), rinsed and air dried. To determine the spot intensity of photocopied images of the films, Image J software with an in build protein array analyser was used. Due to limited resources, only one independent experiment was undertaken (two technical replicates; two membranes per

condition). Statistical analysis was undertaken with the limited number of technical replicates obtained (n=2).

4.2.2.6 Amplex® Red Acetylcholinesterase Assay

For the determination of cellular AChE activity, cells were grown and treated as previously described for the comet assay (4.2.2.4 Comet assay (alkaline), p.232). To determine whether the extract decreases AChE *in vitro* in SH SY-5Y cells, the Amplex® Red kit previously used for the AChE inhibition activity, was used, with minor modifications. Neostigmine (100 µM) was used as a positive control (known AChE inhibitor) after determining its non-toxic concentrations *via* MTT assay (4.2.2.2 Cell viability, p.231).

The protein content of the samples was determined as previously described (4.2.2.1 General cell culture techniques, p.229 ff.) and diluted to 3000 µg/mL. 100 µL of protein sample as well as AChE (positive control), 1x reaction buffer (negative control) and H₂O₂ (10 µM, positive control) were pipetted in triplicates into a black 96 well plate, with clear flat bottoms. To the controls and the samples 100 µL of the reaction mix (previously described in 3.2.2.5 Acetylcholinesterase inhibition potential, p.163) were added and the plate immediately placed into the plate reader. The reaction was monitored over a period of 150 minutes. Four independently grown cell culture samples were collected for this experiment and analysed in the same 96-well assay plate.

4.2.2.7 Statistical analysis

Statistical analysis was carried out using GraphPad Prism 7. Specific methods used for statistical comparison of each experiment are detailed in the results section. At least 3 independent experiments (n) were analysed per assay, unless otherwise stated and results shown as mean ± standard deviation. P-values below 0.05 were considered significant.

4.3 Results and Discussion

4.3.1 Cellular toxicity of RSP extract

4.3.1.1 MTT assay

Initial experiments using MTT for the toxicity determination of the RSP extract, showed questionable and varying results for three independent experiments (Figure 4.9). From the absorbance measurements taken at 560 nm the results appear to show an increase of proliferation when treated with e.g. 5 mg/mL RSP extract. However, morphological observation of the cells under the microscope before addition of the MTT solution after 24 hours treatment showed extensive cell toxicity (rounded up cells and decrease in cell number, Figure A10, p.449) compared to the media control. The results from the MTT assay contradict these observations.

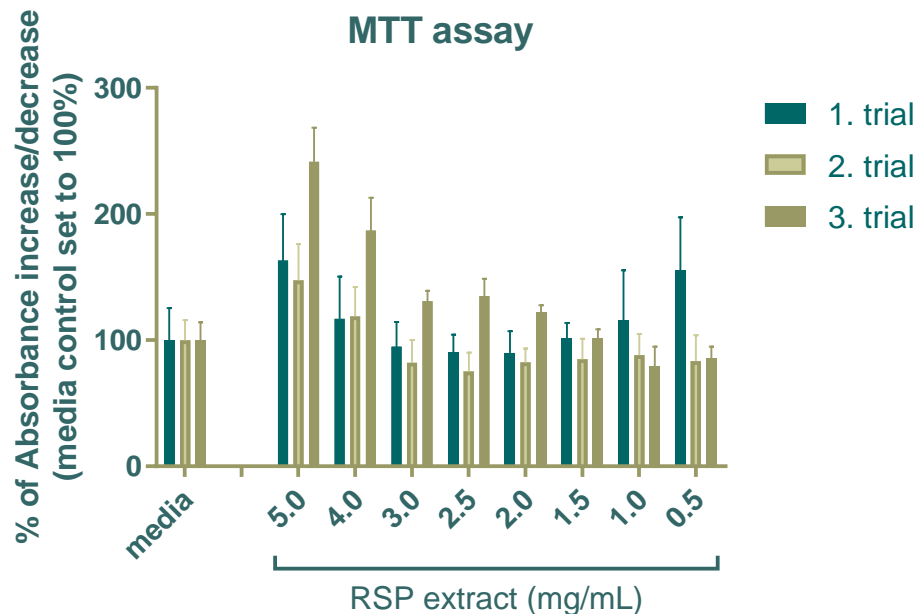


Figure 4.9 | MTT-assay results from SH-SY5Y cells incubated with RSP extract (24 h treatment)

Literature research into this issue revealed the potential of interference of the extract with the MTT solution. In Bruggisser *et al.*⁵⁶⁷ for example flavonoids kaempferol and resveratrol as well as antioxidant substances such as ascorbic acid sodium salt, vitamin E and N-acetylcysteine were able to reduce the tetrazolium ring of MTT (Figure 2.7, p.84). Also, some of the tested plant (*Hypericum*) extracts showed similar effects. The observed interference was

not due to the extract's absorption at the measured wavelength but due to an active reduction of MTT to formazan⁵⁶⁷. To determine whether this could be the case sinapic acid as one of the present phenolic acids was tested in a cell free system at concentrations ranging from 0.005-2.5 mg/mL (Figure 4.10).

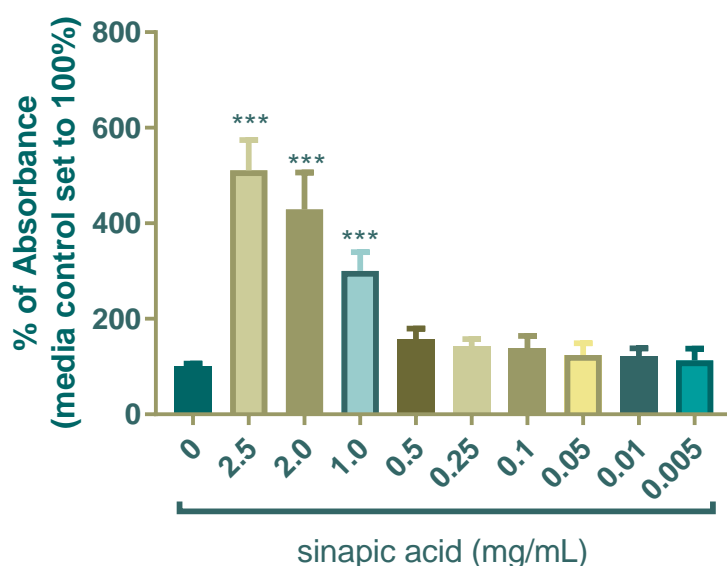


Figure 4.10| MTT reduction by sinapic acid in a cell free system (24 h)

Statistical significant difference determined using One-way ANOVA and Bonferroni's multiple comparison analysis compared to media control: *** $p \leq 0.001$, $n=6$ (only technical replicates)

The results from this experiment showed a significant increase in absorbance readings at high concentrations of sinapic acid (1.0-2.5 mg/mL), suggesting a reduction of the MTT had taken place. No statistical significances were observed for the lower concentrations, however a trend towards a slightly higher absorbance is visible for most of them (Figure 4.10). Repeating statistical analysis excluding the highest 3 concentrations, revealed statistical significance also for 0.1, 0.25 and 0.5 mg/mL (Figure A9, p.450). This significance was lost in the initial graph due to the wide range of absorbance results. These results clearly showed that sinapic acid reduces MTT.

At 5 mg/mL RSP extract, a sinapic acid concentration of 0.02 mg/mL (3.99 $\mu\text{g}/\text{mg}$ RSP extract, Table 3.5, p.171) is present. Although at that concentration sinapic acid alone is not expected to be responsible for the observed increase in absorbance (Figure 4.10), a combination of other

phenolics present in the RSP extract could synergistically have contributed to the observed effect. At the time of that experiment the high level of sinapine in the RSP extract was not known, which is why only sinapic acid was tested. Considering the higher concentration of sinapine in the extract, it could be responsible for the observed interference. More detailed analysis looking into sinapine's reduction potential of MTT in a cell free-system could solve this uncertainty.

However, due to the limited time available, the resazurin cell viability assay was used instead to determine cell toxicity of the extract. To avoid potential interference, wells without cells (prepared equally to cell containing wells) were analysed simultaneously.

4.3.1.2 Resazurin assay

The resazurin assay gave clearer results and agreed with the cell morphology observed under the microscope after treatment with RSP extract (Figure 4.11 vs. Figure A10, p.449). Concentrations of up to 1.5 mg/mL of RSP extract showed no significant decrease in fluorescence intensity compared to the media control. Starting at 2.0 mg/mL, the measured fluorescence intensity significantly decreased compared to the media control ($p < 0.001$). These results suggest a toxicity of the RSP extract towards SH-SY5Y cells starting between 1.5 and 2.0 mg/mL.

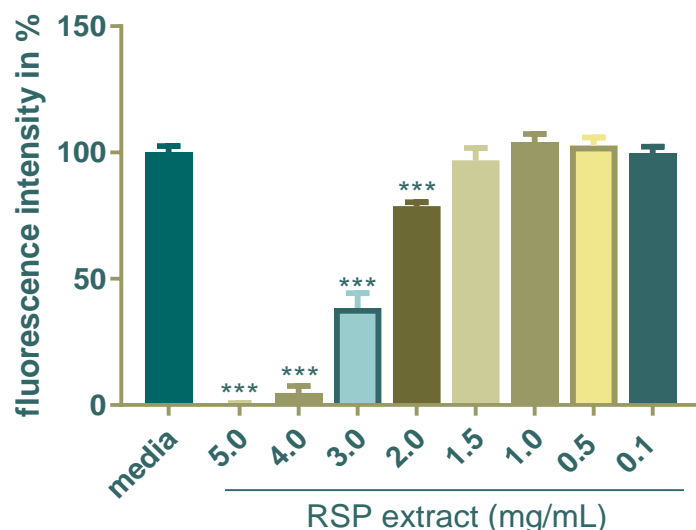


Figure 4.11 | Resazurin cell viability assay using RSP extract (0.1-5.0 mg/mL, 24 h treatment)

Statistical significant difference determined using One-way ANOVA and Bonferroni's multiple comparison analysis compared to media control: *** $p < 0.001$, $n = 3$

Based on the resazurin toxicity results, subsequent experiments using RSP extract were done at concentrations of 1.0 mg/mL or less. Slightly higher concentrations could have been used (1.5 mg/mL, non-toxic), but this was avoided, because a small but insignificant decrease for the fluorescence intensity was observed at that concentration. In addition, the cell morphology started to change after 24 hours treatment with 1.5 mg/mL RSP extract concentration (Figure A10, p.449). Also, the addition of further stressors in combination with the extract could lead to increased toxicity, which is why a maximum of 1.0 mg/mL was chosen to be safe for future research. The IC₅₀ of the RSP extract was determined to be 2.75 mg/mL, which means 2.75 mg/mL of the RSP extract eliminate 50% of the cell population (Figure A11, p.450).

So far, no literature has been found to report on the cell toxicity of RSP extracts towards SH-SY5Y cells. Compared to other natural extracts, the cells show a higher acceptability towards the RSP extract. An ethanol extract of *Bactris guineensis* (L.) H.E. Moore (corozo fruit) for example showed reduced SH-SY5Y cell viability already at 0.15 mg/mL⁵⁶⁸. Similar was true for *Agaricus blazei* (almond mushroom) extract, even at small concentrations such as 0.05 and 0.10 mg/mL showed a significant decrease in cell viability⁵²¹. A greater tolerance towards the RSP extract is advantageous, as higher concentrations can be tested for the potential protection of cells from oxidative stress.

4.3.2 Protection of SH-SY5Y cells by RSP extract from ROS induced by H₂O₂

Following the toxicity determination of the RSP extracts in the neuroblastoma cell line, the potential of RSP extract to alleviate the production of ROS after H₂O₂ induced oxidative stress was analysed. To achieve this objective, the potential of the RSP extract to produce ROS in SH-SY5Y cells was assessed and compared with ROS production (increased fluorescence) caused by H₂O₂ (1 mM, 30 min, Figure 4.12). One-way ANOVA and Bonferroni's multiple comparison analysis of the results (media control vs. treatment) showed a significant increase of ROS production upon treatment with H₂O₂ (1 mM, 30 minutes). In contrast, the RSP extract (0.25-1.0 mg/mL) was not associated with a significant increase in ROS production after 24 hour treatment ($p > 0.05$).

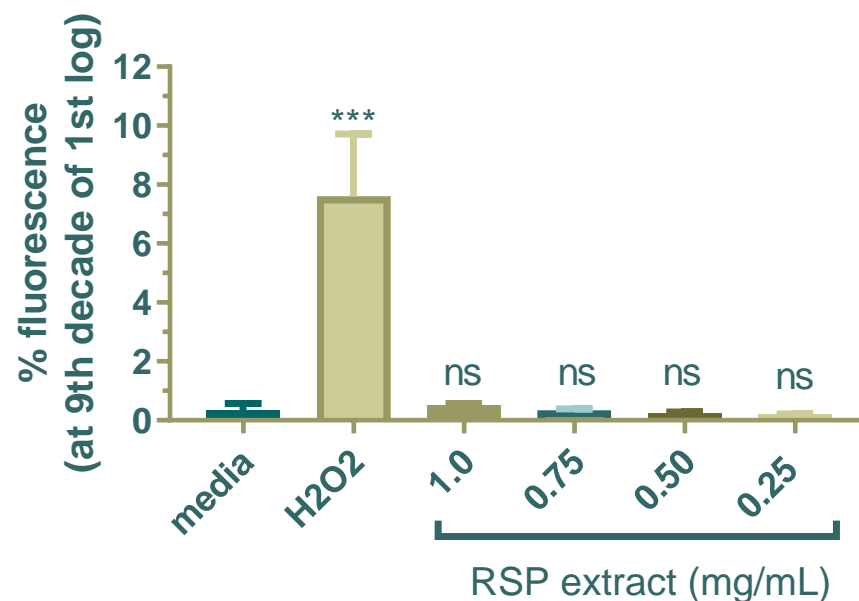


Figure 4.12| ROS production in SH-SY5Y cells caused by H₂O₂ control (1 mM, 30 min) and different concentrations of RSP extract (0.25-1.0 mg/mL)

*Statistical significant difference determined using One-way ANOVA and Bonferroni's multiple comparison analysis compared to media control: ns-not significant; *** $p \leq 0.001$, $n = 3$*

However, in this set of data, the high fluorescence readings obtained for the H₂O₂ control skews the data. When taking a closer look, it appears as if the RSP extract is causing a slight concentration dependent increase in cellular ROS production. When removing the data obtained for the H₂O₂ control, the graph is less skewed (Figure A12, p.451). Although, One-way ANOVA with

Bonferroni's multiple comparison does not show a significant difference in fluorescence between the treated and untreated cells a concentration dependent trend towards an increased ROS production at 1 mg/mL treated cells is visible. Since the increase was not significant all four concentrations were taken for further analysis. Especially as a minor increase in ROS production by the RSP extract treatment could trigger an antioxidant response on a molecular level in the cell, e.g. by activating Nrf2 (Figure 1.29, p.60) that could aid to decrease the oxidative stress caused by the addition of H₂O₂.

In the following experiments, cells were pre-treated with RSP extract (0.25-1.0 mg/mL) for 24 hours and then incubated with H₂O₂ (1 mM) for 30 minutes, to determine whether pre-treatment with the extract can decrease the amount of produced ROS *in vitro*. The results obtained (Figure 4.13, Figure A12 (p.451)- for example of raw data) clearly demonstrated the ability of the RSP extract to inhibit ROS production after H₂O₂ induced oxidative stress. Lower concentrations (0.25 and 0.5 mg/mL) showed a decreasing trend in fluorescence, hence a decrease in ROS production.

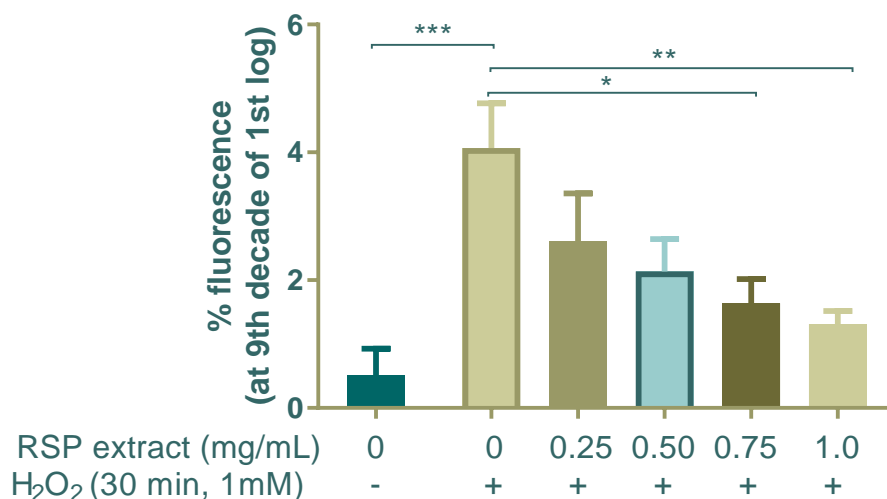


Figure 4.13| ROS production after pre-treatment with RSP extract (24 h) followed by treatment with H₂O₂ (1 mM, 30 minutes)

Statistical significant difference determined using One-way ANOVA and Bonferroni's multiple comparison analysis compared to H₂O₂ control: **p*≤0.05; ***p*≤0.01; ****p*≤0.001, *n*=4

Higher concentrations of RSP extract (0.75 and 1.0 mg/mL) show a statistical (One-way ANOVA and Bonferroni's multiple comparison analysis) significant

decrease in fluorescence compared to the H₂O₂ control. This decrease in fluorescence implies a decrease of ROS production in the SH-SY5Y cells. Thus, the two highest concentrations (0.75 and 1.0 mg/mL) of the RSP extract are successful in significantly preventing ROS production as a result of H₂O₂-induced oxidative stress.

As previously described for the cell viability study, this is the first time, RSP extracts activity towards a decrease of ROS production in SH-SY5Y cells is reported. However, other plant extracts have previously shown similar effects *in vitro*^{520,569}. In a paper by Park *et al.*⁵²⁰, a *Liriope platyphylla* extract (0.5-50 µg/mL) decreased ROS concentrations measured in SH-SY5Y cells stressed with H₂O₂ (100 µM). Similarly, in a paper by Wang *et al.*⁵⁶⁹ phenolic extracts of *Inula helenium*, decreased ROS production at 0.5 and 5 µg/mL significantly. In contrast to these two papers, where pre-treatment with the extracts occurred for one and six hours respectively, we pre-treated the cells for 24 hours with the RSP extract.

ROS are well known to cause oxidative stress (1.4.1 Oxidative stress, p.53 ff.) within a cell system. This oxidative stress can amongst others lead to DNA strand breaks (nuclear). Following the above results, it was decided to extend the experiments to study whether (i) ROS generated by H₂O₂, can inflict SH-SY5Y cellular DNA damage and (ii) RSP extract can provide cellular DNA protection from H₂O₂-induced DNA strand breakage using the comet assay.

4.3.3 Protection of SH-SY5Y cells by RSP extract from H₂O₂-induced DNA strand breakage-Comet assay

To determine whether the RSP extract is not only able to protect pBR322 plasmid DNA from oxidative stress induced damage (3.3.8 Inhibition of supercoiled plasmid DNA strand breakage, p.201 ff.) but also cellular nuclear DNA, here the comet assay was applied. In Figure 4.14 below an overview of the classes of comets scored during this experiment with SH-SY5Y cells, ranging from 0 (no DNA strand breaks) to 4 (significant amount of DNA strand breaks) is given. The scoring was done according to Collins⁵⁴¹ (Table 4.5, p.234). The comets obtained from this cell line look very similar to those obtained from other cell lines, such as lymphocytes in Collins⁵⁴¹.

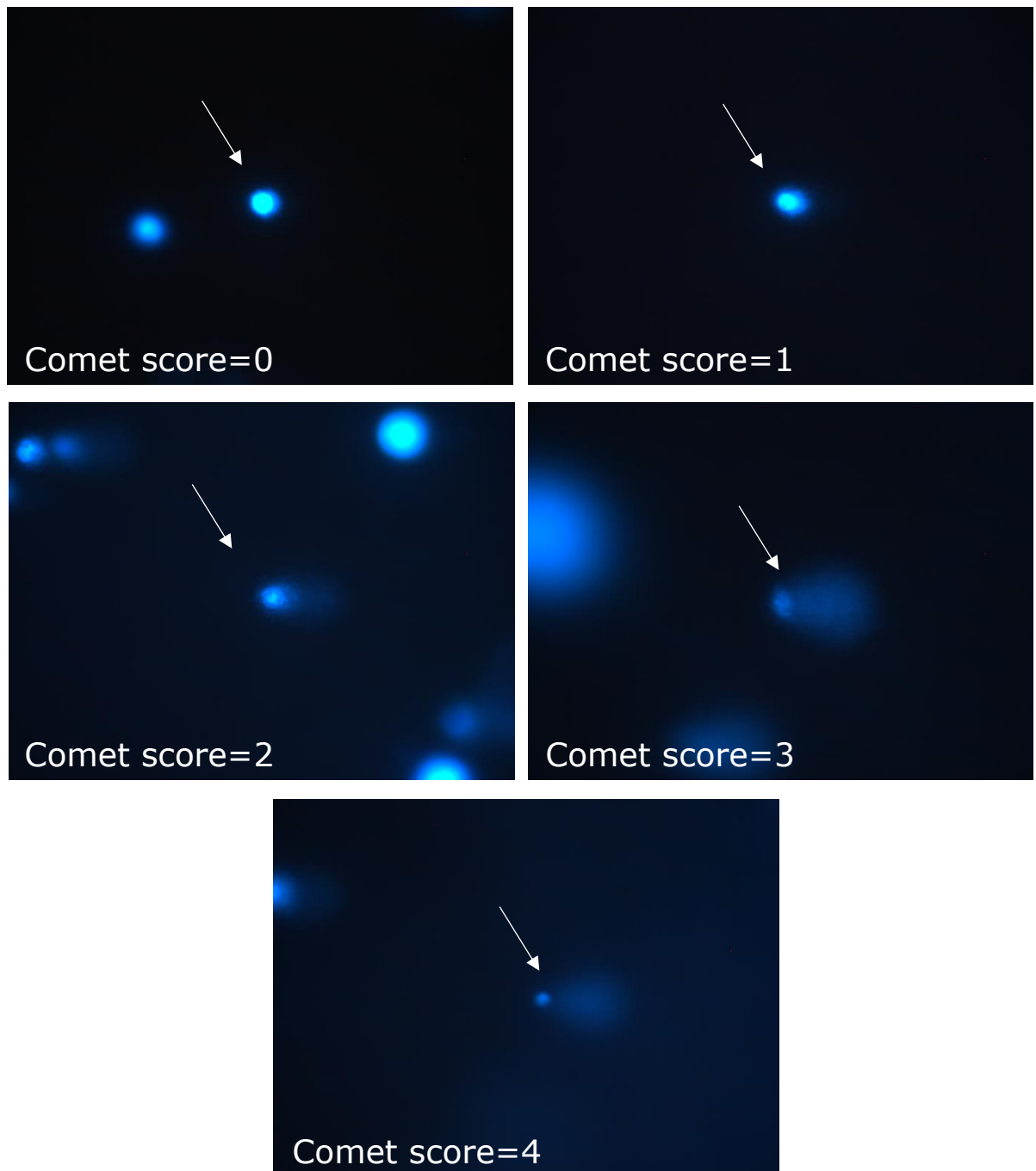


Figure 4.14| Images of comet classes obtained for SH-SY5Y cells
Score 0-4 (Leica DMRB microscope (100x) with Leica DFC 300FX camera (0.63x), size of pictures decreased to fit page)

Before conducting the experiments to study the protective properties of the extracts, the DNA strand breakages caused by different concentrations of H_2O_2 (100-1000 μM) were assessed first. Ideally a concentration of the stressor should be chosen that inflicts a significant amount of damage (arbitrary unit (AU) score between 200 and 300) but does not cause detrimental DNA damage and eventually cell death. In the SH-SY5Y cells, the controls had a mean score value of 6.9, when scoring 100 comets on 3 gels each and determining the mean (Figure 4.15). With increasing concentrations of H_2O_2 , the comet score increases in a concentration dependent manner: 100 μM 44.4 < 200 μM 197.7 < 300 μM 263.8 < 500 μM 360.4 < 1000 μM 382.3.

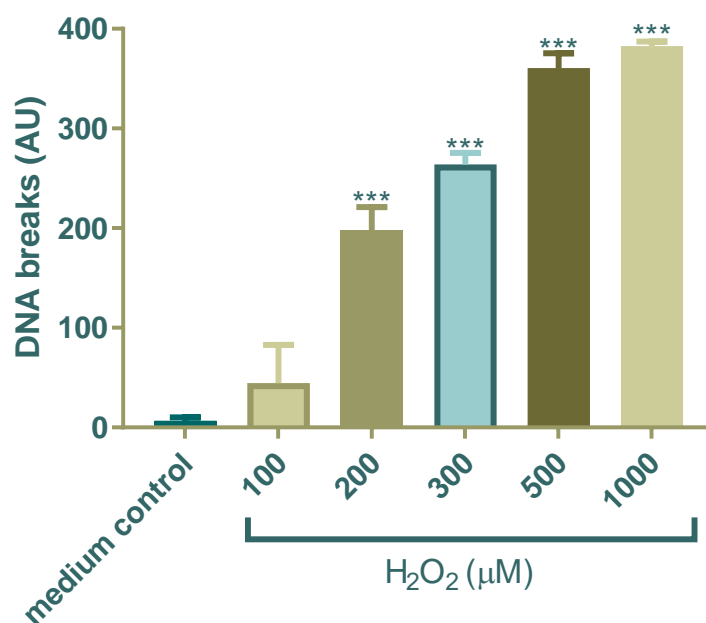


Figure 4.15| Concentration dependent DNA strand breaks induced by H_2O_2 (30 minutes)

Statistical significant difference using One-way ANOVA and Bonferroni's multiple comparison analysis compared to media medium control: *** $p \leq 0.001$, $n=3$

Based on the above results, the decision was made to use a concentration of 300 μM H_2O_2 the protection study of RSP extract. At that concentration a significant amount of DNA damage ($p < 0.001$) compared to the media control was observed, but the DNA is not a strongly damaged as for 1000 μM . Hence a protection study of the DNA by the extract is possible. In addition, another

H₂O₂ concentration of 1000 µM was used as in a previous experiment this concentration was able to induce ROS (4.3.2 Protection of SH-SY5Y cells by RSP extract from ROS induced by H₂O₂, p.241 ff.). RSP extract concentrations used in the comet assay were also based on the results of the ROS experiment, in which 1 mg/mL of the RSP extract showed the best inhibition of ROS production (Figure 4.13, p.242), so this concentration was taken forward for the comet assay. Figure 4.16 shows the results obtained for the comet assay, using both concentrations of H₂O₂ and comparing between media and RSP extract treated cells.

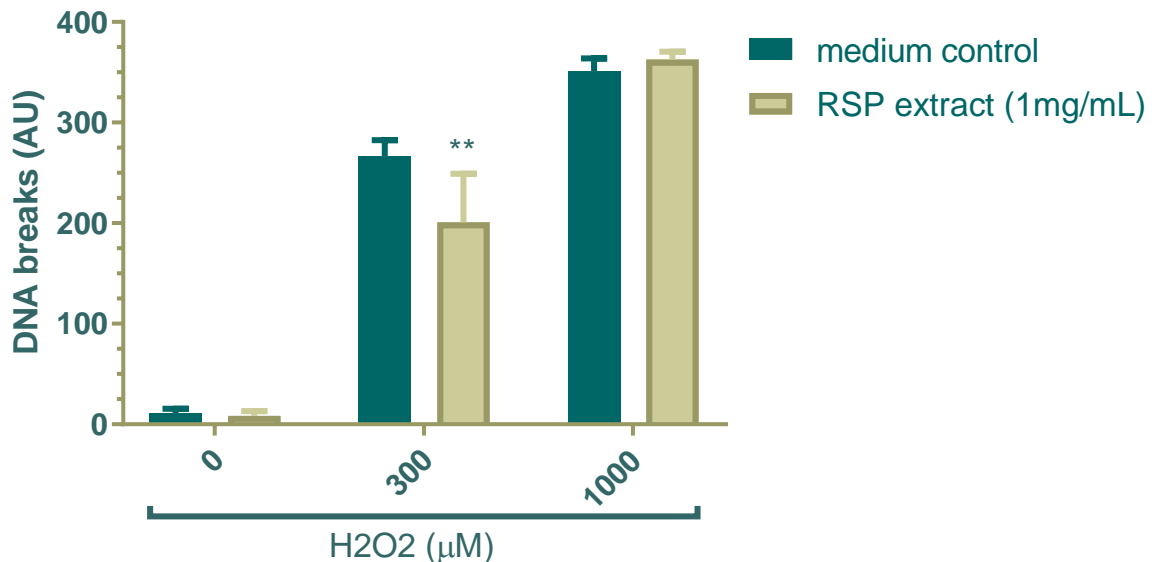


Figure 4.16| Cellular DNA protection from H₂O₂ induced DNA strand breaks by the RSP extract (1mg/mL, 24 h preincubation)

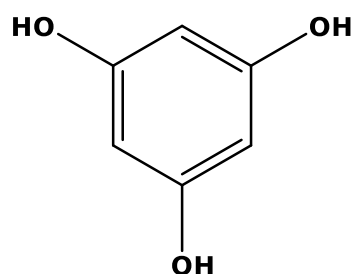
*Protection from 300 µM H₂O₂ induced strand breakage (but not 1000µM), statistical significant difference using Two-way ANOVA and Bonferroni's multiple comparison analysis compared with media control at the same level of H₂O₂ (**p<0.01), n=4*

As previously shown the media control shows little DNA damage (10.6). The same is true for the RSP treated control (no H₂O₂), with a mean comet score of 8.7. No significant difference between both were observed, indicating the presence of the RSP itself does not cause any DNA damage in SH-SY5Y cells. For the H₂O₂ treated cells comet scores showed increasing DNA strand breakage as previously determined (Figure 4.15, p.246). Here, 300 and 1000 µM H₂O₂ gave comet scores of 266 and 351 respectively. When pre-treating cells with the RSP extract (1 mg/mL, 24 hr) followed by the addition of H₂O₂,

a significant ($p < 0.01$) protection from DNA damage was observed for the 300 μM H_2O_2 treatment (Figure 4.16, p.247). In contrast, no protection was observed for 1000 μM H_2O_2 . The latter concentration led to severe stress (DNA strand breakage) that the protective properties of the extract were not effective to protect the cells from the DNA strand breaks.

It is noteworthy to mention that this is the first study in applying RSP extract for the protection of cellular DNA from H_2O_2 induced DNA strand breaks. In general, there is limited supporting evidence in the literature for the use of natural compounds/extracts to prevent DNA strand breakage in SH-SY5Y cells.

Kim *et al.*⁵⁷⁰ had previously demonstrated similar positive comet assay outcome by applying a pre-treatment with phloroglucinol (1,3,5-trihydroxybenzene). Phloroglucinol is a phenolic (phlorotannin) commonly found in *Ecklonia cava* (brown algae) of the family *Laminariaceae*.



phloroglucinol

In their paper phloroglucinol showed to be more toxic towards SH-SY5Y cells than the RSP extract. Concentration starting at 40 $\mu\text{g}/\text{mL}$ showed a decrease in cell viability in the MTT assay. However, they were also able to demonstrate that phloroglucinol can prevent high ROS levels, induced by H_2O_2 (0.8 mM). Similarly, to our findings, they were also able to show the protection from DNA strand breaks using 10 $\mu\text{g}/\text{mL}$ (concentration found to be safe for cells). Also Ghosh *et al.*⁴¹⁹ found DNA protective properties in the comet assay using boysenberry and blackcurrant extracts (phenolic or anthocyanin rich). However, they failed to detail the concentration of H_2O_2 used and for the comet assay they also switched cell lines from SH-SY5Y cells (toxicity/ROS) to HL-60 cell, for which no particular reason was given.

DNA, as well as protein and lipid damage in neuronal cells (Figure 1.27, p.54) are known to play a key role in the development of neurodegenerative disease. Compounds able to protect DNA from strand breakage as well decreasing ROS levels when under oxidative attack, could be potential candidates for the prevention and treatment of these neurological disorders.

More studies into DNA protection of RSP extract are necessary, to determine the mode of action. One explanation for the protection of SH-SY5Y cells by RSP extract seen in both the ROS experiment and the comet assay is their direct antioxidant activity. However, the extracts could also provide cellular protection due to their potential indirect antioxidant activity through the activation of antioxidant pathways within the cell system (1.4.3 Exogenous antioxidants - natural products: direct and indirect antioxidant activity, p.58 ff.). The literature suggests, that a number of different extracts/isolated compounds activate for example the Nrf2 pathway both *in vitro* and *in vivo*. Curcumin (turmeric), sulforaphane (broccoli) and resveratrol (grapes) are only some of the compounds known to activate Nrf2 expressions, followed by the activation of antioxidant and detoxification enzymes^{229,571}. To further investigate the extracts effect *in vitro*, molecular analysis on the extracts effect on cell stress proteins was undertaken.

4.3.1 Study into the cell stress related protein expression induced by RSP extract using micro array technology

As demonstrated in the ROS and comet assay, the RSP extract shows no significant increase in cellular stress (ROS) or DNA damage. To verify these observations at molecular levels, the human cell stress protein array was used. Media control cells were compared to cells incubated with RSP extract for 24 hours. All the cell stress proteins under investigation are listed in Table 4.6.

Table 4.6| Human cell stress proteins included in the protein array⁵⁵⁶

Coordinate	Colour	Analyte/Control	Alternative name
A1, A2, A21, A22, E1, E2		Reference Spot	/
B3, B4		ADAMTS1	/
C3, C4		HIF-2 α	EPAS1
D3, D4		Phospho-p38 (T180/Y182)	
B5, B6		Bcl-2	
C5, C6		Phospho-HSP (S78/S82)	
D5, D6		Phospho-p53 (S46)	
B7, B8		Carbonic Anhydrase IX	CA9
C7, C8		HSP60	
D7, D8		PON1	
B9, B10		Cited-2	
C9, C10		HSP70	
D9, D10		PON2	
B11, B12		COX-2	
C11, C12		IDO	Indoleamine 2,3-dioxygenase
D11, D12		PON3	
B13, B14		Cytochrome c	
C13, C14		Phospho-JNK Pan (T183/Y182)	
D13, D14		Thioredoxin-1	
B15, B16		Dkk-4	
C15, C16		NF κ B1	
D15, D16		SIRT2	Sirtuin 2
B17, B18		FABP-1	L-FABP
C17, C18		p21/CIP1	CDNK1A
D17, D18		SOD2	MnSOD
B19, B20		HIF-1 α	
C19, C20		p27	Kip1
D19, C20		Negative control	Control (-)

Note(s): Colour coding in accordance with Figure 4.17 schematic

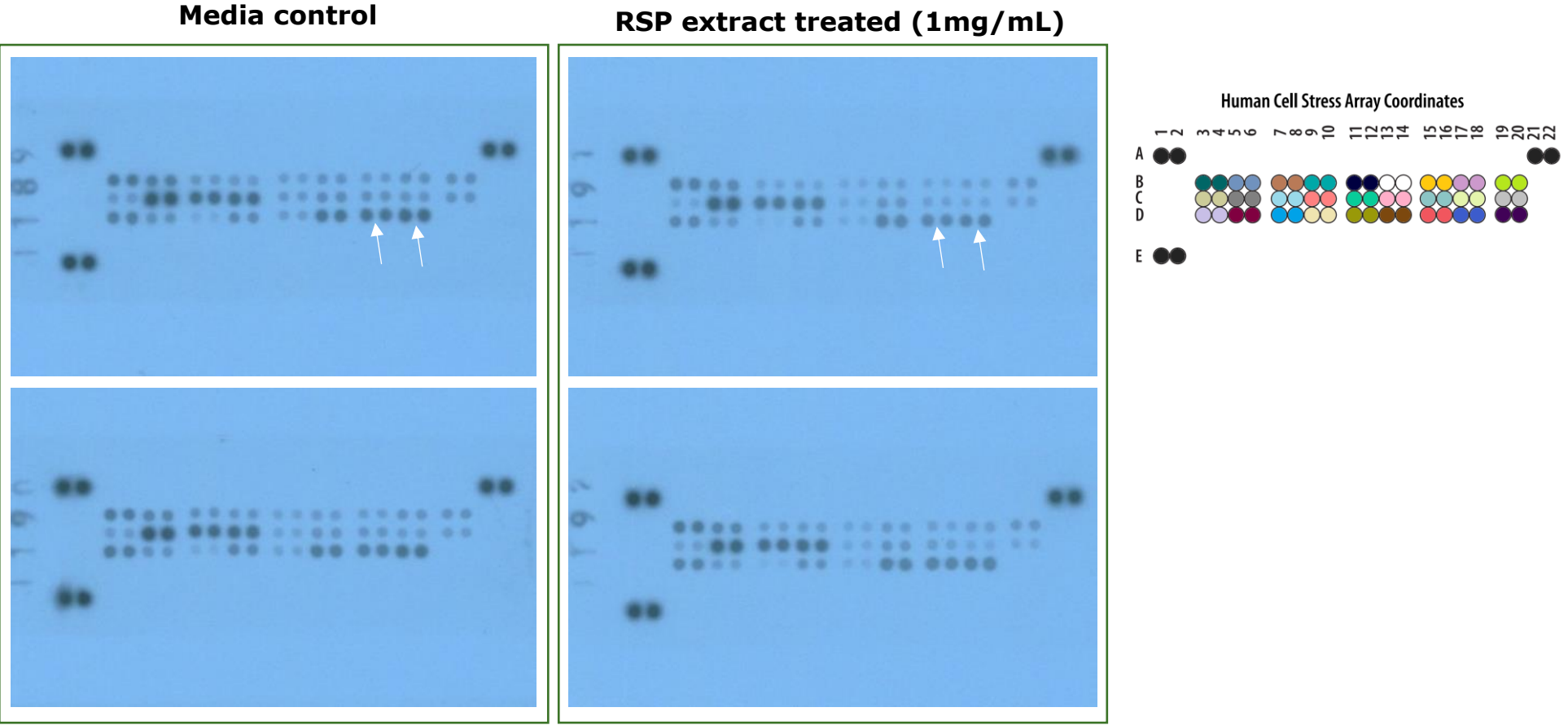


Figure 4.17| Developed films of human cell stress protein arrays

Comparing media control (left) to RSP extract treatment (right). Schematic on far right showed the analysed proteins colour coded in association with Table 4.6

The developed films (Figure 4.17, p.251) of the human cell stress protein array show a slight reduction in intensity for most of the investigated proteins. To verify the visual indication of a decrease in cell stress protein expression after RSP extract (1 mg/mL) treatment, the intensity of the spots was analysed and graphed (Figure 4.18).

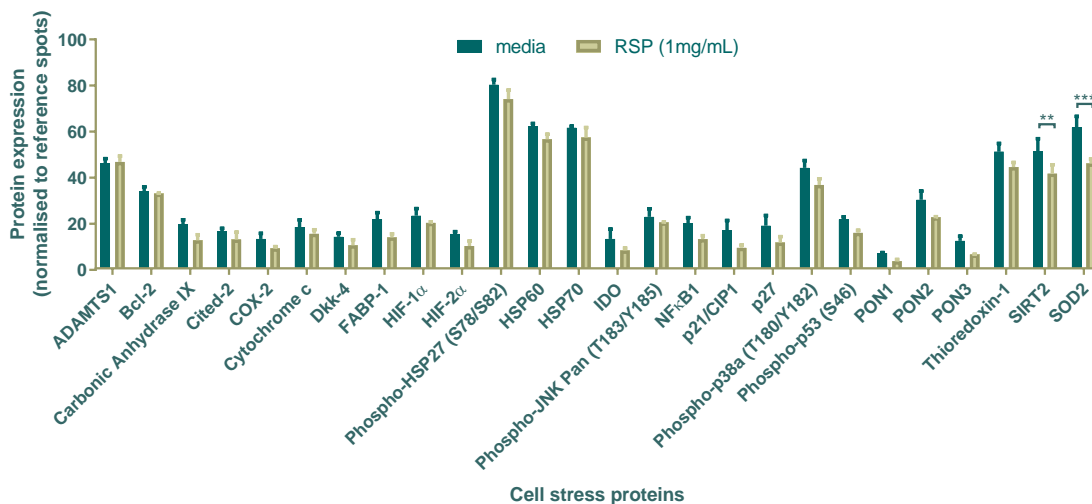


Figure 4.18| Expression of human cell stress proteins in SH-SY5Y cells exposed to RSP extract (1 mg/mL, 24 h) in comparison to media control

Values were normalized to the reference spots, statistical significant difference was determined using multiple *t*-test with Holm-Sidak correction ($\alpha=0.05$), using adjusted *p*-values, ** $p \leq 0.01$, *** $p \leq 0.001$, $n=2$

As indicated by the visual observation, all the cell stress proteins except ADAMTS1 are slightly down regulated after RSP extract treatment. Only SIRT2 and SOD2 (white arrows in Figure 4.17, p.251) were significantly down regulated. However, since the statistics were done using only two replicates for each condition, the results need to be taken carefully. Especially as the two replicates are not from independent experimental set-ups. To get a clear view on the effect of the extract on cell stress protein expression, 3 independent experiments should be conducted.

The enzyme SIRT2 (sirtuin2) is part of the histone deacetylase (HDAC) family of proteins that participate in a number of cellular functions and are important for aging, a major risk factor for many neurodegenerative diseases. In humans 7 sirtuins have been identified (SIRT1-SIRT7)⁵⁷², SIRT2 is a mostly cytoplasmic protein. In non-neuronal cells SIRT2 is associated with cell cycle regulation *via* the deacetylation of cytoplasmic substrates, including α -tubulin

(backbone for many cellular substructures like the mitotic and meiotic spindles and the intracellular cytoskeletal network⁵⁷³)^{574,575}. Literature however found, that in neuronal cells microtubule acetylation is necessary for neuronal cell development and function. In addition, a number of well-known pathological issues in patients with neurological disorders (e.g. the accumulation of misfolded or aggregated proteins, abnormal mitochondrial trafficking and decreased synaptic connectivity) are microtubule-dependent cellular processes⁵⁷⁴. In Outeiro *et al.*⁵⁷², the inhibition of SIRT2 has previously shown to rescue α -synuclein-mediated toxicity in *in vitro* and *in vivo* models of PD. Neuroprotection was also observed in a HD model by SIRT2 inhibition⁵⁷⁶. On the other hand, in a paper by Singh *et al.*⁵⁷⁷ over expression of SIRT2 in SH-SY5Y cells protected from rotenone (mitochondrial-) and diquat (cellular-) induced stress/cell death. In contrast to the papers given above, where SIRT2 inhibition showed positive effects in PD⁵⁷² and HD⁵⁷⁶ models, Singh *et al.*⁵⁷⁷ demonstrated that SIRT2 inhibition enhanced α -synuclein aggregate formation in diquat or rotenone treated cells and overexpression reduced aggregation. The obtained different results are most likely due to the different treatments used to induce α -synuclein aggregates in Outeiro *et al.*⁵⁷² A53T mutant α -synuclein overexpression directly aggregated in cellular and fly models whereas, in Singh *et al.*'s⁵⁷⁷ study, α -synuclein aggregate formation was induced by oxidative stress⁵⁷⁷. Under basal conditions (no rotenone/diquat) no increase of aggregations was seen compared to the control. However, these varying results also show that a lot is still unknown regarding the importance of SIRT2 in neurodegenerative disease.

Nevertheless, Wang *et al.*⁵⁷⁸ showed that SIRT2 expression is increased under caloric restriction as well as oxidative stress. As previously mentioned, SIRT2 has deacetylation properties. When binding to FOXO3a, this leads to the reduced acetylation of this forkhead box O (FOXO) transcription factors, which increases FOXO DNA binding and so increased expression of its target genes, one of which is MnSOD (SOD2). This association is also seen in the protein array results. After treatment of the cells with RSP extract, both SIRT2 and SOD2 protein expression were down regulated.

In humans 3 SOD enzymes exist (SOD1-3). SOD2 is a mitochondrial manganese-dependent superoxide dismutase (MnSOD), containing a single metal ion site⁵⁷⁹. It catalyses the reaction of superoxide ($O_2^{\cdot-}$) to hydrogen peroxide (H_2O_2), before it can oxidize essential components such as DNA, proteins, or lipid (Figure 4.19)⁵⁸⁰.

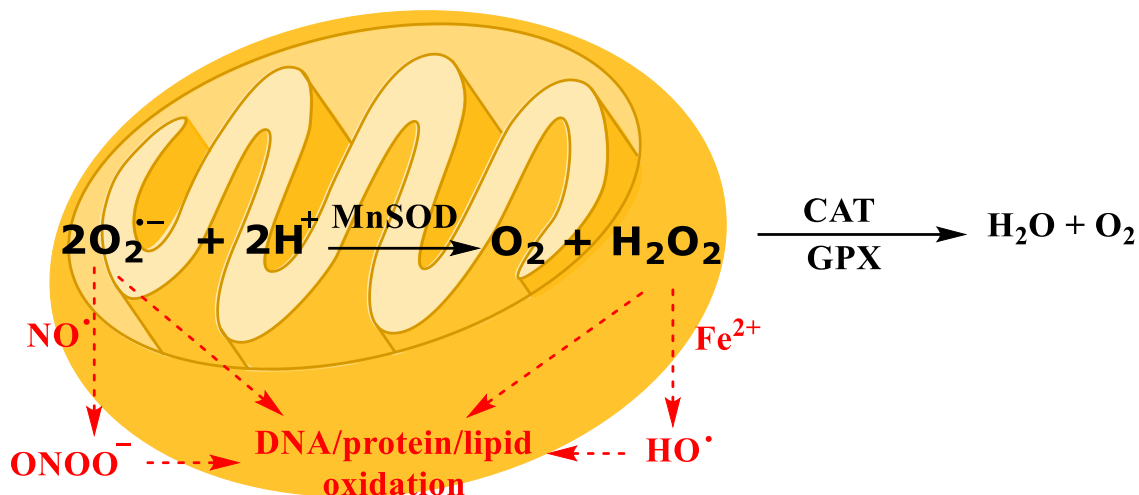


Figure 4.19|Reaction of superoxide to H₂O₂ catalysed by MnSOD (SOD2)

Adapted from^{581,582}

SOD2 is generally upregulated under oxidative stress and is necessary to regulate levels of ROS. After the treatment with RSP extract the protein expression of SOD2 was decreased, which on the one hand means that the extract is not causing SOD2 related cell stress, which would otherwise lead to an increase of SOD2 expression. On the other hand, this downregulation could lead to increased damage when introducing oxidative stressors to the cells, as SOD2 is present in smaller amounts to counter act oxidative insult.

To determine the cells reaction towards oxidative stress, it would be useful to analyse the cell stress proteins under e.g. H_2O_2 -induced insult, when pre-treated with RSP extract and in comparison, to the media control. An experiment like this could give an indication of which proteins are important for the protective effect of the RSP extracts in SH-SY5Y cells. In addition, further studies into the time dependent expression of these proteins could give a greater insight into the expression changes of stress related proteins. Currently the results only represent a single time point after RSP extract treatment (24h). Even though protein arrays are very useful in the detection

of several cell stress related proteins, they do not cover all the relevant cellular proteins which might be involved in the extracts potential to protect cells from oxidative stress induced damage. Since the extracts have previously shown *in vitro* antioxidant activity it would be interesting to determine the expression of a number of proteins involved in cellular antioxidant pathways. A few phytochemicals have previously been shown to not only have direct antioxidant activity but also indirect antioxidant activity, via the upregulation of endogenous antioxidant systems. One interesting pathway could be the Nrf2 (nuclear factor erythroid 2 [NF-E2]-related factor 2)-Keap1 (Kelch-like ECH-associated protein 1)-ARE (antioxidant response element) pathway (1.4.3 Exogenous antioxidants - natural products: direct and indirect antioxidant activity p.58 ff.). This pathway is important in the cytoprotective responses to oxidative and electrophilic stress in cells⁵⁸³ and could be one pathway of action for the RSP extract.

In general, the results obtained in this experiment should be taken cautiously. For the results obtained here, only two membranes for each condition were used. The cells used for all four membranes are from the same cell stock. No biological replicates were performed, using distinguished cell stocks. The replicates obtained here are technical replicates for the experimental set up rather than biological replicates. For verification of the results obtained here, the same experiment should be repeated additional two times, to have 3 biological replicates with two technical replicates each. We also need to consider that neuroblastoma cells were used, not differentiated or primary neurons, which might show slightly different reactions towards the treatment with the RSP extract. However, this is still the first recorded study into the activation of cell stress related proteins after treatment with RSP extract and so enhances knowledge on the possible revalorisation of food "waste" for the potential treatment or prevention of neurodegenerative disease.

4.3.2 AChE inhibition study by RSP extract in SH-SY5Y cells

In chapter "3.3.6 AChE inhibition potential" (p.194) the inhibition of the enzyme AChE by the RSP extract was clearly demonstrated *in vitro*. To determine whether such activity is observed at cellular level, neuroblastoma SH-SY5Y cells were used. The latter were treated with RSP extract (1 mg/mL) and positive control neostigmine (100 μ M) for 24 hours and their AChE inhibition activity monitored. The neostigmine concentration (100 μ M) was chosen after initial toxicity measurement using the MTT assay (Figure A14, p.452). The results obtained for the AChE activity in the cell samples are shown in Figure 4.20 below.

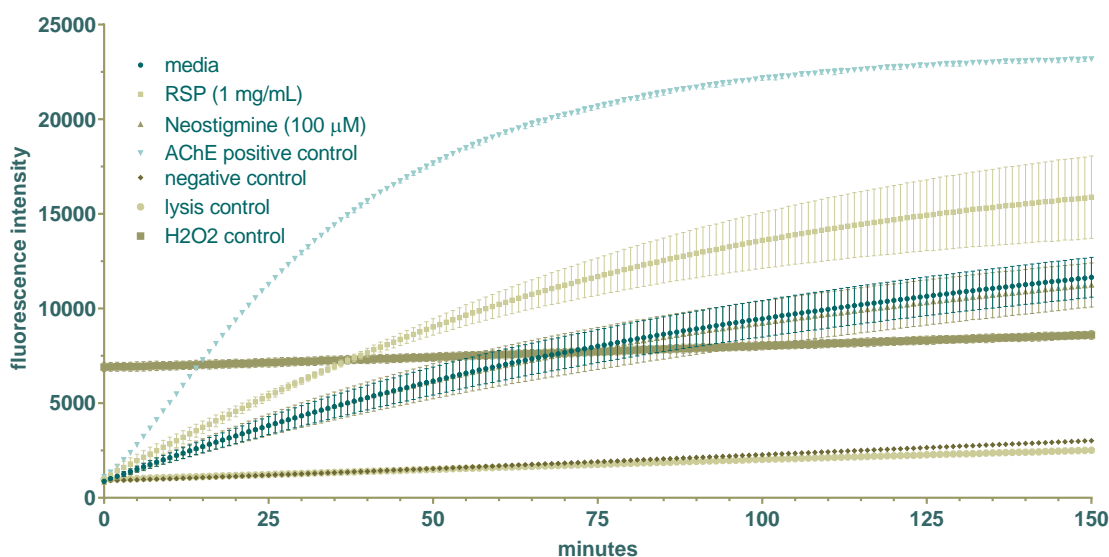


Figure 4.20| AChE activity in SH-SY5Y cells

After treatment with RSP extract (1 mg/mL) and neostigmine (100 μ M) for 24 hours, $n=4$

Treatment of the cells for 24 hours with neostigmine, a known AChE inhibitor shows no significant difference in AChE activity within the assay. In contrast, an increase in AChE activity is observed after treatment with RSP extract. These results contradict the expectations. The hypothesis was to see a decrease in AChE activity for both treatments in comparison to the media control, as both had previously demonstrated AChE inhibition activity (Figure 3.33, p.196). Literature research for a potential explanation of this phenomenon led to the finding of a review by Kračmarová *et al.*⁵⁸⁴ on the possibility of AChE overexpression in AD patients after treatment with AChE

inhibitors. Only measuring the AChE activity after 24 hour treatment could have led to the obtained results. Not many papers were found that analyse compounds AChE inhibition activity in a cell-based system, most research just employs simple *in vitro* methods such as described in chapter 3. In a study by Santillo and Liu⁵⁸⁵, cells were co-incubated with AChE inhibitors, including neostigmine, and the Amplex Red mix and ACh and the AChE activation measured immediately. A similar approach was taken by Li *et al.*⁵⁸⁶, where cells were left to attach overnight, treated for one hour and the reaction mix added thereafter for AChE activity measurement. Those experiments suggest that the AChE inhibition takes place well before the end of the 24 hours treatment undertaken in this study, suggesting shorter time points of treatment (e.g. 30 minutes to 2 hours) and the analysis of AChE activity thereafter would be more appropriate. In the experiments mentioned above cells were not lysed, the assay was conducted in the wells directly, where the cells were seeded, however, Li *et al.*⁵⁸⁶ suggested an interference with the culture media, which is why it was decided to use cell lysates instead. Using cell lysates makes it also possible to analyse data at the same protein concentration. By measuring the AChE activity in the well directly, the assumption is made that the same number of cells was present in all wells. Initially the 24 hours treatment were chosen to keep the experimental set up similar to the previously undertaken experiments discussed above. In hindsight this was the wrong decision. There is still the potential to see AChE inhibition by the extracts within the cell systems by applying shorter treatment time.

4.4 Conclusion/Future Work

In this chapter we were able to demonstrate some of the RSP extracts *in vitro* cell activity. Initially the extracts toxicity towards SH-SY5Y neuroblastoma cells was found to have an IC₅₀ of 2.75 mg/mL. Concentrations below 1.5 mg/mL showed no significant cell toxicity compared to the media control. However, it was decided for subsequent experiments to work with extract concentrations of 1 mg/mL or below, for safety reasons, since at 1.5 mg/mL showed a slight trend towards lower cell viability (Figure A 10, p.449). Using 1 and 0.75 mg/mL of RSP extract showed a significant protection of SH-SY5Y cells from H₂O₂-induced ROS production. Also, lower concentrations (0.25 and 0.5 mg/mL) showed a trend towards cell protection from oxidative stress. In the comet assay the RSP extract (1 mg/mL) showed no increase in DNA damage compared to the media control. Induced DNA damage by H₂O₂ (300 µM) was significantly reduced by pre-treatment with 1 mg/mL of the RSP extract. Higher levels of DNA strand breaks induced by 1000 µM H₂O₂ could not be prevented by the extract. When determining expression of cell stress proteins after treatment with RSP extract, a general down regulation of the analysed proteins was observed. This decreased expression was only significant for SOD2 and SIRT2 proteins. Overall these results indicate that the extract is not causing any harm towards the cells at concentrations of or below 1 mg/mL. Unfortunately, the AChE inhibition activity of the extract found *in vitro* was so far not verified in the cell based assay for the tested time point (24 hours). Additional studies need to investigate AChE activity at time points before 24 hours treatment.

Further studies would include studying the concentration dependent DNA protection as well as DNA repair within the cells. Furthermore, different pathway of action, for the RSP extracts observed effect, should be investigated (e.g. Nrf2, NFκB, ERK1/2). The cell stress protein array showed the downregulation of some tested cell stress proteins, however, there is still the potential of the activation of other maybe antioxidant pathways such as those regulated by the Nrf-2 transcription factor, which might be responsible for the seen effect of the RSP extract. Further studies should also investigate sinapine, as the most abundant compound found in the extract, for its potential positive activity within the same cell line. To produce more

neurodegeneration significant output, it might also be advantageous to repeat the experiment on differentiated cells or primary neurons.

Although cell based *in vitro* assays have the advantage over chemical assays to determine both direct and indirect antioxidant activity, however, they still have their limitations³¹⁹ and are not representative for *in vivo* activity. For this reason, further *in vivo* studies were undertaken in the model organism *C. elegans*, to determine the potential application of RSP extracts for the treatment/prevention of neurodegenerative diseases.

The Potential Application of Rapeseed Pomace Extracts in the Prevention and Treatment of Neurodegenerative Diseases

5 AN *IN VIVO* STUDY OF THE ANTIOXIDANT AND NEUROPROTECTIVE PROPERTIES OF RSP EXTRACT IN *C. ELEGANS* NEMATODE MODELS

Contents

5.1 Introduction	262
5.1.1 <i>C. elegans</i>	
5.1.2 <i>C. elegans</i> disease models and their application in neurodegeneration studies	
5.1.3 Determination of potential pathways of action using <i>C. elegans</i> as model organism	
5.1.4 Objectives	
5.2 Materials and Methods	288
5.2.1 Chemicals and Equipment	
5.2.2 Methods	
5.3 Results and Discussion	312
5.3.1 Toxicity/Food clearance assay	
5.3.2 Machado-Joseph disease <i>C. elegans</i> model	
5.3.3 AChE inhibition hypothesis	
5.3.4 Parkinson's disease <i>C. elegans</i> model	
5.3.5 <i>In vivo</i>	
5.4 Conclusion/Future Work	347

This chapter covers the in vivo work undertaken using the RSP extract. The in vivo model of choice was the nematode C. elegans. After initial toxicity analysis of the RSP extract, its effect towards the phenotypes of one Machado-Joseph disease (MJD, SCA3) and three different Parkinson's disease models was studied. To determine the mechanism of action of the RSP extract, two hypotheses were tested (i) the AChE inhibition and (ii) the antioxidant activity, using reporter and knock out strains.

5.1 Introduction

5.1.1 *C. elegans*

Model systems have become fundamental for the elucidation of mechanisms associated with complex neurodegenerative disease⁵⁸⁷. Currently, the most commonly used research organisms with a functional nervous system are rodents such as mice (*Mus musculus*) and rats (*Rattus norvegicus*) as well as the fruit fly (*Drosophila melanogaster*) and zebrafish (*Danio rerio*)⁵⁰⁶. In addition, there is one more organism whose impact has increased significantly over the last 40 years especially in the field of neuroscience, *Caenorhabditis elegans* (*C. elegans*), the organism of choice for this project. In the *C. elegans* research community, the nematode is often referred to as “the worm”, so following *C. elegans* is referred to as nematode, worm or animal.⁷⁹ *C. elegans* research has increased so much, mainly due to the many advantages over other model organisms, some of which are highlighted in Figure 5.1 and will be further discussed throughout the chapter.

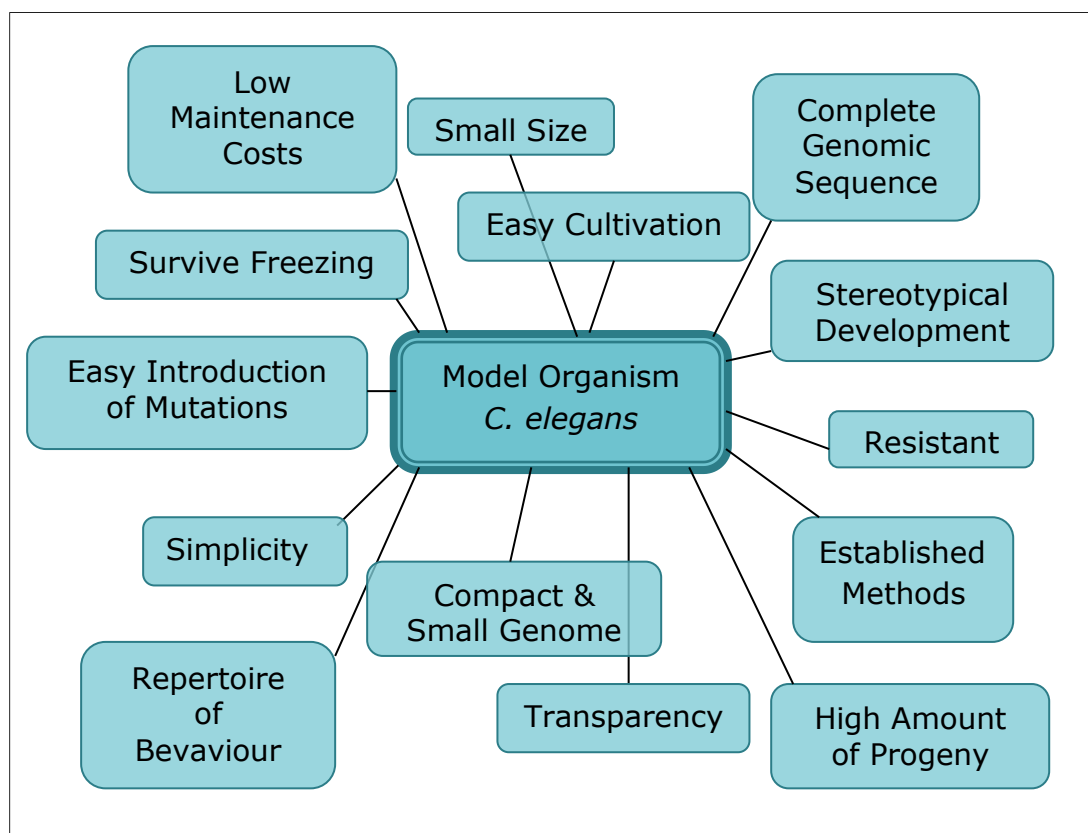


Figure 5.1| Advantages of *C. elegans* as research model organism
Adapted from Pohl⁷⁹

5.1.1.1 General biological properties and genetic background of *C. elegans*

Caenorhabditis elegans (scientific classification: Table 5.1) is a soil living non-hazardous, -infectious, -pathogenic and -parasitic soil living nematode (roundworm) found in many places of the world⁵⁸⁸⁻⁵⁹⁰.

Table 5.1 | Scientific classification of *C. elegans*

Kingdom	Wormia
Phylum	Nematoda
Class	Secernentea
Order	Rhabditida
Family	Rhabditidae
Genus	Caenorhabditis
Species	<i>Caenorhabditis elegans</i>

Note(s): adapted from Wood⁵⁸⁸

In the laboratory worms are fed with OP50, an uracil-requiring mutant of *E. coli*. This strain is used to prevent overgrowth of the bacterial lawn (limited uracil in the nematode growth media (NGM) media), which would obstruct the worms⁵⁹¹.

Just like other nematodes, *C. elegans* has a small, cylindrical body, consisting of only one segment, which becomes conical towards the head and tail region (Figure 5.2)⁵⁹². There are two sexes, males (X0) and self-fertilising hermaphrodites (XX). The wild type (N2) hermaphrodite worms are between 1-1.5 mm⁵⁹³ in length and about 80 µm in diameter once they reach adult age (~day 4 under normal laboratory conditions)^{588,591,593,594}. Both sexes can be distinguished from each other *via* their size and tail shape at the adult stage. Hermaphrodites are slightly larger than males, but in comparison to males they lack the fan shaped tail (Figure 5.2 (arrows), p.264). One anatomical advantageous feature in the *C. elegans*, is its transparency, which is demonstrated in the brightfield microscopy images presented in Figure 5.2. This transparency is sustained throughout the whole life cycle of the worm⁷⁹.

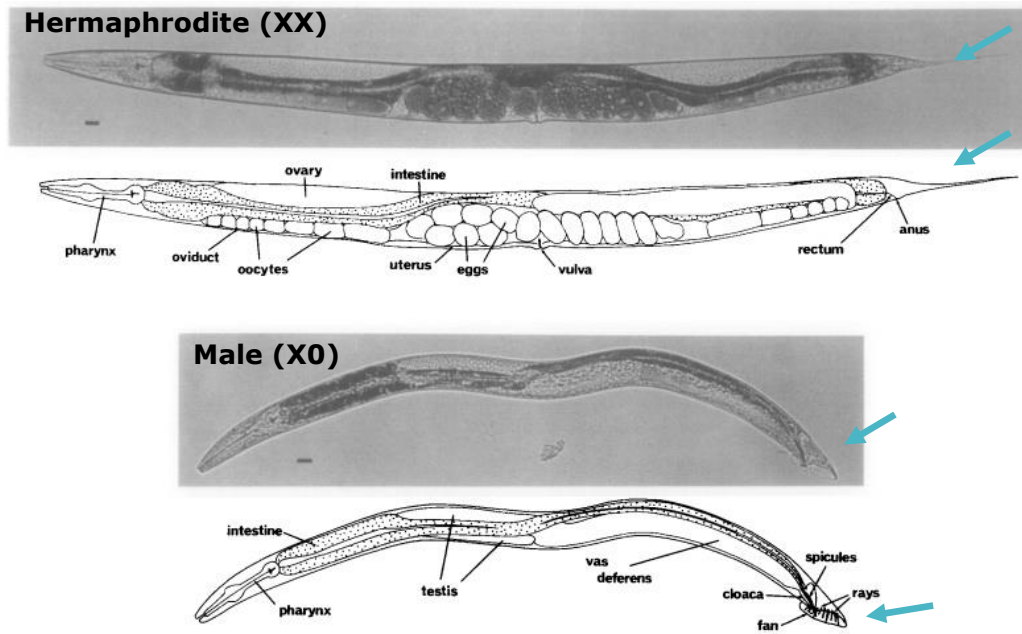


Figure 5.2| Microscopy images (bright-field illumination) and schematics of hermaphrodite and male *C. elegans*

Indicating major anatomical features; Top: adult stage hermaphrodite producing progeny Bottom: adult male, bar =20 μ m; Reprinted with permission from Sulston et al.⁵⁹⁵, with slight modifications

By producing oocytes as well as sperm, hermaphrodites are able to reproduce by self-fertilisation (inbreeding). In addition, they can be fertilised by males, however, hermaphrodites are not able to fertilise each other⁵⁸⁸. Most often males occur through breeding (up to 50 %) whilst hermaphrodites through self-fertilization rarely produce male offspring. However, males offspring can occur, *via* meiotic non-disjunction of the X chromosome (0.1-0.2%), from the hermaphrodite animals⁵⁹⁶. During their reproductive life span, the self-fertilising hermaphrodites can produce about 300 progenies. This number is regulated, by the limited supply of sperm in hermaphrodites. However, when fertilisation occurs through males, the number of progeny can rise to about 1200-1400^{79,588}. In the laboratory and for most experiments, hermaphrodite *C. elegans* are employed. However, males are used regularly for breeding (crossing). Hence for the rest of this thesis, hermaphrodite *C. elegans* will be referred to as *C. elegans* while when referring to males, an indication of the sex will be given.

Under optimal conditions (sufficient food availability), the life cycle (Figure 5.3) of *C. elegans* takes only about 3-4 days from the fertilized egg to the adult stage; this is however dependent on the strain and temperature. The

embryonic development from the zygote (one cell) to the L1 larva (558 cells) only takes 12-14 hours. During that time a total of 671 cells are generated some of which undergo controlled cell death. So, the L1 stage larva hatches with a total number of 558 cells 222 of which are neurons⁵⁹⁷. This complete cell lineage of the embryonic development was tracked from fertilization through hatching as early as 1983 by Sulston *et al.*⁵⁹⁸. To pass from the L1 larva to the adult stage with 959 somatic nuclei only takes another 45-50 hours post-hatching for wild type animals (room temperature).

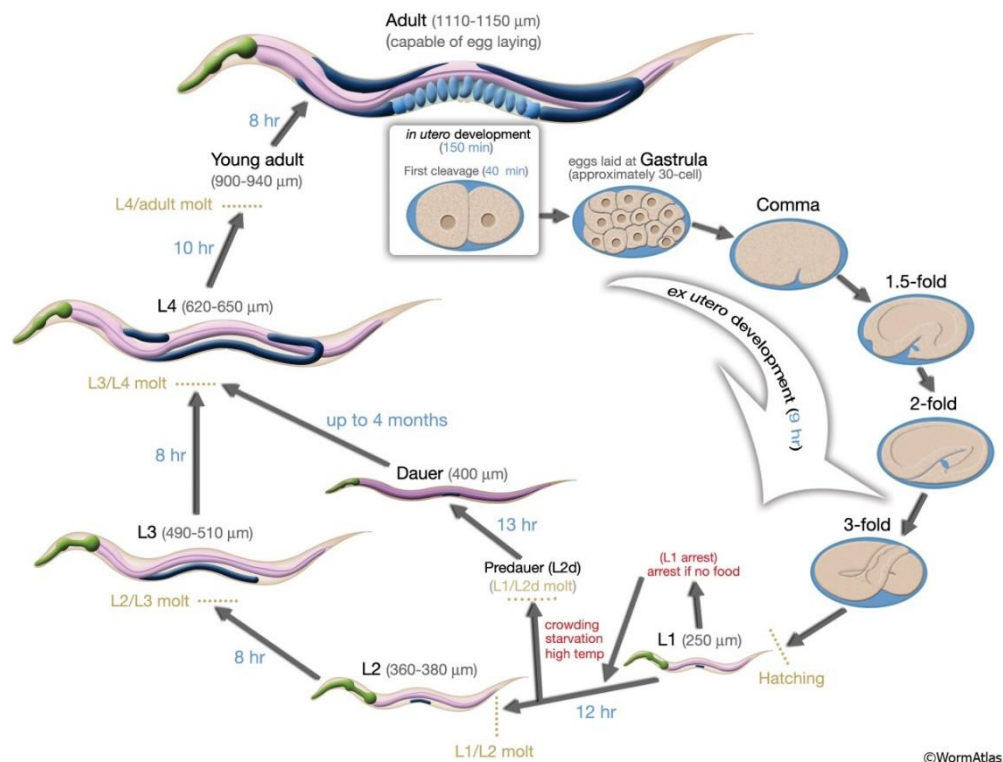


Figure 5.3| Complete life cycle of *C. elegans*

From the egg to the adult stage, with the time the organism spends in every stage, reprinted with permission from WormAtlas⁵⁹²

Thereafter, the worm is fertile for approximately 4 days and usually lives for another 10-15 days afterwards⁵⁸⁸, providing a general lifespan of about 20 days for wild type *C. elegans*. However, there is also a facultative diapause stage called dauer larva, which the L1 larva can enter. This happens if the habitat is crowded, starved of food or when the temperature rises above the optimal conditions. They can survive in this dauer larva stage up to 4 months.⁵⁹² Of great advantage is also the worms (L1s and L2s) potential to survive a slow freezing process (-80°C or liquid nitrogen), this makes it

possible to undertake experiments on the same stock of worms, without the need for continuous culturing.

The adult hermaphrodite consists of only 959 somatic cells, whilst the males are made up of 1031 cells (381 neurons). Of these 959 cells in a hermaphrodite, almost a third, that is 302, are neurons⁵⁹². The anatomy and cell number of *C. elegans* are highly invariant, with each worm having the same number of cells⁵⁹⁹.

The genome of *C. elegans* is diploid and consists of 5 pairs of autosomes (chromosome I-X), all of which have similar sizes, and one pair of x chromosomes (hermaphrodites, XX) or one x chromosome (males, X0)⁶⁰⁰. The whole genomic sequence was first published in 1998 with final changes up until 2002⁶⁰¹. This made *C. elegans* the first completely sequenced multicellular organism.

Genetic mutations are part of the natural course of life and so form part of natural selection. In the laboratory environment however they are exceptionally useful to decipher gene functions. In *C. elegans*, forward (genome-wide mutagenesis) and reverse (target-selected and gene-specific mutagenesis) genetic studies are possible⁶⁰². These methods are used to create and find new mutations together with their phenotypic impact. They are also employed to create disease specific mutants, which can then be used for drug screenings (5.1.2 *C. elegans* disease models and their application in neurodegeneration). Before any such drug screenings, usually the toxicity of drug candidates is tested to determine safe working concentrations within the nematode model. The advantages and disadvantages for using *C. elegans* in toxicity tests are detailed following.

5.1.1.2 *C. elegans* for toxicity screenings

The current 'gold standard' for toxicity tests is still based on mammalian model organisms, however, even these do not always predict accurate and reliable toxic effects for humans. In addition, they are expensive and time consuming as well as ethically questionable. The aim of research in toxicology, is to find alternative methods, which can provide better predictions for human outcomes while reducing costs, time and use of mammals in toxicity assessments⁵⁸⁹. *C. elegans* in conjunction with many

alternative methods (cell culture, mathematical models or *in silico*) or non-mammalian organisms could help to achieve this aim.

C. elegans, unlike cell cultures, toxicity results come from a whole organism with an intact and metabolically active digestive, reproductive, endocrine, sensory and neuromuscular systems⁵⁸⁹. However, *C. elegans* also has its limitations as it lacks certain organs (e.g. heart, lungs and kidney) and the circulatory system found in mammals. Furthermore they lack an adaptive immune system (only have innate immune system), which allows for immune response in mammals.⁶⁰³ One additional concern in the *C. elegans* toxicity studies, is the worm's drug uptake and the question of treatment methods. Different methods of treatment have been used in a variety of studies, hence making comparison amongst them difficult. The most commonly used treatment options and their drug uptake were studied by Zheng *et al.*⁶⁰⁴. Several more advantage and disadvantages of *C. elegans* in toxicity studies are summarised by Hunt⁵⁸⁹. Although toxicity read outs from *C. elegans* alone might not be ideal to determine safe concentrations of compounds in humans or other mammals, it is still valuable for determining toxicity within the species to obtain safe working concentrations for further studies in the model organism. To determine the toxicity of compounds in *C. elegans*, a number of different assays can be used. For lethality or developmental delay, the food clearance assay can be employed⁶⁰⁵.

Food clearance assay for the determination of toxicity and developmental delay

This assay determines toxicity using the feeding behaviour of developing *C. elegans*. Initially worm eggs or L1 larvae are coalesced with the OP50 food source and the drug/compound of interest in multi-well (96-) plates. To avoid metabolism of the drug by the *E. coli*, the latter are most often inactivated *via* UV radiation, freeze-thawing or heat. The nature of the OP50 solution (brown-yellowish in colour) leads to an optical absorbance of the final mixture (worms, OP50 and drug) at 595 nm. This optical density is then monitored for 7 consecutive days, to determine developmental delay as well as toxicity (Figure 5.4, p.268). Healthy developing animals will start consuming the OP50 food source, after hatching. During normal development, the OD of the

wells will start to decrease on day 3-4 (start at egg stage), where the worms reach their adult stage. This is followed with a significant drop on day 5 as seen for the s-media control and the 1% DMSO treated animals in Figure 5.4 (■ and ■ respectively). This drop on day 5 is associated with the worm's production of progeny and their requirement for additional OP50. However, when increasing the DMSO concentration to e.g. 2% the curve has a slightly different trend (▲). At this DMSO concentration, the optical density decreases approximately 1 day delayed. The latter is due to developmental delay of the animals, they reach adulthood one day later and hence produce progeny later. This impact is even more obvious at 3% DMSO (▼). At this concentration an even stronger developmental delay of about 2.5 days can be observed. When increasing the concentration even further (e.g. 5% Figure 5.22, p.312), the OD does not decrease over the 7 days, which indicates toxicity.

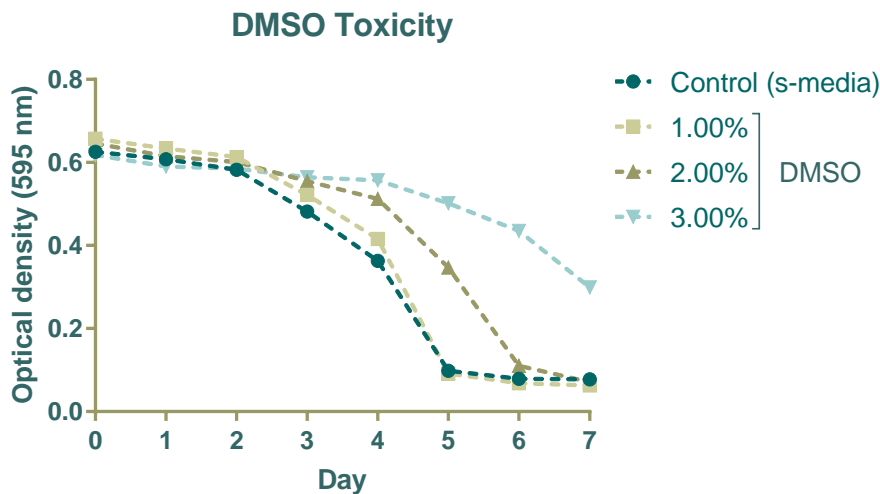


Figure 5.4| Food clearance assay example readout for DMSO toxicity test

Adapted from Pohl⁷⁹

This assay is particularly valuable for toxicity analysis, as it determines toxicity and developmental delay within one experiment using a simple readout of optical absorbance. It is relatively easy to perform and avoids long scoring of dead or alive animals manually. By using multi-well plates, replicates as well as different drug concentrations can be analysed in the same experiment. Additional experiments will also look into other readouts of potential toxicity, such as motility and numbers of neurons (5.1.2 *C. elegans* disease models and their application in neurodegeneration studies).

5.1.2 *C. elegans* disease models and their application in neurodegeneration studies

For *C. elegans* as a model organism in neuroscience, the same advantages over other model organisms (Figure 5.1 p.262) apply as for general use of the nematode in research. However, there are also some additional and important benefits that need to be emphasised. The nervous system of *C. elegans* is fully differentiated and consists of a constant number of 302 neurons, including a large somatic nervous system (282 neurons) and a small pharyngeal nervous system (20 neurons)⁶⁰⁶. Of great advantage is also the unique position and identity of every single neuron, making them reproducible from worm to worm. A complete connectivity map for these cells is available^{79,607,608}. Due to the worms' transparency, protein inclusions as well as neuronal cell death can be visualized using microscopy techniques, or be measured/quantified via different optical techniques and software programmes¹¹⁶. Many human related neurodegenerative disease associated genes can and have been expressed in this model organism, including the creation of Huntington's, Parkinson's, Alzheimer's as well as Machado-Joseph disease models⁶⁰⁹⁻⁶¹¹. The availability of such models together with its many other advantages (Figure 5.1, p.262) makes *C. elegans* very attractive and useful for drug discovery screenings as well as drug target analysis in neuroscience and aging.

Several models of *C. elegans* have been created for most neurodegenerative diseases including AD, ALS, HD, PD and MJD, which were reviewed by Chen *et al.* in 2015⁶¹⁰. Here in this project, the focus was on two neurodegenerative disease states namely, MJD and PD with the aim to determine the potential use of RSP extract in the treatment/prevention of such neurodegenerative diseases. The MJD model was chosen due to preliminary positive results obtained from the RSP extract in this disease⁷⁹. In addition, we decided to expand our study in the use of RSP extract using PD models. In particular in PD oxidative stress has been associated with the course of the disease^{209,612,613} and so these models provide a good model for testing the activity of RSP extract *in vivo*.

5.1.2.1 *C. elegans* model of Machado-Joseph Disease (SCA3)

The *C. elegans* model of MJD was established in 2011 by A. Teixeira-Castro *et al.*⁶¹⁴. This model (AT3q130), expresses human ataxin-3, with 130 CAG (polyQ) repeats, in all neurons. In addition, two other models (AT3q14 and AT3q75) were created expressing shorter lengths of the CAG repeats (14 and 75 respectively). The expression of the different length ataxin-3 proteins is controlled by the promoter of the F25B3.3 gene. This gene is a *C. elegans* ortholog of the Ca²⁺-regulated Ras nucleotide exchange factor (RasGRP), which is exclusively expressed in the nervous system. Normal length (q14) and mutant (q75/130) ataxin-3 were tagged at the C-terminus with the yellow fluorescent protein (YFP) for visualization of the protein within the model organism⁶¹⁴.

When comparing the three created models, both models with shorter polyQ sequences (AT3q14 and AT3q75), showed a diffuse neuronal distribution of ataxin-3, the AT3q130 model however is associated with the presence of discrete aggregates (foci) in some neurons but diffuse expression in other nerve cells (Figure 5.5). Also observed, was a decreased life span and lethargy of the worms, compared to the other two models (AT3q14 and AT3q75).⁶¹⁴

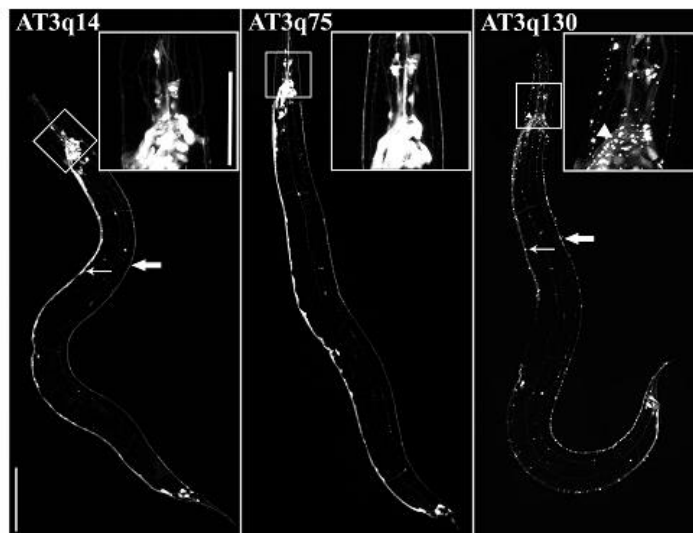


Figure 5.5|Comparison of AT3q14, AT3q75 and ATq130 *C. elegans* strain

Showing heterogeneity as well as discrete foci for AT3q130 in certain neurons, whilst the other two show a diffuse distribution of ataxin-3 (arrows show foci formation in AT3q130 at ventral nerve cord (VNC, thin arrow), dorsal nerve cord (DNC, thick arrow) and pharyngeal nerve ring (arrow head)), scale bar 100 μ m, reprinted with copyright agreement from Teixeira-Castro *et al.*⁶¹⁴

In addition to the visible protein aggregation phenotype observed in the neurons, the MJD model (AT3q130) was also tested for neuronal dysfunction, using behavioural assays. In *C. elegans* neuronal dysfunctions are closely associated with motility, since innervations of muscle cells in the nematode require more than 60 neurons. In cases where ataxin-3 aggregations had led to neuronal dysfunctions, a reduced motility can be expected together with a lack of coordination. This was confirmed when testing the motility behaviour for AT3q130 animals using the classic motility assay by Teixeira-Castro *et al.* (Figure 5.6)⁶¹⁴.

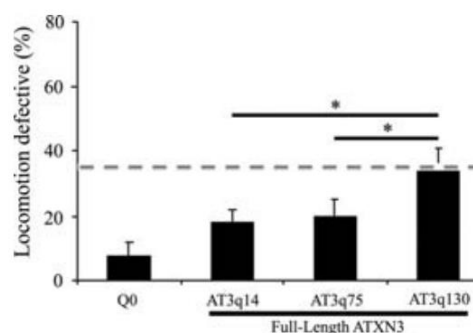


Figure 5.6| Locomotion defect of AT3q130 in the classical motility assay

*Increase in polyQ-length is associated with a higher percentage of locomotion deficiency of age-synchronised young adult worms (day 4, post-hatching), reproduced with copyright permission from Teixeira-Castro et al.*⁶¹⁴

When comparing AT3q130 with control animals (Q0) of the same age, a significant motility deficiency was observed, when using the classical motility assay as read out (5.2.2.5 AT3q130 strain methods; I Motility determination, p.306). The susceptibility to mutant ataxin-3 aggregations and toxicity was also found to be neuron-type specific, as seen in human MJD patients. These findings make this model exceptionally interesting for research in MJD, since the presence of those two phenotypical characteristics (aggregations and motility deficiency) strikingly recapitulates key aspects of polyQ diseases in human patients⁶¹⁵. Having these two phenotypical read outs makes it possible to test compounds and determine their effect on either of them, increasing the amount of information gained for the tested compounds from this MJD model strain.

Previous research in the same lab group⁶¹⁶, employed this model to screen a library of over 1000 mainly FDA/EMA-approved small molecules, to identify

compounds which can suppress the mutant ATXN3 pathogenesis *in vivo*. In that study citalopram (selective serotonin reuptake inhibitor) was found to achieve this aim. Citalopram was able to decrease the motility deficiency of the AT3q130 strain significantly in 4 day old animals. This improvement was continuously seen even for 6-14 day old animals. In addition to improving the locomotion defect, citalopram was also able to decrease the number of aggregates per total area in the disease strain. These effects caused by citalopram were shown to be due to its action on serotonergic neurotransmission and modulation of serotonin mediated signalling. To prove that the inhibition of serotonin transporter by citalopram was responsible for the observed effect with a potential target of citalopram being MOD-5 (serotonin transporter orthologue of the vertebrate SERT). Both, pharmacological and pharmacogenetic inhibition of MOD-5 were shown to restore motility and decreased the aggregation load of AT3q130 *via* modulation of serotonin transmission⁶¹⁶. Similar approaches can hopefully be applied to determine the mode of action for the RSP extract in the MJD model.

5.1.2.2 *C. elegans* models of Parkinson's Disease

As previously described, PD can be caused by a number of different genetic and environmental factors (1.3.3 Parkinson's Disease (PD), p.47 ff.), however the exact pathogenic pathways are still under investigation⁶¹⁷. Just like for AD, ALS, HD and other polyQ disease, *C. elegans* has been widely employed to study the role of these genetic and environmental factors contributing to the pathology of PD as well as to find potential treatment options.

Maulik *et al.*⁶¹⁸ and Chege *et al.*²⁰⁶ summarize a number of commonly used *C. elegans* strains for PD research, including mutant and non-mutant strains (i) expressing human (wild type) α -synuclein in body wall muscles (e.g. NL5901, OW13), (ii) expressing wild type (UA44, BY273) or mutant (A53T) human α -synuclein (JVR107, JVR203) in neurons, (iii) studying leucine-rich repeat kinase (LRRK) and putative kinase 1 (PINK1) mutations and their contribution (SGC851, SGC856, JVR104, BR3646) (iv) examining the involvement of PARKIN (PARK2; *C. elegans* homolog pdr-1, VC1024), (v) overexpressing of tyrosine hydroxylase (UA57) and (vi) those using chemicals such as 6-OHDA, MPTP/MPP⁺, insecticides or different metals as

inducer for DAergic neuron loss (N2, BZ555, BY250). Most of the above models have one feature in common, the loss or defect of DAergic neurons. Out of the 302 neurons in *C. elegans*, 8 are DAergic neurons, 6 in the head and 2 in the tail region of the animal. They have ciliated dendrites, which contact the cuticle and likely convey mechanosensory information. Ablation of these neurons, using lasers, and genetic studies had linked them to foraging, movement and egg-laying behaviors⁶¹⁹. In the head there are four cephalic sensilla (CEP) neurons, two dorsal (CEPDL/R (left and right)) and two ventral (CEPVL/R) both of which are bilaterally paired. Their dendrites extend to the tip of the nose (Figure 5.7).

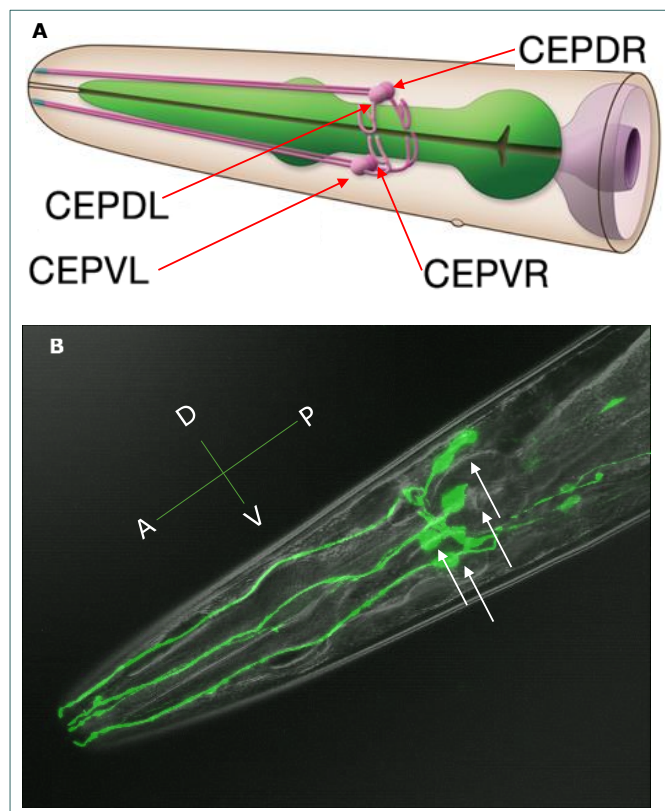


Figure 5.7 | *C. elegans* CEP neurons

A: schematic of CEP neurons, reprinted with permission from WormAtlas⁶²⁰, B: confocal image of BZ555 (egIs1 [dat-1p::GFP]) showing Brightfield image on top of fluorescent image taken of same worm in same position (A, anterior; P, posterior; D, dorsal; V, ventral) by Andreia Teixeira-Castro

In addition to the four CEP neurons situated just anteriorly of the terminal bulb of the pharynx, there are also two bilaterally paired anterior deirid neurons. These are situated posteriorly to the terminal bulb of the pharynx (Figure 5.8).

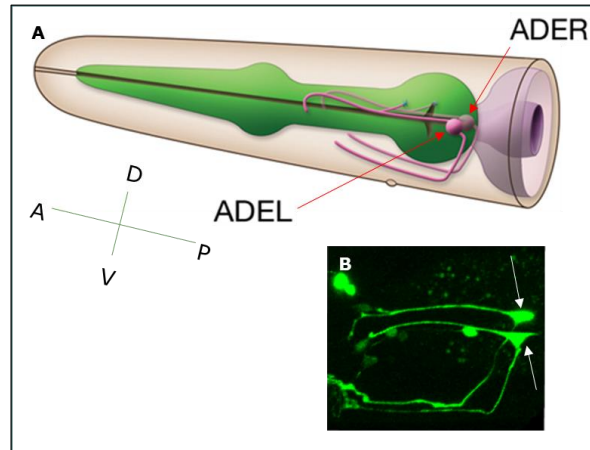


Figure 5.8| *C. elegans* ADE neurons

A: schematic of ADE neurons, reprinted with permission from WormAtlas⁶²⁰ B: confocal fluorescent imaging of ADE neurons in BZ555 (egIs1 [dat-1p::GFP]) animals (A, anterior; P, posterior; D, dorsal; V, ventral) by Andreia Teixeira-Castro

Besides the 6 DAergic neurons situated in the anterior, there are two posterior deirid neurons (PDE), positioned next to dorsal body wall muscle along the lateral side of the posterior body (Figure 5.9).

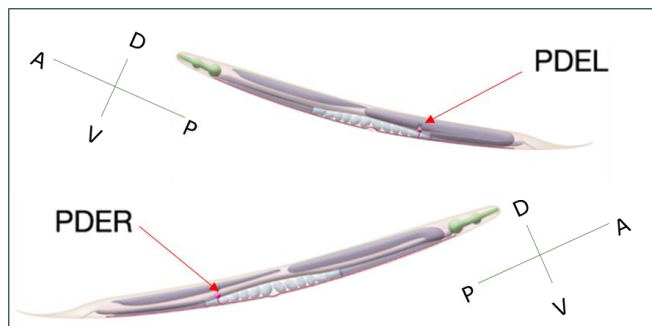


Figure 5.9| *C. elegans* PDE neurons

Schematic of both the left and the right PDE neurons (A, anterior; P, posterior; D, dorsal; V, ventral) , reprinted with permission from WormAtlas⁶²⁰

These three classes of DAergic neurons (CEP, ADE and PDE) are mechanoreceptor neurons (MRNs) responsible for sensing the mechanosensory stimuli from the food source (e.g. bacteria) and facilitate the motor circuit for necessary behavioural changes i.e. basal slowing response (well fed animals). This behaviour change is dependent on intact CEP, ADE, and PDE neurons and dopamine synthesis^{621,622}. At a molecular level, these neurons have all the essential components involved in dopamine neurotransmission, including the proteins responsible for dopamine biosynthesis (Figure 5.10), vesicular packaging, and inactivation. Males have 6 additional DAergic neurons in the tail, mainly responsible for mating behaviour^{619,623}.

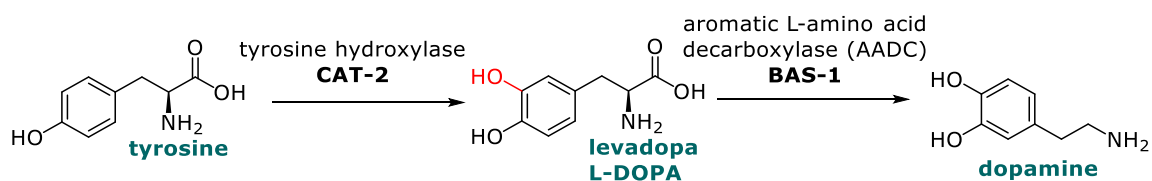
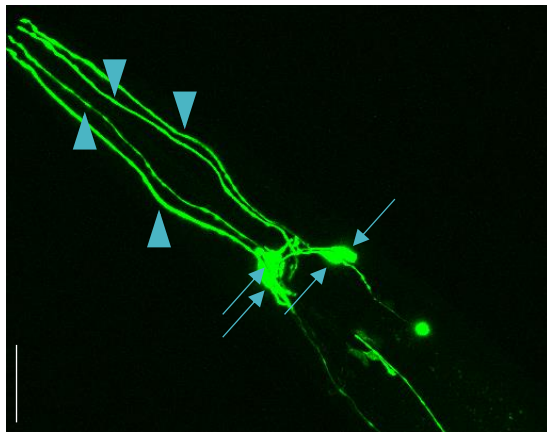


Figure 5.10| DA biosynthesis

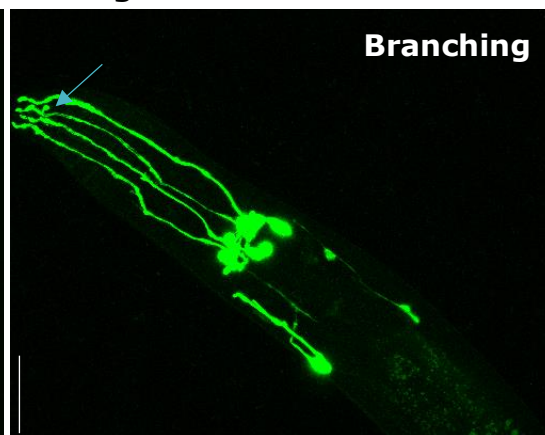
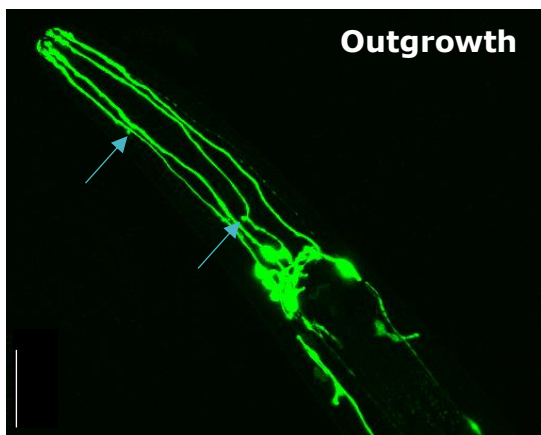
These DAergic neurons are lost in PD and so form the focus of PD studies in *C. elegans*. Most of the models reported by Maulik *et al.*⁶¹⁸ showed specific DAergic neuron damage or loss. This damage can be minor i.e. outgrowth or branching of the DAergic neuronal dendrites, or more significant i.e. blebbing of the dendrites or complete loss of DAergic neurons and their dendrites (Figure 5.11, p.276)^{624,625}. The reason why this damage occurs in patients is not completely elucidated yet. However, in *C. elegans* significant DAergic neuron damage can be created using chemical induced or genetic models of PD, as described by Maulik *et al.*⁶¹⁸.



Wild type looking CEP neurons:

All 4 CEP neurons (arrows) + dendrites (arrow heads)

Minor damage



Major damage

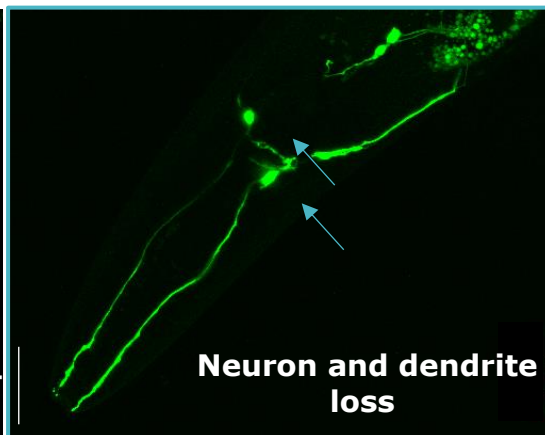
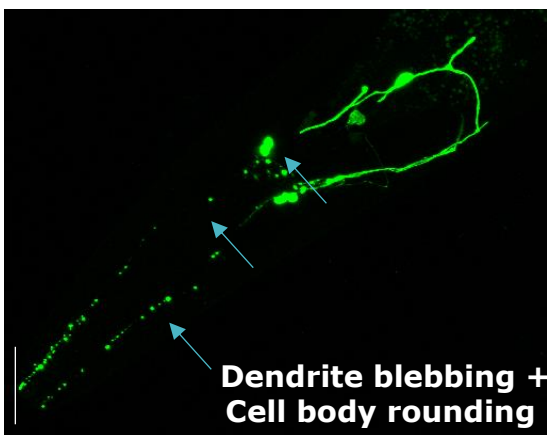


Figure 5.11| DAergic neuronal damage observed in genetic (UA44 and UA57) and chemical induced (6-OHDA) *C. elegans* models of PD
Scale bar 30 μ m, confocal imaging by Andreia Teixeira-Castro

To study the effect of RSP extract in PD, three different *C. elegans* PD models were used, two genetic models; UA44, expressing human wildtype α -synuclein in combination with GFP in DAergic neurons; UA57, overexpressing tyrosine hydroxylase in combination with GFP in DAergic neurons and one chemical induced model employing BZ555, expressing GFP in DAergic

neurons treated with 6-OHDA. Further details on all three strains and the conditions used in the experiments are discussed following.

Chemically induced *C. elegans* PD model using 6-OHDA

To induce PD like phenotypes i.e. DAergic neuronal loss in *C. elegans* the two commonly used chemicals are 6-OHDA and MPTP/MPP+, but also other chemicals e.g. metals such as methyl mercury (MeHg), manganese and aluminium^{206,626} or rotenone and paraquat have previously be reported to induce DAergic neuron loss. Here in our study 6-OHDA, a hydroxylated analogue of the natural neurotransmitter dopamine was used (Figure 5.12)⁶²⁷.

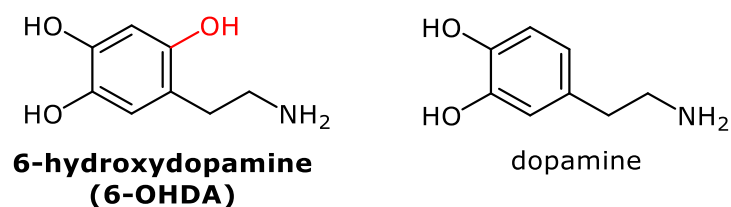


Figure 5.12| Chemical structure for 6-hydroxydopamine (6-OHDA) compared to dopamine (DA)

Due to its structural similarities, 6-OHDA can be recognized by the DA reuptake transporter and be transported specifically into DAergic neurons. The exact chain of actions by which 6-OHDA is causing DAergic neurotoxicity and cell death is currently still under investigation. However, there are a few considerations on how 6-OHDA acts within the cells and oxidative stress is assumed to play a significant role. One of the theories is that 6-OHDA causes oxidative stress, due to the blocking of complex I of the respiratory chain⁶²⁷. In addition, it has also been shown that 6-OHDA reduces glutathione (GSH) and superoxide dismutase (SOD) enzyme activity⁶²⁸ while increasing the levels of malondialdehyde⁶²⁹, a marker for lipid peroxidation, often associated with cellular ROS. *C. elegans* exposed to 6-OHDA, have shown gradual DAergic neuronal death⁶¹⁹. Selective DAergic neurodegeneration manifests itself as blebbing of processes, cell body rounding and eventual disintegration of DAergic neuronal cell bodies and dendrites loss. Reasons and pathways of DAergic neuronal death induced by 6-OHDA are still under investigation^{619,630}. Several factors have been identified which regulate 6-OHDA induced toxicity in *C. elegans*, including dopamine receptor modulation, autophagy

inactivation, and ER chaperone function. In addition, as previously mentioned 6-OHDA also induces mitochondria disruption⁶²⁶.

For easy visualization of DAergic neuron loss, BZ555 worms will be employed for this experiment. This strain expresses GFP in all DAergic neurons (using Pdat-1 promoter) allowing visualisation of the 8 DAergic neurons under investigation. For note, the expression of GFP alone does not cause significant DAergic loss⁶²⁶.

Genetic α -synuclein *C. elegans* PD model (UA44)

The UA44 (bal11, Pdat-1:: α -syn, Pdat-1::GFP) model, co-expresses human wildtype α -synuclein and GFP in the dopaminergic neurons, using the dopaminergic neuron specific Pdat-1 promoter^{470,625}. The observed neuronal loss in this strain is age dependent. Young larval-stage animals show little degeneration, whereas older worms (day 6 till 10) show significant neuronal (DAergic) damage^{625,631,632}. This model was first described by Cao *et al.* in 2005⁶²⁵, where they showed that the co-expression of TorsinA, reduced neurodegeneration. TorsinA is a human protein, expressed in DAergic neurons and a component of Lewy bodies, often associated with neurodegenerative disease. Since then, the same model has been used in other studies, to (i) identify neuroprotective genes^{633,634}, (ii) show the importance of antioxidant enzymes (e.g. glutaredoxin 1 (Grx1))⁶³⁵ in preventing exacerbate neurodegeneration and (iii) test compounds for their neurodegeneration preventative properties e.g. spermidine⁴⁷⁰, alpha-linolenic acid⁶³⁶ and valproic acid⁶³⁷. The DAergic neuron loss can be scored using fluorescence microscopy, due to the co-expression of GFP in the DAergic neurons. In some studies, the UA44 strain is used in conjunction with 6-OHDA, which leads to an earlier onset of DAergic neuronal loss⁶³⁶.

In addition to DAergic neuron loss, the UA44 strain also shows a decrease in basal slowing response. Wild type well-fed worms will slow down in their movement, once they enter a bacteria lawn. This behaviour is dependent on intact DAergic neuro signalling. The damage of DAergic neurons in the UA44 strain leads to a loss of basal slowing response, which increases with age⁶³⁵.

Genetic tyrosine hydroxylase overexpressing *C. elegans* PD model (UA57)

The UA57 (*bals4*, *Pdat-1::GFP* and *Pdat-1::CAT-2*) strain overexpresses tyrosine hydroxylase (CAT-2) which is a rate-limiting enzyme for the production of dopamine. CAT-2 performs hydroxylation of the aromatic ring of the amino acid tyrosine (highlighted red in Figure 5.10) to form L-DOPA. By increasing the concentration of CAT-2 this reaction is enhanced and leads to increased levels of DA. The strain co-expresses GFP in the dopaminergic neurons, using the same DAergic neuron specific *Pdat-1* promoter as for the UA44 strain. This strain was first introduced in a study by Cao *et al.* in 2005⁶²⁵. Similar to the UA44 strain, UA57 animals show age dependent DAergic neurodegeneration, less than 25% of seven day old animals retain all four CEP neurons. In contrast to the positive results of torsin co-overexpression in the UA44 strain, there was no significant increase in worms with wild type CEP neurons in the double mutant torsin/UA57 strain⁶²⁵.

Overexpression of CAT-2 leads to an increase in dopamine synthesis. Under normal conditions, DA is rapidly stored in vesicles by vesicular monoamine transporter 2 (VMAT2), where a lower pH stabilizes it, limiting the concentrations of cytoplasmic DA^{617,638}. Increased production of DA can lead to excessive amount of cytoplasmic DA, which can cause a diversion from the normal metabolic sequence (oxidation *via* MAO-A and ADH to generate non-toxic 3,4-dihydroxyphenylacetic acid and hydrogen peroxide) and generate intermediates (dopamine-*o*-quinone and (dop)aminochrome) and further metabolites (e.g. leukodopamineochrome-*o*-semiquinone radical) all of which are endogenous neurotoxins. The latter are able to reduce oxygen to superoxide anion radicals or impact mitochondria, via NADH oxidation or directly affecting mitochondrial complex I which can result in neuro toxicity^{188,617,638,639}. Metal ions (e.g. copper(II) and iron (III)) can aid in the catalysis of cytoplasmic dopamine oxidation^{188,640}. A paper by Chege *et al.*²⁰⁶ gives a great overview of the issues associated with PD, including CAT-2, 6-OHDA and α -synuclein. Previous research has employed this model to identify compounds that prevent or treat the observed DAergic neuronal loss in *C. elegans* e.g. extracts from *Sorbus alnifolia* (traditional medicine in Korea)⁶⁴¹ as well as *Chondrus crispus* (red seaweed)⁶⁴² were tested.

5.1.3 Determination of potential pathways of action using *C. elegans* as model organism

In chapters 3 experiments using the RSP extracts were carried out to study AChE inhibition, DNA plasmid protection and antioxidant activity. Furthermore, *in vitro* studies, at cellular level, had shown the ability of the RSP extract to (i) prevent ROS formation and (ii) protect DNA from oxidative damage. Previous preliminary experiments using two RSP extracts, had shown positive improvements of the *C. elegans* MJD motility phenotype⁷⁹. These results led to the research question of 'How does the RSP extract induce these observed effects?' To address this question, multiple hypotheses for the mode of action of the RSP extract were considered. Two of these were thoroughly studied in this project using the *C. elegans* model:

1. "The extracts AChE inhibition activity is responsible for the observed effects" (5.1.3.1)
2. "The extracts antioxidant activity is causing the positive results" (5.1.3.2)

5.1.3.1 AChE neurotransmission

ACh is the most widely used neurotransmitter in the *C. elegans* nervous system⁶⁴³. Acetylcholine neurotransmission is stopped by enzymatic hydrolysis by AChE, in the synaptic cleft (Figure 3.10, p.147). The produced choline is transported back into the presynaptic neuron and is again available for the synthesis of further ACh (3.1.3 Acetylcholinesterase (AChE)/Acetylcholinesterase inhibitors). AChE inhibitors are used in the treatment of various disease to improve the neurotransmission by Ach. In chapter 3 (3.3.6 AChE inhibition potential, p.194 ff.) the AChE inhibition potential of both RSP extract and sinapine was discussed. To determine whether AChE inhibition can improve the MJD disease phenotype (motility deficiency), pharmacological and pharmacogenetic methods were employed. For the pharmacological option neostigmine, a known AChE inhibitor will be used to treat the disease MJD model, to determine whether pharmacologic treatment using AChE inhibitors can help to reduce the locomotion deficiency. The pharmacogenetic method employed two AChE *C. elegans* knock out strains (*ace-1* and *ace-2*), which were crossed with the MJD disease model to discover if genetic deletion of either of the two genes responsible for most of

the production of AChE could alleviate the disease phenotype. At the end the results can be compared to the results of the pharmacological model to confirm or negate the first hypothesis.

C. elegans has four so far known ace genes, ace-1 to 4, compared to only one gene encoding AChE in vertebrates. These four genes encode three different pharmacological classes of AChE (A-C)^{644,645}. The gene ace-1 encodes AChE class A and produces about half of the AChE activity in the nematode^{646,647}. Ace-1 mutants (knock out, Figure A15, p.453 f.) were found to be developmentally and behaviourally indistinguishable from wild type

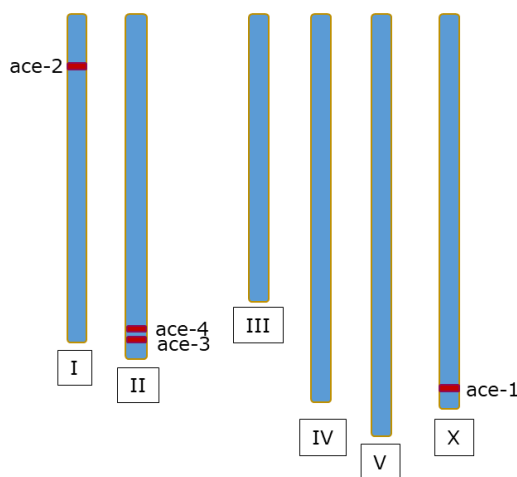


Figure 5.13 | Genes for AChE (ace1-4) in the *C. elegans* genome

animals (N2). The gene can be found towards the end of the X chromosome⁶⁴⁶ and has 42% identity with human AChEs⁶⁴⁵. A second ace gene, ace-2, which is located on chromosome I (not linked to ace-1), is a structural gene for AChE class B. A homozygous deletion (Figure A16, p.455 f.) of ace-2 also produces normal coordinated animals, thus suggesting that ace-1 is partially

redundant functionally with ace-2. A double mutant of ace-1;ace-2 however leads to an uncoordinated phenotype with approximate 98% decrease of AChE in worms⁶⁴⁸. The expression pattern for both ace enzymes is different, with ace-1 being expressed in muscle cells and a few neurons, whereas ace-2 is mainly expressed in the neurons⁶⁴⁴.

A third class of AChE, class C, in *C. elegans* is encoded by the third ace gene, ace-3, and is located on chromosome II. Ace-3 is thought to account for less than 5% of AChE activity⁶⁴⁹. Worms homozygous for ace-3 have no obvious behavioural phenotype. Also, double mutants ace-1;ace-3 and ace-2;ace-3 have shown little difference in their movement from the wild type animals (except slightly slower behaviour on backwards movement). However, the triple mutant ace-1;ace-2;ace-3, lacks all three AChE classes (A,B,C), resulting in paralysis and late embryonic or early larval lethality (after hatching).⁶⁵⁰ In conclusion, ace function in *C. elegans* seems to be essential,

at least ace-3 function is necessary for viability, whereas for intact motor function either ace-1 or ace-2 are necessary. A fourth ace-4 gene exists, located just ahead of the ace-3 gene. This gene is believed to encode a non-functional protein (biochemically undetectable activity)⁶⁴⁵.

The information found on these AChE knockout strains, had led to the decision that for crossings with the motility deficient MJD model only single mutants for ace-1 and ace-2 are viable options to determine if a genetic decrease of AChE activity is able to alleviate the locomotion defective phenotype. This experimental set-up would assist in determining whether hypothesis 1 is a possible explanation for the effect of RSP extracts in *C. elegans*. The hypothesis will further be tested using various concentrations of neostigmine, a pharmacological AChE inhibitor, in the MJD model.

5.1.3.2 Antioxidant and detoxification pathway

It has been shown, that antioxidant molecules can act not only by simply scavenging free radicals, but also by modulating the activity and/or expression of endogenous antioxidants (indirect antioxidant activity), such as super-oxide dismutase (SOD), catalase (CAT) and glutathione peroxidase (GPX) as well as other genes related to the clearance of ROS and xenobiotics (1.4.3 Exogenous antioxidants - natural products: direct and indirect antioxidant activity, p.58 ff.). That way, antioxidants can improve the endogenous defence system against oxidative stress and exogenous toxins. To determine the indirect antioxidant activity of compounds/extracts *in vivo* in *C. elegans*, a few options are available. Due to its transparent and thin (~80 µm) nature, *C. elegans* is easily amenable to the use of fluorescent probes. These can help to visualize oxidative stress within the nematodes *in vivo*. When these fluorescent probes are bound to certain antioxidant genes, reporter strains are created. Those reporter strains make use of e.g. the green fluorescent protein (GFP⁶⁵¹) to visualize gene expression patterns. These include amongst others the visualization of proteins associated with oxidative stress⁶⁵².

Although the anatomy of *C. elegans* is rather simple, it has a complex ROS biology including several redox-active enzymes, similar to other model organisms and humans. These include genes for superoxide dismutase (sod), catalase (ctl), glutathione-S-transferase (gst) and glutathione peroxidase

(gpx)⁶⁵³⁻⁶⁵⁵, responsible for detoxification and oxidative stress resistance. Reporter strains for 3 genes were employed for this project (gst-4, sod-3 and gcs-1) and are described in more detail following.

Phase II metabolic enzyme glutathione S-transferases (GST-4)

Glutathione S-transferases (GSTs) are a group of cellular detoxification enzymes (phase II). This multifunctional enzyme family helps to detoxify both exogenously and endogenously derived toxic compounds by catalysing the conjugation of various electrophiles with glutathione (GSH), an important antioxidant. After catalysis with GSH, less toxic and more hydrophilic molecules are obtained, which can be metabolised and excreted. Organisms usually express various GSTs, with different substrate specificity and localization, leading to specialized functions. Based on data base sequence comparison, *C. elegans* is thought to have over 50 GSTs^{656,657}.

The gene *gst-4* (sequence K08F4.7), situated at the beginning of the second half of chromosome IV, induces a nematode specific GST, known to be upregulated under oxidative stress caused by e.g. paraquat⁶⁵⁸ or hyperbaric oxygen⁶⁵⁹. It is an antioxidant response element (ARE) containing gene and so a direct target of the transcription factor *skn-1* (ortholog of Nrf2), which can upregulate the expression due to oxidative stress and reactive electrophilic compounds⁶⁶⁰.

In 2002, Link and Johnson⁶⁵⁹, created a reporter strain for *gst-4* called CL2166 by introducing an oxidative stress-inducible reporter transgene using GFP as fluorescence indicator. This reporter was used by Leiers *et al.*⁶⁵⁶ in 2003 for further studies and showed increased fluorescence intensity after treatment with oxidative stressors plumbagin (200 μ M), paraquat (100 mM) and juglone (200 μ M)⁶⁵⁶. Although short time exposure of these compounds can induce *gst-4* activation, exposure to high concentrations of plumbagin⁶⁶¹, paraquat and juglone⁶⁶² for longer time periods can be toxic or lead to developmental delay in the nematode. Thus, compounds that can induce the expression of *gst-4* without having negative side effects are of significant interest for the treatment of oxidative stress related diseases. Literature review has shown that for example trans-cinnamaldehyde D-(+)-camphor, phytochemicals found in *Cinnamomum osmophloeum*, demonstrated

increased *gst-4* expression along with antioxidant activity against juglone-induced oxidative stress in *C. elegans*⁶⁶³. Similar results were reported for curcumin, found in turmeric⁶⁶⁴; coffee extracts⁶⁶⁵ and garlic-derived thioallyl compounds⁶⁶⁶. Some of these tested compounds/ extracts were also found to induce *sod-3*, one of the other antioxidant related genes of interest in this study.

Antioxidant enzymes superoxide dismutase -3

Superoxide dismutase (SOD) is another group of redox-active enzyme that protects against oxidative stress by catalysing the reaction of $O_2^{\bullet-}$ into H_2O_2 , which can be further converted to H_2O and O_2 by catalase, glutathione peroxidase or other enzymes (Figure 4.19, p.254)⁶⁶⁷. *C. elegans* has five *sod* genes (*sod-1-5*). *Sod-1*, 4 and 5 express Cu/ZnSODs, whereas *sod-2* and 3 are mitochondrial MnSODs⁶⁵⁴. The *sod-3* gene can be found in the end of the x chromosome.

As previously seen for the *gst-4*, also for *sod-3* a reporter strain was created (CF1553 (SOD-3::GFP)), for which the expression of GFP is controlled by the *sod-3* promoter⁶⁶⁸. Overexpression of *sod-3* three leads to increased catalyses of $O_2^{\bullet-}$, which can lead to decreased oxidative stress. *Sod-3* is a target gene of *daf-16*, a with aging and longevity associated gene^{669,670}. Other natural extracts/ compounds have previously been shown to activate *sod-3*, epigallocatechin gallate (EGCG, found in tea) for example significantly increased SOD-3 expression in the *sod-3* reporter strain model while also decreasing oxidative stress, as shown by Zhang *et al.*⁶⁷¹.

GCS-1, enzyme of the cellular glutathione (GSH) biosynthetic pathway

Reduced glutathione (GSH), a linear tripeptide, is a very abundant non-protein thiol in many organisms, known to be a potent reducing agent. Many other cellular functions have been recently ascribed to GSH, triggering intense scientific interest in its biological properties. Impaired GSH synthesis is associated with various disease and disorders, including neurodegeneration and aging. GSH depletion and increased levels of oxidative stress in the brain are common. However, currently no drugs are available to increase brain GSH

levels, which might be associated with the issue that e.g. orally dosed GSH is rapidly degraded in the gut. Also GSH administered through intravenous injection is rapidly oxidized (half-life of 2–3 min), making the treatment with GSH unsuccessful^{672,673}. GSH is produced intracellularly from three amino acids through two consecutive steps catalysed by γ -glutamylcysteine ligase (GCL, also known as γ -glutamylcysteine synthetase GCS) and GSH synthetase (GS) (Figure 5.14).

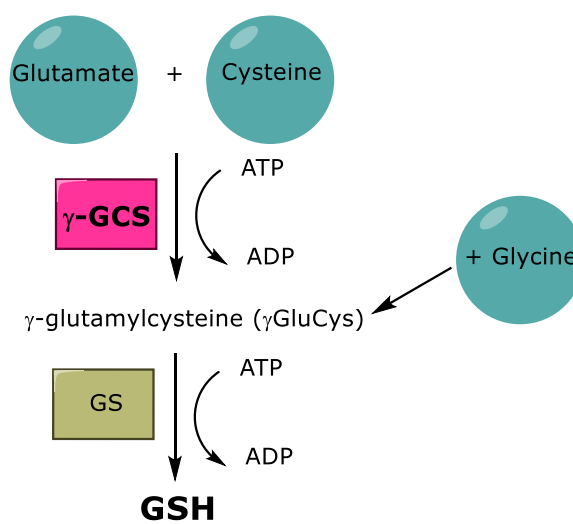


Figure 5.14| GSH synthesis from Glu, Cys and Gly catalysed through γ -GCS and GS

Adapted from Franco *et al.*⁶⁷⁴

Due to its catalytic action, γ -GCS seems to play a key role in regulating GSH homeostasis and thus has an impact on the capacity of cells to cope with the potential detrimental effects of oxidative stress. Hence, compounds which have the potential to up regulate the expression and activity of γ -GCS are considered potential treatment options⁶⁷⁵. In *C. elegans*, *gcs-1*, which is induced by SKN-1 (homologue of human transcription factor Nrf2), is the gene encoding γ -glutamyl-cysteine synthetase (heavy chain). *Gcs-1* is expressed at low levels under normal conditions in the intestines and ASI neurons (set of two ciliated neurons), but it is upregulated strongly by oxidative stress^{676,677}. *Gcs-1* regulation (just like *gst-4* and *sod-3*) can be visualized using a reporter strain in which the *gcs-1* promoter drives expression of GFP (*gcs-1p::GFP*)²⁰⁷. Previous research has shown that willow bark extract is able to induce *gcs-1* expression in intestinal cells in a *skn-1* dependent manner⁶⁷⁸.

Use of knockout mutants for further pathway of action elucidation

Using these three reporter strains will help to elucidate whether the RSP extracts activity observed in the model organism could be associated with its indirect antioxidant activity on either of those genes. Should one of these proteins be significantly increased due to overexpression on the gene level, knockout mutants for these genes can be employed to determine the necessity of these genes for the positive effect of RSP extract in the disease models. However, to be able to test whether the gene is necessary for the RSP extract effect, the potential knockout strains (Table 5.2) need to be crossed with the disease strains. Here in this to work, the knockout strains themselves need to have a wild type phenotype (no motility deficiency or DAergic neuron loss,) because this would interfere with the assay.

Table 5.2| Potential knock out strains for sod-3, gst-4 and gcs-1

Name	gene	Nucleotide change
GA186	sod-3(tm760) X.	715 bp deletion
RB1823	gst-4&msp-38(ok2358) IV.	1548 bp deletion
VC337	gcs-1(ok436)/mIn1 [mIs14 dpy-10(e128)] II.	837 bp deletion

Once the double mutant strains are created (e.g. sod-3(ko);AT3q130), the motility assay can be repeated, both under control (DMSO control) as well as RSP extract treatment. If the RSP extract would be mostly independent of sod-3 activation, the motility assay would show a significant improvement of motility behaviour for both strains (AT3q130 and sod-3(ko);AT3q130) when treated with the RSP extract (Figure 5.15 A). However, if the RSP extract is acting mostly through activation of sod-3, there would be no motility improvement in the double mutant, as the gene, that RSP extract is acting on, is absent and the pathway of action is disrupted (Figure 5.15 B).

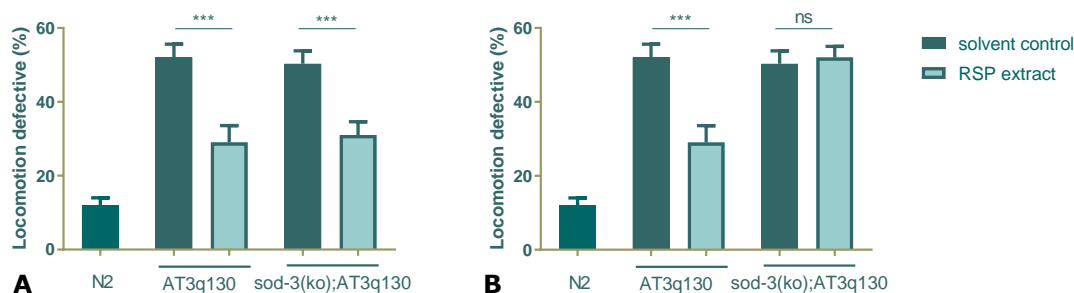


Figure 5.15| Hypothetical results for the RSP extracts' dependence on expression of sod-3 using double mutants (sod-3(ko);AT3q130)
A: independent and B: dependent on sod-3 expression

5.1.4 Objectives

The list below describes the final objectives set out for this project to determine the extracts potential in preventing or treating neurodegenerative disease:

- Assess the extracts *in vivo* toxicity
- Determine the extracts effect an MJD *C. elegans* model on the:
 - o motility deficiency and
 - o neuronal ataxin 3 aggregations
- evaluate the extracts effect on three different models of PD (neuronal lose)
- measure the extracts activity on antioxidant reporter strains
- determine whether the AChE inhibition activity could be responsible for the seen activity via pharmacogenetic and pharmacological pathways
- establish whether the knock out of the most activated reporter gene from the reporter strains can inhibit the extracts activity

5.2 Materials and Methods

5.2.1 Chemicals and Equipment

The following chemicals/kits (Table 5.3) and equipment (Table 5.4) was used in the aid of the experiments in this chapter.

Table 5.3| Chemicals, reagents and kits

Chemicals	Provider
NaC	Sigma Aldrich
KH ₂ PO ₄	Sigma Aldrich
Na ₂ HPO ₄ *7H ₂ O	Sigma Aldrich
MgSO ₄ *7H ₂ O	Sigma Aldrich
Bleach (5% sodium hypochlorite, non-germicidal)	Sainsbury's/Pavão
NaOH	Sigma Aldrich
DMSO	Sigma Aldrich
Nystatin	Sigma Aldrich
Penicillin-Streptomycin	Sigma Aldrich
Ethanol	Sigma Aldrich
Cholesterol	Sigma Aldrich
Bacto Peptone	BD Bioscience
Bacto Agar	BD Bioscience
Glycerol	Evans Medical limited BD
Proteinase K	Thermo Scientific
Agarose (molecular biology grade)	GeneON for 50bp-50kb
Tris base	Sigma Aldrich
Glacial acetic acid	Sigma Aldrich
EDTA	Sigma Aldrich
Levamisol	Sigma Aldrich
PCR master mix M750C	Pomega
GreenSafe Premium dye	nzytech
GelRed dye	Fisher Scientific
Bacto Tryptone	BD Bioscience
Bacto Yeast Extract	BD Bioscience
KCl	Sigma Aldrich
MgCl ₂	Sigma Aldrich
Triton-X100	Acros Organics
Tween-20	Fisher Scientific
Gelatin	BDH
Tripotassium citrate	Sigma Aldrich
FeSO ₄ *7H ₂ O	Sigma Aldrich
Na ₂ EDTA	Sigma Aldrich
MnCl ₂ *4H ₂ O	Sigma Aldrich
CuSO ₄ *5H ₂ O	Sigma Aldrich
Citric acid monohydrate	Sigma Aldrich
KOH	Sigma Aldrich
ZnSO ₄ *7H ₂ O	Sigma Aldrich
Sucrose	Fisher Scientific

Bromophenol

Sigma Aldrich

Table 5.4| Equipment

Equipment	Manufacturer/Details
Incubator	SANYO
Vacuum system	Vacunsafe Comfort, BS Integra Biosciences
Centrifuge	Thermo, Heraeus Multifuge 3L-R
Water bath	Memmert, WNE22
Plate reader	Tecan Infinite 200; Tecan iControl software
Agitator	Shel Lab, SI Series
Flow chamber (RGU)	Microflow M51424/2 classII
Microscope	Olympus, SZX16
Confocal microscope	Olympus FV1000
Shaking incubator (OP50)	Shel Lab, SI series
Shaker (RGU)	Stuart SI1600
Incubator (RGU)	Panasonic MMIR-154-PE
Thermocycler	Eppendorf Mastercycler epgradient S
Centrifuge	Heraeus Pico 17
Gel pouring chamber and tank	Bio-RAD Sub-Cell GT
Power pack	Consort E835 (300V-500mA)
PCR thermocycler (ICVS)	Eppendorf mastercycler epgradient S
PCR thermocycler (RGU)	iCycler BioRad 582BR
Gel camera/software	BIO-RAD Gel Doc TM EZ Imager, software: Image lab 4.1 bio-rad

5.2.2 Methods

The methods employed in this chapter (Figure 5.16) were used to study the effect of RSP extract on the *in vivo* model organism *C. elegans*. Different disease models for both MJD and PD were employed, to evaluate the potential use of RSP extract for the treatment or prevention of neurodegenerative disease.

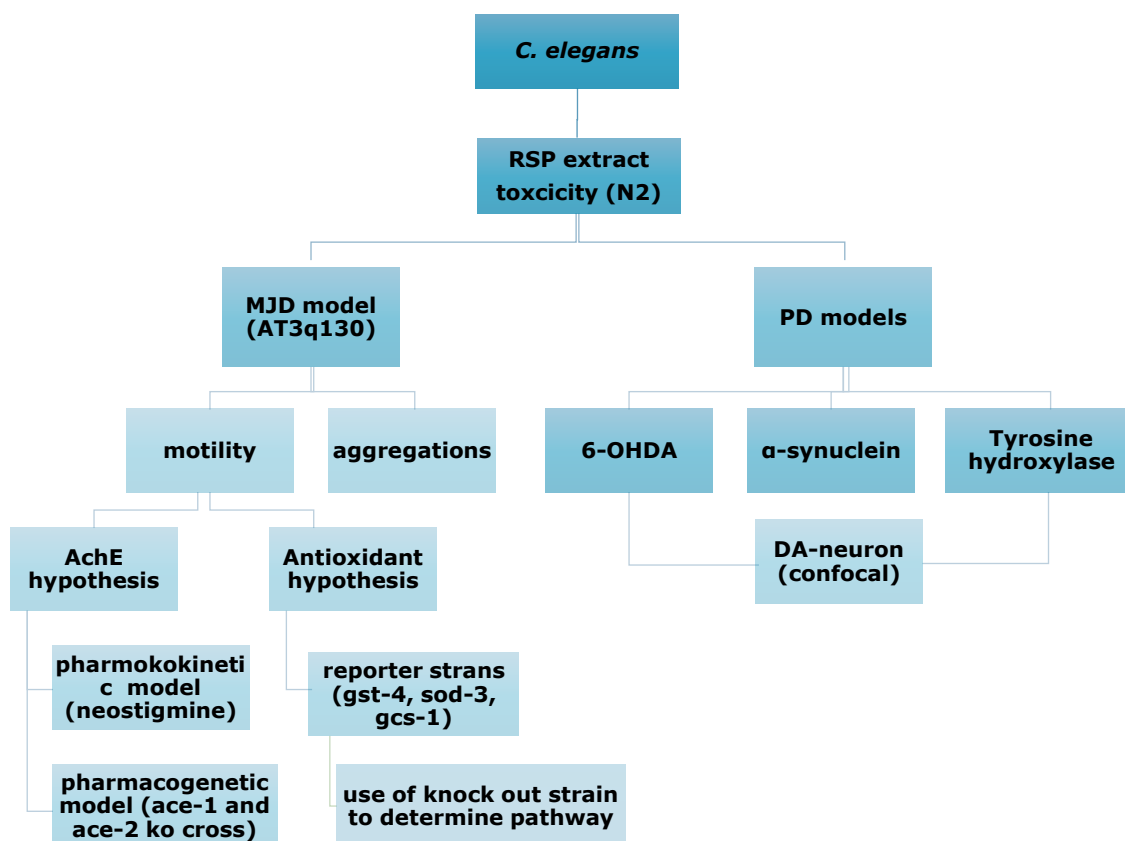


Figure 5.16| Overview of methods used to determine the extracts activity in different *C. elegans* models

5.2.2.1 General maintenance/Strains

C. elegans strains (Table 5.5) were maintained on nematode growth medium (NGM, Table A5, p.457 f.) seeded with living *E. Coli* bacteria (OP50) as food source⁵⁹¹, unless otherwise noted. The OP50 solution for seeding was obtained by inoculating LB with OP50 bacteria and culturing overnight (16 h at 37°C, 150 rpm). OP50 solution was immediately seeded onto dried NGM plates or stored at 4°C. After seeding the plates were dried for 2-4 days and then used for *C. elegans* maintenance or stored at 4°C. The NGM plates with worms were maintained at 20°C (SANYO incubator), unless described

differently. Worms were transferred (3-6 adult animals) every 4-5 days for general maintenance. Table 5.5 below lists the used stains, with abbreviations referred to throughout the thesis, their genotype and place of origin, whereas Table 5.6 lists the strains created *via* crossing during this project.

List of strains

Table 5.5| List of strains

Name	Abbreviation	Genotype	origin
Wild type	N2	<i>wt</i>	CGC ^a
AM510 (Teixeira- Castro et al., 2011)	AT3q14	<i>rmIs228[PF25B3.3::AT3 v1-1q14::yfp]</i>	ICVS made
AM685 (Teixeira- Castro et al., 2011)	AT3q130	<i>rmls263[PF25B3.3::AT3 v1-1q130::yfp] II</i>	ICVS made
Ace-1	Ace-1	NA	CGC ^a (6x BC by F.Pohl)
Ace-2	Ace-2	NA	CGC ^a (6x BC by F.Pohl)
BZ555	BZ555	<i>egIs1 [dat-1p::GFP]</i>	
UA44	UA44	<i>baIn11[pdat-1::aSyn + pdat-1::GFP]</i>	Caldwell Lab ^b
UA 57	UA 57	<i>baIs4 [dat-1p::GFP + dat-1p::CAT-2]</i>	Caldwell Lab ^b
RB1823	Gst-4(ko)	<i>gst-4&msp-38(ok2358) IV.</i>	CGC ^a (6x BC by F.Pohl and V. Lindsay)
CF1553	Sod-3	<i>muIs84 [(pAD76) sod-3p::GFP + rol-6(su1006)]</i>	CGC ^a
LD1171	Gcs-1	<i>ldIs3 [gcs-1p::GFP + rol-6(su1006)]</i>	CGC ^a
CL2166	Gst-4	<i>dvIs19 [(pAF15)gst-4p::GFP::NLS] III</i>	CGC ^a

Note(s): ^aCGC, funded by NIH Office of Research Infrastructure Programs (P40 OD010440); ^b Guy and Kim Caldwell, The University of Alabama

Table 5.6| List of strains created

Name	Created by
<i>AT3q130;ace-1</i>	F.Pohl (ICVS)
<i>AT3q130;ace-2</i>	F.Pohl, A.Teixeiro-Castro (ICVS)
<i>UA44;gst-4(ko)</i>	V. Lindsay (ICVS)

All strains used, were outcrossed to N2 (Table 5.5) at least six times to avoid them carrying mutations in genes in addition to the gene of interest⁶⁷⁹.

5.2.2.2 Freezing and thawing of worm cultures

Adult *C. elegans* (3-6, strain dependent) were picked onto new NGM plates (2-3) and left to have progeny (4 - 5 days) until their OP50 food source was just depleted, the plates had plenty of L1s and L2s as well as some eggs (plate has not been depleted too long) and no contaminations. Worms were washed off the plates using M9 (Table A5, p.457 ff.) solution into 15 mL falcon tubes, centrifuged (2000 x g, 1 min) the supernatant discarded, and the worms washed 2-3 more times until the supernatant was clear. After the last centrifuge step, all but 3 mL/4.5 mL (2/3 plates) of M9 solution were discarded. An equal amount of freezing solution (complete, Table A5, p.457 ff.) was added, the vial agitated, to evenly distribute the worms, and the worm suspension aliquoted (1 mL each) into clearly labelled cryovials, which were cooled down slowly, using either a styrofoam or Mr. Frosty™ Freezing container in the freezer (-80°C).

After one month, a test thaw for each frozen strain was undertaken until which the worms are continuously cultured under normal conditions. To thaw the worms and look for survival, the vials were thawed and then pipetted onto the NGM plates around the OP50 seeding. Plates were left to dry overnight and checked for survival the next day. Living worms were picked and placed onto new plates, to prevent contamination. If there were no surviving worms (unsuccessful freezing), the freezing process was repeated using the plates continuously cultured with the strains.

5.2.2.3 Backcrossing and creation of double mutant strains-“worm crossings”

Worm lysis

Single or multiple worm lysis was undertaken by adding 10% Proteinase K (20mg/mL) to *C. elegans* lysis buffer (50 mM KCl, 10 mM Tris (pH 8.3), 2.5 mM MgCl₂, 0.45% NP-40/Triton-X100, 0.45% Tween-20, 0.01% gelatine). Depending on single or multiple worm lysis, 4 or 20 µL lysis buffer were pipetted into the lid of PCR tubes and 1 or 10 worms picked into the buffer respectively. PCR tubes were closed and then subject to a brief spin in the centrifuge to bring the solution and worms to the bottom of the tube, which were then frozen (-80°C) for 30 minutes. There after the tubes were placed in the thermocycler (Eppendorf Mastercycler eppgradient S) using the following

lysis program: 65 minutes at 65°C, 15 minutes at 95°C followed by cool down to 4°C. Lysed worms were stored in the fridge (4°C) until needed for further experiments or it was immediately added to the PCR.

Primer design and preparation for PCR

For the back crosses (*ace-1*, *ace-2* and *gst-4* (ko)) and the intended crossings of *ace-1* and *ace-2* with AT3q130 worms, and *gst-4* (ko) with UA44 worms, primers were needed, to determine the genotype of the crossed animals. These were created using the Primer3-PCR primer design tool⁶⁸⁰. The gene sequences of the *ace-1* (VC505, ok663), *ace-2* (RB1942, ok2545) and *gst-4* (ko) (RB1823, ok2358) genes are shown in Figure A15 (p.453 f.), Figure A16 (p.455 f.) and Figure A17 (p.457 ff.) respectively.

Table 5.7 shows the sequence of the three designed primers; one forward (for-1) and two reverse (rev-1 and rev-2), with primer rev-2 located in the middle of the allele deletion. The primers were obtained from STAB vida (Portugal) or Sigma-Aldrich (*gst-4* (ko)).

Table 5.7| Primers for crosses and back-crosses

GENE	PRIMER	SEQUENCE (5'- 3')
ace-1	for-1	TGTTGAAGAAGCATGCGAAA
	rev-2	TAGGGGTGTGAACATGCAAA
	rev-1	GAGATTGCCAACTGGTGGTT
ace-2	for-1	TGAAAAGTAGCCGCATCAAA
	rev-2	ACGATATCGGGATGGAGTTG
	rev-1	CAACAGCTTGCTCTTCGTTG
gst-4 (ko)	for-1	TTGGGCAAGAATTTCCAGAG
	rev-2	GGCTTCACTCACTTGGCTTC
	rev-1	AAAGATCTGGGGCAGTGATG

Stock primers solutions (1 µg/µL) were prepared in milliQ water, based on the weight of primer obtained. From the respective stock solution, a working solution of 10 µM was prepared in milliQ water by considering the molecular weight of each primer. Working solutions and stock solutions were kept at -20°C when not in use.

PCR optimization

The following procedure describes the PCR reaction optimization for ace-1. The same process was repeated for ace-2 and gst-4 (ko). For the PCR optimization 3 PCR master mixes were prepared as described in Table 5.8. The amount of master mix prepared was adjusted, depending on the number of samples (e.g. x30, last column Table 5.8). For Mix 1 PCR master mix 2x (Pomega M750C) was mixed with milliQ water, primers for-1 and rev-2 (10 µM) as well as worm lysate. In comparison, Mix 2 contained for-1 and rev-2 and Mix 3 all three primers. The 3 different mixtures were prepared to determine if it would be necessary to run Mix 1 and Mix 2 for the following PCRs or whether Mix 3 itself would be sufficient.

Table 5.8| PCR master mixes

	Mix 1 (µL)	Mix 2 (µL)	Mix 3 (µL)	x30 for all samples, for each mix (µL)
PCR master mix 2x	12.5	12.5	12.5	375
For-1(10 µM)	0.5	0.5	0.5	15
Rev-2 (10 µM)	0.5	-	0.5	15-0-15 (Mix 1-Mix 2-Mix 3)
Rev-1 (10 µM)	-	0.5	0.5	0-15-15 (Mix 1-Mix 2-Mix 3)
Worm lysate	1.5	1.5	1.5	In PCR tubes
Water milliQ	10	10	9.5	300-300-285 (Mix 1-Mix 2-Mix 3)

For the PCR optimisation eight different annealing temperatures (53.1, 54.2, 55.0, 55.8, 56.7, 58.4, 59.1 and 59.8°C) were tested within the following PCR program: 5 minutes 95°C, then 1 minute 95°C, 1 minute temperature gradient (8 different temperatures), 1.5 minutes 72°C which was repeated 35 times, followed by 10 minutes 72°C and a cool down to 4°C using an Eppendorf thermocycler (Mastercycler epgradient S). The temperature and mixtures (Mix1+Mix2 or Mix3) found to give the best results ("5.3.3.2 Pharmacogenetic approach using two *C. elegans* mutants (knock out) for the AChE gene", p.325) was used for all subsequent PCRs.

Gel electrophoresis of PCR products

For the gel electrophoresis of the PCR products, a 1% agarose gel (w/v) was prepared by dissolving an appropriate weight of agarose (molecular biology grade, GeneON for 50bp-50kb) in 1x TAE buffer (1960 mL deionized water and 40 mL 50x TAE buffer (242 g Tris base, 57.1 mL glacial acetic acid, 100 mL EDTA (0.5 M, pH 8) made up to a total of 1000 mL with deionized water)) in the microwave. The gel was left to cool down till hand warm, green safe dye (3 µL/100 mL, nzytech Greensafe Premium) was added, mixed and then poured into the appropriate size gel tray fitted with combs and let to set for 20-30 minutes. Thereafter the tray was immersed in the gel tank (BIO-RAD Sub-Cell GT) containing 1x TEA buffer. After the PCR run, 5 µL loading dye (20 g sucrose in 50 mL deionized water, with bromophenol for desired colour) were added to all the DNA samples obtained and 25 µL loaded into the wells. A DNA ladder (Gene Ruler™ DNA Ladder Mix: 100 µL DNA ladder, 100 µL 6x loading dye, 400 µL dH₂O; storage at -20°C) was run for DNA size determination. The gel was electrophorized at 125 V for about 90 min. The gels were visualized using a BIO-RAD Gel Doc TMEZ Imager and Image lab 4.1 bio-rad software.

The expected DNA lengths after PCR and gel electrophoresis for wild type, mutant and heterozygous worms for *ace-1*, *ace-2* and *gst-4* (ko) are presented in Table 5.9.

Table 5.9|Expected DNA fragments for genotyped *ace-1*, *ace-2* and *gst-4* (ko) worms

GENE	WT	MUT	HETEROZYGOUS
ace-1	263bp+1004bp	396bp	263bp+396bp+1004bp
ace-2	243bp+1869bp	399bp	243bp+399bp+1869bp
gst-4 (ko)	531bp+1983bp	435bp	531bp+435bp+1983bp

Outcrossing

Some of the strains, obtained from the CGC (*ace-1*, *ace-2*, *gst-4* (ko)) were 0 x backcrossed (BC). To avoid genes mutations in addition to the gene of interest they had to be backcrossed to N2 worms, before undertaking any further experiments or crosses with other strains (AT3q130 and UA444). The

following paragraph describes the process of backcrossing using *ace-1* animals, the same procedure was undertaken when backcrossing *ace-2* and *gst-4* (ko) worms. The gene for *ace-1* is located on the x chromosome, which only hermaphrodites are diploid (x/x) for, males are haploid (x/0).

For the first backcrossing 13 male N2 (genotype: wt/0), were placed onto OP50 seeded 60 mm NGM plates, together with three L₄ stage hermaphrodite *ace-1* worms (genotype: *ace-1/ace-1*) and left to breed at 15 °C for 2 days (Figure 5.17 (1xBC)). Thereafter the three hermaphrodites (now around day five of development) were isolated onto three separate OP50 seeded 60mm NGM plates and left to lay eggs (2-3 days, 20°C). From these, one plate was chosen that contained a significant number of male worms as indicator for successful breeding. From this plate, 13 males (genotype: *ace-1/0*) were bred with three L₄ stage N2 hermaphrodites (wt/wt) for 2 days at 15°C (Figure 5.17 (2xBC)). There after the three hermaphrodites were again isolated onto separate 60mm plates and left to lay eggs (2-3 days at 20°C). One of these plates was selected (significant number of male progeny) and 10 hermaphrodites (L4 stage) isolated. These 10 hermaphrodites can have the following genotypes: wt/wt (from self-fertilization) or *ace-1/wt* (occurred after successful breeding). The worms were left to lay eggs for 2-3 days. The 10 isolated adults are then used for single worm PCR, to determine their individual genotypes. From one of the plates, that showed an adult with a heterozygous (*ace-1/wt*) genotype 16 hermaphrodites were isolated and left to lay eggs on 16 separate plates. Single worm PCR was again undertaken to detect their genotype, which can be one of three: *ace-1/ace-1*, *ace-1/wt* or wt/wt in the ratio 1:2:1 according to Mendel's first law (law of segregation of genes⁶⁸¹, Table 5.10).

Table 5.10| Genetic cross of hermaphrodite self-fertilization

♀	wt	<i>ace-1</i>
wt	wt/wt	wt/ <i>ace-1</i>
<i>ace-1</i>	wt/ <i>ace-1</i>	<i>ace-1/ace-1</i>

Note(s): heterozygous worms (wt/ace-1), on X-chromosome

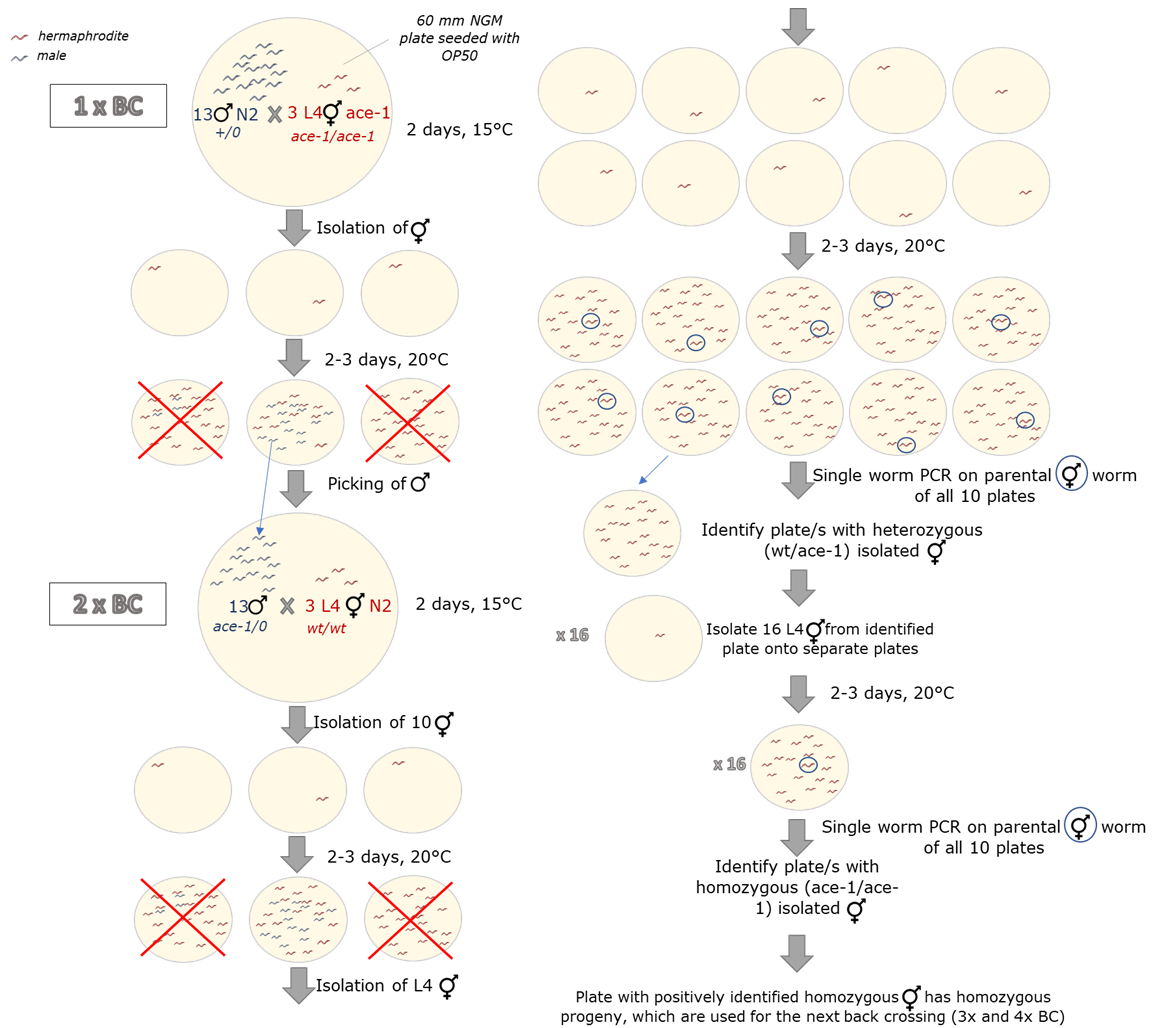


Figure 5.17| Backcrossing schematic for *ace-1* worms, deletion of *ace-1* on the X chromosome

Three L₄ stage hermaphrodites from one of the plates, which showed the *ace-1/ace-1* genotype, were then chosen to start the 3rd backcrossing, together with 13 N₂ males, as previously described for the first backcrossing. The 3x and 4x as well as the 5x and 6x back crossing were conducted in the same way as the 1x and 2x respectively. Two-, four- and six times back crossed animals were frozen (5.2.2.2 Freezing and thawing of worm cultures p.292), to secure the different stages of back crossing.

Crossing

To explain the crossing between two *C. elegans* mutants, the example of crossing *ace-1* worms with AT3q130 is presented, the other crosses (*ace-2* (6xBC)xAT3q130 and *gst-4(ko)*(6xBC)xUA44 were undertaken using the same crossing method (Figure 5.18, p.300). For the first crossing 13 male N₂



(wt/0 for *ace-1*; wt/wt for AT3q130) were transferred onto 60 mm NGM plates and left to breed with three L4 stage hermaphrodite AT3q130 animals (wt/wt for *ace-1*; q130/q130 for AT3q130) (2 days, 15 °C). Thereafter the three hermaphrodites (now around day 5 of development) were isolated onto 3 separate 60 mm plates and were left to lay eggs (2-3 days, 20°C). From one of the three plates, containing a significant number of males, 13 males (wt/0 for *ace-1*; wt/q130 for AT3q130) were bred with 3 *ace-1* L4 stage hermaphrodites (*ace-1/ace-1* for *ace-1*, 6xBC; wt/wt for AT3q130) for 2 days at 15°C. There after the hermaphrodites were isolated again onto 60 mm plates and left to lay eggs (2-3 days at 20°C). One of the plates, containing a significant number of males, was selected and 3 L4 stage hermaphrodites, showing YFP fluorescence when observed using a fluorescent microscope, were isolated. This confirms the successful crossing and provides the following genotype for the three chosen hermaphrodites: wt/*ace-1* for *ace-1* and wt/q130 for AT3q130. The three isolated worms were left to lay eggs (2-3 days, 20°C). Following, from one of the three plates 24 hermaphrodites (L₄) were isolated, showing both low and high intensity fluorescence, both wt/q130 and q130/q130 (for AT3q130) genotype worms were selected (Table 5.11, both and respectively), for the chance of picking an *ace-1/ace-1* genotype (bold in Table 5.11).

Table 5.11 | Genetic cross for progeny of the 24 isolated animals*

♀	<i>ace-1</i> q130	<i>ace-1</i> wt	wt q130	wt wt
<i>ace-1</i> q130	<i>ace-1/ace-1</i> q130/q130	<i>ace-1/ace-1</i> wt/q130	wt/ <i>ace-1</i> q130/q130	wt/ <i>ace-1</i> wt/q130
<i>ace-1</i> wt	<i>ace-1/ace-1</i> q130/wt	<i>ace-1/ace-1</i> wt/wt	wt/ <i>ace-1</i> q130 /wt	wt/ <i>ace-1</i> wt/wt
wt q130	<i>ace-1</i> /wt q130/q130	<i>ace-1</i> /wt wt/ q130	wt/wt q130 / q130	wt/wt wt/ q130
wt wt	<i>ace-1</i> / wt q130/ wt	<i>ace-1</i> / wt wt / wt	wt / wt q130 / wt	wt/ wt wt / wt

Note(s):* heterozygous for both genes: genotype wt/*ace-1*|wt/q130 green highlighted genotypes showed YFP fluorescence (bright for homozygous and less bright for heterozygous animals); genotypes needed for further experiments are highlighted with red/orange boarder

The probability of obtaining the desired double mutant (genotype *ace-1/ace-1|q130/q130*) was 1:16, and 1:12 after selecting for fluorescence. To enhance the probability of picking the *ace-1/ace-1* genotype, a total number of at least 24 worms were isolated and left to lay eggs for 2-3 days (20°C). Thereafter all the parental worms were genotyped for the *ace-1* gene, using single worm PCR, to identify the parents, homozygous for the *ace-1* gene. These would also produce homozygous offspring for this gene.

The plates with homozygous (*ace-1*) parental worms were then observed using fluorescence microscopy, to determine plates with exclusively fluorescent worms. Plates with only fluorescent worms, verify, that the parent had the required genotype for the ataxin-3 gene (*q130/q130*), thus giving the wanted double mutant genotype of *ace-1/ace-1|q130/q130* (Table 5.11 ) to all of their offspring. In addition, the wild type (*ace-1*) homozygous AT3q130 worms (*wt/wt|q130/q130*) were isolated (Table 5.11 ). The acquired newly created worms were cultured (5.2.2.1 General maintenance/Strains, p.290 f.) and frozen (5.2.2.2 Freezing and thawing of worm cultures, p.292), to secure the positive outcome of the crossing, and their use in future experiments.

The Potential Application of Rapeseed Pomace Extracts in the Prevention and Treatment of Neurodegenerative Diseases

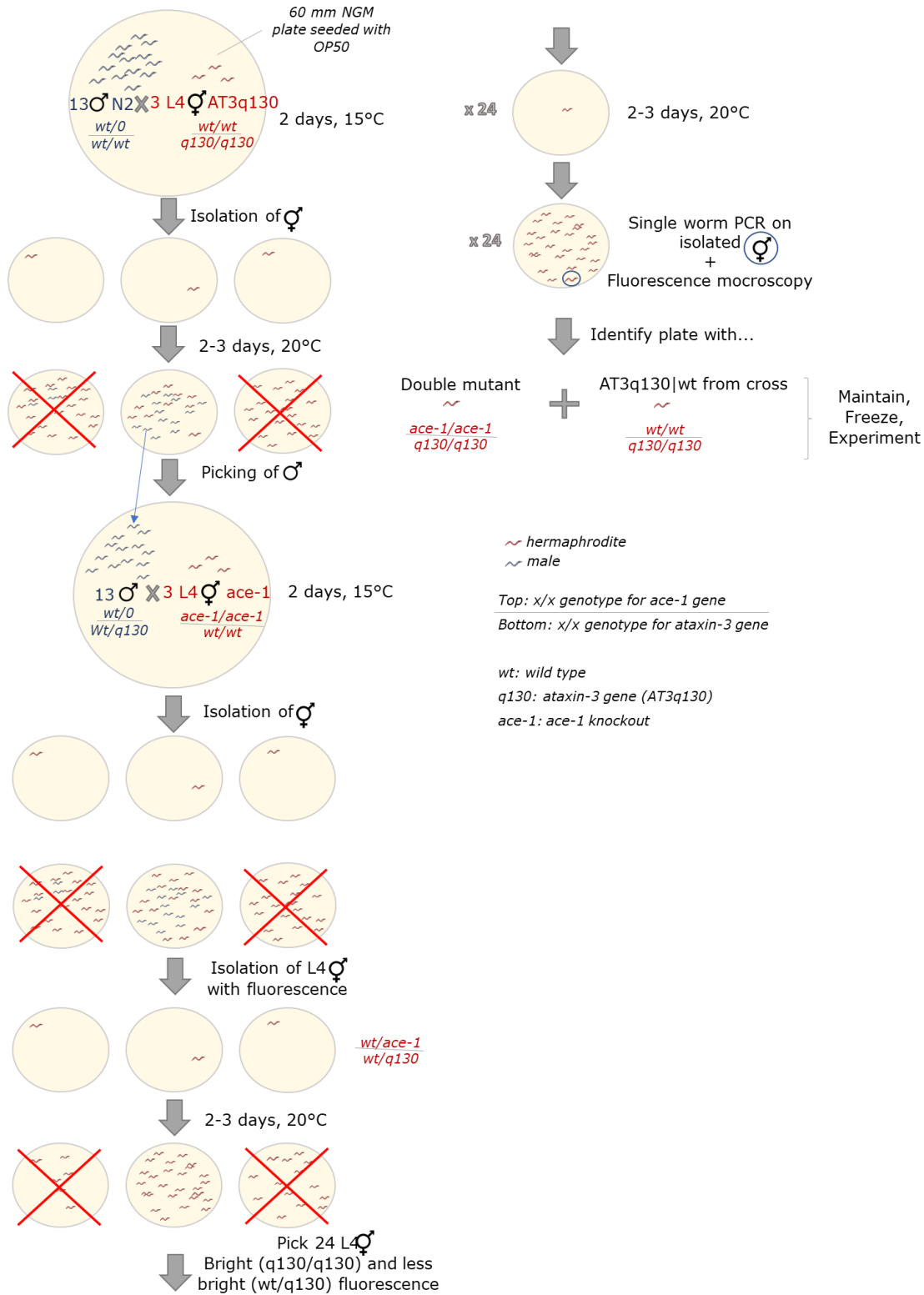


Figure 5.18| Schematic depicting the crossing for *ace-1* (on chromosome X) \times AT3q130 (on chromosome II) worms for the creation of double mutants

5.2.2.4 Toxicity assay/Food clearance assay

To evaluate toxicity of the RSP extract towards *C. elegans* the food clearance assay was applied. The latter was performed in liquid culture using a 96-well format as previously described^{605,616} with minor modifications. The steps adopted for the toxicity evaluation are depicted in Figure 5.19 (p.302). and described following (I.-III.).

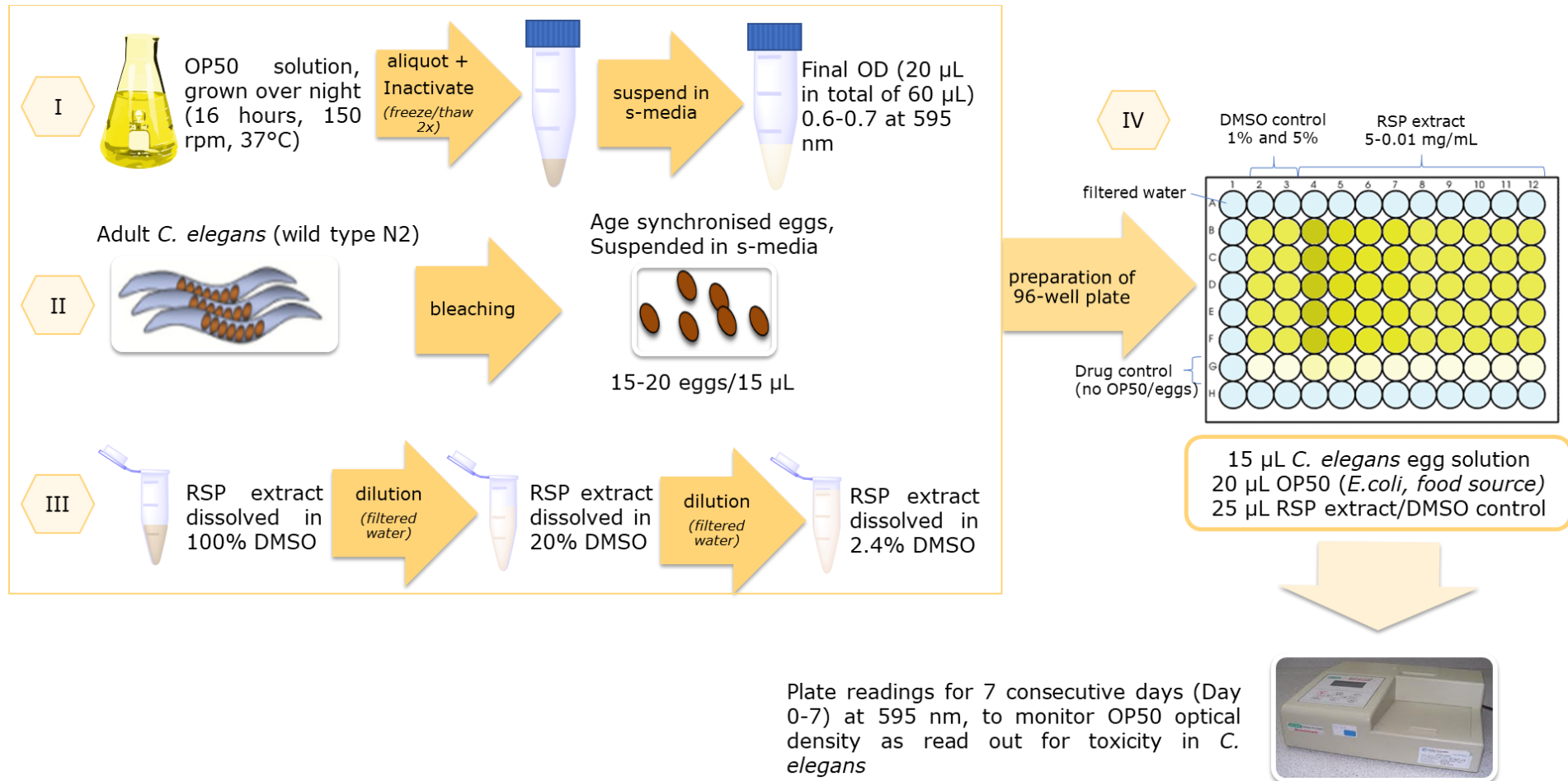


Figure 5.19| Food clearance assay/Toxicity assay for evaluating the toxicity of the RSP extract in *C. elegans*

I. Preparation of inactivated OP50 solution

Inactivated OP50 solution was prepared by growing the OP50 bacteria in Luria Broth (LB, Table A5, p.457) media (overnight (16 h) at 37°C and 150 rpm). The solution was aliquoted into falcon tubes (50 mL) and pelleted by centrifugation (4000 x g, 30 min). The supernatant was discarded and the OP50 pellet inactivation *via* 2 cycles of freeze (liquid nitrogen)/thawing (water bath, 70°C). For storage, pellets were frozen in liquid nitrogen and stored at -80°C. On the day of the assay, the pellet/s was/were thawed and re-suspended in s-medium complete (Table A5, p.457) containing 0.08% cholesterol (5 mg/mL), 0.5% streptomycin/penicillin and 0.5% nystatin (100x). The optical density (OD) of the diluted OP50 pellet was adjusted to a final OD between 0.6-0.7 at 595 nm (20 µL OP50 plus 40 µL s-media in 96-well plate).

II. Preparation of synchronised *C. elegans* egg population

To screen the RSP extract for toxicity, the Bristol strain (N2) was employed. Four days prior to the setup of the toxicity experiment, three to four gravid adult N2 animals were picked onto a new OP50 seeded NGM plates. The number of plates was adjusted depending on the number of toxicity assays (eggs needed).

On the day of the experiment, early progeny of the picked animals had grown into gravid adult *C. elegans*. The plate/s were washed using M9 (Table A5, p.457 f.) solution and animals collected in falcon tubes (15 mL) and worms left to settle to the bottom (5 min). The M9 solution was carefully removed by aspiration using flame sterilised glass pipette attached to a pump (Vacusafe Comfort, BS Integra Biosciences). The worms were then treated using alkaline hypochlorite (bleaching) solution (Table A5, p.457 f.), until the adult worms had dissolved (4-6 min) to obtain an age synchronised egg population. After the bleaching process, the bleaching solution was carefully removed after centrifugation (2000 x g, 1 min) with the eggs at the bottom of the falcon tube and M9 was added for washing. The eggs were again centrifuged (2000 x g, 1 minute) and the washing process repeated twice more. After removing the M9 following the last wash, the eggs were re-

suspended in s-medium complete (Table A5, p.457 f.) to an appropriate number of eggs (15-20 eggs in 15 μ L).

III. Preparation of RSP extract and DMSO controls

The extract was dissolved in DMSO to create a stock solution (100 mg/mL). This stock solution was diluted using filtered water to obtain different concentrations of RSP extract stock solutions at 20 % DMSO, which were further diluted to obtain final concentrations of the extract between 0.024-12 mg/mL, each at 2.4% DMSO. Aliquots of these solutions were stored at -20°C until further use. The final concentration of DMSO in all the RSP extract samples was 1% and final extract concentrations tested ranged from 0.01-5 mg/mL (see well set-up below and Figure 5.19, p.302). A 2.4% and 12% DMSO control were prepared in addition for final concentrations of 1% (vehicle/solvent control) and 5% (toxic condition) DMSO respectively.

In addition, neostigmine and sinapine were tested in the toxicity assay. Stocks were made up with DMSO, using similar procedures as described for the RSP extract. Using final DMSO concentration of 1% and neostigmine and sinapine concentrations ranged from 0.01-10 mM and 0.001-1.0 mg/mL respectively.

IV. Set-up of 96-well plate for toxicity assay

After the preparation of all the solutions, 15 µL of the egg solution (15-20 eggs) together with 20 µL inactivated OP50 bacteria and 25 µL of the RSP extract or DMSO control solutions were added to the wells (5 wells for each condition) of a 96-well plate (clear flat bottom). To avoid interference from the absorbance of the RSP extract at 595 nm, one well per condition was used as drug control. These were filled with 35 µL s-media complete and 25 µL of the RSP extract or DMSO control solutions. The outside wells of each plate were filled with filtered water to avoid dehydration of the plate throughout the time of the experiment (7 days). After the preparation of the 96-well plate, the initial optical density (day 0) at 595 nm was measured and the plates wrapped into moist paper towels (avoid dehydration) and aluminium foil (avoid light). The eggs/worms in the 96-well plates were grown at 20°C and 180 rpm (Shel Lab) for 7 days. The optical density (595 nm) was measured daily to monitor the rate by which the OP50 food suspension was consumed, as a read out for worm growth and development, survival and fecundity.

5.2.2.5 AT3q130 strain methods

I. Motility determination

For the motility assay N2, AT3q14 (NC7) and AT3q130 (RSP extract treated and DMSO control treated (1%)) worms were grown in liquid culture using inactivated OP50 as food source as described above (5.2.2.4 Toxicity assay/Food clearance assay) with minor modifications. The optical density was increased to between 0.9-1.0 at 595 nm, to ensure the availability of enough OP50 for the duration of 4 days. In addition, the number of eggs used per well was adjusted per strain (N2 20-30, AT3q14 30-40 and AT3q130 40-60). A total number of 6 wells were used per condition on each 96-well plate. On day four of incubation (20°C and 180 rpm (Shel Lab)) worms (gravid adult) were transferred from the wells to unseeded NGM plates, equilibrated to 20°C. Plates were allowed to dry for approximately one hour, before conducting the motility assay as previously described⁶¹⁴. Briefly, worms (3-10) were picked and transferred into the middle of an evenly seeded (OP50) NGM plate (30 mm). The worms were given 1 minute to crawl, worms that had not crawled out of a circle 10 mm in diameter were scored as motility deficient (Figure 5.20, p.307). The circle was kept constant by using a circle drawn onto a lid of a 30 mm plate, which was put underneath the seeded NGM plate before transferring worms into the middle. The motor behaviour assays were run in quintuplicate (n=5) with at least 50 animals per condition in each experiment, giving a total n≥250 per tested genotype and/or extract concentration.

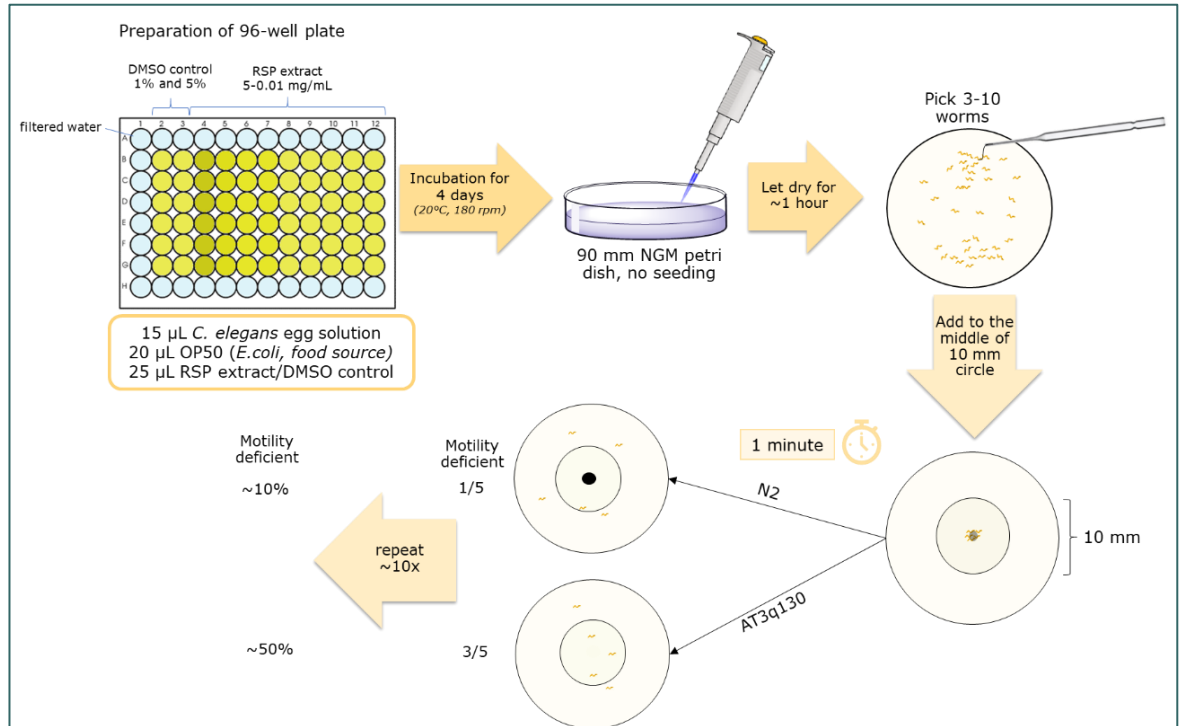


Figure 5.20| Schematic of the motility assay of N2 and AT3q130 worms

II. Confocal microscopy

For confocal dynamic imaging and quantification of ataxin-3, animals (AT3q130) were mounted onto 3% agarose pads (agarose prepared in M9) on microscopy slides and treated with levamisole (10 mM, antihelminthic), covered with a cover slip and all four sides sealed with 3% agarose to avoid dehydration. Slides were left at 20°C for ~two hours for the levamisole to immobilize the worms for confocal imaging. All images were captured on an Olympus FV1000 (Japan) confocal microscope, under a 60x oil (NA= 1.35) objective. Z-series images were acquired for vehicle (1% DMSO)- and extract-treated (4 mg/mL) animals, using a 515/514 nm laser excitation line for YFP. The pinhole was adjusted to 1.0 Airy unit of optical slice, and a scan was acquired every ~0.5 µm along the z-axis. The quantification of the aggregates was performed as previously described by Teixeira-Castro *et al.*^{614,616}. Two parameters were measured: area of aggregates/total area and number of aggregates/total area in 3 repeated experiments (n=3). Values shown are the mean (normalized to vehicle treated control) of ten or more animals per group.

5.2.2.6 PD strain methods

For the experiments using the PD strains, DMSO controls (1%) as well as RSP extract treated worms were analysed for the prevention of DAergic neuron loss in one chemical induced model of PD, using 6-OHDA and BZ555 animals, and 2 genetic models (UA44, UA57). For the extract a concentration of 4 mg/mL was chosen (explanation see 5.3.2 Machado-Joseph disease *C. elegans* model). For all PD models, treatment was performed on NGM plates.

I. Preparation of OP50 seeding with treatment

The seeding for *C. elegans* treatment on NGM plates was prepared by thawing the for the drug assay (in liquid media) prepared inactivated OP50 pellets (5.2.2.4 I. Preparation of inactivated OP50 solution, p.303) and adding approximately 4 mL of s-media complete (Table A5, p.457 f.) containing streptomycin/penicillin and nystatin. To this, 50 μ L of concentrated vehicle control (DMSO) or RSP extract were added and the solution made up to a total of 5 mL for final concentrations of 1% DMSO and 4 mg/mL RSP extract. Dried unseeded NGM plates (60 mm) were seeded with 200 μ L of the prepared seeding and allowed to dry in the flow chamber for 20-30 minutes in the dark. Treatment plates were used immediately after or stored for use (4°C) for up to two days. All plates seeded with treatment, with or without worm populations, were stored in the dark to prevent potential light sensitive compounds from decomposition.

II. Exposure to 6-OHDA (BZ555)

An age synchronized egg population was obtained *via* bleaching for BZ555 worms, as described before (5.2.2.4 II. Preparation of synchronised *C. elegans* egg population p.303). About 200 eggs were put onto freshly vehicle (1% DMSO) and RSP extract (4 mg/mL) OP50 seeded plates (day 0, Figure 5.21, p.309). Approximately 48 hours later worms (between L2-L3 stage of development) were washed off the plates and washed in filtered deionized water (supplemented with 1 % LB) 2-3 times until the washing liquid was clear (no more OP50 present). Worms were redistributed in approximately 500 μ L filtered deionized water (1% LB). In a 12 well plate, 250 μ L 6-OHDA (final concentration 10 and 25 mM), 250 μ L ascorbic acid (final concentration 2 and 5 mM respectively, antioxidant) and 500 μ L of the worm solution were

incubated for one hour (20°C, ~50 rpm). After one hour, the worms were diluted and washed (2-3) times with filtered deionized water (1% LB). Thereafter worms were transferred back onto respective vehicle or RSP extract OP50 seeded plates. On day 5 approximately 72 hours after 6-OHDA treatment worms were prepared for confocal imaging, as described previously (5.2.2.5 II. Confocal microscopy, p.307). DAergic neurons in 10-12 animals were counted and representative pictures taken for all conditions. The experiment was repeated 3 times (n=3), with a total number of n≥30 worms scored.

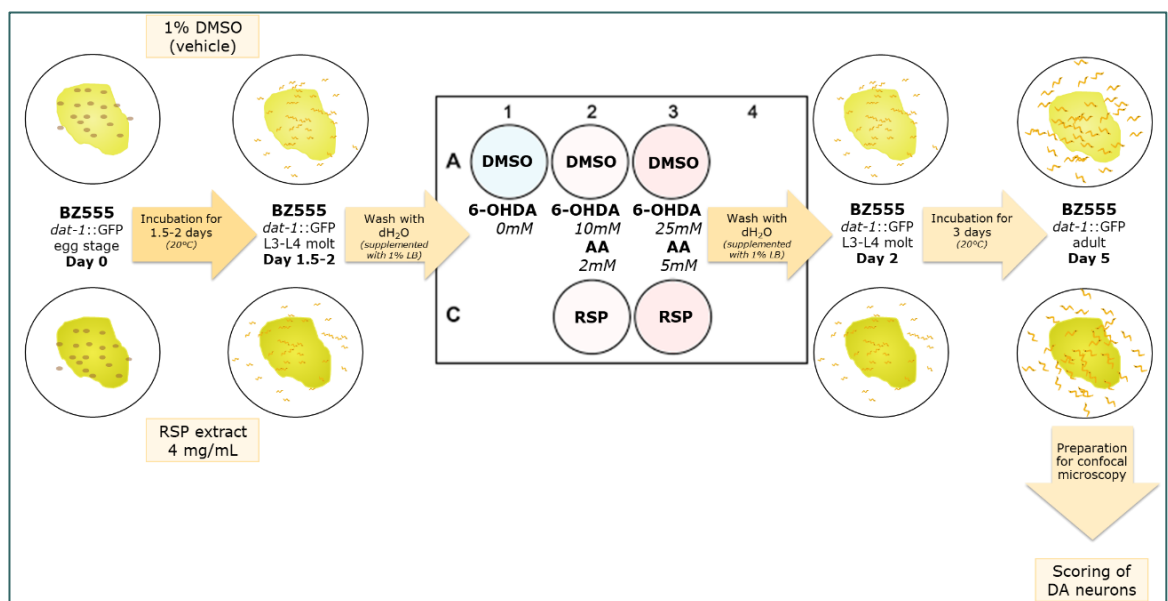


Figure 5.21 | 6-OHDA induced PD model experimental setup using BZ555 animals

Comparing treated (4 mg/mL RSP extract) to vehicle treated (DMSO (1%)) animals using two different concentrations of 6-OHDA (10 and 25 mM) in conjunction with ascorbic acid (AA-ascorbic acid, 1 and 5 mM respectively)

III. Age dependent neurodegeneration (UA57, UA44)

To determine age dependent neurodegeneration in PD models of *C. elegans*, BZ555 (control for DAergic neurons), UA44 (alpha-syn.) and UA57 (CAT-2) age synchronised egg populations were obtained, through synchronisation *via* egg laying, by picking 10 gravid animals onto freshly seeded vehicle (1% DMSO; BZ555, UA57, UA44) and RSP extract (4 mg/mL; UA57, UA44) seeded plates. They were left to lay eggs and then taken off, for only the eggs to remain. Starting on day three/four, adult worms were transferred onto

freshly seeded plates (treated/untreated) each day until about day 7, when the egg laying slowly decrease and worms were only transferred once before the end of the experiment on day 10. Worms (10-12) were prepared for confocal microscopy on day 7 and 10 as described above (5.2.2.5 II. Confocal microscopy, p.307) and DAergic neurons were counted, and representative pictures of each condition taken. The experiment was repeated 3 times (total number of worms scored $n \geq 30$).

5.2.2.7 Reporter strains/Fluorescence microscopy

An age synchronised egg population was obtained *via* egg laying methodology as described before (5.2.2.6 III. Age dependent neurodegeneration (UA57, UA44) p.309). Ten gravid adults from each strain (CL2166, CF1553, LD1171) were picked onto three freshly vehicle and RSP extract seeded plates (5.2.2.6 I. Preparation of OP50 seeding with treatment, p.308) and left to lay eggs. The plates were seeded fresh on the day of the egg laying. After about 1-2 hours (~50 eggs), the adult worms were removed and only the eggs remained. On day four (96 hours later), the worms were prepared for fluorescence microscopy as previously described (5.2.2.5 II. Confocal microscopy, p.307) using sodium azide (2 mM), to anesthetize the worms. On the slide, the worms (10-12) were orientated facing the same direction, using an eyelash. Excess azide was removed and the worms covered with a cover slide and sealed as previously described. Bright field (1.662 ms exposure time, ISO1600) images and fluorescence (ISO1600, GFP filter) images were taken for both, the vehicle and RSP extract treated animals with the same settings. However, fluorescence exposure time was set to a different value for each strain (CL2166, CF1553, LD1171), so that vehicle treated worms were barely visible; the same settings were used to analyse the RSP extract treated worms, to distinguish between their difference in intensity. Exposure time of the same strain in different experiments varied. Fluorescence intensity of each worm was measured using Fiji (ImageJ, 1.51n), divided by the total area of the respective animal. Statistical analysis was undertaken on the raw data, and after normalized to the mean of the vehicle treated worms for graphical representation. The results of one representative experiment are shown. A total of three biological replicates ($n=3$) with a total of ≥ 30 animals were analysed per strain.

5.2.2.8 Statistical analysis

Statistical analysis was carried out using GraphPad Prism 7. Specific methods used for statistical comparison of each experiment are detailed in the results section. At least 3 independent experiments (n) were analysed per assay, unless otherwise stated and results shown as mean \pm standard deviation. P-values below 0.05 were considered significant.

5.3 Results and Discussion

5.3.1 Toxicity/Food clearance assay

To test the extracts potential toxicity towards *C. elegans* the food clearance assay was employed. This assay had previously been used to test a whole library of individual compounds⁶¹⁶ as well as plant extracts³³¹. The RSP extract was tested with concentrations ranging from 0.01-5 mg/mL, together with two DMSO controls, 5%, known to be toxic to the worms and 1%, known to not cause any developmental delay or toxicity. The final concentration of DMSO in all RSP extract samples was similarly equal to 1%. Previously, the safe working concentration of DMSO ($\leq 1\%$) was determined using the same food clearance assay⁷⁹. The results obtained for the toxicity determination of the RSP extract in *C. elegans* (Figure 5.22) show that the extract is not toxic up to the tested maximum concentration of 5 mg/mL.

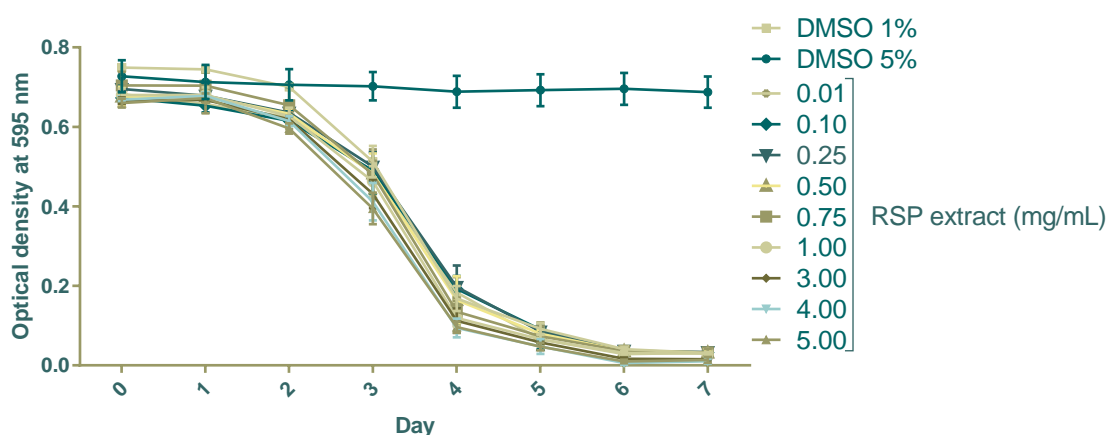


Figure 5.22 | Toxicity assessment of RSP extract (0.01-5.0 mg/mL) using the food clearance assay, DMSO as negative (1%) and positive (5%) control

The optical density curves for all the tested concentrations are consistent with the 1% DMSO control (—■), known to be safe for the animal⁷⁹. The food is being cleared in the expected manner, starting on day 2-3 where worms are between L3 and L4 of development. Further decrease in optical density on day 4 is associated with an increased number of worms in the wells, due to the number of progenies. The 5% DMSO control shows no clearing of the well, with an optical density around 0.75 throughout the entire experiment, confirming its toxic effect towards the model organism.

For the solvent DMSO, both mammalian cells and *C. elegans* nematodes showed similar susceptibility at concentrations over 1%. Hence, less than or equal to 1% DMSO is used as solvent. In contrast, the RSP extract was found to be less toxic in *C. elegans* than in SH-SY5Y cells (Figure 4.11 p.239). The use of immortalized cell line such as SH-SY5Y have previously shown false positives and negatives for toxicity determination and can often not be used to predict a response at the organism level^{589,682}. *C. elegans*, when compared to the SH-SY5Y cell line, provides an insight into *in vivo* toxicity, with the advantage of an intact and metabolically active digestive, endocrine, sensory, reproductive and neuromuscular system. In addition, some similarities in the mode of toxicity have been observed between *C. elegans* and mammals, e.g. the toxicity of organophosphate pesticides is linked to AChE inhibition^{589,683}. Although *C. elegans* also has its limitations as model organism for drug screenings (5.1.1.2 *C. elegans* for toxicity screenings, p.266), the toxicity evaluation was necessary to determine a safe working concentration for the RSP extract within the *C. elegans* model. Based on the toxicity results, all the subsequent experiments using RSP extract were performed using concentrations up to 5 mg/mL.

Other natural compounds/extracts have previously been tested for toxicity using the food clearance assay. Tsai *et al.*⁶⁸⁴ for example tested the toxicity of betulin, a naturally occurring triterpen found in the outer bark of birch trees with various biological activities. Concentrations up to 0.5 mM (0.22 mg/mL) were found to not cause developmental delay or toxicity in the model organism, when starting treatment in the L1 stage of development. In contrast, 2.5 mM (1.1 mg/mL) showed significant toxicity. In a report from Chalorak *et al.*⁶⁸⁵ the extracts from *Holothuria scabra* were found to be safe up to the highest tested concentration of 0.5 mg/mL. For different solvent extracts of the roots and leaves from *Damnacanthus officinarum* (Yang *et al.*⁶⁸⁶) 0.8 mg/mL were found to be acceptable as a safe concentration. One difference, between the food clearance assays undertaken in those references and our study, was the stage of development in which the assay was initiated, whilst Tsai *et al.*⁶⁸⁴, Chalorak *et al.*⁶⁸⁵ and Yang *et al.*⁶⁸⁶ all used L1s for the start of the experiment, in our study the treatment started in the egg stage of development. Personal preliminary analysis of different compounds using

both egg and L1 stage of development as starting point for the food clearance assay had indicated slight variations for some of the tested compounds when starting at different stages of development. Some compounds which were safe at certain concentrations showed developmental delay when starting the assay in the L1 stage, none of them however, showed extreme toxicity⁷⁹. Due to the fact that the following experiments would start treatment in the egg stage, the toxicity was also tested starting at the same stage of development. In general, the results indicate that *C. elegans* is tolerant towards the RSP extracts and all the tested concentrations can be taken forward for further experiments using the disease models.

5.3.1.1 Toxicity of sinapine and neostigmine in *C. elegans*

After identifying sinapine as one of the most abundant compounds in the RSP extract, also the toxicity of sinapine was tested in the food clearance assay, ranging from concentrations between 0.001 to 1.0 mg/mL. The toxicity of sinapine was determined, to identify safe concentrations for further studies on its effect in the disease model/s. Similar to the RSP extract, no toxicity of sinapine towards the model organism was found (Figure 5.23), even at double the concentration (1 mg/mL) of sinapine present in 5 mg/mL RSP extract (545.5 µg sinapine/5 mg RSP extract. For the following experiments (e.g. motility assay), concentrations of up to at least 1.0 mg/mL could be tested.

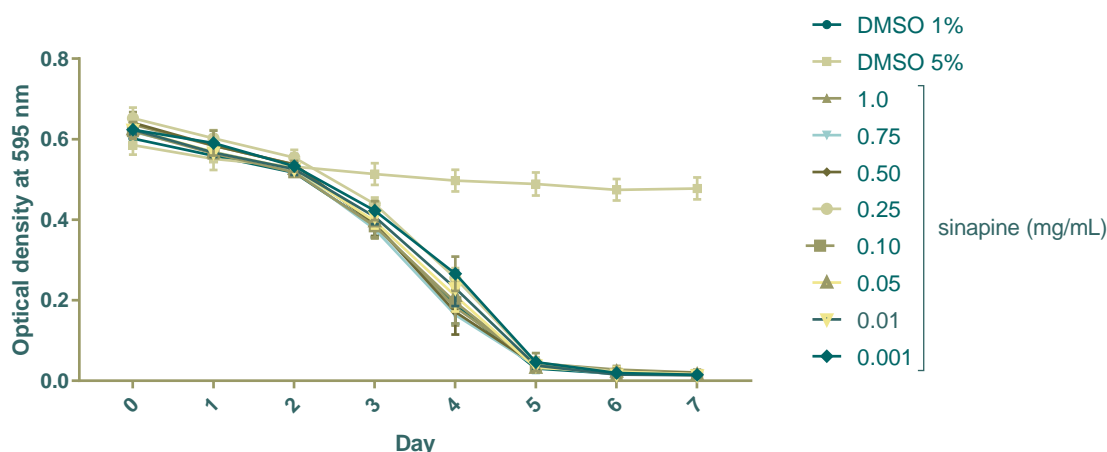


Figure 5.23|Toxicity assessment of sinapine (0.001-1.0 mg/mL) using the food clearance assay, DMSO as negative (1%) and positive (5%) control

So far there is limited research in the toxicity evaluation of sinapine in model organisms. As previously indicated, research using sinapine has been

undertaken in Asian countries, using rodent cerebral homogenate and blood serum as well as in the *Drosophila* model, but toxicity values were not provided^{401,403}. In the *Drosophila* model 10 and 50 mg/L (0.01 and 0.05 mg/mL respectively) of sinapine had shown increased longevity. In the rodent cerebral homogenate and blood serum also low concentrations showed AChE inhibition (3.66 μ M (1.13 μ g/mL) and 22.1 μ M (6.86 μ g/mL) respectively). Both studies used much smaller concentrations of sinapine than the concentration (1 mg/mL) tested here. In a different much older study in 1987, sinapine was found to have no depressive effect on the digestive and metabolic utilization in the diet of rats and did not show signs of toxicity towards the latter⁶⁸⁷.

Furthermore, also neostigmine in form of neostigmine bromide was subject to toxicity studies in *C. elegans*, for further investigations into the extract's potential mechanism of action, i.e. AChE inhibition. Neostigmine is a currently used drug (AChE inhibitor) for the treatment of myasthenia gravis, concentrations tolerated in patients are well known. Oral administration of 15-30 mg are commonly used for adults, that can be repeated for a total daily dose of between 75-300 mg. Subcutaneous injections or intramuscular injection use lower doses of between 1.0-2.5 mg, which are repeated to usually total daily doses of 5-20 mg (adults)⁶⁸⁸.

Just like for the extract and sinapine, all the tested concentrations (0.01-10 mM; 0.03-3.0 mg/mL) showed no toxicity towards the N2 animals (Figure 5.24). As no toxicity or developmental delay was observed, following concentrations up to 10 mM will be tested in the MJD model (AT3q130).

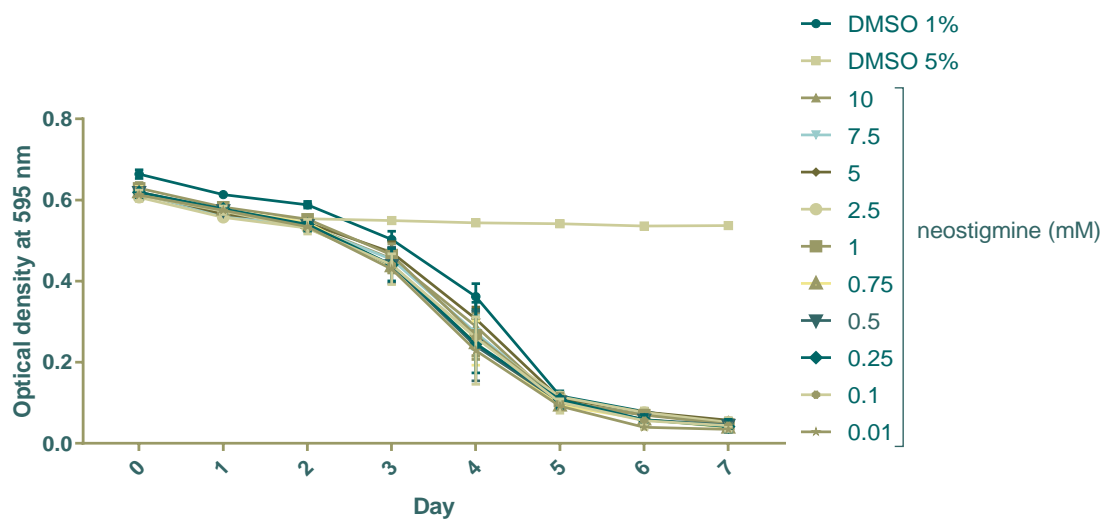


Figure 5.24| Toxicity assessment of neostigmine (0.01-10 mM) using the food clearance assay, DMSO as negative (1%) and positive (5%) control

In a paper by Kalinnikova *et al.*⁶⁸⁹, toxic effects of neostigmine were seen in worms' in form of paralysis only at very high concentrations of neostigmine (≥ 6 mM). This toxic effect was assessed using the worms' motility ability. The food clearance assay in comparison assesses toxicity *via* the development of the nematode, using food consumption as read out. During this experiment the worms are not assessed on the motility behaviour. The slightly different toxicity results in our and Kalinnikovas study can be explained by the two different methods used. In general, both studies agree that very high concentrations of neostigmine are necessary to show toxic effects in *C. elegans*. To verify the findings by Kalinnikova *et al.*⁶⁸⁹ all concentrations (0.01-10 mM) were take forward for further studies in the MJD model. This might verify an increased locomotion defect, when using high concentrations of neostigmine, which was not detected using the food clearance assay, with the latter determining toxicity *via* development and fecundity.

5.3.2 Machado-Joseph disease *C. elegans* model

The first neurodegenerative disease model used to assess the potential of the RSP to prevent/treat neurodegenerative disease was the MJD model. Preliminary studies using the same model and RSP extracts (SOX and UAE-ethanol/water 95/5%, 2012 RSP harvest) had shown improvement in the motility deficient phenotype using an automated system, to track the movement of worms in liquid media (swimming behaviour)⁷⁹. To determine if the same positive outcome could be repeated when assessing the worms crawling behaviour, here the manual motility assay was employed and AT3q130 animals treated with the RSP extract. In addition, also the impact of the RSP extract on the ataxin-3 aggregation load in the neurons was assessed.

5.3.2.1 Motility assessment of RSP extract treated AT3q130 strain

Since the concentrations of RSP extract up to 5 mg/mL were found to be safe for *C. elegans* in the toxicity assay, RSP extract concentrations ranging from 0.1 to 5 mg/mL were used to determine their effect on the MJD model. All but the smallest concentration (0.1 mg/mL) tested showed a positive dose dependent improvement of the motility deficient phenotype (Figure 5.25).

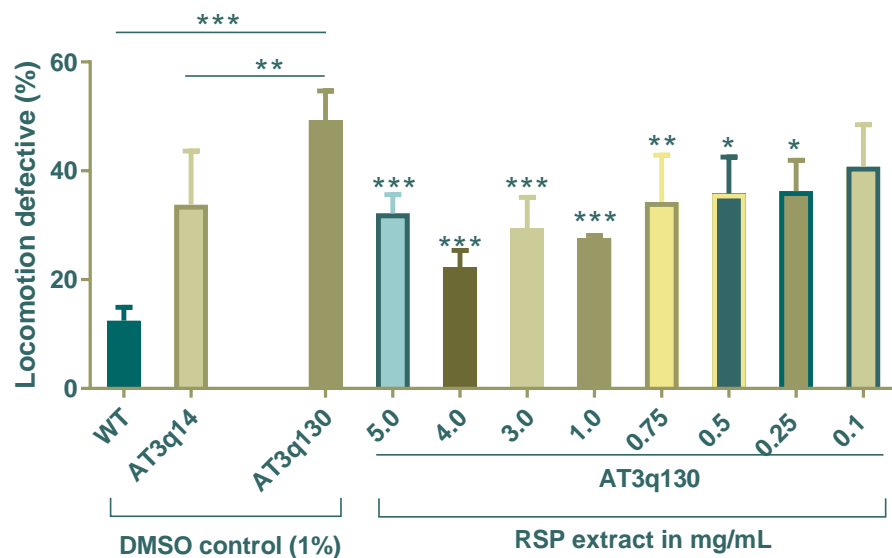


Figure 5.25| RSP extract improves locomotion defective behaviour of MJD (AT3q130) animals

Comparison between treated (RSP extract 0.1-5.0 mg/mL) and untreated animals (1% DMSO solvent control) in comparison to wild type (N2) and AT3q14 controls (1% DMSO). Statistical significant difference was determined using One-way ANOVA and Bonferroni's multiple comparison analysis compared to AT3q130 control: *** $p \leq 0.001$, ** $p \leq 0.01$, * $p \leq 0.05$, $n = 5$

The highest RSP extract concentrations (1.0-5.0 mg/mL) showed the best motility improvement with $p \leq 0.0006$. At the lower concentrations (0.25, 0.5 and 0.75 mg/mL RSP extract) this significance was reduced as expected ($p < 0.05$ but $p > 0.001$). At 0.1 mg/mL the significance was lost ($p > 0.05$), however a slight improvement in motility was still observed for the mean values i.e. untreated 49.31% compared to 40.76% for 0.1 mg/mL RSP treated animals.

To determine whether the presence of sinapine within the RSP extract could be responsible for the seen motility improvement, concentrations of sinapine ranging from 0.001 to 1.00 mg/mL sinapine were tested in the motility assay using the MJD (AT3q130) model (Figure 5.26).

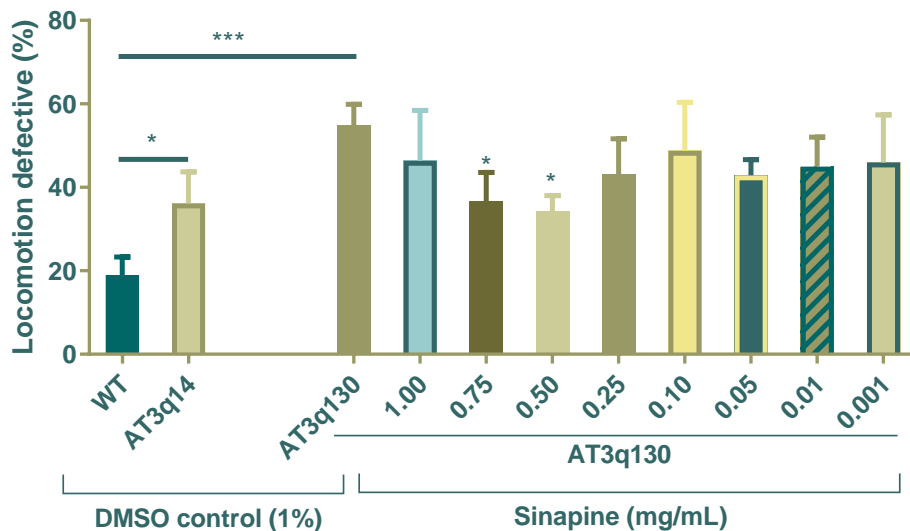


Figure 5.26| Sinapine shows limited positive effect in MJD strain (AT3q130)

Locomotion defective behaviour of AT3q130 animals, comparison between treated (sinapine 0.001-1.00 mg/mL) and vehicle treated (DMSO (1%) solvent control) animals in comparison to wild type (N2) and AT3q14 controls (1% DMSO). Statistical significant difference was determined using One-way ANOVA and Bonferroni's multiple comparison analysis compared to AT3q130 control: * $p < 0.05$, *** $p < 0.001$, $n = 5$

Only two of the tested concentrations of sinapine (0.75 and 0.50 mg/mL) showed a significant improvement of the phenotype. This improvement however was not as significant as some of the RSP extract concentrations i.e. $p \leq 0.05$ (e.g. 0.5 mg/mL sinapine) compared to $p \leq 0.001$ (e.g. 4 mg/mL RSP extract) (Figure 5.25, p.317). Interestingly, the tested concentrations that showed significant difference (0.50 and 0.75 mg/mL) are equivalent to 4.58 and 6.87 mg/mL of RSP extract respectively. This is comparable to the results

seen with the RSP extract where significant motility improvement was demonstrated at 4.0 and 5.0 mg/mL concentrations. RSP extract concentrations above 5.0 mg/mL were not tested, due to lack of toxicity data. These results indicated that the sinapine within the RSP extract could be partially responsible for the positive activity in the MJD model. The lower improvement ($p > 0.01$) from sinapine when compared with the RSP extract, may be due to the presence of other compounds within the RSP extract contributing to the activity. Further studies into the identity of compounds, whether already known (3.3.3 LC-MS/MS analysis of final RSP extract, p.170 ff. or 3.3.4 Additional secondary metabolite analysis, p.175 ff.) or not would be necessary to fully elucidate the mode of action of the RSP extract.

Only limited research information is available on this MJD model since this strain is not currently available from the CGC. However, a few other compounds have shown to improve the locomotion defective phenotype. In Teixeira-Castro *et al.*⁶¹⁴ both valproic acid (6 mM) and 17-(dimethylaminoethyl- lamino)-17-demethoxygeldanamycin (17-DMAG (1 and 10 μ M), induces heat shock response) showed improvement of the phenotype. Valproic acid from 71.75% to 37.9% on day 10 of adulthood and 17-DMAG from around 40% to 20% in 4 day old animals. In a more recent study by the same group a commercially available compound library, containing mainly FDA/EMA-approved drugs, was screened for potential drug candidates for MJD in *C. elegans*. Throughout that study 48 compounds, with different specific pharmacological activity, such as modulators of neurotransmission (adrenergic 14%, serotonergic 14%, cholinergic 4%, dopaminergic 4% and histaminergic 5%), anti-infectious (14%), cardiovascular (9%), anti-inflammatory (9%), analgesic (4%), hormone-related (7%) and other actions, were found to induce more than 50% improvement⁶¹⁶. With an improvement from a mean of 49.31% for the AT3q130 model to 22.29% for AT3q130 animals treated with 4 mg/mL of RSP extract, improvement of the locomotion defect was more than 50% and so fits into the above mentioned criteria.

To determine whether the effect from the RSP extract was disease specific, also N2 (WT) and AT3q14 (AT3WT, normal length of q repeats in ataxin-3) animals were treated with the RSP extract (Figure 5.27), at a concentration

(4 mg/mL) that showed the best results in the MJD model (Figure 5.25 p. 317).

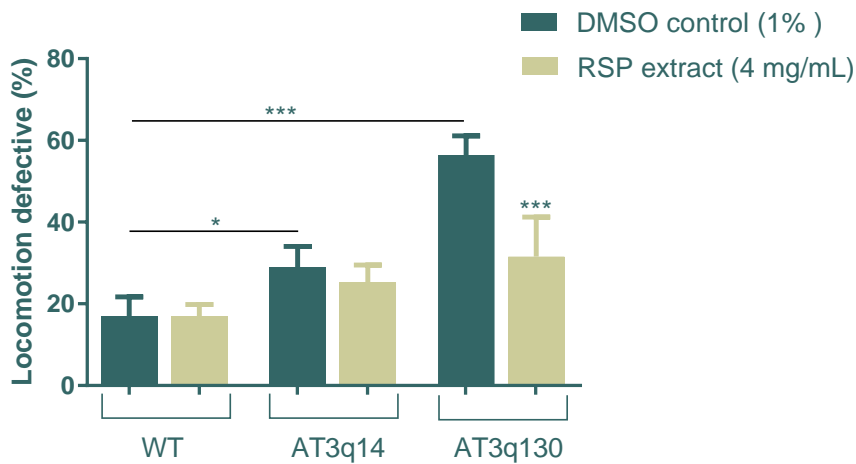


Figure 5.27 | RSP extracts effect on MJD strain is disease specific

Comparison of locomotion defective behaviour of N2, AT3q14 and AT3q130 untreated (1% DMSO vehicle control) and RSP extract treated (4 mg/mL) animals. Statistical significant difference determined using One-way ANOVA and Bonferroni's multiple comparison analysis compared to AT3q130 control: *** $p \leq 0.001$, * $p \leq 0.05$, $n = 6$

The results obtained, show that neither the wt animals ($p > 0.999$) nor the AT3q14 ($p = 0.761$) animals are significantly affected by the presence of the RSP extract, whereas the MJD model is ($p < 0.001$). Therefore this observation leads to the conclusion, that the effect is disease specific, targeting mutant ataxin-3 mediated pathogenesis as described in Teixeira-Castro *et al.*⁶¹⁶ regarding their hit compound citalopram. To determine whether the observed motility improvement is associated with a decrease in the number or the area of ataxin-3 aggregations, animals were also studied using confocal microscopy methodology as discussed following.

5.3.2.2 Ataxin-3 aggregation load after RSP extract treatment of AT3q130 animals

To determine if the observed positive activity of the RSP extract is related to a change in the number or the area of protein aggregations in AT3q130 neurons *in vivo*, confocal microscopy imaging was undertaken. The results obtained are presented in Figure 5.28 (p.321). In this study no significant changes in either number or the area of ATXN3 aggregates (per total area) were observed. This suggests that the RSP extract has a different mode of action when compared to e.g. citalopram in the identical model, where a decrease in number and/or area of aggregates was reported together with

and increased ATXN3 solubility (assessed by biochemical fractionation). However, these changes were not associated with an overall change in protein levels of ATXN3⁶¹⁶.

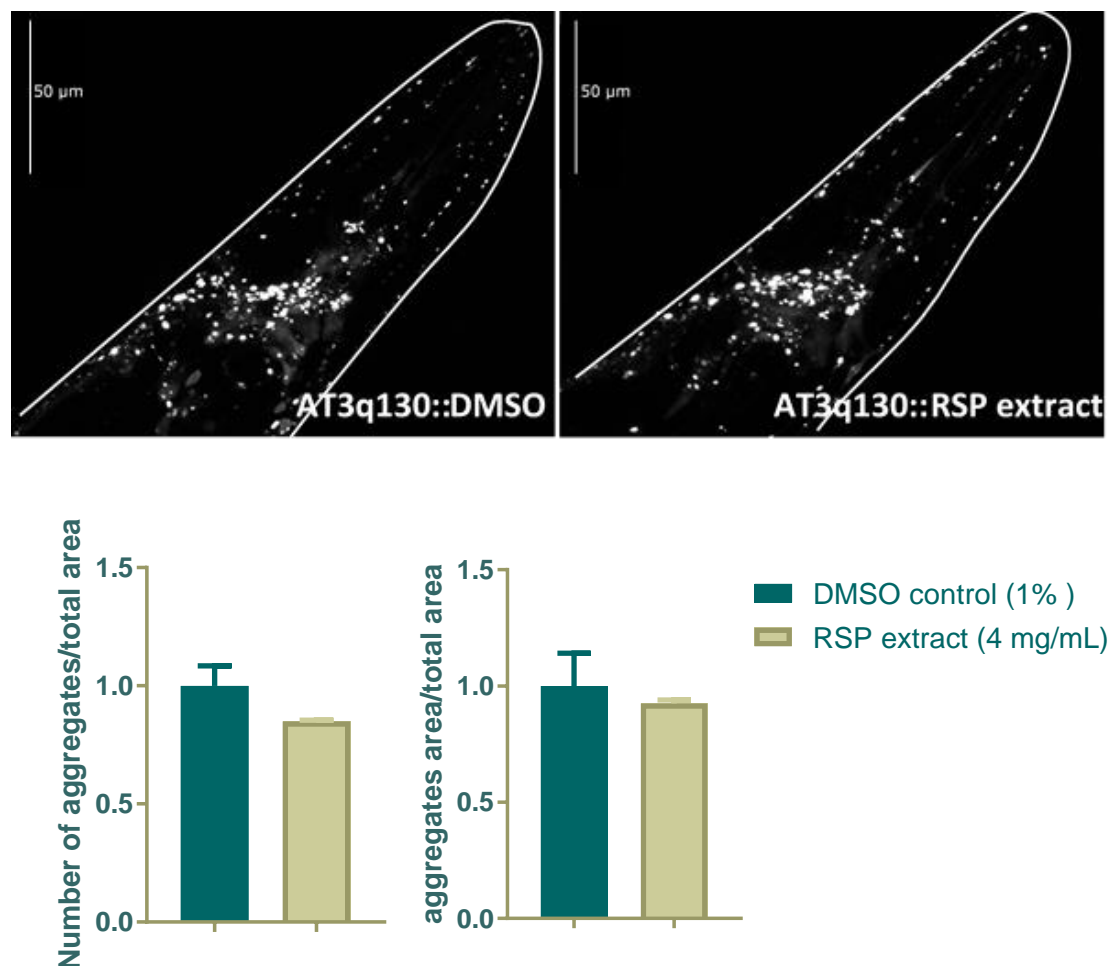


Figure 5.28| No changes in the ataxin-3 aggregation load induce by RSP extract in the MJD model

Aggregation load (number and area of aggregation) of AT3q130 animals upon treatment with RSP extract (4 mg/mL) compared to solvent control (1% DMSO). For aggregate quantification: $n \geq 10$ number of animals per experiment, $n = 3$ number of experiments, no significant difference, $p > 0.05$ (ANOVA, Bonferroni's multiple comparisons test). Data normalized to the 1% DMSO control. Confocal microscopy pictures are representative for the three independent experiments; confocal imaging by Andreia Teixeira-Castro.

Considering the previously undertaken *in vitro* studies ("3. Phytochemical Characterisation and Neuroprotective Properties of RSP Extract", p.133 ff.), other potential modes of action can be identified and tested in the *C. elegans* model system. Previously, the RSP extract for example showed antioxidant and radical scavenging activity indicating their direct antioxidant activity (3.3.2 Antioxidant activity of final RSP extract, p.168 ff.). In addition the

extract might also exhibit indirect antioxidant activity (through the activation of Nrf2/skn-1, followed by phase II enzymes see 1.4.3 Exogenous antioxidants - natural products: direct and indirect antioxidant activity, p.58 ff. and 5.1.3 Determination of potential pathways of action using *C. elegans* as model organism, p.280 ff.), as previously shown for other natural products^{54,224,690}. This hypothesis was further investigated in "5.3.5 *In vivo* study of antioxidant activity: the indirect antioxidant activity pathway theory". In addition, *in vitro* analysis also indicated AChE inhibition activity by the extract/sinapine, which could also be responsible for the seen motility improvements and this was further investigated as discussed following.

5.3.3 AChE inhibition hypothesis

Two different approaches were initiated (pharmacological and pharmacogenetic) to verify the AChE inhibition hypothesis (5.1.3 Determination of potential pathways of action using *C. elegans* as model organism p.280 ff.). The pharmacological approach used the treatment of AT3q130 worms with neostigmine (AChE inhibitor), whereas the pharmacogenetic model employed AChE knock out strains crossed with the AT3q130 model.

5.3.3.1 Pharmacological approach using neostigmine as AChE inhibitor *in vivo*

For this approach neostigmine was employed, to evaluate whether AChE inhibition could be responsible for the observed motility improvements with the RSP extract in the AT3q130 model. Neostigmine is a well-known AChE inhibitor used in the clinic for the treatment of myasthenia gravis, and was also applied as positive control in the *in vitro* analysis of AChE inhibition activity of the RSP extract (3.3.6 AChE inhibition potential, p.194). The food clearance assay (Figure 5.24, p.316) showed no toxicity of neostigmine towards *C. elegans* up to 10 mM. Therefore, neostigmine concentrations from 0.01 to 10 mM were applied in the motility assay initially (Figure 5.29, p.323).

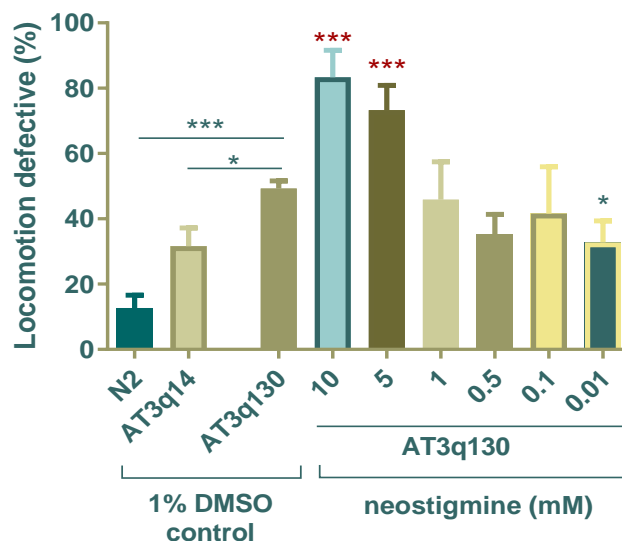


Figure 5.29| Locomotion defective behaviour of AT3q130 animals after neostigmine treatment

Comparison between treated (neostigmine 0.01-10 mM) and untreated animals in comparison to wild type (N2) and AT3q14 controls. Statistical significant difference determined using One-way ANOVA and Bonferroni's multiple comparison analysis compared to AT3q130 control: *** $p \leq 0.001$, ** $p \leq 0.01$, * $p \leq 0.05$, *** $p \leq 0.001$ (increase of motility deficiency, worsening of phenotype) $n=5$

Although 10 mM neostigmine did not show to have an effect on the worm's development and fecundity (Figure 5.24), there is a significant increase in locomotion defect when treating AT3q130 animals with this concentration. The locomotion defect increases significantly from $49.32 \pm 2.32\%$ (■) to $83.37 \pm 8.28\%$ (■ $p < 0.0001$). A worsening effect on the phenotype is also visible for 5 mM (■ $73.27 \pm 7.58\%$, $p = 0.0004$). Similar results were obtained by Kalinnikova *et al.*⁶⁸⁹, where 6, 12, 24 mM neostigmine (90 minute exposure) showed increasing uncoordinated behaviour while swimming, after mechanical stimulus) due to aldicarb-like toxic effects.

Interestingly at lower neostigmine concentrations (0.1-1.0 mM) non-significant difference between treated and untreated animals was observed. Only at 0.01 mM (■) a significant ($p = 0.0225$) positive improvement of the locomotion behaviour was observed. Due to the improving phenotype at the lowest concentration of neostigmine, further studies were initiated that included 10 μM (0.01 mM), 1 μM and 0.1 μM (Figure 5.30).

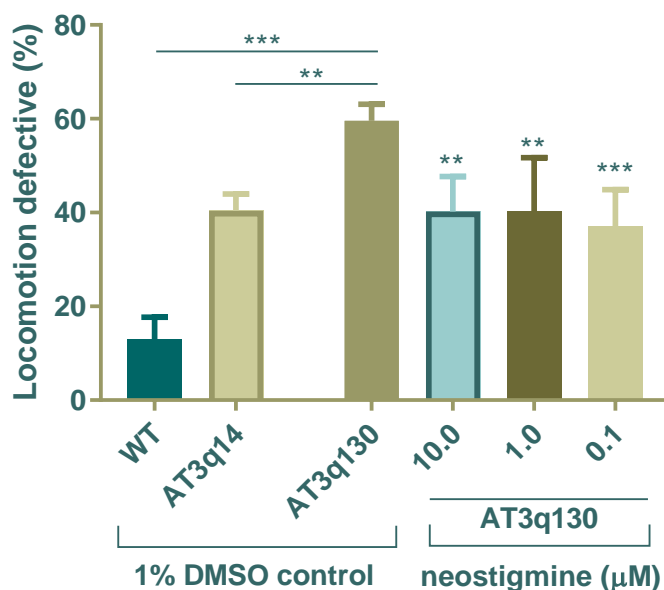


Figure 5.30| Locomotion defective behaviour of AT3q130 animals after lower concentrations of neostigmine treatment

Locomotion defective behaviour of AT3q130 animals, comparison between treated (neostigmine 0.1-10 μM) and untreated animals in comparison to wild type (N2) and AT3q14 controls. Statistical significant difference determined using One-way ANOVA and Bonferroni's multiple comparison analysis compared to AT3q130 control: *** $p \leq 0.001$, ** $p \leq 0.01$, $n = 5$

The results obtained for the lower neostigmine concentrations demonstrated significant motility improvement of the AT3q130 model for all 3 tested

concentrations (0.1, 1.0 and 10.0 μM). However, this improvement (ATq130 59.55% compared to between 37.0-40.2% for the neostigmine treatment) is not as significant as seen for the RSP extract treatment (Figure 5.25, p.317). Literature research on the potential use of AChE inhibitors for the treatment of MJD is very limited. In a small (21 participants) double-blind, triple-crossover trial of oral physostigmine in inherited ataxias, published by Kark *et al.* in 1981⁶⁹¹, physostigmine showed to be more effective than the placebo. More than half of the patients (13) showed statistically significant responses to physostigmine. However, the results were not consistent, certain aspects of ataxia improved in some patients, whereas other aspects improved in other patients. This report was a follow up on a study published in 1977 by the same lead Author, where similar positive results were observed⁶⁹². In contrast, in a later study (1997) using physostigmine, by Wessel *et al.*⁶⁹³, no significant effect on cerebellar symptoms were detected when using a transdermal system (patch). Of note, in both studies by Kark, oral administration was used. Those results seem to be contradicting and no further research into other AChE inhibitors was found during literature review.

Considering the outcome of our *C. elegans* study here, the hypothesis, that the RSP extract's AChE inhibition activity could be responsible for the improved motility phenotype, cannot be negated. To further shed light on this hypothesis, also a pharmacogenetic approach was employed, which is described following.

5.3.3.2 Pharmacogenetic approach using two *C. elegans* mutants (knock out) for the AChE gene

The two strains (*ace-1* and *ace-2*), used to determine whether the extract's AChE inhibition potential might be responsible for the motility improvement in the MJD model of *C. elegans*, were obtained from the CGC (Table 5.5). The strains acquired from the CGC had to be back crossed, before crossing them with the AT3q130 model. To perform either of the crosses, the PCR protocol had to be optimized, so the genotype of backcrossed animals could be identified. The results for the PCR optimization for *ace-1* and *ace-2* (short), the outcrossing and the crossing with the AT3q130 disease strain are detailed in the appendix (subsection A5, p.458 ff.)

Motility analysis

After successful crossing of AT3q130 and *ace-1* and *ace-2* mutant strains, motility testing was conducted to either prove or disprove the AChE hypothesis through pharmacogenetics methodology. Figure 5.31 represents the motility results obtained for the motility assays with (A) AT3q130;*ace-1* and (B) AT3q130;*ace-2* double mutants.

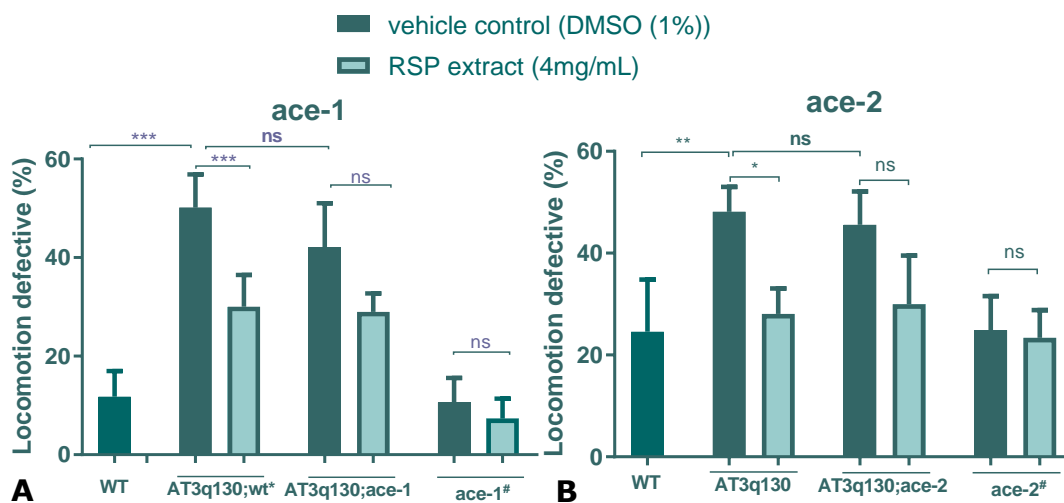


Figure 5.31 | Locomotion defective behaviour of AT3q130 animals compared to double mutant

A: AT3q130;*ace-1*, B: AT3q130;*ace-2* treated (RSP extract (4 mg/mL)) and untreated (DMSO (1%)), including controls (WT, *ace-1/2* 6xBC (treated and untreated)). *AT3q130/wild type animals for *ace-1* gene obtained after crossing, #*ace-1/2* mutants (6xBC). Statistical significant difference determined using One-way ANOVA and Bonferroni's multiple comparison analysis: *** $p \leq 0.001$, ** $p \leq 0.01$, * $p \leq 0.05$, $n = 5$

The results for the motility assays, done using the AT3q130/*ace-1/2* cross, are inconclusive. The improvement for the AT3q130;wt to the RSP extract treated animals is still significant for both experiments and verifies previously obtained results (Figure 5.25, p.317). However, the difference between the AT3q130;wt animals and the AT3q130/*ace-1/2* worms is not significant (ns), suggesting that knock out of the *ace-1* gene, which is responsible for approximately half of the AChE production in *C. elegans*, or *ace-2* does not have a significant effect on the AT3q130 motility deficiency. However, although the difference is not significant, there is a visible trend towards reduced motility impairment, with e.g. mean values of 50.12% and 42.11% for AT3q130;wt and AT3q130;*ace-1* respectively, which could indicate a minor involvement of AChE activity in the phenotypic behaviour

improvement. When treating the double mutants with the RSP extract also no significant difference was detected compared to the untreated control (DMSO (1%)). This is most likely due to the relatively large standard deviation seen for most of the strains/conditions e.g. the AT3q130;ace-1 animals ($42.11 \pm 8.895\%$). To test whether the ace-1/2 worms have a motility deficient phenotype themselves, they were also tested, treated and untreated. Statistical analysis comparing WT (N2) to ace-1 and ace-2 worms did not show any significant difference in locomotion behaviour ($p > 0.9999$) in our assay, although Melstrom and Williams⁶⁴⁹ had previously suggested a decrease in the rate of movement for ace-1 animals. This might be due to the sensitivity of the used experiment. Here a manual motility assay was used (5.2.2.5 I Motility determination, p.306) whereas in Melstrom and Williams a tracking system was used which can monitor 50-80 worms simultaneously to determine the average distance of movement per worm per second in μm . Furthermore, as previously shown for WT and AT3q14 animals, the RSP extract is not able to significantly improve the motility behaviour of the mutants (ace-1 and ace-2) motility behaviour. The AT3q130;wt, obtained after the crossing with ace-1, shows the same phenotype as the AT3q130 used in the previous experiments, with means and standard deviations of $50.12 \pm 6.75\%$ and $49.31 \pm 5.351\%$ (Figure 5.25, p.317) respectively. This suggested that for further experiments the regular AT3q130 worms could be used. For the ace-2 motility assays the AT3q130 and not the from the back crossing obtained AT3q130;wt was used, because the stain was lost during a freezer shut down. To verify the results with the back crossed version, further crosses (AT3q130xace-2) will be initiated and the motility assay repeated, to verify the results.

In general, the results obtained from both these motility assays using the double mutant strains together with the neostigmine data are inconclusive. Although neostigmine showed a significant improvement of the motility deficient phenotype (Figure 5.30, p.324), both double mutants showed a lacked of significant changes (Figure 5.31, p.326). However, the fact that in both cases a slight trend towards motility improvement was observed led to the conclusion that AChE might play a role in the effect observed by the RSP extracts but further investigation is required. No comparison to previous

literature can be done, as this is the first study looking into the importance of AChE inhibition *via* drug treatment and decreased expression *via* gene knockout in the context of MJD.

To further investigate our hypothesis, it would be useful determine if the RSP extract can actually decrease the AChE activity *in vivo* within the MJD model as well as in wild type (N2) animals. To do so either the Amplex Red Assay kit or the Ellman's assay could be employed, after lysis of worm pellets to determine the AChE activity in worms untreated (DMSO (1%)) compared to treated (RSP extract) animals in conjunction with control animals treated with an AChE inhibitor (e.g. neostigmine) or the mutant strains. Different time point of treatment should be considered, as previously mentioned (4.3.2 AChE inhibition study by RSP extract in SH-SY5Y cells, p.256). The Ellman assay has previously been used to determine AChE activity in *C. elegans* by Shashikumar *et al.*⁶³⁶. The latter used the assay to show that induced inhibition of AChE activity by 6-OHDA, can be recovered by co-incubation with alpha-linolenic acid. Similarly the AChE activity Amplex Red Kit has been used previously⁶⁹⁴. In addition, it would be interesting to create triple mutants of both AT3q130;ace-1 and AT3q130;ace-2 animals with ace-3. The addition of knocking out an extra gene encoding approximately 5% more AChE⁶⁴⁵, in *C. elegans*, might lead to an additional improvement which could turn out to be significant. In contrast, the creation of a triple mutant using AT3q130, ace-1 and ace-2 would most likely not be useful, due to the fact that the double mutant (ace-1;ace-2) are relatively uncoordinated⁶⁴⁸ and so might interfere with the already motility impaired AT3q130 model.


5.3.4 Parkinson's disease *C. elegans* model

To determine the activity of RSP extract in an additional model of neurodegenerative disease in *C. elegans*, three PD models were selected. One was chemically induced (6-OHDA) and two were genetically induced, age dependent, models (UA57(CAT-2) and UA44(α -syn)). All three can be characterised by a significant loss of dopaminergic neurons compared to control strains (BZ555). The results obtained from these strains after treatment with RSP extract (4 mg/mL, Figure 5.25 p.317) together with untreated (1% DMSO, solvent control) conditions are presented following.

5.3.4.1 Chemical induced PD model using 6-OHDA

For the investigation of dopaminergic (DAergic) neuronal loss the mutant BZ555 strain was employed, in which the DAergic neurons can be visualized using fluorescence microscopy, due to their co-expression of GFP in combination with the Pdat-1 promoter. This *C. elegans* model, treated with 6-OHDA (chemical inducer of DAergic neuronal loss), has previously been used in a number of publications. Reports show varying conditions of treatment (i) different concentrations of 6-OHDA, (ii) different treatment times and (iii) the presence or absence of ascorbic acid^{618,684,695,696}. Due to these varying protocols, the assay first had to be optimized (data not shown). The use of both 10 and 25 mM 6-OHDA together with ascorbic acid, 2 and 5 mM respectively, exhibited a significant phenotype for the loss of DAergic neuron (Figure 5.32 F and G). In conclusion, these concentrations were used for further analysis of the RSP extracts potential to prevent the induced neuronal loss.

The results obtained for the study on the RSP extract's DAergic neuron protection potential are presented in Figure 5.32 (p.331), showing confocal imaging (A-E) as well as graphical representation of the three independent experiments (F and G). The graph represents an overview of the mean values for each of the independent experiments for each strain/condition.

For each experiment 10 or more animals were scored per strain and treatment (F and G). The left graph (F) in Figure 5.32 shows the total number of DAergic neurons (total of 8: 4 CEP, 2 ADE and 2 PDE) found in control animals treated with the control solvent (DMSO (1%) ) , in comparison to

the animals treated with both concentrations of 6-OHDA (10 mM and 25 mM). Looking at these three bars reveals a clear dose dependent DAergic neuronal loss after 6-OHDA induced stress. This phenotype was rescued, when pre- and post-treating the animals with the RSP extract (4 mg/mL) for both concentrations of 6-OHDA (10 mM and 20 mM). A similar effect was seen when only looking at the four CEP neurons (G Figure 5.32). In both cases the effect is more significant when introducing higher concentrations of 6-OHDA (25 mM). To determine whether even higher concentrations of 6-OHDA would show an increased DAergic loss, 30 and 50 mM were tested in the initial optimization process, but either of them led to developmental delay or morphological changes of the worms. Counting the DAergic neurons in these worms would not have been reliable, as the absence of DAergic neurons could be due to the 6-OHDA treatment or the developmental delay or morphological changes. In comparison, at the chosen 10 and 25 mM the animals developed normally in comparison to control animals. The most obvious DAergic loss after treatment with 6-OHDA was observed in the CEP neurons, together with the loss of CEP neuron dendrites, which are highlighted by the arrow in Figure 5.32 (A-E, p.331). To verify this observation graphically the percentage of animals with intact CEP, ADE and PDE neurons are plotted in Figure 5.33 (p.332). The biggest differences were seen when animals were treated with 25 mM 6-OHDA, where 78% (mean) of worms still showed intact ADE and PDE neurons, but only 37% exhibited intact CEP neurons. Already Nass *et al.*⁶¹⁹ identified the higher sensitivity of CEP neurons towards 6-OHDA (CEP>ADE>>PDE), showing earliest and most detected morphological changes occurring in the CEP processes/dendrites. Both, the dendrite and cell body loss of CEP neurons were prevented with RSP extract treatment (Figure 5.32, p.331).

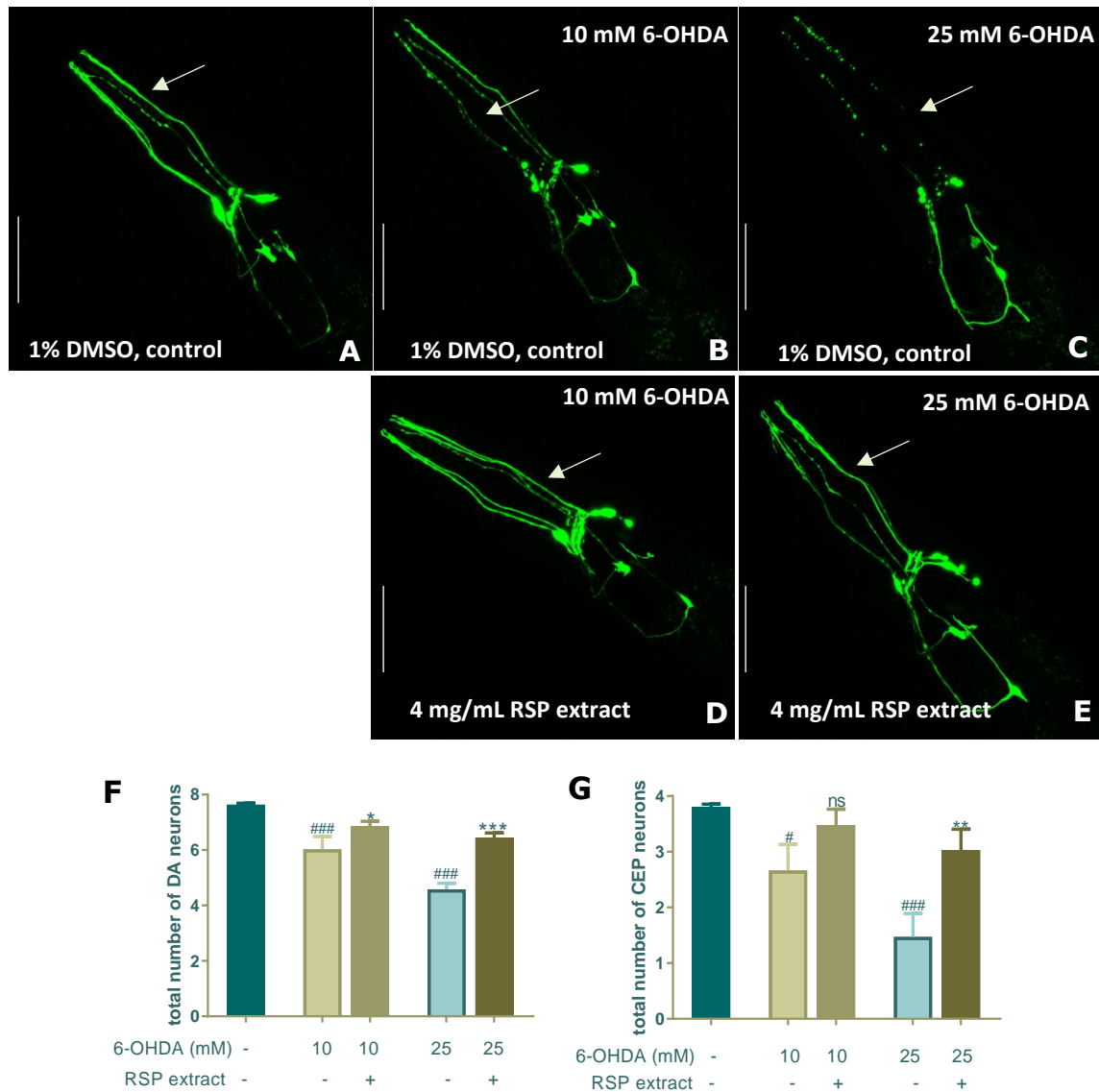


Figure 5.32| Protective effects of RSP extract on the DAergic neurodegeneration in *C. elegans*

GFP expression of treated/untreated transgenic strain BZ555 (*Pdat-1::GFP*) (A)-(C) 1% DMSO (solvent control) treated BZ555 with; A 0 mM 6-OHDA and 0 mM AA, B 10 mM 6-OHDA and 2 mM AA, C 25 mM 6-OHDA and 5 mM AA. (D)-(E) 4 mg/mL RSP extract pre- and post- treated BZ555; D 10 mM 6-OHDA and 2 mM AA, E 25 mM 6-OHDA and 5 mM AA. The fluorescence signals of DAergic neurons (CEP and ADE) were photographed using confocal fluorescence microscopy. (F) Total number of DAergic neurons and (G) total number of CEP neurons in treated/untreated transgenic strain BZ555. Significant differences were determined by One-way ANOVA and Bonferroni's multiple comparison analysis, # $p < 0.05$, ### $p < 0.001$ compared with vehicle alone (no 6-OHDA), * $p < 0.05$, ** $p < 0.01$ and *** $p < 0.001$ compared with respective 6-OHDA control, $n \geq 10$ for each independent experiment ($n = 3$). Scale bar 50 μm in all represented pictures; confocal imaging and neuron counting by Andreia Teixeira-Castro.

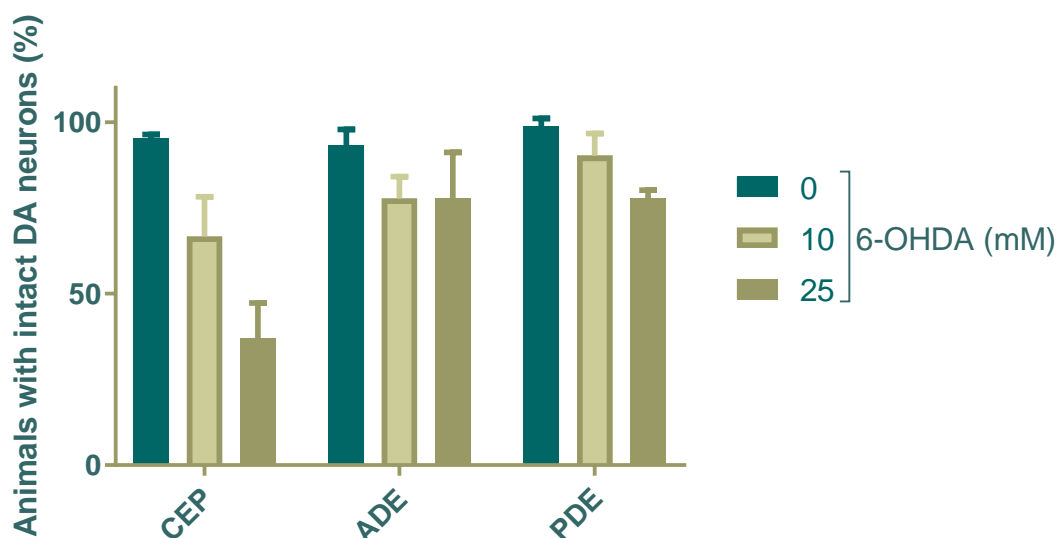


Figure 5.33| DAergic neuron loss is dependent on 6-OHDA concentration as well as class of DAergic neurons

Same data as in Figure 3.37 F and G, distinguishing between the three classes of DAergic neurons and their susceptibility to 6-OHDA

As with previous results so far, there has been no literature evidence that identifies the positive effects of RSP extract on PD models of *C. elegans*. However, this model was used with other natural extracts/compound and they showed similar effects as the RSP extract. Li *et al.*⁶⁹⁶ for example observed, that polysaccharide from *Astragalus membranaceus*, a Chinese medicine, were able to decrease 6-OHDA (50 mM and 10 mM AA) induced neurotoxicity (DAergic neuron loss) in the same model of *C. elegans* (BZ555). Similar positive results were also found for (i) alpha-linolenic acid (ALA)⁶³⁶, a plant-derived dietary polyunsaturated fatty acid (using UA44 animals in conjunction with 6-OHDA), (ii) methanolic extracts of red seaweed (*Chondrus crispus*, using UA57 animals in conjunction with 6-OHDA)⁶⁴² and (iii) betulin⁶⁸⁴, a triterpene found in the outer bark of birch trees for 6-OHDA induced PD model and for (iv) a methanol extract from *Sorbus alnifolia*⁶⁴¹ in a MPP⁺ induced PD *C. elegans* model. A very interesting recent article by Chalorak *et al.*⁶⁸⁵ also used the BZ555 6-OHDA model (50 mM). They were able to show that *Holothuria scabra* (sea cucumber, found in the Indo-Pacific region including Thailand) extracts also presented the potential to protect DAergic neurons from 6-OHDA induced damage. Three (whole body-butanol, whole body-ethyl acetate, body wall-ethyl acetate) of their six extracts showed this protection. Even more interesting however is the fact that they also employed Levodopa, a common used drug to treat PD in human patients.

Levodopa provided the best protection from 6-OHDA induced damage. Levodopa increases the concentration of dopamine in the cells and might so lead to a decreased uptake of 6-OHDA into *C. elegans* DAergic neurons.

These very positive results from the RSP extract in the chemical induced PD model then led to further investigation into the effect of the RSP extract on two additional genetic models, the results of which are described following.

5.3.4.2 Two genetic Parkinson's disease *C. elegans* models

The two additional *C. elegans* PD models UA44 and UA57 (5.1.2.2 *C. elegans* models of Parkinson's Disease, p.272) used in this project, are age dependent phenotypes, with DAergic neuron loss occurring towards the middle of their life. Both strains showed a significant DAergic neuron loss phenotype on day 7 (Figure 5.34, p.335, A₇). The same analysis was repeated for day 10 old animals (Figure 5.34, p.335 A₁₀). In this case, again both strains show a decreased number of DAergic neurons when compared to the BZ555 control. For easier visualization of data, all the worms from the 3 independent experiments were drawn together with n≥30 animals per strain and One-way ANOVA with Bonferroni's multiple comparison was used to determine significant differences between the strains. When analysing the results, while taking replicates and independent experimental trials into consideration, two-way ANOVA also showed a significant statistical difference between the strain. However, this difference was not seen for all the independent trials (Bonferroni's multiple comparison analysis). The lack of significant difference for each trial is probably due to the very small and limited number of DAergic neurons. Thus, this experiment was repeated three times.

Surprisingly there does not seem to be a big difference between the number of surviving DAergic neurons on day 7 compared to day 10 (Figure A18, p.463). This may be due to the fact that it was not possible to analyse the same animals on day 7 and 10. In addition, this is also the time of *C. elegans* life span, when worms are starting to die due to their natural life cycle a limited number of worms is available. Another explanation for this phenomenon was the fact that potentially worms scored on day 10 were healthier (survival till day 10), which might be associated with a smaller loss of DAergic neurons. Taken together, this could explain why there is no

significant difference between day 7 and day 10 old animals (Figure A23, p.466).

When treating both strains from the start of their development (egg stage) till day 7 (Figure 5.34, p.335 B₇), the RSP extract treated animals showed a decreased loss of DAergic neurons. Again, for easier graphical presentation, the total number of worms were plotted and analysed together, with $n \geq 30$ per treatment condition. The RSP extract treatment was significant for both strains, UA44 ($p \leq 0.05$) and UA57 ($p \leq 0.001$). As mentioned previously when analysing the results grouped for trials and treatment, two-way ANOVA showed a significant treatment effect. Which was not present in each trial separately, which is why we decided to run 3 independent experiment.

In contrast, when treating the animals till day 10, both strains show a significant difference between vehicle and RSP extract treated worms of $p \leq 0.001$ (Figure 5.34, B₁₀). This is most likely cause by the lower standard deviation of the results on day 10.

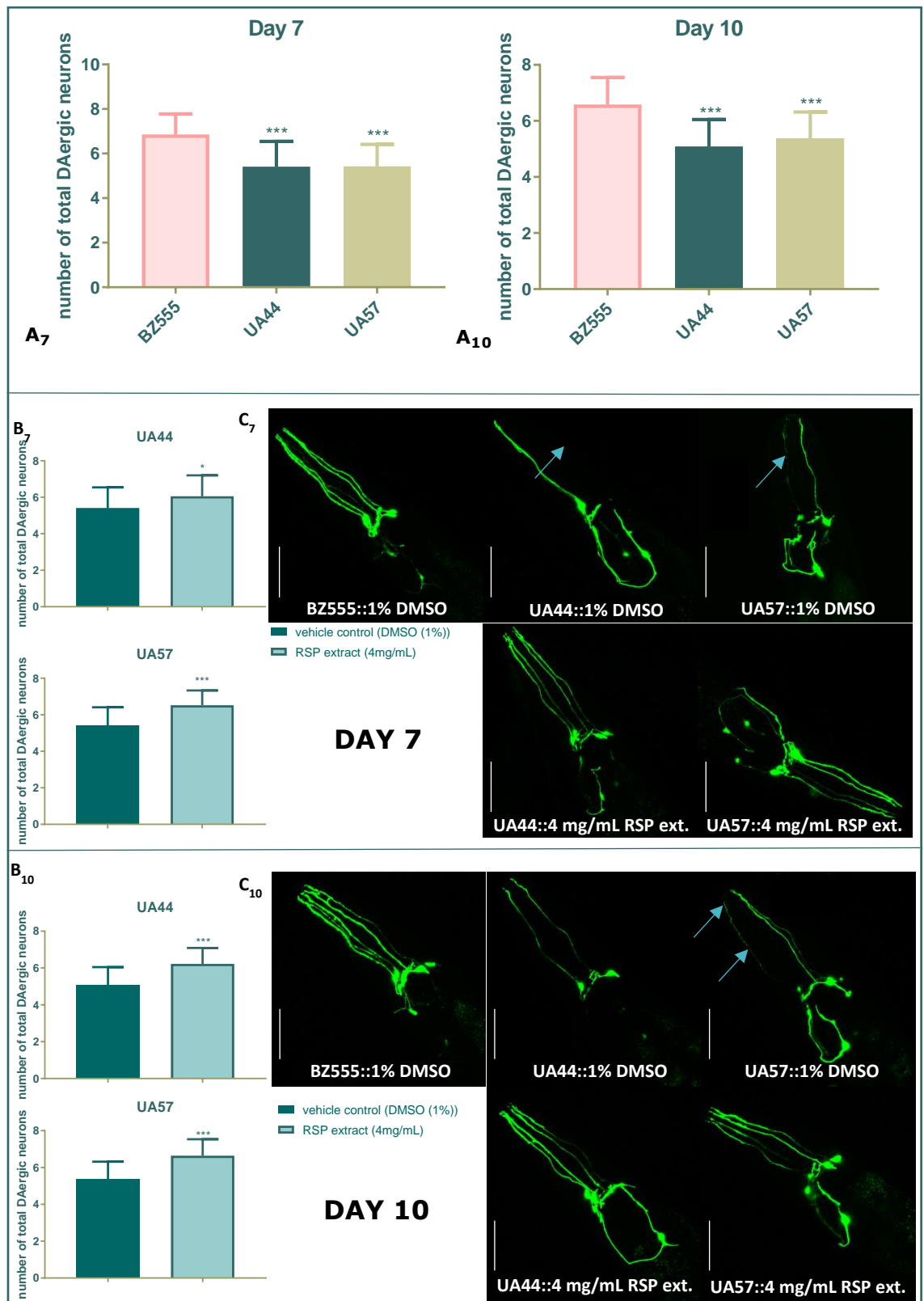


Figure 5.34| Effect of RSP extract treatment in genetic *C. elegans* PD strains

Dopaminergic neuron cell count for BZ555 (control), vehicle treated (1% DMSO) as well as UA 44 and UA57, vehicle (1%DMSO) and RSP extract (4 mg/mL) treated on day 7 (top) and 10 (bottom). Data are expressed as the mean \pm std. of all worms ($n \geq 30$)

with results obtained from three independent experiments ($n \geq 10$ each). A_{7+10} : comparison between the three strains indicates age dependent neuronal loss for UA44 and UA57 on day 7 and 10, B_{7+10} : comparison between untreated (1% DMSO) and treated (4 mg/mL RSP extract) disease strains (UA44 and UA57). Right (C_{7+10}): Confocal microscopy pictures, showing CEP neurons, the pictures are representative for the three independent experiments. Blue arrows indicating dendrite loss, blebbing and abrupt gaps. Scale bar 50 μm in all represented pictures. Significant differences between the three strains (A_7+A_{10}) were determined by One-way ANOVA and Bonferroni's multiple comparison analysis. For statistical analysis of the treatment unpaired *t*-test (two-tailed) was undertaken for each strain, $*p < 0.05$ and $**p < 0.01$, $***p < 0.001$. Confocal imaging and neuron counting by Andreia Teixeira-Castro.

The same can be observed for both time points in the confocal images (Figure 5.34 C_{7+10}). BZ555 animals clearly showed the presence of the four CEP neurons with their dendrites intact. In contrast both UA44 and UA57 animals had lost some of the CEP neurons and dendrite, showed blebbing and abrupt gaps or breaks in the dendrites on day 7 (top) and 10 (bottom). The animals pre-treated with the RSP extract show less CEP neuron and dendrite loss.

It is noteworthy to mention that this is the very first reported evidence that demonstrates the use of RSP extract to alleviate PD related DAergic neuron loss in *C. elegans* strains. However, other natural compounds have previously been tested and shown positive results. For example in a paper by Büttner *et al.*⁴⁷⁰ spermidine (polyamine), was found to show DAergic neuron protection in the α -synuclein strain (UA44). In addition, it also showed positive effects in a α -synuclein *Drosophila melanogaster* model of PD. Also, valproic acid (synthetic compound) has been found to induce DAergic neuron protection in the UA44 strain. In general, reported literature on the UA44 strain is limited, probably partially due to the fact that this strain is not available through the CGC, but can only be obtained from the laboratory where the strain was created (Caldwell lab). Although the UA57 strain is available through the CGC, research using natural compound in this model is nevertheless still limited but a few studies were found in the literature. For example, methanolic plant extracts from *Sorbus alnifolia*⁶⁴¹ and *Chondrus crispus*⁶⁴² (red seaweed, using UA57 animals in conjunction with 6-OHDA) showed protective properties. In a very recent study by Manalo and Medina⁶⁹⁷, caffeine was found to protect DAergic neurons against degeneration promoted by excessive dopamine production through over expression of tyrosine hydroxylase.

In previous experiments (5.3.3 AChE inhibition hypothesis) it was shown that the AChE inhibition hypothesis cannot be negated in the MJD model, however

results were not positive enough to evaluate the same AChE inhibition hypothesis in the PD model. In addition to its AChE inhibition activity however, the RSP extract also possesses valuable direct antioxidant activity *in vitro* and was able to reduce ROS production in H₂O₂ stress induced SH-SY5Y neuroblastoma cells, which can be associated with its antioxidant activity. This led to the second hypothesis (5.1.3 Determination of potential pathways of action using *C. elegans* as model organism, p.280 ff.), that the observed positive effect of the RSP extract on the disease strains, may be caused by its antioxidant property.

5.3.5 *In vivo* study of antioxidant activity: the indirect antioxidant activity pathway theory

To test the hypothesis whether the RSP extracts antioxidant activity is responsible for all or at least some of the observed positive phenotypical improvements in the 4 different disease models (1 MJD, 3 PD) two methods were employed. One made use of reporter strains, which show increase GFP fluorescence in association with increased expression of certain genes of interest (5.3.5.1 *C. elegans* reporter strains). The second method entails the use of a knockout strain, in which one of the important genes necessary for oxidative stress resistance and detoxification (*gst-4(ko)*) is knocked out. The latter was crossed with the genetic disease model (UA44) to determine whether the gene in question (*gst-4*) is required for the activity of the RSP extract.

5.3.5.1 *C. elegans* reporter strains for antioxidant related genes

Antioxidant activity can either be direct or indirect (1.4.3 Exogenous antioxidants - natural products: direct and indirect antioxidant activity p.58 ff.). The RSP extract has previously demonstrated direct antioxidant activity in several *in vitro* experiments (3.3.2 Antioxidant activity of final RSP extract, p.168 ff.). To determine whether the extract also exhibits indirect antioxidant activity *in vivo*, three *C. elegans* reporter strains for stress response genes (*sod-3*, *gst-4* and *gcs-1*) were employed. Worms were treated with the extract from the egg stage till adulthood and were then analysed using fluorescence microscopy while comparing to vehicle treated (DMSO (1%)) control animals. Fluorescent imaging and the intensity analysis of one of the independent experiments are depicted in Figure 5.35 (p.339).

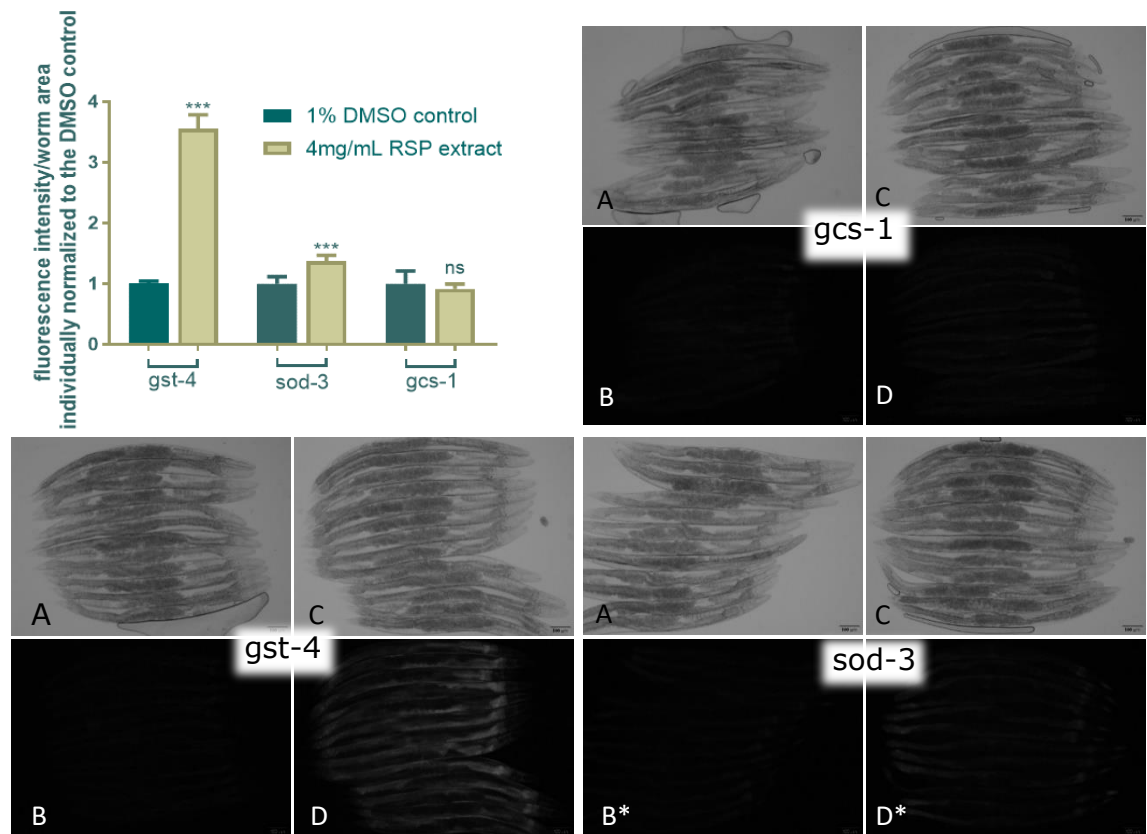


Figure 5.35|RSP extract treatment activates antioxidant pathways *gst-4* and *sod-3* in *C. elegans*

Graphical results of the fluorescence intensity divided by the total area of each worm ($n \geq 9$) normalized to the respective pathway 1% DMSO control, statistical comparison via Two-way ANOVA and Bonferroni's multiple comparisons test. The graph shows one representative example of the three experimental replicates. The pictures and the graph presented are from the same experimental day and represent all three pathways, *gst-4*, *sod-3*, *gcs-1*. A: bright field image of 1% DMSO control, B: GFP fluorescence picture of 1% DMSO control, C: bright field image of 4 mg/mL RSP extract treated animals, D: GFP fluorescence pictures of 4 mg/mL RSP extract treated animals. 10x objective, ISO 1600, exposure time set according to DMSO control (worm outlines barely visible), scale bar (bottom right corner in light microscopy pictures) 100 μ m, *for better representation depicted in larger size in the appendix (Figure A24, p.467)

The graph (top left) in Figure 5.35 presents the results obtained for the reporter strains, each strain normalized to its respective DMSO control. The results are shown for one of the three independent experiments. The additional two experiments showed very similar results. The graph as well as the microscopy pictures (*gst-4* B compared to D) indicate a significant ($p \leq 0.001$) activation of *gst-4* in the reporter strain in comparison to the DMSO (1%) control. The fluorescence intensity is more than 3 times higher. Also *sod-3* is significantly activated after treatment with the RSP extract, however the activation is not as visual as for the *gst-4* reported. In the fluorescent microscopy pictures for *sod-3* (Figure 5.35 bottom right and Figure A24,

p.467) a slight activation can be observed in the tail and head region of the animals. In contrast to *gst-4* and *sod-3*, no activation of *gcs-1* was observed.

These results suggest that the RSP extract not only has direct antioxidant properties but can also exert indirect antioxidant activity, *via* the activation of antioxidant pathways *in vivo* within *C. elegans*. However, only certain pathways appear to be significantly activated (*sod-3* and *gst-4*). Similarly curcumin (20 μ M) has been shown to increase the expression of *gst-4*, however it did not significantly induce *sod-3*⁶⁶⁴. The same was true for garlic-derived thioallyl compounds S-allylcysteine (SAC) and S-allylmercaptocysteine (SAMC) as reported by Ogawa *et al.*⁶⁶⁶. Also coffee extracts showed an increase in the expression of *gst-4* reporter strain in Dostal *et al.*⁶⁶⁵. When using a different reporter strain (MJCU032 {kEx32 [*gst-4p::gfp*, pDP#MM016B]}), Hasegawa *et al.*⁶⁹⁸ showed that also allyl isothiocyanate, found in wasabi can induce *gst-4* expression. Although some of the previously mentioned compounds were not able to induce *sod-3* expression there are other natural compounds that do, e.g. flavonoids quercetin, kaempferol and naringenin also found in the RSP extract⁶⁹⁹. Naringenin was tested for its direct antioxidant activity in the FRAP and the DPPH assay in this project and was found to have no or very little activity (2.3.11 Determination of antioxidant activity of single compounds within the extract as well as their mixtures, p.127 ff.), suggesting that compound do not necessarily need to have direct antioxidant activity to show indirect activation of antioxidant pathways. However, some compounds and extracts appear to have both direct and indirect activity^{700,701}.

For better understanding of these antioxidant pathways it is important to know, that harmful compounds such as juglone, paraquat and H₂O₂ can activate these pathways. However, at high concentrations these compounds can be harmful for the organism. In contrast, the RSP extract can induce these pathways without causing adverse effects, e.g. not toxicity and negative impact on fecundity or motility behaviour were observed (Figure 5.22, p.312, Figure 5.25, p.317). Furthermore, the RSP extract even improves the observed devastating phenotypes (motility deficiency and DAergic neuronal loss). Further studies are necessary to determine exactly which compound/s in the extract is/are responsible for the activation of the

gst-4 and *sod-3* antioxidant genes. The first compound that should be tested in this endeavour is sinapine, as it is the most abundant compound in the RSP extract. Fu *et al.*³⁹⁶ had shown that sinapine from *Brassica rapa var. rapa L* was able to increase SOD/CAT activation after a decrease caused by carbon tetrachloride (CCl₄, hepatotoxin) in mice.

The strong expression increase of *gst-4*, suggests the importance of this gene for the RSP extracts activity. To further investigate whether *gst-4* activation is necessary to observe the positive effect of the RSP extract treatment, further studies using a *gst-4* knock out (ko) strain were undertaken, which are described following.

5.3.5.2 Determination of the significance of the *gst-4* gene on the RSP extracts effect using a *gst-4* knock out strain

After determining the activation of *gst-4* and *sod-3* using the reporter strains above, the aim of the subsequent experiment was to determine whether the modulation these genes are necessary for the positive effect in the disease models after RSP extract treatment. Due to the fact that the *gst-4* activation was more significantly increased than the *sod-3* activity the decision was made to test the importance of *gst-4* first. To do so a *gst-4* knockout (*gst-4* (ko)) strain was obtained from the CGC (5.1.3.2 Antioxidant and detoxification pathway, p.282). The received strain was not back crossed and had to go through the same procedure as *ace-1* and *ace-2* previously (5.3.3.2 Pharmacogenetic approach using two *C. elegans* mutants (knock out) for the AChE gene, p.325 ff.) using the method described in "5.2.2.3 Backcrossing and creation of double mutant strains-"worm crossings"" (p.292 ff.). After obtaining the 6xBC *gst-4*(ko) strain, it was crossed (Figure 5.18, p.300) with the UA44 (PD) disease model, to obtain double mutants, lacking the gene for the expression of *gst-4*. This double mutant strain was thereafter tested for DAergic neuronal morphology with the treatment of RSP extract and under control conditions (1% DMSO).

DAergic neuron loss and its prevention using RSP extract in UA44;gst-4(ko) double mutants

To determine whether *gst-4* expression is necessary for positive effect of the RSP extract in the PD model, animals were treated as previously described on NGM plates. In addition to the BZ555 (control) and the UA44 (control for DAergic neuron loss) this time also the double mutant was analysed for DAergic neuronal loss under vehicle (DMSO (1%)) treated conditions. Both UA44 and UA44;*gst-4*(ko) were also treated using the RSP extract (4 mg/mL) (Figure 5.36).

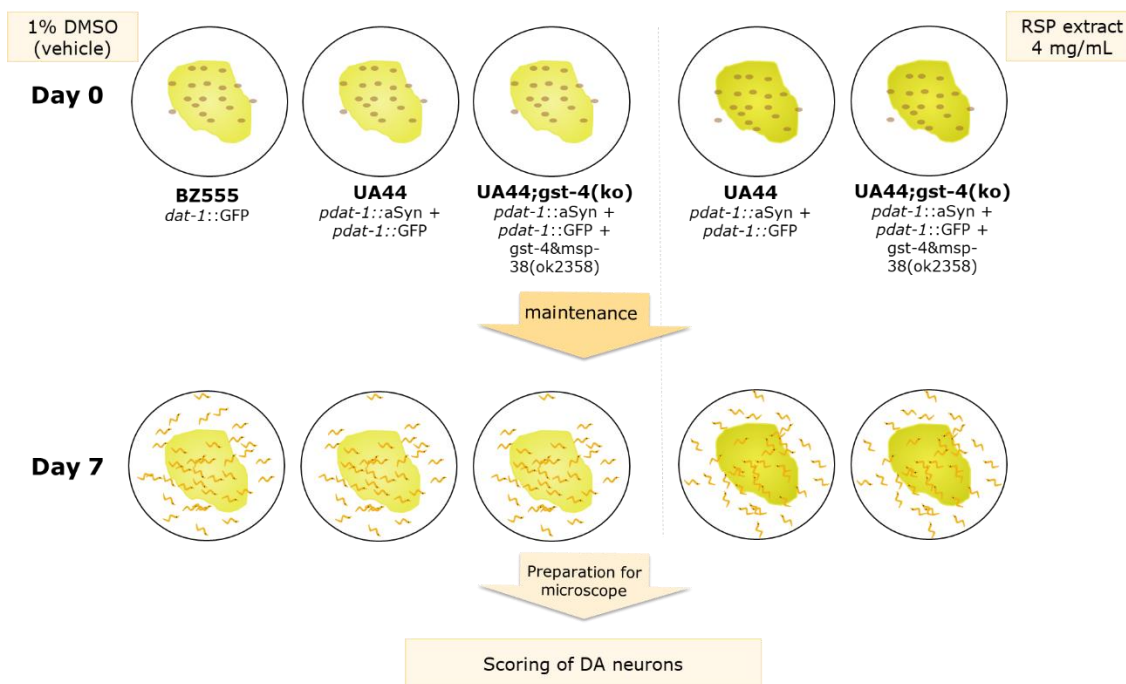


Figure 5.36| Conditions and strains used to determine the RSP extracts dependence on *gst-4* in the UA44 strain

In the previous experiment, when assessing the DAergic neuron loss of both UA44 and UA57, there was no significant difference between day 7 and day 10 old animals, therefore only day 7 old animals were assessed following (Figure A23, p.466).

Figure 5.37 (p.343) presents the results obtained as mean±standard deviation off the total number of worms ($n \geq 24$), collected from 2 independent experiments ($n \geq 12$ each). The number of experiments was reduced, due to the high significance observed after only 2 independent experiments. The knockout of the *gst-4* gene however does not appear to have an impact on the neuronal phenotype of the UA44 strain, hence no significant difference

was observed between UA44 and UA44;*gst-4*(ko) DMSO (1%) treated animals. As previously shown, the RSP extract treatment is able to reduce the DAergic neuronal loss significantly in the UA44 strain ($p \leq 0.001$). In contrast, when treating UA44;*gst-4*(ko) animals with the RSP extract, the number of DAergic neurons is not significantly higher than the number of DAergic neurons for the vehicle treated animals (Figure 5.37).

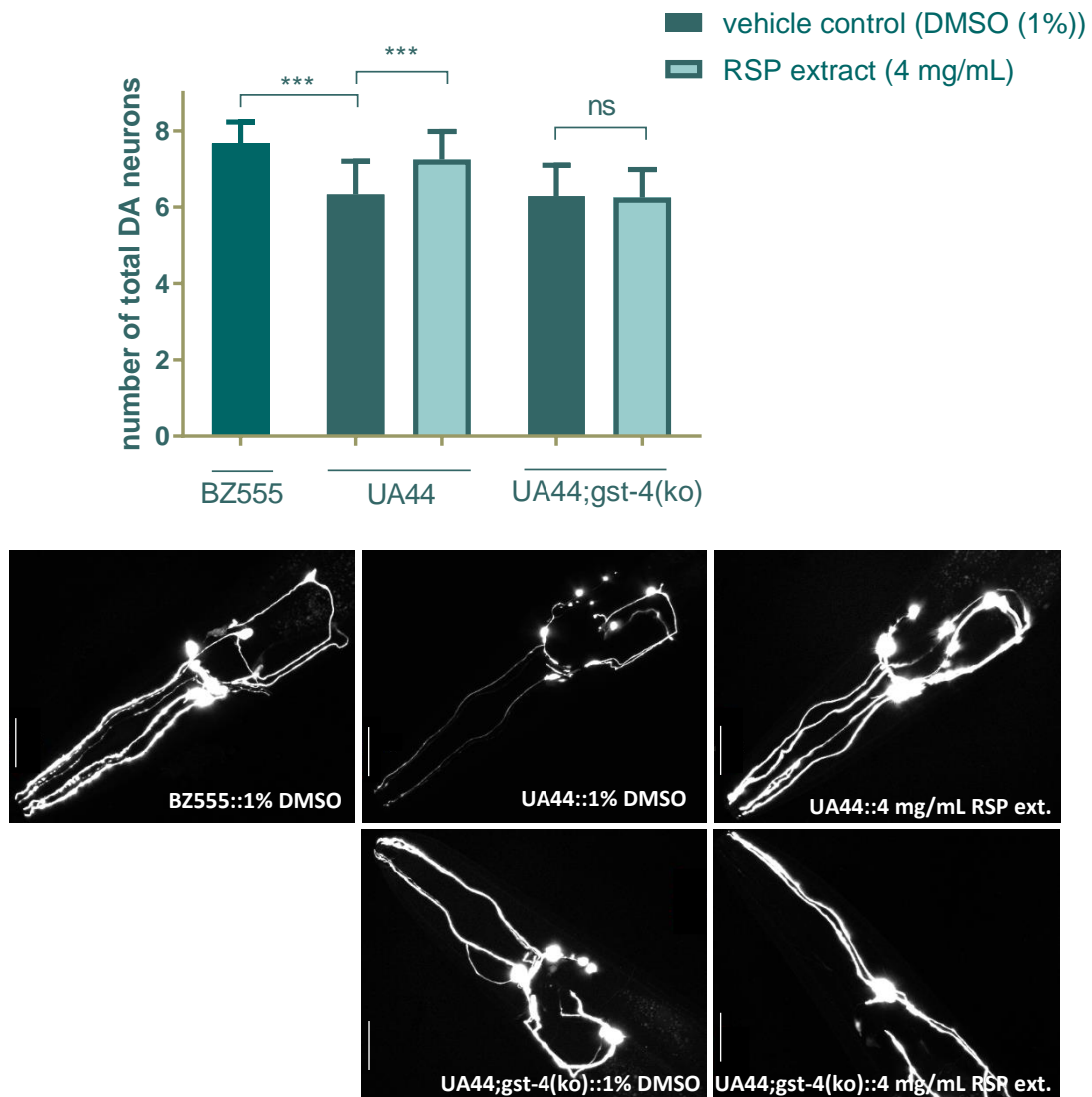


Figure 5.37 | Protection of DAergic neurons in UA44 strain dependent on *gst-4* activation

DAergic neuron loss in BZ555, UA44 and UA44;*gst-4*(ko) animals comparing treated (RSP extract (4 mg/mL) and untreated (DMSO (1%))). Top: 2 independent experiments (n) were conducted with 12 replicates per strain each. For statistical analysis all 24 worms per condition were accumulated. Statistical significant difference was determined using One-way ANOVA and Bonferroni's multiple comparison analysis: *** $p \leq 0.001$. Bottom: confocal imaging of DA neurons, scale bar 30 μ m. Confocal imaging and neuron counting by Andreia Teixeira-Castro, experimental set-up by Victoria Lindsay.

These results clearly suggest the strong dependence of the DAergic neuronal protection of the RSP extract on the activation of *gst-4*. In the absence of the gene, no protection is observed. Further studies using an *AT3q130;gst-4(ko)* double mutant are currently under investigation, to determine if *gst-4* activation is also necessary for the improved motility in the MJD model.

Literature research indicated a lack of current knowledge in this area, no publications were found indicating the activation of *gst-4* by RSP extracts or the importance of *gst-4* activation as the pathway of action of PD/MJD medical treatment. Hence, these findings are extremely interesting, as they do not only present the potential application of RSP extract in the prevention or treatment of neurodegenerative disease, but they also indicate the importance of antioxidant/detoxification pathways in neurodegeneration. This could lead to the search of additional *gst-4* activators with the potential to treat/prevent PD/MJD or even other neurodegenerative disease, since oxidative stress has been associated with most of them^{192,702}.

Further research is required to investigate through which pathway *gst-4* is activated in *C. elegans* by the RSP extract. Although *gst-4* is often associated with the activation of transcription factor *skn-1* (Nrf2, Figure 1.29, p.60) there are however other potential pathways by which it can be activated e.g. through the epidermal growth factor (EGF) signalling pathway that was responsible for activation of *gst-4* by royalactin (Figure 5.38, p.345) as presented by Detienne *et al.*⁶⁶⁰.

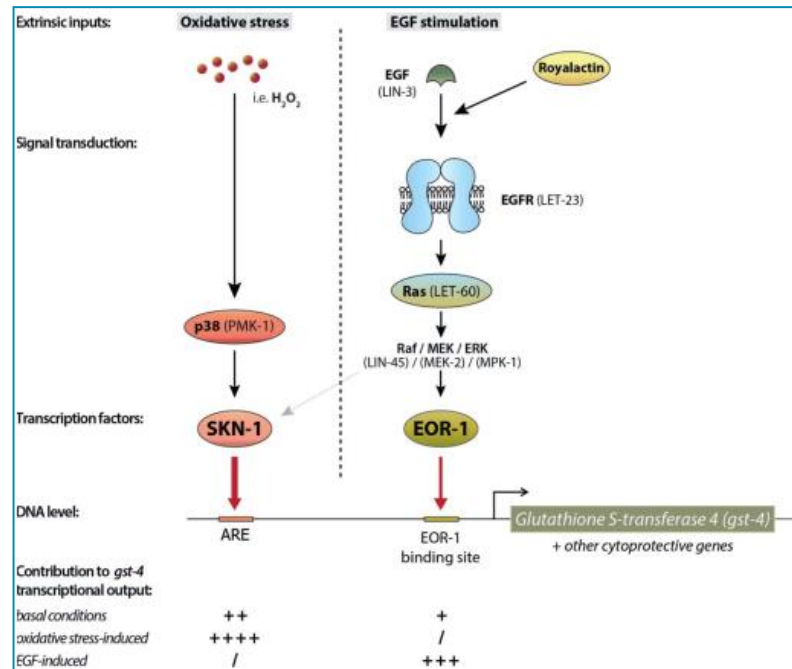


Figure 5.38 | Activation pathway of *gst-4* through epidermal growth factor (EGF) signalling by royalactin

Reprinted with permission from Taylor and Francis from Detienne *et al.*⁶⁶⁰

Additional quantitative real-time PCR of the genes of interest or western blot analysis of protein expression could shed further light on the issue of pathway elucidation. One paper by Chege *et al.*²⁰⁶ elegantly summarizes most of the results obtained throughout our project for the PD models, in written as well as in graphical form (Figure 5.39). They highlighted the three different PD models (6-OHDA, CAT-2 and α -synuclein) used here and how they induce DAergic neuronal damage through the production of ROS followed by lipid, protein and DNA/RNA damage. In addition, some mechanisms of potential counter action are presented, one of which is activation of GST (Figure 5.39), but also includes correct metal homeostasis. *In vitro* studies of the RSP extract showed its copper chelating properties, which might add to the extracts activity *in vivo* by keeping copper homeostasis in check.

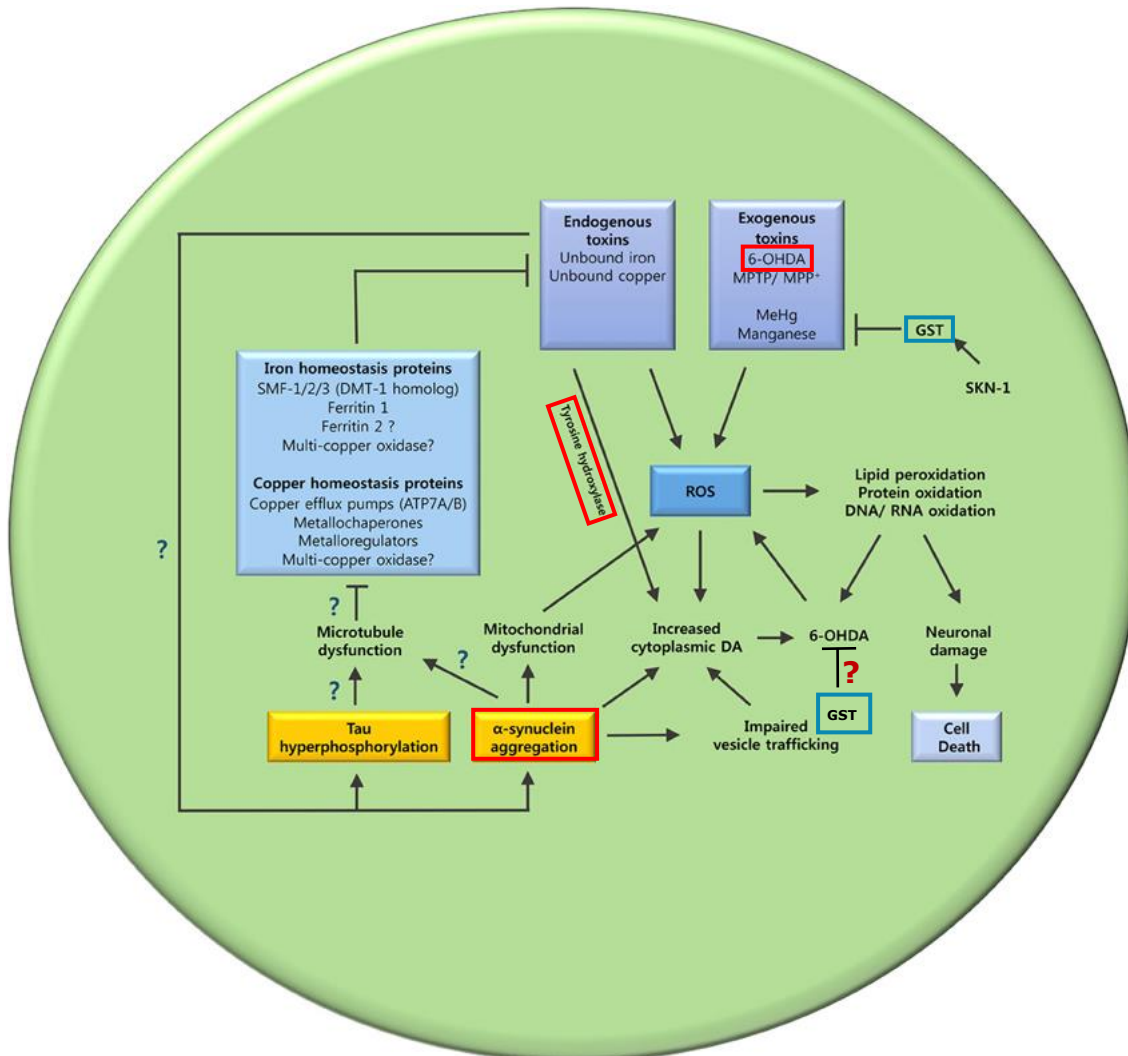


Figure 5.39| Oxidative stress and metal homeostasis implications in PD

Reprinted (minor modifications) with permission by corresponding author Gawain McColl from Chege and McColl²⁰⁶

5.4 Conclusion/Future Work

The *in vivo* experiments, using *C. elegans*, regarding the RSP extract treatment have shown very interesting and promising results. Whilst indicating no toxicity towards the model organism up to 5 mg/mL, the RSP extract was able to partially rescue the motility deficient phenotype of MJD as well as the DAergic neuron loss in three different PD models. These results indicate that the RSP extract might not only be able to help to prevent one single neurodegenerative disease but has the potential to prevent neurodegeneration in general. In particular, since the extract showed to prevent disease phenotypes related to protein aggregations (ataxin-3 (MJD) and α -synuclein (PD)), exogenous toxins (6-OHDA) and endogenous toxin production (CAT-2). All these different mechanisms have been closely associated with neurodegeneration in other neurodegenerative disease, e.g. AD, ALS and MS. Therefore, these results provide a solid basis for further studies into the potential use of the RSP extract to prevent and treat other neurodegenerative disease. As indicated previously, there are several additional *C. elegans* models for all the different neurodegenerative diseases, including AD, ALS, HD as well as prion related disease⁶¹⁰. All these models present different behaviours or show phenotypical changes, which can be assessed to give additional valuable insights into the RSP extracts potential in neurodegenerative research. Due to the observed potential of the RSP extract to reduce A β ₄₂ aggregation *in vitro* (Figure 3.35), one interesting model would be either of the A β ₄₂ AD *C. elegans* models, e.g. strain CL4176 (*Pmyo-3::A β ₄₂*), in which the A β ₄₂ is inducible *via* temperature upshift. This model has previously been used to show that coffee⁶⁶⁵, as well as tea seed pomace (*Camellia tenuifoliacan*) extracts²³⁸ can reduce the by A β ₄₂ induced paralysis.

In addition, we also showed the importance of the indirect antioxidant activity of the extracts with the activation of *gst-4* and *sod-3* in the reported strains. This activity could be investigated further by (i) including reporter strains for other antioxidant/detoxification pathways e.g. CAT, GSH GPx and other SODs/GSTs or (ii) determining the expression increase on a genetic level i.e. quantitative real-time PCR of mRNA expressions after RSP extract treatment (work in progress, data not shown).

Crossing the *gst-4(ko)* strain with the UA44 PD model, to create the double mutant, revealed the significant importance of the RSP extracts on the presence of the intact *gst-4* gene. In the absence of the gene, the RSP extract does not show the decreased DAergic neuronal loss. Further studies could on the one hand identify if additional antioxidant genes are necessary for the observed effect. *Sod-3* for example was also significantly upregulated in the reporter strains and could be another important gene of interest. On the other hand, as *gst-4* has already been shown to be of significant interest, further studies should determine through which pathway it is activated. Most often *gst-4* is described to be dependent on *skn-1* (Nrf2) activation. However, further research has suggested the potential dependence on epidermal growth factor (EGF) and EOR-1 signalling in *C. elegans*. So was royal actin treatment for example *skn-1* independent but *eor-1* dependent⁶⁶⁰. The *skn-1* dependence of the RSP extract effect can be determine by (i) using rt-qPCR, (ii) use of reporter strains (LD1) or (iii) the use of knockout strains *skn-1* (*zu67*) and *eor-1(cs28)*⁶⁶⁰.

The overview in Figure 5.39 (p.346) describes the downstream detrimental effects caused by the production of ROS (lipid, protein and DNA/RNA damage), which then lead to the DAergic neuronal loss. To better understand the background of the used models (MJD and PD), further studies should initially determine the effect that the endogenous and exogeneous toxins have on the ROS production and the cellular components (DNA/RNA, proteins, lipids). As previously indicated to determine ROS levels in *C. elegans*, the same dye, used for the SH-SY5Y cell line, can be employed and ROS be analysed in N2 compared to the disease strains, to determine whether the genetic modification or the external stressors (6-OHDA) induce increased levels of ROS. In addition, the disease models can be analysed, comparing treated to untreated, to determine if the RSP extract treatment is able to decrease ROS production *in vivo* as well as *in vitro*.

To determine lipid damage, one of the most widely studied compounds is malondialdehyde (MDA), a lipid peroxidation product. MDA can be detected *via* HPLC⁷⁰³, the thiobarbituric acid (TBA) method⁷⁰⁴ or assay kits⁶⁹⁶. Also other lipid peroxidation products can be determined, such as lipid hydroperoxides and 4-hydroxynonenal²⁰⁶. Furthermore, the level of DNA

damage could be determined in the different PD and the MJD models. To determine whether the extract is able to prevent DNA damage *in vivo*, the comet assay⁷⁰⁵ or a number of stressors known to induce DNA damage can be employed⁷⁰⁶. These stressors e.g. UV irradiation, γ -IR, hydroxyurea, camptothecin or nitrogen mustard (HN₂) can induce different DNA lesions, which have a negative impact on embryonic viability and larva lethality, which can be measured by observation of the progeny⁷⁰⁶. Overall the so far obtained results for the RSP extract in *C. elegans* look very promising and grant further research into their potential use for the treatment or prevention of neurodegenerative disease, especially when being able to determine the active component or components.

The Potential Application of Rapeseed Pomace Extracts in the Prevention and Treatment of Neurodegenerative Diseases

6 OVERALL CONCLUSION ON THE POTENTIAL OF THE RSP EXTRACT

Neurodegenerative diseases are on the rise and currently no cures are available. Thus, with the constantly growing world population, the issues associated with these diseases will further increase. Research into these diseases with the aim to find drug treatments has become increasingly important. However, so far research has been unsuccessful in determining the RSP extracts molecular mechanisms behind these diseases and to find successful cures. In this project, we aimed to find potential treatments/preventions using an extract obtained from a natural waste/by-product called rapeseed pomace (RSP). The decision was made to employ a food by-product that is currently being used only as animal feed. Because of the growing world population, the need for food resources has been increasing and so the use of food products themselves to extract natural products from to treat diseases is not a desirable undertaking. However, using food production by-products has many advantages that include: (i) reduces the amount of waste accumulated, (ii) does not impact the amount of food available for consumption and (iii) adds extra value to the by-product. During this project the Soxhlet extraction method was found to produce the most antioxidant active RSP extract, with practical handling properties (dry powder sample). The 95% aqueous ethanolic extract, obtained from defatted (petroleum ether extraction) RSP, showed *in vitro* antioxidant activity in a number of different assays in addition to acetylcholinesterase inhibition activity, plasmid DNA protection under oxidative stress, copper chelating properties and the prevention of self-mediated β -amyloid aggregation. To determine whether the extract would show similar positive results in a cellular system, SH-SY5Y neuroblastoma cells were employed. Here the extract showed low toxicity (non-toxic till 1.5 mg/mL), the protection of cells from hydrogen peroxide induced ROS production as well as the prevention of DNA strand breakage. Investigation of activity of the extract at the molecular protein level, showed that SIRT2 and SOD2, associated with cell stress, were down regulated after RSP extract treatment of the cells.

Although all these promising results showed potential for the RSP extract to aid in the prevention of neurodegeneration associated with oxidative stress, further in depth *in vivo* studies were necessary to explore the extract's full potential. Thus, the Machado-Joseph disease (MJD) *C. elegans* model was applied where the extract significantly improved the motility deficient

phenotype. However, this improvement in motility was not related to a decrease in number or area of ataxin-3 aggregations within the *C. elegans* MJD model system. To determine whether the RSP extract was selective in ameliorating MJD, we also employed three Parkinson's disease *C. elegans* strains, all of them demonstrated typically PD associated dopamine(DA)ergic neuron loss. Once treated with the RSP extract, this DAergic neuronal loss was significantly decreased. Hence, the neuroprotective effect of RSP extract does not appear to be specific to a certain neurodegenerative disease but seems to affect neurodegeneration in general. Further studies using other disease strains would support this conclusion. Additional studies, using *C. elegans*, were initiated to determine the mechanism of action of the RSP extract. Whilst the results for the AChE inhibition hypothesis were inconclusive, investigations into the importance of antioxidant response genes appeared very promising. In the *C. elegans* reporter strains, GFP expression increase for *sod-3* and *gst-4* and subsequent studies using *gst-4* knockout strains, suggested the importance of the *gst-4* gene for the show positive effect seen with the RSP extract.

Overall this study investigated the chemical composition of the RSP extract together with its *in vitro* and *in vivo* activity. However, before the extract can enter clinical trials, a number of further experiments are necessary. These include more detailed studies into the pathway of action, as well as studies determining a potential active ingredient (e.g. sinapine) which is responsible for the observed activity. Furthermore, studies using mammalian models (e.g. mice or rats) would give a second input on toxicity data and determine whether the RSP extract is active in other models of neurodegenerative diseases. If positive activities of the extract as a total or potentially isolated compounds can be shown, then the extract/compounds would have good chances of getting into clinical studies or could be used as food additive with positive impact on neuro protection such as seen previously for ginkgo biloba. However, very often, when moving up the ladder of model complexity, the positive activity of drugs is lost. Even if this were the case, further studies into determining why the RSP extract is only active in certain model organisms could enhance the knowledge of neurodegenerative disease and might help to create better animal model for future drug testing. In general, the RSP extract shows overall promising potential for the

The Potential Application of Rapeseed Pomace Extracts in the Prevention and Treatment of Neurodegenerative Diseases

treatment/prevention of neurodegenerative disease and further research is recommended.

7 REFERENCES

1. Yeap Foo, L. & Lu, Y. Isolation and identification of procyanidins in apple pomace. *Food Chem.* **64**, 511–518 (1999).
2. Petrovska, B. B. Historical review of medicinal plants' usage. *Pharmacogn. Rev.* **6**, 1–5 (2012).
3. Merriam Co., C. & G. Natural product. *Webster's Revised Unabridged Dictionary* (1913). Available at: <http://www.thefreedictionary.com/Natural+product>. (Accessed: 26th January 2015)
4. Newman, D. J. & Cragg, G. M. Natural products as sources of new drugs over the 30 years from 1981 to 2010. *J. Nat. Prod.* **75**, 311–35 (2012).
5. Ngo, L. T., Okogun, J. I. & Folk, W. R. 21st century natural product research and drug development and traditional medicines. *Nat. Prod. Rep.* **30**, 584–92 (2013).
6. Lahlou, M. The Success of Natural Products in Drug Discovery. *Pharmacol. Pharm.* **4**, 17–31 (2013).
7. Molinari, G. Natural products in drug discovery: present status and perspectives. in *Advances in experimental medicine and biology* **655**, 13–27 (2009).
8. Wilson, M. A. *et al.* Blueberry polyphenols increase lifespan and thermotolerance in *Caenorhabditis elegans*. *Aging Cell* **5**, 59–68 (2006).
9. Muthaiyah, B., Essa, M. M., Chauhan, V. & Chauhan, A. Protective effects of walnut extract against amyloid beta peptide-induced cell death and oxidative stress in PC12 cells. *Neurochem. Res.* **36**, 2096–103 (2011).
10. Fontana, A. R., Antonioli, A. & Bottini, R. Grape pomace as a sustainable source of bioactive compounds: Extraction, characterization, and biotechnological applications of phenolics. *J. Agric. Food Chem.* **61**, 8987–9003 (2013).
11. Vergara-Salinas, J. R. *et al.* Effect of pressurized hot water extraction on antioxidants from grape pomace before and after enological fermentation. *J. Agric. Food Chem.* **61**, 6929–36 (2013).
12. Laws, B. *Fifty Plants that Changed the Course of History*. (Quid Publishing, 2016).

13. United Nations Department of Economic and Social Affairs Population Division (2017). *World Population Prospects: The 2017 Revision, Key Findings and Advance Tables. Working Paper No. ESA/P/WP/248.*
14. Chakraborty, S. & Newton, A. C. Climate change, plant diseases and food security: an overview. *Plant Pathol.* **60**, 2–14 (2011).
15. Sharma, S. K. *et al.* Utilization of food processing by-products as dietary, functional, and novel fiber: A review. *Critical Reviews in Food Science and Nutrition* **56**, 1647–1661 (2015).
16. Dou, Z. *et al.* Assessing U.S. food wastage and opportunities for reduction. *Glob. Food Sec.* **8**, 19–26 (2016).
17. Buzby, J. C., Farah-Wells, H. & Hyman, J. The Estimated Amount, Value, and Calories of Postharvest Food Losses at the Retail and Consumer Levels in the United States. *Econ. Inf. Bull.* 1–33 (2014).
18. Schieber, A., Stintzing, F. C. & Carle, R. By-products of plant food processing as a source of functional compounds — recent developments. *Trends Food Sci. Technol.* **12**, 401–413 (2001).
19. Parfitt, J., Stanley, C. & Thompson, L. *WRAP-Guidance for Food and Drink Manufacturers and Retailers on the Use of Food Surplus as Animal Feed.* (2016).
20. Westendorf, M. L. & Wohlt, J. E. Brewing by-products: their use as animal feeds. *Vet. Clin. North Am. Food Anim. Pract.* **18**, 233–52 (2002).
21. Wahlberg, M. L. *Alternative Feeds for Beef Cattle.* (2009).
22. Carré, P. & Pouzet, A. Rapeseed market, worldwide and in Europe. *OCL - Oilseeds fats, Crop. Lipids* **21**, (2014).
23. Fuller, S., Beck, E., Salman, H. & Tapsell, L. New Horizons for the Study of Dietary Fiber and Health: A Review. *Plant Foods Hum. Nutr.* **71**, (2016).
24. Xu, Y. *et al.* A recyclable protein resource derived from cauliflower by-products: Potential biological activities of protein hydrolysates. *Food Chem.* **221**, 114–122 (2017).
25. Liadakis, G. N., Tzia, C., Oreopoulou, V. & Thomopoulos, C. D. Protein Isolation from Tomato Seed Meal, Extraction Optimization. *J. Food Sci.*

- 60**, 477–482 (1995).
26. Ribeiro, B. D., Barreto, D. W. & Coelho, M. A. Z. Enzyme-Enhanced Extraction of Phenolic Compounds and Proteins from Flaxseed Meal. *ISRN Biotechnol.* **2013**, 1–6 (2013).
 27. Yu, X., Gouyo, T., Grimi, N., Bals, O. & Vorobiev, E. Ultrasound enhanced aqueous extraction from rapeseed green biomass for polyphenol and protein valorization. *Comptes Rendus Chim.* **19**, 766–777 (2016).
 28. Deng, J. *et al.* Extraction Optimization and Functional Properties of Proteins from Kiwi Fruit (*Actinidia chinensis* Planch.) Seeds. *Int. J. Food Prop.* **17**, 1612–1625 (2014).
 29. Bennett, R. N. & Wallsgrave, R. M. Secondary metabolites in plant defence mechanisms. *New Phytol.* **127**, 617–633 (1994).
 30. Agostini-Costa, T. da S., Vierira, R., Bizzo, H. R., Silveira, D. & Gimenes, M. A. Secondary Metabolites. in *Chromatography and Its Applications* (ed. Dhanarasu, S.) 131–164 (IntechOpen, 2012).
 31. Wink, M. Preface. in *Annual plant reviews volume 40, Biochemistry of plant Secondary Metabolites* (ed. Wink, M.) **40**, XIII–XV (Blackwell Publishing L, 2010).
 32. Wink, M. Introduction: Biochemistry, Physiology and Ecological Functions of Secondary Metabolites. in *ANNUAL PLANT REVIEWS Volume 40 Biochemistry of Plant Secondary Metabolites* (ed. Wink, M.) 1–19 (Wiley-Blackwell, 2010).
 33. Björkman, M. *et al.* Phytochemicals of Brassicaceae in plant protection and human health - Influences of climate, environment and agronomic practice. *Phytochemistry* **72**, 538–556 (2011).
 34. Matsuura, H. N. & Fett-Neto, A. G. Plant Alkaloids: Main Features, Toxicity, and Mechanisms of Action. in *Plant Toxins. Toxinology* (eds. Gopalakrishnakone, P., Carlini, C. & Ligabue-Braun, R.) 1–15 (Springer, 2015).
 35. Iriti, M. & Faoro, F. Chemical diversity and defence metabolism: How plants cope with pathogens and ozone pollution. *Int. J. Mol. Sci.* **10**, 3371–3399 (2009).

36. Roberts, M. F., Strack, D. & Wink, M. Biosynthesis of Alkaloids and Betalains. in *Annual Plant Reviews Volume 40: Biochemistry of Plant Secondary Metabolism* (ed. Wink, M.) 20–91 (Wiley-Blackwell).
37. Wink, M. Occurrence and Function of Natural Products in Plants. *Phytochem. Pharmacogn.* (2011).
38. Springob, K. & Kutchan, T. M. Introduction to the Different Classes of Natural Products. in *Plant-derived Natural Products* (eds. Osbourn, A. E. & Lanzotti, V.) 3–50 (Springer Science+Business Media, LLC, 2009).
39. Shahid, M., Yusuf, M., and Mohammad, F. Plant phenolics: A Review on Modern extraction techniques. in *Recent Progress in Medicinal Plants, Volume 41: Analytical and Processing Techniques* (eds. Govil, J. N. & Pathak, M.) (Studium Press, 2016).
40. Cartea, M. E., Francisco, M., Soengas, P. & Velasco, P. Phenolic Compounds in Brassica Vegetables. *Molecules* **16**, 251–280 (2010).
41. Shahidi, F. & Ambigaipalan, P. Phenolics and polyphenolics in foods, beverages and spices: Antioxidant activity and health effects – A review. *J. Funct. Foods* **18**, 820–897 (2015).
42. Firuzi, O., Moosavi, F., Hosseini, R. & Saso, L. Modulation of neurotrophic signaling pathways by polyphenols. *Drug Des. Devel. Ther.* **10**, 23–42 (2015).
43. Maeda, H. & Dudareva, N. The Shikimate Pathway and Aromatic Amino Acid Biosynthesis in Plants. *Annu. Rev. Plant Biol.* **63**, 73–105 (2012).
44. Jeffery, E. H. *et al.* Variation in content of bioactive components in broccoli. *J. Food Compos. Anal.* **16**, 323–330 (2003).
45. Generalić, I. *et al.* Seasonal Variations of Phenolic Compounds and Biological Properties in Sage (*Salvia officinalis* L.). *Chem. Biodivers.* **9**, 441–457 (2012).
46. Ambriz-Pérez, D. L., Leyva-López, N., Gutierrez-Grijalva, E. P. & Heredia, J. B. Phenolic compounds: Natural alternative in inflammation treatment. A Review. *Cogent Food Agric.* **2**, 1–14 (2016).
47. Macé, S., Truelstrup Hansen, L. & Rupasinghe, H. P. V. Anti-Bacterial Activity of Phenolic Compounds against *Streptococcus pyogenes*. *Med.*

(Basel, Switzerland) **4**, (2017).

48. Bouyahya, A., Abrini, J., El-Baabou, A., Bakri, Y. & Dakka, N. Determination of Phenol Content and Antibacterial Activity of Five Medicinal Plants Ethanolic Extracts from North-West of Morocco. *J. Plant Pathol. Microbiol.* **07**, 1–4 (2016).
49. Balea, Ș. S., Pârvu, A. E., Pop, N., Marín, F. Z. & Pârvu, M. Polyphenolic Compounds, Antioxidant, and Cardioprotective Effects of Pomace Extracts from Fetească Neagră Cultivar. *Oxid. Med. Cell. Longev.* **2018**, 1–11 (2018).
50. Cao, Y. *et al.* Two new phenolic constituents from the root bark of *Morus alba* L. and their cardioprotective activity. *Nat. Prod. Res.* **32**, 391–398 (2018).
51. Liu, L., Zubik, L., Collins, F. W., Marko, M. & Meydani, M. The antiatherogenic potential of oat phenolic compounds. *Atherosclerosis* **175**, 39–49 (2004).
52. Szydłowska-Czerniak, A. & Tułodziecka, A. Antioxidant capacity of rapeseed extracts obtained by conventional and ultrasound-assisted extraction. *JAOCs, J. Am. Oil Chem. Soc.* **91**, 2011–2019 (2014).
53. Jara-Palacios, M. J. *et al.* Study of Zalema Grape Pomace: Phenolic Composition and Biological Effects in *Caenorhabditis elegans*. *J. Agric. Food Chem.* **61**, 5114–5121 (2013).
54. Christensen, L. P. & Christensen, K. B. The Role of Direct and Indirect Polyphenolic Antioxidants in Protection Against Oxidative Stress. in *Polyphenols in Human Health and Disease* (eds. Watson, R. R., Preedy, V. R. & Zibadi, S.) **1**, 289–309 (Academic Press (Elsevier), 2014).
55. Minatel, I. O. *et al.* Phenolic Compounds: Functional Properties, Impact of Processing and Bioavailability. in *Phenolic Compounds - Biological Activity* (ed. Soto-Hernández, M.) 1–24 (IntechOpen, 2017).
56. Weinreb, O., Amit, T., Mandel, S. & Youdim, M. B. H. Neuroprotective molecular mechanisms of (-)-epigallocatechin-3-gallate: a reflective outcome of its antioxidant, iron chelating and neuritogenic properties. *Genes Nutr.* **4**, 283–96 (2009).

57. Levites, Y., Youdim, M. B. H., Maor, G. & Mandel, S. Attenuation of 6-hydroxydopamine (6-OHDA)-induced nuclear factor-kappaB (NF-κB) activation and cell death by tea extracts in neuronal cultures. *Biochem. Pharmacol.* **63**, 21–29 (2002).
58. Lee, J. W. *et al.* Green tea (-)-epigallocatechin-3-gallate inhibits beta-amyloid-induced cognitive dysfunction through modification of secretase activity via inhibition of ERK and NF-kappaB pathways in mice. *J. Nutr.* **139**, 1987–93 (2009).
59. Lin, Y.-R., Chen, H.-H., Ko, C.-H. & Chan, M.-H. Neuroprotective activity of honokiol and magnolol in cerebellar granule cell damage. *Eur. J. Pharmacol.* **537**, 64–9 (2006).
60. Krikorian, R. *et al.* Blueberry Supplementation Improves Memory in Older Adults †. *J. Agric. Food Chem.* **58**, 3996–4000 (2010).
61. Manganaris, G. A., Goulas, V., Vicente, A. R. & Terry, L. A. Berry antioxidants: small fruits providing large benefits. *J. Sci. Food Agric.* **94**, 825–33 (2014).
62. Lau, F. C., Bielinski, D. F. & Joseph, J. A. Inhibitory effects of blueberry extract on the production of inflammatory mediators in lipopolysaccharide-activated BV2 microglia. *J. Neurosci. Res.* **85**, 1010–7 (2007).
63. Collins, J. J., Evason, K. & Kornfeld, K. Pharmacology of delayed aging and extended lifespan of *Caenorhabditis elegans*. *Exp. Gerontol.* **41**, 1032–9 (2006).
64. Smith, J. V. & Luo, Y. Elevation of oxidative free radicals in Alzheimer's disease models can be attenuated by Ginkgo biloba extract EGb 761. *J. Alzheimers. Dis.* **5**, 287–300 (2003).
65. Wu, Y. *et al.* Amyloid-beta-induced pathological behaviors are suppressed by Ginkgo biloba extract EGb 761 and ginkgolides in transgenic *Caenorhabditis elegans*. *J. Neurosci.* **26**, 13102–13 (2006).
66. Wang, J. *et al.* Moderate consumption of Cabernet Sauvignon attenuates Abeta neuropathology in a mouse model of Alzheimer's disease. *FASEB J.* **20**, 2313–20 (2006).
67. Wang, J. *et al.* Grape derived polyphenols attenuate tau neuropathology

- in a mouse model of Alzheimer's disease. *J. Alzheimers. Dis.* **22**, 653–61 (2010).
68. Pinelo, M., Fabbro, P., Manzocco, L., Nunez, M. & Nicoli, M. Optimization of continuous phenol extraction from byproducts. *Food Chem.* **92**, 109–117 (2005).
69. Alonso-Salces, R. M. *et al.* Pressurized liquid extraction for the determination of polyphenols in apple. *J. Chromatogr. A* **933**, 37–43 (2001).
70. Vulic, J. J. *et al.* Polyphenolic content and antioxidant activity of the four berry fruits pomace extracts - Open Access Library. *Acta Period. Technol.* 271–279 (2011).
71. Li, R. *et al.* Phenolics and antioxidant activity of Saskatoon berry (*Amelanchier alnifolia*) pomace extract. *J. Med. Food* **17**, 384–92 (2014).
72. Servili, M. *et al.* High-performance liquid chromatography evaluation of phenols in olive fruit, virgin olive oil, vegetation waters, and pomace and 1D- and 2D-nuclear magnetic resonance characterization. *J. Am. Oil Chem. Soc.* **76**, 873–882 (1999).
73. Cardoso, S. M. *et al.* Characterisation of phenolic extracts from olive pulp and olive pomace by electrospray mass spectrometry. *J. Sci. Food Agric.* **85**, 21–32 (2005).
74. Onyilagha, J. *et al.* Leaf flavonoids of the cruciferous species, *Camelina sativa*, *Crambe* spp., *Thlaspi arvense* and several other genera of the family Brassicaceae. *Biochem. Syst. Ecol.* **31**, 1309–1322 (2003).
75. Szydłowska-Czerniak, A. Rapeseed and its products-sources of bioactive compounds: a review of their characteristics and analysis. *Crit. Rev. Food Sci. Nutr.* **53**, 307–30 (2013).
76. Saeidnia, S. & Gohari, A. R. Importance of *Brassica napus* as a medicinal food plant. *J. Med. Plants Res.* **6**, 2700–2703 (2012).
77. Lin, L. *et al.* Evidence of health benefits of canola oil. *Nutr. Rev.* **71**, 370–385 (2013).
78. United States Department of Agriculture Economic Research Service. *USDA Economic Research Service - Oil Crops Yearbook.* (2016).

79. Pohl, F. Searching for Therapeutic Strategies in a *C. elegans* model of Machado-Joseph Disease. *Master Thesis* (The Robert Gordon University, 2013).
80. Szydłowska-Czerniak, A., Trokowski, K., Karlovits, G. & Szłyk, E. Determination of Antioxidant Capacity, Phenolic Acids, and Fatty Acid Composition of Rapeseed Varieties. *J. Agric. Food Chem.* **58**, 7502–7509 (2010).
81. Kortesiemi, M. *et al.* NMR metabolomics of ripened and developing oilseed rape (*Brassica napus*) and turnip rape (*Brassica rapa*). *Food Chem.* **172**, 63–70 (2015).
82. Mag, T. K. Canola oil processing in Canada. *J. Am. Oil Chem. Soc.* **60**, 380–384 (1983).
83. Yue, J. *et al.* Nutritional and Antioxidant Properties of Rapeseed (*Brassica Napus*) Cultivars with High and Low Erucic Acid Content. *J. Food Nutr. Res.* **2**, 918–924 (2014).
84. Simopoulos, A. P. The importance of the ratio of omega-6/omega-3 essential fatty acids. *Biomed. Pharmacother.* **56**, 365–79 (2002).
85. Rapeseed Oil Production. *Food and Agriculture Organization of the United Nations Statistics Division* (2016). Available at: <http://faostat3.fao.org/browse/Q/QD/E>. (Accessed: 10th August 2017)
86. Rapeseed Crop Production. *Food and Agriculture Organization of the United Nations Statistics Division* (2017). Available at: <http://www.fao.org/faostat/en/?#data/QC/visualize>. (Accessed: 10th August 2017)
87. Wanasundara, U. N. & Shahidi, F. Canola extract as an alternative natural antioxidant for canola oil. *J. Am. Oil Chem. Soc.* **71**, 817–822 (1994).
88. Szydłowska-Czerniak, A., Amarowicz, R. & Szłyk, E. Antioxidant capacity of rapeseed meal and rapeseed oils enriched with meal extract. *Eur. J. Lipid Sci. Technol.* **112**, 750–760 (2010).
89. Szydłowska-Czerniak, A., Karlovits, G., Hellner, G., Dianoczki, C. & Szłyk, E. Effect of enzymatic and hydrothermal treatments of rapeseeds on quality of the pressed rapeseed oils Part I: Antioxidant capacity and antioxidant content. *Process Biochem.* **45**, 7–17 (2010).

90. Szydłowska-Czerniak, A., Bartkowiak-Broda, I., Karlović, I., Karlovits, G. & Szlyk, E. Antioxidant capacity, total phenolics, glucosinolates and colour parameters of rapeseed cultivars. *Food Chem.* **127**, 556–63 (2011).
91. Thiyam, U., Kuhlmann, A., Stöckmann, H. & Schwarz, K. Prospects of rapeseed oil by-products with respect to antioxidative potential. *Comptes Rendus Chim.* **7**, 611–616 (2004).
92. Kozłowska, H., Naczka, M., Shahidi, F. & Zadernowski, R. Phenolic Acids and Tannins in Rapeseed and Canola. in *Canola and Rapeseed* 193–210 (Springer US, 1990).
93. Naczka, M., Amarowicz, R., Sullivan, A. & Shahidi, F. Current research developments on polyphenolics of rapeseed/canola: a review. *Food Chem.* **62**, 489–502 (1998).
94. Teh, S.-S. & Birch, E. J. Effect of ultrasonic treatment on the polyphenol content and antioxidant capacity of extract from defatted hemp, flax and canola seed cakes. *Ultrason. Sonochem.* **21**, 346–353 (2014).
95. Amarowicz, R., Naczka, M. & Shahidi, F. Antioxidant activity of various fractions of non-tannin phenolics of canola hulls. *J. Agric. Food Chem.* **48**, 2755–9 (2000).
96. Nićiforović, N. & Abramović, H. Sinapic Acid and Its Derivatives: Natural Sources and Bioactivity. *Compr. Rev. Food Sci. Food Saf.* **13**, 34–51 (2014).
97. Thiyam, U., Stöckmann, H., Zum Felde, T. & Schwarz, K. Antioxidative effect of the main sinapic acid derivatives from rapeseed and mustard oil by-products. *Eur. J. Lipid Sci. Technol.* **108**, 239–248 (2006).
98. Bhullar, K. S. & Rupasinghe, H. P. V. Polyphenols: Multipotent therapeutic agents in neurodegenerative diseases. *Oxid. Med. Cell. Longev.* **2013**, (2013).
99. Fang, J. *et al.* Tissue-Specific Distribution of Secondary Metabolites in Rapeseed (*Brassica napus* L.). *PLoS One* **7**, e48006 (2012).
100. Velasco, P., Soengas, P., Vilar, M., Cartea, M. E. & Rio, M. del. Comparison of Glucosinolate Profiles in Leaf and Seed Tissues of Different *Brassica napus* Crops. *J. Am. Soc. Hortic. Sci.* **133**, 551–558 (2008).

101. Velasco, P. *et al.* Phytochemical fingerprinting of vegetable Brassica oleracea and Brassica napus by simultaneous identification of glucosinolates and phenolics. *Phytochem. Anal.* **22**, 144–152 (2011).
102. Hussain, N. *et al.* Detection of Tocopherol in Oilseed Rape (Brassica napus L.) Using Gas Chromatography with Flame Ionization Detector. *J. Integr. Agric.* **12**, 803–814 (2013).
103. Leckband, G., Frauen, M. & Friedt, W. NAPUS 2000. Rapeseed (Brassica napus) breeding for improved human nutrition. *Food Res. Int.* **35**, 273–278 (2002).
104. Gruszka, J. & Kruk, J. RP-LC for Determination of Plastoquinone, Tocotrienols and Tocopherols in Plant Oils. *Chromatographia* **66**, 909–913 (2007).
105. Choe, E. & Min, D. B. Mechanisms of Antioxidants in the Oxidation of Foods. *Compr. Rev. Food Sci. Food Saf.* **8**, 345–358 (2009).
106. Gül, M. K. & Şeker, M. Comparative analysis of phytosterol components from rapeseed (Brassica napus L.) and olive (Olea europaea L.) varieties. *Eur. J. Lipid Sci. Technol.* **108**, 759–765 (2006).
107. Segura, R., Javierre, C., Lizarraga, M. A. & Ros, E. Other relevant components of nuts: phytosterols, folate and minerals. *Br. J. Nutr.* **96 Suppl 2**, S36-44 (2006).
108. Zago, E. *et al.* Influence of rapeseed meal treatments on its total phenolic content and composition in sinapine, sinapic acid and canolol. *Ind. Crops Prod.* **76**, 1061–1070 (2015).
109. Siger, A., Czubinski, J., Dwiecki, K., Kachlicki, P. & Nogala-Kalucka, M. Identification and antioxidant activity of sinapic acid derivatives in *Brassica napus* L. seed meal extracts. *Eur. J. Lipid Sci. Technol.* **115**, n/a-n/a (2013).
110. Yang, S. *et al.* Identification and Determination of Phenolic Compounds in Rapeseed Meals (Brassica napus L.). *J. Agric. Chem. Environ.* **4**, 14–23 (2015).
111. Hassas-Roudsari, M., Chang, P. R., Pegg, R. B. & Tyler, R. T. Antioxidant capacity of bioactives extracted from canola meal by subcritical water, ethanolic and hot water extraction. *Food Chem.* **114**, 717–726 (2009).

112. Misra, B. B. Cataloging the Brassica napus seed metabolome. *Cogent Food Agric.* **2**, 1–16 (2016).
113. Khattab, R., Eskin, M., Aliani, M. & Thiyam, U. Determination of Sinapic Acid Derivatives in Canola Extracts Using High-Performance Liquid Chromatography. *J. Am. Oil Chem. Soc.* **87**, 147–155 (2010).
114. Liu, Y. G., Zhou, M. Q. & Liu, M. L. A survey of nutrients and toxic factors in commercial rapeseed meal in China and evaluation of detoxification by water extraction. *Anim. Feed Sci. Technol.* **45**, 257–270 (1994).
115. Raikos, V. *et al.* Proteomic and Glucosinolate Profiling of Rapeseed Isolates from Meals Produced by Different Oil Extraction Processes. *J. Food Process. Preserv.* **41**, 1–8 (2017).
116. Dimitriadi, M. & Hart, A. C. Neurodegenerative disorders: insights from the nematode *Caenorhabditis elegans*. *Neurobiol. Dis.* **40**, 4–11 (2010).
117. Zhaurova, K. Genetic Causes of Adult-Onset Disorders. *Nat. Educ.* **1**, 49 (2008).
118. Jaul, E. & Barron, J. Age-Related Diseases and Clinical and Public Health Implications for the 85 Years Old and Over Population. *Front. public Heal.* **5**, 335 (2017).
119. Joyner, P. M. & Cichewicz, R. H. Bringing natural products into the fold - exploring the therapeutic lead potential of secondary metabolites for the treatment of protein-misfolding-related neurodegenerative diseases. *Nat. Prod. Rep.* **28**, 26–47 (2011).
120. Brown, R. C., Lockwood, A. H. & Sonawane, B. R. Neurodegenerative diseases: an overview of environmental risk factors. *Environ. Health Perspect.* **113**, 1250–6 (2005).
121. Pandey, R., Gupta, S., Shukla, V., Tandon, S. & Shukla, V. Antiaging, antistress and ROS scavenging activity of crude extract of *Ocimum sanctum* (L.) in *Caenorhabditis elegans* (Maupas, 1900). *Indian J. Exp. Biol.* **51**, 515–21 (2013).
122. Skovronsky, D. M., Lee, V. M.-Y. & Trojanowski, J. Q. Neurodegenerative Diseases: New Concepts of Pathogenesis and Their Therapeutic Implications. *Annu. Rev. Pathol. Mech. Dis.* **1**, 151–170 (2006).

123. DeStefano, A. L. *et al.* A familial factor independent of CAG repeat length influences age at onset of Machado-Joseph disease. *Am. J. Hum. Genet.* **59**, 119–27 (1996).
124. Wijesekera, L. C. & Leigh, P. N. Amyotrophic lateral sclerosis. *Orphanet J. Rare Dis.* **4**, 3 (2009).
125. Wenning, G. K., Colosimo, C., Geser, F. & Poewe, W. Multiple system atrophy. *Lancet. Neurol.* **3**, 93–103 (2004).
126. National Institute of Neurological Disorders and Stroke. Parkinson's Disease Information Page. (2018). Available at: <https://www.ninds.nih.gov/Disorders/All-Disorders/Parkinsons-Disease-Information-Page>. (Accessed: 21st August 2018)
127. Lantz, M. S. & Buchalter, E. N. Pick's Disease. *Clin. Geriatr.* **16**, 14–17 (2005).
128. Christoph, G. Dipl.-Med. and Senior Physician at Klinikum Niederlausitz GmbH Klinik für Geriatrie. personal communication (2013).
129. Huntington's Disease Society of America. What is HD? (2018). Available at: <http://hdsa.org/what-is-hd/#stages>. (Accessed: 21st August 2018)
130. Fujikake, N. *et al.* Heat shock transcription factor 1-activating compounds suppress polyglutamine-induced neurodegeneration through induction of multiple molecular chaperones. *J. Biol. Chem.* **283**, 26188–97 (2008).
131. Barnes, D. E. & Yaffe, K. The projected effect of risk factor reduction on Alzheimer's disease prevalence. *Lancet Neurol.* **10**, 819–828 (2011).
132. World Health Organization. *Global Health Estimates 2016: Deaths by Cause, Age, Sex, by Country and by Region 2000-2016*. (2018).
133. Prince, M. *et al.* *Dementia UK Second edition*. (2014).
134. Querfurth, H. W. & LaFerla, F. M. Mechanisms of Disease Alzheimer's Disease. *new Engl. J. of Med. Rev.* **362**, 329–344 (2010).
135. Munoz, D. G. & Feldman, H. Causes of Alzheimer's disease. *Cmaj* **162**, 65–72 (2000).
136. Price, D. L., Tanzi, R. E., Borchelt, D. R. & Sisodia, S. S. Alzheimer's disease: Genetic Studies and Transgenic Models. *Annu. Rev. Genet.* **32**, 461–493 (1998).

137. Yacoubian, T. A. Neurodegenerative Disorders: Why Do We Need New Therapies? in *Drug Discovery Approaches for the Treatment of Neurodegenerative Disorders* (ed. Adejare, A.) 1–16 (Academic Press, 2017).
138. Blessed, G., Tomlinson, B. E. & Roth, M. The association between quantitative measures of dementia and of senile change in the cerebral grey matter of elderly subjects. *Br. J. Psychiatry* **114**, 797–811 (1968).
139. LaFerla, F. M. & Oddo, S. Alzheimer's disease: A β , tau and synaptic dysfunction. *Trends Mol. Med.* **11**, 170–176 (2005).
140. Masters, C. L. *et al.* Alzheimer's disease. *Nat. Rev. Dis. Prim.* **1**, 15056 (2015).
141. Arriagada, P. V, Growdon, J. H., Hedley-Whyte, E. T. & Hyman, B. T. Neurofibrillary tangles but not senile plaques parallel duration and severity of Alzheimer's disease. *Neurology* **42**, 631–9 (1992).
142. Atwood, C. S., Martins, R. N., Smith, M. A. & Perry, G. Senile plaque composition and posttranslational modification of amyloid- β peptide and associated proteins. *Peptides* **23**, 1343–1350 (2002).
143. Bachurin, S. O., Bovina, E. V. & Ustyugov, A. A. Drugs in Clinical Trials for Alzheimer's Disease: The Major Trends. *Medicinal Research Reviews* **37**, 1186–1225 (2017).
144. Crowther, D. C. *et al.* Intraneuronal A β , non-amyloid aggregates and neurodegeneration in a Drosophila model of Alzheimer's disease. *Neuroscience* **132**, 123–135 (2005).
145. Selkoe, D. J. Toward a comprehensive theory for Alzheimer's disease. Hypothesis: Alzheimer's disease is caused by the cerebral accumulation and cytotoxicity of amyloid beta-protein. *Ann. N. Y. Acad. Sci.* **924**, 17–25 (2000).
146. Zolochewska, O., Bjorklund, N., Woltjer, R., Wiktorowicz, J. E. & Tagliavola, G. Postsynaptic Proteome of Non-Demented Individuals with Alzheimer's Disease Neuropathology. *J. Alzheimer's Dis.* **65**, 659–682 (2018).
147. Rapoport, S. I., Pettigrew, K. D. & Schapiro, M. B. Discordance and

- concordance of dementia of the Alzheimer type (DAT) in monozygotic twins indicate heritable and sporadic forms of Alzheimer's disease. *Neurology* **41**, 1549–53 (1991).
148. Giri, M., Zhang, M. & Lü, Y. Genes associated with Alzheimer's disease: an overview and current status. *Clin. Interv. Aging* **11**, 665–81 (2016).
 149. Wentzell, J. & Kretzschmar, D. Alzheimer's Disease and tauopathy studies in flies and worms. *Neurobiol. Dis.* **40**, 21–28 (2010).
 150. Gatz, M. *et al.* Role of Genes and Environments for Explaining Alzheimer Disease. *Arch. Gen. Psychiatry* **63**, 168 (2006).
 151. Keowkase, R. *et al.* Neuroprotective effects and mechanism of cognitive-enhancing choline analogs JWB 1-84-1 and JAY 2-22-33 in neuronal culture and *Caenorhabditis elegans*. *Mol. Neurodegener.* **5**, 59 (2010).
 152. Chen, R. *et al.* Treatment effects between monotherapy of donepezil versus combination with memantine for Alzheimer disease: A meta-analysis. *PLoS One* **12**, e0183586 (2017).
 153. Littlejohn, G., Guymer, E., Littlejohn, G. & Guymer, E. Modulation of NMDA Receptor Activity in Fibromyalgia. *Biomedicines* **5**, 15 (2017).
 154. Danysz, W. & Parsons, C. G. The NMDA receptor antagonist memantine as a symptomatological and neuroprotective treatment for Alzheimer ' s disease ... The NMDA receptor antagonist memantine as a symptomatological and neuroprotective treatment for Alzheimer ' s disease : preclinical e. *Int. J. Geriatr. Psychiatry* **18**, S23–S32 (2003).
 155. Cummings, J., Lee, G., Mortsdorf, T., Ritter, A. & Zhong, K. Alzheimer's disease drug development pipeline: 2017. *Alzheimer's Dement. Transl. Res. Clin. Interv.* **3**, 367–384 (2017).
 156. Cummings, J. L., Morstorf, T. & Zhong, K. Alzheimer's disease drug-development pipeline: few candidates, frequent failures. *Alzheimers. Res. Ther.* **6**, 37 (2014).
 157. Macedo-Ribeiro, S., Pereira de Almeida, L., Carvalho, A. L. & Rego, A. C. Polyglutamine Expansion Diseases – the Case of Machado-Joseph Disease. in *Interaction Between Neurons and Glia in Aging and Disease* (eds. Malva, J., Rego, A. C., Cunha, R. & Oliveira, C.) 391–426 (Springer US, 2007).

158. Ranum, L. P. *et al.* Spinocerebellar ataxia type 1 and Machado-Joseph disease: incidence of CAG expansions among adult-onset ataxia patients from 311 families with dominant, recessive, or sporadic ataxia. *Am. J. Hum. Genet.* **57**, 603–8 (1995).
159. Lima, M., Bruges-Armas, J. & Bettencourt, C. Non-Mendelian Genetic Aspects in Spinocerebellar Ataxias (SCAS): The Case of Machado-Joseph Disease (MJD). in *Spinocerebellar Ataxia* (ed. Gazulla, J.) 27–40 (InTech, 2012).
160. Bettencourt, C. & Lima, M. Machado-Joseph Disease: from first descriptions to new perspectives. *Orphanet J. Rare Dis.* **6**, 35 (2011).
161. Coutinho, P. & Andrade, C. Autosomal dominant system degeneration in Portuguese families of the Azores Islands. A new genetic disorder involving cerebellar, pyramidal, extrapyramidal and spinal cord motor functions. *Neurology* **28**, 703–9 (1978).
162. Lopes-Cendes, I. *et al.* Molecular characteristics of Machado-Joseph disease mutation in 25 newly described Brazilian families. *Brazilian J. Genet.* **20**, 717–724 (1997).
163. Kawaguchi, Y. *et al.* CAG expansions in a novel gene for Machado-Joseph disease at chromosome 14q32.1. *Nat. Genet.* **8**, 221–228 (1994).
164. Gusella, J. F. & MacDonald, M. E. Molecular genetics: Unmasking polyglutamine triggers in neurodegenerative disease. *Nat. Rev. Neurosci.* **1**, 109–115 (2000).
165. Kato, T. *et al.* Sisters homozygous for the spinocerebellar ataxia type 6 (SCA6)/CACNA1A gene associated with different clinical phenotypes. *Clin. Genet.* **58**, 69–73 (2000).
166. Carvalho, D. R., La Rocque-Ferreira, A., Rizzo, I. M., Imamura, E. U. & Speck-Martins, C. E. Homozygosity Enhances Severity in Spinocerebellar Ataxia Type 3. *Pediatr. Neurol.* **38**, 296–299 (2008).
167. Myers, R. H., Madden, J. J., Teague, J. L. & Falek, A. Factors related to onset age of Huntington disease. *Am. J. Hum. Genet.* **34**, 481–8 (1982).
168. Matos, C. A., de Macedo-Ribeiro, S. & Carvalho, A. L. Polyglutamine diseases: The special case of ataxin-3 and Machado-Joseph disease.

- Prog. Neurobiol.* **95**, 26–48 (2011).
169. Hayashi, M., Kobayashi, K. & Furuta, H. Immunohistochemical study of neuronal intranuclear and cytoplasmic inclusions in Machado-Joseph disease. *Psychiatry Clin. Neurosci.* **57**, 205–213 (2003).
170. van Alfen, N. *et al.* Intermediate CAG repeat lengths (53,54) for MJD/SCA3 are associated with an abnormal phenotype. *Ann. Neurol.* **49**, 805–7 (2001).
171. Maciel, P. *et al.* Improvement in the molecular diagnosis of Machado-Joseph disease. *Arch. Neurol.* **58**, 1821–7 (2001).
172. Mirkin, S. M. Expandable DNA repeats and human disease. *Nature* **447**, 932–940 (2007).
173. Jalles, A. Searching for therapeutic compounds in a transgenic Caenorhabditis. (Universidade do Minho, Braga, Portugal, 2011).
174. Costa, M. do C. *et al.* Ataxin-3 Plays a Role in Mouse Myogenic Differentiation through Regulation of Integrin Subunit Levels. *PLoS One* **5**, e11728 (2010).
175. Hochstrasser, M. Origin and function of ubiquitin-like proteins. *Nature* **458**, 422–429 (2009).
176. Markossian, K. A. & Kurganov, B. I. Protein folding, misfolding, and aggregation. Formation of inclusion bodies and aggresomes. *Biochemistry. (Mosc).* **69**, 971–84 (2004).
177. Rodrigues, A.-J. *et al.* Absence of ataxin-3 leads to cytoskeletal disorganization and increased cell death. *Biochim. Biophys. Acta - Mol. Cell Res.* **1803**, 1154–1163 (2010).
178. Rodrigues, A.-J. *et al.* Functional genomics and biochemical characterization of the *C. elegans* orthologue of the Machado-Joseph disease protein ataxin-3. *FASEB J.* **21**, 1126–1136 (2007).
179. Bauer, P. O. & Nukina, N. The pathogenic mechanisms of polyglutamine diseases and current therapeutic strategies. *J. Neurochem.* **110**, 1737–1765 (2009).
180. Nóbrega, C. & de Almeida, L. P. Machado-Joseph Disease / Spinocerebellar Ataxia Type 3. in *Spinocerebellar Ataxia* (ed. Gazulla, J.)

(InTech, 2012).

181. Shao, J. & Diamond, M. I. Polyglutamine diseases: emerging concepts in pathogenesis and therapy. *Hum. Mol. Genet.* **16**, R115–R123 (2007).
182. Kalia, L. V & Lang, A. E. Parkinson's disease. *Lancet (London, England)* **386**, 896–912 (2015).
183. Jankovic, J. Parkinson's disease: clinical features and diagnosis. *J. Neurol. Neurosurg. Psychiatry* **79**, 368–76 (2008).
184. Smeyne, M. & Smeyne, R. J. Glutathione metabolism and Parkinson's disease. *Free Radic. Biol. Med.* **62**, 13–25 (2013).
185. Kalia, L. V, Kalia, S. K., McLean, P. J., Lozano, A. M. & Lang, A. E. α -Synuclein oligomers and clinical implications for Parkinson disease. *Ann. Neurol.* **73**, 155–69 (2013).
186. Goedert, M., Spillantini, M. G., Del Tredici, K. & Braak, H. 100 years of Lewy pathology. *Nat. Rev. Neurol.* **9**, 13–24 (2013).
187. Wang, Q., Liu, Y. & Zhou, J. Neuroinflammation in Parkinson's disease and its potential as therapeutic target. *Transl. Neurodegener.* **4**, 19 (2015).
188. Segura-Aguilar, J. *et al.* Protective and toxic roles of dopamine in Parkinson's disease. *J. Neurochem.* **129**, 898–915 (2014).
189. Goetz, C. G. The history of Parkinson's disease: Early clinical descriptions and neurological therapies. *Cold Spring Harb. Perspect. Med.* **1**, 1–15 (2011).
190. Birkmayer, W. & Hornykiewicz, O. Der L-Dioxyphenylalanin (=L-DOPA)-Effekt beim Parkinson-Syndrom des Menschen: Zur Pathogenese und Behandlung der Parkinson-Akinese. *Arch. für Psychiatr. und Nervenkrankheiten* **203**, 560–574 (1962).
191. Poewe, W., Antonini, A., Zijlmans, J. C., Burkhard, P. R. & Vingerhoets, F. Levodopa in the treatment of Parkinson's disease: an old drug still going strong. *Clin. Interv. Aging* **5**, 229–38 (2010).
192. Gandhi, S. & Abramov, A. Y. Mechanism of oxidative stress in neurodegeneration. *Oxid. Med. Cell. Longev.* **2012**, 428010 (2012).

193. Uttara, B., Singh, A. V, Zamboni, P. & Mahajan, R. T. Oxidative stress and Neurodegenerative Diseases: A Review of Upstream and Downstream Antioxidant Therapeutic Options. *Curr. Neuropharmacol.* **7**, 65–74 (2009).
194. Sureda, F. X. *et al.* Antiapoptotic drugs: a therapeutic strategy for the prevention of neurodegenerative diseases. *Curr. Pharm. Des.* **17**, 230–45 (2011).
195. Lublin, A. L. & Link, C. D. Alzheimer's disease drug discovery: in vivo screening using *Caenorhabditis elegans* as a model for β -amyloid peptide-induced toxicity. *Drug Discov. Today. Technol.* **10**, e115-9 (2013).
196. Bautista-Aguilera, O. M. *et al.* Multipotent cholinesterase/monoamine oxidase inhibitors for the treatment of Alzheimer's disease: design, synthesis, biochemical evaluation, ADMET, molecular modeling, and QSAR analysis of novel donepezil-pyridyl hybrids. *Drug Des. Devel. Ther.* **8**, 1893–1910 (2014).
197. Aliev, G. *et al.* Flavones from the Root of *Scutellaria baicalensis* Georgi - Drug of the Future in Neurodegeneration and Neuroprotection? in *Systems Biology of Free Radicals and Antioxidants* (ed. Laher, I.) 2305–2323 (Springer-Verlag Berlin Heidelberg, 2014).
198. Rafii, M. S. & Aisen, P. S. Recent developments in Alzheimer's disease therapeutics. *BMC Med.* **7**, 7 (2009).
199. Harman, D. Aging: A Theory Based on Free Radical and Radiation Chemistry. *J. Gerontol.* **11**, 298–300 (1956).
200. Patten, D. A., Germain, M., Kelly, M. A. & Slack, R. S. Reactive Oxygen Species: Stuck in the Middle of Neurodegeneration. *J. Alzheimer's Dis.* **20**, S357–S367 (2010).
201. Knight, J. A. Free radicals: Their history and current status in aging and disease. *Ann. Clin. Lab. Sci.* **28**, 331–346 (1998).
202. Poljsak, B., Šuput, D. & Milisav, I. Achieving the balance between ROS and antioxidants: when to use the synthetic antioxidants. *Oxid. Med. Cell. Longev.* **2013**, 956792 (2013).
203. Pohl, F. & Kong Thoo Lin, P. The Potential Use of Plant Natural Products and Plant Extracts with Antioxidant Properties for the

Prevention/Treatment of Neurodegenerative Diseases: In Vitro, In Vivo and Clinical Trials. *Molecules* **23**, 3283 (2018).

204. Tang, L.-L., Wang, R. & Tang, X.-C. Huperzine A protects SHSY5Y neuroblastoma cells against oxidative stress damage via nerve growth factor production. *Eur. J. Pharmacol.* **519**, 9–15 (2005).
205. Choi, D.-Y. Y., Lee, Y.-J. J., Hong, J. T. & Lee, H.-J. J. Antioxidant properties of natural polyphenols and their therapeutic potentials for Alzheimer's disease. *Brain Res. Bull.* **87**, 144–153 (2012).
206. Chege, P. M. & McColl, G. *Caenorhabditis elegans*: a model to investigate oxidative stress and metal dyshomeostasis in Parkinson's disease. *Front. Aging Neurosci.* **6**, 1–15 (2014).
207. Wang, J. *et al.* RNAi Screening Implicates a SKN-1-Dependent Transcriptional Response in Stress Resistance and Longevity Deriving from Translation Inhibition. *PLoS Genet.* **6**, e1001048 (2010).
208. Martínez, M. C. & Andriantsitohaina, R. Reactive Nitrogen Species: Molecular Mechanisms and Potential Significance in Health and Disease. *Antioxid. Redox Signal.* **11**, 669–702 (2009).
209. Gilgun-Sherki, Y., Melamed, E. & Offen, D. Oxidative stress induced-neurodegenerative diseases: the need for antioxidants that penetrate the blood brain barrier. *Neuropharmacology* **40**, 959–975 (2001).
210. Augustyniak, A. *et al.* Natural and synthetic antioxidants: An updated overview. *Free Radic. Res.* **44**, 1216–1262 (2010).
211. Mirończuk-Chodakowska, I., Witkowska, A. M. & Zujko, M. E. Endogenous non-enzymatic antioxidants in the human body. *Adv. Med. Sci.* **63**, 68–78 (2018).
212. Carocho, M. & Ferreira, I. C. F. R. A review on antioxidants, prooxidants and related controversy: Natural and synthetic compounds, screening and analysis methodologies and future perspectives. *Food Chem. Toxicol.* **51**, 15–25 (2013).
213. Kennedy, D. O. & Wightman, E. L. Herbal Extracts and Phytochemicals: Plant Secondary Metabolites and the Enhancement of Human Brain Function. *Adv. Nutr. An Int. Rev. J.* **2**, 32–50 (2011).

214. Scipioni, M., Kay, G., Megson, I. & Kong Thoo Lin, P. Novel vanillin derivatives: Synthesis, anti-oxidant, DNA and cellular protection properties. *Eur. J. Med. Chem.* **143**, 745–754 (2018).
215. Harvey, A. L., Edrada-Ebel, R. & Quinn, R. J. The re-emergence of natural products for drug discovery in the genomics era. *Nat. Rev. Drug Discov.* **14**, 111–129 (2015).
216. Mathur, S. & Hoskins, C. Drug development: Lessons from nature. *Biomed. reports* **6**, 612–614 (2017).
217. Harbourne, N., Marete, E., Jacquier, J. C. & O’Riordan, D. Stability of phytochemicals as sources of anti-inflammatory nutraceuticals in beverages — A review. *Food Res. Int.* **50**, 480–486 (2013).
218. Khlifi, D. & Sghaier, R. M. Anti-Inflammatory and Acetylcholinesterase Inhibition Activities of *Globularia Alypum*. *J. Med. Bioeng.* **2**, 232–237 (2013).
219. Wink, M. & Abbas, S. Epigallocatechin Gallate (EGCG) from Green Tea (*Camellia sinensis*) and Other Natural Products Mediate Stress Resistance and Slows Down Aging Processes in *Caenorhabditis elegans*. in *Tea in Health and Disease Prevention* (ed. Preedy, V. R.) 1105–1115 (Elsevier Science Publishing Co Inc, 2013).
220. Sun-Waterhouse, D. The development of fruit-based functional foods targeting the health and wellness market: a review. *Int. J. Food Sci. Technol.* **46**, 899–920 (2011).
221. Brusotti, G., Cesari, I., Dentamaro, a, Caccialanza, G. & Massolini, G. Isolation and characterization of bioactive compounds from plant resources: the role of analysis in the ethnopharmacological approach. *J. Pharm. Biomed. Anal.* **87**, 218–28 (2014).
222. Upadhyay, S. & Dixit, M. Role of Polyphenols and Other Phytochemicals on Molecular Signaling. *Oxid. Med. Cell. Longev.* **2015**, 15 (2015).
223. Björkman, M. *et al.* Phytochemicals of Brassicaceae in plant protection and human health--influences of climate, environment and agronomic practice. *Phytochemistry* **72**, 538–56 (2011).
224. Dinkova-Kostova, A. T. & Talalay, P. Direct and indirect antioxidant properties of inducers of cytoprotective proteins. *Mol. Nutr. Food Res.* **52**,

128–138 (2008).

225. Xu, D.-P. *et al.* Natural Antioxidants in Foods and Medicinal Plants: Extraction, Assessment and Resources. *Int. J. Mol. Sci.* **18**, (2017).
226. Kostova, I. Synthetic and natural coumarins as antioxidants. *Mini Rev. Med. Chem.* **6**, 365–374 (2006).
227. Magesh, S., Chen, Y. & Hu, L. Small molecule modulators of Keap1-Nrf2-ARE pathway as potential preventive and therapeutic agents. *Med. Res. Rev.* **32**, 687–726 (2012).
228. Ahn, Y.-H. *et al.* Electrophilic tuning of the chemoprotective natural product sulforaphane. *Proc. Natl. Acad. Sci. U. S. A.* **107**, 9590–5 (2010).
229. Stefanson, A. L. & Bakovic, M. Dietary regulation of Keap1/Nrf2/ARE pathway: focus on plant-derived compounds and trace minerals. *Nutrients* **6**, 3777–801 (2014).
230. Lee, J., Jo, D.-G., Park, D., Chung, H. Y. & Mattson, M. P. Adaptive Cellular Stress Pathways as Therapeutic Targets of Dietary Phytochemicals: Focus on the Nervous System. *Pharmacol. Rev.* **66**, 815–868 (2014).
231. Smith, R. *et al.* The Role of the Nrf2/ARE Antioxidant System in Preventing Cardiovascular Diseases. *Diseases* **4**, 34 (2016).
232. Santos, J. S., Alvarenga Brizola, V. R. & Granato, D. High-throughput assay comparison and standardization for metal chelating capacity screening: A proposal and application. *Food Chem.* **214**, 515–522 (2017).
233. Gao, Z., Huang, K., Yang, X. & Xu, H. Free radical scavenging and antioxidant activities of flavonoids extracted from the radix of *Scutellaria baicalensis* Georgi. *Biochim. Biophys. Acta - Gen. Subj.* **1472**, 643–650 (1999).
234. Huang, W.-H., Lee, A.-R. & Yang, C.-H. Antioxidative and anti-inflammatory activities of polyhydroxyflavonoids of *Scutellaria baicalensis* GEORGI. *Biosci. Biotechnol. Biochem.* **70**, 2371–2380 (2006).
235. Dhanalakshmi, C., Manivasagam, T., Nataraj, J., Justin Thenmozhi, A. & Essa, M. M. Neurosupportive Role of Vanillin, a Natural Phenolic Compound, on Rotenone Induced Neurotoxicity in SH-SY5Y Neuroblastoma Cells. *Evid. Based. Complement. Alternat. Med.* **2015**,

- 626028 (2015).
236. Braidy, N. *et al.* Neuroprotective effects of a variety of pomegranate juice extracts against MPTP-induced cytotoxicity and oxidative stress in human primary neurons. *Oxid. Med. Cell. Longev.* **2013**, 685909 (2013).
 237. Wu, Y.-L. *et al.* Treatment with Caffeic Acid and Resveratrol Alleviates Oxidative Stress Induced Neurotoxicity in Cell and Drosophila Models of Spinocerebellar Ataxia Type3. *Sci. Rep.* **7**, 11641 (2017).
 238. Wei, C.-C. *et al.* Antioxidant Activity, Delayed Aging, and Reduced Amyloid- β Toxicity of Methanol Extracts of Tea Seed Pomace from *Camellia tenuifolia*. *J. Agric. Food Chem.* **62**, 10701–7 (2014).
 239. Abbas, S. & Wink, M. Epigallocatechin gallate inhibits beta amyloid oligomerization in *Caenorhabditis elegans* and affects the daf-2/insulin-like signaling pathway. *Phytomedicine* **17**, 902–9 (2010).
 240. Jahromi, S. R., Haddadi, M., Shivanandappa, T. & Ramesh, S. R. Attenuation of neuromotor deficits by natural antioxidants of *Decalepis hamiltonii* in transgenic *Drosophila* model of Parkinson's disease. *Neuroscience* **293**, 136–150 (2015).
 241. Lee, H. E. *et al.* Neuroprotective effect of sinapic acid in a mouse model of amyloid β (1-42) protein-induced Alzheimer's disease. *Pharmacol. Biochem. Behav.* **103**, 260–6 (2012).
 242. Karakida, F. *et al.* Cerebral protective and cognition-improving effects of sinapic acid in rodents. *Biol. Pharm. Bull.* **30**, 514–9 (2007).
 243. Haque, E., Javed, H., Azimullah, S., Abul Khair, S. B. & Ojha, S. Neuroprotective potential of ferulic acid in the rotenone model of Parkinson's disease. *Drug Des. Devel. Ther.* **9**, 5499–5510 (2015).
 244. Radojković, M. *et al.* Optimization of solid-liquid extraction of antioxidants from black mulberry leaves by response surface methodology. *Food Technol. Biotechnol.* **50**, 167–176 (2012).
 245. Azwanida, N. N. A Review on the Extraction Methods Use in Medicinal Plants, Principle, Strength and Limitation. *Med. Aromat. Plants* **04**, 1–6 (2015).
 246. Kim, H. K., Choi, Y. H. & Verpoorte, R. NMR-based metabolomic analysis

of plants. *Nat. Protoc.* **5**, 536–549 (2010).

247. Romanik, G., Gilgenast, E., Przyjazny, A. & Kamiński, M. Techniques of preparing plant material for chromatographic separation and analysis. *J. Biochem. Biophys. Methods* **70**, 253–261 (2007).
248. Eliasson, L., Labrosse, L. & Ahrné, L. Effect of drying technique and particle size of bilberry press cake on the extraction efficiency of anthocyanins by pressurized carbon dioxide extraction. *LWT - Food Sci. Technol.* **85**, 510–516 (2017).
249. Vongsak, B. *et al.* Maximizing total phenolics, total flavonoids contents and antioxidant activity of *Moringa oleifera* leaf extract by the appropriate extraction method. *Ind. Crops Prod.* **44**, 566–571 (2013).
250. Vaidya, B. N. & Brearley, T. A. Antioxidant Capacity of Fresh and Dry Leaf Extracts of Sixteen *Scutellaria* Species. *J. Med. Act. Plants* **2**, 42–49 (2014).
251. Mulinacci, N. *et al.* Storage method, drying processes and extraction procedures strongly affect the phenolic fraction of rosemary leaves: An HPLC/DAD/MS study. *Talanta* **85**, 167–176 (2011).
252. Handa, S. S. *et al.* *Extraction Technologies for Medicinal and Aromatic Plants*. (International Centre for Science and High Technology, 2008).
253. Mankanjuola, S. A. Influence of particle size and extraction solvent on antioxidant properties of extracts of tea, ginger, and tea-ginger blend. *Food Sci. Nutr.* **5**, 1179–1185 (2017).
254. Kossah, R., Nasbimana, C., Zhang, H. & Chen, W. Optimization of Extraction of Polyphenols from Syrian Sumac (*Rhus coriaria* L.) and Chinese Sumac (*Rhus typhina* L.) Fruits. *Res. J. Phytochem.* **4**, 146–153 (2010).
255. Khan, M. K., Abert-Vian, M., Fabiano-Tixier, A.-S., Dangles, O. & Chemat, F. Ultrasound-assisted extraction of polyphenols (flavanone glycosides) from orange (*Citrus sinensis* L.) peel. *Food Chem.* **119**, 851–858 (2010).
256. Azmir, J. *et al.* Techniques for extraction of bioactive compounds from plant materials: A review. *J. Food Eng.* **117**, 426–436 (2013).
257. Cowan, M. M. Plant products as antimicrobial agents. *Clin. Microbiol. Rev.*

- 12**, 564–82 (1999).
258. Puri, M., Sharma, D. & Barrow, C. J. Enzyme-assisted extraction of bioactives from plants. *Trends Biotechnol.* **30**, 37–44 (2012).
259. Ngo, T. Van, Scarlett, C. J., Bowyer, M. C., Ngo, P. D. & Vuong, Q. Van. Impact of Different Extraction Solvents on Bioactive Compounds and Antioxidant Capacity from the Root of *Salacia chinensis* L. *J. Food Qual.* **2017**, 1–8 (2017).
260. Ruenroengklin, N. *et al.* Effects of various temperatures and pH values on the extraction yield of phenolics from litchi fruit pericarp tissue and the antioxidant activity of the extracted anthocyanins. *Int. J. Mol. Sci.* **9**, 1333–1341 (2008).
261. Wong, B. Y., Tan, C. P. & Ho, C. W. Effect of solid-to-solvent ratio on phenolic content and antioxidant capacities of 'Dukung Anak' (*Phyllanthus niruri*). *Int. Food Res. J.* **20**, 325–330 (2013).
262. Irshad, M., Zafaryab, M., Singh, M. & Rizvi, M. M. a. Comparative Analysis of the Antioxidant Activity of *Cassia fistula* Extracts. *Int. J. Med. Chem.* **2012**, 157125 (2012).
263. He, R. *et al.* Antioxidant activities of rapeseed peptides produced by solid state fermentation. *Food Res. Int.* **49**, 432–438 (2012).
264. Bochoráková, H. *et al.* Main flavonoids in the root of *Scutellaria baicalensis* cultivated in Europe and their comparative antiradical properties. *Phytother. Res.* **17**, 640–4 (2003).
265. Ahmad, A., Alkarkhi, A. F. M., Hena, S. & Khim, L. H. Extraction, Separation and Identification of Chemical Ingredients of *Elephantopus Scaber* L. Using Factorial Design of Experiment. *Int. J. Chem.* **1**, 36–49 (2009).
266. Gerhardt. Soxtherm Instruction Manual. 38 (2009).
267. Wagener, S. The Extraction and Activities of Phytochemicals Derived from Rapeseed Pomace. (The Robert Gordon University, 2013).
268. Londoño-Londoño, J. *et al.* Clean recovery of antioxidant flavonoids from citrus peel: Optimizing an aqueous ultrasound-assisted extraction method. *Food Chem.* **119**, 81–87 (2010).

269. Charpe, T. W. & Rathod, V. K. Extraction of glycyrrhizic acid from licorice root using ultrasound: Process intensification studies. *Chem. Eng. Process. Process Intensif.* **54**, 37–41 (2012).
270. Rao, P. R. & Rathod, V. K. Mapping study of an ultrasonic bath for the extraction of andrographolide from *Andrographis paniculata* using ultrasound. *Ind. Crops Prod.* **66**, 312–318 (2015).
271. Chemat, F. *et al.* Ultrasound assisted extraction of food and natural products. Mechanisms, techniques, combinations, protocols and applications. A review. *Ultrason. Sonochem.* **34**, 540–560 (2017).
272. Rutkowska, M., Namieśnik, J. & Konieczka, P. Ultrasound-Assisted Extraction. in *The Application of Green Solvents in Separation Processes* (eds. Pena-Pereira, F. & Tobiszewski, M.) 301–324 (Elsevier Inc., 2017).
273. Medina-Torres, N., Ayora-Talavera, T., Espinosa-Andrews, H., Sánchez-Contreras, A. & Pacheco, N. Ultrasound Assisted Extraction for the Recovery of Phenolic Compounds from Vegetable Sources. *Agronomy* **7**, 47 (2017).
274. Muñiz-Márquez, D. B. *et al.* Ultrasound-assisted extraction of phenolic compounds from *Laurus nobilis* L. and their antioxidant activity. *Ultrason. Sonochem.* **20**, 1149–1154 (2013).
275. Pacheco-Palencia, L. A., Duncan, C. E. & Talcott, S. T. Phytochemical composition and thermal stability of two commercial açai species, *Euterpe oleracea* and *Euterpe precatoria*. *Food Chem.* **115**, 1199–1205 (2009).
276. Hossain, M. B., Barry-Ryan, C., Martin-Diana, A. B. & Brunton, N. P. Optimisation of accelerated solvent extraction of antioxidant compounds from rosemary (*Rosmarinus officinalis* L.), marjoram (*Origanum majorana* L.) and oregano (*Origanum vulgare* L.) using response surface methodology. *Food Chem.* **126**, 339–346 (2011).
277. Srivastava, A., Akoh, C. C., Yi, W., Fischer, J. & Krewer, G. Effect of storage conditions on the biological activity of phenolic compounds of blueberry extract packed in glass bottles. *J. Agric. Food Chem.* **55**, 2705–2713 (2007).
278. Maisuthisakul, P. & Gordon, M. H. Characterization and storage stability

- of the extract of Thai mango (*Mangifera indica* Linn. Cultivar Chok-Anan) seed kernels. *J. Food Sci. Technol.* **51**, 1453–62 (2014).
279. Jha, D. K., Panda, L., Lavanya, P., Ramaiah, S. & Anbarasu, A. Detection and Confirmation of Alkaloids in Leaves of *Justicia adhatoda* and Bioinformatics Approach to Elicit Its Anti-tuberculosis Activity. *Appl. Biochem. Biotechnol.* **168**, 980–990 (2012).
280. Oleszek, W. . Chromatographic determination of plant saponins. *J. Chromatogr. A* **967**, 147–162 (2002).
281. María, R. *et al.* Preliminary phytochemical screening, total phenolic content and antibacterial activity of thirteen native species from Guayas province Ecuador. *J. King Saud Univ. - Sci.* **30**, 500–505 (2017).
282. Thomas, A. W. & Frieden, A. The Gelatin-Tannin Reaction. *Ind. Eng. Chem.* **15**, 839–841 (1923).
283. Ajanal, M., Gundkalle, M. B. & Nayak, S. U. Estimation of total alkaloid in Chitrakadivati by UV-Spectrophotometer. *Anc. Sci. Life* **31**, 198–201 (2012).
284. Li, L. *et al.* Studies on quantitative determination of total alkaloids and berberine in five origins of crude medicine 'sankezhen'. *J. Chromatogr. Sci.* **53**, 307–311 (2015).
285. Mawlong, I., Sujith Kumar, M. S., Gurung, B., Singh, K. H. & Singh, D. A simple spectrophotometric method for estimating total glucosinolates in mustard de-oiled cake. *Int. J. Food Prop.* **20**, 3274–3281 (2017).
286. Changling, Y., Bing, F., Yuqin, J. & Zhijing, H. Determination of Total Glucosinolates in Cruciferous Seeds by Semimicro-gravimetry and Spectrophotometry with Tetrachloropalladate. *Fett Wiss. Technol. Sci. Technol.* **89**, 342–345 (1987).
287. Wang, S. *et al.* Rutin inhibits β -amyloid aggregation and cytotoxicity, attenuates oxidative stress, and decreases the production of nitric oxide and proinflammatory cytokines. *Neurotoxicology* **33**, 482–90 (2012).
288. Chang, C. L., Lin, C. S. & Lai, G. H. Phytochemical characteristics, free radical scavenging activities, and neuroprotection of five medicinal plant extracts. *Evidence-based Complement. Altern. Med.* **2012**, (2012).

289. Carro, M. Di, Ianni, C. & Magi, E. Determination of Terpenoids in Plant Leaves by GC-MS: Development of the Method and Application to *Ocimum basilicum* and *Nicotiana glauca*. *Anal. Lett.* **46**, 630–639 (2013).
290. Harman-Ware, A. E., Sykes, R., Peter, G. F. & Davis, M. Determination of Terpenoid Content in Pine by Organic Solvent Extraction and Fast-GC Analysis. *Front. Energy Res.* **4**, 2 (2016).
291. Zhao, Y., Sun, Y. & Li, C. Simultaneous Determination of Ginkgo Flavonoids and Terpenoids in Plasma: Ammonium Formate in LC Mobile Phase Enhancing Electrospray Ionization Efficiency and Capacity. *J. Am. Soc. Mass Spectrom.* **19**, 445–449 (2008).
292. Terpinč, P., Čeh, B., Ulrih, N. P. & Abramovič, H. Studies of the correlation between antioxidant properties and the total phenolic content of different oil cake extracts. *Ind. Crops Prod.* **39**, 210–217 (2012).
293. Russell, W. R., Labat, A., Scobbie, L., Duncan, G. J. & Duthie, G. G. Phenolic acid content of fruits commonly consumed and locally produced in Scotland. *Food Chem.* **115**, 100–104 (2009).
294. Ferreres, F. *et al.* Tronchuda cabbage (*Brassica oleracea* L. var. *costata* DC) seeds: Phytochemical characterization and antioxidant potential. *Food Chem.* **101**, 549–558 (2007).
295. Lee, J., Durst, R. W. & Wrolstad, R. E. Determination of Total Monomeric Anthocyanin Pigment Content of Fruit Juices, Beverages, Natural Colorants, and Wines by the pH Differential Method: Collaborative Study. *J. AOAC Int.* **88**, 1269–1278 (2015).
296. Brito, A., Areche, C., Sepúlveda, B., Kennelly, E. J. & Simirgiotis, M. J. Anthocyanin characterization, total phenolic quantification and antioxidant features of some Chilean edible berry extracts. *Molecules* **19**, 10936–10955 (2014).
297. Thunig, J., Hansen, S. H. & Janfelt, C. Analysis of Secondary Plant Metabolites by Indirect Desorption Electrospray Ionization Imaging Mass Spectrometry. *Anal. Chem.* **83**, 3256–3259 (2011).
298. Stashenko, E. E., Andrés Ordóñez, S., Marín, N. A. & Martínez, J. R. Determination of the volatile and semi-volatile secondary metabolites,

- and aristolochic acids in *Aristolochia ringens* Vahl. *J. Chromatogr. Sci.* **47**, 817–21 (2009).
299. Karthika, K. & Paulsamy, S. TLC and HPTLC Fingerprints of Various Secondary Metabolites in the Stem of the Traditional Medicinal Climber, *Solena amplexicaulis*. *Indian J. Pharm. Sci.* **77**, 111–6 (2015).
300. Cozzolino, D. Infrared Spectroscopy as a Versatile Analytical Tool for the Quantitative Determination of Antioxidants in Agricultural Products, Foods and Plants. *Antioxidants* **4**, 482–497 (2015).
301. López-Alarcón, C. & Denicola, A. Evaluating the antioxidant capacity of natural products: A review on chemical and cellular-based assays. *Anal. Chim. Acta* **763**, 1–10 (2013).
302. Huang, D., Ou, B., Prior, R. L. & Rior, R. O. L. P. The chemistry behind antioxidant capacity assays. *J. Agric. Food Chem.* **53**, 1841–56 (2005).
303. Apak, R. *et al.* Comparative Evaluation of Various Total Antioxidant Capacity Assays Applied to Phenolic Compounds with the CUPRAC Assay. *Molecules* 1496–1547 (2007).
304. Leopoldini, M., Marino, T., Russo, N. & Toscano, M. Antioxidant Properties of Phenolic Compounds: H-Atom versus Electron Transfer Mechanism. doi:10.1021/jp037247d
305. Ou, B., Hampsch-Woodill, M. & Prior, R. L. Development and validation of an improved oxygen radical absorbance capacity assay using fluorescein as the fluorescent probe. *J. Agric. Food Chem.* **49**, 4619–26 (2001).
306. Wayner, D. D., Burton, G. W., Ingold, K. U. & Locke, S. Quantitative measurement of the total, peroxy radical-trapping antioxidant capability of human blood plasma by controlled peroxidation. The important contribution made by plasma proteins. *FEBS Lett.* **187**, 33–7 (1985).
307. Bors, W., Michel, C. & Saran, M. Inhibition of the bleaching of the carotenoid crocin a rapid test for quantifying antioxidant activity. *Biochim. Biophys. Acta - Lipids Lipid Metab.* **796**, 312–319 (1984).
308. Ghiselli, A., Serafini, M., Natella, F. & Scaccini, C. Total antioxidant capacity as a tool to assess redox status: critical view and experimental data. *Free Radic. Biol. Med.* **29**, 1106–1114 (2000).

309. Prior, R. L. Oxygen radical absorbance capacity (ORAC): New horizons in relating dietary antioxidants/bioactives and health benefits. *J. Funct. Foods* **18**, 797–810 (2015).
310. Xie, J. & Schaich, K. M. Re-evaluation of the 2,2-diphenyl-1-picrylhydrazyl free radical (DPPH) assay for antioxidant activity. *J. Agric. Food Chem.* **62**, 4251–60 (2014).
311. Ndhlala, A. R., Ncube, B. & Van Staden, J. Developments in Antioxidants - Retrospective and Prospective Insights. in *Systems Biology of Free Radicals and Antioxidants* (ed. Laher, I.) 489–503 (Springer-Verlag Berlin Heidelberg, 2014).
312. Shahidi, F., Alasalvar, C. & Liyana-Pathirana, C. M. Antioxidant Phytochemicals in Hazelnut Kernel (*Corylus avellana* L.) and Hazelnut Byproducts. *J. Agric. Food Chem.* **55**, 1212–1220 (2007).
313. Sonani, R. R., Singh, N. K., Kumar, J., Thakar, D. & Madamwar, D. Concurrent purification and antioxidant activity of phycobiliproteins from *Lyngbya* sp. A09DM: An antioxidant and anti-aging potential of phycoerythrin in *Caenorhabditis elegans*. *Process Biochem.* **49**, 1757–1766 (2014).
314. Folin, O. & Denis, W. On phosphotungstic-phosphomolybdic compounds as color reagents. *J. Biol. Chem.* **12**, 239–243 (1912).
315. Folin, O. & Ciocalteu, V. On Tyrosine and Tryptophane in Proteins. *J. Biol. Chem.* **73**, 627–648 (1927).
316. Singleton, V. L., Rossi Jr., J. A. & Rossi J A Jr. Colorimetry of Total Phenolics with Phosphomolybdic-Phosphotungstic Acid Reagents. *Am. J. Enol. Vitic.* **16**, 144–158 (1965).
317. European Communities. Commission Regulation (EEC) No 2676/90 of 17 September 1990 determining Community methods for the analysis of wines. *Off. J. Eur. Communities* **33**, (1990).
318. European Commission. List and description of methods of analysis referred to in the first paragraph of Article 120g of Council Regulation (EC) No 1234/2007. *Off. J. Eur. Union* **53**, 12–13 (2010).
319. Amorati, R. & Valgimigli, L. Advantages and limitations of common testing

- methods for antioxidants. *Free Radic. Res.* **49**, 633–649 (2015).
320. Stevanato, R., Sabrina Fabris & Momo, F. New Enzymatic Method for the Determination of Total Phenolic Content in Tea and Wine. *J. Agric. Food Chem.* **52**, 6287–6293 (2004).
321. Benzie, I. F. F. An automated, specific, spectrophotometric method for measuring ascorbic acid in plasma (EFTSA). *Clin. Biochem.* **29**, 111–116 (1996).
322. Benzie, I. F. F. & Strain, J. J. The Ferric Reducing Ability of Plasma (FRAP) as a Measure of "Antioxidant Power": The FRAP Assay. *Anal. Biochem.* **239**, 70–76 (1996).
323. Prior, R. L., Wu, X. & Schaich, K. Standardized Methods for the Determination of Antioxidant Capacity and Phenolics in Foods and Dietary Supplements. *J. Agric. Food Chem.* **53**, 4290–4302 (2005).
324. Benzie, I. F. F. & Szeto, Y. T. Total antioxidant capacity of teas by the ferric reducing/ antioxidant power assay. *J. Agric. Food Chem.* **47**, 633–636 (1999).
325. Gan, R.-Y. *et al.* Screening of Natural Antioxidants from Traditional Chinese Medicinal Plants Associated with Treatment of Rheumatic Disease. *Molecules* **15**, 5988–5997 (2010).
326. Guo, Y.-J. *et al.* Antioxidant capacities, phenolic compounds and polysaccharide contents of 49 edible macro-fungi. *Food Funct.* **3**, 1195 (2012).
327. Blois, M. S. Antioxidant determinations by the use of a stable free radical. *Nature* **181**, 1199–1200 (1958).
328. Csepregi, K., Neugart, S., Schreiner, M. & Hideg, É. Comparative evaluation of total antioxidant capacities of plant polyphenols. *Molecules* **21**, 1–17 (2016).
329. Roy, M. K. *et al.* ORAC and DPPH assay comparison to assess antioxidant capacity of tea infusions: Relationship between total polyphenol and individual catechin content. *Int. J. Food Sci. Nutr.* **61**, 109–124 (2010).
330. Dudonné, S., Vitrac, X., Coutière, P., Woillez, M. & Mérillon, J.-M. Comparative Study of Antioxidant Properties and Total Phenolic Content

of 30 Plant Extracts of Industrial Interest Using DPPH, ABTS, FRAP, SOD, and ORAC Assays. *J. Agric. Food Chem.* **57**, 1768–1774 (2009).

331. Chen, J. *et al.* Extracts of Tsai Tai (*Brassica chinensis*): enhanced antioxidant activity and anti-aging effects both in vitro and in *Caenorhabditis elegans*. *Food Funct.* **7**, 943–952 (2016).
332. Ferreira, A., Proença, C., Serralheiro, M. L. M. & Araújo, M. E. M. The in vitro screening for acetylcholinesterase inhibition and antioxidant activity of medicinal plants from Portugal. *J. Ethnopharmacol.* **108**, 31–7 (2006).
333. Shahidi, F., Alasalvar, C. & Liyana-Pathirana, C. M. Antioxidant phytochemicals in hazelnut kernel (*Corylus avellana* L) and hazelnut byproducts. *J. Agric. Food Chem.* **55**, 1212–1220 (2007).
334. Glazer, A. N. Phycoerythrin fluorescence-based assay for reactive oxygen species. *Methods Enzymol.* **186**, 161–168 (1990).
335. Cao, G., Alessio, H. M. & Cutler, R. G. Oxygen-radical absorbance capacity assay for antioxidants. *Free Radic. Biol. Med.* **14**, 303–11 (1993).
336. Zulueta, A., Esteve, M. J. & Frígola, A. ORAC and TEAC assays comparison to measure the antioxidant capacity of food products. *Food Chem.* **114**, 310–316 (2009).
337. Niki, E. Free radical initiators as source of water- or lipid-soluble peroxy radicals. in *Methods in Enzymology* (eds. Packer, L. & Glazer, A. N.) **186**, 100–108 (Elsevier Inc., 1990).
338. Chandrasekara, A., Rasek, O. A., John, J. A., Chandrasekara, N. & Shahidi, F. Solvent and Extraction Conditions Control the Assayable Phenolic Content and Antioxidant Activities of Seeds of Black Beans, Canola and Millet. *J. Am. Oil Chem. Soc.* **93**, 275–283 (2016).
339. Vergara-Salinas, J. R., Pérez-Jiménez, J., Torres, J. L., Agosin, E. & Pérez-Correa, J. R. Effects of Temperature and Time on Polyphenolic Content and Antioxidant Activity in the Pressurized Hot Water Extraction of Deodorized Thyme (*Thymus vulgaris*). *J. Agric. Food Chem.* **60**, 10920–9 (2012).
340. Ky, I., Lorrain, B., Kolbas, N., Crozier, A. & Teissedre, P.-L. Wine by-Products: Phenolic Characterization and Antioxidant Activity Evaluation of

- Grapes and Grape Pomaces from Six Different French Grape Varieties. *Molecules* **19**, 482–506 (2014).
341. Schaich, K. M., Tian, X. & Xie, J. Hurdles and pitfalls in measuring antioxidant efficacy: A critical evaluation of ABTS, DPPH, and ORAC assays. *J. Funct. Foods* **14**, 111–125 (2015).
342. Russell, W. R. *et al.* High-protein, reduced-carbohydrate weight-loss diets promote metabolite profiles likely to be detrimental to colonic health. *Am. J. Clin. Nutr.* **93**, 1062–1072 (2011).
343. Neacsu, M. *et al.* Bound phytophenols from ready-to-eat cereals: Comparison with other plant-based foods. *Food Chem.* **141**, 2880–2886 (2013).
344. Wanasundara, U., Amarowicz, R. & Shahidi, F. Isolation and Identification of an Antioxidative Component in Canola Meal. *J. Agric. Food Chem* **42**, 1285–1290 (1994).
345. Sagdic, O. *et al.* RP-HPLC–DAD analysis of phenolic compounds in pomace extracts from five grape cultivars: Evaluation of their antioxidant, antiradical and antifungal activities in orange and apple juices. *Food Chem.* **126**, 1749–1758 (2011).
346. Liu, Q., Wu, L., Pu, H., Li, C. & Hu, Q. Profile and distribution of soluble and insoluble phenolics in Chinese rapeseed (*Brassica napus*). *Food Chem.* **135**, 616–22 (2012).
347. Waterhouse, A. L. A. L., Waterhouse & L., A. Determination of Total Phenolics. in *Current Protocols in Food Analytical Chemistry* (eds. Wrolstad, R. E. *et al.*) (John Wiley & Sons, Inc., 2003).
348. Arya, A. *et al.* In vitro Antioxidant, PTP-1B Inhibitory Effects and in vivo Hypoglycemic Potential of Selected Medicinal Plants. *Int. J. Pharmacol.* **9**, 50–57 (2013).
349. Huang, D., Ou, B., Hampsch-Woodill, M., Flanagan, J. a. & Prior, R. L. High-Throughput assay of oxygen radical absorbance capacity (ORAC) using a multichannel liquid handling system coupled with a microplate fluorescence reader in 96-well format. *J. Agric. Food Chem.* **50**, 4437–4444 (2002).
350. Russell, W. R., Scobbie, L., Labat, A. & Duthie, G. G. Selective bio-

- availability of phenolic acids from Scottish strawberries. *Mol. Nutr. Food Res.* **53**, S85–S91 (2009).
351. Kroon, P. A., Faulds, C. B., Ryden, P., Robertson, J. A. & Williamson, G. Release of Covalently Bound Ferulic Acid from Fiber in the Human Colon. *J. Agric. Food Chem.* **45**, 661–667 (1997).
352. Gawlik-Dziki, U., Świeca, M. & Dziki, D. Comparison of phenolic acids profile and antioxidant potential of six varieties of spelt (Triticum spelta L.). *J. Agric. Food Chem.* **60**, 4603–4612 (2012).
353. Pohl, F. *et al.* Revalorisation of rapeseed pomace extracts: An in vitro study into its anti-oxidant and DNA protective properties. *Food Chem.* **239**, 323–332 (2018).
354. Krygier, K., Sosulski, F. & Hogge, L. Free, esterified, and insoluble-bound phenolic acids. 2. Composition of phenolic acids in rapeseed flour and hulls. *J. Agric. Food Chem.* **30**, 334–336 (1982).
355. Krygier, K., Sosulski, F. & Hogge, L. Free, esterified, and insoluble-bound phenolic acids. 1. Extraction and purification procedure. *J. Agric. Food Chem.* **30**, 330–334 (1982).
356. Sosulski, F., Krygier, K. & Hogge, L. Free, esterified, and insoluble-bound phenolic acids. 3. Composition of phenolic acids in cereal and potato flours. *J. Agric. Food Chem.* **30**, 337–340 (1982).
357. Mackintosh of Glendaveny. Extra Virgin Cold Pressed Rapeseed Oil. Available at: <https://www.mackintoshofglendaveny.co.uk/contact.html>. (Accessed: 5th June 2018)
358. Arranz, S., Saura-Calixto, F., Shaha, S. & Kroon, P. A. High Contents of Nonextractable Polyphenols in Fruits Suggest That Polyphenol Contents of Plant Foods Have Been Underestimated. *J. Agric. Food Chem.* **57**, 7298–7303 (2009).
359. White, B. L., Howard, L. R. & Prior, R. L. Release of Bound Procyanidins from Cranberry Pomace by Alkaline Hydrolysis. *J. Agric. Food Chem.* **58**, 7572–7579 (2010).
360. Personal Communication. Dr Wendy Russell, Rowett Institute, Aberdeen University. (2018).

361. Sardar, P. & Kempken, F. Characterization of indole-3-pyruvic acid pathway-mediated biosynthesis of auxin in *Neurospora crassa*. *PLoS One* **13**, e0192293 (2018).
362. Kankara, S. S., Mustafa, M., Ibrahim, H. M., Nulit, R. & Go, R. Effect of Drying Methods, Solid-Solvent Ratio, Extraction Time and Extraction Temperature on Phenolic Antioxidants and Antioxidant Activity of *Guiera senegalensis* J.F. Gmel (Combretaceae) Leaves Water Extract. *Am. J. Phytomedicine Clin. Ther.* **2**, 1378–1392 (2014).
363. Prat, D., Hayler, J. & Wells, A. A survey of solvent selection guides. *Green Chem.* **16**, 4546–4551 (2014).
364. Cvjetko, M., Lepojević, Ž., Zeković, Z., Vidović, S. & Milošević, S. ANTIOXIDANT PROPERTIES OF RAPESEED. *Zb. Rad. Fak. u Leskovcu* **19**, 27–33 (2009).
365. Kostadinovic-Velickovska, S. & Mitrev, S. Characterization of Fatty Acid Profile, Polyphenolic Content and Antioxidant Activity of Cold Pressed and Refined Edible Oils from Macedonia. *J. Food Chem. Nutr.* **1**, 16–21 (2013).
366. Jun, H.-I., Wiesenborn, D. P. & Kim, Y.-S. Antioxidant activity of phenolic compounds from canola (*Brassica napus*) seed. *Food Sci. Biotechnol.* **23**, 1753–1760 (2014).
367. Zou, Y., Kim, A. R., Kim, J. E., Choi, J. S. & Chung, H. Y. Peroxynitrite scavenging activity of sinapic acid (3,5-dimethoxy-4-hydroxycinnamic acid) isolated from *Brassica juncea*. *J. Agric. Food Chem.* **50**, 5884–5890 (2002).
368. Pari, L. & Mohamed Jalaludeen, A. Protective role of sinapic acid against arsenic - Induced toxicity in rats. *Chem. Biol. Interact.* **194**, 40–47 (2011).
369. Kim, D. H. *et al.* Sinapic acid attenuates kainic acid-induced hippocampal neuronal damage in mice. *Neuropharmacology* **59**, 20–30 (2010).
370. Picone, P., Nuzzo, D. & Di Carlo, M. Ferulic acid: a natural antioxidant against oxidative stress induced by oligomeric A-beta on sea urchin embryo. *Biol. Bull.* **224**, 18–28 (2013).
371. Han, H. Y. *et al.* Down-regulation of prostate specific antigen in LNCaP cells by flavonoids from the pollen of *Brassica napus* L. *Phytomedicine* **14**,

338–343 (2007).

372. Lopez-Lazaro, M. Distribution and Biological Activities of the Flavonoid Luteolin. *Mini-Reviews Med. Chem.* **9**, 31–59 (2009).
373. Lee, C.-F. *et al.* Kaempferol induces ATM/p53-mediated death receptor and mitochondrial apoptosis in human umbilical vein endothelial cells. *Int. J. Oncol.* **48**, 2007–2014 (2016).
374. Chen, A. Y. & Chen, Y. C. A review of the dietary flavonoid, kaempferol on human health and cancer chemoprevention. *Food Chem.* **138**, 2099–2107 (2013).
375. Wijngaard, H. H., Rößle, C. & Brunton, N. A survey of Irish fruit and vegetable waste and by-products as a source of polyphenolic antioxidants. *Food Chem.* **116**, 202–207 (2009).
376. Sharma, O. P. & Bhat, T. K. DPPH antioxidant assay revisited. *Food Chem.* **113**, 1202–1205 (2009).
377. Phani Kumar, G. *et al.* DNA damage protecting and free radical scavenging properties of Terminalia arjuna bark in PC-12 cells and plasmid DNA. *Free Radicals Antioxidants* **3**, 35–39 (2013).
378. Phaniendra, A., Jestadi, D. B. & Periyasamy, L. Free radicals: properties, sources, targets, and their implication in various diseases. *Indian J. Clin. Biochem.* **30**, 11–26 (2015).
379. Isa, N. M. *et al.* In vitro anti-inflammatory, cytotoxic and antioxidant activities of boesenbergin A, a chalcone isolated from Boesenbergia rotunda (L.) (fingerroot). *Brazilian J. Med. Biol. Res.* **45**, 524–30 (2012).
380. Wu, X. *et al.* Lipophilic and hydrophilic antioxidant capacities of common foods in the United States. *J. Agric. Food Chem.* **52**, 4026–37 (2004).
381. Wu, X. *et al.* Development of a database for total antioxidant capacity in foods: a preliminary study. *J. Food Compos. Anal.* **17**, 407–422 (2004).
382. Prior, R. L., Sintara, M. & Chang, T. Multi-radical (ORACMR5) antioxidant capacity of selected berries and effects of food processing. *J. Berry Res.* **6**, 159–173 (2016).
383. Leyser, L. The Study into the synergistic Effect of Phenolics From

- Rapeseed Pomace Extracts. (Hochschule Bonn-Rhein-Sieg, 2017).
384. Mudnic, I. *et al.* Antioxidative and vasodilatory effects of phenolic acids in wine. *Food Chem.* **119**, 1205–1210 (2010).
385. Rice-Evans, C. A., Miller, N. J. & Paganga, G. Structure-antioxidant activity relationships of flavonoids and phenolic acids. *Free Radic. Biol. Med.* **20**, 933–956 (1996).
386. Sevgi, K., Tepe, B. & Sarikurkcu, C. Antioxidant and DNA damage protection potentials of selected phenolic acids. *Food Chem. Toxicol.* **77**, 12–21 (2015).
387. Ambrosewicz-Walacik, M., Tańska, M. & Rotkiewicz, D. Phospholipids of Rapeseeds and Rapeseed Oils: Factors Determining Their Content and Technological Significance—A Review. *Food Rev. Int.* **31**, 385–400 (2015).
388. Gan, C.-Y. & Latiff, A. A. Optimisation of the solvent extraction of bioactive compounds from *Parkia speciosa* pod using response surface methodology. *Food Chem.* **124**, 1277–1283 (2011).
389. Chen, C. Sinapic Acid and Its Derivatives as Medicine in Oxidative Stress-Induced Diseases and Aging. *Oxid. Med. Cell. Longev.* 1–10 (2015).
390. Mayengbam, S., Achary, A. & Thiyam-Hollander, U. Endogenous Phenolics in Hulls and Cotyledons of Mustard and Canola: A Comparative Study on Its Sinapates and Antioxidant Capacity. *Antioxidants* **3**, 544–558 (2014).
391. Fang, J., Reichelt, M., Kai, M. & Schneider, B. Metabolic Profiling of Lignans and Other Secondary Metabolites from Rapeseed (*Brassica napus* L.). *J. Agric. Food Chem.* **60**, 10523–10529 (2012).
392. Henry, Fils & Garot. Acide sulfo-sinapique. *J. Pharm. des Sci. Accessoires* **11**, 473–474 (1825).
393. Gadamer, J. Über die Bestandteile des schwarzen und des weissen Senfsamens. *Arch. Pharm. (Weinheim)*. **235**, 44–114 (1897).
394. Baumert, A. *et al.* Formation of a complex pattern of sinapate esters in *Brassica napus* seeds, catalyzed by enzymes of a serine carboxypeptidase-like acyltransferase family? *Phytochemistry* **66**, 1334–

1345 (2005).

395. Milkowski, C. & Strack, D. Sinapate esters in brassicaceous plants: biochemistry, molecular biology, evolution and metabolic engineering. *Planta* **232**, 19–35 (2010).
396. Fu, R., Zhang, Y., Guo, Y., Peng, T. & Chen, F. Hepatoprotection using *Brassica rapa* var. *rapa* L. seeds and its bioactive compound, sinapine thiocyanate, for CCl₄-induced liver injury. *J. Funct. Foods* **22**, 73–81 (2016).
397. Dubie, J., Stancik, A., Morra, M. & Nindo, C. Antioxidant Extraction from Mustard (*Brassica juncea*) Seed Meal Using High-Intensity Ultrasound. *J. Food Sci.* **78**, E542–E548 (2013).
398. Ferreres, F. *et al.* Metabolic and Bioactivity Insights into *Brassica oleracea* var. *acephala*. *J. Agric. Food Chem.* **57**, 8884–8892 (2009).
399. Lifang, L., Ling, H. & Yuxin, W. Use of sinapine in preparing medicine for preventing and curing senile dementia. (2006).
400. 冯宝民 *et al.* Method for preparing sinapine thiocyanate from rapeseed cakes and application. (2016).
401. He, L. *et al.* Inhibitory effects of sinapine on activity of acetylcholinesterase in cerebral homogenate and blood serum of rats. *China J. Chinese Mater. medica* **33**, 813–5 (2008).
402. Yang & He. Neuroprotective Effects of Sinapine on PC12 Cells Apoptosis Induced by Sodium Dithionite. *Chin. J. Nat. Med.* **6**, 205–209 (2008).
403. Li, Q. & Gu, R. The Effects of Sinapine from Cruciferous Plants on the Life-Span of *Drosophila Melangaster*. *Chinese J. Appl. Environ. Biol.* **01**, (1999).
404. Clauß, K. *et al.* Overexpression of Sinapine Esterase BnSCE3 in Oilseed Rape Seeds Triggers Global Changes in Seed Metabolism. *Plant Physiol.* **155**, 1127–1145 (2011).
405. Thiyam, U., Pickardt, C., Ungewiss, J. & Baumert, A. De-oiled rapeseed and a protein isolate: characterization of sinapic acid derivatives by HPLC–DAD and LC–MS. *Eur. Food Res. Technol.* **229**, 825–831 (2009).

406. Oszmiański, J., Kolniak-Ostek, J. & Wojdyło, A. Application of ultra performance liquid chromatography-photodiode detector-quadrupole/time of flight-mass spectrometry (UPLC-PDA-Q/TOF-MS) method for the characterization of phenolic compounds of *Lepidium sativum* L. sprouts. *Eur. Food Res. Technol.* **236**, 699–706 (2013).
407. Holst, B. & Williamson, G. A critical review of the bioavailability of glucosinolates and related compounds. *Nat. Prod. Rep.* **21**, 425–447 (2004).
408. Bruce, T. J. A. Glucosinolates in oilseed rape: Secondary metabolites that influence interactions with herbivores and their natural enemies. *Ann. Appl. Biol.* **164**, 348–353 (2014).
409. Becker, T. & Juvik, J. The Role of Glucosinolate Hydrolysis Products from Brassica Vegetable Consumption in Inducing Antioxidant Activity and Reducing Cancer Incidence. *Diseases* **4**, 22 (2016).
410. Cavaiuolo, M. & Ferrante, A. Nitrates and glucosinolates as strong determinants of the nutritional quality in rocket leafy salads. *Nutrients* **6**, 1519–38 (2014).
411. Zhao, F., Evans, E. J., Bilsborrow, P. E. & Syers, J. K. Influence of nitrogen and sulphur on the glucosinolate profile of rapeseed (*brassica napus* l). *J. Sci. Food Agric.* **64**, 295–304 (1994).
412. Houghton, C. A., Fassett, R. G. & Coombes, J. S. Sulforaphane and Other Nutrigenomic Nrf2 Activators: Can the Clinician’s Expectation Be Matched by the Reality? *Oxid. Med. Cell. Longev.* **2016**, 1–17 (2016).
413. Giacoppo, S. *et al.* An overview on neuroprotective effects of isothiocyanates for the treatment of neurodegenerative diseases. *Fitoterapia* **106**, 12–21 (2015).
414. Goodman, I., Fouts, J. R., Bresnick, E., Menegas, R. & Hitchings, G. H. A Mammalian Thioglycosidase. *Science (80-.)*. **130**, 450–451 (1959).
415. Shapiro, T. A., Fahey, J. W., Wade, K. L., Stephenson, K. K. & Talalay, P. Chemoprotective glucosinolates and isothiocyanates of broccoli sprouts: metabolism and excretion in humans. *Cancer Epidemiol. Biomarkers Prev.* **10**, 501–8 (2001).
416. Li, F., Hullar, M. A. J., Beresford, S. A. A. & Lampe, J. W. Variation of

- glucoraphanin metabolism in vivo and ex vivo by human gut bacteria. *Br. J. Nutr.* **106**, 408–16 (2011).
417. Vig, A. P., Rampal, G., Thind, T. S. & Arora, S. Bio-protective effects of glucosinolates – A review. *LWT - Food Sci. Technol.* **42**, 1561–1572 (2009).
418. Kong, J.-M., Chia, L.-S., Goh, N.-K., Chia, T.-F. & Brouillard, R. Analysis and biological activities of anthocyanins. *Phytochemistry* **64**, 923–933 (2003).
419. Ghosh, D., McGhie, T. K., Zhang, J., Adaim, A. & Skinner, M. Effects of anthocyanins and other phenolics of boysenberry and blackcurrant as inhibitors of oxidative stress and damage to cellular DNA in SH-SY5Y and HL-60 cells. *J. Sci. Food Agric.* **86**, 678–686 (2006).
420. Coutinho, M. R., Quadri, M. B., Moreira, R. F. P. M. & Quadri, M. G. N. Partial Purification of Anthocyanins from *Brassica oleracea* (Red Cabbage). *Sep. Sci. Technol.* **39**, 3769–3782 (2004).
421. Suzuki, M., Nagata, T. & Terahara, N. New Acylated Anthocyanins from *Brassica campestris* var. *chinensis*. **8451**, 10–12 (2014).
422. Scalzo, R. Lo, Genna, A., Branca, F., Chedin, M. & Chassaigne, H. Anthocyanin composition of cauliflower (*Brassica oleracea* L. var. *botrytis*) and cabbage (*B. oleracea* L. var. *capitata*) and its stability in relation to thermal treatments. *Food Chem.* **107**, 136–144 (2008).
423. Lin, L.-Z., Sun, J., Chen, P. & Harnly, J. UHPLC-PDA-ESI/HRMS/MSn Analysis of Anthocyanins, Flavonol Glycosides, and Hydroxycinnamic Acid Derivatives in Red Mustard Greens (*Brassica juncea* Coss Variety). *J. Agric. Food Chem.* **59**, 12059–12072 (2011).
424. Nie *et al.* *Brassica napus* possesses enhanced antioxidant capacity via heterologous expression of anthocyanin pathway gene transcription factors. *Russ. J. Plant Physiol.* **60**, 108–115 (2013).
425. Li, X., Gao, M.-J., Pan, H.-Y., Cui, D.-J. & Gruber, M. Y. Purple Canola: *Arabidopsis PAP1* Increases Antioxidants and Phenolics in *Brassica napus* Leaves. *J. Agric. Food Chem.* **58**, 1639–1645 (2010).
426. Fuleki, T. & Francis, F. J. Quantitative Methods for Anthocyanins. 1.

- Extraction and Determination of Total Anthocyanin in Cranberries. *J. Food Sci.* **33**, 72–77 (1968).
427. Singh, N. *et al.* Brain iron homeostasis: from molecular mechanisms to clinical significance and therapeutic opportunities. *Antioxid. Redox Signal.* **20**, 1324–63 (2014).
428. Scheiber, I. F., Mercer, J. F. B. & Dringen, R. Metabolism and functions of copper in brain. *Prog. Neurobiol.* **116**, 33–57 (2014).
429. Delangle, P. & Mintz, E. Chelation therapy in Wilson’s disease: from d-penicillamine to the design of selective bioinspired intracellular Cu(i) chelators. *Dalt. Trans.* **41**, 6359–6370 (2012).
430. Yager, J. Y. & Hartfield, D. S. Neurologic manifestations of iron deficiency in childhood. *Pediatr. Neurol.* **27**, 85–92 (2002).
431. Cicero, C. E. *et al.* Metals and neurodegenerative diseases. A systematic review. *Environ. Res.* **159**, 82–94 (2017).
432. Zhang, Y.-H. *et al.* Efficacy and Toxicity of Clioquinol Treatment and A-beta42 Inoculation in the APP/PS1 Mouse Model of Alzheimer’s Disease. *Curr. Alzheimer Res.* **10**, 494–506 (2013).
433. Lan, J. & Jiang, D. H. Desferrioxamine and vitamin E protect against iron and MPTP-induced neurodegeneration in mice. *J. Neural Transm.* **104**, 469–481 (1997).
434. Carter, P. Spectrophotometric determination of serum iron at the submicrogram level with a new reagent (ferrozine). *Anal. Biochem.* **40**, 450–458 (1971).
435. Colović, M. B., Krstić, D. Z., Lazarević-Pašti, T. D., Bondžić, A. M. & Vasić, V. M. Acetylcholinesterase inhibitors: pharmacology and toxicology. *Curr. Neuropharmacol.* **11**, 315–35 (2013).
436. Santos, M. A., Chand, K. & Chaves, S. Recent progress in repositioning Alzheimer’s disease drugs based on a multitarget strategy. *Futur Med. Chem.* **8**, (2016).
437. Francis, P. T., Palmer, A. M., Snape, M. & Wilcock, G. K. The cholinergic hypothesis of Alzheimer’s disease: a review of progress. *J. Neurol. Neurosurg. Psychiatry* **66**, 137–47 (1999).

438. Davies, P. & Maloney, A. J. F. Selective Loss of Central Cholinergic Neurons in Alzheimer'S Disease. *Lancet* **308**, 1403 (1976).
439. Bartus, R. T., Dean, R. L., Beer, B. & Lippa, A. S. The cholinergic hypothesis of geriatric memory dysfunction. *Science* **217**, 408–14 (1982).
440. Nino, J., Hernández, J. A., Correa, Y. M., Mosquera, O. M. & Niño, J. In vitro inhibition of acetylcholinesterase by crude plant extracts from Colombian flora. *Mem. Inst. Oswaldo Cruz* **101**, 783–785 (2006).
441. Ellman, G. L., Courtney, D., Andres, V. J. & Featherstone, R. M. A New and Rapid Colorimetric Determination of Acetylcholinesterase Activity. *Biochem. Pharmacol.* **7**, 88–95 (1961).
442. Badawy, M. E. I. & El-Aswad, A. F. Bioactive paper sensor based on the acetylcholinesterase for the rapid detection of organophosphate and carbamate pesticides. *Int. J. Anal. Chem.* **2014**, 536823 (2014).
443. Molecular Probes Invitrogen detection technologies. Amplex ® Red Acetylcholine / Acetylcholinesterase Assay Kit (A12217). *Molecular Probes manual* 1–4 (2004).
444. Sweeney, P. *et al.* Protein misfolding in neurodegenerative diseases: implications and strategies. *Transl. Neurodegener.* **6**, 1–13 (2017).
445. Velandar, P. *et al.* Natural product-based amyloid inhibitors. *Biochem. Pharmacol.* **139**, 40–55 (2017).
446. Vassar, P. S. & Culling, C. F. Fluorescent stains, with special reference to amyloid and connective tissues. *Arch. Pathol.* **68**, 487–98 (1959).
447. Wallin, C. *et al.* Alzheimer's disease and cigarette smoke components: effects of nicotine, PAHs, and Cd(II), Cr(III), Pb(II), Pb(IV) ions on amyloid-β peptide aggregation. *Sci. Rep.* **7**, 1–14 (2017).
448. Niidome, T. *et al.* Mulberry leaf extract prevents amyloid beta-peptide fibril formation and neurotoxicity. *Neuroreport* **18**, 813–816 (2007).
449. Ono, K. *et al.* Effects of grape seed-derived polyphenols on amyloid beta-protein self-assembly and cytotoxicity. *J. Biol. Chem.* **283**, 32176–87 (2008).

450. Ma, H. *et al.* Effects of a Standardized Phenolic-Enriched Maple Syrup Extract on β -Amyloid Aggregation, Neuroinflammation in Microglial and Neuronal Cells, and β -Amyloid Induced Neurotoxicity in *Caenorhabditis elegans*. *Neurochem. Res.* **41**, 2836–2847 (2016).
451. Madabhushi, R. *et al.* DNA Damage and Its Links to Neurodegeneration. *Neuron* **83**, 266–282 (2014).
452. Wei, Q.-Y., Zhou, B., Cai, Y.-J., Yang, L. & Liu, Z.-L. Synergistic effect of green tea polyphenols with trolox on free radical-induced oxidative DNA damage. *Food Chem.* **96**, 90–95 (2006).
453. Fredotović, Ž. *et al.* Chemical composition and biological activity of *Allium cepa* L. and *Allium × cornutum* (Clementi ex Visiani 1842) methanolic extracts. *Molecules* **22**, (2017).
454. Ushijima, Y., Ohniwa, R. & Morikawa, K. In vitro DNA Protection Assay Using Oxidative Stress. *BIO-PROTOCOL* **5**, e1538 (2015).
455. Patil, A. & Modak, M. Comparative Evaluation of Oxidative Stress Modulating and DNA Protective Activities of Aqueous and Methanolic Extracts of *Acacia catechu*. *Medicines* **4**, 1–12 (2017).
456. Yates, K. *et al.* Determination of Sinapine in Rapeseed Pomace Extract: its antioxidant and acetylcholinesterase inhibition properties. *Food Chem.* (2018). doi:10.1016/J.FOODCHEM.2018.10.045
457. The commission of the European Communities. 96/23/EC Commission Decision of 12 August 2002 implementing Council Directive 96/23/EC concerning the performance of analytical methods and the interpretation of results (notified under document number C(2002) 3044)(Text with EEA relevance) (2002/657/EC). *Off. J. Eur. Communities* **L221**, 8–36 (2002).
458. Ben Lagha, A., Haas, B. & Grenier, D. Tea polyphenols inhibit the growth and virulence properties of *Fusobacterium nucleatum*. *Sci. Rep.* **7**, 1–10 (2017).
459. Bolognesi, M. L. *et al.* Bis(7)-tacrine derivatives as multitarget-directed ligands: Focus on anticholinesterase and anti-amyloid activities. *ChemMedChem* **5**, 1215–1220 (2010).
460. de Camargo, A. C., Regitano-d’Arce, M. A. B., Biasoto, A. C. T. & Shahidi, F. Low molecular weight phenolics of grape juice and winemaking

byproducts: antioxidant activities and inhibition of oxidation of human low-density lipoprotein cholesterol and DNA strand breakage. *J. Agric. Food Chem.* **62**, 12159–71 (2014).

461. Szwajgier, D. & Borowiec, K. Phenolic acids from malt are efficient acetylcholinesterase and butyrylcholinesterase inhibitors. *J. Inst. Brew.* **118**, 40–48 (2012).
462. Szwajgier, D., Borowiec, K. & Pustelniak, K. The Neuroprotective Effects of Phenolic Acids: Molecular Mechanism of Action. *Nutrients* **9**, 1–21 (2017).
463. Ju, D.-T. *et al.* Nerve Regeneration Potential of Protocatechuic Acid in RSC96 Schwann Cells by Induction of Cellular Proliferation and Migration through IGF-IR-PI3K-Akt Signaling. *Chin. J. Physiol.* **58**, 412–419 (2015).
464. Yang, E.-J. *et al.* Syringin from stem bark of *Fraxinus rhynchophylla* protects A β (25–35)-induced toxicity in neuronal cells. *Arch. Pharm. Res.* **33**, 531–538 (2010).
465. Guo, C. *et al.* Protocatechualdehyde Protects Against Cerebral Ischemia-Reperfusion-Induced Oxidative Injury Via Protein Kinase C ϵ /Nrf2/HO-1 Pathway. *Mol. Neurobiol.* **54**, 833–845 (2017).
466. Khan, K. A. *et al.* Impact of caffeic acid on aluminium chloride-induced dementia in rats. *J. Pharm. Pharmacol.* **65**, 1745–1752 (2013).
467. Szwajgier, D. Anticholinesterase activity of selected phenolic acids and flavonoids – interaction testing in model solutions. *Ann. Agric. Environ. Med.* **22**, 690–694 (2015).
468. Shyamala, B. N., Madhava Naidu, M., Sulochanamma, G. & Srinivas, P. Studies on the antioxidant activities of natural vanilla extract and its constituent compounds through in vitro models. *J. Agric. Food Chem.* **55**, 7738–7743 (2007).
469. González-Correa, J. A. *et al.* Neuroprotective effect of hydroxytyrosol and hydroxytyrosol acetate in rat brain slices subjected to hypoxia-reoxygenation. *Neurosci. Lett.* **446**, 143–146 (2008).
470. Büttner, S. *et al.* Spermidine protects against α -synuclein neurotoxicity. *Cell cycle* **13**, 3903–8 (2014).

471. Yang, Y. *et al.* Induction of autophagy by spermidine is neuroprotective via inhibition of caspase 3-mediated Beclin 1 cleavage. *Cell Death Dis.* **8**, e2738 (2017).
472. Iida, A. *et al.* Protective effects of *Nitraria retusa* extract and its constituent isorhamnetin against amyloid β -induced cytotoxicity and amyloid β aggregation. *Biosci. Biotechnol. Biochem.* **79**, 1548–1551 (2015).
473. Churches, Q. I. *et al.* Naturally occurring polyphenolic inhibitors of amyloid beta aggregation. *Bioorg. Med. Chem. Lett.* **24**, 3108–3112 (2014).
474. Barreca, D. *et al.* Neuroprotective effects of phloretin and its glycosylated derivative on rotenone-induced toxicity in human SH-SY5Y neuronal-like cells. *BioFactors* **43**, 549–557 (2017).
475. Yang, I. J., Lee, D. U. & Shin, H. M. Anti-inflammatory and antioxidant effects of coumarins isolated from *Foeniculum vulgare* in lipopolysaccharide-stimulated macrophages and 12-*O*-tetradecanoylphorbol-13-acetate-stimulated mice. *Immunopharmacol. Immunotoxicol.* **37**, 308–317 (2015).
476. Raza, S. S. *et al.* Neuroprotective effect of naringenin is mediated through suppression of NF- κ B signaling pathway in experimental stroke. *Neuroscience* **230**, 157–171 (2013).
477. Braidy, N. *et al.* Neuroprotective Effects of Citrus Fruit-Derived Flavonoids, Nobiletin and Tangeretin in Alzheimer's and Parkinson's Disease. *CNS Neurol. Disord. - Drug Targets* **16**, 387–397 (2017).
478. Rattanajarasroj, S. & Unchern, S. Comparable Attenuation of A β 25–35-Induced Neurotoxicity by Quercitrin and 17 β -Estradiol in Cultured Rat Hippocampal Neurons. *Neurochem. Res.* **35**, 1196–1205 (2010).
479. Cho, J. Antioxidant and neuroprotective effects of hesperidin and its aglycone hesperetin. *Arch. Pharm. Res.* **29**, 699–706 (2006).
480. Liu, Y., Zhang, L. & Liang, J. Activation of the Nrf2 defense pathway contributes to neuroprotective effects of phloretin on oxidative stress injury after cerebral ischemia/reperfusion in rats. *J. Neurol. Sci.* **351**, 88–92 (2015).

481. Millán, S. *et al.* Identification and quantification of glucosinolates in rapeseed using liquid chromatography-ion trap mass spectrometry. *Anal. Bioanal. Chem.* **394**, 1661–1669 (2009).
482. Kim, S.-J. & Ishii, G. Effect of storage temperature and duration on glucosinolate, total vitamin C and nitrate contents in rocket salad (*Eruca sativa* Mill.). *J. Sci. Food Agric.* **87**, 966–973 (2007).
483. Taviano, M. F. *et al.* Contribution of the Glucosinolate Fraction to the Overall Antioxidant Potential, Cytoprotection against Oxidative Insult and Antimicrobial Activity of *Eruca sativa* Mill. Leaves Extract. *Pharmacogn. Mag.* **13**, 738–743 (2017).
484. Navarro, S. L., Li, F. & Lampe, J. W. Mechanisms of action of isothiocyanates in cancer chemoprevention: an update. *Food Funct.* **2**, 579 (2011).
485. Matthäus, B. & Fiebig, H. J. Simultaneous Determination of Isothiocyanates, Indoles, and Oxazolidinethiones in Myrosinase Digests of Rapeseeds and Rapeseed Meal by HPLC. *J. Agric. Food Chem.* **44**, 3894–3899 (1996).
486. Youngs, C. G. & Wetter, L. R. Microdetermination of the major individual isothiocyanates and oxazolidinethione in rapeseed. *J. Am. Oil Chem. Soc.* **44**, 551–554 (1967).
487. Kähkönen, M. & Heinonen, M. Antioxidant Activity of Anthocyanins and Their Aglycons. *J. Agric. Food Chem.* **51**, 628–633 (2003).
488. Dai, W. *et al.* Genetic analysis for anthocyanin and chlorophyll contents in rapeseed. *Ciência Rural* **46**, 790–795 (2016).
489. Lee, J., Rennaker, C. & Wrolstad, R. E. Correlation of two anthocyanin quantification methods: HPLC and spectrophotometric methods. *Food Chem.* **110**, 782–786 (2008).
490. Andjelković, M. *et al.* Iron-chelation properties of phenolic acids bearing catechol and galloyl groups. *Food Chem.* **98**, 23–31 (2006).
491. Říha, M. *et al.* In vitro evaluation of copper-chelating properties of flavonoids. *RSC Adv.* **4**, 32628–32638 (2014).
492. DTNB | Dojindo. Available at: <http://www.dojindo.eu.com/store/p/207->

DTNB.aspx. (Accessed: 30th May 2018)

493. Phytochemical profile of a blend of black chokeberry and lemon juice with cholinesterase inhibitory effect and antioxidant potential. *Food Chem.* **134**, 2090–2096 (2012).
494. Anticholinesterase potential of flavonols from paper mulberry (*Broussonetia papyrifera*) and their kinetic studies. *Food Chem.* **132**, 1244–1250 (2012).
495. Papandreou, M. A. *et al.* Effect of a polyphenol-rich wild blueberry extract on cognitive performance of mice, brain antioxidant markers and acetylcholinesterase activity. *Behav. Brain Res.* **198**, 352–358 (2009).
496. Ono, K., Hasegawa, K., Naiki, H. & Yamada, M. Curcumin has potent anti-amyloidogenic effects for Alzheimer's β -amyloid fibrils in vitro. *J. Neurosci. Res.* **75**, 742–750 (2004).
497. Weinberg, R. P. *et al.* Oil Palm Phenolics Inhibit the *In Vitro* Aggregation of β -Amyloid Peptide into Oligomeric Complexes. *Int. J. Alzheimers. Dis.* **2018**, 1–12 (2018).
498. Gao, C., Tian, C., Zhou, R., Zhang, R. & Lu, Y. Phenolic composition, DNA damage protective activity and hepatoprotective effect of free phenolic extract from *Sphallerocarpus gracilis* seeds. *Int. Immunopharmacol.* **20**, 238–247 (2014).
499. Yates, K. *et al.* Determination of sinapine in rapeseed pomace extract: Its antioxidant and acetylcholinesterase inhibition properties. *Food Chem.* **276**, 768–775 (2019).
500. Carboni, E. & Lingor, P. Insights on the interaction of alpha-synuclein and metals in the pathophysiology of Parkinson's disease. *Metallomics* **7**, 395–404 (2015).
501. Holzgrabe, U., Kapková, P., Alptüzün, V., Scheiber, J. & Kugelmann, E. Targeting acetylcholinesterase to treat neurodegeneration. 161–179 (2007).
502. Lashuel, H. A., Overk, C. R., Oueslati, A. & Masliah, E. The many faces of α -synuclein: from structure and toxicity to therapeutic target. *Nat. Rev. Neurosci.* **14**, 38–48 (2013).

503. Gordon, J., Amini, S. & White, M. K. General overview of neuronal cell culture. *Methods Mol. Biol.* **1078**, 1–8 (2013).
504. Kovalevich, J. & Langford, D. Considerations for the use of SH-SY5Y neuroblastoma cells in neurobiology. in *Neuronal Cell Culture: Methods and Protocols* (eds. Amini, S. & White, K. M.) 9–21 (Springer Science+Business Media, 2013).
505. Bahmad, H. *et al.* Modeling Human Neurological and Neurodegenerative Diseases: From Induced Pluripotent Stem Cells to Neuronal Differentiation and Its Applications in Neurotrauma. *Front. Mol. Neurosci.* **10**, 1–17 (2017).
506. Gitler, A. D., Dhillon, P. & Shorter, J. Neurodegenerative disease: models, mechanisms, and a new hope. *Dis. Model. Mech.* **10**, 499–502 (2017).
507. Jorfi, M., D’Avanzo, C., Kim, D. Y. & Irimia, D. Three-Dimensional Models of the Human Brain Development and Diseases. *Adv. Healthc. Mater.* **7**, 1–20 (2018).
508. Marton, R. M. & Paşca, S. P. Neural Differentiation in the Third Dimension: Generating a Human Midbrain. *Cell Stem Cell* **19**, 145–146 (2016).
509. Biedler, J. L., Helson, L. & Spengler, B. a. Morphology and Growth , Tumorigenicity , and Cytogenetics of Human Neuroblastoma Cells in Continuous Culture Morphology and Growth , Tumorigenicity , and Cytogenetics of Human Neuroblastoma Cells in Continuous Culture1. *Cancer Res.* **33**, 2643–2652 (1973).
510. Biedler, J. L., Roffler-Tarlov, S., Schachner, M. & Freedman, L. S. Multiple Neurotransmitter Synthesis by Human Neuroblastoma Cell Lines and Clones. *Cancer Res.* **38**, 3751–3757 (1978).
511. Koriyama, Y., Furukawa, A., Muramatsu, M., Takino, J. & Takeuchi, M. Glyceraldehyde caused Alzheimer’s disease-like alterations in diagnostic marker levels in SH-SY5Y human neuroblastoma cells. *Sci. Rep.* **5**, 1–7 (2015).
512. Xicoy, H., Wieringa, B. & Martens, G. J. M. The SH-SY5Y cell line in Parkinson’s disease research: a systematic review. *Mol. Neurodegener.* **12**, 1–11 (2017).

513. Krishna, A. *et al.* Systems genomics evaluation of the SH-SY5Y neuroblastoma cell line as a model for Parkinson's disease. *BMC Genomics* **15**, 1–23 (2014).
514. Yu, Z. *et al.* Neurodegeneration-associated TDP-43 interacts with fragile X mental retardation protein (FMRP)/Staufen (STAU1) and regulates SIRT1 expression in neuronal cells. *J. Biol. Chem.* **287**, 22560–72 (2012).
515. Filograna, R. *et al.* Analysis of the Catecholaminergic Phenotype in Human SH-SY5Y and BE(2)-M17 Neuroblastoma Cell Lines upon Differentiation. *PLoS One* **10**, e0136769 (2015).
516. Teppola, H., Sarkanen, J.-R., Jalonen, T. O. & Linne, M.-L. Morphological Differentiation Towards Neuronal Phenotype of SH-SY5Y Neuroblastoma Cells by Estradiol, Retinoic Acid and Cholesterol. *Neurochem. Res.* **41**, 731–47 (2016).
517. Cheung, Y. T. *et al.* Effects of all-trans-retinoic acid on human SH-SY5Y neuroblastoma as in vitro model in neurotoxicity research. *Neurotoxicology* **30**, 127–135 (2009).
518. Liu, P. *et al.* Protection of SH-SY5Y neuronal cells from glutamate-induced apoptosis by 3,6'-disinapoyl sucrose, a bioactive compound isolated from radix polygala. *J. Biomed. Biotechnol.* **2012**, 1–5 (2012).
519. Seoposengwe, K. *et al.* In vitro neuroprotective potential of four medicinal plants against rotenone-induced toxicity in SH-SY5Y neuroblastoma cells. *BMC Complement. Altern. Med.* **13**, 1–11 (2013).
520. Park, H. R. *et al.* Neuroprotective effects of Liriope platyphylla extract against hydrogen peroxide-induced cytotoxicity in human neuroblastoma SH-SY5Y cells. *BMC Complement. Altern. Med.* **15**, 171 (2015).
521. Venkatesh Gobi, V. *et al.* Agaricus blazei extract attenuates rotenone-induced apoptosis through its mitochondrial protective and antioxidant properties in SH-SY5Y neuroblastoma cells. *Nutr. Neurosci.* **21**, 97–107 (2018).
522. González-Sarrías, A., Núñez-Sánchez, M. Á., Tomás-Barberán, F. A. & Espín, J. C. Neuroprotective Effects of Bioavailable Polyphenol-Derived Metabolites against Oxidative Stress-Induced Cytotoxicity in Human Neuroblastoma SH-SY5Y Cells. *J. Agric. Food Chem.* **65**, 752–758 (2017).

523. Gay, N. H. *et al.* Neuroprotective Effects of Phenolic and Carboxylic Acids on Oxidative Stress-Induced Toxicity in Human Neuroblastoma SH-SY5Y Cells. *Neurochem. Res.* **43**, 619–636 (2018).
524. Hynes, J., Floyd, S., Soini, A. E., Connor, R. O. & Papkovsky, D. B. Fluorescence-Based Cell Viability Screening Assays Using Water-Soluble Oxygen Probes. *J. Biomol. Screen.* **8**, 264–272 (2003).
525. Stoddart, M. J. Cell Viability Assays: Introduction. in *Mammalian Cell Viability* (ed. Stoddart, M. J.) 1–6 (Humana Press, 2011).
526. Duque, A. & Rakic, P. Different effects of bromodeoxyuridine and [3H]thymidine incorporation into DNA on cell proliferation, position, and fate. *J. Neurosci.* **31**, 15205–17 (2011).
527. Berridge, M. V., Herst, P. M. & Tan, A. S. Tetrazolium dyes as tools in cell biology: New insights into their cellular reduction. *Biotechnol. Annu. Rev.* **11**, 127–152 (2005).
528. Stockert, J. C., Horobin, R. W., Colombo, L. L. & Blázquez-Castro, A. Tetrazolium salts and formazan products in Cell Biology: Viability assessment, fluorescence imaging, and labeling perspectives. *Acta Histochem.* **120**, 159–167 (2018).
529. Riss, T. L. *et al.* Cell Viability Assays. in *Assay Guidance Manual* (eds. Sittampalam, G. S. *et al.*) 355–386 (Eli Lilly & Company and the National Center for Advancing Translational Sciences, 2004).
530. Pearse, A. G. E. Intracellular Localisation of Dehydrogenase Systems Using Monotetrazolium Salts and Metal Chelation of their Formazans. *J. Histochem. Cytochem.* **5**, 515–527 (1957).
531. Nakayama, G. R., Caton, M. C., Nova, M. P. & Parandoosh, Z. Assessment of the Alamar Blue assay for cellular growth and viability in vitro. *J. Immunol. Methods* **204**, 205–208 (1997).
532. O'Brien, J., Wilson, I., Orton, T. & Pognan, F. Investigation of the Alamar Blue (resazurin) fluorescent dye for the assessment of mammalian cell cytotoxicity. *Eur. J. Biochem.* **267**, 5421–5426 (2000).
533. Pace, R. T. & Burg, K. J. L. Toxic effects of resazurin on cell cultures. *Cytotechnology* **67**, 13–17 (2015).

534. Reiniers, M. J. *et al.* Preparation and Practical Applications of 2',7'-Dichlorodihydrofluorescein in Redox Assays. *Anal. Chem.* **89**, 3853–3857 (2017).
535. Eruslanov, E. & Kusmartsev, S. Identification of ROS Using Oxidized DCFDA and Flow-Cytometry. in *Advanced Protocols in Oxidative Stress II* (ed. Armstrong, D.) 57–72 (Human Press (Springer), 2010).
536. Adan, A., Alizada, G., Kiraz, Y., Baran, Y. & Nalbant, A. Flow cytometry: basic principles and applications. *Crit. Rev. Biotechnol.* **37**, 163–176 (2017).
537. Coppedè, F. & Migliore, L. DNA damage in neurodegenerative diseases. *Mutat. Res. Mol. Mech. Mutagen.* **776**, 84–97 (2015).
538. Mecocci, P., MacGarvey, U. & Beal, M. F. Oxidative damage to mitochondrial DNA is increased in Alzheimer's disease. *Ann. Neurol.* **36**, 747–751 (1994).
539. Su, J. H., Deng, G. & Cotman, C. W. Neuronal DNA damage precedes tangle formation and is associated with up-regulation of nitrotyrosine in Alzheimer's disease brain. *Brain Res.* **774**, 193–199 (1997).
540. Migliore, L. *et al.* Chromosome and oxidative damage biomarkers in lymphocytes of Parkinson's disease patients. *Int. J. Hyg. Environ. Health* **204**, 61–66 (2001).
541. Collins, A. R. The comet assay for DNA damage and repair: Principles, Applications, and Limitations. *Mol. Biotechnol.* **26**, 249–261 (2004).
542. Ostling, O. & Johanson, K. J. Microelectrophoretic study of radiation-induced DNA damages in individual mammalian cells. *Biochem. Biophys. Res. Commun.* **123**, 291–8 (1984).
543. Singh, N. P., McCoy, M. T., Tice, R. R. & Schneider, E. L. A simple technique for quantitation of low levels of DNA damage in individual cells. *Exp. Cell Res.* **175**, 184–91 (1988).
544. Olive, P. L. & Banáth, J. P. The comet assay: a method to measure DNA damage in individual cells. *Nat. Protoc.* **1**, 23–29 (2006).
545. Azqueta, A., Slyskova, J., Langie, S. A. S., O'Neill Gaivão, I. & Collins, A. Comet assay to measure DNA repair: approach and applications. *Front.*

Genet. **5**, 1–8 (2014).

546. Azqueta, A. & Collins, A. R. The essential comet assay: A comprehensive guide to measuring DNA damage and repair. *Arch. Toxicol.* **87**, 949–968 (2013).
547. Şardaş, S. *et al.* Use of alkaline Comet assay (single cell gel electrophoresis technique) to detect DNA damages in lymphocytes of operating room personnel occupationally exposed to anaesthetic gases. *Mutat. Res. Toxicol. Environ. Mutagen.* **418**, 93–100 (1998).
548. Kumar, K. *et al.* Evaluation of sperm DNA quality in men presenting with testicular cancer and lymphoma using alkaline and neutral Comet assays. *Andrology* **6**, 230–235 (2018).
549. Silva, J. P., Gomes, A. C. & Coutinho, O. P. Oxidative DNA damage protection and repair by polyphenolic compounds in PC12 cells. *Eur. J. Pharmacol.* **601**, 50–60 (2008).
550. Duty, S. M. *et al.* The relationship between environmental exposures to phthalates and DNA damage in human sperm using the neutral comet assay. *Environ. Health Perspect.* **111**, 1164–9 (2003).
551. Soloneski, S., Ruiz de Arcaute, C., Nikoloff, N. & Larramendy, M. L. Genotoxicity of the herbicide imazethapyr in mammalian cells by oxidative DNA damage evaluation using the Endo III and FPG alkaline comet assays. *Environ. Sci. Pollut. Res.* **24**, 10292–10300 (2017).
552. Muraleedharan, A., Menon, V., Rajkumar, R. P. & Chand, P. Assessment of DNA damage and repair efficiency in drug naïve schizophrenia using comet assay. *J. Psychiatr. Res.* **68**, 47–53 (2015).
553. McGlynn, A. P. *et al.* The bromodeoxyuridine comet assay: detection of maturation of recently replicated DNA in individual cells. *Cancer Res.* **59**, 5912–6 (1999).
554. McKenna, D. J., Doherty, B. A., Downes, C. S., McKeown, S. R. & McKelvey-Martin, V. J. Use of the Comet-FISH Assay to Compare DNA Damage and Repair in p53 and hTERT Genes following Ionizing Radiation. *PLoS One* **7**, e49364 (2012).
555. Sutandy, F. X. R., Qian, J., Chen, C.-S. & Zhu, H. Overview of protein

- microarrays. *Curr. Protoc. protein Sci.* **Chapter 27**, Unit 27.1 (2013).
556. R&D Systems Inc. Proteome Profiler™ Array-Human Cell Stress Array Kit. 1–11 (2014).
557. Beere, H. M. 'The stress of dying': the role of heat shock proteins in the regulation of apoptosis. *J. Cell Sci.* **117**, 2641–2651 (2004).
558. Litvinov, D., Mahini, H. & Garelnabi, M. Antioxidant and anti-inflammatory role of paraoxonase 1: implication in arteriosclerosis diseases. *N. Am. J. Med. Sci.* **4**, 523–32 (2012).
559. Smith, T. G., Robbins, P. A. & Ratcliffe, P. J. The human side of hypoxia-inducible factor. *Br. J. Haematol.* **141**, 325–334 (2008).
560. Fearn, A. *et al.* The NF- κ B1 is a key regulator of acute but not chronic renal injury. *Cell Death Dis.* **8**, e2883 (2017).
561. Vegarud, G., Vegarud, G., Undeland, I. & Scheers, N. Effects of Marine Oils, Digested with Human Fluids, on Cellular Viability and Stress Protein Expression in Human Intestinal Caco-2 Cells. *Nutrients* **9**, 1213 (2017).
562. Smith, W. W. *et al.* α -Synuclein Phosphorylation Enhances Eosinophilic Cytoplasmic Inclusion Formation in SH-SY5Y Cells. *J. Neurosci.* **25**, 5544–5552 (2005).
563. BIO RAD. Microplate Assay Protocol. in *DC Protein Assay Instruction Manual* 3–4 (2013).
564. Barron, G. A., Bermano, G., Gordon, A. & Kong Thoo Lin, P. Synthesis, cytotoxicity and DNA-binding of novel bisnaphthalimidopropyl derivatives in breast cancer MDA-MB-231 cells. *Eur. J. Med. Chem.* **45**, 1430–1437 (2010).
565. Duthie, S. J., Narayanan, S., Blum, S., Pirie, L. & Brand, G. M. Folate Deficiency In Vitro Induces Uracil Misincorporation and DNA Hypomethylation and Inhibits DNA Excision Repair in Immortalized Normal Human Colon Epithelial Cells Folate Deficiency In Vitro Induces Uracil Misincorporation and DNA Hypomethylation and. 37–41 (2009).
566. Heuser, V. D., Erdtmann, B., Kvitko, K., Rohr, P. & da Silva, J. Evaluation of genetic damage in Brazilian footwear-workers: Biomarkers of exposure, effect, and susceptibility. *Toxicology* **232**, 235–247 (2007).

567. Bruggisser, R., Daeniken, K. von, Jundt, G., Schaffner, W. & Tullberg-Reinert, H. Interference of Plant Extracts, Phytoestrogens and Antioxidants with the MTT Tetrazolium Assay. *Planta Med.* **68**, 445–448 (2002).
568. López, S. *et al.* Cytoprotective action against oxidative stress in astrocytes and neurons by *Bactris guineensis* (L.) H.E. Moore (corozo) fruit extracts. *Food Chem. Toxicol.* **109**, 1010–1017 (2017).
569. Wang, J., Zhao, Y. M., Zhang, B. & Guo, C. Y. Protective Effect of Total Phenolic Compounds from *Inula helenium* on Hydrogen Peroxide-induced Oxidative Stress in SH-SY5Y Cells. *Indian J. Pharm. Sci.* **77**, 163–9 (2015).
570. Kim, H. S., Lee, K., Kang, K. A., Lee, N. H. & Hyun, J. W. Phloroglucinol exerts protective effects against oxidative stress-induced cell damage in SH-SY5Y cells. *J Pharmacol Sci* **119**, 186–192 (2012).
571. Hodges, R. E. & Minich, D. M. Modulation of Metabolic Detoxification Pathways Using Foods and Food-Derived Components: A Scientific Review with Clinical Application. *J. Nutr. Metab.* **2015**, 760689 (2015).
572. Outeiro, T. F. *et al.* Sirtuin 2 Inhibitors Rescue α -Synuclein-Mediated Toxicity in Models of Parkinson's Disease. *Science (80-.).* **317**, 516–519 (2007).
573. Findeisen, P. *et al.* Six Subgroups and Extensive Recent Duplications Characterize the Evolution of the Eukaryotic Tubulin Protein Family. *Genome Biol. Evol.* **6**, 2274–2288 (2014).
574. Maxwell, M. M. *et al.* The Sirtuin 2 microtubule deacetylase is an abundant neuronal protein that accumulates in the aging CNS. *Hum. Mol. Genet.* **20**, 3986–96 (2011).
575. Favero, G., Franceschetti, L., Rodella, L. F. & Rezzani, R. Sirtuins, aging, and cardiovascular risks. *Age (Dordr).* **37**, 9804 (2015).
576. Luthi-Carter, R. *et al.* SIRT2 inhibition achieves neuroprotection by decreasing sterol biosynthesis. *Proc. Natl. Acad. Sci.* **107**, 7927–7932 (2010).
577. Singh, P., Hanson, P. S. & Morris, C. M. Sirtuin-2 Protects Neural Cells

- from Oxidative Stress and Is Elevated in Neurodegeneration. *Parkinsons Dis.* **2017**, 2643587 (2017).
578. Wang, F., Nguyen, M., Qin, F. X.-F. & Tong, Q. SIRT2 deacetylates FOXO3a in response to oxidative stress and caloric restriction. *Aging Cell* **6**, 505–514 (2007).
579. Perry, J. J. P. *et al.* Contribution of human manganese superoxide dismutase tyrosine 34 to structure and catalysis. *Biochemistry* **48**, 3417–24 (2009).
580. Flynn, J. M. & Melov, S. SOD2 in mitochondrial dysfunction and neurodegeneration. *Free Radic. Biol. Med.* **62**, 4–12 (2013).
581. Kim, Y., Gupta Vallur, P., Phaëton, R., Mythreye, K. & Hempel, N. Insights into the Dichotomous Regulation of SOD2 in Cancer. *Antioxidants* **6**, 86 (2017).
582. Tribble, D. L. *et al.* Fatty streak formation in fat-fed mice expressing human copper-zinc superoxide dismutase. *Arterioscler. Thromb. Vasc. Biol.* **17**, 1734–40 (1997).
583. Espinosa-Diez, C. *et al.* Antioxidant responses and cellular adjustments to oxidative stress. *Redox Biol.* **6**, 183–97 (2015).
584. Kračmarová, A., Drtinová, L. & Pohanka, M. Possibility of Acetylcholinesterase Overexpression in Alzheimer Disease Patients After Therapy With Acetylcholinesterase Inhibitors. *ACTA MEDICA (Hradec Králové)* **58**, 37–42 (2015).
585. Santillo, M. F. & Liu, Y. A fluorescence assay for measuring acetylcholinesterase activity in rat blood and a human neuroblastoma cell line (SH-SY5Y). *J. Pharmacol. Toxicol. Methods* **76**, 15–22 (2015).
586. Li, S. *et al.* Identification of acetylcholinesterase inhibitors using homogenous cell-based assays in quantitative high-throughput screening platforms. *Biotechnol. J.* **12**, 1–12 (2017).
587. Eaton, S. L. & Wishart, T. M. Bridging the gap: large animal models in neurodegenerative research. *Mamm. Genome* **28**, 324–337 (2017).
588. Wood, W. B. 1 Introduction to *C. elegans* Biology. in *The Nematode Caenorhabditis elegans* (ed. Wood, W. B.) 1–16 (Cold Spring Harbor

Laboratory Press, 1988).

589. Hunt, P. R. The *C. elegans* model in toxicity testing. *J. Appl. Toxicol.* **37**, 50–59 (2017).
590. Edgley, M. (Riddle lab). What is *C. elegans*? An introduction for those unfamiliar with 'the worm'. *College of Biological Science* (2015). Available at: <https://cbs.umn.edu/cgc/what-c-elegans>. (Accessed: 7th August 2018)
591. Brenner, S. The genetics of *Caenorhabditis elegans*. *Genetics* **77**, 71–94 (1974).
592. Altun, Z. F. & Hall, D. H. Introduction. in *WormAtlas* (2009).
593. Riddle, D. L., Blumenthal, T., Meyer, B. J. & Priess, J. R. *Introduction to C. elegans. C. elegans II* (Cold Spring Harbor Laboratory Press, 1997).
594. Artal-Sanz, M., de Jong, L. & Tavernarakis, N. *Caenorhabditis elegans*: A versatile platform for drug discovery. *Biotechnol. J.* **1**, 1405–1418 (2006).
595. Sulston, J. E. & Horvitz, H. R. Post-embryonic cell lineages of the nematode, *Caenorhabditis elegans*. *Dev. Biol.* **56**, 110–156 (1977).
596. Corsi, A. K., Wightman, B. & Chalfie, M. A Transparent Window into Biology: A Primer on *Caenorhabditis elegans*. *Genetics* **200**, 387–407 (2015).
597. Hall, D. H., Herndon, L. A. & Altun, Z. Introduction to *C. elegans* Embryo Anatomy. in *WormAtlas* (2017).
598. Sulston, J. E., Schierenberg, E., White, J. G. & Thomson, J. N. The embryonic cell lineage of the nematode *Caenorhabditis elegans*. *Dev. Biol.* **100**, 64–119 (1983).
599. Pazdernik, N. & Schedl, T. Introduction to germ cell development in *Caenorhabditis elegans*. *Adv. Exp. Med. Biol.* **757**, 1–16 (2013).
600. Hodgkin, J. Karyotype, ploidy, and gene dosage. *WormBook* (2005).
601. The *C. elegans* Sequencing Consortium. Genome Sequence of the Nematode *C. elegans*: A Platform for Investigating Biology. *Science* (80- .). **282**, 2012–2018 (1998).
602. Kutscher, L. M. & Shaham, S. Forward and reverse mutagenesis in *C.*

- elegans. in *WormBook* (ed. The C. elegans research Community) 1–26 (2014).
603. O'Reilly, L. P., Luke, C. J., Perlmutter, D. H., Silverman, G. A. & Pak, S. C. C. elegans in high-throughput drug discovery. *Adv. Drug Deliv. Rev.* **69–70**, 247–53 (2014).
604. Zheng, S. Q., Ding, A. J., Li, G. P., Wu, G. S. & Luo, H. R. Drug Absorption Efficiency in Caenorhabditis elegans Delivered by Different Methods. *PLoS One* **8**, 1–9 (2013).
605. Voisine, C. *et al.* Identification of potential therapeutic drugs for huntington's disease using Caenorhabditis elegans. *PLoS One* **2**, e504 (2007).
606. Altun, Z. F. & Hall, D. H. Nervous system, general description. in *WormAtlas* (2011).
607. Silverman, G. A. *et al.* Modeling molecular and cellular aspects of human disease using the nematode Caenorhabditis elegans. *Pediatr. Res.* **65**, 10–8 (2009).
608. Chew, Y. L. *et al.* Recordings of Caenorhabditis elegans locomotor behaviour following targeted ablation of single motorneurons. *Sci. Data* **4**, 170156 (2017).
609. Kaletta, T. & Hengartner, M. O. Finding function in novel targets: C. elegans as a model organism. *Nat. Rev. Drug Discov.* **5**, 387–399 (2006).
610. Chen, X., Barclay, J. W., Burgoyne, R. D. & Morgan, A. Using C. elegans to discover therapeutic compounds for ageing-associated neurodegenerative diseases. *Chem. Cent. J.* **9**, 1–20 (2015).
611. Link, C. D. Transgenic invertebrate models of age-associated neurodegenerative diseases. *Mech. Ageing Dev.* **122**, 1639–1649 (2001).
612. Rao, A. V. & Balachandran, B. Role of Oxidative Stress and Antioxidants in Neurodegenerative Diseases. **5**, 291–309
613. Chakraborty, S., Bornhorst, J., Nguyen, T. T. & Aschner, M. Oxidative stress mechanisms underlying Parkinson's disease-associated neurodegeneration in C. elegans. *Int. J. Mol. Sci.* **14**, 23103–28 (2013).
614. Teixeira-Castro, A. *et al.* Neuron-specific proteotoxicity of mutant ataxin-

- 3 in *C. elegans*: rescue by the DAF-16 and HSF-1 pathways. *Hum. Mol. Genet.* **20**, 2996–3009 (2011).
615. Christie, N. T. M., Lee, A. L., Fay, H. G., Gray, A. A. & Kikis, E. A. Novel Polyglutamine Model Uncouples Proteotoxicity from Aging. *PLoS One* **9**, e96835 (2014).
616. Teixeira-Castro, A. *et al.* Serotonergic signalling suppresses ataxin 3 aggregation and neurotoxicity in animal models of Machado-Joseph disease. *Brain* 1–15 (2015). doi:10.1093/brain/awv262
617. Bisaglia, M., Greggio, E., Beltramini, M. & Bubacco, L. Dysfunction of dopamine homeostasis: clues in the hunt for novel Parkinson's disease therapies. *FASEB J.* **27**, 2101–2110 (2013).
618. Maulik, M., Mitra, S., Bult-Ito, A., Taylor, B. E. & Vayndorf, E. M. Behavioral Phenotyping and Pathological Indicators of Parkinson's Disease in *C. elegans* Models. *Front. Genet.* **8**, (2017).
619. Nass, R., Hall, D. H., Miller, D. M. & Blakely, R. D. Neurotoxin-induced degeneration of dopamine neurons in *Caenorhabditis elegans*. *Proc. Natl. Acad. Sci. U. S. A.* **99**, 3264–9 (2002).
620. CEPDL, CEPDR, CEPVL, CEPVR. *WormAtlas* Available at: <http://www.wormatlas.org/neurons/IndividualNeurons/CEPframeset.html>. (Accessed: 1st August 2018)
621. Sawin, E. R., Ranganathan, R. & Horvitz, H. R. *C. elegans* locomotory rate is modulated by the environment through a dopaminergic pathway and by experience through a serotonergic pathway. *Neuron* **26**, 619–31 (2000).
622. Goodman, M. B. Mechanosensation. in *WormBook* (ed. The *C. elegans* Research Community) (2006).
623. Chase, D. L. & Koelle, M. R. Biogenic amine neurotransmitters in *C. elegans*. in *WormBook* (eds. The *C. elegans* Research & Community) (2007).
624. Guha, S., Caldwell, G. & Kapahi, P. Morphological Analysis of Dopaminergic Neurons with Age Using *Caenorhabditis elegans* GFP Reporter Strains. *BIO-PROTOCOL* **Bio101**, (2018).

625. Cao, S., Gelwix, C. C., Caldwell, K. A. & Caldwell, G. A. Torsin-Mediated Protection from Cellular Stress in the Dopaminergic Neurons of *Caenorhabditis elegans*. *J. Neurosci.* **25**, 3801–3812 (2005).
626. Martinez, B. A., Caldwell, K. A. & Caldwell, G. A. *C. elegans* as a model system to accelerate discovery for Parkinson disease. *Curr. Opin. Genet. Dev.* **44**, 102–109 (2017).
627. Schober, A. Classic toxin-induced animal models of Parkinson's disease: 6-OHDA and MPTP. *Cell Tissue Res.* **318**, 215–224 (2004).
628. Perumal, A. S., Gopal, V. B., Tordzro, W. K., Cooper, T. B. & Cadet, J. L. Vitamin E attenuates the toxic effects of 6-hydroxydopamine on free radical scavenging systems in rat brain. *Brain Res. Bull.* **29**, 699–701 (1992).
629. Kumar, R., Agarwal, A. K. & Seth, P. K. Free radical-generated neurotoxicity of 6-hydroxydopamine. *J. Neurochem.* **64**, 1703–7 (1995).
630. Offenburger, S.-L. *et al.* 6-OHDA-induced dopaminergic neurodegeneration in *Caenorhabditis elegans* is promoted by the engulfment pathway and inhibited by the transthyretin-related protein TTR-33. *PLoS Genet.* **14**, e1007125 (2018).
631. Berkowitz, L. A. *et al.* Application of a *C. elegans* dopamine neuron degeneration assay for the validation of potential Parkinson's disease genes. *J. Vis. Exp.* (2008).
632. Ray, A., Martinez, B. A., Berkowitz, L. A., Caldwell, G. A. & Caldwell, K. A. Mitochondrial dysfunction, oxidative stress, and neurodegeneration elicited by a bacterial metabolite in a *C. elegans* Parkinson's model. *Cell Death Dis.* **5**, e984 (2014).
633. Hamamichi, S. *et al.* Hypothesis-based RNAi screening identifies neuroprotective genes in a Parkinson's disease model. (2008).
634. Muñoz-Lobato, F. *et al.* Protective role of DNJ-27/ERdj5 in *Caenorhabditis elegans* models of human neurodegenerative diseases. *Antioxid. Redox Signal.* **20**, 217–35 (2014).
635. Johnson, W. M. *et al.* Glutaredoxin deficiency exacerbates neurodegeneration in *C. elegans* models of Parkinson's disease. *Hum. Mol. Genet.* **24**, 1322–1335 (2015).

636. Shashikumar, S., Pradeep, H., Chinnu, S., Rajini, P. S. & Rajanikant, G. K. Alpha-linolenic acid suppresses dopaminergic neurodegeneration induced by 6-OHDA in *C. elegans*. *Physiol. Behav.* **151**, 563–569 (2015).
637. Kautu, B. B., Carrasquilla, A., Hicks, M. L., Caldwell, K. A. & Caldwell, G. A. Valproic acid ameliorates *C. elegans* dopaminergic neurodegeneration with implications for ERK-MAPK signaling. *Neurosci. Lett.* **541**, 116–9 (2013).
638. Tabrez, S. *et al.* A synopsis on the role of tyrosine hydroxylase in Parkinson's disease. *CNS Neurol. Disord. Drug Targets* **11**, 395–409 (2012).
639. Bisaglia, M., Soriano, M. E., Arduini, I., Mammi, S. & Bubacco, L. Molecular characterization of dopamine-derived quinones reactivity toward NADH and glutathione: Implications for mitochondrial dysfunction in Parkinson disease. *Biochim. Biophys. Acta - Mol. Basis Dis.* **1802**, 699–706 (2010).
640. Zucca, F. A. *et al.* Interactions of iron, dopamine and neuromelanin pathways in brain aging and Parkinson's disease. (2017).
641. Cheon, S.-M. *et al.* *Sorbus alnifolia* protects dopaminergic neurodegeneration in *Caenorhabditis elegans*. *Pharm. Biol.* **55**, 481–486 (2016).
642. Liu, J., Banskota, A., Critchley, A., Hafting, J. & Prithiviraj, B. Neuroprotective Effects of the Cultivated *Chondrus crispus* in a *C. elegans* Model of Parkinson's Disease. *Mar. Drugs* **13**, 2250–2266 (2015).
643. Pereira, L. *et al.* A cellular and regulatory map of the cholinergic nervous system of *C. elegans*. *Elife* **4**, 1253–1266 (2015).
644. Combes, D., Fedon, Y., Toutant, J. P. & Arpagaus, M. Acetylcholinesterase genes in the nematode *Caenorhabditis elegans*. *Int. Rev. Cytol.* **209**, 207–239 (2001).
645. Combes, D., Fedon, Y., Grauso, M., Toutant, J.-P. & Arpagaus, M. Four Genes Encode Acetylcholinesterases in the Nematodes *Caenorhabditis elegans* and *Caenorhabditis briggsae*. cDNA Sequences, Genomic Structures, Mutations and in vivo Expression. *J. Mol. Biol.* **300**, 727–742

- (2000).
646. Johnson, C. D. *et al.* An acetylcholinesterase-deficient mutant of the nematode *Caenorhabditis elegans*. *Genetics* **97**, 261–79 (1981).
 647. Johnson, C. D. & Russell, R. L. Multiple molecular forms of acetylcholinesterase in the nematode *Caenorhabditis elegans*. *J. Neurochem.* **41**, 30–46 (1983).
 648. Culotti, J. G., Von Ehrenstein, G., Culotti, M. R. & Russell, R. L. A second class of acetylcholinesterase-deficient mutants of the nematode *Caenorhabditis elegans*. *Genetics* **97**, 281–305 (1981).
 649. Melstrom, P. C. & Williams, P. L. Measuring Movement to Determine Physiological Roles of Acetylcholinesterase Classes in *Caenorhabditis elegans*. *J. Nematol.* **39**, 317–20 (2007).
 650. Johnson, C. D., Rand, J. B., Herman, R. K., Stern, B. D. & Russell, R. L. The acetylcholinesterase genes of *C. elegans*: identification of a third gene (*ace-3*) and mosaic mapping of a synthetic lethal phenotype. *Neuron* **1**, 165–73 (1988).
 651. Chalfie, M., Tu, Y., Euskirchen, G. & Ward, W. W. Green Fluorescent Protein as a Marker for Gene Expression. *Science* (80-.). **263**, 802–805 (1994).
 652. Hobert, O. & Loria, P. Use of GFP in *Caenorhabditis elegans*. in *Green Fluorescent Protein-Properties, Applications, and Protocols* (eds. Chalfie, M. & Kain, St. R.) 203–226 (John Wiley & Sons, Inc., 2005).
 653. Ighodaro, O. M. & Akinloye, O. A. First line defence antioxidants-superoxide dismutase (SOD), catalase (CAT) and glutathione peroxidase (GPX): Their fundamental role in the entire antioxidant defence grid. *Alexandria J. Med.* (2017).
 654. Braeckman, B. P., Smolders, A., Back, P. & De Henau, S. In Vivo Detection of Reactive Oxygen Species and Redox Status in *Caenorhabditis elegans*. *Antioxid. Redox Signal.* **25**, 577–92 (2016).
 655. Miranda-Vizueté, A. & Veal, E. A. *Caenorhabditis elegans* as a model for understanding ROS function in physiology and disease. *Redox Biol.* **11**, 708–714 (2017).

656. Leiers, B. *et al.* A stress-responsive glutathione S-transferase confers resistance to oxidative stress in *Caenorhabditis elegans*. *Free Radic. Biol. Med.* **34**, 1405–1415 (2003).
657. Salinas, A. E. & Wong, M. G. Glutathione S-transferases--a review. *Curr. Med. Chem.* **6**, 279–309 (1999).
658. Tawe, W. N., Eschbach, M.-L., Walter, R. D. & Henkle-Dührsen, K. *Identification of stress-responsive genes in Caenorhabditis elegans using RT-PCR differential display.* *Nucleic Acids Research* **26**, (1998).
659. Link, C. D. & Johnson, C. J. Reporter Transgenes for Study of Oxidant Stress in *Caenorhabditis elegans*. in 497–505 (2002).
660. Detienne, G., Van de Walle, P., De Haes, W., Schoofs, L. & Temmerman, L. SKN-1-independent transcriptional activation of glutathione S-transferase 4 (GST-4) by EGF signaling. *Worm* **5**, e1230585 1-10 (2016).
661. Hunt, P. R. *et al.* Extension of Lifespan in *C. elegans* by Naphthoquinones That Act through Stress Hormesis Mechanisms. *PLoS One* **6**, e21922 (2011).
662. Senchuk, M. M., Dues, D. J. & Van Raamsdonk, J. M. Measuring Oxidative Stress in *Caenorhabditis elegans*: Paraquat and Juglone Sensitivity Assays. *Bio Protoc.* **7**, 1–16 (2017).
663. Hsu, F.-L. *et al.* In vivo antioxidant activities of Essential Oils and Their Constituents from Leaves of the Taiwanese *Cinnamomum osmophloeum*. *J. Agric. Food Chem.* **60**, 3092–3097 (2012).
664. Yu, C. W., Wei, C. C. & Liao, V. H. Curcumin-mediated oxidative stress resistance in *Caenorhabditis elegans* is modulated by age-1, akt-1, pdk-1, osr-1, unc-43, sek-1, skn-1, sir-2.1, and mev-1. *Free Radic Res* **48**, 371–379 (2014).
665. Dostal, V., Roberts, C. M. & Link, C. D. Genetic mechanisms of coffee extract protection in a *Caenorhabditis elegans* model of A β -amyloid peptide toxicity. *Genetics* **186**, 857–866 (2010).
666. Ogawa, T., Kodera, Y., Hirata, D., Blackwell, T. K. & Mizunuma, M. Natural thioallyl compounds increase oxidative stress resistance and lifespan in *Caenorhabditis elegans* by modulating SKN-1/Nrf. *Sci. Rep.* **6**, 21611

- (2016).
667. Cabreiro, F. *et al.* Increased life span from overexpression of superoxide dismutase in *Caenorhabditis elegans* is not caused by decreased oxidative damage. *Free Radic. Biol. Med.* **51**, 1575–82 (2011).
668. Libina, N., Berman, J. R. & Kenyon, C. *Tissue-Specific Activities of C. elegans DAF-16 in the Regulation of Lifespan tissues play an important role in establishing the ani-mal's rate of aging. First, the C. elegans genome con-tains more than 35 insulin-like genes expressed in a.* *Cell* **115**, (2003).
669. Salgueiro, W. G. *et al.* Insights into the differential toxicological and antioxidant effects of 4-phenylchalcogenil-7-chloroquinolines in *Caenorhabditis elegans*. *Free Radic. Biol. Med.* **110**, 133–141 (2017).
670. Moreno-Arriola, E. *et al.* *Caenorhabditis elegans*: A useful model for studying metabolic disorders in which oxidative stress is a contributing factor. *Oxid. Med. Cell. Longev.* **2014**, 705253 (2014).
671. Zhang, L., Jie, G., Zhang, J. & Zhao, B. Significant longevity-extending effects of EGCG on *Caenorhabditis elegans* under stress. *Free Radic. Biol. Med.* **46**, 414–421 (2009).
672. Aoyama, K. & Nakaki, T. Impaired glutathione synthesis in neurodegeneration. *Int. J. Mol. Sci.* **14**, 21021–44 (2013).
673. Zhu, Y., Carvey, P. M. & Ling, Z. Age-related changes in glutathione and glutathione-related enzymes in rat brain. *Brain Res.* **1090**, 35–44 (2006).
674. Franco, R., Schoneveld, O. J., Pappa, A. & Panayiotidis, M. I. The central role of glutathione in the pathophysiology of human diseases. *Arch. Physiol. Biochem.* **113**, 234–258 (2007).
675. Liao, V. H. C. & Yu, C. W. *Caenorhabditis elegans gcs-1* confers resistance to arsenic-induced oxidative stress. *BioMetals* **18**, 519–528 (2005).
676. An, J. H. & Blackwell, T. K. SKN-1 links *C. elegans* mesendodermal specification to a conserved oxidative stress response. *Genes Dev.* **17**, 1882–93 (2003).
677. Oliveira, R. P. *et al.* Condition-adapted stress and longevity gene regulation by *Caenorhabditis elegans* SKN-1/Nrf. *Aging Cell* **8**, 524–41

(2009).

678. Ishikado, A. *et al.* Willow bark extract increases antioxidant enzymes and reduces oxidative stress through activation of Nrf2 in vascular endothelial cells and *Caenorhabditis elegans*. *Free Radic. Biol. Med.* **65**, 1506–15 (2013).
679. Lesa, G. M. Isolation of *Caenorhabditis elegans* gene knockouts by PCR screening of chemically mutagenized libraries. *Nat. Protoc.* **1**, 2231–2240 (2006).
680. Untergasser, A. *et al.* Primer3—new capabilities and interfaces. *Nucleic Acids Res.* **40**, e115–e115 (2012).
681. Mendel, G. Versuche über Pflanzen-Hybriden. *Verhandlungen des Naturforschenden Vereines Brünn* **4**, 3–47 (1866).
682. Bhattacharya, S., Zhang, Q., Carmichael, P. L., Boekelheide, K. & Andersen, M. E. Toxicity Testing in the 21st Century: Defining New Risk Assessment Approaches Based on Perturbation of Intracellular Toxicity Pathways. *PLoS One* **6**, e20887 (2011).
683. McVey, K. *et al.* *Caenorhabditis elegans*: An Emerging Model System for Pesticide Neurotoxicity. *J. Environ. Anal. Toxicol.* **S4**, 1–9 (2012).
684. Tsai, C.-W. *et al.* Neuroprotective Effects of Betulin in Pharmacological and Transgenic *Caenorhabditis elegans* Models of Parkinson's Disease. *Cell Transplant.* **26**, 1903–1918 (2017).
685. Chalorak, P. *et al.* *Holothuria scabra* extracts exhibit anti-Parkinson potential in *C. elegans*: A model for anti-Parkinson testing. *Nutr. Neurosci.* **21**, 427–438 (2018).
686. Yang, X. *et al.* The neuroprotective and lifespan-extension activities of *Damnacanthus officinarum* extracts in *Caenorhabditis elegans*. *J. Ethnopharmacol.* **141**, 41–47 (2012).
687. VERMOREL, M. *et al.* Valorization of rapeseed meal. 5. Effects of sinapine and other phenolic compounds on food intake and nutrient utilization in growing rats. *Reprod. Nutr. Développement* **27**, 781–790 (1987).
688. British National Formulary - NICE. Neostigmine. *BNF* (2018). Available at: <https://bnf.nice.org.uk/drug/neostigmine.html>. (Accessed: 25th July

- 2018)
689. Kalinnikova, T. B. *et al.* Acetylcholine Deficiency in *Caenorhabditis elegans* Induced by Hyperthermia Can Be Compensated by ACh-esterase Inhibition or Activation of GAR-3 mAChRs. *Environ. Nat. Resour. Res.* **3**, 98 (2013).
 690. Dinkova-Kostova, A. T., Kostov, R. V. & Kazantsev, A. G. The role of Nrf2 signaling in counteracting neurodegenerative diseases. *FEBS J.* (2018).
 691. Kark, P. R. A., Budellis, M. M. R. & Wachsner, R. Double-blind, cross-over trial of low doses of oral physostigmine in inherited ataxias. *Neurology* **31**, 288–292 (1981).
 692. Kark, R. A., Blass, J. P. & Spence, M. A. Physostigmine in familial ataxias. *Neurology* **27**, 70–2 (1977).
 693. Wessel, K., Langenberger, K., Nitschke, M. F. & Kömpf, D. Double-blind crossover study with physostigmine in patients with degenerative cerebellar diseases. *Arch. Neurol.* **54**, 397–400 (1997).
 694. Sammi, S. R. *et al.* Citrus hystrix-derived 3,7-dimethyloct-6-enal and 3,7-dimethyloct-6-enyl acetate ameliorate acetylcholine deficits. *RSC Adv.* **6**, 68870–68884 (2016).
 695. Fu, R. *et al.* Spatial control of cells, peptide delivery and dynamic monitoring of cellular physiology with chitosan-assisted dual color quantum dot FRET peptides. *Acta Biomater* **6**, e85305 (2010).
 696. Li, H. *et al.* Astragalus Polysaccharide Suppresses 6-Hydroxydopamine-Induced Neurotoxicity in *Caenorhabditis elegans*. *Oxid. Med. Cell. Longev.* **2016**, 4856761 (2016).
 697. Manalo, R. V. M. & Medina, P. M. B. Caffeine Protects Dopaminergic Neurons From Dopamine-Induced Neurodegeneration via Synergistic Adenosine-Dopamine D2-Like Receptor Interactions in Transgenic *Caenorhabditis elegans*. *Front. Neurosci.* **12**, 137 (2018).
 698. Hasegawa, K., Miwa, S., Tsutsumiuchi, K., Miwa, J. & Ahringer, J. Allyl Isothiocyanate that Induces GST and UGT Expression Confers Oxidative Stress Resistance on *C. elegans*, as Demonstrated by Nematode Biosensor. *PLoS One* **5**, e9267 (2010).

699. Grünz, G. *et al.* Structural features and bioavailability of four flavonoids and their implications for lifespan-extending and antioxidant actions in *C. elegans*. *Mech. Ageing Dev.* **133**, 1–10 (2012).
700. Tumer, T. B., Rojas-Silva, P., Poulev, A., Raskin, I. & Waterman, C. Direct and indirect antioxidant activity of polyphenol- and isothiocyanate-enriched fractions from *Moringa oleifera*. *J. Agric. Food Chem.* **63**, 1505–13 (2015).
701. Bajpai, V. K. *et al.* Antioxidant efficacy and the upregulation of Nrf2-mediated HO-1 expression by (+)-lariciresinol, a lignan isolated from *Rubia philippinensis*, through the activation of p38. *Sci. Rep.* **7**, 46035 (2017).
702. Federico, A. *et al.* Mitochondria, oxidative stress and neurodegeneration. *J. Neurol. Sci.* **322**, 254–262 (2012).
703. Khoschsorur, G. *et al.* Evaluation of a sensitive HPLC method for the determination of Malondialdehyde, and application of the method to different biological materials. *Chromatographia* **52**, 181–184 (2000).
704. Alcántar-Fernández, J., Navarro, R. E., Salazar-Martínez, A. M., Pérez-Andrade, M. E. & Miranda-Ríos, J. *Caenorhabditis elegans* respond to high-glucose diets through a network of stress-responsive transcription factors. *PLoS One* **13**, e0199888 (2018).
705. Imanikia, S. *et al.* The application of the comet assay to assess the genotoxicity of environmental pollutants in the nematode *Caenorhabditis elegans*. *Environ. Toxicol. Pharmacol.* **45**, 356–61 (2016).
706. Kim, H.-M. & Colaiácovo, M. DNA Damage Sensitivity Assays in *Caenorhabditis elegans*. *BIO-PROTOCOL* **5**, e1487 (2015).
707. Jäger, S. *et al.* Preparation of herbal tea as infusion or by maceration at room temperature using mistletoe tea as an example. *Sci. Pharm.* **79**, 145–55 (2011).
708. Mandal, S. C., Mandal, V. & Das, A. K. Classification of Extraction Methods. in *Essentials of Botanical Extraction* 83–136 (2015).
709. Spigno, G., Tramelli, L. & De Faveri, D. M. Effects of extraction time, temperature and solvent on concentration and antioxidant activity of

- grape marc phenolics. *J. Food Eng.* **81**, 200–208 (2007).
710. Figueroa-Pérez, M. G. *et al.* Diabetic nephropathy is ameliorated with peppermint (*Mentha piperita*) infusions prepared from salicylic acid-elicited plants. *J. Funct. Foods* **43**, 55–61 (2018).
711. Sharifi, N., Mahernia, S. & Amanlou, M. Comparison of Different Methods in Quercetin Extraction from Leaves of *Raphanus sativus* L. *Pharm. Sci.* **23**, 59–65 (2017).
712. Musuyu Muganza, D. *et al.* In vitro antiprotozoal and cytotoxic activity of 33 ethnopharmacologically selected medicinal plants from Democratic Republic of Congo. *J. Ethnopharmacol.* **141**, 301–308 (2012).
713. Valdés, A., Vidal, L., Beltrán, A., Canals, A. & Garrigós, M. C. Microwave-Assisted Extraction of Phenolic Compounds from Almond Skin Byproducts (*Prunus amygdalus*): A Multivariate Analysis Approach. *J. Agric. Food Chem.* **63**, 5395–5402 (2015).
714. Lovrić, V., Putnik, P., Kovačević, D. B., Jukić, M. & Dragović-Uzelac, V. Effect of Microwave-Assisted Extraction on the Phenolic Compounds and Antioxidant Capacity of Blackthorn Flowers. *Food Technol. Biotechnol.* **55**, 243–250 (2017).
715. Dhanani, T., Shah, S., Gajbhiye, N. A. & Kumar, S. Effect of extraction methods on yield, phytochemical constituents and antioxidant activity of *Withania somnifera*. *Arab. J. Chem.* **10**, S1193–S1199 (2017).
716. Tikhomiroff, C. & Jolicoeur, M. Screening of *Catharanthus roseus* secondary metabolites by high-performance liquid chromatography. *J. Chromatogr. A* **955**, 87–93 (2002).
717. Lu, Y., Hu, R. & Pan, Y. Integrated Countercurrent Extraction of Natural Products: A Combination of Liquid and Solid Supports. *Anal. Chem.* **82**, 3081–3085 (2010).
718. Fki, I., Allouche, N. & Sayadi, S. The use of polyphenolic extract, purified hydroxytyrosol and 3,4-dihydroxyphenyl acetic acid from olive mill wastewater for the stabilization of refined oils: a potential alternative to synthetic antioxidants. *Food Chem.* **93**, 197–204 (2005).
719. Rockenbach, I. I. *et al.* Characterization of flavan-3-ols in seeds of grape pomace by CE, HPLC-DAD-MSn and LC-ESI-FTICR-MS. *Food Res. Int.* **48**,

848–855 (2012).

720. Brandão, G. H. A. *et al.* Extraction of bioactive alkaloids from *Melocactus zehntneri* using supercritical fluid. *J. Supercrit. Fluids* **129**, 28–35 (2017).
721. Vieitez, I., Maceiras, L., Jachmanián, I. & Alborés, S. Antioxidant and antibacterial activity of different extracts from herbs obtained by maceration or supercritical technology. *J. Supercrit. Fluids* **133**, 58–64 (2018).
722. Farag, R. S., Badei, A. Z. M. A., Hewedi, F. M. & El-Baroty, G. S. A. Antioxidant activity of some spice essential oils on linoleic acid oxidation in aqueous media. *J. Am. Oil Chem. Soc.* **66**, 792–799 (1989).
723. Urbizu-González, A. L., Castillo-Ruiz, O., Martínez-Ávila, G. C. G. & Torres-Castillo, J. A. Natural variability of essential oil and antioxidants in the medicinal plant *Turnera diffusa*. *Asian Pac. J. Trop. Med.* **10**, 121–125 (2017).
724. Ruiz-Terán, F., Perez-Amador, I. & López-Munguía, A. Enzymatic Extraction and Transformation of Glucovanillin to Vanillin from Vanilla Green Pods. *J. Agric. Food Chem.* **49**, 5207–5209 (2001).
725. Sowbhagya, H. B. & Chitra, V. N. Enzyme-Assisted Extraction of Flavorings and Colorants from Plant Materials. *Crit. Rev. Food Sci. Nutr.* **50**, 146–161 (2010).

APPENDICES

Contents

A2 Secondary Metabolite Composition and Antioxidant Activity of Rapeseed Pomace Extracts – comparison between 2 harvest years and 3 extraction techniques	424
A3 Phytochemical Characterisation and Neuroprotective Properties of RSP Extract <i>in vitro</i>	441
A4 Cell Protective Properties of RSP Extract in SH-SY5Y Neuroblastoma Cell Line	447
A5 An <i>in vivo</i> Study of the Antioxidant and Neuroprotective Properties of RSP Extract in <i>C. elegans</i> Nematode Models	452

This last section forms the appendix. It contains information, important for the project which didn't fit into the context of the chapters above. The Appendix is separated into four sections (A2-A5), based onto the first chapters of this thesis. Hence each subsection in this appendix contains information important for the chapter indicated e.g. A2 "Secondary Metabolite Composition and Antioxidant Activity of Rapeseed Pomace Extracts – comparison between 2 harvest years and 3 extraction techniques" contains information relevant for Chapter 2.

A2 Secondary Metabolite Composition and Antioxidant Activity of Rapeseed Pomace Extracts – Secondary Metabolite Composition and Antioxidant Activity of Rapeseed Pomace Extracts – comparison between 2 harvest years and 3 extraction techniques

Table A1| Explanation of various extraction techniques used for plant and plant by-products, food waste/food production waste (adapted from various sources^{245,247,252,258,273,707,708})

Extraction technique	explanation	advantages	disadvantages	used in
maceration	Soaking of plant material in solvent containing stoppered container at room temperature for long period (at least 3 days) with agitation, followed by straining and filtering, "cold extraction"	<ul style="list-style-type: none"> - Easy - No expensive equipment - Flexible choice of solvents/mixtures - cheap 	<ul style="list-style-type: none"> - Time consuming - Amount of solvent - Choice of container (resistance to solvent for long time, take up of compounds to be extracted, contamination for following extraction) 	249,709
Infusion	Similar to maceration; boiling water/oil/alcohol is placed over sample remains suspended in solvent for a shorter amount of time (minutes), usually prepared for immediate use.	<ul style="list-style-type: none"> - Easy - No expensive equipment needed - Cheap - Made for immediate use 	<ul style="list-style-type: none"> - Amount of solvent - High temp. Might impact on metabolites - Solvent choice limited if used immediately 	320,710

<i>Digestion</i>	Form of maceration, using gentle heat throughout the extraction process with solvent, used when higher temperatures are not objectionable, increasing solvent efficiency	<ul style="list-style-type: none"> - Easy - Cheap - Better extraction via heat - No expensive equipment 	711	
<i>Percolation</i>	Starting material is moistened and left for a few hours, the packed into the percolator, more solvent added and the percolator left to macerate for about 1 day and then the outlet is opened, and the extract left to drip out into the collection vessel slowly, additional solvent can be added. The process is finished by filtration or decanting.	<ul style="list-style-type: none"> - Easy - Cheap 	<ul style="list-style-type: none"> - Percolator necessary - High amount of solvent 	249
<i>Decoction</i>	Plant material is placed in cold water and the boiled for certain amount of time, sometimes with a specific volume of water to sample ratio (1:4 or 1:16 sample:water); and the water evaporated to parts of its original volume, the extract is then cooled a strained/filtered. Used for water soluble, heat stable compounds.	<ul style="list-style-type: none"> - Easy - Cheap - Water as solvent 	<ul style="list-style-type: none"> - Only for heat resistant compounds 	249,712

Soxhlet
(traditional and automated)

Sample is placed in a cellulose thimble, which is placed into the solvent, extraction can be done using different temperatures and times, solvent is partially evaporated and used for rinsing the sample within the automated system.

- Can be automated
- Easy
- Solvent can be re-used, as it is collected in reservoir
- Reduced extraction time due to heat and automated system
- Rinse cycle displaces the transfer equilibrium
- Reduced extraction time due to microwave radiation (fast)
- Less solvent use possible
- Energy efficient, uniform heating
- Easy to handle

- Amount and temperature of solvent
- Soxhlet equipment needed
- Extraction time can be long
- Volume of solvent

249,262,35
3

Microwave-assisted

Sample extraction is facilitated using microwave energy, which interacts polar and polarizable materials, such as polar solvents, causing them to heat up; a vapour pressure within the cell can be generated which can break cell walls to release compounds of interest.

- Reduced extraction time due to microwave radiation (fast)
- Less solvent use possible
- Energy efficient, uniform heating
- Easy to handle

- Microwave equipment needed
- Thermal degradation possible of e.g. tannins and anthocyanins
- Selective for polar compounds

713-715

Ultra sound-assisted/sonication
(bath or probe)

Uses ultra sound in the range of 20kHz to 2000kHz, which increases the surface contact between solvent and sample via acoustic cavitation. Disruption of plant cell walls can facilitate compound release.

- Reduced extraction time and solvent amount
- Relatively cheap
- Sonic bath available in most Laboratories
 - Safe to use (atmospheric pressure)
 - Temperature changeable

- High ultra sound energy can have effect on phytochemicals
- Filtration required after processing

255,715,71
6

Counter-current

A wet raw material is pulverized to obtain a slurry, it is brought in contact with the solvent in a cylindrical extractor in which the slurry is mixed with the solvent and then separated through different outlets.

- Efficient
- Quick
- No high temperatures
- Less solvent

- Equipment necessary

717,718

Accelerated solvent/pressurized fluid

Uses the help of pressure to reduce the needed temperature for extraction, samples are packed within layers of inert material such as sand and filters in an extraction cell. The solvent is passed through the cell under high pressure and relatively low temperature and the extract collected.

- Very efficient extraction
- Can be automated
- Very low amount of solvent
- Lower temperature possible due to high pressure
- Short extraction time
- No filtering required

- High cost of equipment
- Sample preparation in cells time consuming

276,719

Supercritical fluid

A technique using supercritical fluid, such as CO₂ at their respective supercritical fluid temperature and pressure (<31.1°C and 7380kPa for CO₂). Supercritical fluids behave like gasses but show solvating characteristics of liquid. Also, Argon can be used as solvent.

- Very efficient
- No organic solvent needed
- CO₂ low cost and toxicity
- Less heat required
- Fast

- High cost of equipment
- Polarity limitations of CO₂, addition of organic solvents can counter-act issue
- Number of parameters to optimise

720,721

Steam

Often used for the extraction of essential oils from plant material, using steam, which is passed through the plant material, vaporized compounds travel to the condenser and are collected after separation from water.

Isolation of volatile compounds (essential oils, amines, organic acids)

- High energy consumption
- High temperatures
- System need to be set up

722,723

- Need of enzymes
- Enzymes usually have an optimal temperature, change from this can impact extraction efficiency

- Eco-friendly
- Specificity and regioselectivity
- Use of mild processing conditions
- Lower amount of solvent
- Can be assisted by other techniques such as microwave

This method uses enzymes, which work as catalysts, to enhance the extraction; they can also break cell walls and membranes, helping to release compounds of interest

Enzyme-assisted

Table A2| Comprehensive secondary metabolite composition of 6 RSP extracts.

		2012		2014		t-test	2012		2014		t-test	2012		2014		t-test
		FA					ALK					ACD				
		mean	std	mean	std		mean	std	mean	std		mean	std	mean	std	
Benzoic Acids	benzoic acid	5.081	0.083	3.888	0.728	*	9.219	1.201	12.531	0.373	*	7.008	1.069	7.266	1.090	
	salicylic acid	0.238	0.031	0.420	0.156		0.239	0.055	0.286	0.035		0.536	0.055	0.757	0.067	*
	m-hydroxybenzoic acid	0.573	0.089	0.498	0.041		0.000	0.000	0.000	0.000		0.000	0.000	0.000	0.000	
	p-hydroxybenzoic acid	3.843	0.066	5.201	0.888		4.209	0.411	6.049	0.566	*	8.473	0.154	6.824	0.227	***
	2,3-dihydroxybenzoic acid	0.100	0.001	0.121	0.007	**	0.181	0.007	0.228	0.018	*	0.404	0.019	0.437	0.017	
	2,4-dihydroxybenzoic acid	0.000	0.000	0.000	0.000		0.000	0.000	0.000	0.000		0.000	0.000	0.000	0.000	
	2,5-dihydroxybenzoic acid	0.460	0.014	0.481	0.082		0.000	0.000	0.000	0.000		3.704	0.228	2.375	0.078	***
	2,6-dihydroxybenzoic acid	0.000	0.000	0.000	0.000		0.000	0.000	0.000	0.000		0.000	0.000	0.000	0.000	
	protocatechuic acid	2.521	0.040	5.396	0.812	**	16.543	3.762	24.116	1.203	*	17.143	0.534	17.423	0.935	
	3,5-dihydroxybenzoic acid	0.000	0.000	0.000	0.000		0.000	0.000	0.000	0.000		0.000	0.000	0.000	0.000	
	o-anisic acid	0.000	0.000	0.000	0.000		0.000	0.000	0.000	0.000		0.000	0.000	0.000	0.000	
	m-anisic acid	0.000	0.000	0.000	0.000		0.000	0.000	0.000	0.000		0.000	0.000	0.000	0.000	
	p-anisic acid	0.585	0.046	1.016	0.110	**	1.310	0.127	2.682	0.146	***	0.208	0.010	0.313	0.020	**
	gallic acid	0.000	0.000	0.838	0.066	***	0.000	0.000	0.000	0.000		0.000	0.000	0.259	0.016	***
	vanillic acid	1.826	0.162	2.551	0.336	*	1.608	0.192	2.275	0.123	**	14.737	0.353	13.770	0.344	*
syringic acid	2.386	0.039	5.658	1.032	**	1.195	0.151	1.320	0.066		4.864	0.245	4.500	0.121		

	3,4-dimethoxybenzoic acid	0.000	0.000	0.000	0.000		0.000	0.000	0.000	0.000		0.000	0.000	0.000	0.000	
Benzaldehydes	p-hydroxybenzaldehyde	0.217	0.016	0.153	0.027	*	0.715	0.101	0.849	0.073		0.604	0.048	0.560	0.024	
	protocatachaldehyde	2.141	0.067	2.463	0.349		19.539	5.718	23.332	2.033		11.956	0.700	12.066	0.712	
	3,4,5-trihydroxybenzaldehyde	0.000	0.000	0.000	0.000		0.000	0.000	0.159	0.144		0.000	0.000	0.000	0.000	
	vanillin	0.714	0.003	0.536	0.078	*	1.682	0.209	1.825	0.063		1.201	0.128	1.269	0.092	
	isovanillin	0.000	0.000	0.000	0.000		0.000	0.000	0.000	0.000		0.000	0.000	0.000	0.000	
	syringin	0.965	0.011	0.746	0.107	*	1.841	0.228	2.049	0.003		1.826	0.282	1.812	0.215	
	3-methoxybenzaldehyde	0.000	0.000	0.000	0.000		0.000	0.000	0.000	0.000		0.000	0.000	0.000	0.000	
	3,4-dimethoxybenzaldehyde	0.000	0.000	0.000	0.000		0.000	0.000	0.000	0.000		0.028	0.002	0.027	0.004	
	3,4,5-trimethoxybenzaldehyde	0.000	0.000	0.000	0.000		0.000	0.000	0.000	0.000		0.000	0.000	0.000	0.000	
Cinnamic Acids	cinnamic acid	2.512	0.053	1.366	0.174	***	0.489	0.015	0.490	0.033		0.450	0.013	0.488	0.021	
	o-coumaric acid	0.000	0.000	0.000	0.000		0.000	0.000	0.000	0.000		0.000	0.000	0.000	0.000	
	m-coumaric acid	0.145	0.252	0.000	0.000		0.080	0.139	0.000	0.000		0.000	0.000	0.000	0.000	
	p-coumaric acid	2.162	0.008	1.933	0.340		10.754	6.601	6.842	5.163		0.249	0.009	0.285	0.028	
	caffeic acid	5.538	0.119	7.540	1.275		13.427	0.769	20.661	2.090	**	6.510	0.381	6.759	0.339	
	ferulic acid	12.251	0.302	9.570	1.627	*	64.554	39.367	38.645	2.074		1.527	0.166	1.232	0.056	*
	sinapic acid	224.235	3.577	161.400	25.548	*	917.650	43.784	1072.136	32.380	**	11.312	1.378	10.540	1.249	
	3-methoxycinnamic acid	0.000	0.000	0.000	0.000		0.000	0.000	0.000	0.000		0.000	0.000	0.000	0.000	

	4-methoxycinnamic acid	0.000	0.000	0.000	0.000		0.000	0.000	0.000	0.000		0.000	0.000	0.000	0.000	
	3,4-dimethoxycinnamic acid	0.066	0.006	0.051	0.011		0.381	0.035	0.926	0.019	***	0.000	0.000	0.000	0.000	
	3,4,5-trimethoxycinnamic acid	0.031	0.003	0.025	0.003		0.131	0.019	0.284	0.013	***	0.000	0.000	0.000	0.000	
Phenylpropionic acids	phenylpropionic acid	0.000	0.000	0.000	0.000		0.000	0.000	0.000	0.000		1.871	0.091	1.548	0.216	
	2-hydroxyphenylpropionic acid	0.000	0.000	0.000	0.000		0.000	0.000	0.000	0.000		0.000	0.000	0.000	0.000	
	3-hydroxyphenylpropionic acid	0.000	0.000	0.000	0.000		0.000	0.000	0.000	0.000		0.000	0.000	0.000	0.000	
	4-hydroxyphenylpropionic acid	0.000	0.000	0.000	0.000		0.000	0.000	0.000	0.000		0.000	0.000	0.000	0.000	
	3,4-dihydroxyphenylpropionic acid	0.000	0.000	0.000	0.000		0.000	0.000	0.000	0.000		1.243	0.048	1.309	0.040	
	4-hydroxy-3-methoxyphenylpropionic acid	0.000	0.000	0.000	0.000		0.000	0.000	0.113	0.195		0.291	0.039	0.282	0.025	
	3-methoxyphenylpropionic acid	0.000	0.000	0.000	0.000		0.000	0.000	0.000	0.000		0.000	0.000	0.000	0.000	
Benzenes	phenol	0.000	0.000	0.000	0.000		0.000	0.000	0.000	0.000		0.821	0.062	1.020	0.172	
	1,2-hydroxybenzene	0.000	0.000	0.000	0.000		0.000	0.000	0.000	0.000		0.000	0.000	0.000	0.000	
	1,3-hydroxybenzene	0.000	0.000	0.000	0.000		0.000	0.000	0.000	0.000		0.000	0.000	0.000	0.000	
	1,2,3-trihydroxybenzene	0.000	0.000	0.000	0.000		0.000	0.000	0.000	0.000		0.000	0.000	0.000	0.000	
Acetophenones	4-hydroxyacetophenone	0.000	0.000	0.000	0.000		0.000	0.000	0.000	0.000		0.031	0.005	0.034	0.004	
	4-hydroxy-3-methoxyacetophenone	0.000	0.000	0.000	0.000		0.000	0.000	0.000	0.000		0.088	0.009	0.077	0.005	
	4-hydroxy-3,5-dimethoxyacetophenone	0.125	0.009	0.088	0.018	*	0.257	0.045	0.336	0.021		0.308	0.060	0.277	0.020	
	3,4-dimethoxyacetophenone	0.000	0.000	0.000	0.000		0.000	0.000	0.000	0.000		0.000	0.000	0.000	0.000	

	3,4,5-trimethoxyaceto-phenone	0.00 0	0.00 0	0.00 4	0.00 1	**	0.00 0	0.00 0	0.000	0.00 0		0.000	0.00 0	0.000	0.00 0	
Phenylacetic acids	phenylacetic acid	0.56 2	0.03 1	0.43 3	0.05 2	*	1.18 7	0.11 0	1.322	0.05 9		0.115	0.00 2	0.124	0.00 2	**
	3-hydroxyphenyl-acetic acid	0.00 0	0.00 0	0.00 0	0.00 0		0.00 0	0.00 0	0.000	0.00 0		0.000	0.00 0	0.000	0.00 0	
	4-hydroxyphenyl-acetic acid	0.37 6	0.08 0	0.60 8	0.12 1		3.27 8	0.29 3	4.052	0.39 0		1.794	0.18 5	2.747	0.84 4	
	3,4-dihydroxyphenyl-acetic acid	0.00 0	0.00 0	0.00 0	0.00 0		0.00 0	0.00 0	0.000	0.00 0		0.000	0.00 0	0.000	0.00 0	
	4-hydroxy-3-methoxyphenyl-acetic acid	0.00 0	0.00 0	0.00 0	0.00 0		0.00 0	0.00 0	0.000	0.00 0		0.000	0.00 0	0.000	0.00 0	
	4-methoxyphenyl-acetic acid	0.00 0	0.00 0	0.00 0	0.00 0		0.00 0	0.00 0	0.000	0.00 0		0.000	0.00 0	0.000	0.00 0	
Mandelic Acids	mandelic acid	0.00 0	0.00 0	0.00 0	0.00 0		0.00 0	0.00 0	0.000	0.00 0		0.000	0.00 0	0.000	0.00 0	
	3-hydroxymandelic acid	0.12 2	0.01 3	0.09 6	0.00 6	*	2.92 3	0.43 6	3.938	0.21 4	*	2.350	0.32 0	3.049	0.13 8	*
	4-hydroxymandelic acid	0.00 0	0.00 0	0.00 0	0.00 0		0.00 0	0.00 0	0.000	0.00 0		0.000	0.00 0	0.000	0.00 0	
	3,4-dihydroxymandelic acid	0.00 0	0.00 0	0.00 0	0.00 0		0.00 0	0.00 0	0.000	0.00 0		0.000	0.00 0	0.000	0.00 0	
	4-hydroxy-3-methoxymandelic acid	0.00 0	0.00 0	0.00 0	0.00 0		0.00 0	0.00 0	0.000	0.00 0		0.000	0.00 0	0.000	0.00 0	
Phenylpyruvic Acids	phenylpyruvic acid	0.00 0	0.00 0	0.00 0	0.00 0		0.00 0	0.00 0	0.000	0.00 0		0.000	0.00 0	0.000	0.00 0	
	4-hydroxyphenylpyruvic acid	1.67 4	0.26 2	7.46 3	3.97 9		7.88 5	4.03 7	17.92 1	1.56 2	*	13.57 0	0.32 5	13.86 2	2.49 1	
Phenylactic Acids	phenylactic acid	0.80 2	0.06 2	0.57 2	0.05 1	**	0.48 6	0.01 7	0.235	0.01 3	**	0.534	0.05 1	0.192	0.03 9	**
	4-hydroxyphenylactic acid	0.53 1	0.03 8	0.58 5	0.06 6		0.40 8	0.06 0	0.447	0.07 1		0.558	0.09 2	0.611	0.25 6	
Phenolics Others	anthranilic acid	0.00 0	0.00 0	0.00 0	0.00 0		0.22 9	0.06 0	0.454	0.01 3	**	0.000	0.00 0	0.043	0.00 7	**
	quinadilic acid	0.00 0	0.00 0	0.00 0	0.00 0		0.00 0	0.00 0	0.000	0.00 0		0.000	0.00 0	0.000	0.00 0	
	chlorogenic acid	0.99 0	0.19 4	1.02 0	0.09 4		0.00 0	0.00 0	0.000	0.00 0		0.000	0.00 0	0.000	0.00 0	
	0-hydroxyhippuric acid	0.01 6	0.00 2	0.01 1	0.00 2		0.06 4	0.00 4	0.073	0.00 3	*	0.000	0.00 0	0.000	0.00 0	

	ethylferulate	0.000	0.000	0.000	0.000		0.000	0.000	0.000	0.000		0.000	0.000	0.000	0.000	
	4-hydroxyl 3-methoxyl benzyl alcohol	0.030	0.005	0.057	0.010	*	0.012	0.010	0.013	0.003		0.039	0.022	0.019	0.002	
	p-cresol	0.000	0.000	0.000	0.000		0.000	0.000	0.000	0.000		0.000	0.000	0.000	0.000	
	4-ethylphenol	0.000	0.000	0.000	0.000		0.000	0.000	0.000	0.000		0.000	0.000	0.000	0.000	
	4-methylcatechol	0.000	0.000	0.000	0.000		0.004	0.001	0.000	0.000	***	0.012	0.001	0.014	0.002	
	tyrosol	0.000	0.000	0.000	0.000		0.000	0.000	0.000	0.000		0.000	0.000	0.000	0.000	
	hydroxytyrosol	0.000	0.000	0.000	0.000		0.000	0.000	0.000	0.000		0.000	0.000	0.000	0.000	
Phenolic Dimers	ellagic acid	0.000	0.000	0.000	0.000		0.000	0.000	0.000	0.000		0.000	0.000	0.000	0.000	
	ferulic dimer (5-5 linked)	0.000	0.000	0.000	0.000		3.744	3.481	0.383	0.042		0.000	0.000	0.000	0.000	
	ferulic dimer (8-8 linked)	0.000	0.000	0.000	0.000		0.000	0.000	0.000	0.000		0.000	0.000	0.000	0.000	
	ferulic dimer (8-5 linked)	0.000	0.000	0.000	0.000		1.852	1.562	0.000	0.000		0.000	0.000	0.000	0.000	
	Hydrogenated Ferulic Dimer H5-5	0.000	0.000	0.000	0.000		0.000	0.000	0.000	0.000		0.000	0.000	0.000	0.000	
	reservatrol	0.000	0.000	0.000	0.000		0.000	0.000	0.000	0.000		0.000	0.000	0.000	0.000	
	indole	0.000	0.000	0.000	0.000		0.000	0.000	0.000	0.000		0.000	0.000	0.000	0.000	

Indoles	indole-3-acetic acid	0.117	0.010	0.105	0.006		0.211	0.023	0.326	0.020	**	0.112	0.031	0.123	0.012	
	indole-3-acrylic acid	0.000	0.000	0.000	0.000		0.014	0.003	0.019	0.002		0.000	0.000	0.000	0.000	
	indole-3-propionic acid	0.000	0.000	0.000	0.000		0.000	0.000	0.000	0.000		0.000	0.000	0.000	0.000	
	indole-3-carbinol	0.000	0.000	0.000	0.000		0.000	0.000	0.000	0.000		0.000	0.000	0.000	0.000	
	indole-3-carboxylic acid	0.824	0.026	0.609	0.056	**	0.967	0.178	1.314	0.090	*	0.097	0.034	0.074	0.005	

	indole-3-pyruvic acid	3.040	0.392	53.540	87.112		76.168	131.927	197.678	37.956		381.396	71.970	223.575	123.479	
	indole-3-methyl	0.000	0.000	0.000	0.000		0.000	0.000	0.000	0.000		0.000	0.000	0.000	0.000	
	indole-3-lactic acid	0.000	0.000	0.000	0.000		0.000	0.000	0.000	0.000		0.000	0.000	0.000	0.000	
Amines	spermine	0.016	0.003	0.012	0.001		0.015	0.002	0.017	0.002		0.013	0.002	0.014	0.001	
	spermidine	3.796	0.691	3.669	0.126		2.742	0.012	2.666	0.111		2.583	0.097	2.422	0.209	
	tyromine	0.000	0.000	0.000	0.000		0.000	0.000	0.000	0.000		0.000	0.000	0.000	0.000	
	pyrrolidine	0.000	0.000	0.000	0.000		0.000	0.000	0.000	0.000		0.000	0.000	0.000	0.000	
	histamine	0.000	0.000	0.000	0.000		0.000	0.000	0.000	0.000		0.000	0.000	0.000	0.000	
	piperidine	0.000	0.000	0.000	0.000		0.000	0.000	0.000	0.000		0.000	0.000	0.000	0.000	
	cadaverine	0.000	0.000	0.000	0.000		0.000	0.000	0.000	0.000		0.000	0.000	0.000	0.000	
	putresine	0.000	0.000	0.000	0.000		0.000	0.000	0.000	0.000		0.000	0.000	0.000	0.000	
	5-OHtryptophan	0.000	0.000	0.000	0.000		0.000	0.000	0.000	0.000		0.000	0.000	0.000	0.000	
Flavanoids/Coumarins	Coumarin	0.000	0.000	0.000	0.000		0.000	0.000	0.000	0.000		0.000	0.000	0.000	0.000	
	Psoralen	0.000	0.000	0.000	0.000		0.000	0.000	0.000	0.000		0.006	0.000	0.000	0.000	***
	8-methylpsoralen	0.000	0.000	0.000	0.000		0.000	0.000	0.000	0.000		0.000	0.000	0.000	0.000	
	Bergapten	0.000	0.000	0.000	0.000		0.000	0.000	0.000	0.000		0.000	0.000	0.000	0.000	
	Tangeretin	0.008	0.001	0.003	0.000	**	0.003	0.001	0.003	0.000		0.003	0.000	0.002	0.000	**
	Cyanidin-3-Galactoside	0.000	0.000	0.000	0.000		0.000	0.000	0.000	0.000		0.000	0.000	0.000	0.000	
	Peonidin-3-Glucoside	0.000	0.000	0.000	0.000		0.000	0.000	0.000	0.000		0.000	0.000	0.000	0.000	

Petunidin-3-Glucoside	0.000	0.000	0.000	0.000		0.000	0.000	0.000	0.000		0.000	0.000	0.000	0.000	
Malvin-3-Glucoside	0.000	0.000	0.000	0.000		0.000	0.000	0.000	0.000		0.000	0.000	0.000	0.000	
Coumesterol	0.000	0.000	0.000	0.000		0.000	0.000	0.000	0.000		0.000	0.000	0.000	0.000	
Catechin	0.000	0.000	0.000	0.000		0.497	0.861	0.341	0.226		0.000	0.000	0.000	0.000	
Epicatechin	0.000	0.000	0.091	0.033	**	0.986	1.493	0.456	0.385		0.000	0.000	0.000	0.000	
Gallocatechin	0.000	0.000	0.000	0.000		0.000	0.000	0.000	0.000		0.000	0.000	0.000	0.000	
Epigallocatechin	0.000	0.000	0.000	0.000		0.000	0.000	0.000	0.000		0.000	0.000	0.000	0.000	
Epigallocatechin Gallate	0.000	0.000	0.000	0.000		0.000	0.000	0.000	0.000		0.000	0.000	0.000	0.000	
Isoliquiritigenin	0.012	0.007	0.000	0.000	*	0.004	0.004	0.000	0.000		0.000	0.000	0.000	0.000	
Phloretin	0.011	0.004	0.021	0.004	*	0.004	0.003	0.007	0.001		0.009	0.001	0.006	0.006	
Imperatorin	0.000	0.000	0.000	0.000		0.000	0.000	0.000	0.000		0.000	0.000	0.000	0.000	
Eriocitrin	0.000	0.000	0.000	0.000		0.000	0.000	0.000	0.000		0.000	0.000	0.000	0.000	
Naringenin	0.052	0.007	0.034	0.008	*	0.053	0.011	0.211	0.078	*	0.023	0.002	0.031	0.002	**
Naringin	0.000	0.000	0.000	0.000		0.000	0.000	0.000	0.000		0.000	0.000	0.000	0.000	
Hesperitin	0.000	0.000	0.000	0.000		0.000	0.000	0.000	0.000		0.000	0.000	0.000	0.000	
Kaempferol	0.193	0.010	0.754	0.527		0.105	0.008	0.195	0.013	***	141.301	6.773	152.623	5.535	
Morin	0.000	0.000	0.000	0.000		0.000	0.000	0.000	0.000		0.000	0.000	0.000	0.000	
Quercetin	0.103	0.035	0.072	0.012		0.453	0.403	0.397	0.086		3.678	0.299	5.496	0.300	**
Myricetin	0.000	0.000	0.000	0.000		0.000	0.000	0.000	0.000		0.000	0.000	0.000	0.000	
Quercetin-3-Glucoside	0.137	0.032	0.443	0.116	*	0.114	0.009	0.562	0.203	*	0.000	0.000	0.000	0.000	
Taxifolin	0.000	0.000	0.000	0.000		0.121	0.073	0.131	0.037		0.475	0.211	0.374	0.062	
Genstein	0.000	0.000	0.000	0.000		0.000	0.000	0.000	0.000		0.000	0.000	0.000	0.000	

Scopoletin	0.017	0.029	0.000	0.000		0.000	0.000	0.000	0.000		0.028	0.049	0.011	0.019	
Umbelliferone	0.000	0.000	0.000	0.000		0.000	0.000	0.000	0.000		0.000	0.000	0.000	0.000	
7,8-dihydroxy-6-methyl coumarin	0.000	0.000	0.000	0.000		0.000	0.000	0.000	0.000		0.000	0.000	0.000	0.000	
Neohesperidin	0.000	0.000	0.000	0.000		0.000	0.000	0.000	0.000		0.000	0.000	0.000	0.000	
Hesperidin	0.000	0.000	0.000	0.000		0.000	0.000	0.000	0.000		0.000	0.000	0.000	0.000	
Quercitrin	0.012	0.013	0.000	0.000		0.000	0.000	0.000	0.000		0.000	0.000	0.000	0.000	
Biochanin A	0.018	0.011	0.000	0.000		0.005	0.005	0.000	0.000		0.000	0.000	0.000	0.000	
Poncirin	0.000	0.000	0.000	0.000		0.000	0.000	0.000	0.000		0.000	0.000	0.000	0.000	
Didymin	0.000	0.000	0.000	0.000		0.000	0.000	0.000	0.000		0.000	0.000	0.000	0.000	
Phloridzin	0.090	0.002	0.084	0.012		0.000	0.000	0.000	0.000		0.000	0.000	0.000	0.000	
Daidzein	0.000	0.000	0.000	0.000		0.000	0.000	0.000	0.000		0.000	0.000	0.000	0.000	
Galangin	0.218	0.238	0.000	0.000		0.000	0.000	0.000	0.000		0.000	0.000	0.073	0.007	***
Luteolin	0.596	0.070	0.305	0.377		0.189	0.021	4.353	6.836		0.043	0.014	0.168	0.190	
Equol	0.000	0.000	0.000	0.000		0.000	0.000	0.000	0.000		0.000	0.000	0.000	0.000	
Fisetin	0.048	0.027	0.000	0.000	*	0.000	0.000	0.000	0.000		0.000	0.000	0.000	0.000	
Luteolinidin	0.055	0.049	0.000	0.000		0.071	0.004	0.064	0.004		0.034	0.004	0.032	0.003	
Neoeriocitrin	0.000	0.000	0.000	0.000		0.000	0.000	0.000	0.000		0.000	0.000	0.000	0.000	
Isorhamnetin	1.213	0.386	0.718	0.027		0.601	0.327	0.491	0.015		15.737	0.413	18.571	1.166	*
Formononetin	0.008	0.001	0.000	0.000	***	0.000	0.000	0.000	0.000		0.000	0.000	0.000	0.000	
Apigenin	1.273	1.960	0.039	0.029		0.139	0.200	0.124	0.192		0.025	0.010	0.020	0.002	
Gossypin	0.000	0.000	0.000	0.000		0.000	0.000	0.000	0.000		0.235	0.027	0.128	0.112	
Glycitein	0.000	0.000	0.000	0.000		0.000	0.000	0.000	0.000		0.000	0.000	0.000	0.000	
2OHBAlc	0.000	0.000	0.000	0.000		0.000	0.000	0.000	0.000		0.000	0.000	0.000	0.000	

coniferyl alcohol	0.000	0.000	0.000	0.000		1.848	0.371	2.057	0.536		0.000	0.000	0.000	0.000	
BCA	0.000	0.000	0.000	0.000		0.000	0.000	0.000	0.000		0.000	0.000	0.000	0.000	
BGCA	0.000	0.000	0.000	0.000		0.000	0.000	0.000	0.000		0.000	0.000	0.000	0.000	
BGDCA	0.010	0.017	0.000	0.000		0.000	0.000	0.000	0.000		0.000	0.000	0.000	0.000	
BGUDCA	0.000	0.000	0.000	0.000		0.000	0.000	0.000	0.000		0.000	0.000	0.000	0.000	
BGChDCA	0.009	0.015	0.000	0.000		0.000	0.000	0.000	0.000		0.000	0.000	0.000	0.000	
BTCA	0.000	0.000	0.000	0.000		0.000	0.000	0.000	0.000		0.000	0.000	0.000	0.000	
BTDCA	0.007	0.012	0.000	0.000		0.000	0.000	0.000	0.000		0.000	0.000	0.000	0.000	
BTUDCA	0.002	0.004	0.000	0.000		0.000	0.000	0.000	0.000		0.000	0.000	0.000	0.000	
BTChDCA	0.007	0.013	0.000	0.000		0.000	0.000	0.000	0.000		0.000	0.000	0.000	0.000	
BDCA	0.319	0.124	0.228	0.094		0.172	0.021	0.088	0.063		0.264	0.014	0.040	0.069	**
BChDCA	0.000	0.000	0.000	0.000		0.000	0.000	0.000	0.000		0.000	0.000	0.000	0.000	
seco	0.000	0.000	0.000	0.000		0.000	0.000	0.000	0.000		0.000	0.000	0.000	0.000	
mata	0.000	0.000	0.000	0.000		0.000	0.000	0.000	0.000		0.000	0.000	0.000	0.000	
e-diol	0.000	0.000	0.000	0.000		0.000	0.000	0.000	0.000		0.000	0.000	0.000	0.000	
e-lac	0.078	0.017	0.039	0.014	*	0.061	0.005	0.006	0.000	***	0.045	0.004	0.000	0.000	***
syrg	1.234	0.072	0.559	0.485		0.000	0.000	0.000	0.000		0.000	0.000	0.000	0.000	
pino	0.486	0.069	0.000	0.000	***	0.238	0.074	0.000	0.000	**	0.000	0.000	0.000	0.000	
lari	0.475	0.026	0.154	0.071	**	0.000	0.000	0.000	0.000		0.000	0.000	0.000	0.000	
OH-mata	0.000	0.000	0.000	0.000		0.000	0.000	0.000	0.000		0.000	0.000	0.000	0.000	

Note(s): Statistical significance determined without correction for multiple comparisons, with $\alpha=0.05\%$. Each row was analysed individually, without assuming a consistent SD, multiple t-test, analysing each extraction separately, GraphPad Prism

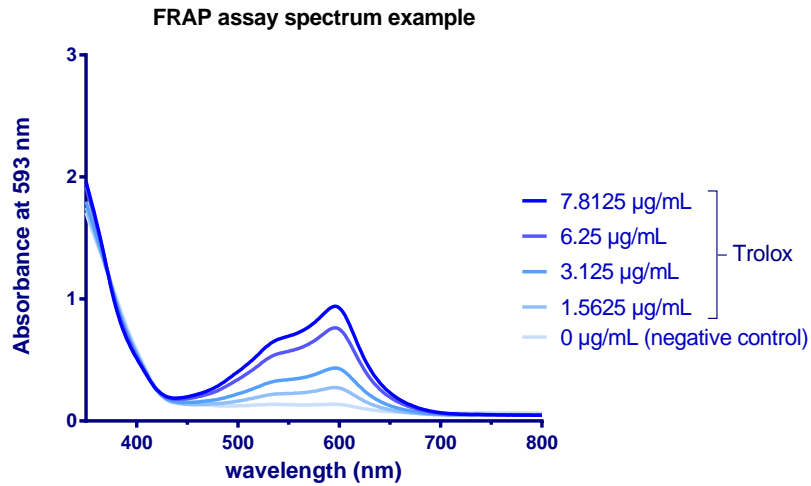


Figure A1 | Example absorbance measurement for FRAP assay (350-800 nm)

Determining 593 nm as absorbance maximum and wavelength used for the experiment

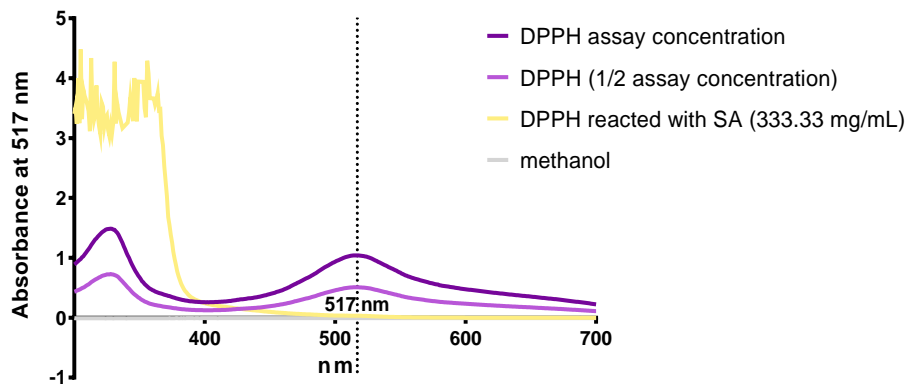


Figure A2 | Absorbance spectra for DPPH assay

Solution before and after reaction with a radical scavenger (SA) and the methanol negative control

Table A3 | Secondary metabolite composition of various *Brassica* plants

Secondary metabolite	cabbage		kale	broccoli	cauliflower	RSP	
	red	white				2012	2014
Sinapic acid	2891	445.3	2001	134.9	34.42	1153	1244
Coumaric acid	m			na	na	0.226	/
	o	372.0	/	8.195	2.575	3.767	/
	p				2.632	5.673	13.17
Ferulic acid	185.7	4.724	106.4	50.10	6.545	78.33	49.45
Benzoic acid	2.846	3.805	7.728	5.987	5.445	21.31	23.69
quercetin	6.039	0.8761	125.8	/	/	0.012	/
kaempferol	/	/	/	19.88	0.1466	141.6	153.6
p-hydroxybenzoic acid	20.88	2.385	12.03	4.618	9.464	16.53	18.07
indol-3-pyruvic acid	/	/	/	/	/	460.6	474.8

Note(s): Concentrations for all the samples given in mg/kg dry weight plant material

A3 Phytochemical Characterisation and Neuroprotective Properties of RSP Extract Phytochemical Characterisation and Neuroprotective Properties of RSP Extract *in vitro*

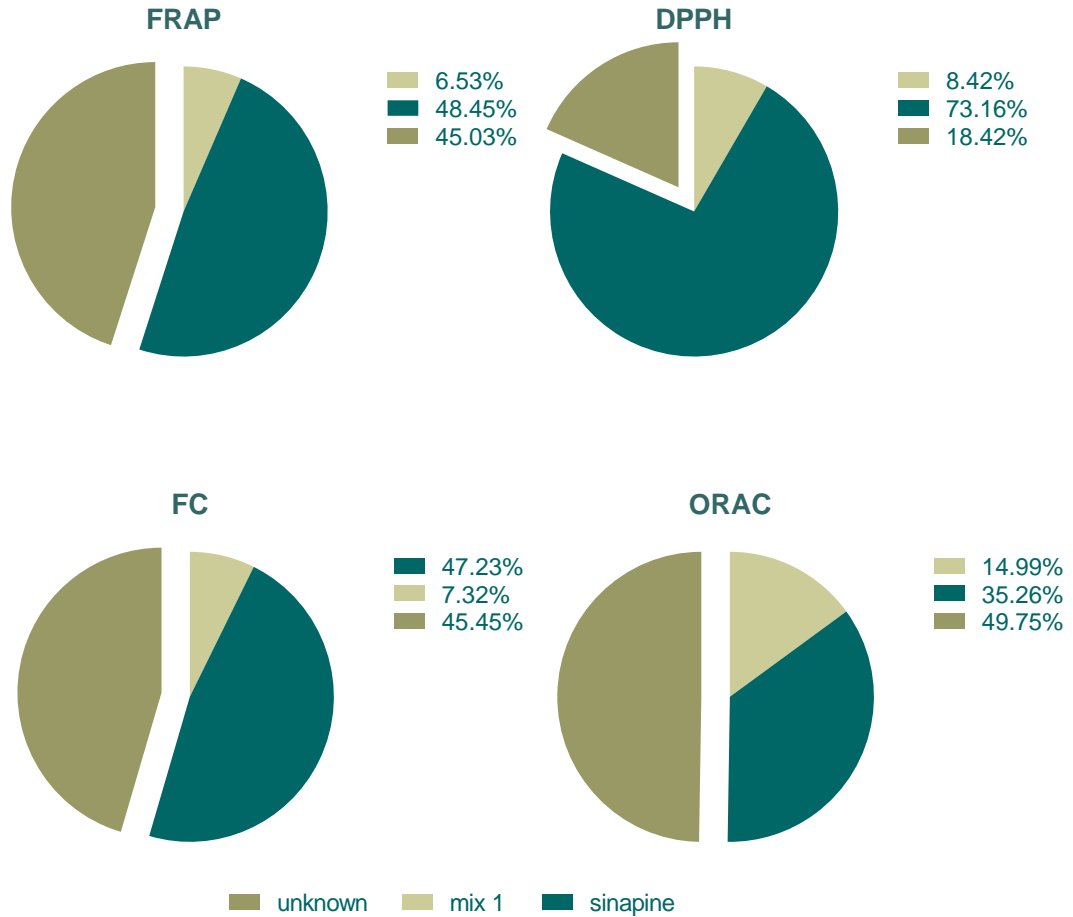


Figure A3| Comparison of sinapine and phenolic acid mixture (mix1) contribution to antioxidant activity of the extract in %, highlighting the unknown fraction

The Potential Application of Rapeseed Pomace Extracts in the Prevention and Treatment of Neurodegenerative Diseases

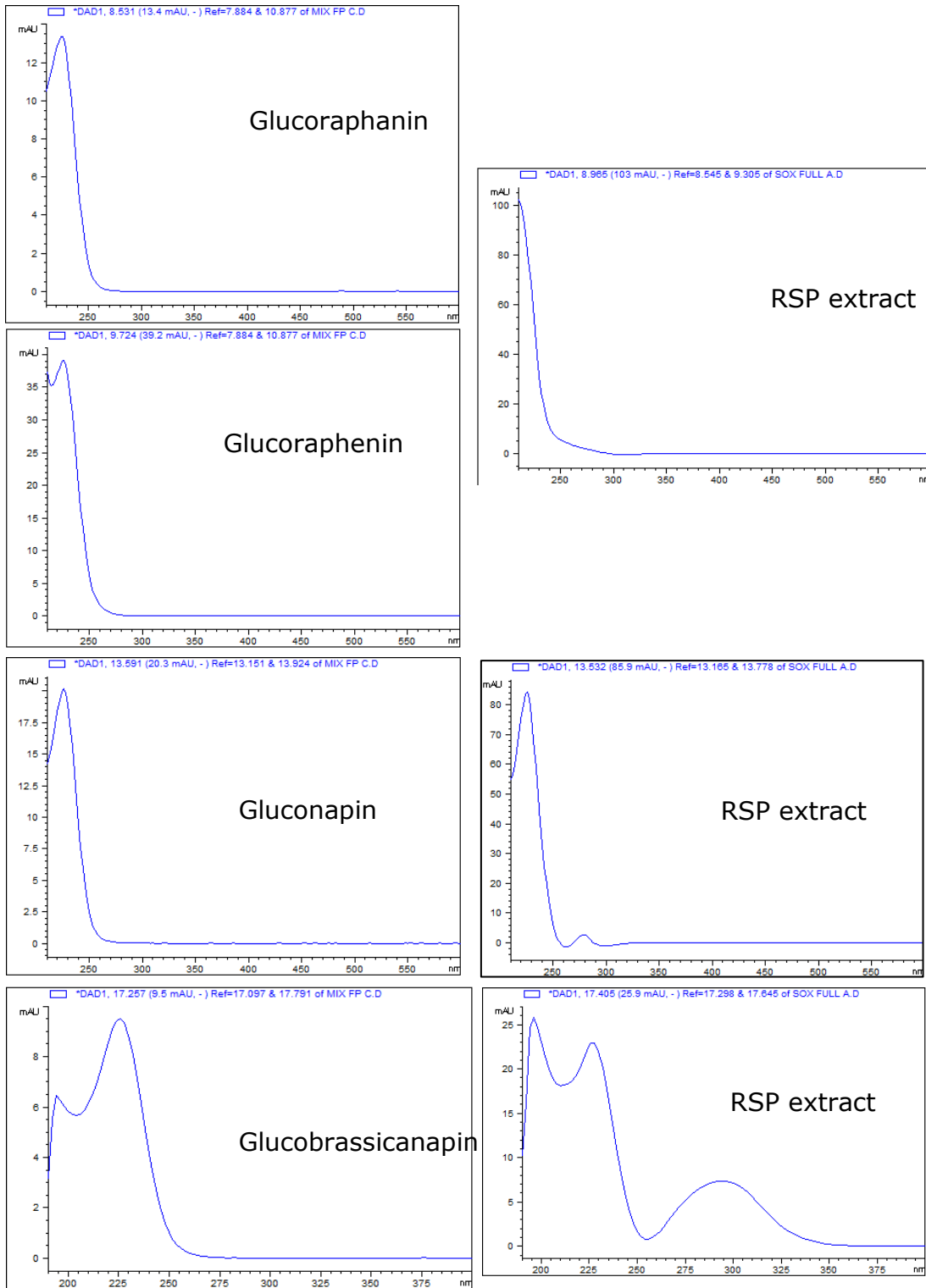


Figure A4| DAD spectra of GLS standards compared to DAD spectra of RSP extract at same retention time

Appendices

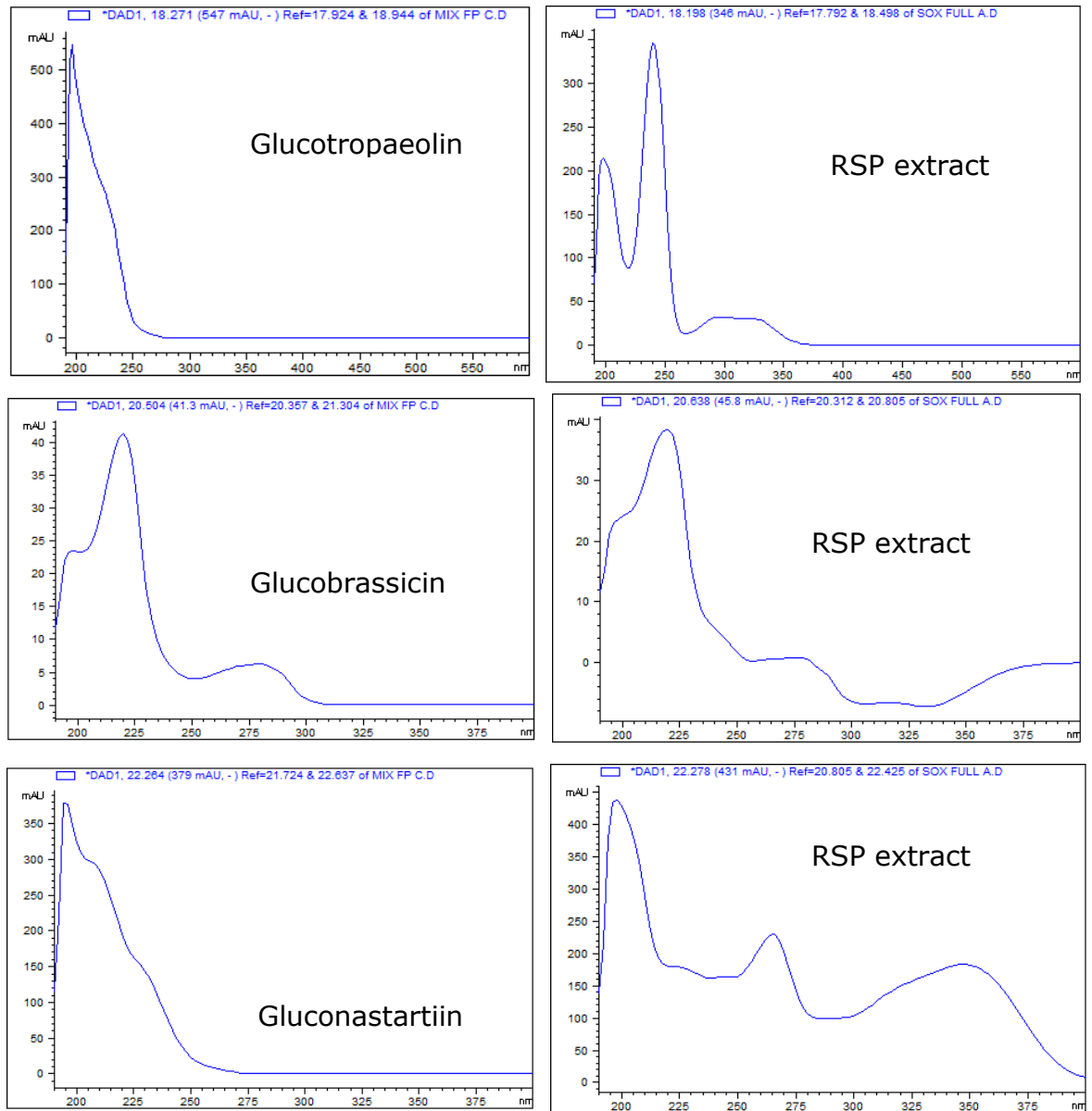


Figure A4| continued

The Potential Application of Rapeseed Pomace Extracts in the Prevention and Treatment of Neurodegenerative Diseases

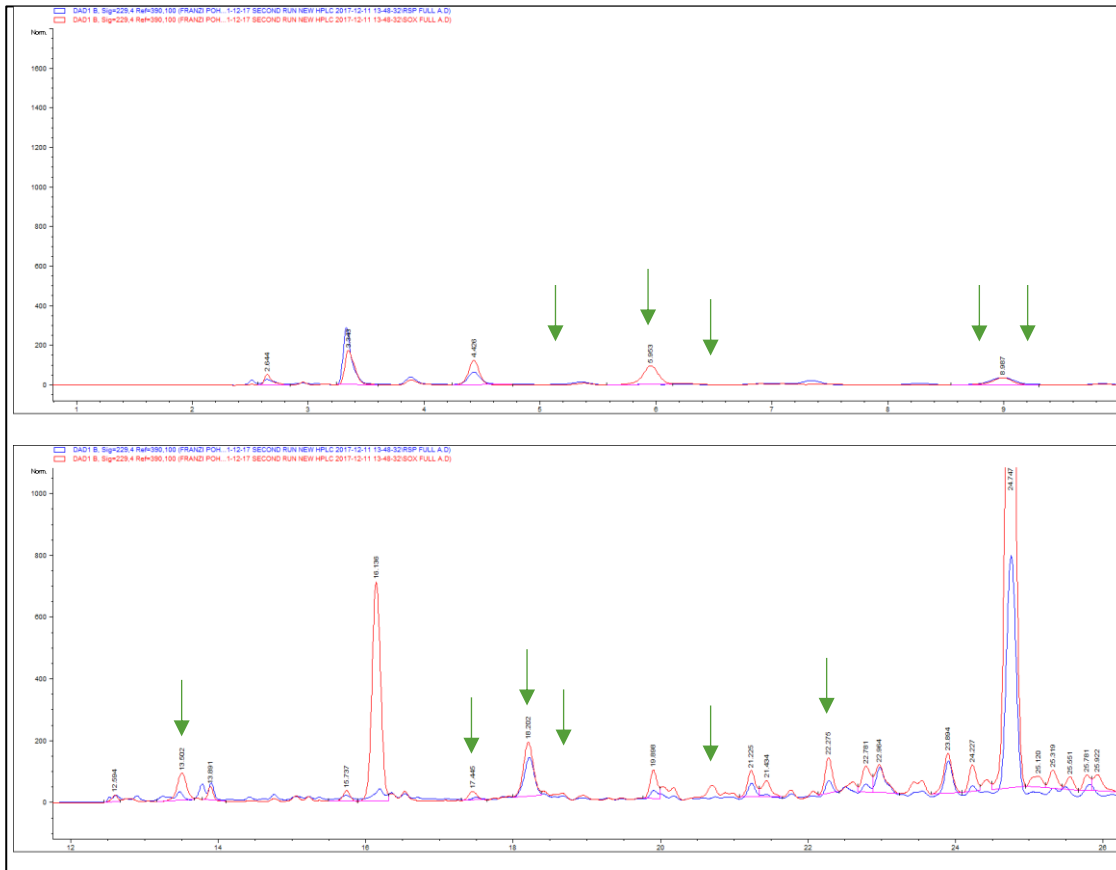


Figure A5| Comparison of chromatogram obtained for the RSP extract (red) and the RSP (blue), arrows indicating where the standards would be

Back calculation of GLSs in cold pressed RSP from GLS content of RSP extract on example of Progoitrin:

$$\text{yield} = 76 \text{ mg extract} / 1 \text{ g RSP}$$

$$\text{Progoitrin in RSP extract} = 2.197 \text{ mg/g extract}$$

$$2.197 \text{ mg progoitrin} / 1 \text{ g extract} = 0.167 \text{ mg progoitrin} / 76 \text{ mg RSP extract}$$

$$0.167 \text{ mg progoitrin} / 76 \text{ mg} = 0.167 / 1 \text{ g RSP}$$

Figure A6| Calculation of GLS in RSP from results obtained in RSP extract, using the extraction yield

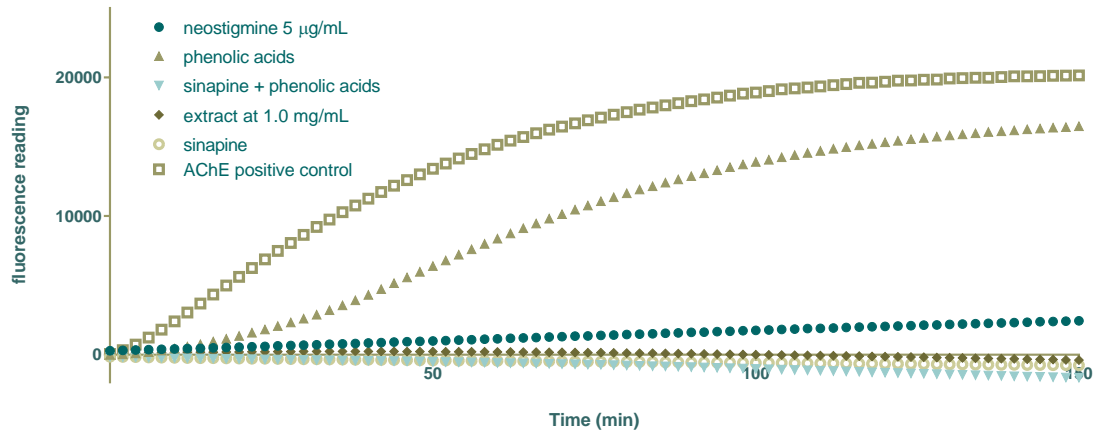


Figure A7| AChE inhibition activity of RSP extract at 1 mg/mL together with sinapine, a mixture of sinapine and phenolic acids and the phenolic acids at the extract specific concentration

Table A4|Emission values for the self-mediated β -amyloid experiment

sample	Mean excitation	control	Corrected mean	significance
Peptide	146.9	28.43 [#]	140.5 ± 19.74	
	174.9			
	185.0			
curcumin	64.21	28.43	33.9 ± 2.154	***
	59.99			
	62.85			
Extract (0.0455 mg/mL)	145.8	28.39	108.6 ± 7.873	*
	134.87			
	130.52			
Extract (0.455 mg/mL)	126.91	28.43 [#]	95.44 ± 7.475	**
	115.35	73.68	50.19 ± 7.475	***
	129.34			

Note(s): Excitation wavelength 446 nm and emission wavelength 490 nm, [#]same ThT control; statistical significant difference analysis via One-way ANOVA and Bonferroni's multiple comparisons analysis between the β -amyloid control and treatments, $p \leq 0.05$ *, $P \leq 0.01$ **, $p \leq 0.001$ ***

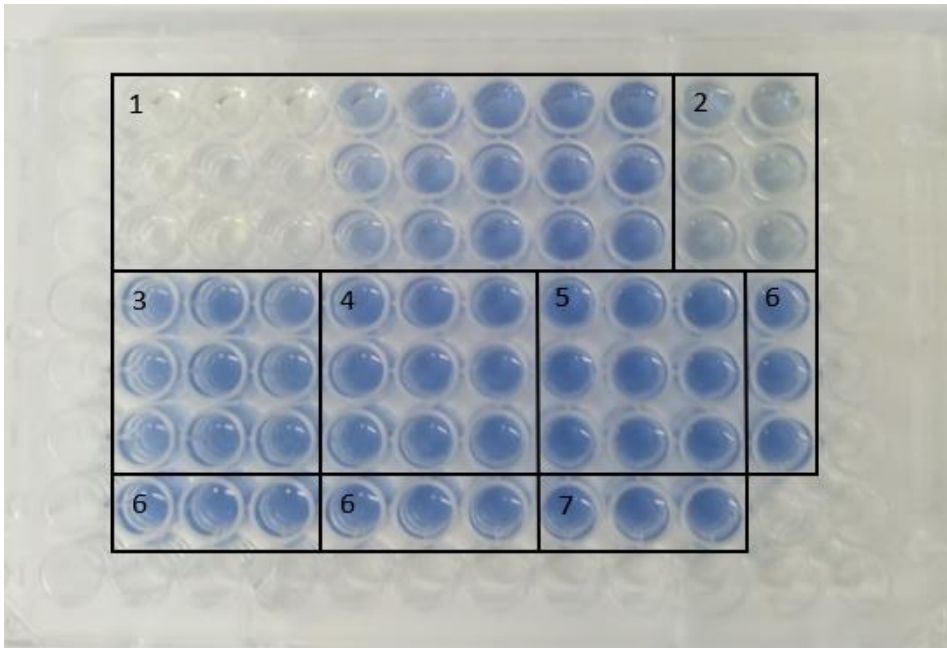


Figure A8| 96-well plate iron chelating

(1) EDTA calibration curve (5-50 µg/mL), (2) positive control (green tea), (3) RSP extract 1 mg/mL, (4) RSP extract 0.5 mg/mL, (5) sinapine 120 µg/mL, (6) sinapine 60 µg/mL and (7) negative control

A4 Cell Protective Properties of RSP Extract in SH-SY5Y Neuroblastoma Cell Line

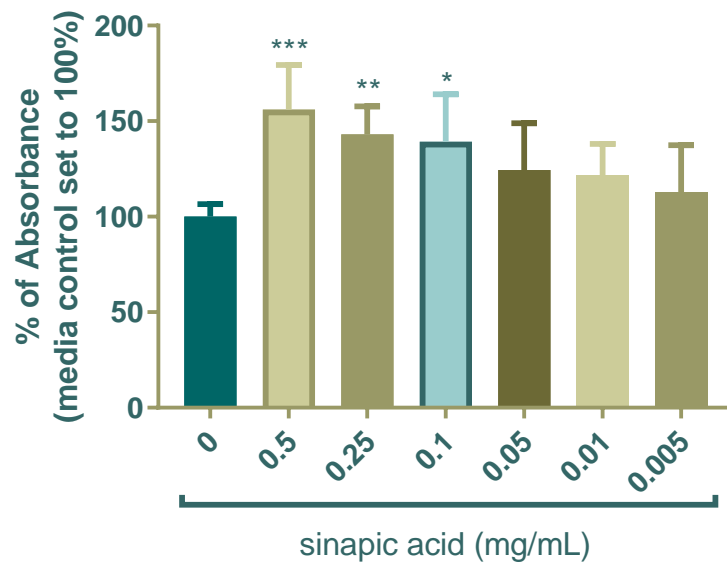


Figure A9 | MTT reduction by sinapic acid in a cell free system

The Potential Application of Rapeseed Pomace Extracts in the Prevention and Treatment of Neurodegenerative Diseases

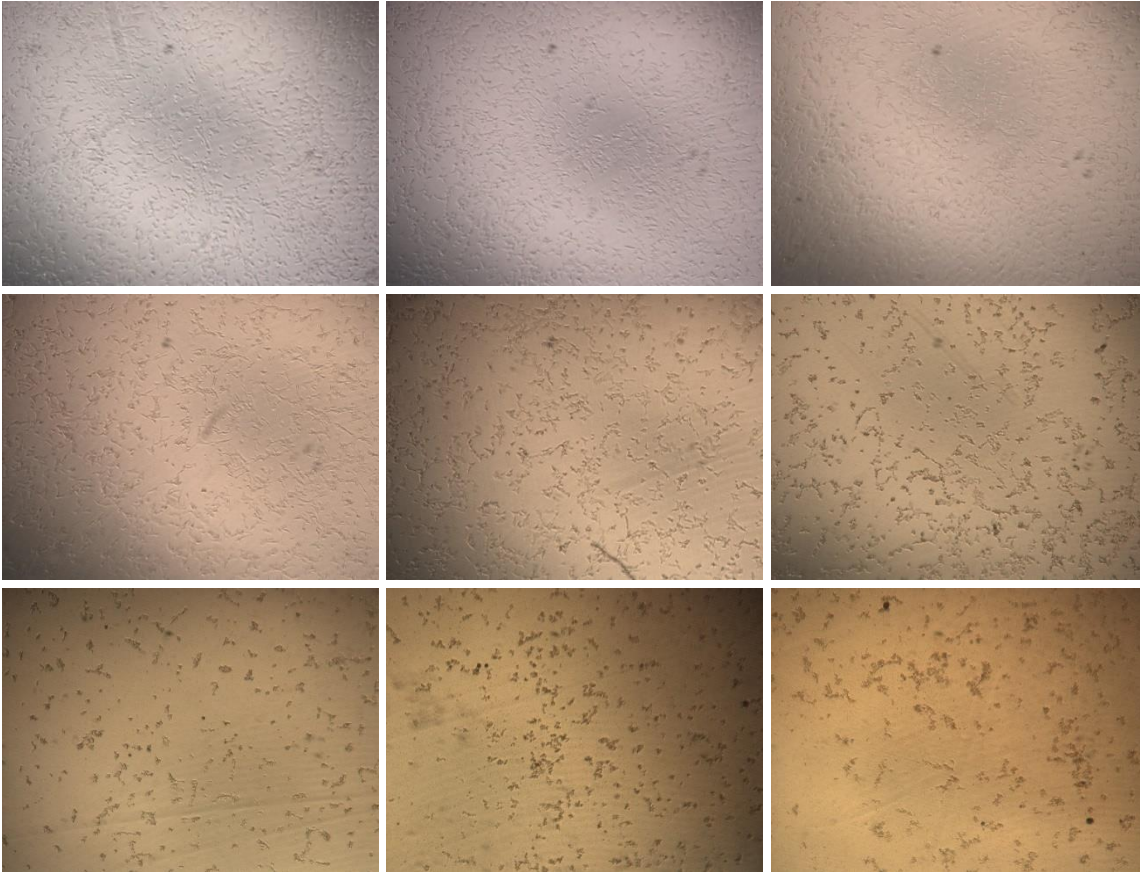


Figure A10 | Morphology of cells under treatment with RSP extract
Concentrations 0, 0.5, 1.0, 1.5, 2.0, 2.5, 3.0, 4.0 and 5.0 mg/mL from top left to bottom right (40x magnification, picture size adjusted to fit page)

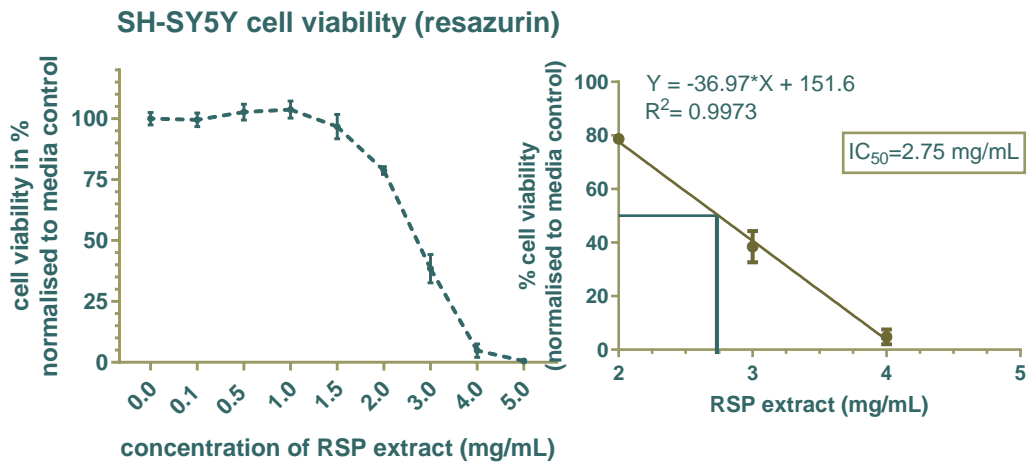
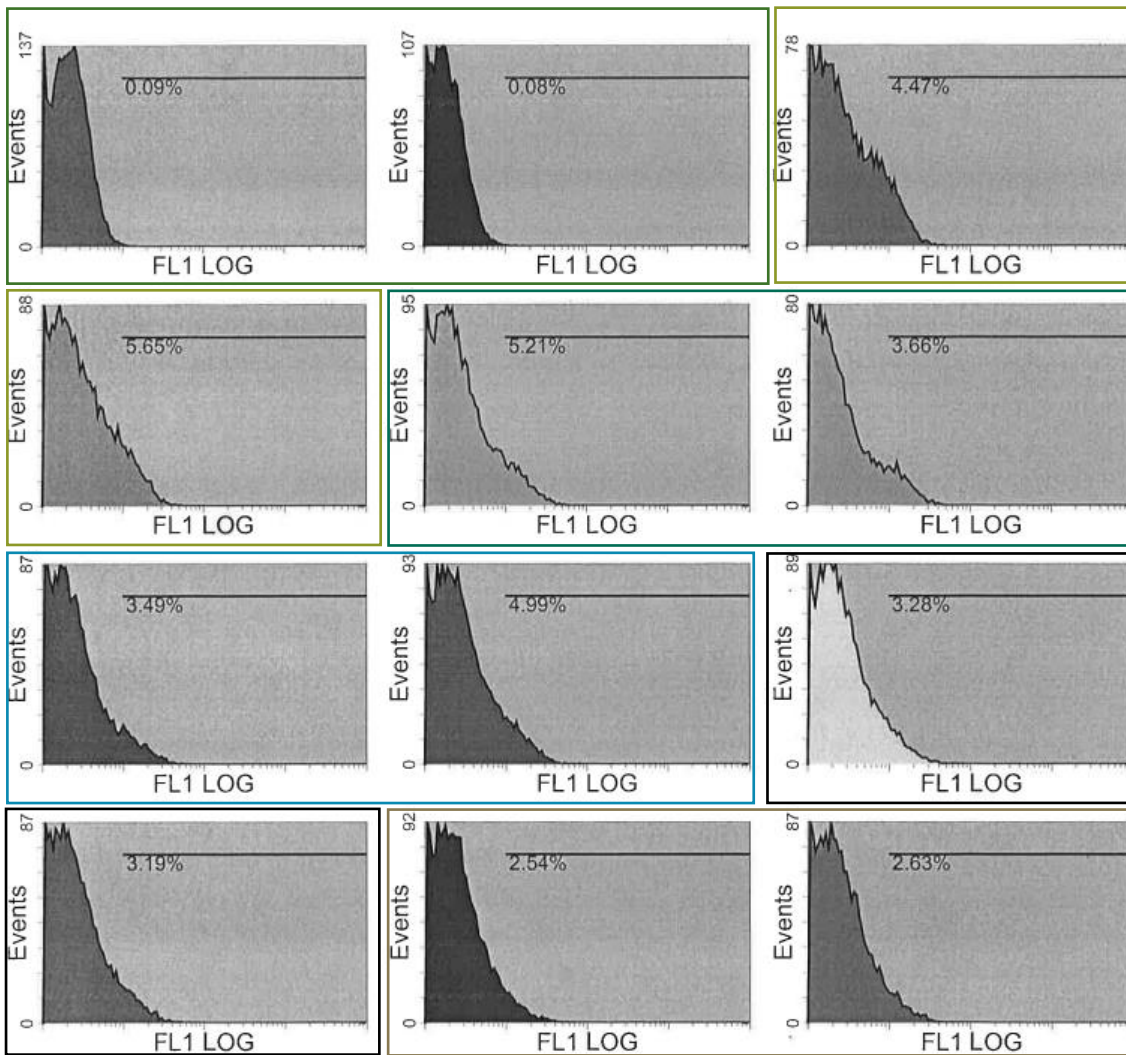


Figure A11 | IC₅₀ determination of the RSP extract

The Potential Application of Rapeseed Pomace Extracts in the Prevention and Treatment of Neurodegenerative Diseases

Overlay Plot 1



Overlay Plot 1		Statistic	Value
Data Source			
media a.LMD Ungated FL1 LOG	LM1	0.09	
media b.LMD Ungated FL1 LOG	LM1	0.08	
H2O2 a.LMD Ungated FL1 LOG	LM1	4.47	
H2O2 b.LMD Ungated FL1 LOG	LM1	5.65	
0.25 a.LMD Ungated FL1 LOG	LM1	5.21	
0.25 b.LMD Ungated FL1 LOG	LM1	3.66	
0.5 a.LMD Ungated FL1 LOG	LM1	3.49	
0.5 b.LMD Ungated FL1 LOG	LM1	4.99	
0.75 a.LMD Ungated FL1 LOG	LM1	3.28	
0.75 b.LMD Ungated FL1 LOG	LM1	3.19	
1 a.LMD Ungated FL1 LOG	LM1	2.54	
1 b.LMD Ungated FL1 LOG	LM1	2.63	

Figure A12| Raw data obtained from flowcytometry, showing Events (number of cells) related to their fluorescence intensity on a logarithmic scale (FL1 LOG)

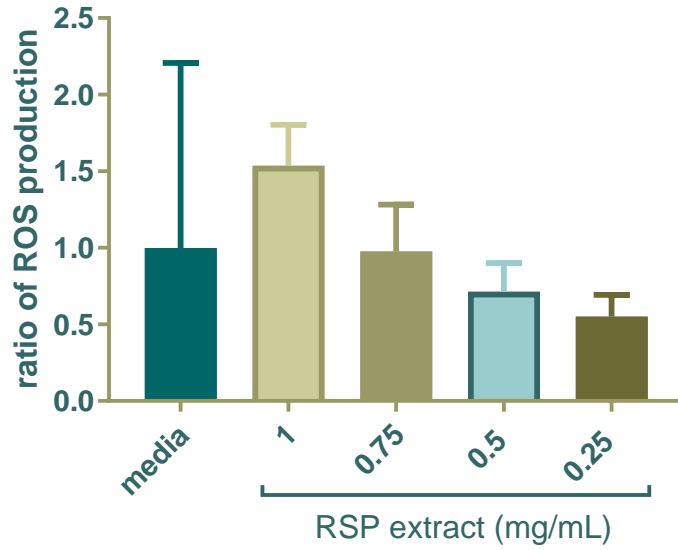


Figure A13| ROS production in SH-SY5Y cells caused by different concentrations of RSP extract (0.25-1.0 mg/mL)

Statistical significant difference determined using One-way ANOVA and Bonferroni's multiple comparison analysis compared to media control: no significant differences, n=3

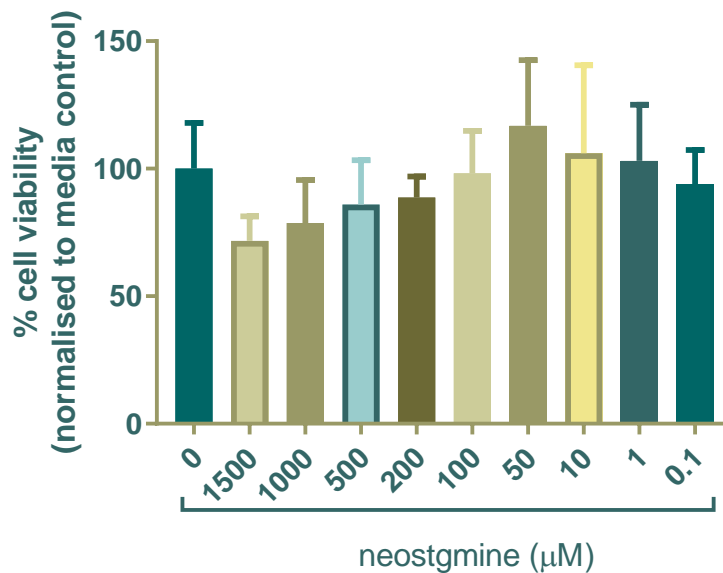


Figure A14|MTT assay neostigmine, no significant differences between all tested concentrations

A5 An *in vivo* Study of the Antioxidant and Neuroprotective Properties of RSP Extract in *C. elegans* Nematode Models

Gene: ace-1

Chromosome: X

Variation type of mutant: allele deletion (608bp)

red = mutation

actg = flanking sequence view wild type, with 250 bp flanks

green = chosen primer region

>ok663 *wild type*, with 250 bp flanks

```
gttcctagtttctcaacgtagatatcatgttcaatagaatcgcatataaaataaaataaaacgaaatcac
ctattcttatgatcatatctttcttttgattttcgatttttcgtgttcctgtcaccttgcgcatcgttcccttggttata
cttgcccagatggtgaaaaaggccattaggatcaagacgtcacattttccacatggtggtgctgctggaccggga
aaaatctgaaattgtttatcttttagatcgcaaaatatacacaatctgcgaaattccttcttgatctacagctctcc
cggcggccaaacgattatgatttgttgaagaagcatgcgaaattccttactattcttcttttctgcctcggtaaatt
tttcttgattttgcattttaaattgacattgattttaatatttttaacatttaagcaaaaataactcataatgatc
caaaacaaccaAATATCATAATAAAACACTCCTAAAAGATTTTTCATAATATCCTGTCAAATTT
TTGAAAAATAAGAACTTTTGAGGAAATCCAAAGCAGTTTGCATGTTACACCCCTACAAT
GTTTTAATGAATGAATAAGTAAAACAAAATTAAGTATAAAAAATGTAGGAAAAAATTTTT
TTGGTCTGACTTCCAAAATTATGAGCTTCAAAAAGTAAATTATCACTTTTTGACAGTA
AATAAAAAATTTTCGAAATTTTAAAGAAACGTTTTATTATGATATTCGGTCATTTGGCACT
ATAGAAATAGTTTAAAACAGTTTCCCCACTGGCGCTACCCACCTTTGAAAAAATTTAGA
AATTTTCTGGTAAGCGAAAATTAATACTAGTTTTTTTGGCAACAACTTCTAAATTATA
TTGGAACTAATTTGATAATTGTTTAAAATTTAAGATGTTTCTAAATGTTCAATGACTTTTT
TTGCAAATTTTCGAAAAGTTTAAAATTTTAAATTTCTAACTGCGATCGAAATTAACCATA
TATAAATACTGTTTATTGAATTTTTGGTTTTTGATTTAAAATTTCTTTTGGAGTACATATGT
agtattatacataaataagcaataactctttcaaaaatcacactaatttgagtttgaaattgtttgatttttaaaat
atataaacgttttttctgttccagacgatattagctgttgatctcattcacctccatgatggctccccacttttgcgga
agaagttttatcacaaccggttaaccattgacaaggtttcaaggattccatttgcaaacaccagttggcaatct
caggtacatttcttatatgatgcgcaaaactcattgtatcattttgcaggttataaaaccgaaaccaagcaacat
ggagaatacctttgaatgcgacaactccaccgaacagttgtattcagagtgaggacacttactttggagactttatg
gttcactatgtggaatgccaacactaaattatccgaagattgtctgtatttgatgtatgtgcctggaaaagtgga
accaaataagaattggctgta
```

>ok663 *ok663* with 250 bp flanks

```
gttcctagtttctcaacgtagatatcatgttcaatagaatcgcatataaaataaaataaaacgaaatc
acctattcttatgatcatatctttcttttgattttcgatttttcgtgttcctgtcaccttgcgcatcgttcccttggtt
tatacttgcccagatggtgaaaaaggccattaggatcaagacgtcacattttccacatggtggtgctgctggacc
```

cgggaaaaatctgaaatttgttatatttttagatcgcaaatatacacaatctgcaaattccttcttgatctaca
 gctctcccgcggtccaacgattatgatttgttgaagaagcatgcaaaattccttactattcttcattttctgccttc
 ggtaaattttcttgattttgcattttaaattggcatttgatttattaatatttttaacatttaagcaaaaatacactc
 ataatgatccaaaacaacca|agtattatacataatagcaataccttttcaaaaatcacactaatttgagttg
 aaattgtttgattatttataaaatataaaacgttttttctgttcagacgatattagctgttgatctcattcacctc
 catgatggctccccacttttggcgaagaagtttatcacaaccggtaaccattgacaaggttcaaggtattcc
 attgcagaaccaccagttggcaatctcaggtacatttcttatatgcatgcaaaactcattgatcattttgcaggt
 taaaaaacgaaaccaagcaaccatggagaataccttgaatgcaaaactccaccgaacagttgtattcaga
 gtgaggacacttacttggagactttatggtccactatgtggaatgccaacactaaattatccgaagattgtctgt
 attgaaatgtgatgtgcctggaaaagtggaccaataaagaaattggctgta

Figure A15|ace-1 molecular details (sequence reported on (+) strand)

The Potential Application of Rapeseed Pomace Extracts in the Prevention and Treatment of Neurodegenerative Diseases

Gene: ace-2

Chromosome: I

Variation type of mutant: allele deletion (1470bp)

red = mutation

actg = flanking sequence view wild type, with 250 bp flanks

green = chosen primer region

>ok2545 *wild type*, with 250 bp flanks

```
accaatttcagtgatgttatttgtgaataaattatcgattttttattgaaaattaaaaagttcttgattgttgttttaa
gaacatacaatttcttgaaaacatatcaatctattgataaaaattatattttcataagatgtatttttattgattttcca
tagaaaacaaaaaaaaatgtatttcaattattgattttcatgaaaaatcaattttgtcataaactaatcgataaa
tttgtttaaataacgattttttgaaatttctcgaaaaaatatggtagaaaaagtgaaaagtagccgcatca
aatccctcaaaaacatttttttaccattttctgatattttcagaatttctgatcaatcgattttaatacaaaatac
ccaagcaatatctcacctgtaggtaaagtagtacataaaacatttcaaaaatggtatccgatatcaaatcgca
aatcaataagagagcaagtaaaAACAAGTCTCCCAAGAATCGAGCAACTCCATCCCGATATC
GTCTTCAGGTACACTACTAGTCGATACATGCTCATAAGAATTCATAAATGCATTCAATA
CAAGTTTCGAACCAGCAAATATGGCATGAATGCTCTCATTGATTCTTCATAATGATCTC
GTGTAATCAGGGCTCGATTATGAGGATCTTCAGCCGATATTGTGTGATTGAATGCAAAT
CCATATTTGGGAAGTGACATGTAATAGGGTAGCCAGTATGTTCCCTTCGCTTTTTACACTT
CCGAATATTATGTTACGCTCTTTTTGAATTGCTTATTCGCCAGTTTTTGGAAATACGTCG
CCCTGAAAATGTTTACGCATAGTAGGAATAATGGTAGAGTATTACGGGAACTCAAATTT
CTGAAAATCCGTAAGTGCACAACATATTTGACGCGCATAATATCTCGTAGCGAAAACACTAC
AGTAATCTTTAAATGTTTACTTTAGCGCTTGTGTCGATTACCGGCTCCGATTTTCATC
GAATAAACGAATTAACGAATGAAAAAAAACCATTAAAAATAGAGCCCGTAAATCGACA
CAAGCTCTACAGTTGTCATTTCAAGAAATACTGTAGTTTTTCGCTACGAGATATTTTGCGA
GTCAATTATGTTGCGCAATACGCATTTTCAAATTTTGAGTTCCTATGAAAACATCGCAA
AAAATTCATATAACCAGTTCTAAAAGTAGAATAATTATAGAATTTTTTTTCCAAAATTTTC
TATGATTTTTTAAAACTCTACCGCAAAAAAATTGGCAAGACTGAATTTTTTTTTTTGAATT
CCAGCGAAAATGAATGAGTTTCAATAATCAATTGCAAAAATTTTTTTTTTCGAAAATGAAT
TTTCATACACTTTTGTGAAAAAAAATGTTGAAAAAATGTTAAATTACCAATTTTCAGAAA
AGACGTAGTTCAACTCTCCAACCCCGTTAAACTTTTTTTGAGTATTTTTTTAACTTTTGAC
TTTTTTTTGTCCTTTTTTTGGCCGTTTTTAAATGAAACTTTTTTGACCCAATTTTCGGGATGTC
CTATTTTTGCTGATTTTTTTGTGTGTTTTTCTTTTTTCTCATTTTTTCTGGATTTTTTGAA
ATTTCTGGGAATTTCTTTTTCTCTGTTTTTCTCCCTGCACTAACTAAACATAAGCTTAAG
CCTCGGCCTAAGCCTAAGCCTTAGCCTTTTCTTTTTCTTTACCTGGAAGAAATTGGCGTC
CGACGAAACAGGAACGTATGCAAATGTCATCGGTGGCCCAATATCTCCAGAAATATTAT
CAGCTTCTGCTTGAAGTACTAGATGTGCTGGAACACTTCGAAGACACTTGACAATTGCATTC
ATATCCGGTGAGCTACAGTTCACTTTTTTCGCGAGACGAAACGAAAGATCAAGCATTGT
TGGTGGAGTTGCTGATGCCCATGAGTTGATTATTGAGCCACTCTTAAAAgtgtagagagtg
ataattggaattgatggtgtaaactttgcaataatatttcaaaaatatttatgtgaattcggggcaaacagatg
agcagtcgctcgaggcggatccagctgatttctcgaacaaagtgaccggtgaccgatcgctccgaatgctccgat
```

```

attctcgtgaacccaacgaagagcaagctgttgatccattaagcccatgttccttgaatcggagaatcatctcc
gaagtagagaaatccgaatgggccagcctgaaaaaaaaatgcgtacgaagttcaggcttagaaggagatcg
gtgctcatgaataggaaactggccacaagtctaataagtaagttgcaaattgcaggataaaaattcttatattt
tttgttctaaaatcatcccactgaaaatgagaaaactgcctatatttctctcaaagaacactgctaggcaggc
aagtacgcctgtctatcattagagcctaacctaacatt

>ok2545 ok2545 with 250 bp flanks
accaatttcagtgatgattttgtgaataaattatcgattttttattgaaaattaaaaagttcttgattgtttgtttaa
gaacatacaatttcttgaaaacatatcaatctattgataaaaattatattttcataagatgattttttattgattttcca
tagaaaacaaaaaaaaatgtatttcaaattattgattttcatgaaaaatatcaattttgtcataaactaatcgataaa
ttgtttaaaaattaacgatttttttgaaaatttcggaaaaaatatggtagaaaaaagtgaaaagtagccgcatca
aatccctcaaaaacatttttttttacatttttctgatattttcagaatttctgatcaatcgatttttaatacaaacac
ccaagcaatatctcacctgtaggtaaagtagtacatataaacatttcaaaaatgttatccgatataaatcagca
aatcaataagagagcaagtaaaa | gtgttagagagtgataattgaaaattgatggtgtaaacctttgcaataa
tatttctaaaatatttatgtgaattcggggcaaacagatgagcagtcgctcgaggcggatccagctgattctccgaa
caaagtgaccctgaccgatcgctccgaatgctccgatatttctcgtgaacccaacgaagagcaagctgttgatc
cattaagcccatgttccttgaatcggagaatcatctccgaagtagagaaatccgaatgggccagcctgaaaaa
aaatgcgtacgaagttcaggcttagaaggagatcggtgctcatgaataggaaactggccacaagttctaatagt
aagtttgcaaattgcaggataaaaattcttatattttttgttctaaaatcatcccactgaaaatgagaaaactgccta
tatttctctcaaagaacactgctaggcaggcaagtacgcctgtctatcattagagcctaacctaacatt

```

Figure A16 | *ace-2* molecular details (sequence reported on (+) strand)

Gene: *gst-4*, *msp-38*

Chromosome: IV

Variation type of mutant: allele deletion (1548 bp)

red = mutation

actg = flanking sequence view wild type, with 250 bp flanks

green = chosen primer region

>ok2358 wild type, with 250 bp flanks

```
aatttgattcaagattggaattcttcctactgactcgaaaacttcaaacgaaacatctcccagataaaacaatt
gtctgatgacttcacctaactcctcgaacatcgaaacacatcagttatagtgaccattttgcagactaaaaataa
ctactctgccagtgtttaattatagatgcaattgtcactatcttcatcttatcgaccaaccattcacacttcta
atcgtgttaaaactcaattagtggaatattgaaattctatgaaacttcatttgcgacaaaagattgtgtttctc
aaacccaaaattatcaatgggaaaatgagatagacaagaactgggaaaaagtcgaggtaataaattaaag
aaatattgaatattcggcgccataatattaacgaaaataacccaaatgccaattattatccaaaagattaga
agttggcaaacctgggcaagaattccagagattgCACTAAAGTTGTAGCCAAGTTTGATCCAAC
TTATCCAATCTTTTACTAAAATTATCCTTAAGACTATTTAAATTTAGATAGAGAATTGGC
GAGAGTTAGATCCCACTTGGATATGACTTATAGTTAGCCTAACCTGAAGCTATTGCTTG
CTTGATCATTGGTTTATCGCTTGTACTTGGATAACCAGCTCCAATAGTTGTTATTTT
TGCTTTTGTTCATCATTTTTCCACGATTTACACTCTCAAGTGAAACCAACTGTTCTTTGAT
GCCAGACGATGACATTACACTTGATAAGAAAATATATATAAACTGGAATTAACAACAAAT
TGATACATCGATTCAATTACTGAATTCTAATTATGCCAACTATAAGCTATTGTATTTG
ATGCTCGTGCTCTTGCTGAGCCAATCCGTATCATGTTTGAATGCTCAATGTGCCTTAC
GAGGATTATAGAGTTTCAGTGGAAGAATGGTCAAAGCTGAAGCCAAGTGAGTGAAGCC
ATGATTATTTTATAACAATTTTCAACTTTTCAAATTTCCAGCGACTCCATTTGGCCAGC
TTCCCATTTTACAAGTCGATGGAGAACAATTCGGTCAGTCAATGTCTATCACAAGATAC
TTGGCAAGAAAATTTGGTAAGGTTTTGTTGTTTTCTTTTTAAAATGTTTAAACATCTAG
GACTCGCTGAAAAACTGCAGAGGAAGAAGCTTACGCTGATTCAATTGTAGATCAATA
CAGAGATTTTCAATTTTCCGTCAATTCCTTCTTCCGTTTTCTATGGAAGTGACGC
TGATCATATTGTAAGCATTCTTAAAATAGCATCTTAAATTTGGGTATCCTATTCTAGAACA
AAGTACGTTTTGAAGTTGTTGAACCAGCCCGTGATGATTTCTTGCAATAATCAATAAG
TTCTTGCCAAGAGTAAATCAGGATTCTCGTTGGAGACTCATTGACTTGGGCTGATAT
TGTGATTGCTGACAATTTGACAAGTCTCCTGAAGAATGGATTCTTAGATTTCAACAAG
AAAAGAAGTTGGAAGAGTTCTATAACAAGATTCATTCAATTCAGAAATTAAGAATTAC
GTGGCAACAAGAAAGGATAGTATTGTTAAAATCGAATTAATTAAGTCTGAATTATGTA
TGTAGTAAAATAATATCGTTCCTATCACGTCTCCAGAGAGCGTAATAAATTATTATTAT
GTGTTTATCCTGAAGCACCGAACTATCTAATTATCAAATATCTTTGAAAATATTAATG
TTATTCTTAAAGATCCAGTTTGGGAAAACTATGGCAGTGACAGAAAAGTGGCAGGATTT
GAGTAATTGGCATTATTTTATTATTATACAAAACCTGTTTCGCTTGAAGTCTTAATAAAT
ATTCAATCTGCAGATTAACAGAAAAACAGAACATATACTTGGAAAAAGTTTATTGTTT
AGAAACCCAGTTCACACATCCTATGGATTGACTCGATTGGAAGTTCTTGCAGCAAC
CATACCGTCTCCTTGAACCATTACGACGgaattgtttggcagcgccatccggggtgttggtccac
tcaacagtgatacgggtcgttgggtatcctctgtccgaaggcaaaagcatcgcaggaaacagcaagaagcac
agcttctttgggtcgaaaactccacatgggtgatcaactccaagtcttcatattgggtccttgatccatatcc
aatacgcagagccgatgagttgatcaccttgatgtggtcgtgtgctgtcatcgtatggagcattgaagacaatc
ttgtaccgggttgggttgatgtctctggtgggacggattggccatggcgactgttgaaggagttatgaga
actcgcactgaagattatgacaaaatctgccaatttatagcaagcttctcatcactgcccagatctttgttctaga
tttgcattgatgagttcacagaaaaatggaaaatgattattagaataatgatgaattgattattctagaaactc
gtta
```

>ok2358 *ok2358* with 250 bp flanks

```
aatttgattcaagattggaattcttcctactgactcgaaaacttcaaacgaaacatctcccagataaaacaatt
gtctgatgacttcacctaactcctcgaacatcgaaacacatcagttatagtgaccattttgcagactaaaaataa
ctactctgccagtgtttaattatagatgcaattgtcactatcttcatcttatcgaccaaccattcacacttcta
atcgtgttaaaactcaattagtggaatattgaaattctatgaaacttcatttgcgacaaaagattgtgtttctc
aaacccaaaattatcaatgggaaaatgagatagacaagaactgggaaaaagtcgaggtaataaattaaag
aaatattgaatattcggcgccataatattaacgaaaataacccaaatgccaattattatccaaaagattaga
agttggcaaacctgggcaagaattccagagattg|gaattgtttggcagcgccatccggggtgttggtccactc
```

```
aacagtgatacggtcggttggtatcctcttggtccgaaggcaaaagcatcgcaggaacagcaagaagcacag
cttctttgggtcgaaaactccacatggtggatcaactccaagtctcttcatattgggtggtcttgataccatccaat
acgacgagccgatgagttgatcaccttgatgtgggtcggtgtgcttgatcgtatggagcattgaagacaatcttg
```

Figure A17 | *gst-4* (ko) molecular details (sequence reported on (+) strand)

Table A5 | Recipes for *C. elegans* maintenance

Solution	Compound	Weight/Volume
Nematode Growth Media (NGM) -1 L	NaCl	3.0 g
	Bacto peptone	2.5 g
	Bacto agar	17 g
NGM complete (for pouring plates) ~1 L	Autoclaved NGM	1.0 L
	KH ₂ PO ₄ (1 M, pH 6, 0.2 µm filtered)	25 mL
	Cholesterol (5 mg/mL in ethanol)	1.0 mL
	MgSO ₄ (1 M, 0.2 µm filtered)	1.0 mL
	CaCl ₂ (1 M, 0.2 µm filtered)	1.0 mL
s-medium (basal) -1 L	NaCl	5.85 g
	K ₂ HPO ₄	1.0 g
	KH ₂ PO ₄	6.0 g
	Cholesterol (5 mg/ml in ethanol)	1.0 mL
Trace metal solution -500 mL	FeSO ₄ *7H ₂ O	0.346 g
	Na ₂ EDTA	0.93 g
	MnCl ₂ *4H ₂ O	0.098 g
	CuSO ₄ *5H ₂ O	0.012 g
	ZnSO ₄ *7H ₂ O	0.144 g
Potassium citrate (1M) -100 mL (pH 6)	Citric acid monohydrate	21.01 g
	KOH (for pH)	~17 g
s-medium (complete) -40 mL	s-medium (basal)	38.96 mL
	MgSO ₄ (1 M, 0.2 µm filtered)	120 µL
	CaCl ₂ (1 M, 0.2 µm filtered)	120 µL
	Trace metal solution	400 µL
	Potassium citrate	400 µl
Luria Broth (LB) -1 L	Bacto tryptone	10 g
	Bacto yeast	5.0 g
	NaCl	10 g
M9 -1 L	Na ₂ HPO ₄ *7H ₂ O	5.8 g
	KH ₂ PO ₄	3.0 g
	NaCl	5.0 g
	MgSO ₄ *7H ₂ O	0.25 g
Freezing solution -100 mL	NaCl	0.58 g
	KH ₂ PO ₄ (1 M, pH 6, 0.2 µm filtered)	5 mL
	Glycerol	24.0 mL

	Made up to 100 mL with water	~
Freezing solution (complete, prepare on day of freezing)	Freezing solution	100 mL
	MgSO ₄ (1 M, 0.2 µm filtered)	30 µL
Bleaching Solution -10 mL	Bleach	2.0 mL
	NaOH (1M)	2.5 mL
	dH ₂ O	5.5 mL

Note(s): NGM and LB were autoclaved; all other solutions are filtered (0.2 µm, Corning™ filter system) to sterilize, all solutions were thereafter handled using sterile techniques (flame/flow chamber)

PCR optimization for ace-1/ace-2 *C. elegans* strain

For the ace-1 PCR optimization, a usable mix of primers and the optimal annealing temperature for the PCR had to be determined. For this, three different PCR primer mixes were used initially (Mix 1: for₁ and rev₂; Mix 2 for₁ and rev₁; Mix 3 for₁, rev₂ and rev₁), to determine if it would be possible to use a mixture of all three primers in the PCR. To determine the optimum annealing temperature, gradient temperatures from 53.1-59.8°C were tested.

The lowest temperatures from 53.1-56.7°C show too much unspecific binding (extra bands at 300 bp and below 250 bp on top gels Figure A18). At annealing temperatures, 59.1 and 59.8°C the heterozygous band at 396 bp started to lose its intensity, which initiated the continuation of further PCRs with 58.4°C as annealing temperature. Furthermore, the latter two temperatures were also omitted due to the appearance of a contamination visible in the gels blank (B), thus making the validity of the gel questionable.

Table A 6.1 shows the expected bp lengths for the three genotypes and for each mix. At for example 54.2°C, in Mix 1 bands occur for the mutant strain (-) at about 400 bp (expected) as well as below (~300 and 200bp), the latter were not expected. These nonspecific bands disappeared with an increase in annealing temperature. Starting at 58.4°C the anticipated bands for Mix 1 and 2 were present (Table A 6.1). For Mix 3 however the 1004 bp band was missing for both, the wt (+) and the heterozygous (+/-) animals. That had prompted further PCRs using both Mix 1 and Mix 2, and not Mix 3 (containing all three primers) on its own. At annealing temperatures, 59.1 and 59.8°C

the heterozygous band at 396 bp started to lose its intensity, which initiated the continuation of further PCRs with 58.4°C as annealing temperature. Furthermore, the latter two temperatures were also omitted due to the appearance of a contamination visible in the gels blank (B), thus making the validity of the gel questionable.

Table A 6.1 | Expected DNA length* for the three different genotypes

MIX	WT (+)	MUT (-)	HET (+/-)
1	263	-	263
2	1004	396	396, 1004
3	263, 1004	396	263, 396, 1004

*Note(s): *all lengths given in bp
 WT= wild type for the ace-1 gene
 MUT= mutant, knock out for ace-1,
 HET= heterozygous for the ace-1 gene*

The same procedure was adopted with the primers obtained for ace-2, using only Mix 1 and Mix 2, to save time and master mix. The obtained DNA gels also showed some nonspecific binding for the lowest annealing temperature (53.1°C), while all the other temperatures showed the expected bp lengths for the respective genotypes. To be able to run the PCR tubes of ace-1 and ace-2 crosses together in one thermocycler (time saving), the same annealing temperature as for ace-1 (58.4°C) was chosen for ace-2. The gel obtained during PCR optimization for this temperature is depicted in Figure A19.

After optimising the primer mixtures and the PCR annealing temperature, the same settings were used for all the subsequent PCRs for the backcrosses (ace-1 and ace-2) as well as for the crosses between the two different mutants (ace-1/2 with AT3q130).

Backcrossing of mutant strains (ace-1/2)

As described (5.2.2.3 Backcrossing and creation of double mutant strains-“worm crossings”) mutants (ace-1 and ace-2) obtained from the CGC were first back crossed with N2 animals. After the second backcross (2xBC, Figure 5.17, p.297), first the heterozygous animals had to be identified. The two

DNA gels obtained after the PCR amplification and gel electrophoresis are shown in Figure A20. In the gels, the bands obtained for single worms 1-9 (10 was lost in agar) are presented as well as blank controls (B) and controls for all possible genotypes (WT, mut and het). As can be seen in Figure A20, all 9 animals were found to be heterozygous, this is due to the fact that the *ace-1* gene is located on the X-chromosome in *C. elegans*. For the *ace-2* mutants all three genotypes were found and one heterozygous plate was chosen. In the case of *ace-1* (Figure A20) it was decided to pick one of the plates with progeny from worm 5-9 due to contamination found on gel A in the blank (B₁).

From the chosen plate (e.g. #5), 16 or more worms (L4) were isolated onto new seeded NGM plates (60 mm) and left to produce progeny. The parental worms were then again subject to single worm lysis, PCR and gel electrophoresis, to find a plate with 2x back crossed homozygous *ace-1* mutant worms (Figure A21).

In the case of the first back cross (2xBC) of *ace-1* the following plates were identified to be homozygous *ace-1* mutants: plate number 1, 9 and 20 (Figure A21). Worms of one of the latter were picked onto fresh NGM plates for freezing/maintenance and 3 L₄ were chosen for the second round of back crossings (3x and 4x BC). The same procedure was repeated twice more to obtain 6x back crossed *ace-1* and *ace-2* worms.

Crossing of two mutants (*ace-1/2* with AT3q130)

After the final back crossing of both strains (*ace-1* and *ace-2*), they were ready to be crossed with the AT3q130 strain (Figure 5.18 p.300), to determine whether a knockout of either of the two *ace* genes could improve the motility deficient phenotype. After crossing 13 N2 males with 3 hermaphrodite AT3q130 animals (2 days, 15°C) and isolation of the latter (2-3 days 20°C), 13 males were selected again from one of the plates (wt/wt; q130/wt) and crossed with 3 hermaphrodite, 6xBC *ace-1* L₄s (*ace-1/ace-1*; wt/wt). Again the 3 hermaphrodites were separated and left to have progeny for 2-3 days with the possible genotypes shown in Table A 6.2.

Table A 6.2| Genotypical outcome of crossing male obtained from first cross (wt/wt; AT3q130/wt) with ace-1 hermaphrodite (ace-1/ace-1; wt/wt)

	ace-1 wt
wt q130	ace-1/wt q130/wt
wt wt	ace-1/wt wt/wt

From one of the plates with a significant number of males, 3 hermaphrodites (L4) showing fluorescence (■) under the fluorescence microscope are selected and isolated to produce progeny. After another 2-3 days 24 worms of one of the plates were isolated. Worms showing both bright (AT3q130/q130 ■) and less bright (q130/wt ■) fluorescence, were picked, to reduce the number of potential genotypes to 12 (Table 5.11, excluding animals which did not carry the AT3q130 gene), but still maintain good chances of having an ace-1/ace-1 genotype in one of the 24 animals. The 24 isolated worms were left (2-3 days) to produce progeny and were then subject to single worm PCR and gel electrophoresis to determine their ace-1 genotype (Figure A22).

After determining the homozygous mutant ace-1/ace-1 genotype in the parent generation (plate#: 2, 6, 9, 17, 18 and 20, Figure A22) as well as the homozygous wt/wt genotype (1, 4, 5, 8, 13, 15) after crossing, the plates were observed using fluorescence microscopy. The aim of this was to identify plates with 100% fluorescent worms as these were homozygous mutant strains for the ataxin-3 gene. Plates with a mixed culture of bright, less bright and non-fluorescent worms were discarded (heterozygous parental worm). Plates found with the appropriate genotypes (ace-1/ace-1 | q130/q130 and wt/wt | q130/q130), were maintained, frozen and used for future motility assays. Wt/wt | q130/q130 worms were used as back crossed AT3q130 control, because the crossing with the ace mutant worms could have induce a variation in other genes, which might change the motility behaviour. The same crossing process was undertaken for ace-2 worms with AT3q130.

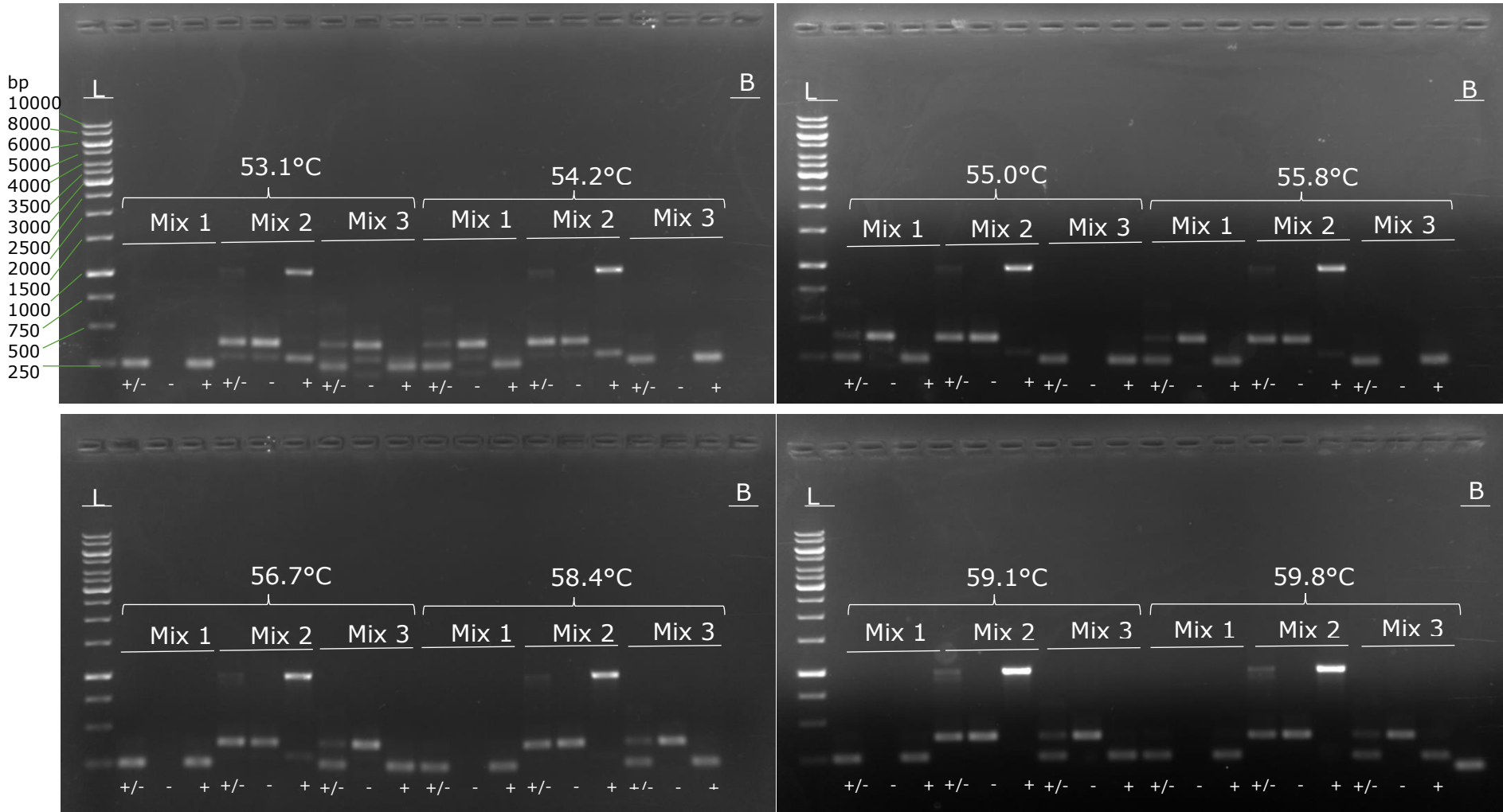


Figure A18| DNA gels for PCR annealing temperature gradient and master mix optimization procedure

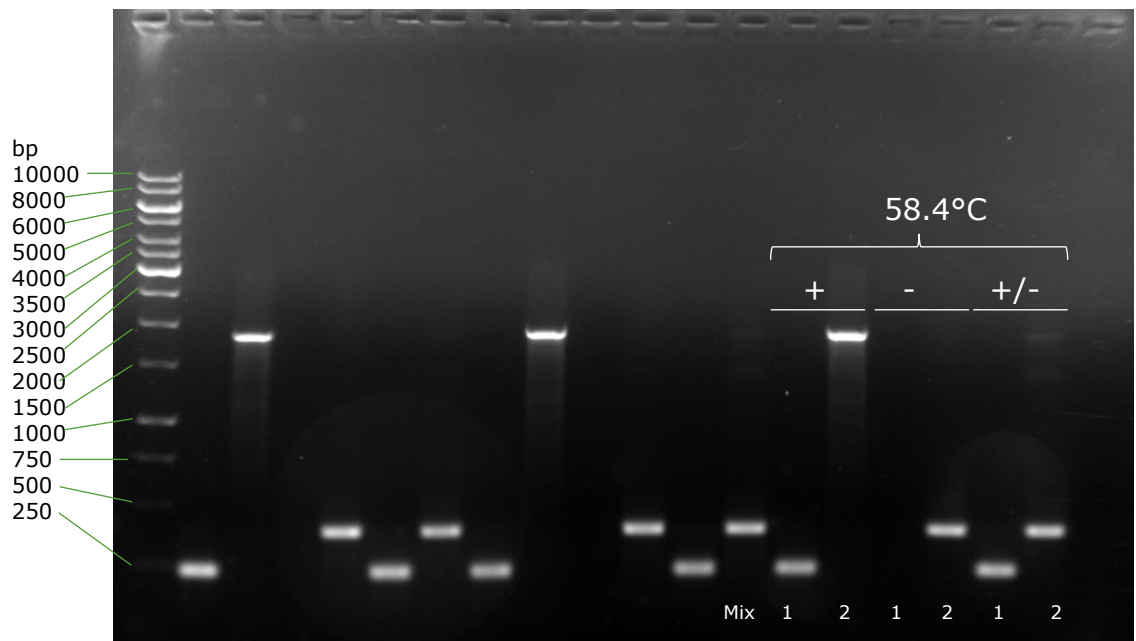


Figure A19| DNA-gel after PCR of *ace-2* gene, showing the chosen temperature (58.4°C) with the expected bands (ladder same as in Figure)

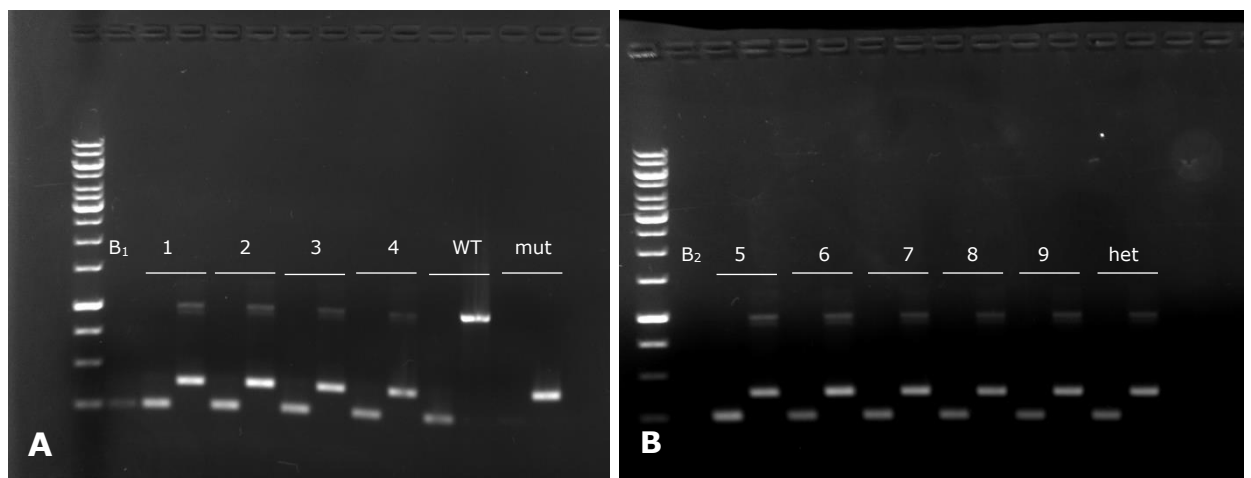


Figure A20| DNA gels depicting initial isolated hermaphrodites after second backcross
 Gel A: blank 1 (B_1), worms 1-4, WT-wild type control and mut- mutant *ace-1* control,
 gel B: blank 2 (B_2), worms 5-9 and het-heterozygous control (ladder same as in Figure 5.31 and 5.32)

The Potential Application of Rapeseed Pomace Extracts in the Prevention and Treatment of Neurodegenerative Diseases

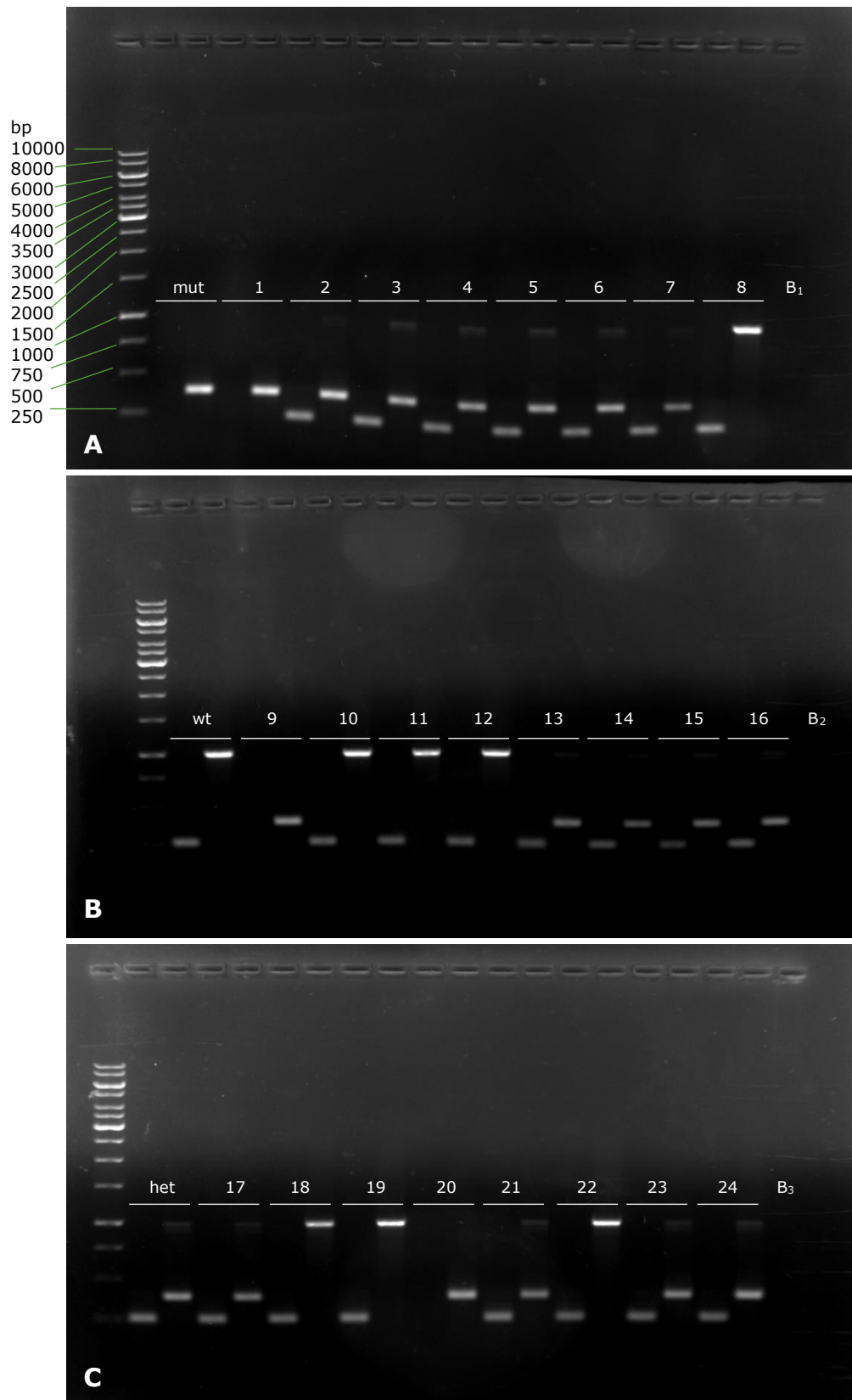


Figure A21| DNA gels depicting single worm PCR of worm isolation after the second backcross, to identify homozygous 2xBC animals
Gel A: *mut*- mutant *ace-1* control, worms 1-8, blank 1 (B_1); gel B: *WT*-wild type control, worms 9-16 blank 2 (B_2); gel C *het*-heterozygous control, worm 17-24 and blank 3 (B_3)

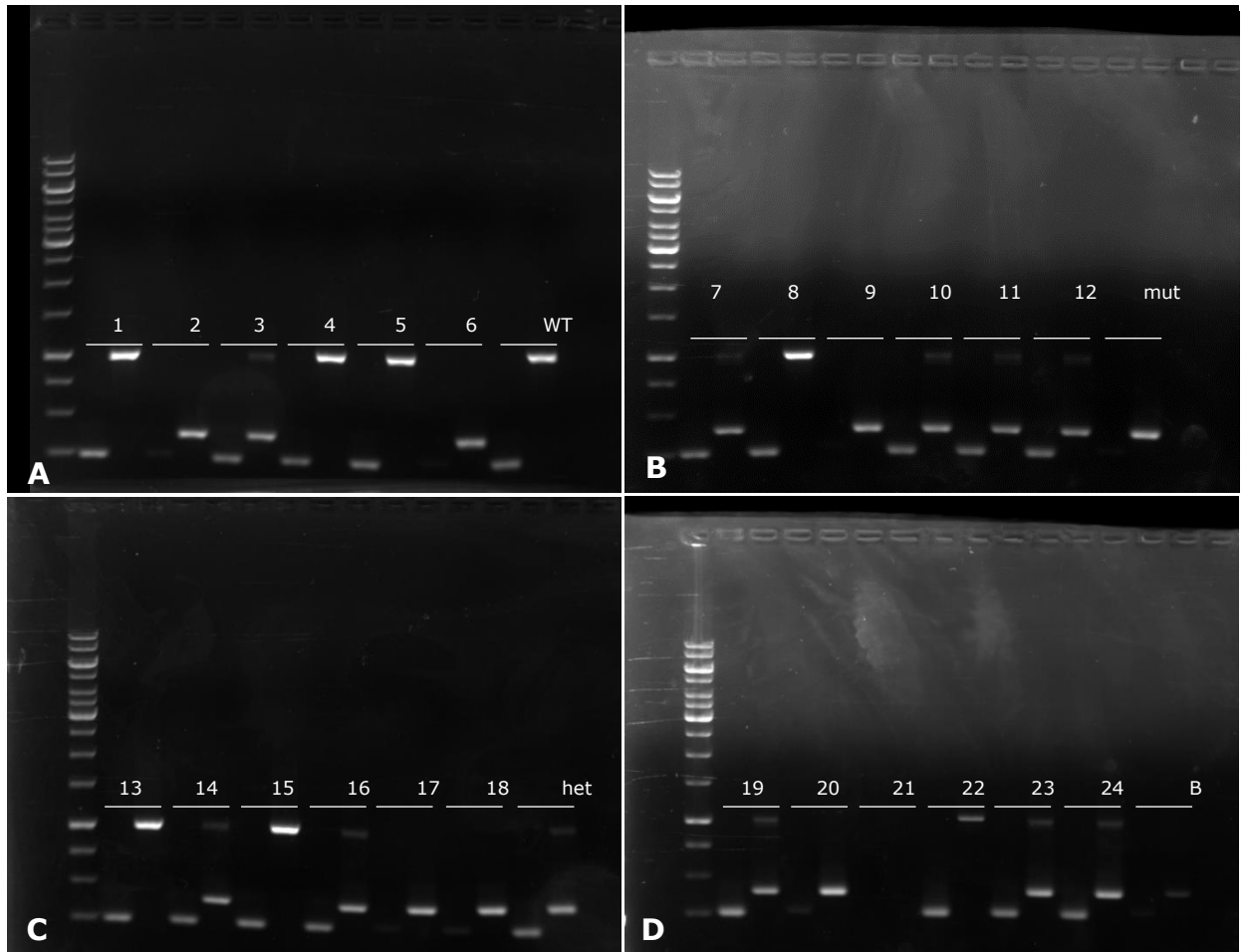


Figure A22 | DNA gels depicting single worm PCR of second worm isolation after crossing (*ace-1*) with AT3q130 animals, to identify homozygous *ace-1* animals

Gel A: worms 1-6, WT-wild type control; gel B: worms 7-12, mut- mutant ace-1 control; gel C worm 13-18, het-heterozygous control; gel D: worms 19-24 and blank (B); ladder same as in Figure A18/21

The Potential Application of Rapeseed Pomace Extracts in the Prevention and Treatment of Neurodegenerative Diseases

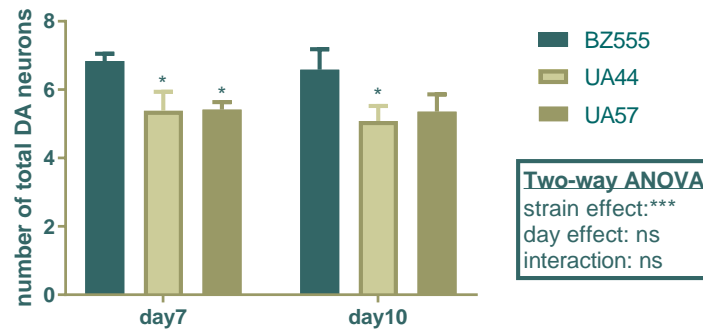


Figure A23 | Comparison between day 7 and day 10 old animals (BZ555, UA44 and UA57)

Statistical significant difference determined using Two-way ANOVA and Bonferroni's multiple comparison analysis: * $p < 0.05$, 3 independent experiments with $n \geq 10$ animals

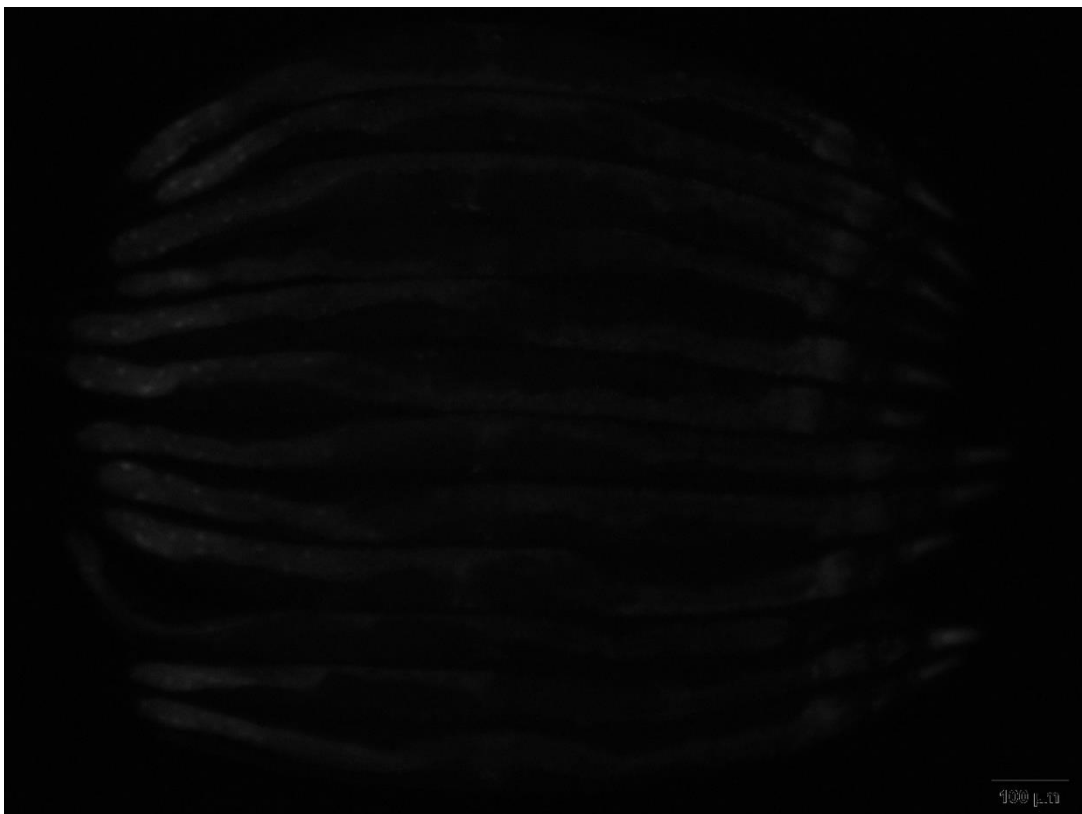


Figure A24| Fluorescence imaging of *sod-3* reporter strain after RSP extract treatment (see Figure Figure 5.35)
Top: DMSO (1%) and bottom RSP extract (4 mg/mL)